2017

Syntheses of Functionalized Cycloparaphenylenes, Furan-Containing Cycloparaphenylenes, and Related Thiophene-Containing Fused Carbon Nanohoop

Behzad Farajidizaji

Syntheses of Functionalized Cycloparaphenylenes, Furan–Containing Cycloparaphenylenes, and Related Thiophene–Containing Fused Carbon Nanohoop

Behzad Farajidizaji

Dissertation submitted to the Eberly College of Arts and Sciences

at West Virginia University

in partial fulfillment of the requirement

for the degree of

Doctor of Philosophy

in

Chemistry

Kung K. Wang, Ph.D., Chair

Jeffrey L. Petersen, Ph.D.

Bjorn C. G. Soderberg, Ph.D.

Brian V. Popp, Ph.D.

Robert K. Griffith, Ph.D

C. Eugene Bennett Department of Chemistry

Morgantown, West Virginia

2017

Keywords: Diels–Alder Reaction, Cycloparaphenylenes, Fused Carbon Nanohoops, Homocoupling, Benzyne, Reductive Deoxygenation, Oxidative Aromatization

ABSTRACT

Syntheses of Functionalized Cycloparaphenylenes, Furan–Containing Cycloparaphenylenes, and Related Thiophene–Containing Fused Carbon Nanohoop

Behzad Farajidizaji

Synthetic pathways for preparing furan-containing cycloparaphenylenes (CPPs) bearing 10, 12, and 15 aromatic units in the macrocyclic ring structures were developed. Several important steps used in these syntheses are the Suzuki–Miyaura cross-coupling reaction between the L-shaped building block and 2-furanylboronic ester the nickel–mediated homocoupling reaction to incorporate two and three 2,2′-bifuran-5,5′-diyl units into functionalized [6]- and [9]cycloparaphenylene (CPP) precursors. Oxidative aromatization of the precursors with 2,3-dichloro-5,6-dicyano-1,4-benzoquinone (DDQ) under mild conditions led to the formation of fully aromatized furan-containing cycloparaphenylenes (CPPs).

The Diels−Alder reaction between the parent benzyne or 3,6-dimethoxybenzyne with furan-2,5-diyl units incorporated into functionalized [8]CPP macrocycle followed by reductive deoxygenation of the Diels−Alder adducts with diiron nonacarbonyl, $Fe_2(CO)_9$ led to the formation of functionalized [12]CPP macrocyclic precursors. Oxidative aromatization with DDQ produced functionalized [12]cycloparaphenylenes bearing four evenly spaced biphenyl and naphthyl units. Additionally, a synthetic pathway for preparing a functionalized [10]CPP has been developed. Tetrahydro[10]CPP was used to investigate the effect of macrocyclic ring size on the reaction rate of oxidative aromatization with DDQ.

Finally, a synthetic pathway for the construction of fused molecular nanohoops bearing two macrocyclic rings with different ring sizes by using two different 1,3-butadienes for the

Diels–Alder reactions with 1,4-benzoquinone has been developed. The key intermediate in this strategy involves having four phenyl groups in *cis* position to one another after the second Diels–Alder reaction. This intermediate led to the formation of a fused carbon nanohoop bearing a tetrahydro[6]cycloparaphenylene (4H[6]CPP) fused to a 4H[10]CPP and a macrocycle bearing a 4H[6]CPP fused to a [6]CPP inserted with two 2,2′-bithiophene-5,5′-diyl units.

Dedicated to

People of Syria and Their Revolution,

Hanyu, Farzad, Paria, and My Parents

Acknowledgment

First, I wish to express my gratitude to my advisor Professor Kung K. Wang, Eberly Distinguished Professor of Chemistry. Professor Wang vision and dedication, for the opportunity to study under his mentorship, and trusting me to help to lay the intellectual, ethical, and scientific foundation of the Wang lab as one of his last students. I am so lucky to have him as my advisor and mentor. He is an excellent example for me in academic and personal life. He is one of the most humble and trustworthy persons I have ever met. I would like to thank oppression in Iran which led me to think about unthinkable and taught me about curiosity, wonder, and beauty of crossing line. I would like my parents and family especially Farzad which always make fun of me and pressured me to the point that I decide to make a turn. I would like to express my deep appreciation to my lovely girlfriend Hanyu. She was always with me in all the time. I would also like to express my appreciation to the formative members of the Wang lab: Dr. Changfeng Huang, Haresh Thakellapall, Shuangjiang Li, Merfat Aljahdli. I would like to express my gratitude to former advisor Dr. Brian V. Popp, his behavior especially in handle the hard situation set the best example for me, I wish one day I will be like him.

I would like to thank my committee members, Professors Dr. Jeffrey L. Petersen, Dr. Bjorn C. G. Soderberg, Dr. Brian V. Popp, and Dr. Robert K. Griffith for taking the time to serve as my committee member. Special thanks to Dr. Petersen for his tremendous work in X-ray structure analysis. I would like to thanks, Dr. Popp for DFT calculation and teaching me 2D NMR. Finally, I would like to thank Dr. Novruz for his NMR experiments for structural elucidation.

Table of Contents

List of Tables

List of Figures

List of Schemes

Chapter 1: Cycloparaphenylene and Related Carbon Nanohoops

Background

Since the first synthesis and structural analysis of carbon nanotubes (CNTs) were reported,[1] much attention has been given to research in this area. Due to their extreme diversity, richness, and unprecedented mechanical and optical properties, CNTs have become a major area of materials research.[2-5] Due to their unprecedented properties, such as thermal and electrical conductivity,[6-9] high aspect ratio,[10] high tensile strength,[11] and unique optical characteristics,[12-14] CNTs are perfect candidates to be considered for the next generation of materials and will be used in many different areas of technology, specifically in nanotechnology.[15] CNTs are used in various applications such as electrical wiring,[16] sensor arrays,[17-21] sensing,[22] biomaterials,[23] field-effect transistors,[24-26] transparent conductive films,[27] interconnect,[28] and other nanoscale applications.[29-34] However, the lack of purification methods for CNTs is one of the most important aspects that limits taking advantage of their unique qualities.[35] Besides, control over chirality and size of CNTs also is a major barrier to the progress of this field.[36,37] In general, CNTs are divided into two categories: single-wall carbon nanotubes (SWCNTs) or multi-wall carbon nanotubes (Figure I-1). Single-wall carbon nanotubes surrounded by another larger nanotube create a multi-wall carbon nanotube.

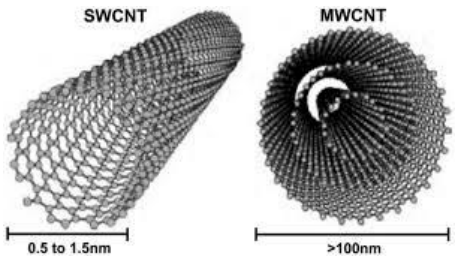

Figure I-1. Single wall carbon nanotube and multi-wall carbon nanotubes.

Carbon Nanotubes: Structure, Properties, and Synthesis

CNTs are formed by wrapping a graphene sheet into a hollow cylindrical structure.[38] CNTs are formed entirely from sp^2-hybridized carbon atoms; based on connectivity and orientation of these sp^2 hybridized carbons, different types (armchair, zigzag, chiral) and sizes of CNTs can be synthesized (Figure I-2). Carbon nanotubes, based on their structures, can have very different electronic properties.

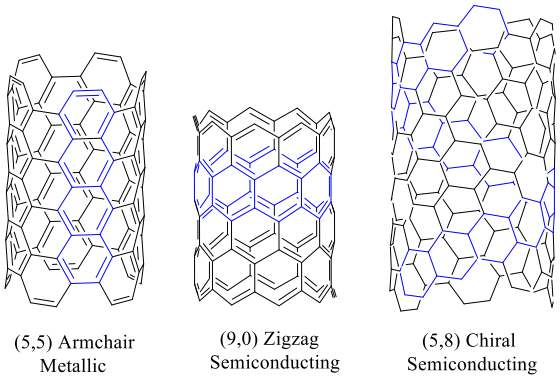

Figure I-2. Various types of carbon nanotubes: (n,n) armchair, (n,0) zigzag and (n,m) chiral.

The electronic properties of SWCNTs are extremely sensitive to the chiral pitch (side wall structure) and tube diameter.[24] CNTs, based on their structure, can either have metallic or semiconductor properties. Due to the ability to vary their band gap, chiral and zigzag CNTs have the potential to replace traditional semiconductors.[9,39] However, armchair CNTs have metallic properties due to m = n; these specific CNTs have a 0 eV band gap. These CNTs can support carrier mobility of approximately 10^4 $cm^2V^{-1}s^{-1}$, which allows them to react in a superconductive fashion. Armchair CNTs support current density 1000 times more than copper.[9]

CNTs have unique optical properties which depend on molecular structure and diameter;[18] Furthermore, CNTs emission wavelength also depends completely on their structures. Careful changes in the shape and size of the CNTs can allow for extensive application in a variety of fields.

The current methods for synthesizing CNTs are arc discharge,[41] laser ablation,[42] and chemical vapor deposition (CVD),[43] which result in a mixture of different types of CNTs, with very different chiralities and diameters. To further complicate things, there are no developed purification techniques that allow for complete isolation of a single type and diameter of CNTs. A synthetic method that permits the formation of a homogeneous CNT is not only desirable but also necessary. These complex challenges provided a tremendous opportunity for chemists to not only address these issues but also to develop new types of chemistry at the same time.

Challenging Unnatural Hydrocarbons

The design and synthesis of rare unnatural products have amazed and puzzled organic chemists for decades. Construction of these novel molecules stretched the boundaries of limitation to discover new chemistry. These unnatural products are often carbon rich. For example, polycyclic aromatic compounds such as circulenes, helicenes, and fullerenes (Figure I-3) are among these unique unnatural products, which share similarity base on the distortion of one or multiple bonds from the plane. Although many of these products have been around for decades, cycloparaphenylenes have just recently joined this group.

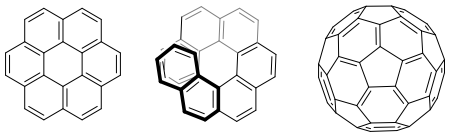

Figure I-3. Polycyclic aromatic compounds.

Cycloparaphenylenes (CPPs) or carbon nanohoops comprise a sequence of benzenes that are connected at *para* positions to make a cyclic ring (Figure I-4).[44.45] At first glance, it is

apparent that the conjugated π-system in a cycloparaphenylene molecule is not planar. A simple planar polyphenylene is not easily connected intramolecularly to form a cyclic structure. Creative synthetic approaches and new chemistry are required to overcome severe distortion in these new classes of compounds. CPPs are the smallest repeating cyclic segment of [*n*,*n*] armchair CNTs and can be used as potential templates for bottom-up synthesize of CNTs.

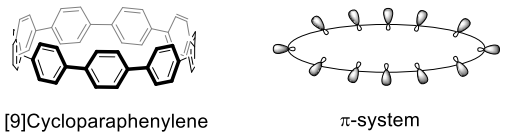

Figure I-4. [9]Cycloparaphenylene and non-planar π-system.

Early Approach Towards Synthesis of Cycloparaphenylenes

In 1943, Parekh and Guha reported an attempt to synthesize [2]CPP by thermal desulfination of macrocycle **I-1** in the presence of copper (Scheme I-1).[46] Unfortunately, only partial desulfination occurred, upon heating with copper, to form **I-2**. The high strain of [2]CPP could be a potential reason that the disulfidation did not procced to completion.

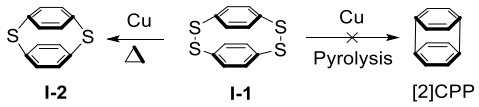

Scheme I-1. Parekh and Guha's Attempted Synthesis of [2]CPP

Almost 60 years after the first attempt, Vögtle adopted the same strategy.[47] The less strained hexaphenyl pentasulfate macrocycle **I-3** was prepared in 65% yield (Scheme I-2). Pyrolysis of macrocycle **I-3** did not produce the desired product, [6]CPP. It was not efficient enough to compensate the strain in highly rigid and bent CPPs.

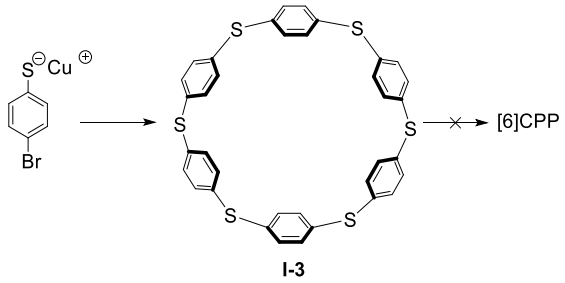

Scheme I-2. Pyrolysis of Macrocyclic **I-3** to Obtain [6]CPP

Furthermore, Vöglte tried the Wittig macrocyclization reaction between dialdehyde **I-4**, and diphosphonium **I-5** and **I-6** at highly dilute conditions to synthesize phenyleneethyleneacetylene macrocycles **I-7** and **I-8**, respectively.[47] In addition, Vöglte also decreased the polymeric side product through this method. Unfortunately, the [4+2] cycloaddition reaction with ene-yne moieties in macrocycles **I-7** and **I-8** was not successful in producing the final four benzenes and the corresponding [8] and [10]CPPs.

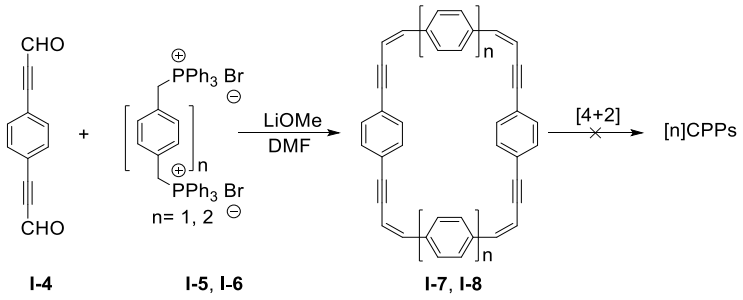

Scheme I-3. Diels−Alder Reaction for the Synthesis of [8] and [10]CPPs

Moreover, Vöglte tried a shotgun approach by using the Cu-mediated Kumada macrocyclization of L-shape *cis*-1,4-diarylcyclohexanes **I-9** (Scheme I-4).[47] Unfortunately, the desired macrocycle was not formed. However, Vöglte envisioned that cyclohexane could be

oxidized to benzene to form the corresponding nanohoops. This strategy was exploited by Itami group later (c. f. Scheme I-9).

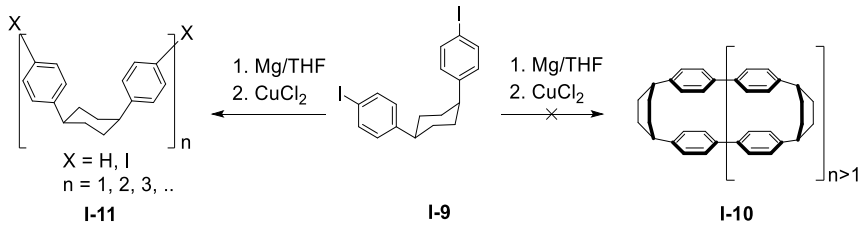

Scheme I-4. Kumada Macrocyclization of Diiodide **I-9**

Finally, Vöglte carried out an intramolecular McMurry coupling reaction on dione **I-12** to form macrocycle **I-13** (Scheme I-5).[47] However, Vöglte's incredible synthesis journey halted at that point, as there was no method for oxidative dehydration to form the desired [5]CPP.

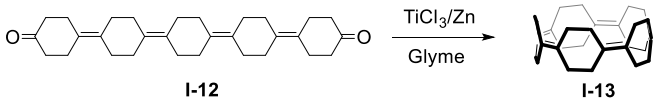

Scheme I-5. Intramolecular McMurry Coupling of Dione **I-12**

Different Strategies for the Synthesis of Cycloparaphenylenes

1. Jasti and Bertozzi Strategy

After almost 70 years of intellectual conception, [n]CPP was successfully synthesized in Bertozzi's lab.[48] Jasti and Bertozzi utilized 1,4-*cis*-dimethoxy-2,5-cyclohexadiene unit **I-14** to form CPP precursor macrocycles (Scheme I-6). Due to the presence of sp^3 hybridized carbons, compound **I-14** contains a curvature in its structure, which is necessary to form a macrocycle and to mask the benzene ring. After a lithium-halogen exchange of diiodobenzene, the 1,4-benzoquinone is transferred via cannula to a lithiated 4-iodobenzene solution. This is followed by methylation with iodomethane in the presence of NaH, which allows the formation of **I-14** in

34% yield over two steps. A portion of *cis*-diiodie **I-14** was converted to bis-boronic ester **I-15** in 82% yield. The Suzuki-Miyaura cross-coupling reaction was carried out between diiodie **I-14** and bis-boronic ester **I-15** in high dilution, which resulted in formation of **I-16** to **I-18**. This shotgun approach also produced of oligomeric by-products in greater quantity than the desire macrocycles. However, the macrocycles were prepared in only four steps.

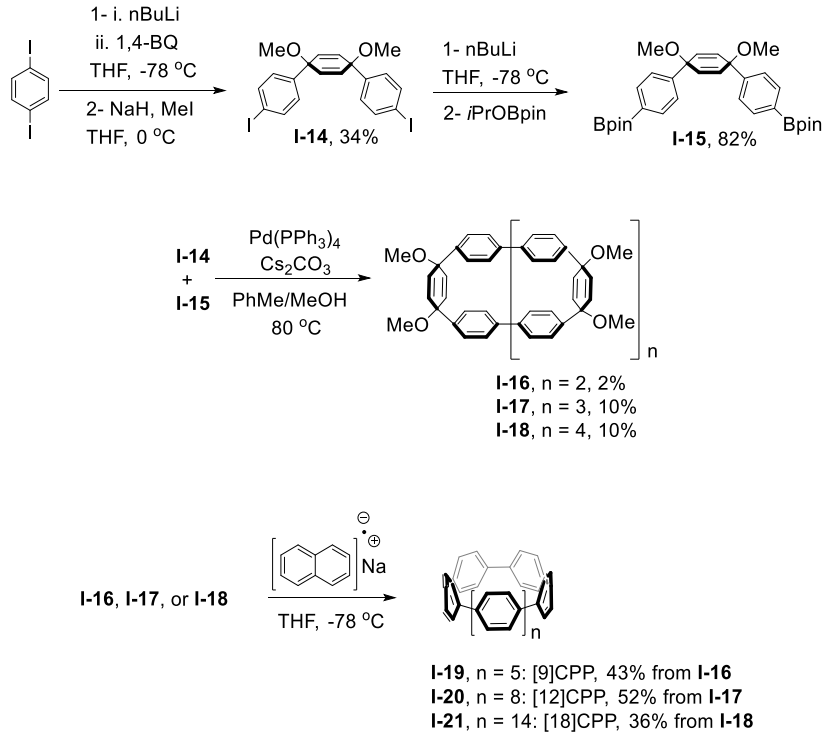

Scheme I-6. The First Synthesis of [9], [12], and [18]CPPs

Treatment of each macrocycle **I-16** to **I-18** with lithium naphthalenide led to the formation of [9], [12], and [18]CPPs in 43%, 52%, 36% yields, respectively.

The final step of preparing [n]CPPs involved the aromatization of 1,4-*cis*-dimethoxy-2,5-cyclohexadiene moiety in macrocycles. However, this is the most challenging step of forming [n]CPPs, due to high strain and susceptibility to rearrangement. When certain reagents are used,

such as Stephens reagent and low valent titanium, [n]CPPs were not formed (Scheme I-7). Under these conditions, carbocation formation led to 1,2 phenyl shift forming undesired macrocycles.

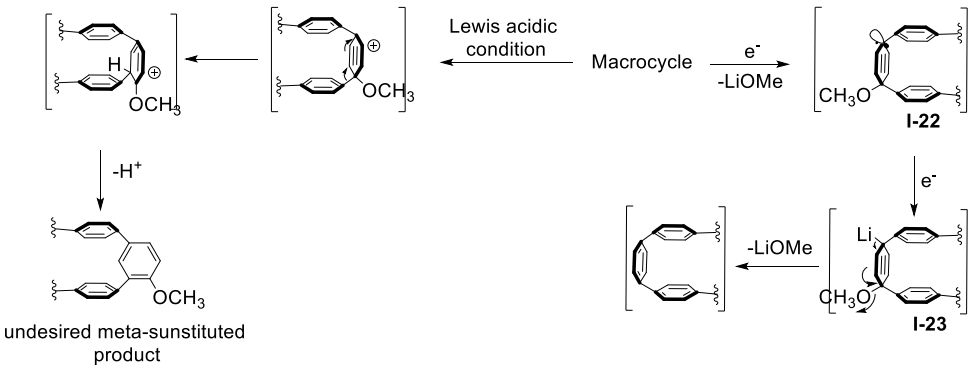

Scheme I-7. Mechanism of Reductive Aromatization

Finally, the successful conversion of macrocycles to [n]CPPs were achieved upon using lithium naphthalenide at -78 °C via electron transfer. The reduction began by a single electron transfer reduction of a C-O bond to form **I-22**, which was followed by a second electron transfer, leading to the formation of alkyllithium moiety **I-23**. This moiety can easily be aromatized by losing lithium methoxide.

The optical data of these CPPs were obtained by using UV-vis and fluorescence spectrometers. All three CPPs have approximately the same absorption maxima (λ_{max}= 338−339 nm). However, their fluorescence showed a red-shift, as the diameter decreased. This phenomenon is exactly the opposite of what is observed in linear parapheneylenes, which showed a red-shift as the oligomer length increased.

Computational studies revealed that the HOMO-LUMO gap in CPPs decreased as the number of benzenes in the ring decreased.[49] This unusual behavior could be explained by loss of π conjugation with decreasing CPP diameter. This unique optical property can be used in new

technologies especially in nanotechnology. Computational studies have also indicated that either [5] or [6]CPP is at the tipping point in electronic structure between a benzenoid and a quinoid structure (Scheme I-8).

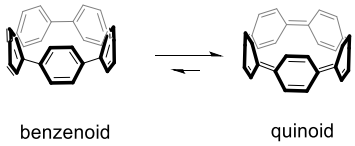

Scheme I-8. Benzenoid to a Quinoid

2. Itami's Selective Synthesis of [12]CPP

In 2009, Itami adjusted Vögtle's approach to the synthesis of [12]CPP.[50] Diiodide **I-24** was prepared by adding 1,4-cyclohexanedione to an excess of 4-iodophenyllithium (Scheme I-9). From this point, two separate reactions were carried out with this product. The first reaction involved conversion of the iodide group to a bis-boronic ester group, yielding **I-25**. The second reaction used MOM as a protecting group to form **I-26**. Following this, the Suzuki-Miyaura cross-coupling reactions were carried out between bis-boronic ester **I-25** and an excess of diiodide **I-26** to form compound **I-27** in 51% yield. The second Suzuki-Miyaura reaction was carried out at highly dilute conditions between diiodide **I-27** and bis-boronic ester **I-25** to form macrocycle **I-28**.

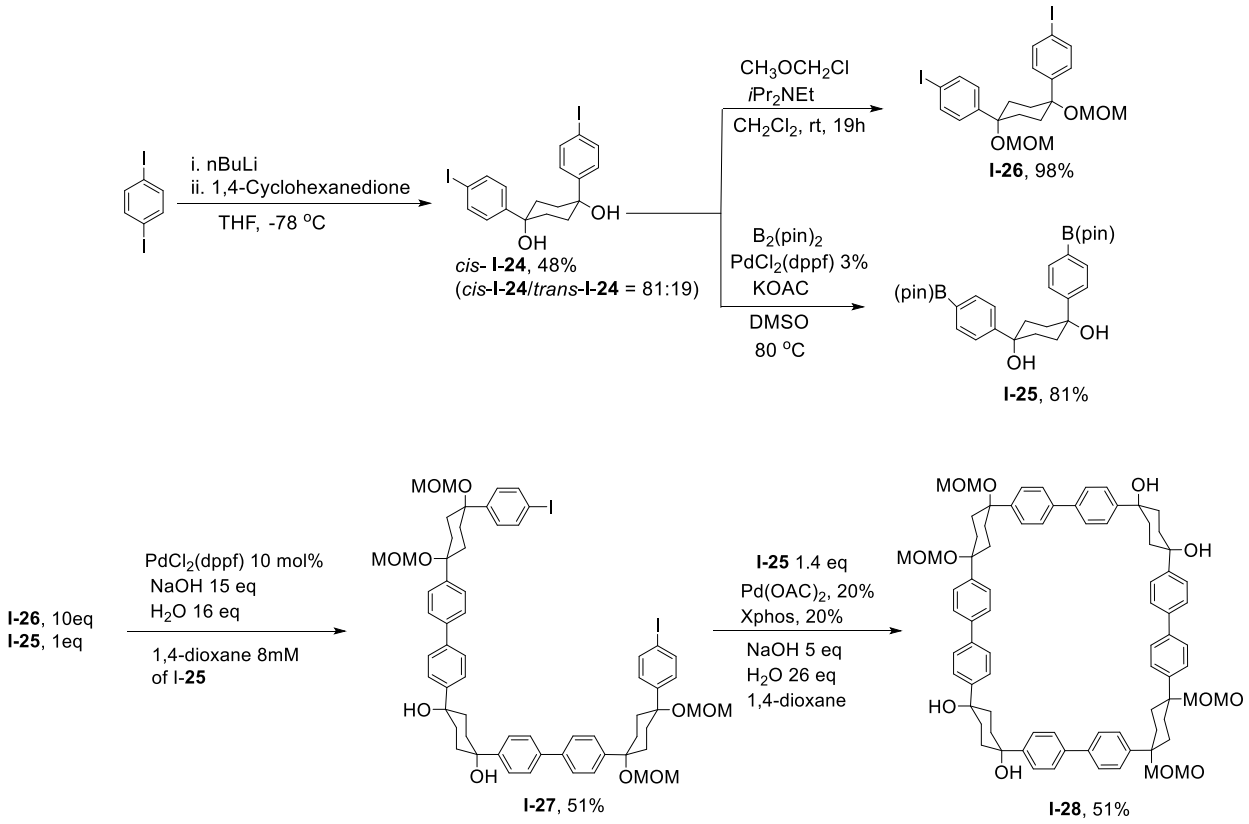

Scheme I-9. Itami's Strategy Toward the Synthesis of Macrocycle **I-28**

Itami used microwave conditions, in the presence of *para*-toluenesulfonic acid, to form [12]CPP **I-29** in 62% yield.

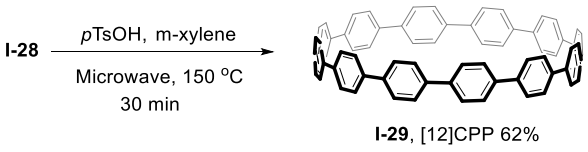

Scheme I-10. Synthesis of [12]CPP

3. Yamago's Strategy

In 2010, Yamago took a new approach to synthesize CPPs. He reported the synthesis of [8]CPP, the smallest and most strained CPP at that time (74 kcal/mol).[51] He was inspired by

palladium and platinum complexes of 4,4'-bipyridyl group, which led to the formation of macrocycles. He envisioned the preparation of *cis*-coordinated, square-shaped tetra(para-substituted oligoaryl)platinum complexes as a key intermediate. The treatment of one equivalent of 4,4'-bis(trimethylstannyl)biphenyl **I-30** with [$PtCl_2$(cod)] (cod = 1,5-cyclooctadiene) led to the formation of a square-shaped macrocycle **I-31** in 57% (Scheme I-11). Upon ligand exchange with 1,1'-bis(diphenylphosphino)ferrocene (dppf), **I-32** was obtained in 91% yield. Reductive elimination of **I-32** was carried out in the presence of bromine, producing [8]CPP in 37% yield over three steps.

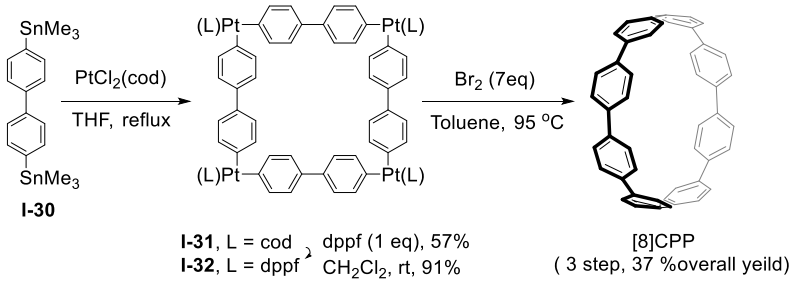

Scheme I-11. Synthesis of [8]CPP Over Three Steps

4. Utilizing the Diels-Alder Reaction as Key Step to Provide the L-Shaped Building Block

In 2014, Dr. Wang's group utilized the Diels-Alder reaction as a critical step to provide *cis* aryl groups as a building block in the synthesis of functionalized carbon nanoohoops.[52] The Horner−Wadsworth−Emmons reaction was used for the synthesis of (*E*,*E*)-1,4-bis(4 bromophenyl)-1,3-butadiene (**I-35**) in 85% yield (Scheme I-12). The Diels-Alder reaction between diene **I-35** and 1,4-benzoquinone was carried out in the presence of $BF_3{\cdot}OEt_2$. This

product was then methylated to produce **I-37** in 91% yield over two steps.

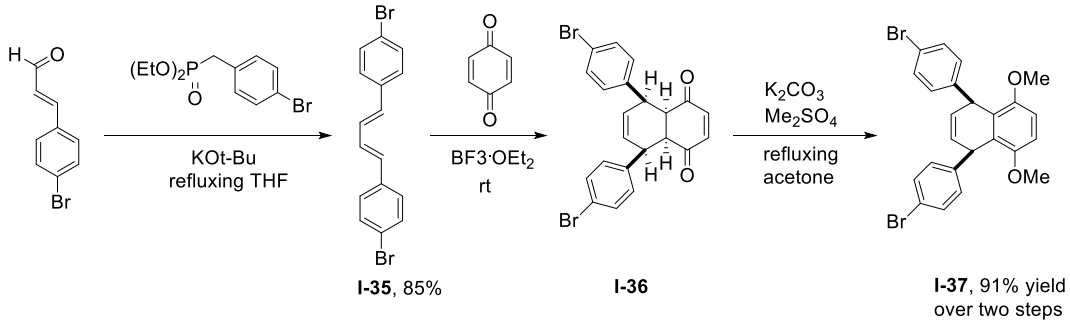

Scheme I-12. Synthesis of Building Block **I-37**

Treatment of **I-37** at 5 mM with $Ni(cod)_2$, (cod = 1,5-cyclooctadiene) in the presence of 2,2′-bipyridyl (bpy), promoted the homocoupling reactions to produce the cyclic dimers *syn*-**I-38** and *anti*-**I-38** in 21% and 6% yield, respectively (Scheme I-13). Furthermore, the cyclic trimers *syn*-**I-39** and *anti*-**I-39** were isolated in 11% yield (*anti*-**I-39** : *syn*-**I-39** = 3:1). To obtain a higher quantity of cyclic trimers, the reaction was carried out at 50 mM. This led to the formation of the cyclic dimers (*syn*-**I-38** : *anti*-**I-38** = 3:1) and the cyclic trimers (*syn*-**I-39** : *anti*-**I-39** = 1:3) in 8% and 18% combined yield, respectively.

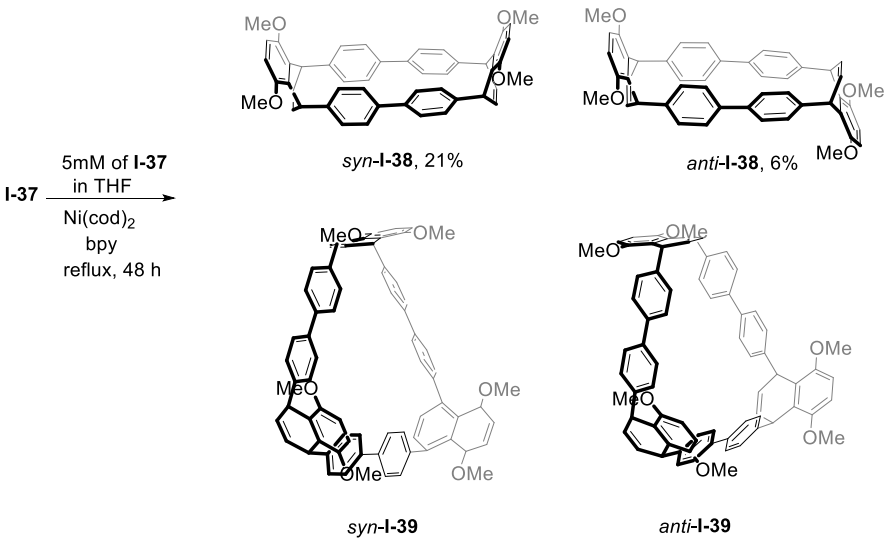

Scheme I-13. Wang's Strategy Toward the Synthesis of CPPs

Oxidative dehydrogenation of cyclic dimer *syn*-**I-37** and *anti*-**I-37** using 2,3-dichloro-5,6-dicyano-1,4-benzoquinone (DDQ) at temperatures ranging between 25-150 °C did not produce fully aromatized functionalized [6]CPP. On the other hand, oxidative dehydrogenation of cyclic trimers *syn*-**I-38** and *anti*-**I-38** occurred smoothly at 70 °C to produced functionalized [9]CPP in 88% yield (Scheme I-14).

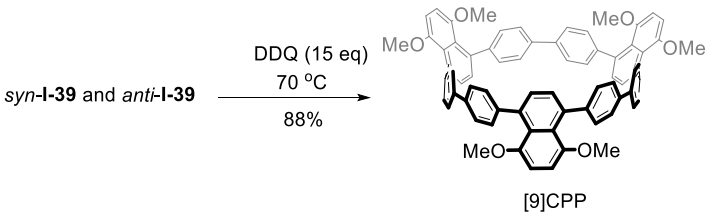

Scheme I-14. Synthesis of Functionalized [9]CPP

Heteroatom-Containing Cycloparaphenylenes

A Nitrogen-Containing Carbon Nanohoop

In 2012, Itami reported the first example of a nitrogen-containing carbon nanohoop.[53] The critical step of synthesizing bipyridyl containing carbon nanoring required the use of a U-shaped **I-41**, which was synthesized in four steps (Scheme I-15).[54]

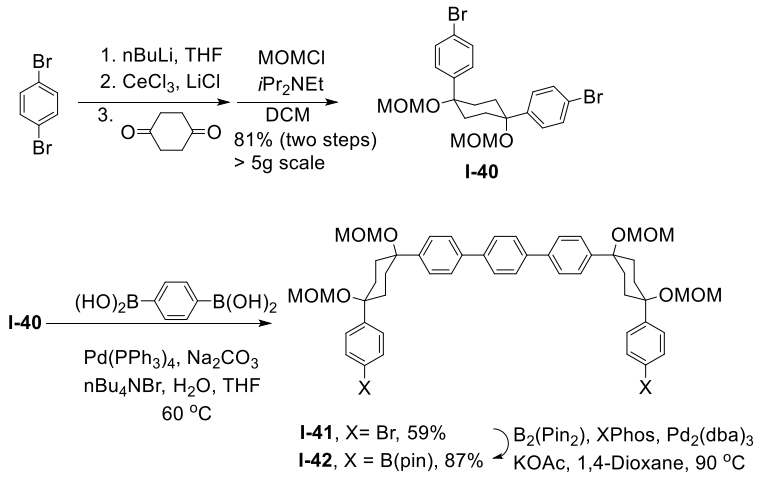

Scheme I-15. Synthesis of U-shaped **I-41**

The Suzuki-Miyaura cross-coupling reaction between U-shaped **I-42** and 5,5'-dibromo-2,2'-bipyridyl (**I-43**) was carried out in 79% yield to form (2+7+2) U-shaped **I-44** in 79% yield (Scheme I-16). The cross-coupling reaction between **I-42** and **I-44** (11+7) led to formation of a square shaped macrocycle **I-45** in 48% yield.

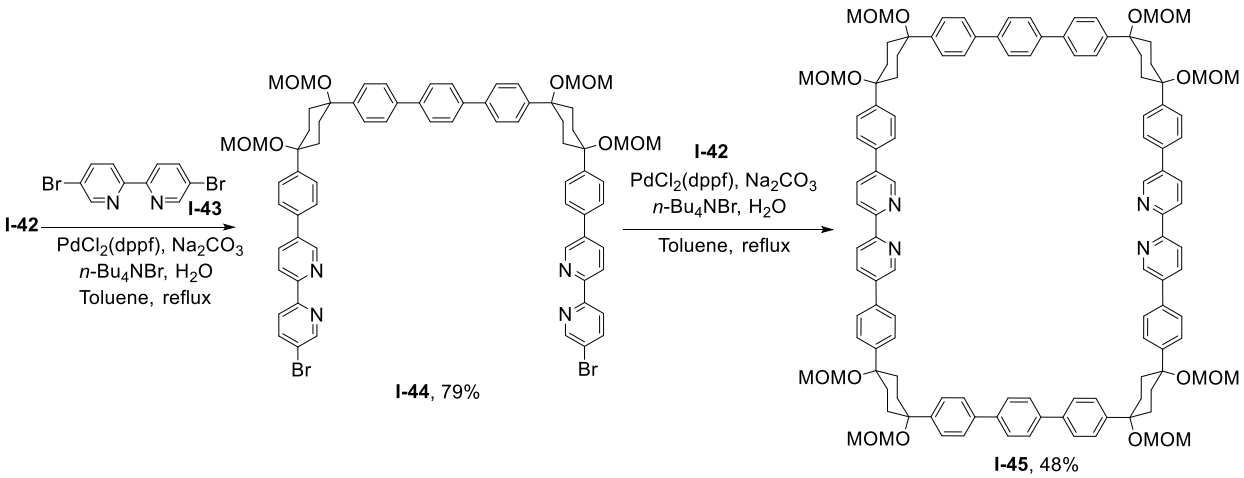

Scheme I-16. Synthesis of Square-Shaped Macrocycle **I-45**

Aromatization of **I-45** in the presence of $NaHSO_4$ (20 eq) and o-chloranil (5 eq) in DMSO/m-xylene at 150 ^oC produced [14,4]CPPy in 56% yield (Scheme I-17). The UV-vis absorption maximum (λ_{abs}) was observed at 344 nm, and fluorescence emission maximum (λ_{em}) was observed at 427 nm. Surprisingly, the shapes of the absorption of [14,4]CPPy and large CPPs are almost identical. This indicates that conjugation has a greater effect than the nitrogen lone pair on the frontier MOs. Introducing HCl to a dilute solution of [14,4]CPPy has a significant impact on optical properties, in particular on the fluorescence of protonated [14,4]CPPy. The acid not only caused the absorption and fluorescence peaks to broaden but also led to a red-shift in both the absorption and fluorescence spectra. This phenomenon may be explained by intramolecular charge transfer. Neutralization, upon addition of NEt_3, resulted in the reproduction of the original spectra of [14,4]CPPy.

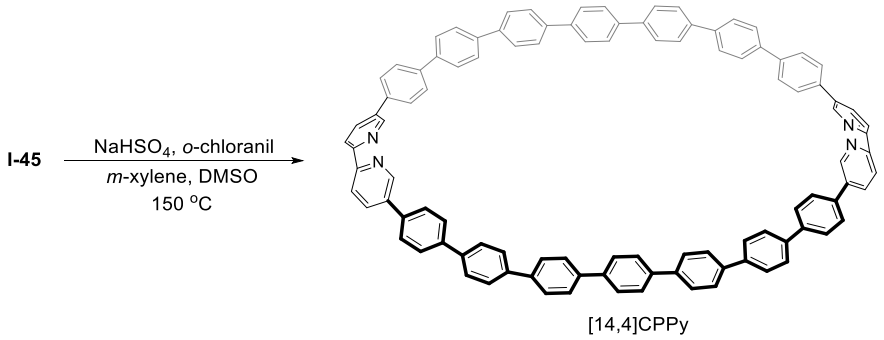

Scheme I-17. Synthesis of [14,4]CPPy

Thiophene-Containing Carbon Nanohoops

In 2015, Itami synthesized thiophene-containing carbon nanohoops.[55] The key steps of this synthesis involved the Glaser-Hay macrocyclization followed by cyclocondensation of 1,3-butadiynes units in macrocycles with $Na_2S \cdot 9H_2O$ under microwave irradiation. Nucleophilic addition of 2-(trimethylsilylethynyl)magnesium bromide to cyclohexane-1,4-dione produced **I-46** in 70% yield (Scheme I-18). The protection of hydroxyl groups, using MOM as the protecting group, followed by deprotection of the acetylene group, in the presence of K_2CO_3, formed the L-shaped unit **I-47** in 80% yield over two steps.

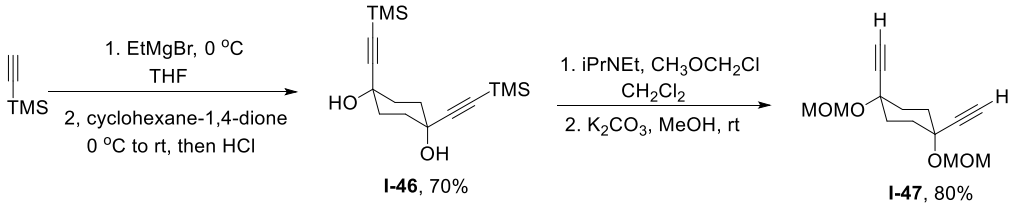

Scheme I-18. Synthesis of the L-Shaped Unit **I-47**

The Glaser-Hay macrocyclization of **I-47** in an open-air flask for two days led to macrocyclic dimers (32%), trimers (31%), tetramers (15%), and pentamers (6%) in 84% yield (Scheme I-19). To prepare the cyclic hexamer, the reaction was carried out at higher

concentration, and hexamers were obtained in 3% yield. It is important to mention that running the reaction at higher concentrations led to a lower combined yield. Cyclocondensation of 1,3-butadiynes units, in the presence of $Na_2S{\cdot}9H_2O$ and microwave irradiation, resulted in the formation of cyclic 1,4-cyclohex-ylene-2',5'-thienylenes ([3]CCyT, [4]CCyT, [5]CCyT, and [6]CCyT) in 86%, 50%, 46%, and 50% yields, respectively.

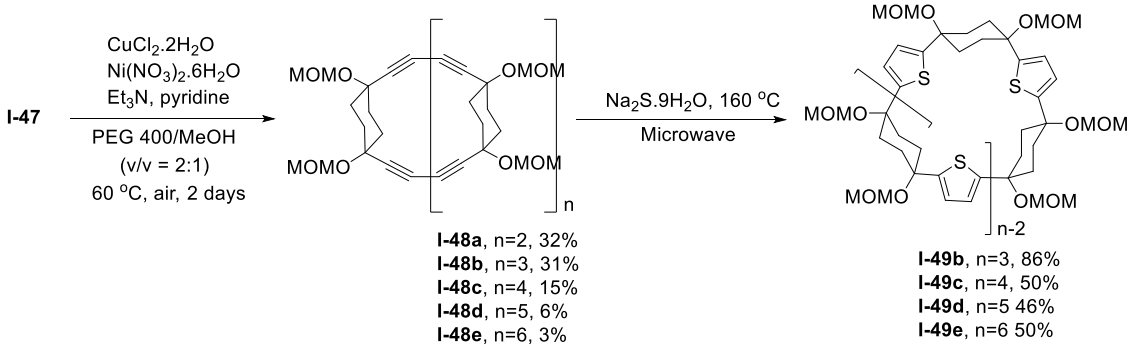

I-48a, n=2, 32%
I-48b, n=3, 31%
I-48c, n=4, 15%
I-48d, n=5, 6%
I-48e, n=6, 3%

I-49b, n=3, 86%
I-49c, n=4, 50%
I-49d, n=5 46%
I-49e, n=6 50%

Scheme I-19. Synthesis of [4]CPT, [5]CPT, and [6]CPT

Aromatization of macrocycles [4]CCyT, [5]CCyT, and[6]CCyT) led to the formation of [4]CPT, [5]CPT,and [6]CPT in 13%, 24%, and 3% yields, respectively (Scheme I-20). Unfortunately, aromatization of [3]CCyT, using the same conditions, did not form the desired [3]CPT. This observation might be rationalized by a lower thermal stability or a higher strain found in [3]CPT.

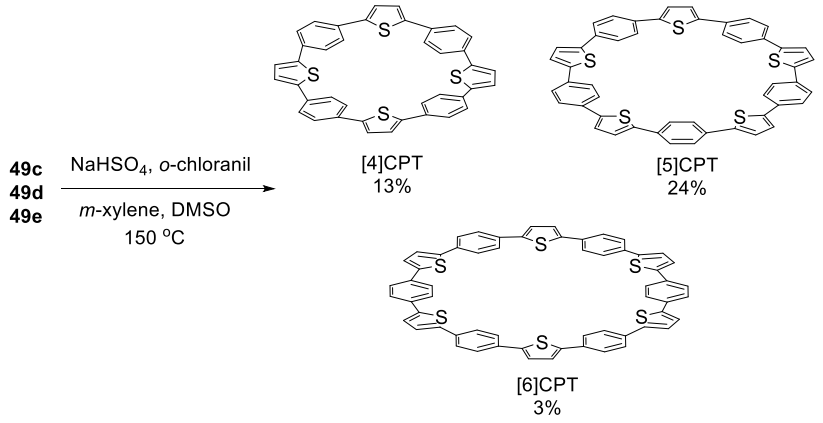

Scheme I-20. **Synthesis of** [4]CPT, [5]CPT, and [6]CPT

The UV-vis absorption maxima (λ_{abs}) were observed at 333, 350, and 362 nm, respectively. Surprisingly, increasing the number of aromatic units resulted in a red-shift, resembling the pattern seen in linear parapheneylenes and opposite to the pattern observed in cycloparaphenylenes. The fluorescence emission maxima (λ_{em}) were observed at 546, 510, 488 nm, respectively with a blue-shift as the ring size increased.

I-References:

(1) Iijima, S. *Nature* **1991**, *354*, 56–58.

(2) Iijima, S.; Ichihashi, T. *Nature* **1993**, *363*, 603−605.

(3) Ajayan, P. M. *Chem. Rev.* **1999**, *99*, 1787−1800.

(4) Scott, L. T.; Jackson, E. A.; Zhang, Q.; Steinberg, B. D.; Bancu, M.; Li, B. *J. Am. Chem. Soc.* **2012**, *134*, 107.

(5) Hitosugi, S.; Nakanishi, W.; Yamasaki, T.; Isobe, H. *Nat. Commun.* **2011**, *2*, 492.

(6) Han, Z.; Fina, A. *Prog. Polym. Sci*. **2011**, *36*, 914−944.

(7) Avouris, P.; Chen, Z.; Perebeinos, V. *Nat. Nanotechnol*. **2007**, *2*, 605−615.

(8) Avouris, P. Acc. *Chem. Res*. **2002**, *35*, 1026−1034.

(9) Collins, P. G.; Avouris, P. *Sci. Am*. **2000**, *283*, 62−69.

(10) Terrones, M. Annu. *Rev. Mater. Res*. **2003**, *33*, 419−501.

(11) Yu, M.-F.; Files, B. S.; Arepalli, S.; Ruoff, R. S. *Phys. Rev. Lett*. **2000**, **84**, 5552−5555.

(12) O'Connell, M. J.; Bachilo, S. M.; Huffman, C. B.; Moore, V. C.; Strano, M. S.; Haroz, E. H.; Rialon, K. L.; Boul, P. J.; Noon, W. H.; Kittrell, C.; Ma, J.; Hauge, R. H.; Weisman, R. B.; Smalley, R. E. *Science* **2002**, *297*, 593−596.

(13) Weisman, R. B.; Bachilo, S. M. *Nano Lett*. **2003**, *3*, 1235−1238.

(14) Kataura, H.; Kumazawa, Y.; Maniwa, Y.; Umezu, I.; Suzuki, S.; Ohtsuka, Y.; Achiba, Y. *Synth. Met.* **1999**, *103*, 2555−2558.

(15) Dresselhaus, M. S.; Dresselhaus, G.; Avouris, P. Carbon Nanotubes. In Topics in Applied Physics; Springer: Berlin, 2001.

(16) Hong, S.; Myung, S. *Nat. Nanotech.* **2007**, *2*, 207.

(17) Sinha, N.; Ma, J.; Yeow, J. T. W. *J. Nanosci. Nanotech.* **2006**, *6*, 573.

(18) Qi, P.; Vermesh, O.; Grecu, M.; Javey, A.; Wang, Q.; Dai, H.; Peng, S.; Cho, K. J. *Nano Lett*. **2003**, *3*, 347−351.

(19) Dionisio, M.; Schnorr, J. M.; Michaelis, V. K.; Griffin, R. G.; Swager, T. M.; Dalcanale, E. *J. Am. Chem. Soc*. **2012**, *134*, 6540−6543.

(20) Rivas, G. A.; Rubianes, M. D.; Rodriguez, M. C.; Ferreyra, N. F.; Luque, G. L.; Pedano, M. L.; Miscoria, S. A.; Parrado, C. *Talanta* **2007**, *74*, 291−307.

(21) Pang, X.; Imin, P.; Zhitomirsky, I.; Adronov, A. *Macromolecules* **2010**, *43*, 10376−1038.

(22) Baughman, R. H.; Zakhidov, A. A.; de Heer, W. A. *Science* **2002**, *297*, 787.

(23) Cha C.; R. Su; Annabi N; Dokmeci M.; Khademhosseini A.; *ACS Nano*. **2013**, 7(4): 2891–2897.

(24) Dai, H. Phys. *World* **2000**, *13* (6), 43−47.

(25) Terrones, M. Annu. *Rev. Mater. Res*. **2003**, *33*, 419−501.

(26) Durkop, T.; Getty, S. A.; Cobas, E.; Fuhrer, M. S. *Nano Lett*. **2004**, *4*, 35−39.

(27) Wu Z., Chen Z., Du X, Logan M., Sippel J, Nikolou M., Kamaras K., Reynolds J., Tanner D., Hebard F., Rinzler A., *Science*, **2004**, *305*, 27.

(28) De Volder, M. F. L.; Tawfick, S. H.; Baughman, R. H.; Hart, A. J. *Science* **2013**, 339, 535−539.

(29) Jariwala, D.; Sangwan, V. K.; Lauhon, L. J.; Marks, T. J.; Hersam, M. C. *Chem. Soc. Rev*. **2013**, *42*, 2824−2860.

(30) Martel, R.; Schmidt, T.; Shea, H. R.; Hertel, T.; Avouris, P. Single. *Appl. Phys. Lett*. **1998**, *73*, 2447-2449.

(31) Zhou, C.; Kong, J.; Dai, H. *Appl. Phys. Lett*. **1999**, *76*, 1597-1599.

(32) Derycke, V.; Martel, R.; Appenzeller, J.; Avouris, P. *Nano Lett*. **2001**, *1*, 453-456.

(33) Bachtold, A.; Hadley, P.; Nakanishi, T.; Dekker, C. *Science* **2001**, *294*, 1317-1320.

(34) Liu, X.; Lee, C.; Zhou, C.; Han, J. *Appl. Phys. Lett.* **2001**, *79*, 3329-3331.

(35) Haddon, R. C.; Sippel, J.; Rinzler, A. G.; Papadimitrakopoulos, F. *MRS Bulletin* **2004**, *29*, 252.

(36) Zhang, G.; Qi, P.; Wang, X.; Lu, Y.; Li, X.; Tu, R.; Bangsaruntip, S.; Mann, D.; Zhang, L.; Dai, H. *Science* **2006**, *314*, 974−977.

(37) Harutyunyan, A. R.; Chen, G.; Paronyan, T. M.; Pigos, E. M.; Kuznetsov, O. A.; Hewaparakrama, K.; Kim, S. M.; Zakharov, D.; Stach, E. A.; Sumanasekera, G. U. *Science* **2009**, *326*, 116−120.

(38) Dai H. *Acc. Chem. Res*. **2002**, 35, 1035−1044.

(39) Yamabe, T.; Okahara, K.; Okada, M.; Tanaka, K. *Synth. Met.* **1993**, *56*, 3142−3147.

(40) Avouris, P.; Freitag, M.; Perebeinos, V. *Nat. Photonics* **2008**, *2*, 341.

(41) Krätschmer, W.; Lamb, L.D.; Fostiropoulos, K.; Huffman, D.R. *Nature* **1999,** *347*, 354−357.

(42) Kroto, H.W.; Heath, J.R.; O'Brien, S.C., Curl, R.F.; Smalley, R.E. *Nature*, **1985**, *318* 162−163.

(43) Kong, J.; Cassell, A.M.; Dai, H. *Chem. Phys. Lett.* **1998**, *292*, 567−574

(44) Hirst, E. S.; Jasti, R. *J. Org. Chem.* **2012**, *77*, 10473−10478.

(45) Golder, M. R.; Jasti, R. *Acc. Chem. Res.* **2015**, *48*, 557−566.

(46) Parekh, V. C.; Guha, P. C. *J. Indian Chem. Soc.* **1934**, *11*, 95.

(47) Friederich, R.; Nieger, M.; Vögtle, F. *Chem. Ber.* **1993**, *126*, 1723−1732.

(48) Jasti, R.; Bhattacharjee, J.; Neaton, J. B.; Bertozzi, C. R. *J. Am. Chem. Soc*. **2008**, *130*, 17646−17647.

(49) Jagadeesh, M. N.; Makur A.; Chandrasekhar, J. *J. Mol. Model*. **2000**, *6*, 226−233.

(50) Takaba, H.; Omachi, H.; Yamamoto, Y.; Bouffard J.; Itami, K. *Angew. Chem., Int. Ed*. **2009**, 48, 6112−6116.

(51) Yamago, S.; Watanabe, Y.; Iwamoto, T. *Angew. Chem., Int. Ed*. **2010**, 49, 757−759.

(52) Huang, C.; Huang, Y.; Akhmedov, N. G.; Popp, B. V.; Petersen, J. L.; Wang, K. K., *Org. Lett*. **2014**, 16, 2672−2675.

(53) Matsui, K.; Segawa, Y.; Itami, K. *Org. Lett*. **2012**, *14*, 1888–1891.

(54) Omachi, H.; Matsuura, S.; Segawa, Y.; Itami, K. *Angew. Chem., Int. Ed*. **2010**, *49*, 10202–10205.

(55) Ito, H.; Mitamura, Y.; Segawa, Y.; Itami, K. *Angew. Chem. Int. Ed*. **2015**, *54*, 159–163.

Chapter 2: Synthesis of Cycloparaphenylenes Bearing Furan-2,5-diyl or 2,2'-Bifuran-5,5'-diyl Units in the Macrocyclic Structures

II-Introduction

Linking multiple units of benzene at the *para* position results in the formation of [*n*]cycloparaphenylens ([*n*]CPPs). Due to their unique connectivity, these [*n*]CPPs have unique optoelectronic and redox characteristics, thus making them inherently useful in nanotechnology and other fields. The [*n*]CPP interior space offers unique host-guest interactions, such as host-gust interaction between [8]-[10]CPPs.[1-3] Additionally, (n,n) single-walled carbon nanotubes (SWCNTs) are comprised of repeating linkages of [*n*]CPPs. The idea of utilizing [*n*]CPPs as a template for a bottom-up approach to synthesizing SWCNTs was first introduced when Smalley and coworkers showed that smaller carbon nanotubes (CNTs) could act as a seed to grow longer CNTs with the same chirality and diameter.[4]

Functionalized CPPs, due to their unique electrochemical and optoelectronic properties,[5] were highly sought after by chemists. The progression of this idea led to the advancement of synthetic methods towards building functionalized CPPs.

Since the Diels-Alder reaction always exclusive regio- and stereoselective, it is a critical reaction to preset phenyl groups in the *cis* position. We recently reported the use of the Diels-Alder reaction between (*E*,*E*)-1,4-bis(4-bromophenyl)-1,3-butadiene (**II-4**) and 1,4-benzoquinone (**II-5**) as a key step to form the functionalized [9]CPP.[6] The extension of the same strategy led to the formation of thiophene-containing cycloparaphenylenes (CPPs).[7] The similar synthetic approach was utilized to synthesize the furan-containing cycloparaphenylenes (CPPs).

These heteroatom-containing cycloparaphenylenes macrocycles, with radially π-conjugated systems, have unique optoelectronic, redox, and solvatochromic properties.[8] At first glance, thiophene and furan are five-membered heterocyclic aromatic compounds. However, their electronic characteristics and chemical reactivates are different. For example, furan and thiophene both are used as organic semiconductors. However, furan containing semiconductors show better performance than their respective thiophene analogs in certain area.[9,10]

The delocalization of the π-system on thiophene is higher than that of furan's, which results in a lower aromaticity in furan than in thiophene. The lower aromaticity in furan leads to different chemical reactivities. For example, the Diels–Alder reactions of benzyne with 2,5-diphenylthiophene has not been reported.[11-13] On the other hand, 2,5-diphenylfuran was found to undergo Diels–Alder reactions with a variety of benzynes in moderate to good yields.[14,15] The differences of these chemical and electronic properties prompted us to develop synthetic pathways to CPPs incorporated with furan-2,5-diyl or 2,2'-bifuran-5,5'-diyl units.

II-Results and Discussion

We now report the synthesis of a furan-containing cycloparaphenylene **II-1** (Figure II-1) bearing 12 aromatic groups including two furan-2,5-diyl units, macrocycles **II-2a** and **II-2b** bearing 10 aromatic groups including two 2,2'-bifuran-5,5'-diyl units, and macrocycles **II-3a** and **II-3b** bearing 15 aromatic groups including three 2,2'-bifuran-5,5'-diyl units.

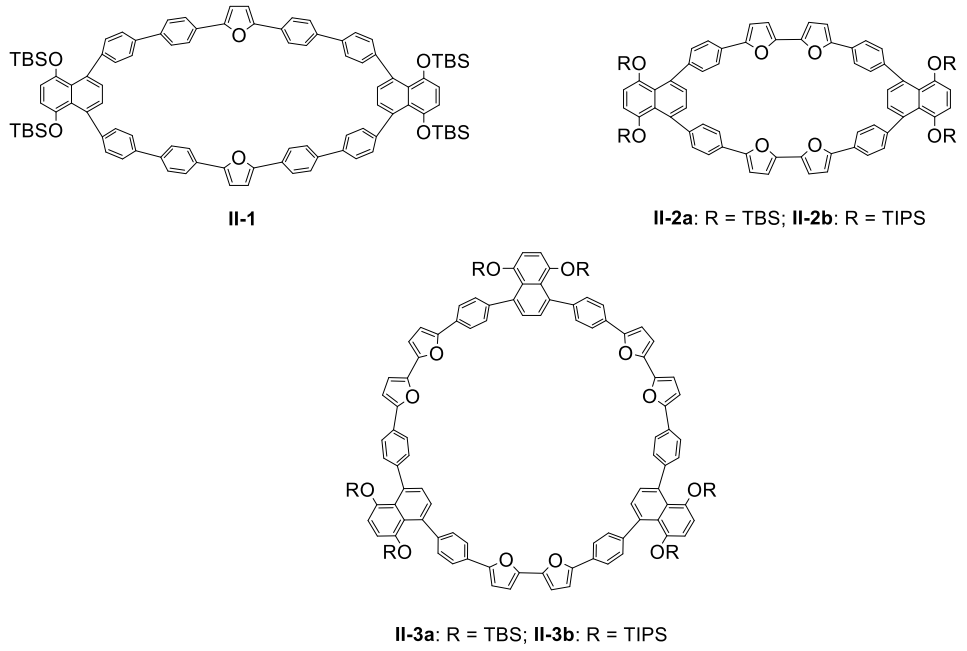

Figure II-1. Structures of the furan-containing CPPs.

The synthetic pathway reported earlier was adopted in this investigation. The Diels–Alder reaction between (*E*,*E*)-1,4-bis(4-bromophenyl)-1,3-butadiene (**II-4**) and 1,4-benzoquinone (**II-5**) in the presence of $BF_3{\cdot}OEt_2$ was used to prepare **II-6** in 92% yield, which positioned 4-bromophenyl groups selectively *cis* to each other (Scheme II-1). The protection of **II-6** was carried out with *tert*-butyldimethylsilyl chloride (TBSCl) in the presence of imidazole to produce **II-7a** in 96% yield. **II-7b** was prepared upon treatment of **II-6** with triisopropylsilyl chloride (TIPSCl) in 71% yield. The presence of silyl groups in **II-7a** and **II-7b** increases their solubilities in organic solvents.

Dibromide **II-7a** was converted to bis-boronic ester **II-9** in 94% yield. The Suzuki–Miyaura coupling reaction between **II-7a** and boronic ester **II-8** was carried out to form **II-11a** in 91% yield, which was followed by bromination with NBS to form dibromide **II-12a** in 92% yield. **II-12b** was prepared in 89% yield as well.

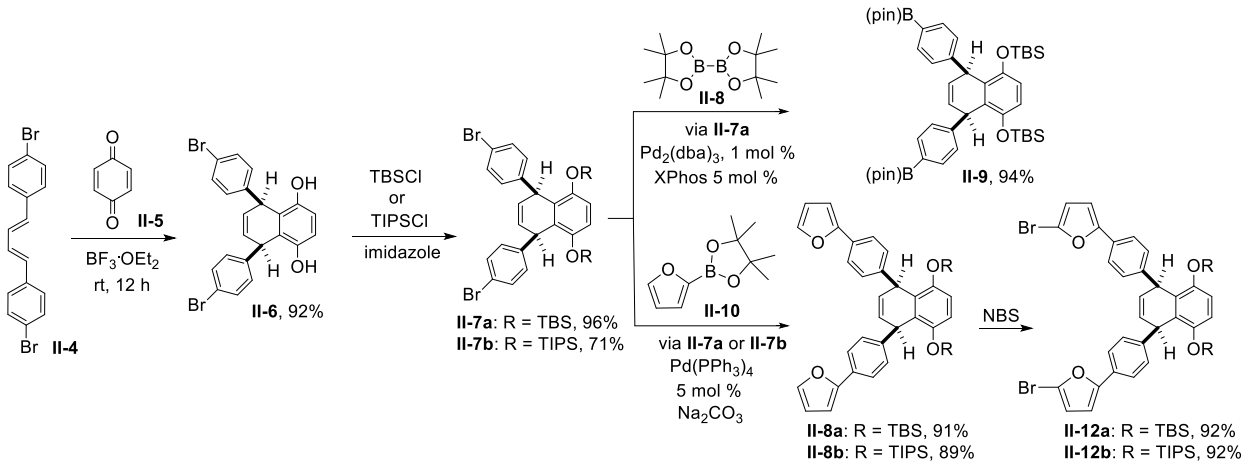

Scheme II-1. Synthesis of Building Blocks **II-9**, **II-12a**, and **II-12b**

The Suzuki–Miyaura cross-coupling reactions between **II-9** and **II-12a** produced a mixture of *syn*-**II-13** and *anti*-**II-13** bearing two furan-2,5-diyl units in 15% combined yield (Scheme II-2). The *syn* isomer bears the two 1,4-bis[(tert-butyldimethylsilyl)oxy]benzene groups on the same side of the macrocyclic ring, whereas the *anti* isomer has them on opposite sides.

Unfortunately, oxidative aromatization of macrocycle *syn*-**II-13** and *anti*-**II-13** to the fully aromatized furan-containing CPP **II-14** with 2,3-dichloro-5,6-dicyano-1,4-benzoquinone (DDQ) at temperature ranging from 100-150 ˚C was not successful and led to the recovery of the starting material. However, attempts to force the reaction to go to completion ended with decomposition at 165 ˚C.

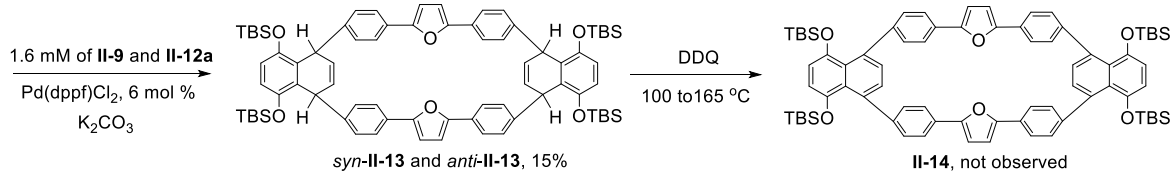

Scheme II-2. Attempted Synthesis of the Furan-Containing CPP **II-14**

The lower aromaticity of furan and higher ring strain may cause the failure. To reduce the ring strain on furan-containing cycloparaphenylene, four additional benzene rings were introduced to macrocycle (Scheme II-3). The Suzuki–Miyaura cross-coupling reactions between bis-boronic ester **II-9** and 1-bromo-4-iodobenzene produced **II-15** in 91% yield, which includes two more benzene rings. Dibromide **II-15** was converted to **II-16** and **II-18** by following the same synthetic approach on Scheme **II-1**.

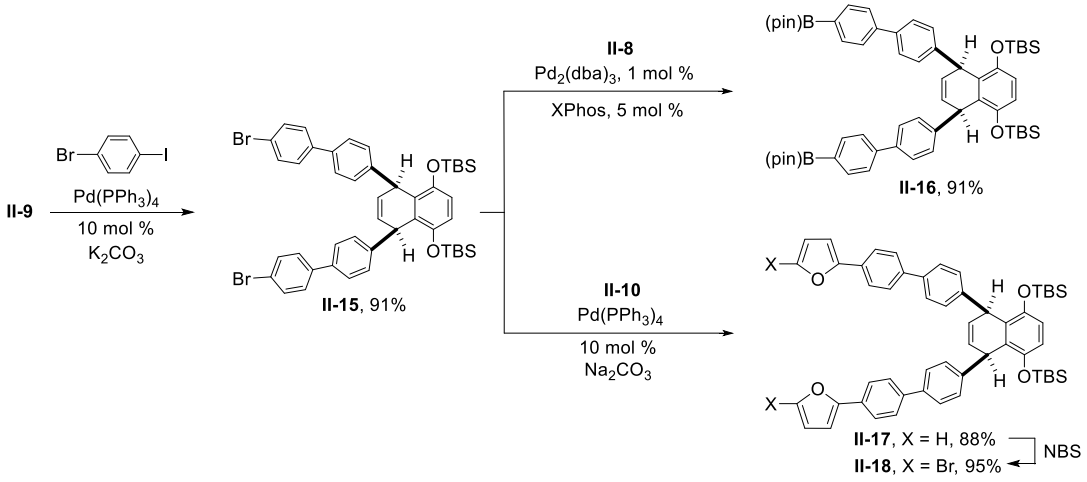

Scheme II-3. Synthesis of Building Block **II-16**, **II-18**

The Suzuki–Miyaura coupling reactions between **II-16** and **II-18** produced a mixture of *syn*-**II-19** and *anti*-**II-19** bearing two furan-2,5-diyl units in 17% combined yield (Scheme II-4). Oxidative aromatization of the mixture of macrocycles *syn*-**II-19** and *anti*-**II-19** with DDQ in chlorobenzene at 70 ^{o}C for 3 hours successfully produced the fully aromatized furan-containing CPP **II-1**, bearing 12 aromatic rings including two furan-2,5-diyl units.

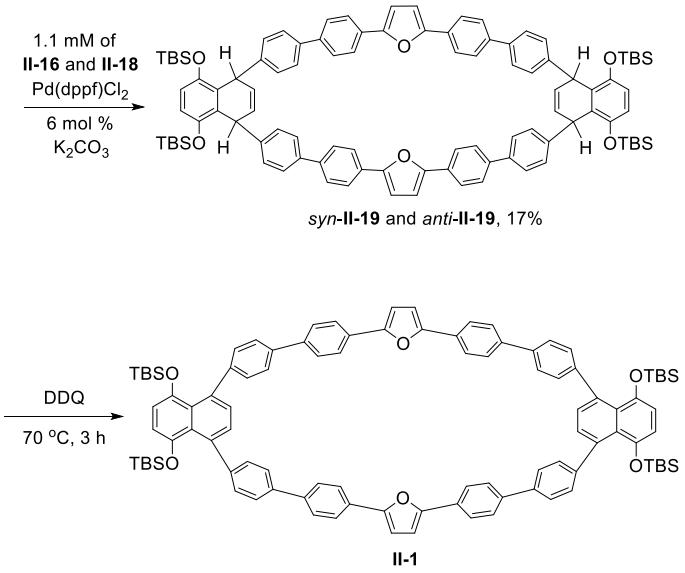

Scheme II-4. Synthesis of the Furan-Containing CPP **II-1**

Treatment of **II-12a** with $Ni(cod)_2$ (cod = 1,5-cyclooctadiene) in the presence of 2,2'-bipyridyl (bpy) promoted the homocoupling reactions to produce the cyclic dimers *syn*-**II-20a** and *anti*-**II-20a** and the cyclic trimer *anti*-**II-21a** (Scheme II-5). In the cyclic trimer *anti*-**II-21a**, two of the three 1,4-bis[(*tert*-butyldimethylsilyl)oxy]benzene groups are on the same side of the macrocyclic ring, whereas the third is on the opposite side (Scheme II-5). The cyclic trimer *syn*-**II-21a** was not isolated. The cyclic dimer *anti*- **II-20a** was separated and isolated in 26% yield. The assignment of the stereochemistry of *anti*-**II-20a** is based on comparing its NMR signals with those of *anti*-**II-20b** with its structure confirmed by X-ray structural elucidation. Treatment of *anti*-**II-20a** with DDQ for oxidative aromatization then produced **II-2a** in 81% yield. A sample containing *syn*-**II-20a** and *anti*-**II-21a** (*syn*-**II-20a** : *anti*-**II-21a** = 2:1) was also isolated in 45% combined yield.

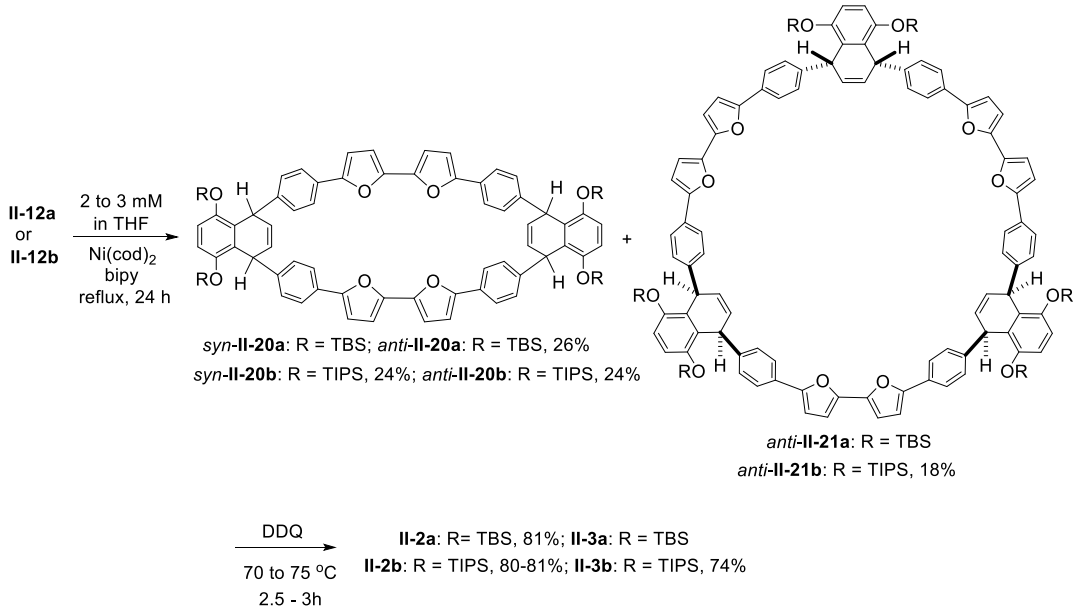

Scheme II-5. Synthesis of the Furan-Containing CPPs

The attempt to separate the *syn*-**II-20a** and *anti*-**II-21a** by silica gel chromatography was not successful. At this point, we carried out oxidative aromatization of the mixture of *syn*-**II-20a** and *anti*-**II-21a** with DDQ to form **II-2a** and **II-3a** in 83% yield. However, the mixture of the **II-2a** and **II-3a** was inseparable. The presence of **II-2a** was confirmed by NMR spectroscopy of the oxidative aromatization product of *anti*- **II-20a**. On the other hand, the presence of the **II-3a** was confirmed by comparing with the NMR spectra of **II-3b**. HRMS of the solution of **II-2a** and **II-3a** showed the presence of both compounds.

The $Ni(cod)_2$-mediated homocoupling reactions of **II-12b** resulted in the formation of the cyclic dimers *syn*-**II-20b** in 24% yield and *anti*-**II-20b** in 24% yield and the cyclic trimer *anti*-**II-21b** in 18% yield (Scheme II-5). These macrocycles were separated by silica gel column chromatography. However, based on probability we expect the formation of approximately 6% of trimer *syn*-**II-21b,** which was not isolated (Scheme II-6).

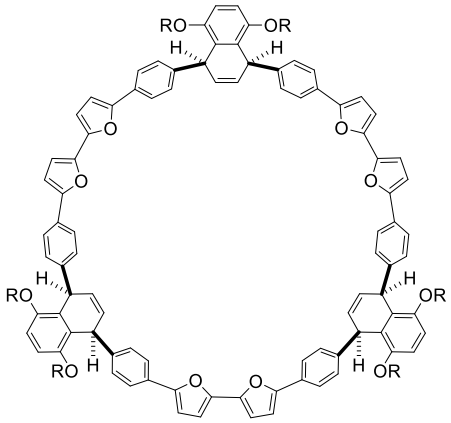

syn-**II-21b**: R = TIPS

Scheme II-6. The Structure of Expected *syn*-**II-21b**

A single crystal of *anti*-**II-20b** suitable for X-ray structure analysis was obtained by recrystallization from a mixture of dichloromethane and acetonitrile (Figure II-2). The X-ray structure of *anti*-**II-20b** indicates that the 2,2'- bifuran-5,5'-diyl units were arranged in the s-*trans* conformation between the two furanyl rings in the crystal lattice. This structural conformation of *anti*-**II-20b** is in similar to that of the acyclic 5,5'-biphenyl end-capped 5,5'-bis([1,1'-biphenyl]-4-yl)-2,2'-bifuran. The torsional angle of the O-C-C-O in the two furanyl rings is 176.5^{o}. Since the stable conformation of 2,2'-bifuran in solution is s-*trans*, most likely the s-*trans* conformation in *anti*-**II-20b** is the stable conformation in solution. The structure of the *anti*-**II-20b** is oval-shaped with the distant between the centers of the two bonds joining the furans of the two bifuran units being 4.15 Å, and the diameter between the centers of the two partially hydrogenated rings in the naphthyl units being 17.47 Å.

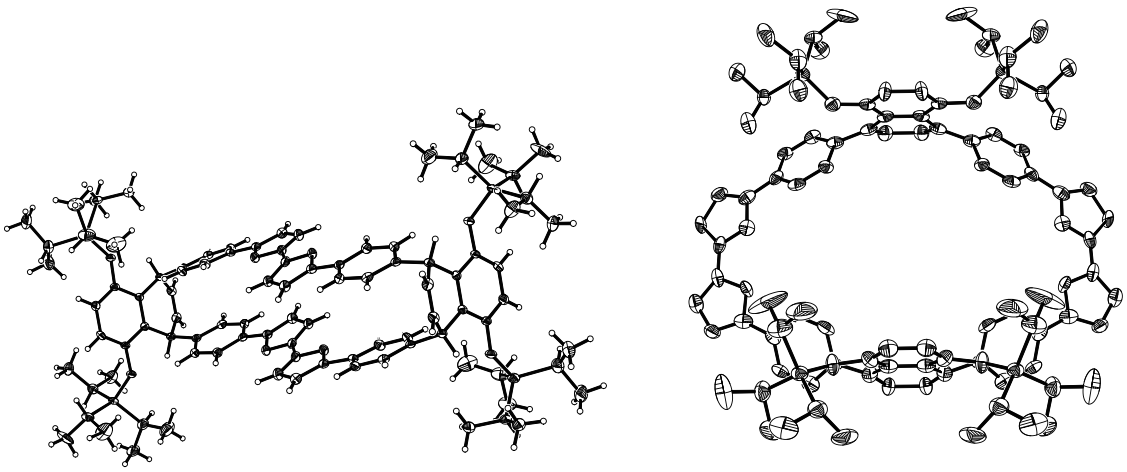

anti-**II-20b** *anti*-**II-2b**

Figure II-2. ORTEP drawings of *anti*-**II-20b** and **II-2b** with hydrogen atoms in **II-2b** omitted for clarity.

Oxidative aromatization of isolated *syn*-**II-20b** with DDQ gave **II-2b** in 81% yield. A similar result was also obtained from oxidation of *anti*-**II-20b** with DDQ to form fully aromatized **II-2b** in 80% yield. *anti*-**II-21b** was treated with DDQ to give **II-3b** in 74% yield.

Fortunately, a single crystal of **II-2b** suitable for X-ray structure analysis was obtained by recrystallization from a chloroform (Figure II-2). The X-ray structure of **II-2b** indicates that the two 1,4-bis[(triisopropylsilyl)oxy]benzene groups were almost parallel to each other and perpendicular to the inner plane of the macrocycle ring. Surprisingly, these groups are on the same side of the macrocyclic ring. The two 2,2'-bifuran-5,5'-diyl units cant toward inner plane of the macrocycle ring in the same direction. The torsional angle of the O-C-C-O in the two furanyl rings is 7.48^{o} in the crystal lattice. The ability of furans to adopt the s-*cis* conformation after aromatization dramatically reduced ring strain. Aromatization forced the macrocycle to substantially change the structure from elliptical to more circular shape. The distance between

the two bifuran units in **II-2b** is 15.15 Å, which is substantially longer than that of *anti*-**II-20b**, and the distance between the two naphthyl units is shortened to 10.49 Å.

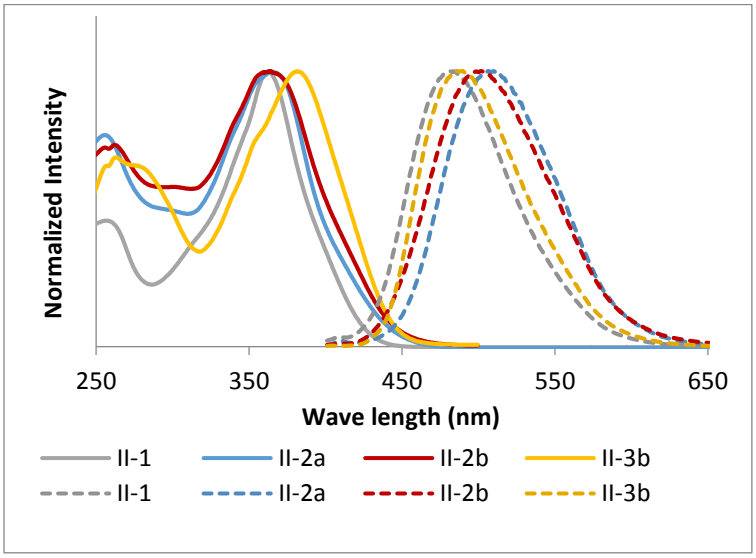

Figure II-3. UV-vis (solid line) and fluorescence (broken line) spectra of the furan-containing CPPs **II-1**, **II-2a**, **II-2b**, and **II-3b**

The λ_{abs} and λ_{em} of **II-1** are also red-shifted from those of 2,5-diphenylfuran, which shows the λ_{abs} at 230 and 327 nm and the λ_{em} at 353 and 372 nm upon excitation at 327 nm in dichloromethane. In comparison with **II-2a** and **II-2b**, the λ_{abs} of the acyclic 5,5'-biphenyl end-capped 2,2'-bifuran appears at 386 nm, and the λ_{em} appear at 431 and 455 nm. For comparison, the parent [10]-, [12]-, and [15]CPPs exhibit the λ_{abs} at 340, 338, and 339 nm, respectively, and the λ_{em} at 470, 450, and 440 nm, respectively in dichloromethane (Table 1).

compound	λ_{abs} (nm)	λ_{em} (nm)	$E_{1/2}$ vs Fc/Fc^+ (V)[a]
II-13	324	388	ND
II-19	355	429	0.54, 0.90, 1.20[b]
II-1	363	481	0.37, 0.81, 1.02[b]
anti-**II-20a**	356	438	ND
II-2a	364.5	510	ND
anti-**II-20b**	356.5	438	0.26, 0.92
syn-**II-20b**	356	434	0.34, 0.93
II-2b	364.5	502	0.28, 0.67,[b] 0.91,[b] 1.17[b]
anti-**II-21b**	368	430	0.26, 0.81, 1.30[b]
II-3b	381.5	486	0.37, 0.81, 1.02,[b] 1.21[b]

[a] Quasi-reversible waves with redox potentials ($E_{1/2}$) identified from differential pulse voltammograms. [b] Irreversible redox event. ND = not determined.

Table 1. UV-vis absorption maxima (λ_{abs}), fluorescence emission maxima (λ_{em}), and voltammetric data.

The electrochemistry of each furan-containing CPP, along with their corresponding reduced precursors were investigated by cyclic and differential pulse voltammetry in dichloromethane. The first oxidation potentials of **II-1**, **II-2b**, and **II-3b** are at 0.37, 0.28 and 0.37 V, respectively relative to Fc/Fc^+. The first oxidation potentials are smaller than 2,5-diphenylfuran which showed at 0.78 V. The first oxidation potential of **II-19** is at 0.54, which is higher than the first oxidation potentials of **II-1**. Surprisingly, the first oxidation potential of *syn*-**II-20** and *anti*-**II-20** are not the same. However, the second oxidation potentials are similar.

II-Conclusion

In summary, synthetic pathways for the furan-containing CPPs **II-1**, **II-2a/b**, and **II-3a/b** and related precursor carbon nanohoops have been developed. The Diels−Alder reaction between diene **II-4** and 1,4-benzoquinone (**II-5**) provides opportunities to stereoselectively place the bromophenyl groups *cis* to each other. The α-bromination of furan allows the use of the homo- and cross-coupling reactions to form the corresponding macrocycles. The optical and electrochemical properties of the macrocyclic furan-containing CPPs and precursors were fully studied. Placing furans in macrocycles provide an opportunity to further functionalized macrocycles.

II-General Experimental Methods

All reactions were conducted in oven-dried (120 °C) glassware under a nitrogen atmosphere. Tetrakis(triphenylphosphine)palladium ($Pd(PPh_3)_4$), tris(dibenzylideneacetone)dipalladium ($Pd_2(dba)_3$), [1,1′-bis(diphenylphosphino)ferrocene]dichloropalladium(II) ($Pd(dppf)Cl_2$), 2-dicyclohexylphosphino-2′,4′,6′-triisopropylbiphenyl (XPhos), 1,4-benzoquinone (**II-5**), bis(pinacolato)diboron (**II-8**), N-bromosuccinimide (NBS), 1-bromo-4-iodobenzene, imidazole, tertbutyldimethylsilyl chloride, triisopropylsilyl chloride, bis(1,5-cyclooctadiene)nickel ($Ni(cod)_2$), 2,2'-bipyridyl (bipy), and 2,3-dichloro-5,6-dicyano-1,4-benzoquinone (DDQ) were purchased from chemical suppliers and were used as received. 1,4-Bis(4-bromophenyl)-1,3-butadiene (4),[S1] and 2-(2-furanyl)-4,4,5,5-tetramethyl-1,3,2-dioxaborolane (10)[S2] were prepared according to the reported procedures. The UV-vis absorption spectra were recorded on a Shimadzu UV-1800 spectrophotometer with 1-nm resolution, and the baseline was corrected with a solvent filled square quartz cell. The fluorescence spectra were recorded on a Shimadzu RF-5301PC spectrofluorophotometer with 2-nm resolution.

Experimental Procedure for Dibromide II-6. To a 500 mL-round bottom flask containing a mixture of 7.24 g of diene **II-4** (19.9 mmol) and 2.59 g of 1,4-benzoquinone (24.0 mmol) in 400 mL of anhydrous dichloromethane under a nitrogen atmosphere was added by using a syringe 8.00 mL of boron trifluoride diethyl etherate (63.4 mmol). The reaction mixture was stirred at rt for 12 h. Ethyl acetate (100 mL) was added, and the solution was washed with water (3 × 100 mL). The organic layer was then passed through a short silica gel column (10 cm high, 5 cm in diameter). The column was further eluted with 300 mL of dichloromethane. The combined eluates were dried over sodium sulfate and concentrated to afford a brown/yellow solid. The solid residue was further purified by flash column chromatography (silica gel/ethyl acetate:hexanes = 1:4 to 1:2) to produce 8.65 g of **II-6** (18.3 mmol, 92% yield) as a yellow solid: mp 170–174 °C; IR 3210, 1484, 1008 cm^{-1} ; ^{1}H NMR ($CDCl_3$, 400 MHz) δ 7.42 (4 H, d, J = 8.2 Hz), 7.14 (4 H, d, J = 8.6 Hz), 6.63 (2 H, s), 5.90 (2 H, d, J = 2.8 Hz), 4.78 (2 H, d, J = 2.8 Hz), 4.21 (2 H, br s); ^{13}C NMR ($CDCl_3$, 100 MHz) δ 147.4, 142.3, 131.9, 129.7, 127.2, 124.8, 120.6, 115.1, 40.8. HRMS (ESI) calcd for $C_{22}H_{16}Br_2O_2$ (M^+) 469.9512, 471.9491, 473.9471, found 469.9516, 471.9495, 473.9474.

Experimental Procedure for Dibromide II-7a. A solution containing 4.70 g (9.95 mmol) of **II-6**, 4.52 g (30.0 mmol) of tert-butyldimethylsilyl chloride, 3.40 g (50.0 mmol) of imidazole in 50 mL of DMF was stirred under nitrogen at rt for 12 h. The reaction mixture was then poured into 200 mL of cold water. The precipitate was collected, washed with 100 mL of water and 50 mL of ethanol, air dried overnight to give 6.70 g (9.56 mmol, 96% yield) of **II-7a** as a brown solid: mp 151–153 °C; IR 1468, 1260, 1250, 773 cm^{-1} ; ^{1}H NMR ($CDCl_3$, 400 MHz) δ 7.28 (4 H, d, J = 8.6 Hz), 6.97 (4 H, d, J = 8.2 Hz), 6.65 (2 H, s), 5.98 (2 H, d, J = 3.2 Hz), 4.79 (2 H, d, J = 2.8 Hz), 0.77 (18 H, s), 0.19 (6 H, s), 0.05 (6 H, s); ^{13}C NMR ($CDCl_3$, 100 MHz) δ 147.2, 143.3,

131.1, 129.4, 128.8, 128.1, 119.4, 116.0, 40.9, 25.6, 18.2, –4.0, –4.2; HRMS (ESI) calcd for $C_{34}H_{44}Br_2O_2Si_2$ (M^+) 698.1241, 700.1221, 702.1200, found 698.1288, 700.1254, 702.1229.

Experimental Procedure for II-9. To a 250-mL flask were added 5.30 g of **II-7a** (7.56 mmol), 4.61 g of bis(pinacolato)diboron (**II-8**, 18.1 mmol), 0.18 g of XPhos (0.38 mmol), and 0.08 g of $Pd_2(dba)_3$ (0.08 mmol). The flask was fitted with a condenser and a rubber septum and then flushed with nitrogen. Then, 1,4-dioxane (200 mL) was introduced via cannula. The flask was flushed with nitrogen for 10 min, and the reaction mixture was heated at 90 °C for 24 h before it was allowed to cool to rt. The solvent was removed in vacuo, and the residue was purified by flash column chromatography (silica gel/ethyl acetate:hexanes = from hexanes only to 1:10) to produce 5.67 g of **II-9** (7.13 mmol, 94% yield) as a white solid: mp 244–247 °C; IR 1468, 1359, 1251, 837 cm^{-1} ; ^1H NMR ($CDCl_3$, 400 MHz) δ 7.59 (4 H, d, J = 8.2 Hz), 7.14 (4 H, d, J = 7.8 Hz), 6.63 (2 H, s), 5.95 (2 H, d, J = 2.8 Hz), 4.84 (2 H, d, J = 2.7 Hz), 1.318 (12 H, s), 1.314 (12 H, s), 0.74 (18 H, s), 0.18 (6 H, s), 0.00 (6 H, s); ^{13}C NMR ($CDCl_3$, 100 MHz) δ 147.7, 147.3, 134.7, 129.1, 127.9, 127.1, 115.7, 83.5, 41.8, 25.7, 24.85, 24.79, 18.2, –4.0, –4.2; HRMS (ESI) calcd for $C_{46}H_{68}B_2O_6Si_2$ (M^+) 793.4771, 794.4735, 795.4769, found 793.4744, 794.4704, 795.4735.

Experimental Procedure for II-11a. To a 500-mL two-neck flask fitted with a condenser and a rubber septum were added 4.24 g of **II-7a** (6.05 mmol), 3.53 g of 2-(2-furanyl)-4,4,5,5-tetramethyl-1,3,2-dioxaborolane (**II-10**, 18.2 mmol), 6.36 g of sodium carbonate (60.0 mmol), and 0.35 g of $Pd(PPh_3)_4$ (0.30 mmol). The flask was flushed with nitrogen, and a mixture of degassed water (50 mL), ethanol (100 mL), and toluene (250 mL) was introduced via cannula. Then nitrogen was bubbled through the solution for another 10 min. The reaction mixture was heated at reflux for 12 h before it was allowed to cool to rt. The solvent was removed in vacuo,

and the residue was purified by flash column chromatography (silica gel/ethyl acetate:hexanes = 1:20 to 1:10) to produce 3.72 g of **II-11a** (5.51 mmol, 91% yield) as a white solid: mp 141–142 °C; IR 1468, 1250, 1007, 777 cm^{-1} ; ^{1}H NMR ($CDCl_3$, 400 MHz) δ 7.52 (4 H, d, J = 8.2 Hz), 7.43 (2 H, d, J = 1.2 Hz), 7.20 (4 H, d, J = 8.2 Hz), 6.71 (2 H, s), 6.57 (2 H, d, J = 3.5 Hz), 6.45 (2 H, dd, J = 3.1, 2.0 Hz), 6.07 (2 H, d, J = 2.7 Hz), 4.91 (2 H, d, J = 2.8 Hz), 0.82 (18 H, s), 0.25 (6 H, s), 0.08 (6 H, s); ^{13}C NMR ($CDCl_3$, 100 MHz) δ 154.3, 147.3, 143.8, 141.5, 129.3, 128.4, 128.0, 123.6, 115.8, 111.5, 104.1, 41.3, 25.7, 18.2, –3.9, –4.2; HRMS (ESI) calcd for $C_{42}H_{50}O_4Si_2$ (M^+) 674.3242, found 674.3275.

Experimental Procedure for Dibromide II-12a. To a solution of **II-11a** (3.50 g, 5.19 mmol) in DMF (50 mL) at 0 °C was added portionwise NBS (1.89 g, 10.6 mmol). The reaction mixture was stirred in dark at rt for 12 h and then poured into 200 mL of cold water. The precipitate was collected, washed with 100 mL of water and air dried overnight. The dried precipitate was purified by flash column chromatography (silica gel/ethyl acetate:hexanes = 1:20 to 1:10) to produce 3.96 g of **12a** (4.75 mmol, 92% yield) as a white solid: mp 89–91 °C; IR 1468, 1252, 836, 773 cm^{-1} ; ^{1}H NMR ($CDCl_3$, 400 MHz) δ 7.42 (4 H, d, J = 8.6 Hz), 7.14 (4 H, d, J = 8.2 Hz), 6.66 (2 H, s), 6.49 (2 H, d, J = 3.6 Hz), 6.33 (2 H, d, J = 3.1 Hz), 6.02 (2 H, d, J = 3.2 Hz), 4.85 (2 H, d, J = 2.7 Hz), 0.77 (18 H, s) 0.20 (6 H, s), 0.04 (6 H, s); ^{13}C NMR ($CDCl_3$, 100 MHz) δ 156.2, 147.3, 144.2, 129.1, 128.0, 127.5, 123.3, 120.7, 115.9, 113.2, 106.6, 41.3, 25.7, 18.2, –4.0, –4.2; HRMS (ESI) calcd for $C_{42}H_{48}Br_2O_4Si_2$ (M^+) 830.1452, 832.1432, 834.1412, found 830.1510, 832.1466, 834.1445.

Experimental Procedure for *syn*-II-13 and *anti*-II-13. To a 1-L two-neck flask fitted with a condenser and a rubber septum were added 1.30 g of **II-12a** (1.56 mmol), 1.25 g of 9 (1.57 mmol), 2.60 g of potassium carbonate (18.8 mmol), and 0.065 g (0.089 mmol) of $Pd(dppf)Cl_2$.

toluene (700 mL), ethanol (150 mL), and water (50 mL) were then introduced. The solution was degassed by bubbling nitrogen through the solution for 30 min and then was heated to reflux for 24 h before it was allowed to cool to rt. The organic layer was separated, and the aqueous layer was extracted with dichloromethane (2 × 200 mL). The combined organic layers were concentrated in vacuo, and the residue was purified by flash column chromatography (silica gel/dichloromethane:hexanes = 1:5 to 1:3) to produce 0.284 g of a mixture of ***syn*-II-13** and ***anti*-II-13** (0.234 mmol, 15% yield, ratio between the two isomers = 1.3:1) as a white solid: mp >200 °C; IR 1468, 1260, 1252, 1066, 892, 766, 750 cm^{-1} ; sample 1: ^{1}H NMR ($CDCl_3$, 400 MHz) δ 7.53 (8 H, d, J = 8.2 Hz), 7.18 (8 H, d, J = 8.2 Hz), 6.68 (4 H, s), 6.60 (4 H, s), 5.96 (4 H, d, J = 2.9 Hz), 4.88 (4 H, d, J = 2.8 Hz), 0.80 (36 H, s), 0.23 (12 H, s), 0.03 (12 H, s); ^{13}C NMR ($CDCl_3$, 100 MHz) δ 153.0, 147.3, 143.4, 129.4, 128.5, 128.03, 128.01, 123.4, 115.7, 106.0, 41.1, 25.7, 18.2, –3.9, –4.3; sample 2: ^{1}H NMR ($CDCl_3$, 600 MHz) δ 7.51 (8 H, d, J = 8.2 Hz), 7.28 (8 H, d, J = 8.2 Hz), 6.63 (4 H, s), 6.59 (4 H, s), 6.09 (4 H, d, J = 2.9 Hz), 4.94 (4 H, d, J = 2.9 Hz), 0.87 (36 H, s), 0.23 (12 H, s), 0.08 (12 H, s); ^{13}C NMR ($CDCl_3$, 150 MHz) δ 153.6, 147.1, 143.0, 129.5, 128.9, 128.5, 123.6, 116.1, 106.4, 41.4, 25.9, 18.4, –3.7, –4.1; HRMS (ESI) calcd for $C_{76}H_{92}O_6Si_4$ (M^+) 1212.5966, found 1212.6008.

Experimental Procedure for Dibromide II-15. To a 500-mL two-neck flask fitted with a condenser and a rubber septum were added 8.90 g of **II-9** (11.2 mmol), 18.85 g of 1-bromo-4-iodobenzene (66.63 mmol), 18.50 g of potassium carbonate (134.1 mmol), and 1.30 g of $Pd(PPh_3)_4$ (1.12 mmol). The flask was flushed with nitrogen, and a mixture of degassed water (50 mL), ethanol (150 mL), and toluene (250 mL) was introduced via cannula. Then nitrogen was bubbled through the solution for another 10 min. The reaction mixture was heated at reflux for 12 h before it was allowed to cool to rt. The solvent was removed in vacuo, and the residue

was purified by flash column chromatography (silica gel/ethyl acetate:hexanes = 1:20 to 1:10) to produce 8.66 g of **II-15** (10.2 mmol, 91% yield) as a white solid: mp 193–195 °C; IR 1469, 1250, 804 cm^{-1} ; ^{1}H NMR ($CDCl_3$, 600 MHz) δ 7.50 (4 H, d, J = 8.2 Hz), 7.36 (4 H, d, J = 8.8 Hz), 7.35 (4 H, d, J = 8.2 Hz), 7.22 (4 H, d, J = 8.2 Hz), 6.67 (2 H, s), 6.05 (2 H, d, J = 2.9 Hz), 4.90 (2 H, d, J = 3.0 Hz), 0.75 (18 H, s), 0.21 (6 H, s), 0.04 (6 H, s); ^{13}C NMR (CDCl3, 150 MHz) δ 147.3, 144.2, 140.2, 137.4, 131.7, 129.2, 128.6, 128.2, 128.0, 126.7, 121.0, 115.8, 41.3, 25.6, 18.2, –3.9, –4.2; HRMS (ESI) calcd for $C_{46}H_{52}Br_2O_2Si_2$ (M^+) 850.1867, 852.1847, 854.1826, found 850.1887, 852.1865, 854.1845.

Experimental Procedure for II-16. To a 250-mL flask were added 4.30 g of **II-15** (5.04 mmol), 3.10 g of bis(pinacolato)diboron (**II-8**, 12.1 mmol), 0.12 g of XPhos (0.25 mmol), and 0.05 g of $Pd_2(dba)_3$ (0.05 mmol). The flask was fitted with a condenser and a rubber septum and then flushed with nitrogen before 1,4-dioxane (150 mL) was introduced via cannula. The flask was again flushed with nitrogen for 10 min, and the reaction mixture was heated at 90 °C for 24 h before it was allowed to cool to rt. The solvent was removed in vacuo, and the residue was purified by flash column chromatography (silica gel/ethyl acetate:hexanes = from hexanes only to 1:10) to produce 4.35 g of **II-16** (4.59 mmol, 91% yield) as a white solid: mp 261–263 °C; IR 1470, 1360, 1250, 810 cm^{-1} ; ^{1}H NMR ($CDCl_3$, 400 MHz) δ 7.83 (4 H, d, J = 7.8 Hz), 7.52 (4 H, d, J = 7.8 Hz), 7.43 (4 H, d, J = 7.8 Hz), 7.23 (4 H, d, J = 8.2 Hz), 6.66 (2 H, s), 6.04 (2 H, d, J = 2.4 Hz), 4.89 (2 H, d, J = 2.3 Hz), 1.35 (24 H, s), 0.74 (18 H, s), 0.20 (6 H, s), 0.03 (6 H, s); ^{13}C NMR ($CDCl_3$, 100 MHz) δ 147.3, 144.1, 144.0, 138.4, 135.1, 129.3, 128.1, 128.0, 127.0, 126.3, 115.7, 83.7, 41.3, 25.6, 24.8, 18.2, –3.9, –4.3; HRMS (ESI) calcd for $C_{58}H_{76}B_2O_6Si_2$ (M^+) 945.5397, 946.5361, 947.5395, found 945.5346, 946.5307, 947.5337.

Experimental Procedure for II-17. To a 250-mL two-neck flask fitted with a condenser and a rubber septum were added 4.40 g of **II-15** (5.16 mmol), 3.03 g of 2-(2-furanyl)-4,4,5,5-tetramethyl- 1,3,2-dioxaborolane (10,15.5 mmol), 6.36 g of sodium carbonate (60.0 mmol), and 0.60 g of $Pd(PPh_3)_4$ (0.52 mmol). The flask was flushed with nitrogen, and a mixture of degassed water (20 mL), ethanol (40 mL), and toluene (80 mL) was introduced via cannula. Then nitrogen was bubbled through the solution for another 20 min. The reaction mixture was heated at reflux for 12 h before it was allowed to cool to rt. The solvent was removed in vacuo, and the residue was purified by flash column chromatography (silica gel/ethyl acetate:hexanes = 1:10 to 1:5) to produce 3.76 g of **II-17** (4.55 mmol, 88% yield) as a white solid: mp 176–178 °C; IR 1467, 1250, 893 cm^{-1} ; ^1H NMR ($CDCl_3$, 400 MHz) δ 7.69 (4 H, d, J = 8.2 Hz), 7.54 (4 H, d, J = 8.2 Hz), 7.47 (2 H, d, J = 1.6 Hz), 7.43 (4 H, d, J = 7.8 Hz), 7.24 (4 H, d, J = 8.2 Hz), 6.68 (2 H, s), 6.65 (2 H, d, J = 3.5 Hz), 6.48 (2 H, dd, J = 3.1, 1.6 Hz), 6.07 (2 H, d, J = 2.8 Hz), 4.92 (2 H, d, J = 2.8 Hz), 0.77 (18 H, s), 0.22 (6 H, s), 0.06 (6 H, s); ^{13}C NMR ($CDCl_3$, 100 MHz) δ 153.9, 147.3, 143.9, 142.0, 140.2, 138.0, 129.44, 129.35, 128.2, 128.1, 127.2, 126.6, 124.1, 115.8, 111.7, 104.9, 41.3, 25.6, 18.2, –3.9, –4.2; HRMS (ESI) calcd for $C_{54}H_{58}O_4Si_2$ (M^+) 826.3868, found 826.3878.

Experimental Procedure for Dibromide II-18. To a solution of 17 (3.67 g, 4.44 mmol) in DMF (50 mL) at 0 °C was added portionwise 1.62 g of NBS (**II-9**.10 mmol). The reaction mixture was stirred in dark at rt for 12 h and then poured into 200 mL of cold water. The precipitate was collected, washed with 100 mL of water and air dried overnight. The dried precipitate was purified by flash column chromatography (silica gel/ethyl acetate:hexanes = 1:20 to 1:10) to produce 4.17 g of **II-18** (4.23 mmol, 95% yield) as a white solid: mp 115–118 °C; IR 1467, 1251, 733 cm^{-1} ; ^1H NMR ($CDCl_3$, 400 MHz) δ 7.64 (4 H, d, J = 8.4 Hz), 7.54 (4 H, d, J =

8.0 Hz), 7.43 (4 H, d, *J* = 8.2 Hz), 7.25 (4 H, d, *J* = 8.6 Hz), 6.70 (2 H, s), 6.59 (2 H, d, *J* = 3.2 Hz), 6.38 (2 H, d, *J* = 3.6 Hz), 6.08 (2 H, d, *J* = 2.8 Hz), 4.94 (2 H, d, *J* = 3.2 Hz), 0.78 (18 H, s), 0.23 (6 H, s), 0.07 (6 H, s); ^{13}C NMR ($CDCl_3$, 100 MHz) δ 155.8, 147.3, 144.0, 140.6, 137.8, 129.3, 128.4, 128.2, 128.1, 127.2, 126.6, 123.8, 121.3, 115.8, 113.4, 107.2, 41.3, 25.6, 18.2, –3.9, –4.2; HRMS (ESI) calcd for $C_{54}H_{56}Br_2O_4Si_2$ (M^+) 982.2078, 984.2058, 986.2038, found 982.2095, 984.2079, 986.2079.

Experimental Procedure for *syn*-II-19 and *anti*-II-19. To a 1-L two-neck flask fitted with a condenser and a rubber septum were added 0.982 g of **II-18** (0.997 mmol), 0.946 g of **II-16** (0.999 mmol), 1.656 g of potassium carbonate (12.00 mmol), and 0.04 g (0.05 mmol) of Pd(dppf)Cl_2. Toluene (600 mL), ethanol (200 mL), and water (100 mL) were then introduced. The solution was degassed by bubbling nitrogen through the solution for 30 min and then was heated at reflux for 24 h before it was allowed to cool to rt. The organic layer was separated, and the aqueous layer was extracted with dichloromethane (2 × 200 mL). The combined organic layers were concentrated in vacuo, and the residue was purified by flash column chromatography (silica gel/dichloromethane:hexanes = 1:6 to 1:3) to produce 0.254 g of a mixture of ***syn*-II-19** and ***anti*-II-19** (0.167 mmol, 17% yield) as a white solid: mp >180 °C; IR 1468, 1260, 765, 750 cm^{-1} ; ^{1}H NMR ($CDCl_3$, 600 MHz) major set δ 7.83 (8 H, d, *J* = 8.5 Hz), 7.63 (8 H, d, *J* = 8.6 Hz), 7.49 (8 H, d, *J* = 8.3 Hz), 7.28 (8 H, d, *J* = 8.3 Hz), 6.77 (4 H, s), 6.68 (4 H, s), 6.07 (4 H, d, *J* = 3.5 Hz), 4.97–4.95 (4 H, from both isomers, br), 0.80 (36 H, s), 0.24 (12 H, from both isomers, s), 0.06 (12 H, from both isomers, s); minor set δ 7.81 (8 H, d, *J* = 8.5 Hz), 7.61 (8 H, d, *J* = 8.5 Hz), 7.47 (8 H, d, *J* = 8.3 Hz), 7.283 (8 H, d, *J* = 8.3 Hz), 6.766 (4 H, s), 6.67 (4 H, s), 6.077 (4 H, d, *J* = 3.5 Hz), 4.965–4.950 (4 H, from both isomers, br), 0.808 (36 H, s), 0.24 (12 H, from both isomers, s), 0.06 (12 H, from both isomers, s); ^{13}C NMR ($CDCl_3$, 150 MHz) both

isomers δ 153.09, 153.0, 147.3, 147.3, 143.7, 143.7, 140.2, 140.0, 138.2, 137.9, 129.4, 129.4, 129.4, 129.3, 128.4, 128.4, 128.2, 128.2, 127.3, 127.1, 126.6, 126.4, 124.02, 123.98, 115.8, 107.1, 41.16, 41.12, 25.7, 18.25, 18.24, –3.86, –3.88, –4.3; HRMS (ESI) calcd for $C_{100}H_{109}O_6Si_4$ (MH^+) 1517.7296, found 1517.7265.

Experimental Procedure for II-1. To a mixture of *syn*-**II-19** and *anti*-**II-19** (0.022 g, 0.014 mmol) in chlorobenzene (2 mL) was added DDQ (0.014 g, 0.061 mmol). The reaction flask was then flushed with nitrogen. The reaction mixture was heated at 70 °C for 3 h before it was allowed to cool to rt. The solution was diluted with 10 mL of dichloromethane and passed through a basic alumina column (5 cm high, 2 cm in diameter), and the column was further eluted with 100 mL of dichloromethane. The combined eluates were concentrated in vacuo, and the residue was washed with 5 mL of cold hexanes to give 0.018 g of **II-1** (0.012 mmol, 82% yield) as a yellow solid: mp >180 °C; IR 1488, 1388, 1252, 838 cm^{-1} ; ^1H NMR ($CDCl_3$, 600 MHz) δ 7.70 (8 H, d, J = 8.5 Hz), 7.52 (8 H, d, J = 8.5 Hz), 7.45 (8 H, d, J = 8.2 Hz), 7.39 (8 H, d, J = 8.2 Hz), 7.11 (4 H, s), 6.93 (4 H, s), 6.69 (4 H, s), 0.74 (36 H, s), 0.00 (24 H, s); ^{13}C NMR ($CDCl_3$, 150 MHz) δ 153.4, 146.6, 143.6, 140.6, 138.4, 137.0, 131.7, 129.7, 128.6, 127.6, 126.9, 126.4, 125.2, 115.2, 106.6, 25.9, 18.5, –4.3, –4.4 ; HRMS (ESI) calcd for $C_{100}H_{104}O_6Si_4$ (M^+) 1512.6905, found 1512.6922.

Experimental Procedure for Cyclic Dimers *syn*-II-20a and *anti*-II-20a and Cyclic Trimer *anti*-II-21a. To a 500 mL-flask were added 0.850 g of **II-12a** (1.02 mmol) and 0.382 g of 2,2′-bipyridyl (2.45 mmol). The flask was flushed with nitrogen and placed in a glovebox under a nitrogen atmosphere before 0.673 g of $Ni(cod)_2$ (2.45 mmol) was added. The flask was fitted with a condenser and a rubber septum and then removed from the glovebox before 350 mL of THF was introduced via cannula. The reaction mixture was heated at reflux for 24 h before it

was allowed to cool to rt. The reaction mixture was passed through a short silica gel column and eluted with dichloromethane (200 mL). The combined eluates were concentrated, and the residue was purified by flash column chromatography (silica gel/dichloromethane:hexanes = 1:10 to 1:3) to produce 0.180 g of *anti*-**II-20a** (0.134 mmol, 26% yield) as a white solid and a mixture of 0.310 g of *syn*-**II-20a** and *anti*-**II-21a** (mole ratio of syn-20a:anti-21a = 2:1, 45% combined yield) as a white solid. *anti*-**II-20a**: mp >210 °C; IR 1471, 1250, 894, 773 cm^{-1} ; ^{1}H NMR ($CDCl_3$, 400 MHz) δ 7.14 (8 H, d, J = 8.2 Hz), 6.79 (8 H, d, J = 8.2 Hz), 6.72 (4 H, s), 6.56 (4 H, dd, J = 4.0, 2.0 Hz), 6.45 (4 H, d, J = 3.2 Hz), 6.27 (4 H, d, J = 3.5 Hz), 5.05 (4 H, m), 0.86 (36 H, s), 0.22 (12 H, s), 0.13 (12 H, s); ^{13}C NMR ($CDCl_3$, 100 MHz) δ 153.1, 146.7, 145.3, 141.4, 132.0, 131.5, 127.6, 127.4, 122.7, 116.1, 106.9, 105.6, 39.1, 25.7, 18.1, –4.17, –4.23; HRMS (ESI) calcd for $C_{84}H_{96}O_8Si_4$ (M^+) 1344.6177, found 1344.6190. The formation of *syn*-**II-20a** and *anti*-**II-21a** was discerned by comparing the ^{1}H NMR spectrum of the mixture with those of *syn*-**II-20b** and *anti*-**II-21b**. The HRMS of the mixture also indicated the formation of *syn*-**II-20a** and *anti*-**II-21a**. *syn*-**II-20a**: HRMS (ESI) calcd for $C_{84}H_{96}O_8Si_4$ (M^+) 1344.6177, found 1344.6187; *anti*-**II-21a**: HRMS (ESI) calcd for $C_{126}H_{144}O_{12}Si_6$ (M^+) 2016.9268, found 2016.9282.

Experimental Procedure for II-2a. To a solution of *anti*-**II-20a** (0.026 g, 0.019 mmol) in chlorobenzene (2 mL) was added DDQ (0.026 g, 0.12 mmol). The reaction flask was then flushed with nitrogen, and the reaction mixture was heated at 75 °C for 2.5 h before it was allowed to cool to rt. The solution was diluted with 30 mL of dichloromethane and passed through a basic alumina column (5 cm high, 2 cm in diameter), and the column was further eluted with 100 mL of dichloromethane. The combined eluates were concentrated in vacuo, and the residue was washed with 5 mL of cold hexanes to give 0.021 g of **II-2a** (0.016 mmol, 81% yield) as a yellow solid: mp >200 °C; IR 1463, 1387, 1255, 920, 838, 780 cm^{-1} ; ^{1}H NMR

($CDCl_3$, 600 MHz) δ 7.62 (8 H, d, J = 8.5 Hz), 7.27 (8 H, d, J = 8.5 Hz), 7.09 (4 H, s), 6.83 (4 H, s), 6.62 (4 H, d, J = 3.4 Hz), 6.53 (4 H, d, J = 3.4 Hz), 0.70 (36 H, s), –0.08 (24 H, s); ^{13}C NMR ($CDCl_3$, 150 MHz) δ 153.2, 146.4, 145.2, 144.1, 137.6, 129.7, 128.4, 128.3, 124.2, 114.9, 106.3, 105.5, 26.0, 18.7, –4.2, –4.3; HRMS (ESI) calcd for $C_{84}H_{92}O_8Si_4$ (M^+) 1340.5864, found 1340.5901.

Experimental Procedure for II-2a and II-3a. To a mixture of *syn*-**II-20a** and *anti*-**II-21a** (0.040 g, mole ratio of *syn*-**II-20a**:*anti*-**II-21a** = 2:1, 0.017 mmol of *syn*-**II-20a** and 0.0085 mmol of *anti*-**II-21a**) in chlorobenzene (3 mL) was added DDQ (0.027 g, 0.12 mmol). The reaction flask was then flushed with nitrogen, and the reaction mixture was heated at 75 °C for 2.5 h before it was allowed to cool to rt. The solution was diluted with 30 mL of dichloromethane and passed through a basic alumina column (5 cm high, 2 cm in diameter), and the column was further eluted with 100 mL of dichloromethane. The combined eluates were concentrated in vacuo, and the residue was washed with 5 mL of cold hexanes to give 0.033 g of a mixture of **II-2a** and **II-3a** (mole ratio of **II-2a**:**II-3a** = 2:1, 83% combined yield) as a yellow solid: ^{1}H NMR of **II-3a** (minor set) of the mixture ($CDCl_3$, 600 MHz) δ 7.78 (12 H, d, J = 8.2 Hz), 7.47 (12 H, d, J = 8.2 Hz), 7.30 (6 H, s), 6.83 (6 H, s), 6.75 (6 H, d, J = 3.4 Hz), 6.65 (6 H, d, J = 3.4 Hz), 0.72 (108 H, s), 0.18 (72 H, s); ^{13}C NMR ($CDCl_3$, 150 MHz) of **II-3a** (minor set) δ 153.6, 146.9, 145.2, 144.4, 137.8, 129.7, 129.5, 128.2, 126.6, 122.8, 114.5, 107.5, 106.1, 26.4, 19.1, –4.2, –4.3.

Experimental Procedure for II-7b. A solution containing 4.70 g (9.95 mmol) of **II-6**, 5.76 g (30.0 mmol) of triisopropylsilyl chloride, 3.40 g (50.0 mmol) of imidazole in 70 mL of DMF under nitrogen was stirred at 70 °C for 12 h. The reaction mixture was then poured into 300 mL of cold water. The precipitate was collected, washed with 50 mL of ethanol, air dried overnight to give 5.55 g (7.07 mmol, 71% yield) of **II-7b** as a brown solid: mp 124–127 °C; IR 1466,

1261, 1011, 882, 751 cm^{-1} ; ^{1}H NMR ($CDCl_3$, 400 MHz) δ 7.27 (4 H, d, J = 8.6 Hz), 6.99 (4 H, d, J = 8.6 Hz), 6.61 (2 H, s), 5.99 (2 H, d, J = 3.1 Hz), 4.84 (2 H, d, J = 2.7 Hz), 1.16 (6 H, septet, J = 7.4 Hz), 0.97 (18 H, d, J = 7.4 Hz), 0.94 (18 H, d, J = 7.4 Hz); ^{13}C NMR ($CDCl_3$, 100 MHz) δ 147.2, 143.4, 131.0, 129.4, 128.3, 128.1, 119.3, 115.7, 41.0, 17.9, 13.2; HRMS (ESI) calcd for $C_{40}H_{56}Br_2O_2Si_2$ (M^+) 782.2180, 784.2160, 786.2139, found 782.2151, 784.2131, 786.2105. Recrystallization of **II-7b** from CH_2Cl_2/acetonitrile produced a single crystal suitable for X-ray structure analysis.

Experimental Procedure for II-11b. To a 250-mL two-neck flask fitted with a condenser and a rubber septum were added 3.20 g of **II-7b** (4.08 mmol), 2.37 g of 2-(2-furanyl)-4,4,5,5-tetramethyl- 1,3,2-dioxaborolane (10, 12.2 mmol), 4.97 g of sodium carbonate (36.0 mmol), and 0.24 g of $Pd(PPh_3)_4$ (0.20 mmol). The flask was flushed with nitrogen, and a mixture of degassed water (20 mL), ethanol (50 mL), and toluene (100 mL) was introduced via cannula. Then nitrogen was bubbled through the solution for another 10 min. The reaction mixture was heated at reflux for 12 h before it was allowed to cool to rt. The solvent was removed in vacuo, and the residue was purified by flash column chromatography (silica gel/ethyl acetate:hexanes = 1:20 to 1:10) to produce 2.75 g of **II-11b** (3.62 mmol, 89% yield) as a white solid: mp 151–153 °C; IR 1465, 1260, 882, 757 cm^{-1} ; ^{1}H NMR ($CDCl_3$, 400 MHz) δ 7.47 (4 H, d, J = 8.2 Hz), 7.41 (2 H, d, J = 2.0 Hz), 7.17 (4 H, d, J = 8.2 Hz), 6.62 (2 H, s), 6.52 (2 H, d, J = 3.1 Hz), 6.42 (2 H, dd, J = 2.8, 1.6 Hz), 6.03 (2 H, d, J = 3.1 Hz), 4.92 (2 H, d, J = 2.4 Hz), 1.17 (6 H, septet, J = 7.4 Hz), 0.97 (18 H, d, J = 7.4 Hz), 0.95 (18 H, d, J = 7.4 Hz); ^{13}C NMR ($CDCl_3$, 100 MHz) δ 154.4, 147.3, 143.9, 141.5, 128.7, 128.3, 128.1, 128.0, 123.6, 115.5, 111.4, 104.1, 41.4, 18.0, 13.2; HRMS (ESI) calcd for $C_{48}H_{62}O_4Si_2$ (M^+) 758.4181, found 758.4189.

Experimental Procedure for II-12b. To a solution of **II-11b** (2.50 g, 3.29 mmol) in DMF (50 mL) at 0 °C was added portionwise 1.20 g of NBS (6.75 mmol). The reaction mixture was stirred in dark at rt for 12 h and then poured into 200 mL of cold water. The precipitate was collected, washed with 100 mL of water and air dried overnight. The dried precipitate was purified by flash column chromatography (silica gel/ethyl acetate:hexanes = 1:20 to 1:10) to produce 2.77 g of **II-12b** (3.02 mmol, 92% yield) as a white solid: mp 185–187 °C; IR 1466, 1262, 883, 764, 751 cm^{-1} ; ^1H NMR ($CDCl_3$, 400 MHz) δ 7.41 (4 H, d, J = 8.6 Hz), 7.15 (4 H, d, J = 8.2 Hz), 6.62 (2 H, s), 6.48 (2 H, d, J = 3.5 Hz), 6.33 (2 H, d, J = 3.5 Hz), 6.03 (2 H, d, J = 3.1 Hz), 4.91 (2 H, d, J = 2.7 Hz), 1.17 (6 H, septet, J = 7.4 Hz), 0.97 (18 H, d, J = 7.4 Hz), 0.94 (18H, d, J = 7.4 Hz; ^{13}C NMR ($CDCl_3$, 100 MHz) δ 156.3, 147.3, 144.3, 128.6, 128.1, 128.0, 127.4, 123.3, 120.7, 115.5, 113.2, 106.5, 41.4, 17.97, 17.96, 13.2; HRMS (ESI) calcd for $C_{48}H_{60}Br_2O_4Si_2$ (M^+) 914.2391, 916.2371, 918.2351, found 914.2403, 916.2383, 918.2362.

Recrystallization of **II-12b** from CH_2Cl_2/acetonitrile produced a single crystal suitable for X-ray structure analysis.

Experimental Procedure for Cyclic Dimers *syn*-II-20b and *anti*-II-20b and Cyclic Trimer *anti*-II-21b. To a 1 L-flask were added 0.917 g of **II-12b** (1.00 mmol) and 0.375 g of 2,2′-bipyridyl (2.40 mmol). The flask was flushed with nitrogen and placed in a glovebox under a nitrogen atmosphere before 0.660 g of $Ni(cod)_2$ (2.40 mmol) was added. The flask was fitted with a condenser and a rubber septum and then removed from the glovebox before 500 mL of THF was introduced via cannula. The reaction mixture was heated at reflux for 24 h before it was allowed to cool to rt. Then the reaction mixture was passed through a short silica gel column and eluted with dichloromethane (200 mL). The combined eluates were concentrated, and the residue was purified by flash column chromatography (silica gel/dichloromethane:hexanes =

1:10 to 1:5) to produce 0.180 g of *anti*-**II-20b** (Rf = 0.65, hexanes:dichloromethane = 4:1, 0.119 mmol, 24% yield) as a white solid, 0.178 g of *syn*-**II-20b** (Rf = 0.15, hexanes:dichloromethane = 4:1, 0.118 mmol, 24% yield) as a white solid, and 0.140 g of *anti*-**II-21b** (Rf = 0.48, hexanes:dichloromethane = 4:1, 0.062 mmol, 18% yield) as a white solid. *anti*-**II-20b**: mp >230 °C; IR 1474, 1259, 882, 765, 750 cm^{-1} ; ^{1}H NMR ($CDCl_3$, 400 MHz) δ 7.13 (8 H, d, J = 8.6 Hz), 6.82 (8 H, d, J = 8.2 Hz), 6.70 (4 H, s), 6.57 (4 H, dd, J = 4.3, 2.0 Hz), 6.45 (4 H, d, J = 3.1 Hz), 6.27 (4 H, d, J = 3.5 Hz), 5.12 (4 H, br s), 1.25 (12 H, septet, J = 7.4 Hz), 1.05 (36 H, d, J = 7.4 Hz), 1.03 (36 H, d, J = 7.0 Hz); ^{13}C NMR ($CDCl_3$, 100 MHz) δ 153.2, 146.9, 145.3, 141.6, 131.6, 131.5, 127.7, 127.3, 122.6, 115.8, 106.8, 105.5, 39.2, 18.11, 18.05, 13.1; HRMS (ESI) calcd for $C_{96}H_{121}O_8Si_4$ (MH^+) 1513.8133, found 1513.8116. *syn*-**II-20b**: mp >240 °C; IR 1469, 1260, 882, 765, 750 cm^{-1} ; ^{1}H NMR ($CDCl_3$, 400 MHz) δ 7.56 (8 H, d, J = 8.2 Hz), 7.16 (8 H, d, J = 8.2 Hz), 6.65 (4 H, s), 6.56 (4 H, d, J = 3.1 Hz), 6.49 (4 H, d, J = 3.5 Hz), 6.06 (4 H, d, J = 2.7 Hz), 4.92 (4 H, d, J = 2.4 Hz), 1.15 (12 H, septet, J = 7.4 Hz), 0.952 (36 H, d, J = 7.4 Hz), 0.948 (36 H, d, J = 7.4 Hz); ^{13}C NMR ($CDCl_3$, 100 MHz) δ 153.5, 147.3, 145.0, 143.7, 128.6, 128.1, 127.9, 127.4, 123.5, 115.2, 107.2, 106.0, 41.1, 18.05, 17.99, 13.1; HRMS (ESI) calcd for $C_{96}H_{120}O_8Si_4$ (M^+) 1512.8055, found 1512.8073. *anti*-**II-21b**: mp >200 °C; IR 1469, 1262, 884, 779 cm^{-1}; ^{1}H NMR ($CDCl_3$, 400 MHz) δ 7.53 (4 H, d, J = 8.2 Hz), 7.49 (8 H, d, J = 7.8 Hz), 7.23 (4 H, d, J = 8.6 Hz), 7.18 (4 H, d, J = 8.2 Hz), 7.14 (4 H, d, J = 8.2 Hz), 6.70– 6.56 (18 H, m), 6.11 (2 H, dd, J = 10.2, 4.3 Hz), 6.08 (2 H, d, J = 3.1 Hz), 6.02 (2 H, dd, J = 9.4, 3.1 Hz), 4.94 (6 H, br s), 1.29–1.08 (18 H, m), 1.04–0.92 (108 H, m); ^{13}C NMR ($CDCl_3$, 100 MHz) δ 153.59, 153.55, 153.50, 147.37, 147.29, 147.23, 145.77, 145.71, 145.69, 143.86, 143.85, 143.81, 129.4, 128.9, 128.3, 128.2, 128.10, 128.07, 127.92, 123.6, 123.5, 115.7, 115.5, 115.3, 107.09, 107.05, 107.00, 106.34, 106.27, 106.19, 41.5, 41.2, 18.03, 18.01, 17.98, 17.95, 13.27, 13.23,

13.17, 0.0; HRMS (ESI) calcd for $C_{144}H_{180}O_{12}Si_6$ (M^+) 2269.2085 found 2269.2096. Recrystallization of *anti*-**II-20b** from CH_2Cl_2/acetonitrile produced a single crystal suitable for X-ray structure analysis.

Experimental Procedure for II-2b. To a solution of *anti*-**II-20b** (0.020 g, 0.013 mmol) in chlorobenzene (2 mL) was added DDQ (0.018 g, 0.079 mmol). The reaction flask was then flushed with nitrogen, and the reaction mixture was heated at 75 °C for 2.5 h before it was allowed to cool to rt. The solution was diluted with 10 mL of dichloromethane and passed through a basic alumina column (5 cm high, 2 cm in diameter), and the column was further eluted with 100 mL of dichloromethane. The combined eluates were concentrated in vacuo, and the residue was washed with 3 mL of cold hexanes to give 0.016 g of **II-2b** (0.011 mmol, 80% yield) as a yellow solid: mp >200 °C; IR 1388, 1259, 912, 777 cm^{-1} ; ^1H NMR ($CDCl_3$, 400 MHz) δ 7.61 (8 H, d, J = 8.2 Hz), 7.29 (8 H, d, J = 8.2 Hz), 7.09 (4 H, s), 6.81 (4 H, s), 6.61 (4 H, d, J = 3.1 Hz), 6.53 (4 H, d, J = 3.1 Hz), 1.01–0.91 (12 H, m), 0.87 (72 H, d, J = 6.7 Hz); ^{13}C NMR ($CDCl_3$, 100 MHz) δ 153.3, 146.8, 145.2, 144.3, 137.7, 129.7, 128.4, 128.1, 127.2, 124.2, 114.1, 106.3, 105.4, 17.9, 13.2; HRMS (ESI) calcd for $C_{96}H_{116}O_8Si_4$ (M^+) 1508.7742, found 1508.7788.

To a solution of *syn*-**II-20b** (0.021 g, 0.014 mmol) in chlorobenzene (2 mL) was added DDQ (0.013 g, 0.056 mmol). The procedure for the oxidative aromatization reaction was carried out as described for *anti*-**II-20b** to afford 0.017g of **II-2b** (0.011 mmol, 81% yield) as a yellow solid. Recrystallization of **II-2b** from chloroform produced a single crystal suitable for X-ray structure analysis.

Experimental Procedure for II-3b. To a solution of *anti*-**II-21b** (0.027 g, 0.012 mmol) in chlorobenzene (2 mL) was added DDQ (0.016 g, 0.071 mmol). The reaction flask was then

flushed with nitrogen, and the reaction mixture was heated at 70 °C for 3 h before it was allowed to cool to rt. The solution was diluted with 10 mL of dichloromethane and passed through a basic alumina column (5 cm high, 2 cm in diameter), and the column was further eluted with 100 mL of dichloromethane. The combined eluates were concentrated in vacuo, and the residue was washed with 5 mL of cold hexanes to give 0.020 g of **II-3b** (0.0088 mmol, 74% yield) as a yellow solid: mp >200 °C; IR 1465, 1389, 1260, 778 cm^{-1} ; ^{1}H NMR ($CDCl_3$, 400 MHz) δ 7.76 (12 H, d, J = 8.2 Hz), 7.47 (12 H, d, J = 8.2 Hz), 7.28 (6 H, s), 6.81 (6 H, s), 6.73 (6 H, d, J = 3.1 Hz), 6.65 (6 H, d, J = 3.5 Hz), 1.04–0.76 (126 H, m); ^{13}C NMR ($CDCl_3$, 100 MHz) δ 153.8, 147.2, 145.2, 144.6, 137.8, 129.7, 129.2, 128.1, 126.7, 123.0, 113.7, 107.5, 106.1, 18.1, 13.2; HRMS (ESI) calcd for $C_{144}H_{175}O_{12}Si_6$ (MH^+) 2264.1694, found 2264.1740.

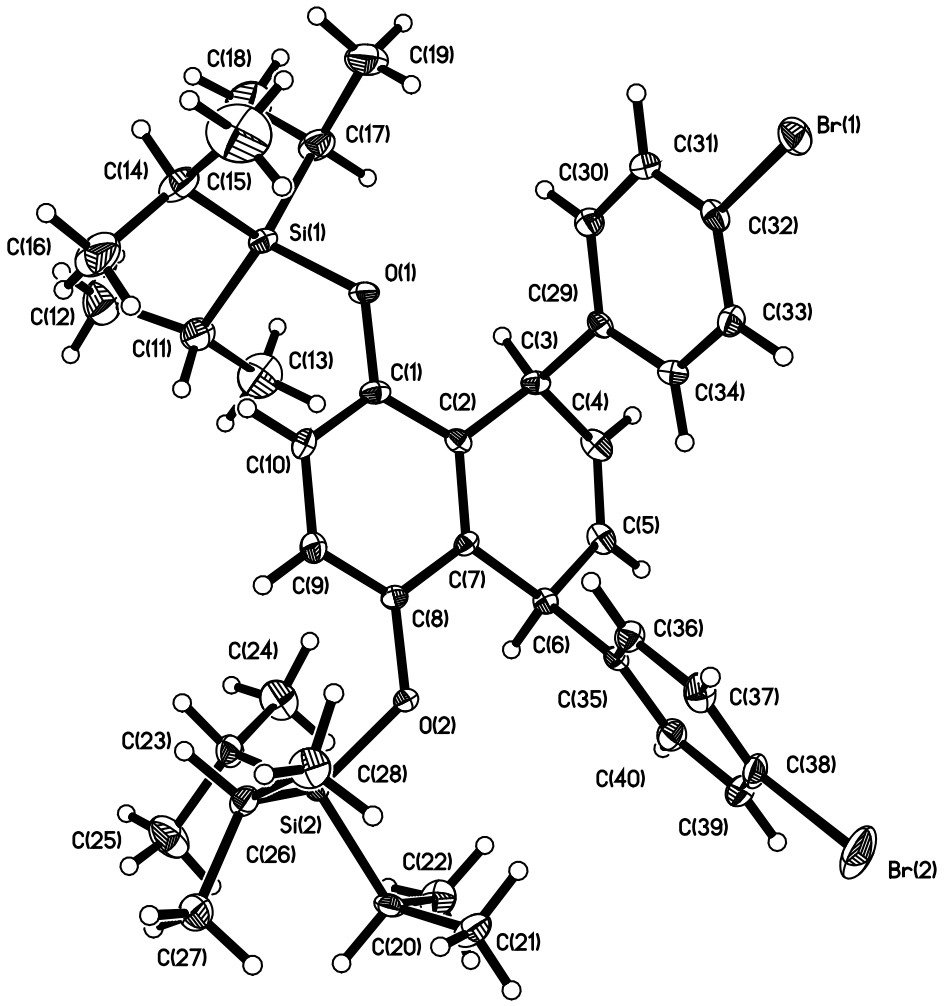

Figure II-4. Perspective view of the molecular structure of **II-7b** $C_{40}H_{56}Br_2O_2Si_2$ (molecule 1) with the atom labeling scheme for the independent non-hydrogen atoms. The thermal ellipsoids are scaled to enclose 50% probability.

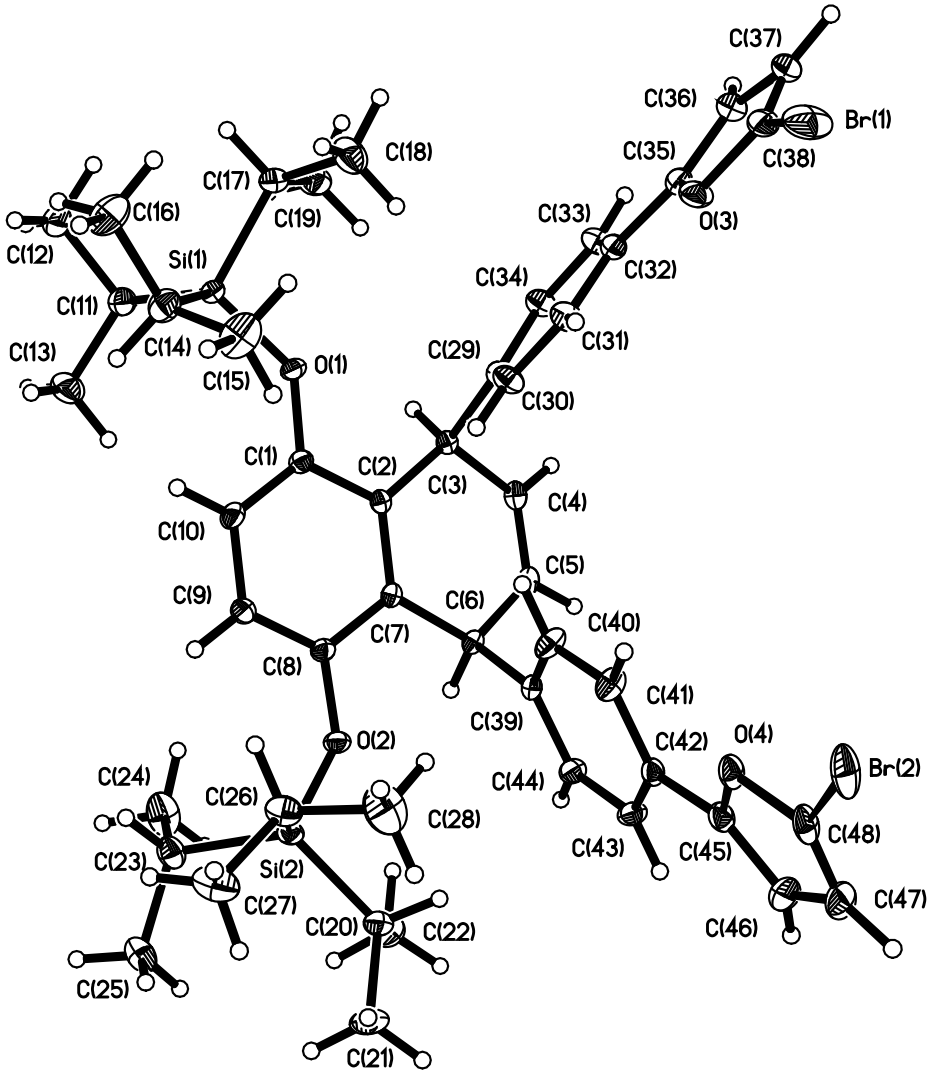

Figure II-5. Perspective view of the molecular structure of **II-12b** $C_{48}H_{60}Br_2O_4Si_2$ with the atom labeling scheme for the independent non-hydrogen atoms. The thermal ellipsoids are scaled to enclose 50% probability.

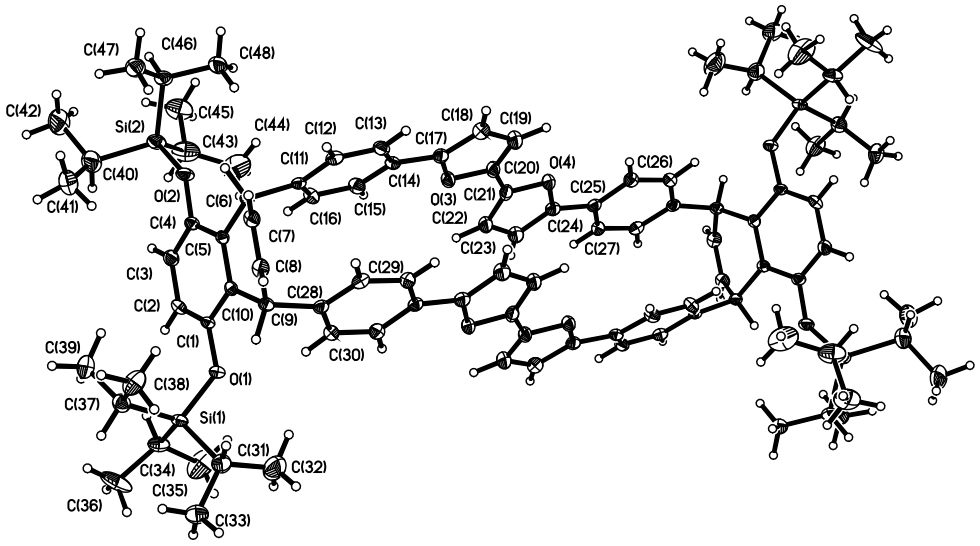

Figure II-6. Perspective view of the molecular structure of *anti*-**II-20b** $C_{98}H_{120}Si_4O_{12}$ with the atom labeling scheme for the independent non-hydrogen atoms. The molecule structure is constrained by the presence a crystallographic center of inversion. The thermal ellipsoids are scaled to enclose 50% probability.

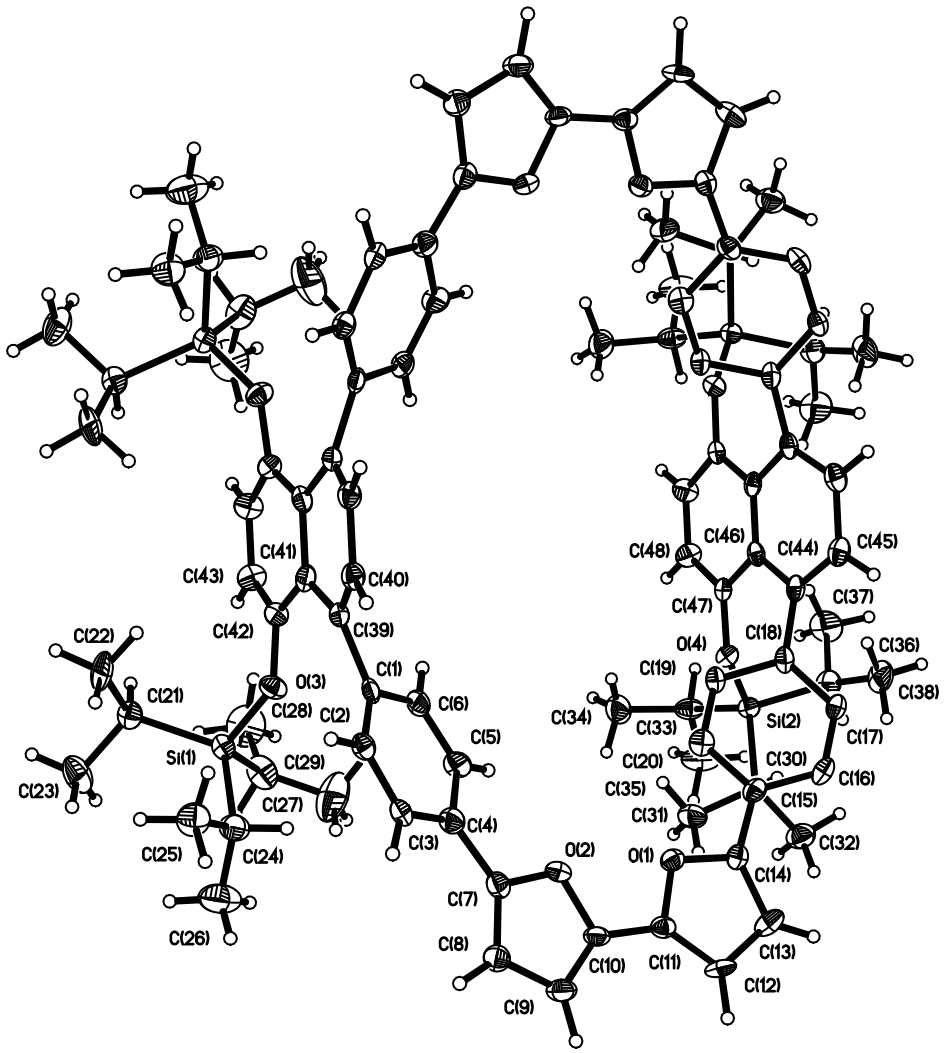

Figure II-7. Perspective view of the molecular structure of $C_{96}H_{116}Si_4O_8$ with the atom labeling scheme for the independent non-hydrogen atoms. The molecular geometry is constrained by a crystallographic mirror plane. The thermal ellipsoids are scaled to enclose 30% probability.

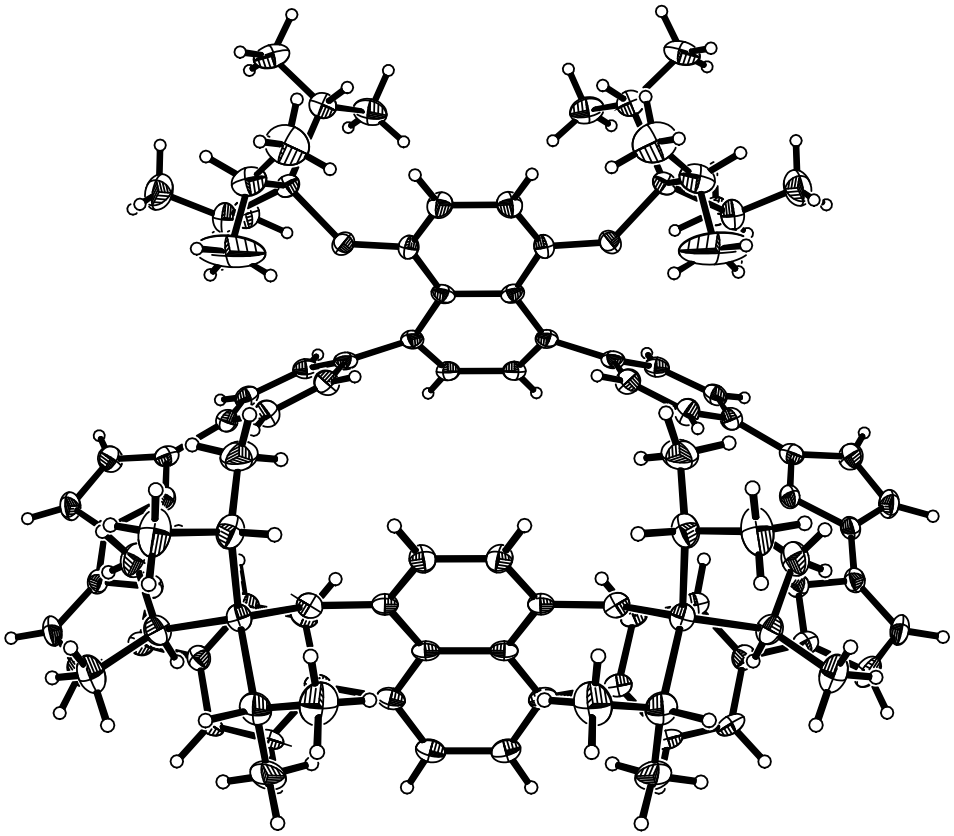

Figure II-8. Perspective view of the molecular structure of $C_{96}H_{116}Si_4O_8$. The molecular geometry is constrained by a crystallographic mirror plane. The thermal ellipsoids are scaled to enclose 30% probability.

II-References:

(1) Xia, J.; Bacon, J. W.; Jast, R. *Chem. Sci*. **2012**, *3*, 3018–3021.

(2) Iwamoto, T.; Watanabe, Y.; Sadahiro, T.; Haino, T.; Yamago, S. *Angew. Chem., Int. Ed*. **2011**, *123*, 8492–8494.

(3) Yuan, K.; Zhou, C. H.; Zhub, Y. C.; Zhao, X. *Phys. Chem. Chem. Phys.* **2015**, *17*, 18802–18812.

(4) Smalley, R. E.; Li, Y.; Moore, V. C.; Price, B. K; Colorado, R.; Schmidt, H. K.; Hauge, R. H.; Barron, A. R.; Tour, J. M. *J. Am. Chem. Soc.* **2006**, *128*, 15824–15829.

(5) Wong, B. M. *J. Phys. Chem. C*, **2009**, *113*, 21921–21927.

(6) Huang, C.; Huang, Y.; Akhmedov, N. G.; Popp, B. V.; Petersen, J. L.; Wang, K. K., *Org. Lett*. **2014**, 16, 2672−2675.

(7) Thakellapalli, H.; Farajidizaji, B.; Butcher, T. W.; Akhmedov, N. G.; Popp, B. V.; Petersen, J. L. Wang, K. K. *Org. Lett.* **2015**, *17*, 3470−3473.

(8) Kuwabara, T.; Orii, J.; Segawa, Y.; Itami, K. *Angew. Chem., Int. Ed*. **2015**, *127*, 9782–9785.

(9) Oniwa, K.; Kanagasekaran, T.; Jin, T.; Akhtaruzzaman, M.; Yamamoto, Y.; Tamura, H.; Hamada, I.; Shimotani, H.; Asao, N.; Ikeda, S.; Tanigaki, K. *J. Mater. Chem*. **2013**, *1*, 4163–4170.

(10) Gidron, O.; Bendikov, B. *Angew. Chem. Int. Ed*. **2014**, *53*, 2546–2555.

(11) Del Mazza, D.; Reinecke, M. G. *J. Org. Chem.* **1988**, *53*, 5799–5806.

(12) Smith, W. B. *J. Phys. Org. Chem*. **2005**, *18*, 477–480.

(13) Li, Y.; Thiemann, Y.; Sawada, T.; Mataka, S.; Tashiro, M. *J. Org. Chem.* **1997**, 62, 7926–7936.

(14) Hart, H.; Ok, D. *J. Org. Chem.* **1986**, *51*, 979–986.

(15) Hart, H.; Lai, C. Y.; Nwokogu, G. C.; Shamouilian, S. *Tetrahedron* **1987**, *43*, 5203–5224.

Chapter 3: Synthesis and Characterization of Functionalized [12]Cycloparaphenylenes Containing Four Alternating Biphenyl and Naphthyl Units

III-Introduction

More complex variations of carbon nanohoops were synthesized (Scheme III-1).[1-4] The key problem to overcome in the synthesis of carbon nanohoops involves innovation on masking benzene rings including curvature necessary to form macrocycles. We envisioned 2,5-diphenylfuran units in a macrocycle reacting via the Diels−Alder reaction with the parent benzyne and 3,6-dimethoxybenzyne to form more complex CPPs. To test this hypothesis, the mixture of partially hydrogenated furan-containing macrocycle *syn*-**III-9** and *anti*-**III-9** was prepared by adopting the synthetic pathway reported previously (Scheme III-2).

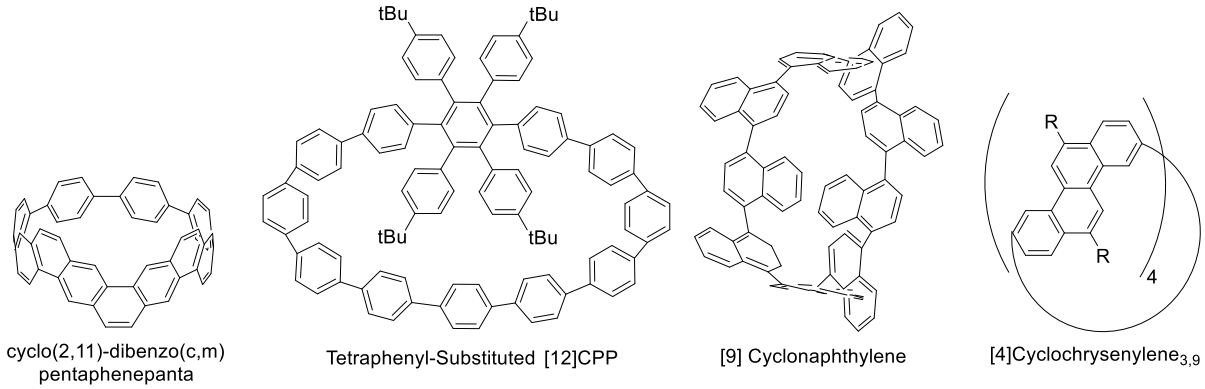

Scheme III-1. More Complex Macrocycles

III-Results and Discussion

The Diels−Alder reaction between (*E*,*E*)-1,4-bis(4-bromophenyl)-1,3-butadiene (**III-1**) and 1,4-benzoquinone (**III-2**), was carried out in the presence of $BF_3{\cdot}OEt_2$. This reaction was followed by protection of the hydronaphthoqinone moiety to form **III-3** bearing 4-bromophenyl

units *cis* to each other, producing 91% yield over the two steps. A portion of dibromide **III-3** was converted to the bis-boronic ester **III-5** as reported previously. The Suzuki–Miyaura coupling reaction between the **III-3** and **III-6** was carried out to form **III-7** in 87% yield. Bromination by NBS was used to prepare **III-8** in 98% yield. The dihydronaphthalene **III-3** provides the curvature necessary for macrocyclization. In addition, the dihydronaphthalene **III-3** can be regarded as a masked naphthalene for the final step of oxidative macrocyclization. The Suzuki–Miyaura cross-coupling reaction between **III-5** and **III-8** formed the mixture of macrocycles *syn*-**III-9** and *anti*-**III-9** (isomer ratio = 2:1) incorporated with two units of 2,5-diphenylfuran in 15% combined yield.

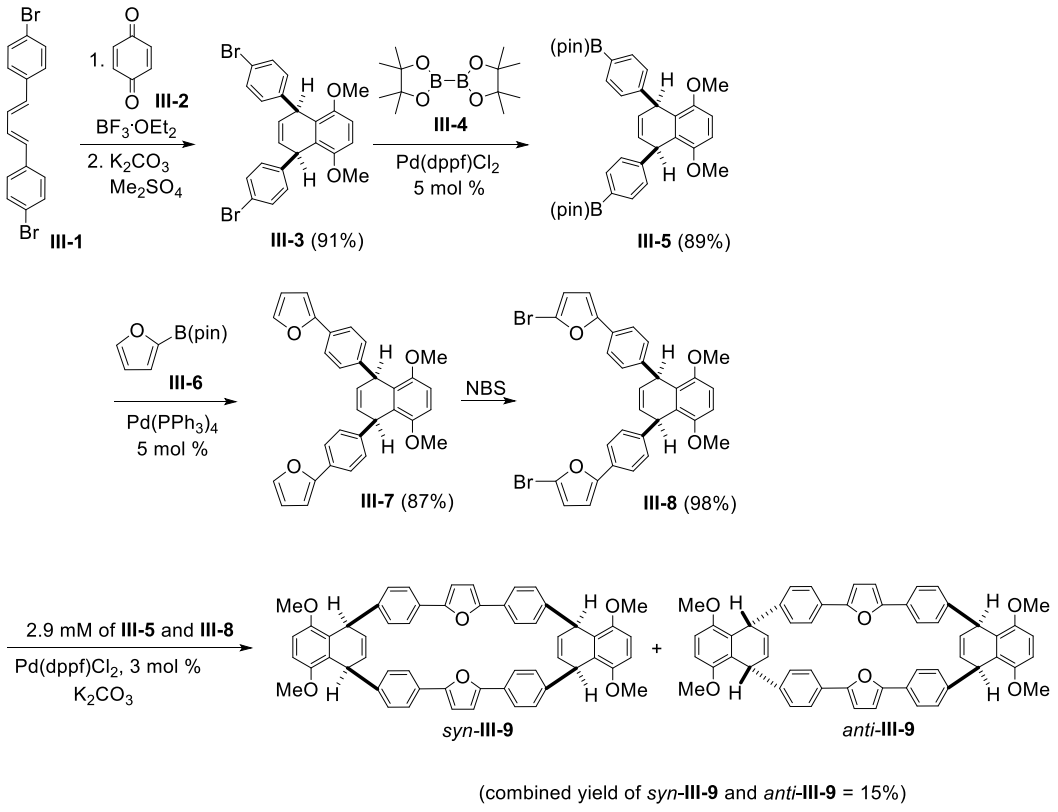

Scheme III-2. Synthesis of the Furan-Containing CPP Precursors *syn*-**III-9** and *anti*-**III-9**

Having macrocycles *syn*-**III-9** and *anti*-**III-9** in hand, we investigate the Diels−Alder reaction between 2,5-diphenylfuran units in macrocycles and the parent benzyne. There are several different conditions to generate benzyne with the harsher and basic conditions reported earlier replaced by milder and neutral conditions (Scheme III-3).

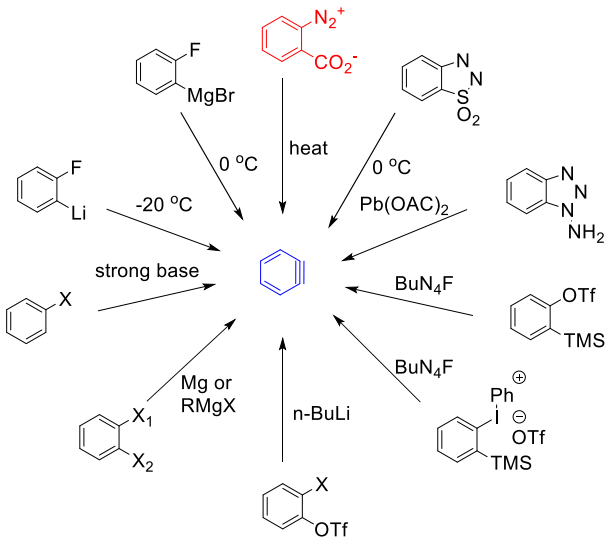

Scheme III-3. Benzyne Generation

Due to the low solubility of macrocycles, we investigated the preparation of benzyne at elevated temperature. It is known that benzenediazonium-2-carboxylate (**III-10**) can under mild thermal decomposition generate benzyne in situ. The [4+2] cycloaddition reaction between 2,5-diphenylfuran and benzyne was reported to form 1,4-diphenyl-1,4-epoxynaphthalene, and other benzynes derivatives also undergo the [4+2] cycloaddition reaction with 2,5-diphenylfuran to lead to 1,4-epoxynaphthalenes. The oxidation state of the adduct was not suitable for undergoing direct elimination of the bridging oxygen. A two-step reaction including reduction of the double bond in 1,4-epoxynaphthalenes followed by a Lewis acid or base treatment could potentially lead to the formation of 1,4-diphenylnaphthalenes. Unfortunately, this strategy did not produce the desired product (Scheme III-4). Searching the literature, we found that reductive deoxygenation

of 1,4-diphenyl-1,4-epoxynaphthalenes with $Fe_2(CO)_9$ was reported to form 1,4-diphenylnaphthalenes.

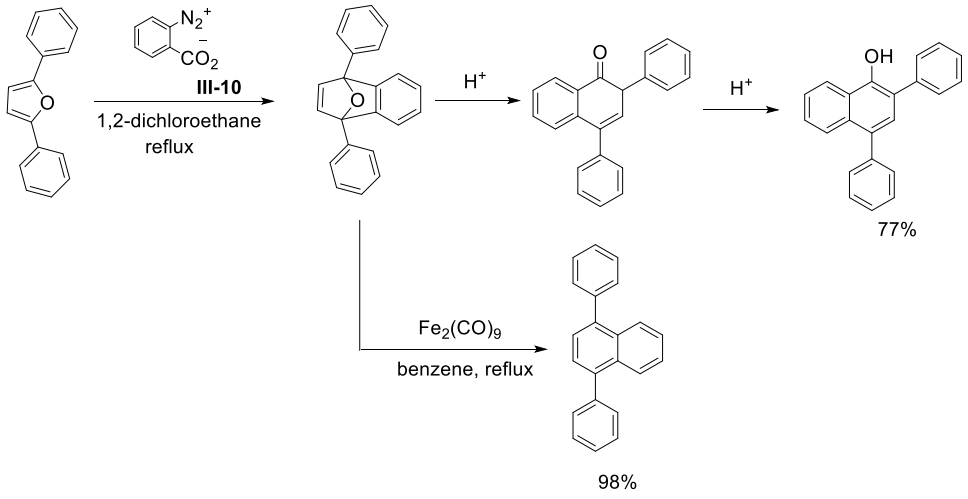

Scheme III-4. Reductive Deoxygenation 1,4-Diphenyl-1,4-Epoxynaphthalene

Benzenediazonium-2-carboxylate (**III-10**) was used to generate the parent benzyne in situ. The Diels−Alder reaction between the two 2,5-diphenylfuran groups in macrocycles *syn*-**III-9** and *anti*-**III-9** with an excess of **III-10** in refluxing 1,2-dichloroethane (DCE) led to the formation of the two 1,4-epoxynaphthalene groups in macrocycles **III-11**. However, our attempts to further separate these products by silica gel column chromatography was unsuccessful and led to 1,2-aryl migration with ring opening of the 1,4-epoxy moieties **III-11** (Scheme III-5). Fortunately, the treatment of the crude reaction products with $Fe_2(CO)_9$ in refluxing benzene under a nitrogen atmosphere was successful in promotion undergone reductive deoxygenation to form a mixture of *syn*-**III-12** and *anti*-**III-12** (isomer ratio = 2:1) in 92% combined yield over two steps (Scheme III-5). Unfortunately, treatment of *syn*-**III-12** and *anti*-**III-12** with **2,3-dichloro-5,6-dicyano-1,4-benzoquinone (DDQ) for oxidative aromatization** at temperatures ranging from 80 to150 °C was not successful.

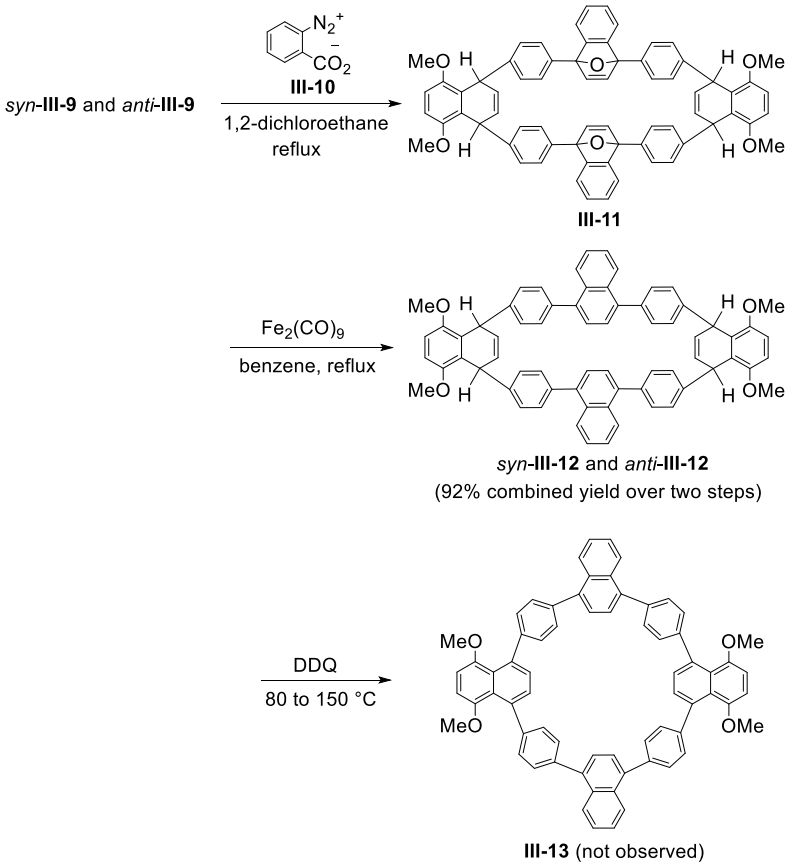

Scheme III-5. Synthesis of [8]CPP Precursors *syn*-**III-12** and *anti*-**III-12** and Attempted Synthesis of [8]CPP **III-13**

The substantial strain energy of fully aromatized [8]CPP, which includes only eight aromatic units contributed to this failure. To overcome this strain energy barrier, we can either use a stronger oxidant or relief the strain energy by expanding the size of the macrocycle ring.

The synthetic pathways reported previously were adopted to incorporating four more benzene units (Scheme III-6). The Suzuki-Miyaura cross-coupling reactions between **III-15** and **III-17** were successful in producing, most likely, a mixture of macrocycles *syn*-**III-18** and *anti*-**III-18**. However, only one of the two isomers was isolated by silica gel column chromatography in 11% yield. We were unable to grow a single crystal to allow for X-ray structure analysis to determine the absolute configuration of **III-18**.

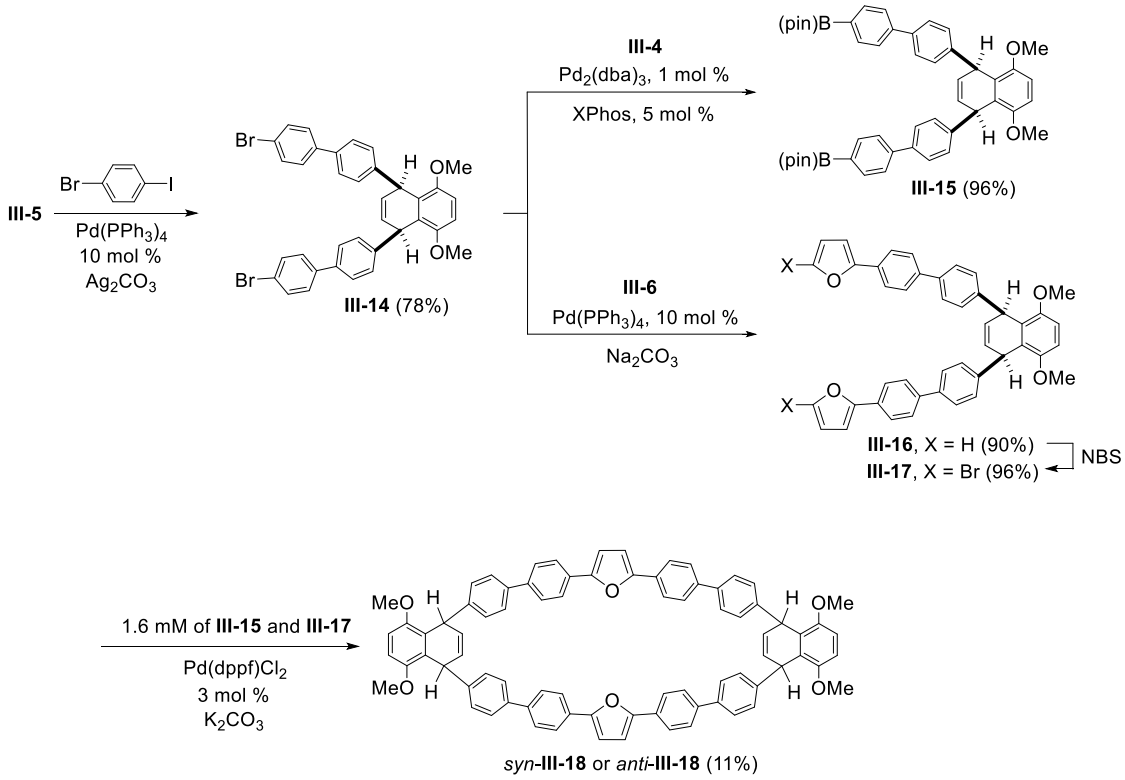

Scheme III-6. Synthesis of the Furan-Containing CPP Precursor *syn*-**III-18** or *anti*-**III-18**

Treatment of **III-18** with **III-10** followed by reductive deoxygenation of the resulting Diels−Alder adduct with $Fe_2(CO)_9$ produced **III-20** in 86% isolated yield (Scheme III-7). Treatment of the **III-20** with DDQ in chlorobenzene at 100 °C for 2.5 h promoted oxidative aromatization successfully to produce the fully aromatized [12]CPP **III-22** in 52% isolated yield, **III-22** has very low solubilities in common deuterated organic solvents. Fortunately, the ^{1}H and gCOSY NMR spectra of **III-22** were obtained in $CDCl_3$ at rt and DMSO-d_6 at 50 °C for structural elucidation. Additionally, the Diels-Alder reaction between **III-18** and an excess 3,6-dimethoxybenzenediazonium-2-carboxylate was carried out in refluxing DCE followed by $Fe_2(CO)_9$ in benzene to give **III-21** in 62% isolated yield. Treatment of **III-21** with DDQ at 85 °C in chlorobenzene for two hours promote oxidative aromatization to form fully aromatized

[12]CPP **III-23** bearing four alternating biphenyl and 5,8-dimethoxynaphth-1,4-diyl units in 88% isolated yield. We were able to elucidate the structure of **III-23** in DMSO-d_6 at 50 °C.

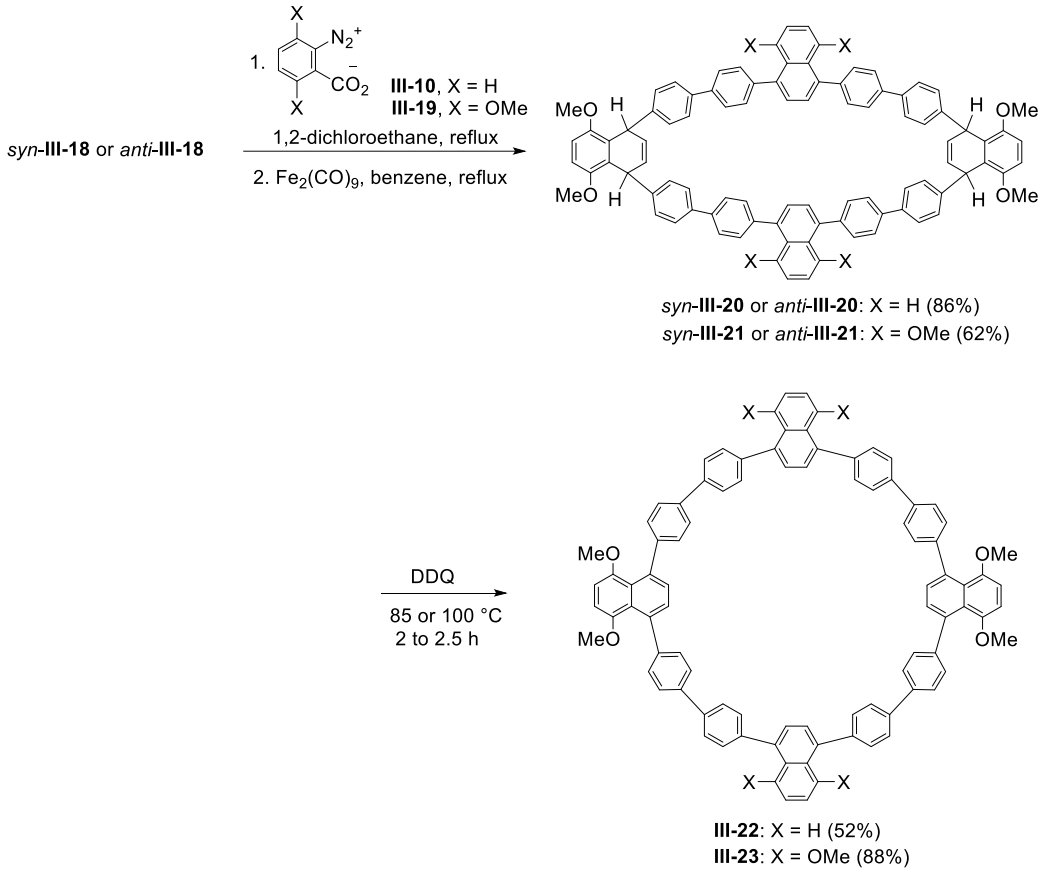

Scheme III-7. Synthesis of [12]CPPs **III-22** and **III-23**

An alternative route to **III-22** could involve oxidative aromatization of **III-18** with DDQ to form the corresponding fully aromatized macrocycle followed by treatment with **III-10** and $Fe_2(CO)_9$. However, the fully aromatized macrocycle of **III-18** showed very low solubility in common organic solvents, making it difficult for purification and isolation. The previously synthesized more soluble version of aromatized **III-18** by replacing the methoxy group with (*tert*-butyldimethylsilyl)oxy groups was used to carry out the Diels-Alder reaction with parent benzyne followed by oxygen extrusion of the intermediate by $Fe_2(CO)_9$. The ^{1}H NMR spectrum

of the crude reaction mixture indicated the formation of a product analogous to **III-22**. However, attempts to purify the desired product was not successful. The resulting 5,8-bis[(*tert*-butyldimethylsilyl)oxy]naphth-1,4-diyl adduct analogous to **III-22** decomposed upon purification either by silica gel or aluminum oxide column chromatography.

The observation that [12]CPPs **III-22** and **III-23**, could be readily produced by oxidative aromatization at the final step. But, the corresponding [8]CPP oxidation with DDQ was not successful. This led us to exploration the effect of macrocyclic ring size on the rate of oxidative aromatization. To determine the rate-determining step in oxidative aromatization, the oval-shaped *syn*-**III-24** or *anti*-**III-24** was prepared from dimerization of **III-14** by using $Ni(cod)_2$ (cod = 1,5-cyclooctadiene) in the presence of 2,2′-bipyridyl (bpy) to promote the homocoupling reactions (Scheme III-8). Oxidative aromatization of **III-24** was carried out at 100 °C in the presence of DDQ for 30 min. The crude ^{1}H NMR spectrum indicated that at 100 °C no significant [10]CPP **III-25** was formed (<2%). Raising the temperature to 120 °C did not indicate any measurable progress on aromatization. This indicated that the oval-shaped 10-membered ring macrocycle requires a higher temperature to overcome the barrier. Finally, increasing temperature to 150 °C for 10 min and analyzing the ^{1}H NMR spectrum revealed the presence of both **III-24** and **III-25** in a 1:1 ratio. There is no indication of the presence of the monodehydrogenated intermediate, clearly showing that the first dehydrogenation step is the rate-determining step of the two-step oxidative aromatization process. The oxidative aromatization of **III-24** in chlorobenzene at 150 °C for two hours gave [10]CPP in 71% yield. This observation explains why smaller ring size and higher ring strain in [8]CPP **III-13** prevent oxidative aromatization taking place.

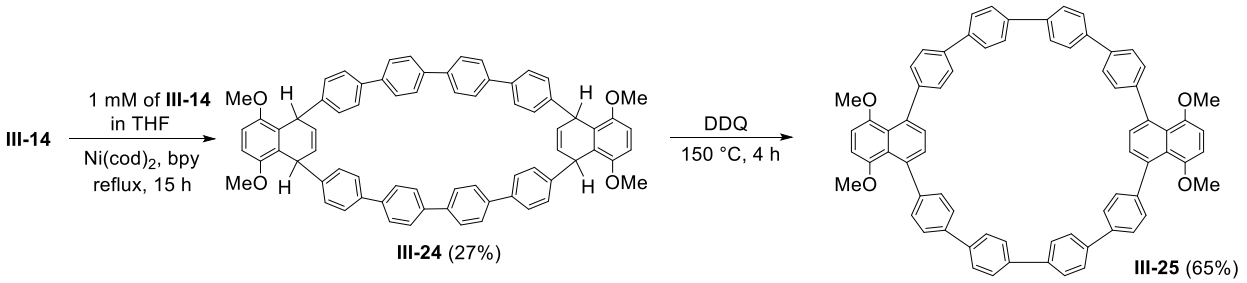

Scheme III-8. Synthesis of [10]CPP **III-25**

The molecular structure of **III-23** contains a C_4 axis, 4 C_2 *i*, σ_h, 2 σ_d, and 2 σ_v. These characters put III-23 in the D_4h group. All eight methoxy groups appear as a singlet, the 5,8-dimethoxynaphth-1,4-diyl units show two singlets, and the 1,4-disubistuted benzene rings gave two doublets in the ^{1}H NMR spectrum.

The DFT-optimized structure of **III-23** indicates that the four 5,8-dimethoxynaphth-1,4-diyl units tilt alternately above and below the plane of the macrocyclic ring with a tilt angle of 125° on average away from the inner plane of the [12]CPP circle (Figure III-3). The dihedral angle between the phenyl groups of the four biphenyl units is 35°, and the dihedral angles between the phenyl groups and the four 5,8-dimethoxynaphth-1,4-diyl groups are 50° on average. The diameter of the ring is calculated to be 16.8 Å, similar to 16.6 Å reported previously for the parent [12]CPP. The conformer with three 5,8-dimethoxynaphth-1,4-diyl units on the same side and the fourth on the opposite side has a slightly higher energy by 1.8 kcal/mol. The conformer with two of the adjacent 5,8-dimethoxynaphth-1,4-diyl units on the same side and the other two on the opposite side is higher in energy by 2.6 kcal/mol. Finally, the conformer which all four 5,8-dimethoxynaphth-1,4-diyl units on the same side has the highest energy by 2.7 kcal/mol. However, the difference between the lowest and highest conformers energy is just only 2.7 kcal/mol. At 50 ^{o}C all four conformers are in rapid equilibrium and interchange, which is

consistent with the observation that only one set of NMR signals were observed in DMSO-d_6 at 50 °C.

The UV−vis spectra of both **III-22** and **III-23** in CH_2Cl_2 showed absorption maxima (λ_{abs}) at 358 nm, which in comparison with the parent [12]CPP at 338, are red-shifted. However, the absorption maxima (λ_{abs}) of **III-22** and **III-23** are slightly blue-shifted from that of the [9]CPP derivate from aromatized trimer of **III-3**. Interestingly, the absorption maximum (λ_{abs}) of **III-25** appeared at 336 nm, which is slightly blue-shifted from that of the parent [10]CPP at 340 nm. The fluorescence maxima (λ_{em}) of **III-22** and **III-23** occurred at 483 and 484 nm, respectively, which are red-shifted with respect to that of the parent [12]CPP at 450 nm and blue-shifted from that of the fully aromatized trimer of **III-3** at 512 nm. For **III-25**, λ_{em} was observed at 453 nm, which is blue-shifted from that of the parent [10]CPP at 470 nm. The red shift of λ_{em} from **III-22** and **III-23** to **III-25** as the ring size decreases reminiscence of previous observations. Finally, the comparison of the hydrogenated CPP precursors **III-20**, **III-21**, and **III-24** with λ_{abs} at 313, 290, and 303 nm and λ_{em} at 414, 461, and 383 nm, respectively, with the UV−vis and fluorescence spectra of the fully aromatized **III-22**, **III-23**, and **III-25** revealed significant red shifts.

III-Conclusion

In summary, the functionalized [12]CPP **III-22** and **III-23** were synthesized by using the Diels−Alder reaction between the furan-containing CPP precursor **III-18** and the benzyne derivatives followed by reductive deoxygenation with $Fe_2(CO)_9$ and oxidative aromatization with DDQ. DFT optimization of four possible conformers of **III-23** reveals each to be of similar energy, with the most stable isomer bearing four 5,8-dimethoxynaphth-1,4-diyl units tilting

alternately above and below the plane of the macrocyclic ring. The UV−vis and fluorescence spectra of the functionalized [12]CPPs **III-22** and **III23** showed redshifts from those of the parent [12]CPP but blue shifts from those of a [9]CPP derivative as the fully aromatized trimer of **III-3**.

III-General Experimental Methods.

All reactions were conducted in oven-dried (120 °C) glassware under a nitrogen atmosphere. Chemicals, including 1,4-benzoquinone (**III-2**), bis(pinacolato)diboron [4, (Bpin)2], [1,1′-bis(diphenylphosphino)ferrocene]dichloropalladium complex with dichloromethane [Pd(dppf)Cl_2·CH_2Cl_2], tetrakis(triphenylphosphine)palladium [Pd(PPh_3)$_4$], tris(dibenzylideneacetone)dipalladium [Pd_2(dba)$_3$], 2-dicyclohexylphosphino-2′,4′,6′-triisopropylbiphenyl (XPhos), N-bromosuccinimide (NBS), diiron nonacarbonyl [$Fe_2(CO)_9$], 2-aminobenzoic acid, isoamyl nitrite, propylene oxide, 2,3-dichloro-5,6-dicyano-1,4-benzoquinone (DDQ), Ni(cod)$_2$, and 2,2′-bipyridyl (bpy), were purchased from chemical suppliers and were used as received. Dibromide **III-3**,[5] bis-boronic ester **III-5**,[6] 2-(2-furanyl)-4,4,5,5 tetramethyl-1,3,2-dioxaborolane (**III-6**),[7] 2-amino-3,6-dimethoxybenzoic acid,[8,9] and benzenediazonium-2-carboxylate (**III-10**)[10] were prepared according to reported procedures. The procedure for the preparation of **III-10** from 2-aminobenzoic acid was adopted for the preparation of 3,6-dimethoxybenzenediazonium-2-carboxylate (**III-19**) from 2-amino-3,6-dimethoxybenzoic acid. Propylene oxide was added as an acid scavenger to remove the potential presence of trace amounts of acids in the samples of **III-10** and **III-19**, which served as the precursors of the corresponding benzynes. The UV−vis absorption spectra were recorded on a spectrophotometer with a 1 nm resolution, and the baseline was corrected with a solvent-filled square quartz cell. The fluorescence spectra were recorded on a spectrofluorophotometer with a 2 nm resolution. Infrared (IR) spectra of solid samples were recorded on a Fourier transform infrared system equipped with a diamond crystal attenuated total reflectance sampling

interface. HRMS spectra were obtained on an FT-ICR mass analyzer coupled with electrospray ionization (ESI).

Experimental Procedure for Bisfuran III-7. To a 250 mL two-neck flask fitted with a condenser and a rubber septum were added 2.50 g of dibromide **III-3** (5.00 mmol), 3.00 g of 2-(2-furanyl)-4,4,5,5-tetramethyl-1,3,2-dioxaborolane (**III-6**, 15.5 mmol), 6.36 g of sodium carbonate (60.0 mmol), and 0.29 g of $Pd(PPh_3)_4$ (0.25 mmol). The flask was flushed with nitrogen, and degassed water (8 mL) and 1,4-dioxane (100 mL) were introduced via cannula. Then nitrogen was bubbled through the solution for an additional 20 min. The reaction mixture was heated at reflux for 12 h before it was cooled to rt. The solvent was removed in vacuo, and the residue was purified by flash column chromatography (silica gel, 1:10 to 1:6 ethyl acetate/hexanes) to produce 2.07 g of **III-7** (4.38 mmol, 87% yield) as a white solid: mp >240 °C; IR 1600, 1475, 1255, 723 cm^{-1}; ^1H NMR ($CDCl_3$, 400 MHz) δ 7.55 (4 H, d, J = 8.8 Hz), 7.44 (2 H, d, J = 1.6 Hz), 7.25 (4 H, d, J = 8.8 Hz), 6.75 (2 H, s), 6.59 (2 H, d, J = 3.2 Hz), 6.45 (2 H, dd, J = 3.4, 1.8 Hz), 6.01 (2 H, d, J = 3.2 Hz), 4.90 (2 H, d, J = 2.8 Hz), 3.61 (6 H, s); ^{13}C NMR ($CDCl_3$, 100 MHz) δ 154.3, 151.4, 144.1, 141.6, 128.49, 128.47, 127.7, 127.5, 123.6, 111.5, 109.2, 104.3, 55.8, 41.0; HRMS (ESI/FT-ICR) m/z $[M - 2\ H]^+$ calcd for $C_{32}H_{24}O_4$ 472.1669; found 472.1673. Recrystallization of **III-7** from pentane produced a single crystal suitable for X-ray structure analysis.

Experimental Procedure for Dibromide III-8. To a solution of **III-7** (1.90 g, 4.02 mmol) in *N*,*N*-dimethylformamide (50 mL) at 0 °C was added in portions NBS (1.44 g, 8.18 mmol). The reaction mixture was stirred in the dark for 12 h and then poured into 100 mL of cold water. The precipitate was collected, washed with 100 mL of water and 10 mL of cold ethanol, and air-dried overnight to give 2.47 g (3.92 mmol, 98% yield) of **III-8** as a white solid: mp >180 °C; IR 1476, 1254, 774 cm^{-1}; ^1H NMR ($CDCl_3$, 400 MHz) δ 7.48 (4 H, d, J = 8.8 Hz), 7.23 (4 H, d, J =

8.8 Hz), 6.74 (2 H, s), 6.53 (2 H, d, *J* = 3.6 Hz), 6.35 (2 H, d, *J* = 3.2 Hz), 5.99 (2 H, d, *J* = 3.2 Hz), 4.89 (2 H, d, J = 2.4 Hz), 3.60 (6 H, s); ^{13}C NMR ($CDCl_3$, 100 MHz) δ 156.2, 151.4, 144.6, 128.5, 127.7, 127.5, 127.3, 123.3, 120.9, 113.2, 109.2, 106.7, 55.7, 41.0; HRMS (ESI/FT-ICR) m/z $[M - 2\ H]^+$ calcd for $C_{32}H_{22}O_4Br_2$ 627.9879, 629.9859, 631.9838; found 627.9885, 629.9865, 631.9845.

Experimental Procedure for *syn*-III-9 and *anti*-III-9. To a two-neck flask fitted with a condenser and a rubber septum were added 1.26 g of dibromide **III-8** (2.00 mmol), 1.19 g of bis-boronic ester **III-5** (2.00 mmol), 3.33 g of potassium carbonate (24.1 mmol), and 0.044 g (0.054 mmol) of $Pd(dppf)Cl_2 \cdot CH_2Cl_2$. Toluene (700 mL), ethanol (150 mL), and water (50 mL) were then introduced. The solution was degassed by bubbling nitrogen through the solution for 30 min and then heated to reflux for 24 h before it was cooled to rt. The organic layer was separated, and the aqueous layer was extracted with dichloromethane (2 × 200 mL). The combined organic layers were concentrated in vacuo, and the residue was purified by flash column chromatography (silica gel, 2:3 to 1:1 dichloromethane/hexanes) to produce 0.246 g of a mixture of *syn*-**III-9** and *anti*-**III-9** (isomer ratio = 2:1, 0.303 mmol, 15% yield) as a white solid: mp 269−270 °C; IR 1478, 1256, 1084 cm^{-1}; ^{1}H NMR ($CDCl_3$, 400 MHz, major isomer) δ 7.58 (8 H, d, *J* = 8.4 Hz), 7.28 (8 H, d, *J* = 8.4 Hz), 6.72 (4 H, s), 6.66 (4 H, s), 5.99 (4 H, d, *J* = 2.4 Hz), 4.93 (4 H, d, J = 2.4 Hz), 3.66 (12 H, s); ^{1}H NMR ($CDCl_3$, 400 MHz, minor isomer) δ 7.582 (8 H, d, *J* = 8.8 Hz), 7.34 (8 H, d, *J* = 8.4 Hz), 6.70 (4 H, s), 6.661 (4 H, s), 6.03 (4 H, d, *J* = 3.6

Hz), 4.96 (4 H, d, *J* = 3.2 Hz), 3.67 (12 H, s); ^{13}C NMR ($CDCl_3$, 100 MHz, major isomer) δ 153.2, 151.3, 143.5, 128.8, 128.0, 127.5, 123.3, 109.0, 106.3, 55.8, 40.8; HRMS (ESI/FT-ICR) m/z $[M]^+$ calcd for $C_{56}H_{44}O_6$ 812.3132; found 812.3133.

Experimental Procedure for *syn*-III-12 and *anti*-III-12. To a two-neck flask containing a solution of *syn*-**III-9** and *anti*-**III-9** (0.096 g, 0.12 mmol) in 1,2-dichloroethane (50 mL) were added 0.046 g (0.31 mmol) of benzenediazonium-2-carboxylate (**III-10**) and propylene oxide (1.5 mL). The reaction mixture was heated at reflux for 2 h before it was cooled to rt. The solvent was removed in vacuo, and 0.343 g of $Fe_2(CO)_9$ (0.94 mmol) was added. The flask was then fitted with a condenser, which was capped with a rubber septum. The flask was flushed with nitrogen for 5 min, and benzene (50 mL) was introduced via cannula. The flask was flushed with nitrogen for an additional 10 min. The mixture was heated at 60 °C for 2 h and then at reflux for 12 h before it was cooled to rt. The reaction mixture was passed through a short Celite column (3 cm), and the column was further eluted with dichloromethane (150 mL). The combined eluates were concentrated, and the residue was washed with diethyl ether and hexanes to produce 0.103 g of a mixture of *syn*-**III-12** and *anti*-**III-12** (isomer ratio = 2:1, 0.110 mmol, 92% yield) as a yellow solid: mp 162−163 °C; IR 1474, 1249, 893 cm^{-1}; ^1H NMR ($CDCl_3$, 600 MHz, major isomer) δ 7.919 (4 H, dd, J = 6.6, 3.0 Hz), 7.28 (4 H, dd, J = 6.6, 3.4 Hz), 6.95 (8 H, d, J = 8.4 Hz), 6.95 (4 H, s), 6.90 (8 H, d, J = 8.0 Hz), 6.77 (4 H, dd, J = 4.2, 2.2 Hz), 6.62 (4 H, s), 5.34 (4 H, m), 3.912 (12 H, s); ^1H NMR ($CDCl_3$, 600 MHz, minor isomer, partial) δ 7.923 (4 H, dd, J = 6.4, 3.2 Hz), 3.916 (12 H, s); ^1H NMR (C_6D_6, 400 MHz, both isomers) δ 8.09−8.05 (4 H, m), 7.11−7.02 (20 H, m), 6.84 (4 H, s), 6.65 (minor isomer) and 6.64 (major isomer) (4 H, two singlets), 6.59 (4 H, dd, J = 4.7, 2.4 Hz), 5.58−5.55 (4 H, br), 3.45 (minor isomer) and 3.44 (major isomer) (12 H, two singlets); ^{13}C NMR ($CDCl_3$, 150 MHz, both isomers) δ 150.9, 141.0, 139.0, 137.6, 132.3, 131.5, 130.7, 129.0, 127.3, 127.1, 126.4, 125.3, 108.9, 56.0, 37.9; ^{13}C NMR (C_6D_6, 100 MHz, both isomers) δ 151.7, 141.91, 141.88, 140.1, 138.8, 132.89, 132.76, 131.62,

131.56, 129.8, 127.2, 126.1, 109.2, 55.8, 38.9; HRMS (ESI/FT-ICR) m/z $[M]^+$ calcd for $C_{68}H_{52}O_4$ 932.3860; found 932.3873.

Experimental Procedure for Dibromide III-14. To a 500 mL flask were added 3.57 g of bis-boronic ester **III-5** (6.00 mmol), 10.3 g of 1-bromo-4-iodobenzene (36.4 mmol), 9.93 g of silver carbonate (36.0 mmol), and 1.04 g of $Pd(PPh_3)_4$ (0.90 mmol). The flask was fitted with a condenser and a rubber septum and then flushed with nitrogen. Tetrahydrofuran (300 mL) was introduced via cannula, and the flask was again flushed with nitrogen for 10 min. The reaction mixture was then heated at reflux for 18 h before it was cooled to rt. The reaction mixture was passed through a silica gel column (15 cm), and the column was further eluted with dichloromethane (100 mL). The combined eluates were concentrated in vacuo, and the residue was purified by flash column chromatography (silica gel, from hexanes to 1:20 ethyl acetate/ hexanes) to produce 3.04 g of **III-14** (4.66 mmol, 78% yield) as a white powder: mp 209−211 °C; IR 1475, 1254, 804 cm^{-1}; ^1H NMR ($CDCl_3$, 400 MHz) δ 7.52 (4 H, d, J = 8.4 Hz), 7.42 (4 H, d, J = 8.4 Hz), 7.41 (4 H, d, J = 8.4 Hz) 7.29 (4 H, d, J = 8.0 Hz), 6.76 (2 H, s), 6.04 (2 H, d, J = 2.8 Hz), 4.95 (2 H, d, J = 2.8 Hz), 3.64 (6 H, s); ^{13}C NMR ($CDCl_3$, 100 MHz) δ 151.4, 144.3, 140.0, 137.3, 131.7, 128.7, 128.5, 127.9, 127.5, 126.5, 121.1, 109.2, 55.8, 40.8; HRMS (ESI/FTICR) m/z $[M]^+$ calcd for $C_{36}H_{28}Br_2O_2$ 650.0451, 652.0430, 654.0410; found 650.0453, 652.0433, 654.0412.

Recrystallization of **III-14** from a mixture of ethyl acetate and hexanes produced a single crystal suitable for X-ray structure analysis.

Experimental Procedure for Bisboronic Ester III-15. To a 250 mL flask were added 1.630 g of **III-14** (2.500 mmol), 1.52 g of bis(pinacolato)diboron (**III-4**, 6.00 mmol), 1.50 g of potassium acetate (15.3 mmol), 0.060 g of XPhos (0.13 mmol), and 0.026 g of $Pd_2(dba)_3$ (0.028 mmol). The

flask was fitted with a condenser and a rubber septum and then flushed with nitrogen. Then 100 mL of 1,4-dioxane was introduced via cannula. The flask was flushed with nitrogen for 10 min, and the reaction mixture was heated at reflux for 24 h before it was cooled to rt. The reaction mixture was passed through a short silica gel column (5 cm), and the column was further eluted with dichloromethane (50 mL). The combined eluates were concentrated in vacuo, and the residue was washed with cold hexanes (2 × 50 mL) to give 1.790 g of **III-15** (2.400 mmol, 96% yield) as a white solid: mp 181−184 °C; IR 1609, 1357, 1091, 657 cm^{-1}; ^{1}H NMR ($CDCl_3$, 400 MHz) δ 7.84 (4 H, d, J = 8.0 Hz), 7.58 (4 H, d, J = 8.4 Hz), 7.49 (4 H, d, J = 8.8 Hz), 7.30 (4 H, d, J = 8.4 Hz), 6.75 (2 H, s), 6.03 (2 H, d, J = 3.2 Hz), 4.94 (2 H, d, J = 2.8 Hz), 3.63 (6 H, s), 1.35 (24 H, s); ^{13}C NMR ($CDCl_3$, 100 MHz) δ 151.4, 144.3, 143.8, 138.3, 135.2, 128.6, 127.8, 127.6, 126.8, 126.2, 109.2, 83.7, 55.8, 40.9, 24.9; HRMS (ESI/FT-ICR) m/z $[M]^+$ calcd for $C_{48}H_{52}B_2O_6$ 745.3981, 746.3945, 747.3978; found 745.3984, 746.3944, 747.3979.

Experimental Procedure for Bisfuran III-16. A two-neck flask containing 1.37 g of **III-14** (2.10 mmol), 1.22 g of 2-(2-furanyl)-4,4,5,5-tetramethyl-1,3,2-dioxaborolane (**III-6**, 6.29 mmol), 2.67 g of sodium carbonate (25.2 mmol), and 0.24 g of $Pd(PPh_3)_4$ (0.21 mmol) was fitted with a condenser and a rubber septum and flushed with nitrogen. Then 50 mL of 1,4-dioxane and 4 mL of degassed water were introduced via cannula. Nitrogen was bubbled through the solution for 20 min. The reaction mixture was heated at reflux for 12 h before it was cooled to rt. The solvent was removed in vacuo, and the residue was purified by flash column chromatography (silica gel, 1:10 to 1:6 ethyl acetate/hexanes) to produce 1.18 g of **III-16** (1.88 mmol, 90% yield) as a white solid: mp 128−130 °C; IR 1477, 1257, 801 cm^{-1}; ^{1}H NMR ($CDCl_3$, 400 MHz) δ 7.71 (4 H, d, J = 8.0 Hz), 7.60 (4 H, d, J = 8.4 Hz), 7.51−7.47 (6 H, m), 7.31 (4 H, d, J = 8.4 Hz), 6.77 (2 H, s), 6.67 (2 H, d, J = 3.6 Hz), 6.48 (2 H, dd, J = 3.4, 1.8 Hz), 6.06 (2 H, d, J = 2.8 Hz), 4.96 (2 H, d, J

= 2.8 Hz), 3.65 (6 H, s); ^{13}C NMR ($CDCl_3$, 100 MHz) δ 153.9, 151.5, 144.1, 142.0, 139.9, 137.9, 129.5, 128.7, 127.9, 127.6, 127.1, 126.5, 124.1, 111.7, 109.2, 104.9, 55.8, 40.9; HRMS (ESI/FTICR) m/z $[M]^+$ calcd for $C_{44}H_{34}O_4$ 626.2452; found 626.2453.

Experimental Procedure for Dibromide III-17. To a solution of **III-16** (1.10 g, 1.76 mmol) in *N*,*N*-dimethylformamide (30 mL) at 0 °C was added in portions NBS (0.64 g, 3.6 mmol). The reaction mixture was stirred in the dark for 12 h and then poured into 100 mL of cold water. The precipitate was collected, washed with 50 mL of water and 5 mL of ethanol, and air-dried overnight to give 1.32 g (1.68 mmol, 96% yield) of **III-17** as a white solid: mp 108−110 °C; IR 1476, 1255, 778 cm^{-1}; ^{1}H NMR ($CDCl_3$, 600 MHz) δ 7.65 (4 H, d, J = 7.8 Hz), 7.59 (4 H, d, J = 8.4 Hz), 7.49 (4 H, d, J = 7.8 Hz), 7.31 (4 H, d, J = 8.4 Hz), 6.77 (2 H, s), 6.61 (2 H, d, J = 3.0 Hz), 6.39 (2 H, d, J = 3.0 Hz), 6.06 (2 H, d, J = 2.4 Hz), 4.96 (2 H, d, J = 2.4 Hz), 3.65 (6 H, s); ^{13}C NMR ($CDCl_3$, 100 MHz) δ 155.8, 151.4, 144.2, 140.3, 137.7, 128.7, 128.5, 127.9, 127.6, 127.2, 126.5, 123.8, 121.4, 113.4, 109.2, 107.2, 55.8, 40.9; HRMS (ESI/FT-ICR) m/z $[M]^+$ calcd for $C_{44}H_{32}Br_2O_4$ 782.0662, 784.0641, 786.0621; found 782.0663, 784.0639, 786.0615.

Experimental Procedure for *syn*-III-18 or *anti*-III-18. To a two-neck flask fitted with a condenser and a rubber septum were added 0.772 g of **III-15** (1.03 mmol), 0.809 g of **III-17** (1.03 mmol), 1.708 g of potassium carbonate (12.36 mmol), and 0.025 g (0.031 mmol) of $Pd(dppf)Cl_2.CH_2Cl_2$. Toluene (650 mL), ethanol (250 mL), and water (80 mL) were introduced. The solution was degassed by bubbling nitrogen through it for 30 min and then was heated to reflux for 24 h before it was cooled to rt. The organic layer was separated, and the aqueous layer was extracted with dichloromethane (2 × 100 mL). The combined organic layers were concentrated in vacuo, and the residue was purified by flash column chromatography (silica gel,

2:3 to 1:1 dichloromethane/hexanes) to produce 0.122 g of a single isomer of either *syn*-**III-18** or *anti*-**III-**

18 (0.109 mmol, 11% yield) as a white solid: mp >280 °C; IR 1479, 1256, 815 cm^{-1}; ^{1}H NMR ($CDCl_3$, 600 MHz) δ 7.83 (8 H, d, J = 8.4 Hz), 7.68 (8 H, d, J = 8.4 Hz), 7.54 (8 H, d, J = 8.4 Hz), 7.32 (8 H, d, J = 7.8 Hz), 6.78 (8 H, s), 6.10 (4 H, d, J = 3.0 Hz), 5.02 (4 H, d, J = 2.4 Hz), 3.70 (12 H, s); ^{13}C NMR ($CDCl_3$, 150 MHz) δ 153.1, 151.4, 143.7, 139.6, 137.8, 129.4, 128.8, 128.2, 127.7, 127.0, 126.2, 124.1, 109.0, 107.2, 55.8, 40.6; HRMS (ESI/FT-ICR) m/z $[M]^+$ calcd for $C_{80}H_{60}O_6$ 1116.4384; found 1116.4381.

Experimental Procedure for *syn*-III-20 or *anti*-III-20. To a two-neck flask containing a solution of a single isomer of either *syn*-**III-18** or *anti*-**III-18** (0.095 g, 0.085 mmol) in 1,2-dichloroethane (50 mL) were added 0.035 g (0.24 mmol) of a freshly prepared benzenediazonium-2-carboxylate **(III-10**) and propylene oxide (1.5 mL). The reaction mixture was heated at reflux for 2 h before it was cooled to rt. The solvent was removed in vacuo, and 0.247 g of $Fe_2(CO)_9$ (0.679 mmol) was added. The flask was fitted with a condenser, which was capped with a rubber septum, and flushed with nitrogen for 5 min. Benzene (30 mL) was introduced via cannula, and the flask was again flushed with nitrogen for 10 min. The reaction mixture was heated at 60 °C for 2 h and then heated to reflux for 12 h before it was cooled to rt. The reaction mixture was passed through a short Celite column (3 cm), and the column was further eluted with dichloromethane (100 mL). The combined eluates were concentrated in vacuo, and the residue was washed with cold hexanes and diethyl ether to give 0.090 g (0.073 mmol, 86% yield) of a single isomer of either *syn*-**III-20** or *anti*-**III-20** as a white solid: mp >250 °C; IR 1483, 1255, 1093, 806 cm^{-1}; ^{1}H NMR ($CDCl_3$, 600 MHz) δ 8.00 (4 H, dd, J = 6.3, 3.3 Hz), 7.38 (4 H, dd, J = 6.6, 3.0 Hz), 7.362 (8 H, d, J = 7.8 Hz), 7.353 (8 H, d, J = 7.8

Hz), 7.19 (4 H, s), 7.09 (8 H, d, *J* = 8.4 Hz), 6.94 (4 H, s), 6.86 (8 H, d, *J* = 8.4 Hz), 6.73 (4 H, dd, *J* = 4.2, 2.4 Hz), 5.31 (4 H, m), 3.90 (12 H, s); ^{1}H NMR (C_6D_6, 600 MHz) δ 8.14 (4 H, dd, *J* = 6.6, 3.4 Hz), 7.393 (8 H, d, *J* = 8.6 Hz), 7.386 (8 H, d, *J* = 8.6 Hz), 7.31 (4 H, s), 7.20 (8 H, d, *J* = 8.2 Hz), 7.20−7.18 (4 H, m), 7.05 (8 H, d, *J* = 8.2 Hz), 6.68 (4 H, s), 6.59 (4 H, dd, *J* = 4.2, 2.3 Hz), 5.57−5.54 (4 H, br), 3.46 (12 H, s); ^{13}C NMR ($CDCl_3$, 150 MHz) δ 150.8, 141.3, 140.2, 139.3, 139.1, 137.6, 132.3, 131.8, 130.7, 130.3, 127.8, 126.9, 126.5, 126.4, 126.2, 125.8, 108.9, 56.0, 37.9; HRMS (ESI/FT-ICR) m/z $[M]^+$ calcd for $C_{92}H_{68}O_4$ 1236.5112; found 1236.5115.

Experimental Procedure for [12]CPP III-22. To a solution of either *syn*-**III-20** or *anti*-**III-20** (0.050 g, 0.040 mmol) in chlorobenzene (4 mL) was added DDQ (0.092 g, 0.41 mmol). The reaction flask was then flushed with nitrogen. The reaction mixture was heated at 100 °C for 2.5 h before it was cooled to rt. Chlorobenzene was removed in vacuo, and the residue was dissolved in dichloromethane (200 mL). The solution was treated with a 1 M sodium bicarbonate solution (3 × 50 mL) and water (2 × 50 mL). The organic layer was concentrated in vacuo, and the residue was washed with 2 mL of cold dichloromethane, 2 mL of diethyl ether, and 5 mL of hexanes to give 0.026 g of 22 (0.021 mmol, 52% yield) as a yellow solid: mp >190 °C; IR 1458, 1254, 819 cm^{-1}; ^{1}H NMR ($CDCl_3$, 600 MHz) δ 8.39 (4 H, dd, *J* = 6.5, 3.5 Hz), 7.68 (8 H, d, *J* = 8.8 Hz), 7.61 (4 H, m), 7.587 (8 H, d, *J* = 8.2 Hz), 7.580 (8 H, d, *J* = 8.2 Hz), 7.34 (8 H, d, *J* = 8.2 Hz), 7.09 (4 H, s), 7.08 (4 H, s), 6.99 (4 H, s), 3.78 (12 H, s); ^{1}H NMR (DMSO-d_6, 600 MHz, 50 °C) δ 8.32 (4 H, dd, *J* = 6.7, 3.5 Hz), 7.79 (8 H, d, *J* = 8.1 Hz), 7.72−7.68 (4 H, m), 7.67 (8 H, d, *J* = 8.6 Hz), 7.60 (8 H, d, *J* = 8.3 Hz), 7.32 (8 H, d, *J* = 8.5 Hz), 7.17 (4 H, s), 7.16 (4 H, s), 7.12 (4 H, s), 3.20 (12 H, s); HRMS (ESI/FT-ICR) m/z $[M]^+$ calcd for $C_{92}H_{64}O_4$ 1232.4799; found 1232.4834.

Experimental Procedure for *syn*-III-21 or *anti*-III-21. To a two-neck flask containing a solution of a single isomer of either *syn*-**III-18** or *anti*-**III-18** (0.065 g, 0.058 mmol) in 1,2-dichloroethane (50 mL) was added propylene oxide (1.0 mL). The reaction mixture was heated at reflux, and 0.085 g (0.41 mmol) of a freshly prepared 3,6-dimethoxybenzenediazonium-2-carboxylate (**III-19**) was added in portions over a period of 1 h. The reaction mixture was heated at reflux for one additional hour before it was cooled to rt. The solvent was removed in vacuo, and 0.17 g of $Fe_2(CO)_9$ (0.47 mmol) was added. The flask was fitted with a condenser, which was capped with a rubber septum, and then flushed with nitrogen for 5 min. Benzene (30 mL) was introduced via cannula, and the flask was flushed with nitrogen for 10 min. The reaction mixture was heated at 60 °C for 2 h and then at reflux for 12 h before it was cooled to rt. The reaction mixture was passed through a short Celite column (5 cm), and the column was further eluted with dichloromethane (100 mL). The combined eluates were concentrated in vacuo, and the residue was washed with cold hexanes and diethyl ether. The residue was purified by flash column chromatography (silica gel, 2:3 to 1:1 dichloromethane/hexanes) to give 0.049 g of a single isomer of either *syn*-**III-21** or *anti*-**III-21** (0.036 mmol, 62% yield) as a white solid: mp >260 °C; IR 1481, 1255, 808 cm^{-1}; ^1H NMR ($CDCl_3$, 600 MHz) δ 7.36 (8 H, br d, J = 8.1 Hz), 7.23 (16 H, d, J = 8.2 Hz), 7.13 (4 H, s), 6.99 (8 H, d, J = 8.3 Hz), 6.89 (4 H, s), 6.76 (4 H, s), 6.52 (4 H, dd, J = 3.8, 1.9 Hz), 5.20 (4 H, dd, J = 3.7, 1.5 Hz), 3.84 (12 H, s), 3.41 (12 H, s); ^{13}C NMR ($CDCl_3$, 150 MHz) δ 151.2, 151.1, 144.3, 141.6, 138.5, 138.4, 137.7, 130.7, 129.6, 129.3, 128.5, 128.1, 126.3, 125.43, 125.35, 108.8, 107.2, 56.1, 55.9, 38.8; HRMS (ESI/FT-ICR) m/z $[M]^+$ calcd for $C_{96}H_{76}O_8$ 1356.5535; found 1356.5551.

Experimental Procedure for [12]CPP 23. To a solution of a single isomer of either *syn*-**III-21** or *anti*-**III-21** (0.045 g, 0.033 mmol) in chlorobenzene (2 mL) was added DDQ (0.075 g, 0.33

mmol). The flask was flushed with nitrogen, and the reaction mixture was heated at 85 °C for 2 h before it was cooled to rt. Chlorobenzene was removed in vacuo, and the residue was dissolved in 200 mL of dichloromethane. The solution was treated with a 1 M sodium bicarbonate solution (3 × 50 mL) and water (2 × 50 mL). The organic layer was separated and concentrated in vacuo, and the residue was washed with 1 mL of cold dichloromethane, 2 mL of diethyl ether, and 5 mL of hexanes to give 0.040 g of **III-23** (0.029 mmol, 88% yield) as a yellow solid: mp >195 °C; IR 1457, 1386, 1254, 760, 699 cm^{-1}; ^{1}H NMR (DMSO-d_6, 600 MHz, 50 °C) δ 7.64 (16 H, d, J = 8.5 Hz), 7.29 (16 H, d, J = 8.7 Hz), 7.13 (8 H, s), 7.09 (8 H, s), 3.68 (24 H, s); ^{13}C NMR (DMSO-d_6, 150 MHz, 50 °C) δ 150.2, 142.9, 136.5, 135.8, 131.0, 127.7, 125.2, 123.8, 107.8, 55.6; HRMS (ESI/FT-ICR) m/z $[M]^+$ calcd for $C_{96}H_{72}O_8$ 1352.5222; found 1352.5229.

Experimental Procedure for Cyclic Dimer III-24. To a 1 L flask were added 0.28 g of dibromide **III-14** (0.43 mmol) and 0.16 g of bpy (1.0 mmol). Then the flask was flushed with nitrogen and placed in a glovebox, and 0.28 g of $Ni(cod)_2$ (1.0 mmol) was added. The flask was fitted with a condenser and a rubber septum and then removed from the glovebox before 450 mL of THF was added via cannula under a nitrogen atmosphere. Then the reaction mixture was heated at reflux for 12 h before it was cooled to rt. The reaction mixture was passed through a short silica gel column, and the column was further eluted with dichloromethane. The combined eluates were concentrated, and the residue was purified by flash column chromatography (silica gel, 3:2 dichloromethane/hexanes) to produce 0.057 g of **III-24** (0.058 mmol, 27% yield) as a white solid: ^{1}H NMR ($CDCl_3$, 400 MHz) δ 7.35 (8 H, d, J = 8.4 Hz), 7.21 (8 H, d, J = 8.4 Hz), 6.99 (8 H, d, J = 8.4 Hz), 6.92 (4 H, s), 6.79 (8 H, d, J = 8.0 Hz), 6.72 (4 H, dd, J = 4.2, 2.2 Hz), 5.27 (4 H, m), 3.88 (6 H, s); ^{13}C NMR ($CDCl_3$, 100 MHz) δ 150.8, 141.2, 139.9, 138.6, 137.3

132.4, 130.8, 127.7, 127.3, 126.8, 125.9, 108.8, 56.0, 37.8; HRMS (ESI/FT-ICR) m/z $[M]^+$ calcd for $C_{72}H_{56}O_4$ 984.4173; found 984.4184.

Experimental Procedure for [10]CPP III-25. To a 20 mL pressure tube were added 0.010 g (0.010 mmol) of **III-24** and 0.016 g (0.07 mmol) of DDQ. The tube was flushed with nitrogen and then 3 mL of chlorobenzene was introduced by using a syringe. The reaction mixture was heated at 150 °C for 2 h before it was cooled to rt. The reaction mixture was diluted with 10 mL of dichloromethane, and immediately passed through a basic aluminum oxide column (4 cm high, 2.5 cm in diameter). The column was eluted with an additional 100 mL of dichloromethane. The combined eluates were concentrated in vacuo to afford 0.007 g of **III-25** (0.007 mmol, 71% yield) as a yellow solid: ^{1}H NMR ($CDCl_3$, 600 MHz) δ 7.58 (8 H, d, J = 8.8 Hz), 7.54 (8 H, d, J = 8.8 Hz), 7.45 (8 H, d, J = 8.2 Hz), 7.27 (8 H, d, J = 8.2 Hz), 7.04 (4 H, s), 6.98 (4 H, s), 3.80 (12 H, s); ^{1}H NMR (C_6D_6, 600 MHz) δ 7.49 (8 H, d, J = 8.5 Hz), 7.46 (8 H, d, J = 8.6 Hz), 7.44 (8 H, d, J = 8.8 Hz), 7.37 (8 H, d, J = 8.5 Hz), 7.00 (4 H, s), 6.70 (4 H, s), 3.45 (12 H, s); ^{13}C NMR (C_6D_6, 150 MHz) δ 151.3, 144.2, 139.6, 138.6, 138.0, 136.5, 133.1, 128.2, 127.6, 127.4, 127.1, 125.3, 107.1, 55.5; HRMS (ESI/FT-ICR) m/z $[M]^+$ calcd for $C_{72}H_{52}O_4$ 980.3860; found 980.3878.

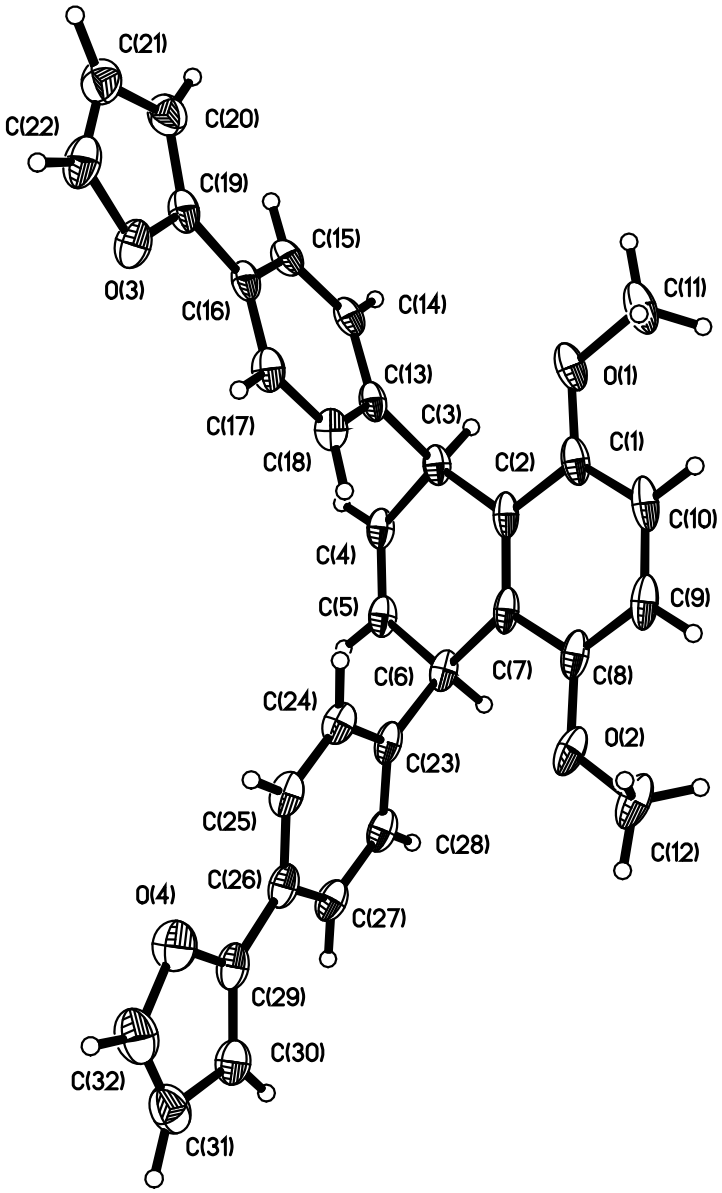

Figure III-1. Perspective view of the molecular structure of **III-7** ($C_{32}H_{26}O_4$) with the atom labeling scheme for the non-hydrogen atoms. The thermal ellipsoids are scaled to enclose 50% probability.

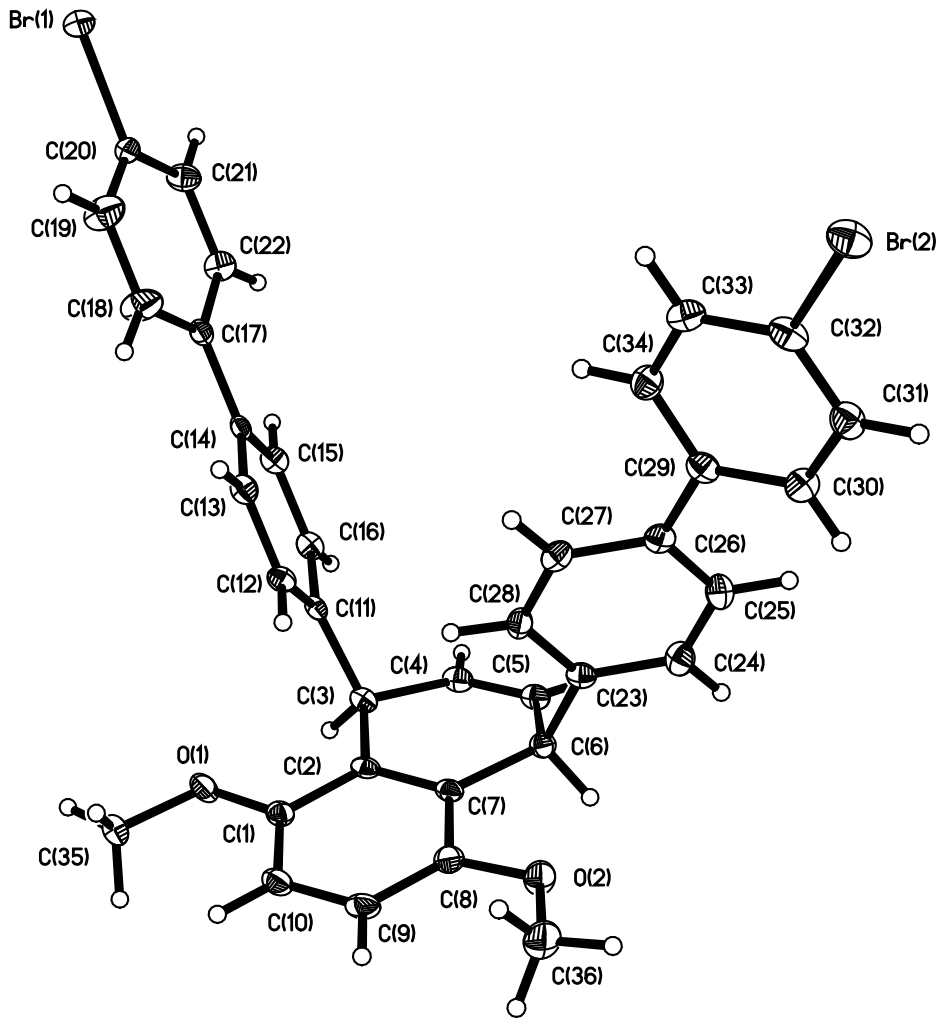

Figure III-2. Perspective view of the molecular structure of **III-14** ($C_{36}H_{28}Br_2O_2$) with the atom labeling scheme for the independent non-hydrogen atoms. The thermal ellipsoids are scaled to enclose 50% probability.

Analyses of the Functionalized [12]CPP III-23

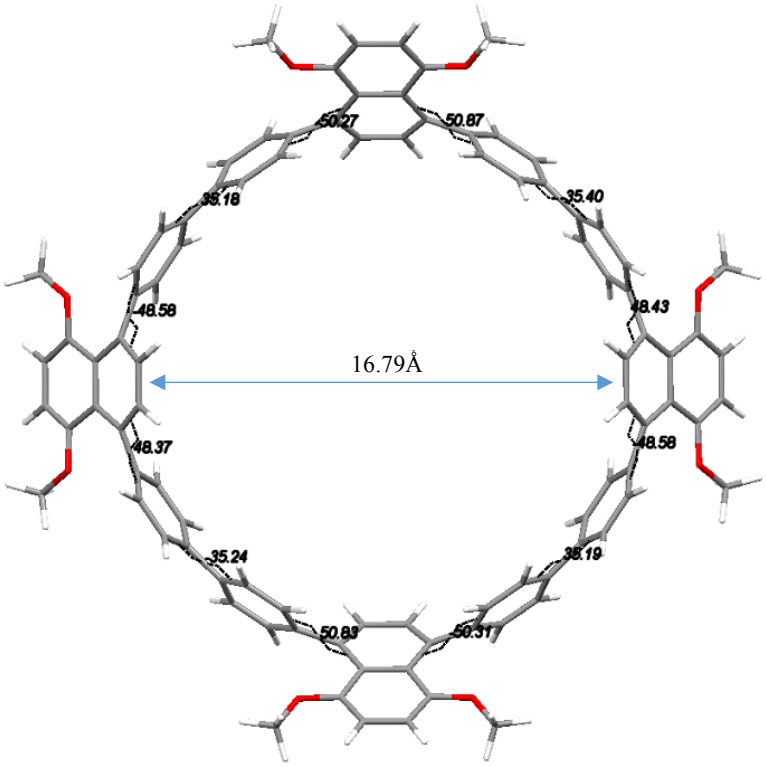

aerial view

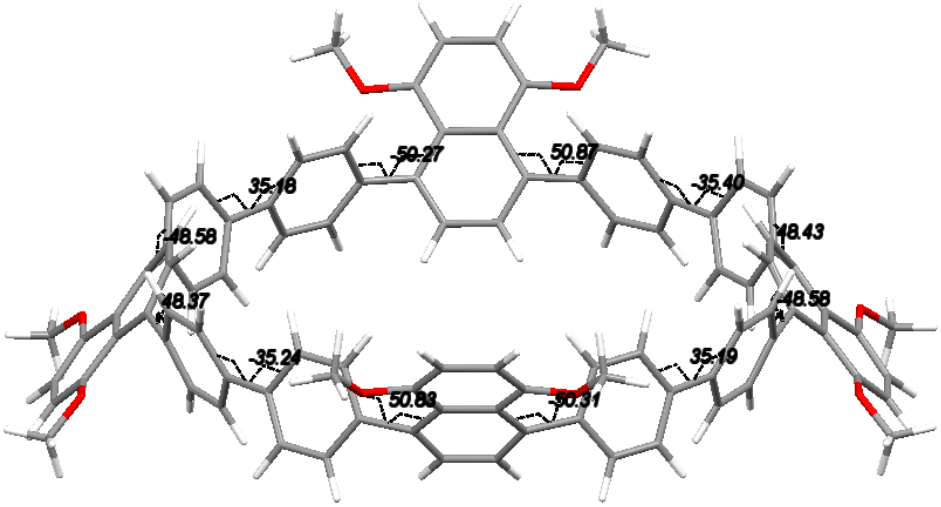

perspective view

Figure III-3. Capped-stick model for the functionalized [12]CPP **III-23** derived from DFT with all aryl-aryl and aryl- dimethoxynaphthyl torsions on the top face noted. The dimethoxynaphthyl moieties cant away from the circle at angles of 124.9° on average for **III-23** four biphenyl moieties have torsional angles of –35.4°, 35.2°, –35.2° and 35.2° for **III-23**.

III-Reference:

(1) Golder, M. R.; Colwell, C. E.; Wong, B. M.; Zakharov, L. N.; Zhen, J.; Jasti, R. *Am. Chem. Soc.* **2016**, *138*, 6577−6582.

(2) Sisto, T. J.; Tian, X.; Jasti, R. *J. Org. Chem.* **2012**, *77*, 5857.

(3) Hitosugi, S.; Yamasaki, T.; Isobe, H. *J. Am. Chem. Soc.* **2012**, *134*, 12442−12445.

(4) Yagi, A.; Segawa, Y.; Itami, K. *J. Am. Chem. Soc.* **2012**, *134*, 2962–2965.

(5) Farajidizaji, B.; Thakellapalli, H.; Li, S.; Huang, C.; Baughman, N. N.; Akhmedov, N. G.; Popp, B. V.; Petersen, J. L.; Wang, K. K. *Chem. Eur. J.* **2016**, *22*, 16420–16424.

(6) Thakellapalli, H.; Farajidizaji, B.; Butcher, T. W.; Akhmedov, N.G.; Popp, B. V.; Petersen, J. L.; Wang, K. K. *Org. Lett.* **2015**, *17*, 3470–3473.

(7) Muroga, T.; Sakaguchi, T.; Hashimoto, T. *Polymer* **2012**, *53*, 4380–4387.

(8) Azadi-Ardakani, M.; Wallace, T. W. *Tetrahedron* **1988**, *44*, 5939–5952.

(9) Almlöf, J. E.; Feyereisen, M. W.; Jozefiak, T. H.; Miller, L. L. J. *Am. Chem. Soc.* **1990**, *112*, 1206–1214.

(10) Asao, N.; Sato, K. *Org. Lett.* **2006**, *8*, 5361–5363.

Chapter 4: Syntheses of Thiophne-Containing Fused Carbon Nanohoop

IV-Introduction

It was recently reported by our research group the successful use of the Diels–Alder reactions between two (*E*,*E*)-1,4-bis(4-bromophenyl)-1,3-butadiene (**IV-1**) and 1,4-benzoquinone (**IV-2**) leading to **IV-3** bearing four 4-bromophenyl groups all *cis* to one another (Scheme IV-1).[1] This compound serves as a key intermediate to form the partially hydrogenated cyclic dimers **IV-4** and **IV-5** and three of the four corresponding cyclic trimers as hydrogenated cycloparaphenylenes (CPPs).[1]

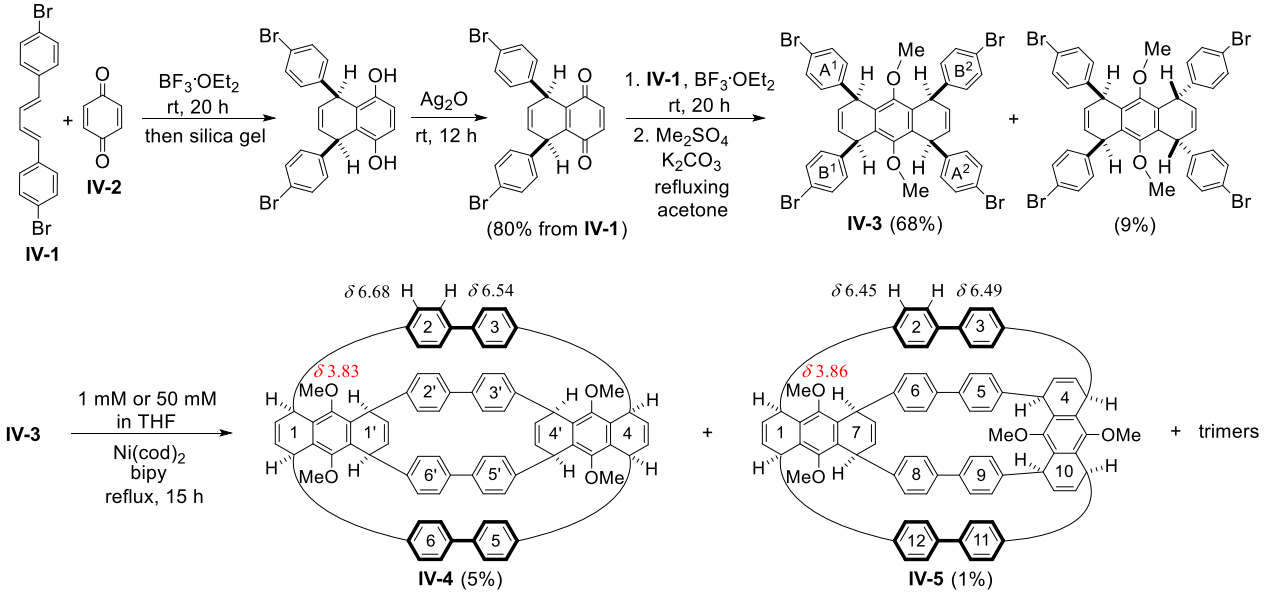

Scheme IV-1. Synthesis of Bent 8H[12]CPP and Fused two 4H[6]CPPs

This synthetic pathway reported earlier was extended in this investigation to form fused molecular nanohoops bearing two macrocyclic rings with different ring sizes. The Diels–Alder reactions between two 1,3-butadienes with 1,4-benzoquinone (**IV-2**) allowed the formation of Diels–Alder adducts with the four aryl groups all *cis* to one another. This strategy was successful

in the construction of macrocycle **IV-6** bearing a tetrahydro[6]cycloparaphenylene (4H[6]CPP) fused to a tetrahydro[10]cycloparaphenylene (4H[10]CPP) and macrocycle **IV-7** bearing a 4H[6]CPP fused to a [6]CPP inserted with two 2,2′-bithiophene-5,5′-diyl units (Figure IV-1).

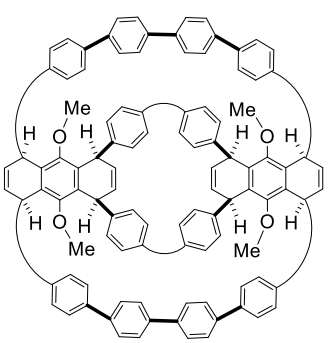

IV-6

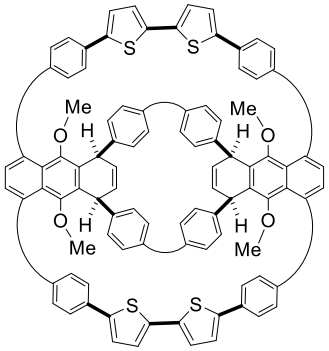

IV-7

Figure IV-1. Fused Macrocycles **IV-6** and **IV-7**.

IV-Result and Discussion

The Diels–Alder reaction between (*E*,*E*)-1,4-bis(4-bromophenyl)-1,3-butadiene (**IV-1**) and 1,4-benzoquinone (**IV-2**), in the presence of $BF_3{\cdot}OEt_2$, followed by oxidation with silver oxide (Ag_2O) produced 1,4-benzoquinone **IV-9** in 80% yield over two steps (Scheme IV-2). To carry out the second Diels–Alder reaction, (*E*,*E*)-1,4-(trimethylsilyl)biphenyl-1,3-butadiene (**IV-11**) was synthesized by the Suzuki–Miyaura coupling reaction between **IV-1** and boronic ester **IV-10** in 89% yield. The trimethylsilyl groups in diene **IV-11** will later be converted to iodo groups.

The second Diels–Alder reaction between the 1,4-benzoquinone moiety in **IV-9** and 1,3-butadiene **IV-11** was carried out in the presence of anhydrous $AlCl_3$. The crude mixture was then methylated to prepare **IV-12** with the two 4-bromophenyl groups and the two 4-[4-(trimethylsilyl)phenyl]phenyl groups all *cis* to one another in 71% yield over two steps.

Interestingly, the *trans* isomer was not seen by NMR spectroscopy. This unique stereoselectivity is either due to the *endo* approach of diene **IV-11** from the same side of the benzoquinone **IV-9** and/or the *exo* approach of the diene **IV-11** from the opposite side. Although both pathways are possible, there is considerable steric interaction in the *endo* approach, suggesting that the *exo* approach provides the thermodynamically more stable transition state. Attempts to obtain a single crystal of initial Diels–Alder adduct between **IV-9** and **IV-11** for X-ray structure analysis failed due to the sensitivity of the α-hydrogens of the resulting ketones to aerobic oxidation.

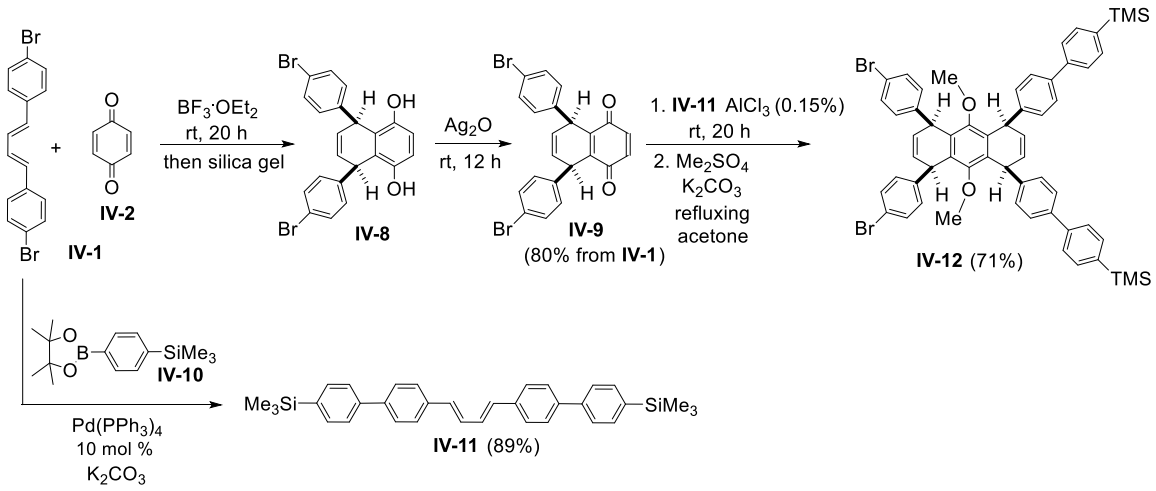

Scheme IV-2. Synthesis of **IV-12**

Treatment of **IV-12** at 1 mM concentration with $Ni(cod)_2$ (cod: 1,5-cyclooctadiene), in the presence of 2,2′-bipyridyl (bpy), promoted homocoupling reactions to produce the cyclic dimers *syn*-**IV-13** and *anti*-**IV-14** in ca. 1:1 ratio in the reaction mixture, observed by NMR spectroscopy (Scheme IV-3). Silica gel chromatography allowed us to separate and isolate *syn*-**IV-13** and *anti*-**IV-14** dimers in 16% and 17% yield, respectively. Dimers *syn*-**IV-13** and *anti*-**IV-14** both contained a tetrahydro[6]CPP segment in the molecular structures. Since both *syn*-**IV-13** and *anti*-**IV-14** have the same number of proton signals and similar chemical shifts, we were not able to

distinguish them at this stage. Treatment of *syn*-**IV-13** and *anti*-**IV-14** with ICl at -78˚C separately replaced the trimethylsilyl groups with iodide groups to form the corresponding tetraiodide *syn*-**IV-15** and *anti*-**IV-16**, respectively.

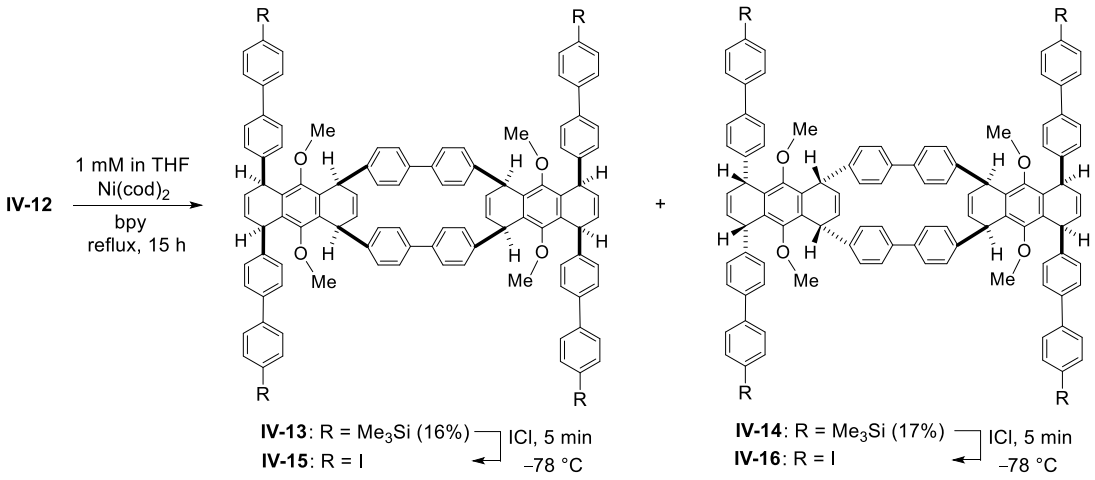

Scheme IV-3. Synthesis of Tetraiodide *syn*-**IV-15** and *anti*-**IV-16**

Without further purification, tetraiodides *syn*-**IV-15** and *anti*-**IV-16** were subjected to $Ni(cod)_2$-mediated homocoupling reactions (Scheme IV-4). Both reactions were analyzed by TLC and NMR. Tetraiodide *anti*-**IV-16** dimer did not produce macrocycle **IV-6**, and broad ^1H NMR signals were observed, indicating that oligomers or polymers of *anti*-**IV-16** were formed. On the other hand, tetraiodides *syn*-**IV-15** successfully formed macrocycle **IV-6** in 46% yield over two steps, indicating that **IV-13** has the all *cis* stereochemistry. Macrocycle **IV-6** contains two partially hydrogenated [6]- and [10]cycloparaphenylene segments (4H[6]–4H[10]CPP).

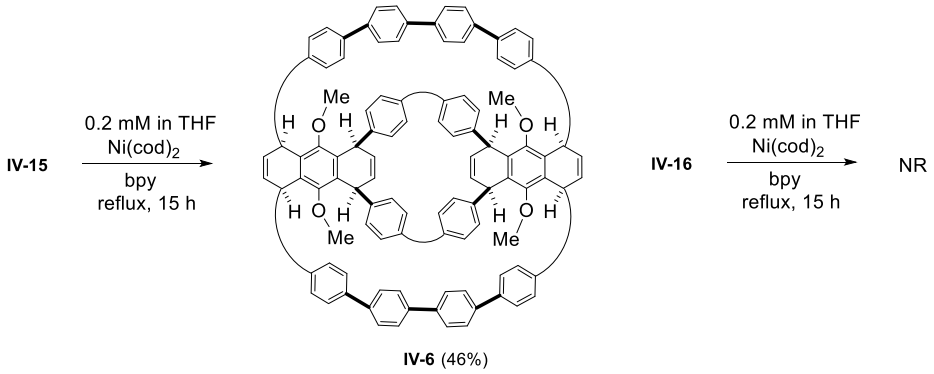

Scheme IV-4. Synthesis of Fused Macrocycle 4H[6]–4H[10]CPP **IV-6**

The DFT-optimized structure of 4H[6]–4H[10]CPP **IV-6** shows that the 4H[6]CPP has the oval-shaped structure and the 4H[10]CPP unit is more severely bent (Figure IV-2).

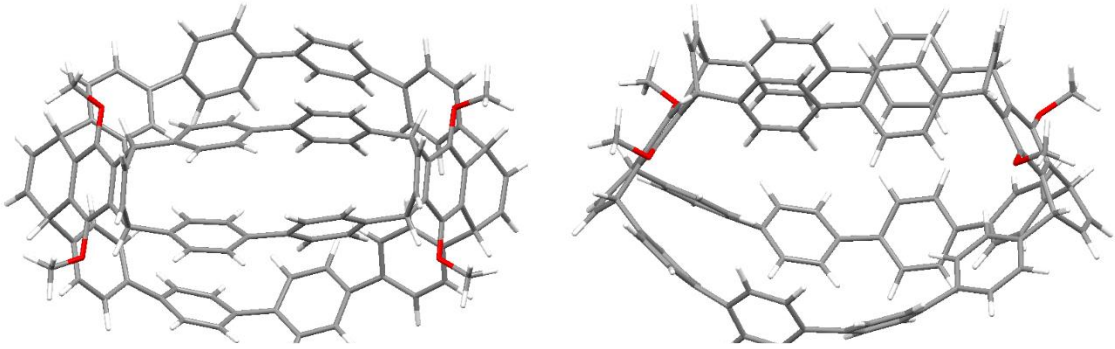

8H[6]–[10]CPPs aerial view 8H[6]–[10]CPPs perspective view

Figure IV-2. DFT-optimized structure of 4H[6]–4H[10]CPP **IV-6**.

The dihedral angle between the central phenyl groups of the two biphenyl units in 4H[6]CPP moiety is 40°, the distance between the centers of the two bonds joining the phenyls of the two biphenyl units is 3.87 Å, and the distance between the centers of the two partially hydrogenated rings in the anthracenyl units is 10.12 Å. The dihedral angle between the central phenyl groups of the two quaterphenyl units in 4H[10]CPP moiety is 34°, the dihedral angles

between the non-central phenyl groups of the two quaterphenyl units are 38 Å and 47 Å. The distance between the centers of the two bonds joining the phenyls of the two quaterphenyl units is 9.37 Å, and the distance between the centers of the two partially hydrogenated rings in the anthracenyl units is 15.50 Å. The two 9,10-dimethoxynanthra-1,4,5,8-tetrayl units cant toward the inner plane at 58°.

The ^{1}H NMR spectrum of the partially hydrogenated 4H[10]CPP segment at 25 °C showed four doublets in aromatic region (Figure VI-3). However, the rate of rotation of the two biphenyl groups in the 4H[6]CPP unit are relatively slow on the ^{1}H NMR scale at rt. These protons appeared in the ^{1}H NMR spectrum as very broad peaks.

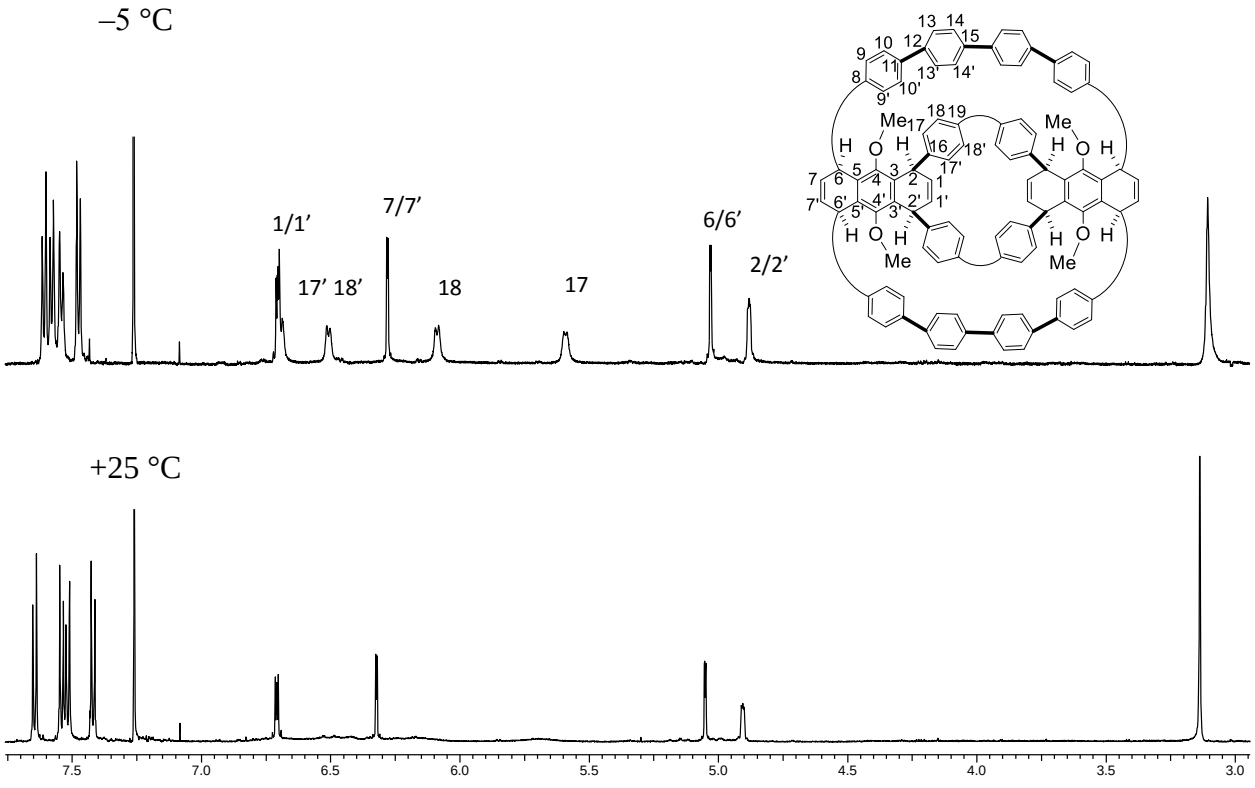

Figure VI-3. ^{1}H NMR spectrum of 4H[6]–4H[10]CPP **IV-6** at –5 °C and 25 °C

The observed broad peaks at rt for the 4H[6]CPP moiety indicate some restricted rotation of the biphenyl units. At –5 °C, the rotation is relatively slow in the NMR time scale, and therefore four distinct signals for hydrogens on carbons 17, 17′, 18, and 18′ were observed. The variable-temperature ^{1}H NMR spectra of 4H[6]–4H[10]CPP was recorded with temperatures ranging from –5 °C to 62 °C (Figure IV-4).

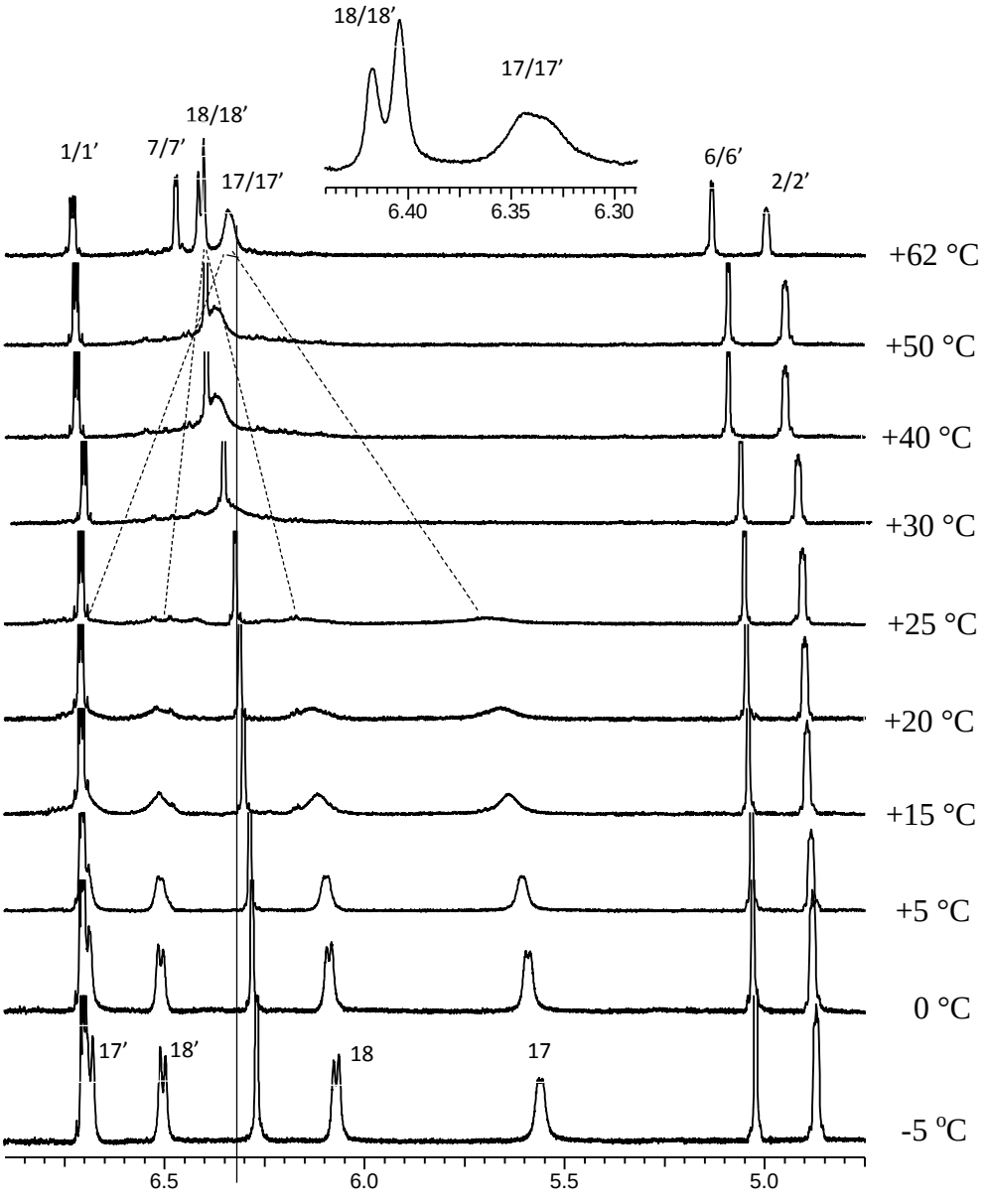

Figure IV-4. Portion of the variable temperature dependent ^{1}H NMR spectrum of 8H[6]–[10]CPPs **IV-6**

The ortho protons of 4H[6]CPP moiety at lower temperatures are anisochronous instead of isochronous at higher temperatures. At low temperature, the macromolecule 4H[6]–4H**[10]CPP IV-6** slower fluctuated therefore **one of the ortho protons for the inner aromatic ring moiety experiences a slightly different magnetic environment and is to some extent deshielded (ca 1 ppm), additionally, the other ortho proton is shielded and appears at 5.58 ppm vs 6.69 ppm (deshielded ortho proton).**

IV-Calculation of activation parameters ($\Delta G^{\ddagger}$, $\Delta H^{\ddagger}$, and $\Delta S^{\ddagger}$)

Macrocycle 4H[6]–4H[10]CPP displays restricted rotation of its inner aromatic groups (4H[6]CPP) as evidenced by the line-shape analysis of the dynamic ^{1}H NMR spectra with the following activation parameters: The activation energy $\Delta G^{\ddagger}$ = 16 kcal/mol, enthalpy $\Delta H^{\ddagger}$ = 18.7 kcal/ mol, and entropy $\Delta S^{\ddagger}$ = 9.9 cal/Kmol were calculated by using the rate constant.

Our previous attempts to oxidatively aromatize 4H[6]CPP were not successful.[2] However, preliminary studies showed that 4H[10]CPP can be oxidatively aromatized by treatment with 2,3-dichloro-5,6-dicyano-1,4-benzoquinone (DDQ) at an elevated temperature (150 °C). Unfortunately, oxidative aromatization of macrocycle **IV-6** at temperatures ranging from 70 to100 °C was not successful and led to the recovery of the starting material. Attempts to force the reaction to completion ended with decomposition at 120 °C.

It was previously reported by our research group the synthesis of cycloparaphenylenes bearing 2,2′-bithiophene-5,5′-diyl and 2,2′-bifuran-5,5′-diyl groups in the macrocyclic ring structures.[3] In both examples, incorporating five-membered heterocycles in the macrocycles reduces the strain dramatically and oxidative aromatization can be carried out at lower tempretures.

To introduce thiophenes into the macrocycles, (*E*,*E*)-1,4-bis(4-iodophenyl)-1,3-butadiene (**IV-17**) was prepared from **IV-1** through the copper-catalyzed halogen exchange, which resulted

in 86% yield (Scheme IV-5).[4] The Diels-Alder reaction between (*E*,*E*)-1,4-bis(4-iodophenyl)-1,3-butadiene (**IV-17**) and 1,4-benzoquinone (**IV-2**) was carried out in refluxing dichloroethane at reflux for 96 h to produce **IV-18** in 84% yield, which upon oxidation by silver(I) oxide produced **IV-19** in 89% yield. A second Diels-Alder reaction was performed between the benzoquinone moiety of **IV-19** and (*E*,*E*)-1,4-bis(4-bromophenyl)-1,3-butadiene (**IV-1**). This was immediately followed by methylation to prepare **IV-20** in 55% yield. The two 4-bromophenyl groups and the two 4-iodophenyl groups are *cis* to on another. Because aryl iodide groups are more reactive toward the Suzuki–Miyaura cross-coupling reactions than aryl bromide groups, we were able to selectively use the aryl iodide groups for the cross-coupling reactions. The Suzuki–Miyaura coupling reactions between **IV-20** and boronic ester **IV-21** formed **IV-22** at 67% yield.

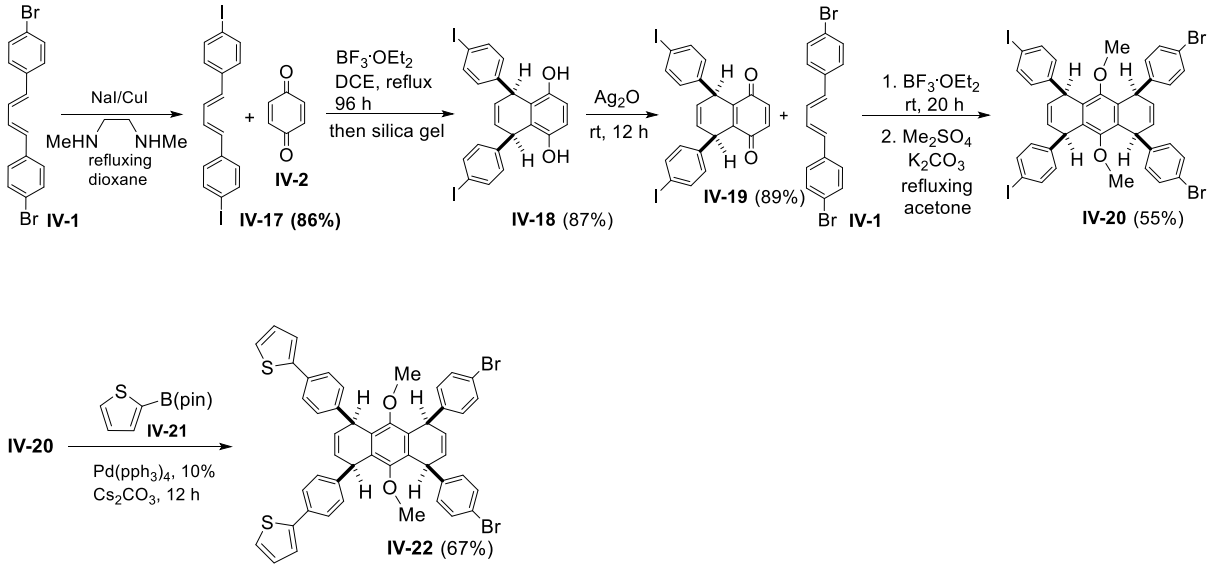

Scheme IV-5. Synthesis of Dibromide-Diiodide **IV-20** and Dibromide **IV-22**

Treatment of compound **IV-22** at 1 mM concentration in THF with $Ni(cod)_2$ (cod: 1,5-cyclooctadiene) in the presence of 2,2′-bipyridyl (bipy) promoted two homocoupling reactions to produce cyclic dimers *syn*-**IV-23** and *anti*-**IV-24** bearing tetrathiophenes in ca. 1:1 ratio in the

reaction mixture in 28% combined yield (Scheme IV-6). Attempts to separate *syn*-**IV-23** and *anti*-**IV-24** tetrathiophenes were unsuccessful. Iodination of the α position of thiophenes was carried out by *N*-iodosuccinimide (NIS) in acidic conditions to form *syn*-**IV-25** and *anti*-**IV-26** in of 87% combined yield. Silica gel chromatography allowed us to separate and isolate *syn*-**IV-25** and *anti*-**IV-26**.

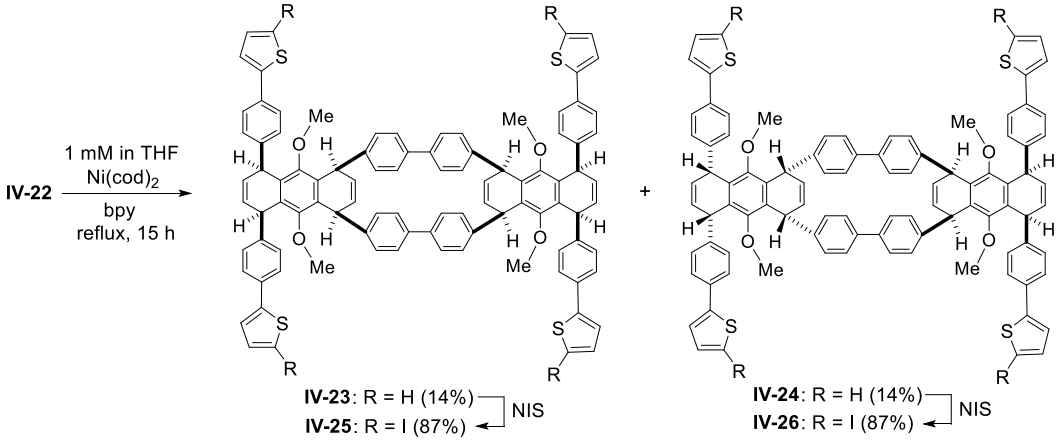

Scheme IV-6. Synthesis of Tetraiodide *syn*-**IV-25** and *anti*-**IV-26**

Both *syn*-**IV-25** and *anti*-**IV-26** dimers were then subjected to $Ni(cod)_2$-mediated homocoupling reactions. The *anti*-**IV-26** dimer did not form a macrocycle. However, the *syn*-**IV-25** dimer successfully formed macrocycle **IV-27** containing two partially hydrogenated 4H[6]CPP fused to a 4H[6]CPP inserted with two 2,2′-bithiophene-5,5′-diyl units in 52% yield.

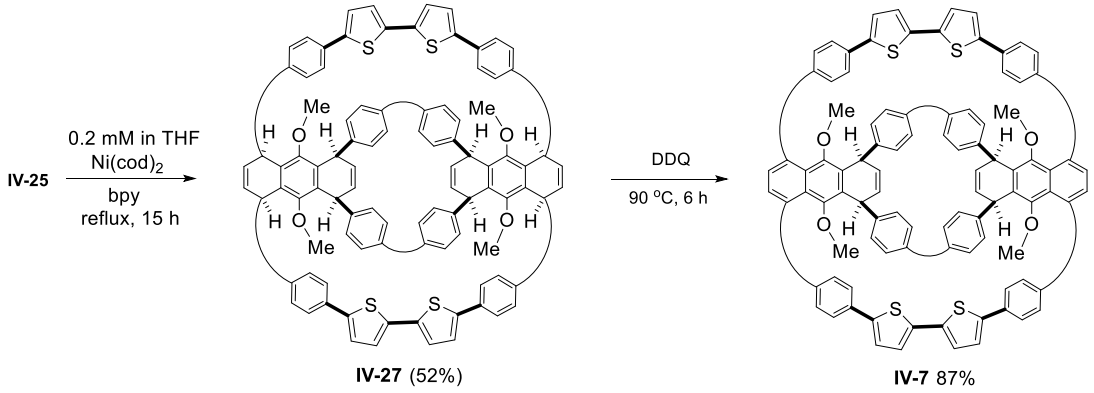

Scheme IV-7. Synthesis of Fused 8H[6]–[6]CPP bearing 2,2′-Bithiophene-5,5′-diyl units **IV-27**

It was gratifying to observe that treatment of macrocycle **IV-27** with DDQ in chlorobenzene at 90 °C for 6 hours was successful in producing **IV-7** in 87% yield.

The DFT-optimized structure of **IV-7** shows that the 4H[6]CPP and the [6]CPP inserted with two 2,2′-bithiophene-5,5′-diyl units have a cone-shaped structure that are fused by two 1,4-dimethoxybenzene units (Figure IV-5).

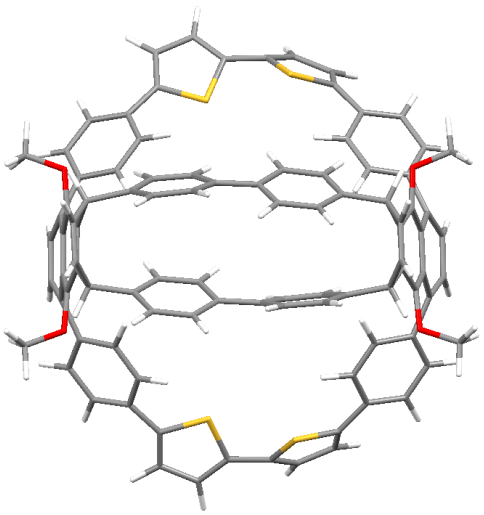

aerial view of **IV-7**

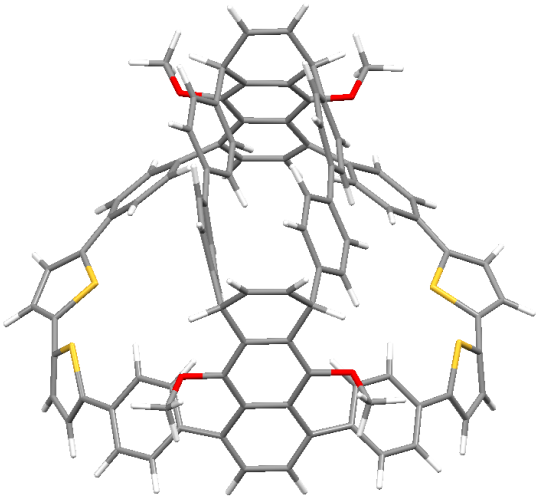

perspective view of **IV-7**

Figure IV-5. DFT-optimized structures of 4H[6]–[6] with two 2,2′-bithiophene-5,5′-diyl units CPP **IV-7**.

IV-Conclusion

The Diels–Alder reactions between two different 1,3-butadienes with 1,4-benzoquinone (**IV-2**) led to a key intermediate with the four aryl groups all *cis* to one another. This stereoselectivity is a key to forming cone-shaped macrocycles. Partially hydrogenated 4H[6]CPP in *syn*-**IV-13** and *syn*-**IV-23** were accessed through the nickel-mediated homocoupling reactions of **IV-12** and **IV-24** respectively. The second nickel-mediated homocoupling reactions tetraiodides **IV-15** and **IV-25** led to the formation of partially hydrogenated 4H[6]CPP fused to 4H[10]CPP (**IV-6**) and compound **IV-7** bearing a 4H[6]CPP fused to a [6]CPP incorporated with two 2,2′-bithiophene-5,5′-diyl units in macrocycle structure respectively. Compound **IV-6** exhibits dynamic behavior at rt. Oxidative aromatization of **IV-25** with DDQ produced compound **IV-7**. The DFT optimized structure of **IV-7** showed at the diameter of 10 membered macrocycle was shorter than reported thiophene containing [10]CPP.

IV-General Experimental Methods

All reactions were conducted in oven-dried (120 °C) glassware. Chemicals, including 1,4-benzoquinone, silver(I) oxide (Ag_2O), boron trifluoride diethyl etherate ($BF_3 \cdot OEt_2$), tetrakis(triphenylphosphine)palladium [$Pd(PPh_3)_4$], bis(1,5-cyclooctadiene)nickel [$Ni(cod)_2$], 2,2′-bipyridyl (bpy), *N*-iodosuccinimide (NIS), anhydrous aluminium chloride ($AlCl_3$), iodine monochloride (ICl), 4,4,5,5-tetramethyl-2-(2-thienyl)-1,3,2-dioxaborolane (**IV-21**), *N*,*N*′-dimethylethylenediamine, and 2,3-dichloro-5,6-dicyano-1,4-benzoquinone (DDQ), were purchased from chemical suppliers and were used as received. (*E,E*)-1,4-Bis(4-bromophenyl)-1,3-butadiene (**IV-1**), dibromide **IV-1′** and 4,4,5,5-tetramethyl-2-[4-(trimethylsilyl)phenyl]-1,3,2-dioxaborolane (**IV-10**) were prepared according to reported procedures.[5] UV-vis absorption spectra were recorded on a spectrophotometer with a 1 nm resolution, and the baseline was corrected with a solvent filled square quartz cell. Fluorescence spectra were recorded on a spectrofluorophotometer with a 2 nm resolution.

Experimental Procedure for IV-11. To a two-neck 250 mL flask containing (*E*,*E*)-1,4-bis(4-bromophenyl)-1,3-butadiene (1.82 g, 5.00 mmol), 4,4,5,5-tetramethyl-2-[4-(trimethylsilyl)phenyl]-1,3,2-dioxaborolane (**IV-1**, 4.14 g, 15.0 mmol), and 2.65 g of sodium carbonate (25.0 mmol) and fitted with a condenser and a rubber septum were added toluene (150 mL), ethanol (30 mL), and water (20 mL). The solution was flushed with nitrogen for 10 min, and then 0.578 g of $Pd(PPh_3)_4$ (0.50 mmol) was added. The solution was again flushed with nitrogen for 20 min and then heated at reflux for 12 h before it was cooled to rt. The solvent was removed in vacuo, and the residue was filtered and then washed with water (2 × 100 mL) and ethanol (3 × 100 mL) to produce **IV-11** (2.24 g, 4.45 mmol, 89% yield) as a pale yellow solid: mp 290–292 °C; IR 1253, 991, 838, 826 cm^{-1}; ^1H NMR ($CDCl_3$, 400 MHz) δ 7.61 (8 H, s), 7.60 (4 H, d, J = 8.6 Hz), 7.53 (4 H, J = 8.6 Hz), 7.03 (2 H, m), 6.73 (2 H, m), 0.31 (18 H, s); ^{13}C NMR ($CDCl_3$, 100 MHz) δ 141.0, 140.2, 139.4, 136.5, 133.8, 132.4, 129.4, 127.3, 126.8, 126.2, –1.1; HRMS (ESI) calcd for $C_{34}H_{38}Si_2$ (M^+) 502.2507, found 502.2530.

Experimental Procedure for IV-12. To a mixture of 0.653 g dibromide **IV-1′**(1.39 mmol), 0.790 g of diene **IV-11** (1.53 mmol), and 0.025 g of $AlCl_3$ (0.187 mmol) under a nitrogen atmosphere was added via cannula anhydrous dichloromethane (50 mL). The reaction mixture was stirred at rt for 24 h before it was passed through a short silica gel column (5 cm high, 3 cm diameter), and the column was further eluted with dichloromethane (2 × 100 mL). The combined eluates were concentrated to afford a yellow solid. The crude solid was used without further purification. To the yellow solid and 0.553 g of potassium carbonate (4.00 mmol) in dry acetone (50 mL) was added 0.40 mL of dimethyl sulfate (4.2 mmol) via a syringe, and the reaction mixture was heated at reflux for 12 h before it was cooled to rt. The reaction mixture was then passed through a short silica gel column (5 cm high, 3 cm diameter), and the column was further

eluted with dichloromethane (2 × 100 mL). The combined organic eluates were concentrated in vacuo. The solid residue was further purified by flash column chromatography (silica gel/dichloromethane:hexanes = 1:6 to 1:3) to produce 0.98 g of **IV-12** (0.98 mmol, 71% yield) as a white solid: mp 140–142 °C; IR 1487, 1249, 850, 810 cm^{-1}; ^{1}H NMR ($CDCl_3$, 400 MHz) δ 7.55 (4 H, d, J = 8.2 Hz), 7.50 (4 H, d, J = 7.8 Hz), 7.33 (4 H, d, J = 8.2 Hz), 7.21 (4 H, d, J = 8.6 Hz), 7.04 (4 H, d, J = 8.2 Hz), 6.86 (4 H, d, J = 8.6 Hz), 6.19 (2 H, d, J = 3.5 Hz), 6.11 (2 H, d, J = 3.1 Hz), 4.93 (2 H, d, J = 3.1 Hz), 4.85 (2 H, d, J = 2.7 Hz), 3.56 (6 H, s), 0.29 (18 H, s); ^{13}C NMR ($CDCl_3$, 100 MHz) δ 152.3, 142.9, 142.8, 141.3, 138.78, 138.74, 133.7, 131.8, 131.1, 130.8, 129.3, 128.6, 128.3, 128.2, 127.9, 127.0, 126.8, 126.3, 119.8, 40.7, 40.4, –1.1; HRMS (ESI) calcd for $C_{58}H_{56}Br_2O_2Si_2$ (M^+) 998.2180, 1000.2160, 1002.2139; found 998.2139, 1000.2169, 1002.2178.

Experimental Procedure for Cyclic Dimers *syn*-IV-13 and *anti*-IV-14. An oven-dried 1 L flask fitted with a condenser was placed in a glovebox. To the flask were then added dibromide **IV-12** (0.560 g, 0.561 mmol), 2,2′-bipyridyl (0.210 g, 1.35 mmol), and bis(1,5-cyclooctadiene)nickel (0.370, 1.35 mmol). The flask was capped with a rubber septum and then removed from the glovebox before 560 mL of anhydrous THF was added via cannula under an argon atmosphere. Then the reaction mixture was heated at reflux for 24 h before it was cooled to rt. The reaction mixture was then passed through a short silica gel column (5 cm high, 3 cm in diameter), and the column was further eluted with THF (2 × 100 mL). The combined eluates were concentrated, and the residue was purified by flash column chromatography (silica gel, dichloromethane:hexanes = 1:10 to 1:4) to produce 0.081 g cyclic dimer *anti*-**IV-14** (0.048 mmol, 17% yield) and 0.075 g cyclic dimer *syn*-**IV-13** (0.045 mmol, 16% yield) as white solids: *anti*-**IV-14**: mp >250 °C; IR 1249, 1114, 840, 809 cm^{-1}; ^{1}H NMR ($CDCl_3$, 600 MHz) δ 7.57 (16

H, s), 7.54 (8 H, d, J = 8.2 Hz), 7.40 (8 H, d, J = 8.2 Hz), 6.84 (4 H, dd, J = 4.4, 2.6 Hz), 6.62 (8 H, d, J = 8.2 Hz), 6.54–6.47 (8 H, br), 6.14 (4 H, d, J = 2.3 Hz), 5.05 (4 H, d, J = 2.3 Hz), 5.02 (4 H, br), 3.59 (12 H, s), 0.30 (36 H, s); ^{13}C NMR ($CDCl_3$, 100 MHz) δ 151.8, 144.2, 141.4, 139.8, 138.9, 138.8, 138.4, 134.4, 133.7, 133.1, 130.7, 128.7, 128.1, 127.9, 127.4, 127.1, 126.4, 126.0, 61.1, 41.5, 38.3, 28.0, –1.1; HRMS (ESI) calcd for $C_{116}H_{112}O_4Si_4Na$ (MNa^+) 1703.75230, found 1703.7534; *syn*-**IV-13**: mp >250 °C; IR 1492, 1247, 807, 757 cm^{-1}; ^{1}H NMR ($CDCl_3$, 600 MHz) δ 7.51 (8 H, d, J = 8.2 Hz), 7.48 (8 H, d, J = 8.2 Hz), 7.39 (16 H, d, J = 8.2 Hz), 6.84 (4 H, dd, J = 4.5, 2.5 Hz), 6.65 (8 H, d, J = 8.6 Hz), 6.52 (8 H, d, J = 7.4 Hz), 6.11 (4 H, d, J = 2.7 Hz), 5.04 (4 H, d, J = 2.3 Hz), 5.00 (4 H, br), 3.57 (12 H, s), 0.13 (34 H, s); ^{13}C NMR ($CDCl_3$, 100 MHz) δ 151.9, 144.2, 141.1, 139.9, 138.8, 138.7, 138.7, 138.6, 134.4, 133.8, 133.3, 130.9, 128.2, 127.9, 127.3, 127.0, 126.22, 126.16, 61.2, 41.6, 38.4, –1.1; HRMS (ESI) calcd for $C_{116}H_{112}O_4Si_4$ (M^+) 1680.7632, found 1680.7616.

Experimental Procedure for IV-6. A solution of 0.018 g of **IV-13** (0.011 mmol) in 10 mL of anhydrous dichloromethane under a nitrogen atmosphere was cooled to −78 °C. To the solution at −78 °C was added dropwise 0.10 mL of a 1 M solution of ICl in dichloromethane. After 5 min at −78 °C, the reaction was quenched with a saturated sodium thiosulfate solution. The reaction mixture was extracted with dichloromethane (3 × 20 mL), dried over sodium sulfate, and concentrated to afford crude **IV-15** as a white solid. Crude **IV-15** in a 100 mL flask, fitted with a condenser, was placed in a glovebox. To the flask were added 0.018 g of 2,2′-bipyridyl (0.113 mmol) and 0.031 g of bis(1,5-cyclooctadiene)nickel (0.113 mmol). The flask was fitted a rubber septum and removed from the glovebox before 50 mL of THF was added via cannula under a nitrogen atmosphere. The reaction mixture was heated at reflux for 24 h before it was cooled to rt. The reaction mixture was then passed through a short silica gel column, and the column was

eluted with dichloromethane (100 mL). The combined eluates were concentrated, and the residue was purified by flash column chromatography (silica gel, dichloromethane:hexanes = 1:5 to 1:2) to produce 0.007 g of **IV-6** (0.005 mmol, 46 % yield from **IV-13**) as white solid: mp >210 °C; IR 1498, 1300, 1065, 791 cm^{-1}; ^{1}H NMR ($CDCl_3$, 400 MHz) δ 7.65 (8 H, d, J = 8.6 Hz), 7.54 (8 H, d, J = 8.6 Hz), 7.52 (8 H, d, J = 8.6 Hz), 7.42 (8 H, d, J = 8.2 Hz), 6.71 (4 H, dd, J = 4.7, 2.7 Hz), 6.32 (4 H, d, J = 2.7 Hz), 5.05 (4 H, d, J = 2.7 Hz), 4.94–4.86 (4 H, m), 3.14 (12 H, s); ^{13}C NMR ($CDCl_3$, 150 MHz) δ 151.5, 143.3, 140.1, 139.8, 139.2, 139.0, 138.6, 134.1, 133.7, 131.6, 130.1, 127.97, 127.94, 127.8, 127.2, 127.1, 126.3, 60.8, 41.2, 38.9; HRMS (ESI) calcd for $C_{104}H_{76}O_4$ (M^+) 1388.5737, found 1388.5793.

Experimental Procedure for Diiodide IV-17. To a solution of (*E*,*E*)-1,4-bis(4-bromophenyl)-1,3-butadiene (**IV-1**) (3.64 g, 10.0 mmol) in dioxane (100 mL) were added CuI (0.381 g, 2.00 mmol), sodium iodide (6.00 g, 40.0 mmol), and *N*,*N*′-dimethylethylenediamine (0.431 mL, 4.00 mmol). The reaction mixture was heated at reflux for 24 h before it was cooled to rt and then poured into 100 mL of a 5% aqueous ammonia solution. The precipitate was collected, washed with water (2 × 100 mL) and cold ethanol (50 mL), and air dried for 8 h to give 3.94 g (8.6 mmol, 86% yield) of **IV-17** as a white solid: mp 257−259 °C; IR 1481, 991, 851, 739 cm^{-1}; ^{1}H NMR ($CDCl_3$, 400 MHz) δ 7.65 (4 H, d, J = 8.2 Hz), 7.17 (4 H, d, J = 8.6 Hz), 6.92 (2 H, dd, J = 11.8, 2.8 Hz), 6.59 (2 H, dd, J = 11.8, 2.7 Hz); ^{1}H NMR (DMSO-d_6, 400 MHz) δ 7.70 (4 H, d, J = 8.2 Hz), 7.32 (4 H, d, J = 8.6 Hz), 7.12 (2 H, dd, J = 11.7, 2.7 Hz), 6.71 (2 H, dd, J = 11.8, 2.7 Hz); ^{13}C NMR (DMSO-d_6, 100 MHz) δ 137.5, 136.5, 132.1, 131.6, 130.0, 128.4, 93.5; HRMS (ESI) calcd for $C_{12}H_{12}I_2$ (M^+) 457.9023, found 457.9029.

Experimental Procedure for Diiodide IV-18. To a solution of 4.600 g of (*E*,*E*)-1,4-bis(4-iodophenyl)-1,3-butadiene (**IV-17**, 10.04 mmol) and 1.300 g of 1,4-benzoquinone (**IV-2**, 12.03

mmol) in 200 mL of anhydrous dichloroethane under an argon atmosphere was added by using a syringe 1.0 mL of boron trifluoride diethyl etherate (4.8 mmol). The reaction mixture was stirred at reflux for 96 h and then washed with water (4 × 100 mL). The organic layer was separated and then passed through a short silica gel column (8 cm high, 5 cm in diameter). The column was further eluted with 200 mL of diethyl ether. The combined eluates were dried over sodium sulfate and concentrated to afford a brown solid. The brown solid was further purified by flash column chromatography (silica gel/ethyl acetate:hexanes = 1:4 to 1:2) to produce 4.95 g of **IV-18** (8.74 mmol, 87% yield) as a yellow solid: mp 153–155 °C; IR 3453–3124 br, 1482, 1286, 1006 cm^{-1}; ^{1}H NMR ($CDCl_3$, 400 MHz) δ 7.62 (4 H, d, J = 8.2 Hz), 7.02 (4 H, d, J = 8.2 Hz), 6.63 (2 H, s), 5.89 (2 H, d, J = 2.4 Hz), 4.76 (2 H, d, J = 2.4 Hz), 4.20 (2 H, s); ^{13}C NMR ($CDCl_3$, 100 MHz) δ 147.4, 143.0, 137.9, 130.0, 127.2, 124.7, 115.1, 92.1, 41.0; HRMS (ESI) calcd for $C_{22}H_{16}I_2O_2$ (M^+) 565.9234, found 565.9240.

Experimental Procedure for Diiodide IV-19. To a mixture of diiodide **IV-18** (2.60 g, 4.59 mmol) and silver oxide (1.28 g, 5.51 mmol) was added 100 mL of anhydrous diethyl ether under a nitrogen atmosphere. The reaction mixture was stirred at rt for 12 h and then passed through a short silica gel column. The column was further eluted with diethyl ether (2 × 50 mL), and the combined eluates were concentrated. The solid residue was further purified by flash column chromatography (silica gel/ethyl acetate:hexanes = 1:10 to 1:5) to afford 2.31 g of **IV-19** (4.09 mmol, 89% yield) as a yellow solid: mp 172–174 °C; IR 1656, 1482, 1293, 864 cm^{-1}; ^{1}H NMR ($CDCl_3$, 400 MHz) δ 7.63 (4 H, d, J = 8.2 Hz), 7.02 (4 H, d, J = 8.6 Hz), 6.69 (2 H, s), 5.89 (2 H, d, J = 2.7 Hz), 4.70 (2 H, d, J=2.7 Hz); ^{13}C NMR ($CDCl_3$, 100 MHz) δ 186.0, 141.6, 141.0, 137.8, 136.5, 130.4, 126.5, 92.5, 40.1; HRMS (ESI) calcd for $C_{22}H_{12}I_2O_2$ (M^+ – 2 H) 561.8921, found 561.8963.

Experimental Procedure for IV-20. To a mixture of (*E*,*E*)-1,4-bis(4-bromophenyl)-1,3-butadiene (**IV-1**, 1.39g, 3.82 mmol) and diiodide **IV-19** (2.05 g, 3.63 mmol) in 100 mL of anhydrous dichloromethane under a nitrogen atmosphere was added by using a syringe 1.00 mL of boron trifluoride diethyl etherate (4.8 mmol). The reaction mixture was stirred at rt for 16 h. The reaction mixture was then passed through a short silica gel column, and the column was further eluted with diethyl ether (2 × 100 mL). The combined eluates were concentrated to afford a yellow solid, which was used without further purification. To the yellow solid and potassium carbonate (2.00 g, 14.5 mmol) in dry acetone (100 mL) was added 1.00 mL of dimethyl sulfate (10.5 mmol) via a syringe, and the reaction mixture was heated at reflux for 12 h before it was cooled to rt. The reaction mixture was then passed through a short silica gel column, and the column was further eluted with dichloromethane (2 × 100 mL). The combined organic eluates were concentrated in vacuo. The solid residue was further purified by flash column chromatography (silica gel/ethyl acetate:hexanes = 1:6 to 1:4) to afford 1.91 g of **IV-20** (2.00 mmol, 55% yield) as a white solid: mp 180–182 °C; IR 1485, 1299, 1008, 809 cm^{-1}; ^{1}H NMR ($CDCl_3$, 400 MHz) δ 7.42 (4 H, d, J = 8.4 Hz), 7.22 (4 H, d, J = 8.4 Hz), 6.80 (4 H, d, J = 8.4 Hz), 6.68 (4 H, d, J = 8.4 Hz), 6.08 (2 H, d, J = 3.2 Hz), 6.06 (2 H, d, J = 3.1 Hz), 4.80 (2 H, d, J = 2.8 Hz), 4.78 (2 H, d, J = 2.8 Hz), 3.52 (6 H, s); ^{13}C NMR ($CDCl_3$, 100 MHz) δ 152.1, 143.3, 142.6, 137.7, 137.1, 131.2, 131.1, 129.5, 129.2, 128.1, 128.0, 120.0, 91.4, 60.4, 40.5, 40.4; HRMS (ESI) calcd for $C_{40}H_{30}Br_2I_2O_2$ (M^+) 955.8676, found 955.8643.

Experimental Procedure for IV-22. To a 100 mL two-neck flask fitted with a condenser and a rubber septum were added **IV-20** (0.60g, 0.63 mmol), 4,4,5,5-tetramethyl-2-(2-thienyl)-1,3,2-dioxaborolane (**IV-21**, 0.265 g, 1.26 mmol), cesium carbonate (0.82 g, 2.5 mmol), and $Pd(PPh_3)_4$ (0.073 g, 0.063 mmol). The flask was flushed with nitrogen, and anhydrous THF (50 mL) was

introduced via cannula. The reaction mixture was heated at 50 °C for 24 h before it was cooled to rt. The reaction mixture was then passed through a short silica gel column, and the column was further eluted with dichloromethane (2 × 50 mL). The combined eluates were concentrated in vacuo. The solid residue was further purified by flash column chromatography (silica gel/ethyl acetate:hexanes = 1:6 to 1:4) to produce 0.366 g of **IV-22** (0.421 mmol, 67% yield) as a white solid: mp 258–260 °C; IR 1486, 1302, 1010, 813 cm^{-1}; ^1H NMR ($CDCl_3$, 400 MHz) δ 7.37 (4 H, d, J = 8.2 Hz), 7.24–7.19 (8 H, m), 7.04 (2 H, dd, J = 4.9, 3.7 Hz), 7.00 (4 H, d, J = 8.2 Hz), 6.83 (4 H, d, J = 8.2 Hz), 6.13 (2 H, d, J = 3.1 Hz), 6.11 (2 H, d, J = 3.1 Hz), 4.89 (2 H, d, J = 3.1 Hz), 4.83 (2 H, d, J = 2.7 Hz), 3.54 (6 H, s); ^{13}C NMR ($CDCl_3$, 100 MHz) δ 152.2, 144.3, 143.2, 142.7, 132.2, 131.5, 131.1, 130.9, 129.3, 128.2, 128.0, 127.9, 125.7, 124.4, 122.8, 119.8, 77.3, 76.7, 60.5, 40.8, 40.4; HRMS (ESI) calcd for $C_{48}H_{38}Br_2O_2S_2$ (M^+) 866.0518, 868.0498, 870.0477; found 866.0525, 868.0503, 870.0486.

Experimental Procedure for Cyclic Dimers *syn*-IV-23 and *anti*-IV-24. To an oven-dried 1 L flask were added dibromide **IV-22** (0.532 g, 0.616 mmol) and 2,2′-bipyridyl (0.234 g, 1.50 mmol). The flask was flushed with argon and placed in a glovebox, and then bis(1,5-cyclooctadiene)nickel (0.420 g, 1.53 mmol) was added. The flask was fitted with a condenser and a rubber septum and then removed from the glovebox before 600 mL of anhydrous THF was added via cannula under an argon atmosphere. Then the reaction mixture was heated at reflux for 18 h before it was cooled to rt. The reaction mixture was then passed through a short silica gel column (5 cm high, 3 cm in diameter), and the column was further eluted with THF (2 × 100 mL). The combined eluates were concentrated, and the residue was purified by flash column chromatography (silica gel, ethyl acetate:hexanes = 1:8 to 1:4) to produce a 1:1 mixture of cyclic dimers *syn*-**IV-23** and *anti*-**IV-24** (0.122 g, 0.086 mmol, 28% yield) as a white solid: IR 1498,

1301, 1066, 815 cm^{-1}; ^1H NMR ($CDCl_3$, 600 MHz) δ 7.569 (8 H, d, J = 8.2 Hz), 7.562 (8 H, d, J = 8.2 Hz), 7.346 (8 H, d, J = 8.4 Hz), 7.343 (8 H, d, J = 8.4 Hz), 7.27 (4 H, dd, J = 3.6, 1.2 Hz), 7.24 (4 H, dd, J = 3.0, 1.2 Hz), 7.23 (4 H, dd, J = 5.1, 1.2 Hz), 7.10 (4 H, dd, J = 5.4, 1.2 Hz), 7.05 (4 H, dd, J = 4.8, 3.6 Hz), 6.94 (4 H, dd, J = 5.3, 3.5 Hz), 6.84 (4 H, dd, J = 4.8, 2.4 Hz), 6.82 (4 H, dd, J = 4.5, 2.7 Hz), 6.65 (8 H, d, J = 8.8 Hz), 6.63 (8 H, d, J = 8.8 Hz), 6.54–6.45 (16 H, br), 6.09 (4 H, d, J = 2.3 Hz), 6.07 (4 H, d, J = 2.9 Hz), 5.03–4.99 (16 H, m), 3.57 (12 H, s), 3.53 (12 H, s); ^{13}C NMR ($CDCl_3$, 100 MHz) δ 151.8, 151.7, 144.48, 144.45, 144.42, 144.36, 139.8, 139.7, 138.6, 138.5, 134.5, 134.4, 133.2, 133.1, 132.4, 130.6, 130.5, 128.3, 128.0, 127.9, 127.7, 127.3, 126.2, 126.1, 126.03, 125.98, 124.5, 124.4, 122.8, 61.16, 61.07, 41.6, 41.5; HRMS (ESI) calcd for $C_{96}H_{72}O_4S_4$ (M^+) 1417.4342, found 1417.4320.

Experimental Procedure for Dimers *syn*-IV-25 and *anti*-IV-26. To a 25 mL flask were added 0.060 g of a 1:1 mixture of *syn*-**IV-23** and *anti*-**IV-24** (0.042 mmol) and *N*-iodosuccinimide (0.076 g, 0.34 mmol). The flask was capped with a rubber septum and flushed with argon for 5 min before 10 mL of $CHCl_3$ and 1 mL of acetic acid were added. The reaction mixture was stirred in the dark at rt for 12 h. A saturated sodium thiosulfate solution (3 mL) was added to the reaction mixture, and the organic layer was separated, dried over Na_2SO_4, and concentrated in vacuo. The residue was purified by flash column chromatography (silica gel/dichloromethane:hexanes = 1:2 to 1:1) to produce 0.035 g of *anti*-**IV-26** (0.036 mmol, 87% yield) and 0.035 g of *syn*-**IV-25** (0.036 mmol, 87% yield) as white solids: *anti*-**IV-26**: mp >185 °C; IR 1498, 1300, 1065, 791 cm^{-1}; ^1H NMR ($CDCl_3$, 600 MHz) δ 7.46 (8 H, d, J = 8.2 Hz), 7.32 (8 H, d, J = 8.8 Hz), 7.19 (4 H, d, J = 4.1 Hz), 6.93 (4 H, d, J = 4.1 Hz), 6.85 (4 H, dd, J = 4.7, 2.3 Hz), 6.61 (8 H, d, J = 8.2 Hz), 6.47 (8 H, br, d, J = 6.4 Hz), 6.08 (4 H, d, J = 2.9 Hz), 5.02–4.99 (4 H, m), 4.99 (4 H, d, J = 2.9 Hz), 3.58 (12 H, s); ^{13}C NMR (CDCl3, 100 MHz) δ

151.7, 150.4, 144.9, 139.7, 138.5, 137.8, 134.6, 133.1, 131.6, 130.3, 128.3, 127.7, 127.3, 126.1, 125.8, 124.2, 71.8, 61.1, 41.5, 38.3; HRMS (ESI) calcd for $C_{96}H_{68}I_4O_4S_4$ (M^+) 1920. 0174, found 1920.0112; *syn*-**IV-25**: mp >180 °C; IR 1497,1420, 1297,1064, 788 cm^{-1}; ^1H NMR ($CDCl_3$, 600 MHz) δ 7.47 (8 H, d, J = 8.2 Hz), 7.33 (8 H, d, J = 8.2 Hz), 7.09 (4 H, d, J = 4.1 Hz), 6.91 (4 H, d, J = 3.5 Hz), 6.83 (4 H, dd, J = 4.4, 2.6 Hz), 6.65 (8 H, d, J = 8.2 Hz), 6.51 (7 H, br), 6.06 (4 H, d, J = 2.3 Hz), 5.04–5.01 (4 H, m), 4.99 (4 H, d, J = 2.3 Hz), 3.54 (12 H, s); ^{13}C NMR ($CDCl_3$, 100 MHz) δ 151.9, 150.3, 144.9, 139.8, 138.6, 137.9, 134.6, 133.2, 131.6, 130.5, 128.3, 127.8, 127.3, 126.2, 125.8, 124.2, 72.3, 61.2, 41.6, 38.5; HRMS (ESI) calcd for $C_{96}H_{68}I_4O_4S_4$ (M^+) 1920.0174, found 1920.0112.

Experimental Procedure for IV-27. To an oven-dried 100 mL flask inside a glovebox were added 0.060 g of *syn*-**IV-25** (0.031 mmol) and 0.029 g of 2,2′-bipyridyl (0.18 mmol), and 0.050 g of bis(1,5-cyclooctadiene)nickel (0.18 mmol). After 25 mL of anhydrous THF was added, the flask was fitted with a condenser and a rubber septum and then removed from the glovebox. Then the reaction mixture was heated at reflux for 24 h before it was cooled to rt. The reaction mixture was then passed through a short silica gel column (3 cm high, 1 cm diameter), and the column was further eluted with THF (2 × 50 mL). The combined eluates were concentrated in vacuo, and the residue was purified by flash column chromatography (silica gel, dichloromethane:hexanes = 1:1 to 2:1) to produce 0.023 g of **IV-27** (0.016 mmol, 52% yield) as a yellow solid: mp >220 °C; IR 1499, 1458, 1300,1065, 799 cm^{-1}; ^1H NMR ($CDCl_3$, 400 MHz) δ 7.66 (8 H, d, J = 8.6 Hz), 7.36 (8 H, d, J = 8.2 Hz), 7.16 (4 H, d, J = 3.5 Hz), 7.06 (4 H, d, J = 3.5 Hz), 6.79 (4 H, dd, J = 4.7, 2.7 Hz), 6.71 (8 H, d, J = 8.6 Hz), 6.14 (4 H, d, J = 2.3 Hz), 5.03–4.98 (4 H, m), 4.94 (4 H, d, J = 2.3 Hz), 3.30 (12 H, s); ^{13}C NMR ($CDCl_3$, 100 MHz) δ 151.7,

154.2, 143.6, 140.1, 138.8, 136.8, 134.6, 133.5, 131.8, 130.9, 128.6, 127.4, 127.1,126.3, 126.0, 122.4, 61.3, 41.4, 38.8; HRMS (ESI) calcd for $C_{96}H_{68}O_4S_4$ (M^+) 1412.3995, found 1412.4028.

Experimental Procedure for IV-7. To a 5 mL flask were added **IV-27** (0.006 g, 0.004 mmol) and DDQ (0.019 g, 0.085 mmol). The flask was flushed with argon, and then 1 mL of chlorobenzene was introduced by using a syringe. The reaction mixture was heated at 90 °C for 6 h before it was cooled to rt. Dichloromethane (50 mL) was added, and the solution was passed through a basic aluminum oxide column (2 cm high, 1 cm in diameter). The column was further eluted with dichloromethane (2 × 50 mL). The combined eluates were concentrated in vacuo, and washed with pentane to afford **IV-27** (0.005 g, 0.004 mmol, 87% yield) as a yellow solid: mp >164 °C; IR 1456, 14.7, 1299, 812 cm^{-1}; ^1H NMR ($CDCl_3$, 600 MHz) δ 7.53 (8 H, d, J = 8.8 Hz), 7.44 (4 H, s), 7.42 (8 H, d, J = 8.2 Hz), 7.06 (4 H, d, J = 3.5 Hz), 6.98 (4 H, dd, J = 4.4, 2.6 Hz), 6.92 (5 H, d, J = 4.1 Hz), 6.90 (8 H, d, J = 8.8 Hz), 6.74 (8 H, br), 5.43 (4 H, br), 3.60 (12 H, s) ; ^{13}C NMR ($CDCl_3$, 100 MHz) δ 149.4, 145.6, 141.2, 140.4, 138.6, 137.3, 137.2, 133.1, 133.0, 132.0 130.6, 127.9, 127.9, 127.4, 127.0, 126.35, 126.26, 122.7, 122.3, 60.3, 38.2; HRMS (ESI) calcd for $C_{96}H_{64}O_4S_4$ (M^+) 1408.3682, found 1408.3579.

IV-Reference:

(1) Huang, C.; Li, S.; Thakellapalli, H.; Farajidizaji, B.; Huang, Y.; Akhmedov, N. G.; Popp, B. V.; Petersen, J. L.; Wang, K. K. *J. Org. Chem.* **2017**, *82*, 1166–1174

(2) Huang, C.; Huang, Y.; Akhmedov, N. G.; Popp, B. V.; Petersen, J. L.; Wang, K. K. *Org. Lett*. **2014**, *16*, 2672–2675

(3) Farajidizaji, B.; Thakellapalli, H.; Li, S.; Huang, C.; Baughman, N. N.; Akhmedov, N. G.; Popp, B. V.; Petersen, J. L.; Wang, K. K. *Chem. Eur. J.* **2016**, *22*, 16420–16424

(4) Klapars, A.; Buchwald, S. L. *J. Am. Chem. Soc.* **2002**, *124*, 14844–14845

(5) Sakamoto Y.; Suzuki, T. *J. Am. Chem. Soc*. **2013**, *135*, 14074−14077

Description of the X-ray Structural Analysis of II-7b ($C_{40}H_{56}Br_2O_2Si_2$)

A colorless crystal of **II-7b** ($C_{40}H_{56}Br_2O_2Si_2$) was covered in a polybutene oil (Sigma-Aldrich) and placed on the end of a MiTeGen loop. The sample was cooled to 100 K with an Oxford Cryostream 700 system and optically aligned on a Bruker AXS D8 Venture fixed-chi X-ray diffractometer equipped with a Triumph monochromator, a Mo Kα radiation source (λ = 0.71073 Å), and a PHOTON 100 CMOS detector. Two sets of 12 frames each were collected using the omega scan method with a 10 s exposure time. Integration of these frames followed by reflection indexing and least-squares refinement produced a crystal orientation matrix for the orthorhombic crystal lattice.

Data collection consisted of the measurement of a total of 372 frames in one run using omega scans with the detector held at 5.00 cm from the crystal. Frame scan parameters are summarized in Table II-1-1 below:

Table II-1-1. Data collection details for **II-7b** ($C_{40}H_{56}Br_2O_2Si_2$)

Run	2θ	ω	φ	χ	Scan Width (°)	Frames	Exposure Time (sec)
1	17.45	-165.55	-10.76	54.79	0.50	372	10.00

The APEX2 software program (version 2014.1-7)[S3] was used for diffractometer control, preliminary frame scans, indexing, orientation matrix calculations, least-squares refinement of cell parameters, and the data collection. The frames were integrated with the Bruker SAINT software package using a narrow-frame algorithm. The integration of the data using an orthorhombic unit cell yielded a total of 44750 reflections to a maximum θ angle of 30.08° (0.71 Å resolution), of

which 22472 were independent (average redundancy 1.991, completeness = 99.3%, R_{int} = 2.63%, R_{sig} = 7.47%) and 18241 (81.17%) were greater than $2\sigma(F^2)$. The final cell constants of a = 14.9169(6) Å, b = 18.4373(8) Å, c = 28.4266(12) Å, volume = 7818.1(6) $Å^3$, are based upon the refinement of the XYZ-centroids of 9986 reflections above 20 σ(I) with 5.934° < 2θ < 59.52°. Data were corrected for absorption effects using the multi-scan method (SADABS). The ratio of minimum to maximum apparent transmission was 0.682. The calculated minimum and maximum transmission coefficients (based on crystal size) are 0.340 and 0.543.

The structure was solved by direct methods and difference Fourier analysis using the programs provided by SHELXL-2013.[S4] The crystallographic asymmetric contains two independent **II-7b** ($C_{40}H_{56}Br_2O_2Si_2$) molecules. Idealized positions for the hydrogen atoms were included as fixed contributions using a riding model with isotropic temperature factors set at 1.2 times (aromatic and methine hydrogens) or 1.5 (methyl hydrogens) times that of the adjacent carbon atom. The positions of the methyl hydrogen atoms were optimized by a rigid rotating group refinement with idealized angles. Full-matrix least-squares refinement, based upon the minimization of $\Sigma w_i |F_o^2 - F_c^2|^2$, with weighting $w_i^{-1} = [\sigma^2(F_o^2) + (0.0\ P)^2 + 0.0\ P]$, where $P = (\text{Max}(F_o^2, 0) + 2\ F_c^2)/3$.[S4] The final anisotropic full-matrix least-squares refinement on F^2 with 853 variables converged at R1 = 3.61% for 18241 observed data with I>2σ(I) and wR2 = 6.59 % for all data. The goodness-of-fit was 0.945.[S5]

A correction for secondary extinction was not applied. The value of the Flack parameter was 0.006(2). The largest peak in the final difference electron density synthesis was 1.086 $e^-/Å^3$ and the largest hole was -0.461 $e^-/Å^3$ with an RMS deviation of 0.073 $e^-/Å^3$. The linear absorption coefficient, atomic scattering factors, and anomalous dispersion corrections were calculated from values found in the International Tables of X-ray Crystallography.[S6]

Table II-1-2. Crystal data for **II-7b** ($C_{40}H_{56}Br_2O_2Si_2$).

Identification code	kw25cms	
Chemical formula	$C_{40}H_{56}Br_2O_2Si_2$	
Formula weight	784.84 g/mol	
Temperature	100(2) K	
Wavelength	0.71073 Å	
Crystal size	0.321 x 0.331 x 0.634 mm	
Crystal system	orthorhombic	
Space group	P $2_12_12_1$ (No. 19)	
Unit cell dimensions	a = 14.9169(6) Å	α = 90°
	b = 18.4373(8) Å	β = 90°
	c = 28.4266(12) Å	γ = 90°
Volume	7818.1(6) $Å^3$	
Z	8	
Density (calculated)	1.334 g/cm^3	
Absorption coefficient	2.167 mm^{-1}	
F(000)	3280	

Table II-1-3. Data collection and structure refinement for **II-7b** ($C_{40}H_{56}Br_2O_2Si_2$).

Theta range used for refinement	2.97 to 30.08°
Index ranges	$-21 \leq h \leq 21$, $-25 \leq k \leq 18$, $-40 \leq l \leq 27$
Reflections collected	44750
Independent reflections	22472 [R(int) = 0.0263]
Coverage of independent reflections	99.3%
Absorption correction	multi-scan
Max. and min. trans.	0.543 and 0.340
Refinement method	Full-matrix least-squares on F^2
Refinement program	SHELXL-2013 (Sheldrick, 2013)
Data / restraints / parameters	22472 / 0 / 853
Goodness-of-fit on F^2	0.945

Final R indices	18241 data; I>2σ(I)	R1 = 0.0361, wR2 = 0.0622
	all data	R1 = 0.0530, wR2 = 0.0659
Largest diff. peak and hole	1.086 and -0.461 $e^-/Å^3$	

Table II-1-4. Atomic coordinates and equivalent isotropic atomic displacement parameters ($Å^2$) for **II-7b (**$C_{40}H_{56}Br_2O_2Si_2$). U(eq) is defined as one third of the trace of the orthogonalized U_{ij} tensor.

	x/a	y/b	z/c	U(eq)
Br1	0.25772(2)	0.85986(2)	0.76772(2)	0.02229(7)
Br2	0.80604(3)	0.54554(2)	0.72114(2)	0.04200(11)
Br3	0.28809(2)	0.99985(2)	0.50861(2)	0.03717(10)
Br4	0.79471(2)	0.70661(2)	0.45823(2)	0.02148(7)
Si1	0.99323(6)	0.12366(4)	0.59293(3)	0.01441(17)
Si2	0.60568(5)	0.86471(4)	0.61309(3)	0.01153(16)
Si3	0.00730(5)	0.29935(4)	0.35599(3)	0.01232(16)
Si4	0.61191(5)	0.03403(4)	0.34311(3)	0.01264(16)
O1	0.99856(13)	0.03983(10)	0.61539(7)	0.0170(4)
O2	0.71455(12)	0.84801(9)	0.62114(6)	0.0134(4)
O3	0.99819(13)	0.21473(10)	0.37632(7)	0.0164(4)
O4	0.71145(13)	0.02479(10)	0.36955(6)	0.0148(4)
C1	0.92794(18)	0.99176(15)	0.61924(10)	0.0135(6)
C2	0.93991(18)	0.92074(15)	0.60292(9)	0.0115(6)
C3	0.03193(19)	0.89639(16)	0.58622(10)	0.0135(6)
C4	0.0271(2)	0.82868(16)	0.55684(10)	0.0169(6)
C5	0.95655(19)	0.78547(16)	0.55513(10)	0.0155(6)
C6	0.87045(18)	0.79815(15)	0.58152(9)	0.0110(5)
C7	0.86642(18)	0.87333(14)	0.60332(9)	0.0109(6)
C8	0.78446(18)	0.89656(14)	0.62185(9)	0.0119(6)
C9	0.77550(19)	0.96575(15)	0.64016(10)	0.0165(6)
C10	0.84720(19)	0.01300(15)	0.63866(10)	0.0168(6)
C11	0.9008(2)	0.12638(16)	0.54823(11)	0.0241(7)
C12	0.8816(3)	0.2020(2)	0.52771(13)	0.0409(10)
C13	0.9137(3)	0.0709(2)	0.50893(12)	0.0380(9)

	x/a	y/b	z/c	U(eq)
C14	0.9744(2)	0.19236(17)	0.64129(12)	0.0256(8)
C15	0.0255(3)	0.1737(3)	0.68633(13)	0.0533(12)
C16	0.8768(3)	0.2087(2)	0.65456(14)	0.0418(10)
C17	0.1074(2)	0.13411(17)	0.56603(11)	0.0236(7)
C18	0.1163(3)	0.1978(2)	0.53154(13)	0.0418(10)
C19	0.1841(2)	0.1376(2)	0.60170(13)	0.0356(9)
C20	0.5573(2)	0.77224(16)	0.60260(10)	0.0166(6)
C21	0.5764(2)	0.72046(16)	0.64372(11)	0.0233(7)
C22	0.5908(2)	0.73739(17)	0.55694(11)	0.0251(7)
C23	0.5945(2)	0.92880(16)	0.56172(10)	0.0188(6)
C24	0.6646(2)	0.91762(19)	0.52241(11)	0.0278(8)
C25	0.4993(2)	0.9290(2)	0.54125(13)	0.0343(9)
C26	0.5556(2)	0.90705(15)	0.66765(10)	0.0158(6)
C27	0.4547(2)	0.89203(17)	0.67261(12)	0.0249(7)
C28	0.6051(2)	0.88688(17)	0.71307(10)	0.0233(7)
C29	0.09324(18)	0.88467(15)	0.62871(10)	0.0129(6)
C30	0.1600(2)	0.93417(16)	0.64014(10)	0.0168(6)
C31	0.2106(2)	0.92642(15)	0.68088(10)	0.0170(6)
C32	0.19448(19)	0.86839(15)	0.71001(9)	0.0151(6)
C33	0.1317(2)	0.81636(15)	0.69855(11)	0.0173(6)
C34	0.0822(2)	0.82462(15)	0.65781(11)	0.0174(6)
C35	0.85423(18)	0.73683(15)	0.61653(10)	0.0129(6)
C36	0.86335(19)	0.74644(16)	0.66458(10)	0.0162(6)
C37	0.8488(2)	0.69033(16)	0.69581(11)	0.0205(7)
C38	0.8248(2)	0.62334(16)	0.67859(12)	0.0224(7)
C39	0.8154(2)	0.61153(16)	0.63085(12)	0.0234(7)
C40	0.8300(2)	0.66830(16)	0.60032(11)	0.0195(7)
C41	0.92671(19)	0.16676(15)	0.37758(10)	0.0130(6)
C42	0.93944(19)	0.09683(15)	0.35935(9)	0.0116(6)
C43	0.03276(19)	0.07404(15)	0.34328(10)	0.0141(6)
C44	0.0305(2)	0.00820(16)	0.31208(10)	0.0165(6)
C45	0.96073(19)	0.96470(16)	0.30862(10)	0.0150(6)
C46	0.87218(19)	0.97589(14)	0.33333(10)	0.0126(6)
C47	0.86608(18)	0.04941(15)	0.35684(9)	0.0116(6)
C48	0.78243(19)	0.07175(14)	0.37366(9)	0.0133(6)

	x/a	y/b	z/c	U(eq)
C49	0.77278(18)	0.13924(15)	0.39488(9)	0.0143(6)
C50	0.84480(19)	0.18662(15)	0.39671(10)	0.0143(6)
C51	0.8967(2)	0.33419(15)	0.33306(10)	0.0167(6)
C52	0.9034(2)	0.41447(16)	0.31857(12)	0.0272(8)
C53	0.8496(2)	0.29080(18)	0.29446(11)	0.0264(7)
C54	0.0446(2)	0.35726(17)	0.40647(10)	0.0204(7)
C55	0.1312(2)	0.32866(19)	0.42932(11)	0.0309(8)
C56	0.9711(2)	0.3669(2)	0.44328(11)	0.0338(9)
C57	0.0995(2)	0.29567(16)	0.31075(10)	0.0160(6)
C58	0.0661(2)	0.26499(16)	0.26355(10)	0.0205(7)
C59	0.1488(2)	0.36790(17)	0.30281(11)	0.0230(7)
C60	0.6317(2)	0.06813(18)	0.28141(10)	0.0234(7)
C61	0.6761(3)	0.1428(2)	0.27967(11)	0.0381(9)
C62	0.5474(3)	0.0674(2)	0.25006(12)	0.0370(9)
C63	0.5634(2)	0.94012(16)	0.34242(12)	0.0223(7)
C64	0.5746(2)	0.90066(17)	0.38971(13)	0.0333(9)
C65	0.5996(3)	0.89287(18)	0.30270(13)	0.0356(9)
C66	0.5403(2)	0.09849(16)	0.37792(11)	0.0188(7)
C67	0.5439(3)	0.08676(19)	0.43136(11)	0.0329(9)
C68	0.4427(2)	0.0995(2)	0.36186(14)	0.0355(9)
C69	0.09399(18)	0.05895(15)	0.38515(10)	0.0147(6)
C70	0.1639(2)	0.10502(17)	0.39731(11)	0.0202(7)
C71	0.2212(2)	0.08841(17)	0.43433(11)	0.0251(7)
C72	0.2076(2)	0.02537(16)	0.45928(10)	0.0205(6)
C73	0.1387(2)	0.97897(17)	0.44854(11)	0.0227(7)
C74	0.0831(2)	0.99568(16)	0.41133(11)	0.0199(7)
C75	0.85312(19)	0.91133(15)	0.36583(10)	0.0125(6)
C76	0.85962(19)	0.91496(15)	0.41445(10)	0.0147(6)
C77	0.84343(19)	0.85455(16)	0.44221(10)	0.0161(6)
C78	0.81885(18)	0.79013(16)	0.42099(10)	0.0156(6)
C79	0.81108(19)	0.78458(15)	0.37272(10)	0.0171(6)
C80	0.82868(19)	0.84548(15)	0.34558(10)	0.0156(6)

Table II-1-5. Interatomic distances (Å) for **II-7b** ($C_{40}H_{56}Br_2O_2Si_2$).

Br1-C32	1.899(3)	Br2-C38	1.897(3)
Br3-C72	1.905(3)	Br4-C78	1.903(3)
Si1-O1	1.674(2)	Si1-C11	1.875(3)
Si1-C17	1.876(3)	Si1-C14	1.890(3)
Si2-O2	1.669(2)	Si2-C20	1.875(3)
Si2-C23	1.886(3)	Si2-C26	1.890(3)
Si3-O3	1.669(2)	Si3-C54	1.873(3)
Si3-C57	1.884(3)	Si3-C51	1.887(3)
Si4-O4	1.673(2)	Si4-C63	1.877(3)
Si4-C66	1.880(3)	Si4-C60	1.886(3)
O1-C1	1.381(3)	O2-C8	1.374(3)
O3-C41	1.386(3)	O4-C48	1.373(3)
C1-C10	1.382(4)	C1-C2	1.401(4)
C2-C7	1.402(4)	C2-C3	1.520(4)
C3-C4	1.504(4)	C3-C29	1.530(4)
C4-C5	1.321(4)	C5-C6	1.506(4)
C6-C7	1.519(4)	C6-C35	1.526(4)
C7-C8	1.399(4)	C8-C9	1.384(4)
C9-C10	1.380(4)	C11-C13	1.527(5)
C11-C12	1.538(5)	C14-C15	1.530(5)
C14-C16	1.534(5)	C17-C19	1.530(5)
C17-C18	1.535(5)	C20-C22	1.532(4)
C20-C21	1.536(4)	C23-C25	1.534(4)
C23-C24	1.545(4)	C26-C28	1.533(4)
C26-C27	1.537(4)	C29-C30	1.389(4)
C29-C34	1.392(4)	C30-C31	1.390(4)
C31-C32	1.374(4)	C32-C33	1.380(4)
C33-C34	1.381(4)	C35-C36	1.384(4)
C35-C40	1.393(4)	C36-C37	1.380(4)
C37-C38	1.376(4)	C38-C39	1.382(4)
C39-C40	1.377(4)	C41-C50	1.387(4)
C41-C42	1.402(4)	C42-C47	1.402(4)
C42-C43	1.524(4)	C43-C44	1.504(4)

C43-C69	1.526(4)	C44-C45	1.318(4)
C45-C46	1.510(4)	C46-C47	1.514(4)
C46-C75	1.533(4)	C47-C48	1.398(4)
C48-C49	1.390(4)	C49-C50	1.386(4)
C51-C53	1.529(4)	C51-C52	1.540(4)
C54-C56	1.527(4)	C54-C55	1.539(4)
C57-C59	1.538(4)	C57-C58	1.539(4)
C60-C61	1.528(5)	C60-C62	1.541(4)
C63-C65	1.525(5)	C63-C64	1.538(5)
C66-C68	1.526(4)	C66-C67	1.535(4)
C69-C70	1.389(4)	C69-C74	1.393(4)
C70-C71	1.389(4)	C71-C72	1.376(4)
C72-C73	1.373(4)	C73-C74	1.379(4)
C75-C76	1.387(4)	C75-C80	1.392(4)
C76-C77	1.386(4)	C77-C78	1.382(4)
C78-C79	1.381(4)	C79-C80	1.387(4)

Table II-1-6. Bond angles (°) for **II-7b** ($C_{40}H_{56}Br_2O_2Si_2$).

O1-Si1-C11	108.54(12)	O1-Si1-C17	101.96(13)
C11-Si1-C17	112.84(15)	O1-Si1-C14	110.39(13)
C11-Si1-C14	111.43(15)	C17-Si1-C14	111.26(15)
O2-Si2-C20	103.22(12)	O2-Si2-C23	107.94(12)
C20-Si2-C23	114.35(14)	O2-Si2-C26	110.38(12)
C20-Si2-C26	110.73(13)	C23-Si2-C26	109.98(13)
O3-Si3-C54	106.96(12)	O3-Si3-C57	105.19(12)
C54-Si3-C57	109.05(14)	O3-Si3-C51	111.50(11)
C54-Si3-C51	109.30(13)	C57-Si3-C51	114.51(13)
O4-Si4-C63	104.65(12)	O4-Si4-C66	109.41(12)
C63-Si4-C66	111.69(14)	O4-Si4-C60	108.22(12)
C63-Si4-C60	110.99(15)	C66-Si4-C60	111.58(14)
C1-O1-Si1	125.91(18)	C8-O2-Si2	128.34(17)
C41-O3-Si3	131.92(17)	C48-O4-Si4	131.20(17)
O1-C1-C10	121.0(3)	O1-C1-C2	118.5(2)

C10-C1-C2	120.6(3)	C1-C2-C7	118.7(2)
C1-C2-C3	119.6(2)	C7-C2-C3	121.6(2)
C4-C3-C2	112.1(2)	C4-C3-C29	110.5(2)
C2-C3-C29	109.6(2)	C5-C4-C3	124.0(3)
C4-C5-C6	124.6(3)	C5-C6-C7	112.2(2)
C5-C6-C35	110.2(2)	C7-C6-C35	113.8(2)
C8-C7-C2	119.7(2)	C8-C7-C6	117.9(2)
C2-C7-C6	122.3(2)	O2-C8-C9	122.2(2)
O2-C8-C7	117.3(2)	C9-C8-C7	120.5(3)
C10-C9-C8	119.7(3)	C9-C10-C1	120.6(3)
C13-C11-C12	110.7(3)	C13-C11-Si1	112.7(2)
C12-C11-Si1	114.7(2)	C15-C14-C16	108.2(3)
C15-C14-Si1	112.6(2)	C16-C14-Si1	116.9(2)
C19-C17-C18	109.0(3)	C19-C17-Si1	114.4(2)
C18-C17-Si1	114.7(2)	C22-C20-C21	108.9(2)
C22-C20-Si2	113.0(2)	C21-C20-Si2	111.9(2)
C25-C23-C24	110.6(3)	C25-C23-Si2	112.2(2)
C24-C23-Si2	114.6(2)	C28-C26-C27	110.5(3)
C28-C26-Si2	113.6(2)	C27-C26-Si2	112.8(2)
C30-C29-C34	117.9(3)	C30-C29-C3	121.3(2)
C34-C29-C3	120.7(3)	C29-C30-C31	121.1(3)
C32-C31-C30	119.2(3)	C31-C32-C33	121.2(3)
C31-C32-Br1	119.9(2)	C33-C32-Br1	118.9(2)
C32-C33-C34	118.9(3)	C33-C34-C29	121.5(3)
C36-C35-C40	117.9(3)	C36-C35-C6	122.2(3)
C40-C35-C6	119.8(3)	C37-C36-C35	121.6(3)
C38-C37-C36	119.0(3)	C37-C38-C39	121.2(3)
C37-C38-Br2	119.4(2)	C39-C38-Br2	119.5(2)
C40-C39-C38	118.9(3)	C39-C40-C35	121.5(3)
O3-C41-C50	121.3(2)	O3-C41-C42	118.2(2)
C50-C41-C42	120.5(3)	C47-C42-C41	119.1(3)
C47-C42-C43	121.7(2)	C41-C42-C43	119.2(2)
C44-C43-C42	112.3(2)	C44-C43-C69	109.0(2)
C42-C43-C69	111.3(2)	C45-C44-C43	123.6(3)
C44-C45-C46	125.0(3)	C45-C46-C47	112.3(2)
C45-C46-C75	109.6(2)	C47-C46-C75	114.7(2)

C48-C47-C42	119.7(3)	C48-C47-C46	117.9(2)
C42-C47-C46	122.3(2)	O4-C48-C49	121.4(2)
O4-C48-C47	118.2(2)	C49-C48-C47	120.3(3)
C50-C49-C48	120.0(3)	C49-C50-C41	120.1(3)
C53-C51-C52	109.9(3)	C53-C51-Si3	118.2(2)
C52-C51-Si3	111.3(2)	C56-C54-C55	110.7(3)
C56-C54-Si3	112.2(2)	C55-C54-Si3	112.2(2)
C59-C57-C58	110.2(2)	C59-C57-Si3	114.7(2)
C58-C57-Si3	111.8(2)	C61-C60-C62	110.0(3)
C61-C60-Si4	113.5(2)	C62-C60-Si4	114.0(2)
C65-C63-C64	109.8(3)	C65-C63-Si4	113.4(2)
C64-C63-Si4	112.7(2)	C68-C66-C67	109.4(3)
C68-C66-Si4	113.1(2)	C67-C66-Si4	114.3(2)
C70-C69-C74	117.8(3)	C70-C69-C43	122.2(3)
C74-C69-C43	120.0(3)	C69-C70-C71	121.0(3)
C72-C71-C70	119.1(3)	C73-C72-C71	121.4(3)
C73-C72-Br3	118.8(2)	C71-C72-Br3	119.7(2)
C72-C73-C74	118.8(3)	C73-C74-C69	121.8(3)
C76-C75-C80	118.2(3)	C76-C75-C46	123.4(3)
C80-C75-C46	118.5(2)	C77-C76-C75	121.1(3)
C78-C77-C76	119.2(3)	C79-C78-C77	121.3(3)
C79-C78-Br4	118.5(2)	C77-C78-Br4	120.2(2)
C78-C79-C80	118.5(3)	C79-C80-C75	121.7(3)

Table II-1-7. Anisotropic atomic displacement parameters ($Å^2$) for **II-7b** ($C_{40}H_{56}Br_2O_2Si_2$). The anisotropic atomic displacement factor exponent takes the form: $-2\pi^2[h^2 a^{*2} U_{11} + ... + 2 h k a^* b^* U_{12}]$.

	U_{11}	U_{22}	U_{33}	U_{23}	U_{13}	U_{12}
Br1	0.02273(16)	0.02355(15)	0.02061(15)	0.00128(13)	-0.0082(1)	0.00270(13)
Br2	0.0465(2)	0.02119(17)	0.0583(3)	0.02059(17)	0.0253(2)	0.00837(17)
Br3	0.0334(2)	0.0416(2)	0.0365(2)	-0.0053(2)	-0.0231(2)	0.01011(18)
Br4	0.02308(16)	0.01783(15)	0.02354(16)	0.00643(13)	-0.0004(1)	-0.0032(1)

	U_{11}	U_{22}	U_{33}	U_{23}	U_{13}	U_{12}
Si1	0.0157(4)	0.0124(4)	0.0151(4)	0.0008(3)	-0.0003(3)	-0.0031(3)
Si2	0.0104(4)	0.0115(4)	0.0128(4)	0.0001(3)	0.0009(3)	0.0006(3)
Si3	0.0151(4)	0.0100(4)	0.0119(4)	-0.0007(3)	-0.0014(3)	-0.0005(3)
Si4	0.0123(4)	0.0118(4)	0.0138(4)	0.0004(3)	-0.0013(3)	0.0012(3)
O1	0.0131(10)	0.0140(10)	0.0238(11)	0.0030(9)	-0.0036(9)	-0.0046(8)
O2	0.0106(9)	0.0097(9)	0.0199(10)	-0.0005(8)	0.0008(8)	-0.0013(8)
O3	0.0139(10)	0.0109(10)	0.0245(11)	0.0042(9)	-0.0036(9)	-0.0013(8)
O4	0.0131(10)	0.0129(9)	0.0182(10)	0.0021(8)	-0.0039(8)	-0.0011(8)
C1	0.0139(14)	0.0147(14)	0.0120(13)	0.0027(12)	-0.0024(11)	-0.0045(12)
C2	0.0095(13)	0.0158(14)	0.0093(13)	0.0027(12)	0.0011(11)	-0.0003(11)
C3	0.0129(14)	0.0149(14)	0.0125(14)	0.0008(12)	0.0004(11)	-0.0031(11)
C4	0.0141(15)	0.0264(17)	0.0102(14)	-0.0027(13)	0.0015(11)	0.0032(12)
C5	0.0156(14)	0.0200(15)	0.0108(13)	-0.0047(12)	0.0001(11)	0.0032(12)
C6	0.0117(13)	0.0130(13)	0.0084(13)	-0.0022(12)	-0.0012(10)	0.0005(11)
C7	0.0133(13)	0.0091(13)	0.0103(13)	-0.0001(11)	-0.0012(11)	-0.0014(11)
C8	0.0116(13)	0.0117(13)	0.0125(13)	0.0013(11)	0.0012(11)	-0.0020(11)
C9	0.0142(15)	0.0146(14)	0.0205(15)	-0.0013(13)	0.0026(12)	0.0022(12)
C10	0.0176(15)	0.0097(14)	0.0230(16)	-0.0019(13)	-0.0005(12)	0.0015(12)
C11	0.0266(17)	0.0208(16)	0.0250(17)	0.0043(15)	-0.0075(14)	-0.0025(14)
C12	0.051(3)	0.035(2)	0.036(2)	0.0102(19)	-0.0120(19)	0.006(2)
C13	0.052(3)	0.040(2)	0.0219(18)	-0.0008(17)	-0.0129(18)	-0.0005(19)
C14	0.0316(19)	0.0181(16)	0.0272(18)	-0.0064(15)	0.0077(15)	-0.0067(14)
C15	0.062(3)	0.076(3)	0.022(2)	-0.016(2)	-0.001(2)	-0.002(3)
C16	0.043(2)	0.0280(19)	0.055(3)	-0.018(2)	0.017(2)	-0.0042(18)
C17	0.0236(17)	0.0196(16)	0.0275(17)	-0.0001(15)	0.0062(14)	-0.0059(14)
C18	0.042(2)	0.040(2)	0.044(2)	0.0119(19)	0.0218(19)	-0.0072(19)
C19	0.0206(18)	0.0333(19)	0.053(2)	-0.0083(19)	0.0006(16)	-0.0071(16)
C20	0.0104(14)	0.0180(15)	0.0213(16)	-0.0036(13)	-0.0007(12)	-0.0029(12)
C21	0.0289(18)	0.0156(16)	0.0254(17)	-0.0005(14)	0.0069(14)	-0.0045(13)
C22	0.0318(19)	0.0224(17)	0.0210(17)	-0.0074(14)	-0.0039(15)	-0.0010(15)
C23	0.0181(16)	0.0179(15)	0.0204(15)	0.0062(13)	0.0001(13)	0.0027(12)
C24	0.0276(18)	0.036(2)	0.0198(17)	0.0103(15)	0.0054(14)	0.0022(15)
C25	0.0232(18)	0.046(2)	0.0335(19)	0.0204(19)	-0.0009(16)	0.0075(16)
C26	0.0174(15)	0.0115(14)	0.0185(15)	0.0001(12)	0.0061(12)	0.0001(12)

	U_{11}	U_{22}	U_{33}	U_{23}	U_{13}	U_{12}
C27	0.0217(17)	0.0207(16)	0.0322(19)	-0.0006(15)	0.0094(15)	0.0023(14)
C28	0.0270(18)	0.0260(17)	0.0169(15)	-0.0037(14)	0.0060(14)	-0.0007(14)
C29	0.0090(13)	0.0158(14)	0.0139(14)	-0.0002(12)	0.0023(11)	0.0020(11)
C30	0.0156(15)	0.0163(15)	0.0186(15)	0.0020(13)	-0.0003(12)	-0.0012(12)
C31	0.0156(14)	0.0140(14)	0.0213(15)	-0.0010(12)	-0.0026(13)	-0.0025(12)
C32	0.0143(14)	0.0186(14)	0.0125(13)	-0.0050(12)	-0.0033(11)	0.0043(12)
C33	0.0177(15)	0.0135(14)	0.0206(16)	0.0036(13)	0.0003(13)	0.0008(12)
C34	0.0129(15)	0.0159(15)	0.0233(16)	0.0008(13)	-0.0026(12)	-0.0032(12)
C35	0.0079(13)	0.0131(14)	0.0176(15)	-0.0016(12)	-0.0010(11)	0.0011(11)
C36	0.0164(15)	0.0142(15)	0.0181(15)	-0.0015(12)	-0.0003(12)	0.0003(12)
C37	0.0207(16)	0.0225(17)	0.0183(16)	0.0041(13)	0.0035(13)	0.0045(13)
C38	0.0170(16)	0.0141(15)	0.0360(19)	0.0120(14)	0.0086(14)	0.0044(12)
C39	0.0200(16)	0.0108(14)	0.0394(19)	-0.0038(14)	-0.0008(15)	0.0010(12)
C40	0.0182(16)	0.0160(15)	0.0244(16)	-0.0040(13)	-0.0021(13)	0.0020(12)
C41	0.0128(14)	0.0128(14)	0.0133(14)	0.0042(12)	-0.0028(11)	-0.0001(11)
C42	0.0148(14)	0.0130(14)	0.0071(13)	0.0025(11)	-0.0011(11)	0.0008(11)
C43	0.0154(14)	0.0122(14)	0.0147(14)	0.0039(12)	0.0009(12)	0.0018(11)
C44	0.0197(15)	0.0211(16)	0.0089(13)	0.0008(12)	0.0032(11)	0.0025(13)
C45	0.0202(15)	0.0154(14)	0.0095(13)	-0.0001(12)	-0.0009(12)	0.0052(12)
C46	0.0160(14)	0.0123(14)	0.0096(13)	0.0018(11)	-0.0024(11)	-0.0003(11)
C47	0.0149(14)	0.0114(13)	0.0086(13)	0.0019(11)	-0.0026(11)	-0.0004(11)
C48	0.0158(14)	0.0125(13)	0.0116(13)	0.0040(11)	-0.0027(11)	-0.0015(11)
C49	0.0138(14)	0.0155(14)	0.0137(13)	0.0019(12)	-0.0005(11)	0.0023(12)
C50	0.0171(15)	0.0113(14)	0.0145(14)	-0.0010(12)	-0.0028(12)	0.0019(11)
C51	0.0161(15)	0.0136(14)	0.0203(15)	0.0025(13)	0.0000(13)	0.0002(12)
C52	0.0242(18)	0.0191(16)	0.038(2)	0.0076(16)	-0.0020(16)	0.0065(14)
C53	0.0233(17)	0.0265(17)	0.0294(18)	0.0039(16)	-0.0099(14)	0.0000(15)
C54	0.0312(18)	0.0157(15)	0.0143(15)	-0.0020(13)	-0.0045(13)	-0.0040(14)
C55	0.037(2)	0.036(2)	0.0197(17)	-0.0002(16)	-0.0077(16)	-0.0035(17)
C56	0.045(2)	0.039(2)	0.0172(16)	-0.0115(16)	0.0038(16)	-0.0013(18)
C57	0.0185(15)	0.0158(14)	0.0138(14)	0.0016(13)	-0.0012(12)	0.0023(13)
C58	0.0289(17)	0.0193(15)	0.0132(15)	0.0016(13)	-0.0014(13)	-0.0001(13)
C59	0.0210(16)	0.0263(17)	0.0218(16)	0.0009(15)	-0.0008(13)	-0.0056(14)
C60	0.0229(17)	0.0321(18)	0.0154(15)	0.0015(14)	-0.0012(13)	0.0028(14)

	U_{11}	U_{22}	U_{33}	U_{23}	U_{13}	U_{12}
C61	0.047(2)	0.047(2)	0.0211(17)	0.0156(17)	-0.0056(16)	-0.0130(19)
C62	0.037(2)	0.051(2)	0.0228(18)	0.0083(18)	-0.0102(16)	0.0013(19)
C63	0.0150(15)	0.0155(15)	0.0364(19)	-0.0031(15)	-0.0080(14)	0.0005(13)
C64	0.037(2)	0.0145(16)	0.049(2)	0.0071(17)	0.0002(18)	-0.0073(15)
C65	0.042(2)	0.0197(17)	0.045(2)	-0.0117(17)	-0.0149(19)	0.0056(16)
C66	0.0175(15)	0.0154(15)	0.0234(16)	0.0005(13)	0.0024(13)	0.0012(12)
C67	0.044(2)	0.0283(19)	0.0264(19)	-0.0033(16)	0.0149(17)	-0.0012(17)
C68	0.0185(18)	0.035(2)	0.053(2)	-0.0126(19)	0.0016(17)	0.0086(16)
C69	0.0114(14)	0.0166(15)	0.0161(14)	-0.0043(13)	0.0018(12)	0.0048(12)
C70	0.0193(16)	0.0171(15)	0.0241(16)	0.0018(13)	0.0004(13)	-0.0042(13)
C71	0.0182(17)	0.0252(17)	0.0319(18)	-0.0051(15)	-0.0049(14)	-0.0044(13)
C72	0.0176(15)	0.0251(16)	0.0187(14)	-0.0038(13)	-0.0089(13)	0.0055(13)
C73	0.0254(17)	0.0215(16)	0.0212(17)	0.0052(14)	-0.0054(14)	-0.0005(13)
C74	0.0169(15)	0.0187(15)	0.0239(16)	0.0006(14)	-0.0053(13)	-0.0036(13)
C75	0.0127(14)	0.0124(14)	0.0123(14)	0.0000(12)	-0.0016(11)	0.0021(11)
C76	0.0167(15)	0.0135(14)	0.0138(14)	-0.0032(12)	-0.0031(12)	-0.0022(12)
C77	0.0175(14)	0.0196(15)	0.0113(13)	0.0000(13)	-0.0011(11)	0.0014(13)
C78	0.0119(14)	0.0149(14)	0.0198(15)	0.0054(13)	0.0003(12)	0.0010(12)
C79	0.0177(15)	0.0116(14)	0.0220(15)	-0.0043(12)	-0.0022(12)	0.0018(12)
C80	0.0178(15)	0.0173(15)	0.0116(13)	-0.0020(12)	0.0000(11)	0.0027(12)

Table II-1-8. Hydrogen atom coordinates and isotropic atomic displacement parameters ($Å^2$) for **II-7b** ($C_{40}H_{56}Br_2O_2Si_2$).

	x/a	y/b	z/c	U(eq)
H3	1.0581	0.9360	0.5665	0.016
H4	1.0779	0.8162	0.5384	0.02
H5	0.9604	0.7434	0.5359	0.019
H6	0.8209	0.7956	0.5579	0.013
H9	0.7203	0.9806	0.6537	0.02
H10	0.8410	1.0606	0.6511	0.02

	x/a	y/b	z/c	U(eq)
H11	0.8451	1.1116	0.5653	0.029
H12A	0.9312	1.2165	0.5072	0.061
H12B	0.8755	1.2371	0.5534	0.061
H12C	0.8259	1.2005	0.5095	0.061
H13A	0.8623	1.0727	0.4875	0.057
H13B	0.9184	1.0222	0.5226	0.057
H13C	0.9687	1.0822	0.4915	0.057
H14	1.0003	1.2391	0.6296	0.031
H15A	1.0151	1.2115	0.7099	0.08
H15B	1.0897	1.1705	0.6794	0.08
H15C	1.0043	1.1270	0.6985	0.08
H16A	0.8513	1.1671	0.6713	0.063
H16B	0.8419	1.2180	0.6260	0.063
H16C	0.8747	1.2516	0.6749	0.063
H17	1.1178	1.0892	0.5471	0.028
H18A	1.1014	1.2431	0.5477	0.063
H18B	1.0752	1.1906	0.5050	0.063
H18C	1.1781	1.2002	0.5198	0.063
H19A	1.2415	1.1318	0.5853	0.053
H19B	1.1770	1.0986	0.6248	0.053
H19C	1.1829	1.1845	0.6178	0.053
H20	0.4908	0.7777	0.6000	0.02
H21A	0.5534	0.6721	0.6362	0.035
H21B	0.5469	0.7386	0.6722	0.035
H21C	0.6413	0.7177	0.6491	0.035
H22A	0.6560	0.7314	0.5585	0.038
H22B	0.5754	0.7686	0.5302	0.038
H22C	0.5624	0.6899	0.5529	0.038
H23	0.6049	0.9786	0.5745	0.023
H24A	0.6585	0.8686	0.5094	0.042
H24B	0.7249	0.9237	0.5354	0.042
H24C	0.6548	0.9534	0.4974	0.042
H25A	0.4959	0.9642	0.5155	0.051
H25B	0.4564	0.9424	0.5659	0.051

	x/a	y/b	z/c	U(eq)
H25C	0.4848	0.8805	0.5293	0.051
H26	0.5621	0.9607	0.6639	0.019
H27A	0.4450	0.8400	0.6773	0.037
H27B	0.4237	0.9078	0.6440	0.037
H27C	0.4311	0.9188	0.6997	0.037
H28A	0.5772	0.9119	0.7397	0.035
H28B	0.6681	0.9016	0.7106	0.035
H28C	0.6017	0.8343	0.7179	0.035
H30	1.1712	0.9740	0.6198	0.02
H31	1.2557	0.9608	0.6885	0.02
H33	1.1226	0.7755	0.7184	0.021
H34	1.0397	0.7885	0.6495	0.021
H36	0.8800	0.7928	0.6763	0.019
H37	0.8553	0.6979	0.7287	0.025
H39	0.7992	0.5650	0.6193	0.028
H40	0.8234	0.6606	0.5675	0.023
H43	1.0592	0.1150	0.3249	0.017
H44	1.0822	-0.0026	0.2939	0.02
H45	0.9666	-0.0769	0.2891	0.018
H46	0.8249	-0.0249	0.3084	0.015
H49	0.7168	0.1529	0.4081	0.017
H50	0.8380	0.2328	0.4111	0.017
H51	0.8550	0.3332	0.3606	0.02
H52A	0.9428	0.4190	0.2911	0.041
H52B	0.9280	0.4428	0.3447	0.041
H52C	0.8436	0.4327	0.3106	0.041
H53A	0.7861	0.3044	0.2934	0.04
H53B	0.8548	0.2389	0.3012	0.04
H53C	0.8776	0.3014	0.2640	0.04
H54	1.0583	0.4064	0.3935	0.024
H55A	1.1492	0.3612	0.4549	0.046
H55B	1.1790	0.3267	0.4057	0.046
H55C	1.1206	0.2799	0.4419	0.046
H56A	0.9551	0.3195	0.4565	0.051

	x/a	y/b	z/c	U(eq)
H56B	0.9181	0.3887	0.4285	0.051
H56C	0.9928	0.3987	0.4685	0.051
H57	1.1452	0.2606	0.3229	0.019
H58A	1.0249	0.2997	0.2489	0.031
H58B	1.0349	0.2190	0.2690	0.031
H58C	1.1174	0.2568	0.2426	0.031
H59A	1.1980	0.3605	0.2805	0.035
H59B	1.1730	0.3854	0.3328	0.035
H59C	1.1068	0.4038	0.2901	0.035
H60	0.6751	0.0336	0.2666	0.028
H61A	0.6892	0.1555	0.2469	0.057
H61B	0.7320	0.1417	0.2978	0.057
H61C	0.6355	0.1790	0.2932	0.057
H62A	0.5075	0.1071	0.2594	0.056
H62B	0.5161	0.0210	0.2538	0.056
H62C	0.5650	0.0737	0.2171	0.056
H63	0.4975	-0.0545	0.3369	0.027
H64A	0.5504	-0.1486	0.3871	0.05
H64B	0.5420	-0.0729	0.4143	0.05
H64C	0.6383	-0.1017	0.3979	0.05
H65A	0.6641	-0.1148	0.3072	0.053
H65B	0.5894	-0.0829	0.2725	0.053
H65C	0.5687	-0.1540	0.3029	0.053
H66	0.5646	0.1482	0.3720	0.023
H67A	0.5177	0.1288	0.4473	0.049
H67B	0.6065	0.0810	0.4413	0.049
H67C	0.5100	0.0430	0.4396	0.049
H68A	0.4151	0.0523	0.3682	0.053
H68B	0.4401	0.1096	0.3280	0.053
H68C	0.4101	0.1374	0.3790	0.053
H70	1.1727	0.1486	0.3801	0.024
H71	1.2690	0.1201	0.4423	0.03
H73	1.1294	-0.0639	0.4664	0.027
H74	1.0361	-0.0368	0.4033	0.024

	x/a	y/b	z/c	U(eq)
H76	0.8754	-0.0404	0.4290	0.018
H77	0.8492	-0.1426	0.4754	0.019
H79	0.7941	-0.2599	0.3584	0.021
H80	0.8239	-0.1578	0.3123	0.019

Description of the X-ray Structural Analysis of II-12b ($C_{48}H_{60}Br_2O_4Si_2$)

A colorless crystal of **II-12b** ($C_{48}H_{60}Br_2O_4Si_2$) was covered in a polybutene oil (Sigma-Aldrich) and placed on the end of a MiTeGen loop. The sample was cooled to 100 K with an Oxford Cryostream 700 system and optically aligned on a Bruker AXS D8 Venture fixed-chi X-ray diffractometer equipped with a Triumph monochromator, a Mo Kα radiation source (λ = 0.71073 Å), and a PHOTON 100 CMOS detector. Two sets of 12 frames each were collected using the omega scan method with a 10 s exposure time. Integration of these frames followed by reflection indexing and least-squares refinement produced a crystal orientation matrix for the monoclinic crystal lattice.

Data collection consisted of the measurement of a total of 1224 frames in four runs using omega scans with the detector held at 5.00 cm from the crystal. Frame scan parameters are summarized in Table II-2-1 below:

Table II-2-1. Data collection details for **II-12b** ($C_{48}H_{60}Br_2O_4Si_2$).

Run	2θ	ω	φ	χ	Scan Width (°)	Frames	Exposure Time (sec)
1	16.35	-165.45	120.00	54.74	0.60	306	40.00
2	16.35	-165.45	-120.00	54.74	0.60	306	40.00
3	16.35	-165.45	0.00	54.74	0.60	306	40.00
4	16.35	-165.45	60.00	54.74	0.60	306	40.00

The APEX2 software program (version 2014.1-7)[S3] was used for diffractometer control, preliminary frame scans, indexing, orientation matrix calculations, least-squares refinement of cell parameters, and the data collection. The frames were integrated with the Bruker SAINT software package using a narrow-frame algorithm. The integration of the data using a monoclinic unit cell

yielded a total of 104359 reflections to a maximum θ angle of 30.13° (0.71 Å resolution), of which 13473 were independent (average redundancy 7.746, completeness = 99.6%, R_{int} = 3.72%, R_{sig} = 2.18%) and 11499 (85.35%) were greater than $2\sigma(F^2)$. The final cell constants of a = 14.1093(5) Å, b = 14.2735(6) Å, c = 22.7675(9) Å, β = 91.2285(12)°, volume = 4584.1(3) $Å^3$, are based upon the refinement of the XYZ-centroids of 9573 reflections above 20 σ(I) with 5.982° < 2θ < 60.19°. Data were corrected for absorption effects using the multi-scan method (SADABS). The ratio of minimum to maximum apparent transmission was 0.794. The calculated minimum and maximum transmission coefficients are 0.504 and 0.736.

The structure was solved by direct methods and difference Fourier analysis using the programs provided by SHELXL-2013.[S4] Idealized positions for the hydrogen atoms were included as fixed contributions using a riding model with isotropic temperature factors set at 1.2 times (aromatic and methine hydrogens) or 1.5 (methyl hydrogens) times that of the adjacent carbon atom. The positions of the methyl hydrogen atoms were optimized by a rigid rotating group refinement with idealized angles. Full-matrix least-squares refinement, based upon the minimization of $\Sigma w_i |F_o^2 - F_c^2|^2$, with weighting $w_i^{-1} = [\sigma^2(F_o^2) + (0.0461\ P)^2 + 3.6921\ P]$, where $P = (\text{Max}\ (F_o^2, 0) + 2\ F_c^2)/3$.[S4] The final anisotropic full-matrix least-squares refinement on F^2 with 517 variables converged at R1 = 3.59% for 11499 observed data with $I>2\sigma(I)$ and wR2 = 9.32% for all data. The goodness-of-fit was 1.039.[S5]

A correction for secondary extinction was not applied. The largest peak in the final difference electron density synthesis was 1.322 $e^-/Å^3$ and the largest hole was -0.364 $e^-/Å^3$ with an RMS deviation of 0.077 $e^-/Å^3$. The linear absorption coefficient, atomic scattering factors, and anomalous dispersion corrections were calculated from values found in the International Tables of X-ray Crystallography.[S6]

Table II-2-2. Crystal data for **II-12b** ($C_{48}H_{60}Br_2O_4Si_2$).

Identification code	kw22cms	
Chemical formula	$C_{48}H_{60}Br_2O_4Si_2$	
Formula weight	916.96 g/mol	
Temperature	100(2) K	
Wavelength	0.71073 Å	
Crystal size	0.175 x 0.304 x 0.427 mm	
Crystal system	orthorhombic	
Space group	P 2_1/c (No. 14)	
Unit cell dimensions	a = 14.1093(5) Å	α = 90°
	b = 14.2735(6) Å	β = 91.2285(12)°
	c = 22.7675(9) Å	γ = 90°
Volume	4584.1(3) $Å^3$	
Z	4	
Density (calculated)	1.329 g/cm^3	
Absorption coefficient	1.862 mm^{-1}	
F(000)	1912	

Table II-2-3. Data collection and structure refinement for **II-12b** ($C_{48}H_{60}Br_2O_4Si_2$).

Theta range used for refinement	2.73 to 30.13°
Index ranges	$-19 \leq h \leq 19$, $-20 \leq k \leq 20$, $-32 \leq l \leq 32$
Reflections collected	104359
Independent reflections	13473 [R(int) = 0.0372]
Coverage of independent reflections	99.6%
Absorption correction	multi-scan
Max. and min. trans.	0.736 and 0.504
Refinement method	Full-matrix least-squares on F^2
Refinement program	SHELXL-2013 (Sheldrick, 2013)
Data / restraints / parameters	13473 / 0 / 517

Goodness-of-fit on F^2	1.039	
Final R indices	11499 data; $I>2\sigma(I)$	R1 = 0.0359, wR2 = 0.0868
	all data	R1 = 0.0465, wR2 = 0.0932
Largest diff. peak and hole	1.322 and -0.364 $e^-/Å^3$	

Table II-2-4. Atomic coordinates and equivalent isotropic atomic displacement parameters ($Å^2$) for **II-12b** ($C_{48}H_{60}Br_2O_4Si_2$). U(eq) is defined as one third of the trace of the orthogonalized U_{ij} tensor.

	x/a	y/b	z/c	U(eq)
Br1	0.93875(2)	0.06168(2)	0.19997(2)	0.03394(6)
Br2	0.46991(2)	0.79674(2)	0.25357(2)	0.02820(5)
Si1	0.23397(3)	0.36900(3)	0.86604(2)	0.01370(8)
Si2	0.73548(3)	0.15148(3)	0.95280(2)	0.01389(8)
O1	0.31068(8)	0.37517(8)	0.92267(5)	0.0156(2)
O2	0.66733(8)	0.23811(8)	0.97680(5)	0.0154(2)
O3	0.04697(8)	0.20041(8)	0.15258(5)	0.0197(2)
O4	0.54503(8)	0.95443(8)	0.20546(5)	0.0175(2)
C1	0.39848(10)	0.33760(10)	0.93416(6)	0.0130(3)
C2	0.44166(10)	0.35990(10)	0.98866(6)	0.0105(2)
C3	0.39126(10)	0.42733(10)	0.02888(6)	0.0111(2)
C4	0.45382(11)	0.45871(10)	0.07989(6)	0.0133(3)
C5	0.53687(11)	0.42077(10)	0.09414(6)	0.0131(3)
C6	0.58367(10)	0.34429(10)	0.05966(6)	0.0110(2)
C7	0.53169(10)	0.32428(10)	0.00222(6)	0.0105(2)
C8	0.57820(10)	0.26774(10)	0.96128(6)	0.0133(3)
C9	0.53505(11)	0.24662(11)	0.90782(7)	0.0173(3)
C10	0.44490(11)	0.28111(12)	0.89444(7)	0.0174(3)
C11	0.27566(11)	0.45062(12)	0.80624(7)	0.0190(3)
C12	0.19973(13)	0.47247(16)	0.75914(8)	0.0296(4)
C13	0.36731(13)	0.42174(14)	0.77678(8)	0.0267(4)
C14	0.21927(12)	0.24485(12)	0.83964(8)	0.0218(3)
C15	0.22233(16)	0.17115(14)	0.88872(9)	0.0322(4)
C16	0.12930(15)	0.23228(15)	0.80123(9)	0.0320(4)

	x/a	y/b	z/c	U(eq)
C17	0.12335(11)	0.42082(12)	0.89711(7)	0.0182(3)
C18	0.07608(14)	0.35954(14)	0.94349(9)	0.0283(4)
C19	0.14245(12)	0.51850(13)	0.92313(8)	0.0233(3)
C20	0.82512(12)	0.14539(12)	0.01496(7)	0.0198(3)
C21	0.89557(14)	0.06343(15)	0.01454(9)	0.0320(4)
C22	0.87728(13)	0.23871(14)	0.02392(9)	0.0281(4)
C23	0.78329(12)	0.18441(12)	0.87870(7)	0.0196(3)
C24	0.78888(17)	0.29107(13)	0.86933(9)	0.0315(4)
C25	0.88036(13)	0.13944(14)	0.86658(8)	0.0253(4)
C26	0.66289(12)	0.04083(12)	0.94628(8)	0.0208(3)
C27	0.71178(13)	0.96527(13)	0.91032(10)	0.0286(4)
C28	0.63481(17)	0.00247(16)	0.00636(10)	0.0384(5)
C29	0.29939(10)	0.39085(10)	0.05467(6)	0.0121(3)
C30	0.27790(11)	0.29616(10)	0.05856(7)	0.0166(3)
C31	0.19853(11)	0.26562(11)	0.08831(7)	0.0181(3)
C32	0.13801(11)	0.32924(11)	0.11476(7)	0.0152(3)
C33	0.15705(11)	0.42508(11)	0.10903(7)	0.0181(3)
C34	0.23644(11)	0.45483(11)	0.07951(7)	0.0168(3)
C35	0.05708(11)	0.29633(11)	0.14771(7)	0.0167(3)
C36	0.98596(11)	0.33958(13)	0.17671(7)	0.0209(3)
C37	0.92809(12)	0.26727(14)	0.20081(7)	0.0234(3)
C38	0.96831(11)	0.18633(13)	0.18516(8)	0.0221(3)
C39	0.59494(10)	0.25661(10)	0.09752(6)	0.0114(2)
C40	0.52084(12)	0.19291(11)	0.10198(7)	0.0179(3)
C41	0.52883(12)	0.11453(11)	0.13802(7)	0.0179(3)
C42	0.61191(11)	0.09833(11)	0.17088(6)	0.0143(3)
C43	0.68622(11)	0.16222(11)	0.16677(7)	0.0179(3)
C44	0.67756(11)	0.24016(11)	0.13038(7)	0.0154(3)
C45	0.61912(11)	0.01714(11)	0.20974(7)	0.0167(3)
C46	0.68190(13)	0.98808(13)	0.25219(8)	0.0244(3)
C47	0.64498(14)	0.90294(13)	0.27615(8)	0.0259(4)
C48	0.56337(13)	0.88707(11)	0.24670(7)	0.0210(3)

Table II-2-5. Interatomic distances (Å) for **II-12b** ($C_{48}H_{60}Br_2O_4Si_2$).

Br1-C38	1.8600(18)	Br2-C48	1.8532(18)
Si1-O1	1.6679(11)	Si1-C17	1.8790(16)
Si1-C14	1.8814(18)	Si1-C11	1.8951(17)
Si2-O2	1.6657(11)	Si2-C20	1.8798(17)
Si2-C26	1.8865(17)	Si2-C23	1.8897(17)
O1-C1	1.3698(17)	O2-C8	1.3659(17)
O3-C38	1.3629(19)	O3-C35	1.381(2)
O4-C48	1.3648(18)	O4-C45	1.378(2)
C1-C10	1.386(2)	C1-C2	1.4071(19)
C2-C7	1.3967(19)	C2-C3	1.5160(19)
C3-C4	1.512(2)	C3-C29	1.526(2)
C4-C5	1.325(2)	C5-C6	1.505(2)
C6-C7	1.5128(19)	C6-C39	1.5259(19)
C7-C8	1.406(2)	C8-C9	1.383(2)
C9-C10	1.392(2)	C11-C13	1.526(2)
C11-C12	1.532(2)	C14-C15	1.535(3)
C14-C16	1.536(2)	C17-C18	1.535(2)
C17-C19	1.536(2)	C20-C22	1.533(3)
C20-C21	1.535(2)	C23-C24	1.539(2)
C23-C25	1.543(2)	C26-C27	1.528(2)
C26-C28	1.533(3)	C29-C30	1.388(2)
C29-C34	1.402(2)	C30-C31	1.391(2)
C31-C32	1.392(2)	C32-C33	1.401(2)
C32-C35	1.457(2)	C33-C34	1.385(2)
C35-C36	1.361(2)	C36-C37	1.433(2)
C37-C38	1.339(3)	C39-C40	1.391(2)
C39-C44	1.392(2)	C40-C41	1.391(2)
C41-C42	1.396(2)	C42-C43	1.394(2)
C42-C45	1.460(2)	C43-C44	1.391(2)
C45-C46	1.362(2)	C46-C47	1.434(2)
C47-C48	1.339(3)		

Table II-2-6. Bond angles (°) for **II-12b** ($C_{48}H_{60}Br_2O_4Si_2$).

O1-Si1-C17	102.63(6)	O1-Si1-C14	111.22(7)
C17-Si1-C14	113.85(8)	O1-Si1-C11	108.46(7)
C17-Si1-C11	107.56(7)	C14-Si1-C11	112.53(8)
O2-Si2-C20	99.86(6)	O2-Si2-C26	109.33(7)
C20-Si2-C26	112.08(8)	O2-Si2-C23	109.14(7)
C20-Si2-C23	115.87(8)	C26-Si2-C23	109.98(8)
C1-O1-Si1	134.12(10)	C8-O2-Si2	132.82(10)
C38-O3-C35	106.05(13)	C48-O4-C45	106.05(13)
O1-C1-C10	122.76(13)	O1-C1-C2	116.90(13)
C10-C1-C2	120.33(13)	C7-C2-C1	119.15(13)
C7-C2-C3	122.26(12)	C1-C2-C3	118.46(12)
C4-C3-C2	112.24(12)	C4-C3-C29	106.99(11)
C2-C3-C29	115.41(12)	C5-C4-C3	124.46(13)
C4-C5-C6	124.36(13)	C5-C6-C7	112.19(12)
C5-C6-C39	109.99(12)	C7-C6-C39	112.10(11)
C2-C7-C8	119.84(13)	C2-C7-C6	122.97(12)
C8-C7-C6	117.19(12)	O2-C8-C9	123.08(13)
O2-C8-C7	116.52(13)	C9-C8-C7	120.39(13)
C8-C9-C10	119.92(14)	C1-C10-C9	120.36(14)
C13-C11-C12	109.51(14)	C13-C11-Si1	115.38(12)
C12-C11-Si1	113.89(12)	C15-C14-C16	110.15(16)
C15-C14-Si1	114.32(12)	C16-C14-Si1	112.08(13)
C18-C17-C19	109.10(14)	C18-C17-Si1	114.29(12)
C19-C17-Si1	111.23(11)	C22-C20-C21	110.72(15)
C22-C20-Si2	111.92(12)	C21-C20-Si2	117.12(12)
C24-C23-C25	109.78(15)	C24-C23-Si2	112.96(12)
C25-C23-Si2	113.05(12)	C27-C26-C28	110.75(16)
C27-C26-Si2	112.50(12)	C28-C26-Si2	112.27(13)
C30-C29-C34	117.86(14)	C30-C29-C3	123.04(13)
C34-C29-C3	118.94(13)	C29-C30-C31	121.02(14)
C30-C31-C32	120.91(14)	C31-C32-C33	118.43(14)
C31-C32-C35	120.47(14)	C33-C32-C35	121.11(14)
C34-C33-C32	120.22(14)	C33-C34-C29	121.47(14)

C36-C35-O3	109.39(14)	C36-C35-C32	134.23(16)
O3-C35-C32	116.37(14)	C35-C36-C37	106.93(16)
C38-C37-C36	105.75(15)	C37-C38-O3	111.87(15)
C37-C38-Br1	132.79(13)	O3-C38-Br1	115.34(13)
C40-C39-C44	118.21(13)	C40-C39-C6	120.53(13)
C44-C39-C6	121.20(13)	C41-C40-C39	121.17(14)
C40-C41-C42	120.39(14)	C43-C42-C41	118.66(14)
C43-C42-C45	121.13(14)	C41-C42-C45	120.19(14)
C44-C43-C42	120.43(14)	C43-C44-C39	121.13(14)
C46-C45-O4	109.47(14)	C46-C45-C42	135.04(16)
O4-C45-C42	115.45(13)	C45-C46-C47	106.97(16)
C48-C47-C46	105.56(15)	C47-C48-O4	111.94(15)
C47-C48-Br2	132.93(13)	O4-C48-Br2	115.05(13)

Table II-2-7. Anisotropic atomic displacement parameters ($Å^2$) for **II-12b (**$C_{48}H_{60}Br_2O_4Si_2$). The anisotropic atomic displacement factor exponent takes the form: $-2\pi^2[h^2 a^{*2} U_{11} + ... + 2 h k a^* b^* U_{12}]$.

	U_{11}	U_{22}	U_{33}	U_{23}	U_{13}	U_{12}
Br1	0.01762(9)	0.03247(11)	0.05191(13)	0.01828(9)	0.00487(8)	-0.00407(7)
Br2	0.05029(12)	0.01638(8)	0.01840(8)	0.00320(6)	0.01197(7)	-0.00632(7)
Si1	0.01142(18)	0.01737(19)	0.01224(18)	-0.0002(2)	-0.0016(1)	0.00037(15)
Si2	0.01365(18)	0.01225(18)	0.01574(19)	-0.0018(1)	-0.0003(1)	0.00313(14)
O1	0.0127(5)	0.0196(5)	0.0143(5)	-0.0027(4)	-0.0036(4)	0.0044(4)
O2	0.0132(5)	0.0167(5)	0.0161(5)	-0.0033(4)	-0.0023(4)	0.0049(4)
O3	0.0122(5)	0.0219(6)	0.0250(6)	0.0064(5)	0.0032(4)	-0.0009(4)
O4	0.0248(6)	0.0137(5)	0.0142(5)	0.0038(4)	0.0056(4)	0.0011(4)
C1	0.0128(6)	0.0128(6)	0.0131(6)	0.0004(5)	-0.0009(5)	0.0010(5)
C2	0.0128(6)	0.0084(6)	0.0105(6)	0.0011(5)	0.0015(5)	-0.0010(5)
C3	0.0132(6)	0.0086(6)	0.0114(6)	0.0010(5)	0.0012(5)	-0.0002(5)
C4	0.0187(7)	0.0091(6)	0.0121(6)	-0.0020(5)	0.0014(5)	-0.0031(5)
C5	0.0179(7)	0.0100(6)	0.0113(6)	-0.0012(5)	-0.0006(5)	-0.0045(5)
C6	0.0125(6)	0.0096(6)	0.0109(6)	0.0016(5)	-0.0010(5)	-0.0023(5)

	U_{11}	U_{22}	U_{33}	U_{23}	U_{13}	U_{12}
C7	0.0131(6)	0.0084(6)	0.0099(6)	0.0013(5)	0.0001(5)	-0.0018(5)
C8	0.0136(6)	0.0128(6)	0.0134(6)	0.0006(5)	-0.0007(5)	0.0025(5)
C9	0.0181(7)	0.0197(7)	0.0140(7)	-0.0043(5)	-0.0007(5)	0.0068(6)
C10	0.0179(7)	0.0216(7)	0.0127(7)	-0.0041(6)	-0.0041(5)	0.0043(6)
C11	0.0175(7)	0.0220(8)	0.0176(7)	0.0026(6)	0.0007(6)	0.0001(6)
C12	0.0253(9)	0.0420(11)	0.0214(8)	0.0106(8)	-0.0010(7)	0.0035(8)
C13	0.0202(8)	0.0337(10)	0.0266(9)	0.0046(7)	0.0069(7)	0.0007(7)
C14	0.0230(8)	0.0210(8)	0.0212(8)	-0.0027(6)	-0.0035(6)	-0.0017(6)
C15	0.0418(11)	0.0207(8)	0.0335(10)	0.0031(7)	-0.0080(8)	-0.0041(8)
C16	0.0312(10)	0.0317(10)	0.0327(10)	-0.0039(8)	-0.0113(8)	-0.0088(8)
C17	0.0128(7)	0.0227(8)	0.0192(7)	-0.0006(6)	-0.0011(5)	0.0010(6)
C18	0.0252(9)	0.0318(9)	0.0281(9)	0.0007(7)	0.0082(7)	-0.0044(7)
C19	0.0209(8)	0.0230(8)	0.0259(8)	-0.0011(7)	0.0003(6)	0.0049(6)
C20	0.0169(7)	0.0230(8)	0.0194(7)	-0.0020(6)	-0.0006(6)	0.0069(6)
C21	0.0269(9)	0.0368(11)	0.0319(10)	-0.0035(8)	-0.0067(7)	0.0182(8)
C22	0.0212(8)	0.0345(10)	0.0282(9)	-0.0069(8)	-0.0054(7)	-0.0020(7)
C23	0.0242(8)	0.0160(7)	0.0188(7)	-0.0019(6)	0.0044(6)	0.0004(6)
C24	0.0477(12)	0.0197(8)	0.0275(9)	0.0023(7)	0.0101(8)	-0.0016(8)
C25	0.0238(8)	0.0284(9)	0.0241(8)	-0.0041(7)	0.0077(7)	-0.0014(7)
C26	0.0190(7)	0.0159(7)	0.0276(8)	-0.0013(6)	0.0013(6)	0.0001(6)
C27	0.0245(9)	0.0161(8)	0.0453(11)	-0.0086(7)	0.0021(8)	-0.0018(7)
C28	0.0448(12)	0.0305(10)	0.0405(12)	0.0048(9)	0.0134(9)	-0.0100(9)
C29	0.0132(6)	0.0122(6)	0.0110(6)	0.0002(5)	-0.0001(5)	0.0000(5)
C30	0.0166(7)	0.0117(7)	0.0217(7)	0.0001(5)	0.0053(6)	0.0010(5)
C31	0.0180(7)	0.0124(7)	0.0242(8)	0.0025(6)	0.0052(6)	0.0001(6)
C32	0.0129(6)	0.0182(7)	0.0145(6)	0.0020(5)	0.0006(5)	-0.0005(5)
C33	0.0157(7)	0.0170(7)	0.0218(7)	-0.0024(6)	0.0040(6)	0.0016(6)
C34	0.0171(7)	0.0120(6)	0.0213(7)	-0.0010(5)	0.0027(6)	0.0008(5)
C35	0.0146(7)	0.0205(7)	0.0151(7)	0.0034(5)	-0.0007(5)	-0.0006(6)
C36	0.0158(7)	0.0272(8)	0.0197(7)	0.0008(6)	0.0017(6)	0.0010(6)
C37	0.0132(7)	0.0382(10)	0.0188(8)	0.0033(7)	0.0022(6)	-0.0027(7)
C38	0.0112(7)	0.0331(9)	0.0219(8)	0.0094(7)	0.0010(6)	-0.0052(6)
C39	0.0141(6)	0.0108(6)	0.0092(6)	0.0004(5)	0.0001(5)	-0.0006(5)
C40	0.0184(7)	0.0168(7)	0.0183(7)	0.0054(6)	-0.0071(6)	-0.0055(6)

	U_{11}	U_{22}	U_{33}	U_{23}	U_{13}	U_{12}
C41	0.0213(7)	0.0140(7)	0.0182(7)	0.0049(6)	-0.0031(6)	-0.0058(6)
C42	0.0184(7)	0.0132(6)	0.0115(6)	0.0023(5)	0.0031(5)	0.0027(5)
C43	0.0127(6)	0.0209(7)	0.0202(7)	0.0072(6)	0.0001(5)	0.0024(6)
C44	0.0124(6)	0.0170(7)	0.0167(7)	0.0043(5)	-0.0001(5)	-0.0011(5)
C45	0.0197(7)	0.0152(7)	0.0155(7)	0.0038(5)	0.0055(5)	0.0028(6)
C46	0.0262(8)	0.0254(8)	0.0217(8)	0.0101(7)	0.0014(6)	0.0046(7)
C47	0.0353(10)	0.0220(8)	0.0207(8)	0.0102(6)	0.0049(7)	0.0081(7)
C48	0.0349(9)	0.0125(7)	0.0161(7)	0.0045(5)	0.0104(6)	0.0045(6)

Table II-2-8. Hydrogen atom coordinates and isotropic atomic displacement parameters ($Å^2$) for **II-12b** ($C_{48}H_{60}Br_2O_4Si_2$).

	x/a	y/b	z/c	U(eq)
H3	0.3749	0.4843	0.0052	0.013
H4	0.4321	0.5091	0.1033	0.016
H5	0.5690	0.4433	0.1284	0.016
H6	0.6487	0.3665	0.0500	0.013
H9	0.5669	0.2086	-0.1198	0.021
H10	0.4150	0.2659	-0.1421	0.021
H11	0.2899	0.5116	-0.1738	0.023
H12A	0.2205	0.5254	-0.2648	0.044
H12B	0.1401	0.4885	-0.2219	0.044
H12C	0.1900	0.4174	-0.2660	0.044
H13A	0.3577	0.3619	-0.2436	0.04
H13B	0.4179	0.4148	-0.1933	0.04
H13C	0.3852	0.4699	-0.2516	0.04
H14	0.2742	0.2315	-0.1861	0.026
H15A	0.1675	0.1794	-0.0861	0.048
H15B	0.2808	0.1786	-0.0878	0.048
H15C	0.2206	0.1083	-0.1286	0.048
H16A	0.1260	0.1676	-0.2132	0.048

	x/a	y/b	z/c	U(eq)
H16B	0.1312	0.2754	-0.2322	0.048
H16C	0.0734	0.2458	-0.1754	0.048
H17	0.0767	0.4287	-0.1362	0.022
H18A	0.1212	0.3475	-0.0241	0.042
H18B	0.0565	0.2999	-0.0743	0.042
H18C	0.0204	0.3920	-0.0415	0.042
H19A	0.0829	0.5455	-0.0634	0.035
H19B	0.1693	0.5590	-0.1070	0.035
H19C	0.1873	0.5132	-0.0436	0.035
H20	0.7873	0.1364	0.0512	0.024
H21A	0.9369	0.0696	-0.0193	0.048
H21B	0.8607	0.0042	0.0118	0.048
H21C	0.9341	0.0642	0.0509	0.048
H22A	0.9124	0.2375	0.0615	0.042
H22B	0.8312	0.2900	0.0241	0.042
H22C	0.9216	0.2482	-0.0081	0.042
H23	0.7376	0.1595	-0.1516	0.024
H24A	0.8333	0.3183	-0.1017	0.047
H24B	0.7259	0.3187	-0.1259	0.047
H24C	0.8110	0.3041	-0.1704	0.047
H25A	0.8977	0.1521	-0.1741	0.038
H25B	0.8765	0.0716	-0.1273	0.038
H25C	0.9285	0.1660	-0.1066	0.038
H26	0.6028	0.0575	-0.0754	0.025
H27A	0.7734	-0.0498	-0.0714	0.043
H27B	0.7211	-0.0117	-0.1297	0.043
H27C	0.6722	-0.0911	-0.0911	0.043
H28A	0.5919	-0.0509	0.0008	0.058
H28B	0.6028	0.0517	0.0285	0.058
H28C	0.6918	-0.0179	0.0282	0.058
H30	0.3180	0.2515	0.0406	0.02
H31	0.1854	0.2004	0.0906	0.022
H33	0.1154	0.4698	0.1254	0.022
H34	0.2485	0.5201	0.0760	0.02

	x/a	y/b	z/c	U(eq)
H36	-0.0235	0.4052	0.1803	0.025
H37	-0.1274	0.2751	0.2232	0.028
H40	0.4638	0.2031	0.0800	0.022
H41	0.4775	0.0717	0.1403	0.021
H43	0.7431	0.1525	0.1890	0.021
H44	0.7289	0.2829	0.1279	0.018
H46	0.7392	0.0184	0.2638	0.029
H47	0.6726	-0.1344	0.3065	0.031

Description of the X-ray Structural Analysis of *anti*-II-20b ($C_{96}H_{120}O_8Si_4 \cdot 2CH_2Cl_2$)

A colorless crystal of *anti*-**II-20b** ($C_{96}H_{120}O_8Si_4 \cdot 2CH_2Cl_2$) was covered in a polybutene oil (Sigma-Aldrich) and placed on the end of a MiTeGen loop. The sample was cooled to 105 K with an Oxford Cryostream 700 system and optically aligned on a Bruker AXS D8 Venture fixed-chi X-ray diffractometer equipped with a Triumph monochromator, a Mo Kα radiation source (λ = 0.71073 Å), and a PHOTON 100 CMOS detector. Two sets of 12 frames each were collected using the omega scan method with a 10 s exposure time. Integration of these frames followed by reflection indexing and least-squares refinement produced a crystal orientation matrix for the triclinic crystal lattice.

Data collection consisted of the measurement of a total of 368 frames in four runs using omega scans with the detector held at 5.00 cm from the crystal. The frame scan parameters are summarized in Table III-3-1 below:

Table III-3-1. Data collection details for *anti*-**II-20b** ($C_{96}H_{120}O_8Si_4 \cdot 2CH_2Cl_2$).

Run	2θ	ω	φ	χ	Scan Width (º)	Frames	Exposure Time (sec)
1	11.01	-170.99	144.00	54.74	2.00	92	80.00
2	11.01	-170.99	0.00	54.74	2.00	92	80.00
3	11.01	-170.99	72.00	54.74	2.00	92	80.00
4	11.01	-170.99	-72.00	54.74	2.00	92	80.00

The APEX2 software program (version 2014.1-7)[S3] was used for diffractometer control, preliminary frame scans, indexing, orientation matrix calculations, least-squares refinement of cell parameters, and the data collection. The frames were integrated with the Bruker SAINT software

package using a narrow-frame algorithm. The integration of the data using a triclinic unit cell yielded a total of 47579 reflections to a maximum θ angle of 27.50° (0.77 Å resolution), of which 10396 were independent (average redundancy 4.577, completeness = 99.8%, R_{int} = 4.70%, R_{sig} = 4.96%) and 7198 (69.24%) were greater than $2\sigma(F^2)$. The final cell constants of a = 12.6079(7) Å, b = 12.8788(7) Å, c = 14.2249(8) Å, α = 87.7467(15)°, β = 82.0261(14)°, γ = 82.0141(16)°, volume = 2264.8(2) $Å^3$, are based upon the refinement of the XYZ-centroids of 9832 reflections above 20 σ(I) with 5.785° < 2θ < 54.91°. Data were corrected for absorption effects using the multi-scan method (SADABS). The ratio of minimum to maximum apparent transmission was 0.914. The calculated minimum and maximum transmission coefficients (based on crystal size) are 0.900 and 0.973, respectively.

The structure was solved by direct methods and difference Fourier analysis using the programs provided by SHELXL-2013.[S4] The crystallographic asymmetric unit contains one independent half molecule of *anti*-**II-20b** ($C_{96}H_{120}O_8Si_4$) and an independent molecule CH_2Cl_2. The two-halves of *anti*-**II-20b** ($C_{96}H_{120}O_8Si_4$) are related by a center of inversion. Idealized positions for the hydrogen atoms were included as fixed contributions using a riding model with isotropic temperature factors set at 1.2 times (methine, methylene and aromatic hydrogens) or 1.5 (methyl hydrogens) times that of the adjacent carbon atom. The positions of the methyl hydrogen atoms were optimized by a rigid rotating group refinement with idealized angles. Full-matrix least-squares refinement, based upon the minimization of $\Sigma w_i |F_o^2 - F_c^2|^2$, with weighting $w_i^{-1} = [\sigma^2(F_o^2) + (0.0717\ P)^2 + 4.1397\ P]$, where $P = (\text{Max}(F_o^2, 0) + 2\ F_c^2)/3$.[S4] The final anisotropic full-matrix least-squares refinement on F^2 with 526 variables converged at R1 = 6.29 % for 7198 observed data with I>2σ(I) and wR2 = 17.57 % for all data. The goodness-of-fit was 1.026.[S5]

A correction for secondary extinction was not applied. The largest peak in the final difference electron density synthesis was 1.160 $e^-/Å^3$ and the largest hole was -0.954 $e^-/Å^3$ with an RMS deviation of 0.080 $e^-/Å^3$. The linear absorption coefficient, atomic scattering factors, and anomalous dispersion corrections were calculated from values found in the International Tables of X-ray Crystallography.[S6]

Table II-3-2. Crystal data for *anti*-**II-20b** ($C_{96}H_{120}O_8Si_4 \cdot 2CH_2Cl_2$).

Identification code	kw30cms	
Chemical formula	$C_{98}H_{124}Cl_4O_8Si_4$	
Formula weight	1684.12 g/mol	
Temperature	105(2) K	
Wavelength	0.71073 Å	
Crystal size	0.116 x 0.240 x 0.451 mm	
Crystal system	triclinic	
Space group	P -1 (No. 2)	
Unit cell dimensions	a = 12.6079(7) Å	α = 87.7467(15)°
	b = 12.8788(7) Å	β = 82.0261(14)°
	c = 14.2249(8) Å	γ = 82.0141(16)°
Volume	2264.8(2) $Å^3$	
Z	1	
Density (calculated)	1.235 g/cm^3	
Absorption coefficient	0.239 mm^{-1}	
F(000)	900	

Table II-3-3. Data collection and structure refinement for *anti*-**II-20b** ($C_{96}H_{120}O_8Si_4 \cdot 2CH_2Cl_2$).

Theta range used for refinement	2.74 to 27.50°
Index ranges	$-16 \le h \le 16$, $-16 \le k \le 16$, $-18 \le l \le 18$
Reflections collected	47579

Independent reflections	10396 [R(int) = 0.0470]	
Coverage of independent reflections	99.8%	
Absorption correction	multi-scan	
Max. and min. trans.	0.973 and 0.900	
Refinement method	Full-matrix least-squares on F^2	
Refinement program	SHELXL-2013 (Sheldrick, 2013)	
Data / restraints / parameters	10396 / 0 / 526	
Goodness-of-fit on F^2	1.026	
Final R indices	7198 data; I>2σ(I)	R1 = 0.0629, wR2 = 0.1514
	all data	R1 = 0.1012, wR2 = 0.1757
Largest diff. peak and hole	1.160 and -0.954 $e^-/Å^3$	

Table II-3-4. Atomic coordinates and equivalent isotropic atomic displacement parameters ($Å^2$) for *anti*-**II-20b** ($C_{96}H_{120}O_8Si_4 \cdot 2CH_2Cl_2$). U(eq) is defined as one third of the trace of the orthogonalized U_{ij} tensor.

	x/a	y/b	z/c	U(eq)
Si1	0.02024(6)	0.77281(5)	0.35871(5)	0.01703(15)
Si2	0.24786(6)	0.27142(6)	0.09507(6)	0.02319(17)
O1	0.97654(14)	0.89870(13)	0.33914(13)	0.0219(4)
O2	0.14073(14)	0.20790(13)	0.10554(13)	0.0214(4)
O3	0.63738(14)	0.52223(13)	0.32539(13)	0.0203(4)
O4	0.46827(14)	0.70840(13)	0.48340(13)	0.0205(4)
C1	0.0205(2)	0.97471(18)	0.28162(18)	0.0174(5)
C2	0.1180(2)	0.00597(19)	0.29451(19)	0.0206(5)
C3	0.1597(2)	0.0842(2)	0.23671(19)	0.0212(5)
C4	0.1034(2)	0.13115(18)	0.16575(18)	0.0170(5)
C5	0.00394(19)	0.10185(17)	0.15294(17)	0.0141(5)
C6	0.94084(19)	0.15351(18)	0.07662(17)	0.0151(5)
C7	0.8805(2)	0.07424(19)	0.03851(18)	0.0187(5)
C8	0.8404(2)	0.00082(19)	0.09486(18)	0.0200(5)

	x/a	y/b	z/c	U(eq)
C9	0.8523(2)	0.99353(18)	0.19903(18)	0.0174(5)
C10	0.96139(19)	0.02347(17)	0.21247(17)	0.0150(5)
C11	0.86332(19)	0.25097(18)	0.11356(17)	0.0154(5)
C12	0.7783(2)	0.29457(19)	0.06530(18)	0.0179(5)
C13	0.7041(2)	0.37694(19)	0.10232(18)	0.0190(5)
C14	0.7121(2)	0.41930(18)	0.18928(18)	0.0180(5)
C15	0.7990(2)	0.37854(19)	0.23619(18)	0.0199(5)
C16	0.8731(2)	0.29594(19)	0.19858(18)	0.0196(5)
C17	0.6306(2)	0.50190(18)	0.23248(18)	0.0188(5)
C18	0.5462(2)	0.5654(2)	0.2033(2)	0.0250(6)
C19	0.4971(2)	0.6284(2)	0.2809(2)	0.0277(6)
C20	0.5543(2)	0.59967(19)	0.3538(2)	0.0219(6)
C21	0.5463(2)	0.62682(19)	0.4515(2)	0.0215(6)
C22	0.5979(2)	0.5852(2)	0.5240(2)	0.0247(6)
C23	0.5508(2)	0.6423(2)	0.6058(2)	0.0248(6)
C24	0.4730(2)	0.71636(19)	0.57918(18)	0.0199(5)
C25	0.3955(2)	0.79542(19)	0.63143(18)	0.0190(5)
C26	0.3122(2)	0.8557(2)	0.59017(19)	0.0209(5)
C27	0.4019(2)	0.8111(2)	0.72633(19)	0.0215(6)
C28	0.7606(2)	0.06309(18)	0.25948(18)	0.0176(5)
C29	0.6747(2)	0.1195(2)	0.21998(18)	0.0202(5)
C30	0.7637(2)	0.07481(19)	0.35612(18)	0.0200(5)
C31	0.8906(2)	0.7151(2)	0.3851(2)	0.0303(7)
C32	0.8017(3)	0.7776(3)	0.4504(3)	0.0573(11)
C33	0.9041(3)	0.5986(2)	0.4078(3)	0.0409(8)
C34	0.1051(2)	0.7639(2)	0.45740(19)	0.0251(6)
C35	0.0378(3)	0.8008(4)	0.5512(2)	0.0541(10)
C36	0.1704(3)	0.6558(2)	0.4711(3)	0.0493(9)
C37	0.1040(2)	0.7098(2)	0.25075(19)	0.0240(6)
C38	0.0406(3)	0.7104(3)	0.1667(2)	0.0339(7)
C39	0.2113(2)	0.7530(2)	0.2199(2)	0.0297(6)
C40	0.3755(2)	0.1760(3)	0.0872(3)	0.0372(7)
C41	0.3668(3)	0.0729(3)	0.0440(3)	0.0435(8)
C42	0.4744(3)	0.2242(3)	0.0366(3)	0.0452(9)

	x/a	y/b	z/c	U(eq)
C43	0.2436(3)	0.3534(3)	0.2034(3)	0.0427(8)
C44	0.1340(3)	0.3843(3)	0.2575(3)	0.0547(10)
C45	0.3031(3)	0.4497(2)	0.1796(3)	0.0429(8)
C46	0.2324(2)	0.3527(2)	0.9839(2)	0.0233(6)
C47	0.2431(2)	0.2862(2)	0.8954(2)	0.0292(6)
C48	0.1246(2)	0.4259(2)	0.9942(2)	0.0294(6)
Cl1	0.38544(7)	0.04707(8)	0.40657(7)	0.0517(2)
Cl2	0.47574(12)	0.91900(9)	0.24414(9)	0.0776(4)
C49	0.4939(3)	0.9541(3)	0.3593(3)	0.0437(8)

Table II-3-5. Interatomic distances (Å) for *anti*-**II-20b** ($C_{96}H_{120}O_8Si_4 \cdot 2CH_2Cl_2$).

Si1-O1	1.6639(18)	Si1-C34	1.870(3)
Si1-C31	1.874(3)	Si1-C37	1.882(3)
Si2-O2	1.6605(18)	Si2-C40	1.877(3)
Si2-C46	1.879(3)	Si2-C43	1.892(3)
O1-C1	1.377(3)	O2-C4	1.372(3)
O3-C20	1.371(3)	O3-C17	1.374(3)
O4-C21	1.380(3)	O4-C24	1.381(3)
C1-C2	1.383(4)	C1-C10	1.394(3)
C2-C3	1.389(4)	C3-C4	1.386(4)
C4-C5	1.396(3)	C5-C10	1.408(3)
C5-C6	1.513(3)	C6-C7	1.513(3)
C6-C11	1.541(3)	C7-C8	1.324(4)
C8-C9	1.508(4)	C9-C10	1.518(3)
C9-C28	1.541(3)	C11-C16	1.389(4)
C11-C12	1.393(3)	C12-C13	1.382(4)
C13-C14	1.393(4)	C14-C15	1.392(4)
C14-C17	1.462(3)	C15-C16	1.386(3)
C17-C18	1.351(4)	C18-C19	1.416(4)
C19-C20	1.354(4)	C20-C21	1.433(4)
C21-C22	1.349(4)	C22-C23	1.415(4)

C23-C24	1.353(4)	C24-C25	1.458(4)
C25-C27	1.388(4)	C25-C26	1.400(4)
C26-C30'	1.383(4)	C27-C29'	1.386(4)
C28-C29	1.391(4)	C28-C30	1.395(4)
C29-C27	1.386(4)	C30-C26	1.383(4)
C31-C32	1.512(5)	C31-C33	1.515(4)
C34-C35	1.532(4)	C34-C36	1.537(4)
C37-C38	1.526(4)	C37-C39	1.536(4)
C40-C41	1.509(5)	C40-C42	1.546(5)
C43-C44	1.496(5)	C43-C45	1.539(4)
C46-C47	1.531(4)	C46-C48	1.536(4)
Cl1-C49	1.763(4)	Cl2-C49	1.770(4)

Primed atoms (') correspond to those generated by the crystallographic center of inversion.

Table II-3-6. Bond angles (°) for *anti*-**II-20b** ($C_{96}H_{120}O_8Si_4 \cdot 2CH_2Cl_2$).

O1-Si1-C34	108.23(11)	O1-Si1-C31	102.10(11)
C34-Si1-C31	115.82(14)	O1-Si1-C37	112.19(11)
C34-Si1-C37	108.75(13)	C31-Si1-C37	109.69(13)
O2-Si2-C40	110.41(12)	O2-Si2-C46	102.08(11)
C40-Si2-C46	113.98(14)	O2-Si2-C43	110.23(13)
C40-Si2-C43	107.12(16)	C46-Si2-C43	112.99(14)
C1-O1-Si1	132.15(16)	C4-O2-Si2	134.84(17)
C20-O3-C17	106.9(2)	C21-O4-C24	106.4(2)
O1-C1-C2	121.4(2)	O1-C1-C10	118.1(2)
C2-C1-C10	120.4(2)	C1-C2-C3	120.3(2)
C4-C3-C2	119.9(2)	O2-C4-C3	122.8(2)
O2-C4-C5	116.7(2)	C3-C4-C5	120.5(2)
C4-C5-C10	119.4(2)	C4-C5-C6	121.1(2)
C10-C5-C6	119.5(2)	C7-C6-C5	109.41(19)
C7-C6-C11	111.3(2)	C5-C6-C11	111.70(19)
C8-C7-C6	120.9(2)	C7-C8-C9	121.5(2)

C8-C9-C10	109.2(2)	C8-C9-C28	112.3(2)
C10-C9-C28	110.5(2)	C1-C10-C5	119.4(2)
C1-C10-C9	121.6(2)	C5-C10-C9	119.0(2)
C16-C11-C12	117.5(2)	C16-C11-C6	121.0(2)
C12-C11-C6	121.5(2)	C13-C12-C11	121.3(2)
C12-C13-C14	120.9(2)	C15-C14-C13	118.0(2)
C15-C14-C17	120.2(2)	C13-C14-C17	121.7(2)
C16-C15-C14	120.6(2)	C15-C16-C11	121.5(2)
C18-C17-O3	109.4(2)	C18-C17-C14	135.3(3)
O3-C17-C14	115.3(2)	C17-C18-C19	107.3(3)
C20-C19-C18	106.6(2)	C19-C20-O3	109.8(2)
C19-C20-C21	136.0(2)	O3-C20-C21	114.1(2)
C22-C21-O4	109.9(2)	C22-C21-C20	132.9(2)
O4-C21-C20	117.1(2)	C21-C22-C23	106.9(2)
C24-C23-C22	107.3(3)	C23-C24-O4	109.5(2)
C23-C24-C25	132.9(3)	O4-C24-C25	117.6(2)
C27-C25-C26	117.9(2)	C27-C25-C24	119.6(2)
C26-C25-C24	122.5(2)	C30'-C26-C25	120.6(2)
C29'-C27-C25	121.2(2)	C29-C28-C30	117.6(2)
C29-C28-C9	121.9(2)	C30-C28-C9	120.5(2)
C27-C29-C28	121.1(2)	C26-C30-C28	121.4(2)
C32-C31-C33	113.6(3)	C32-C31-Si1	115.8(2)
C33-C31-Si1	114.7(2)	C35-C34-C36	110.4(3)
C35-C34-Si1	111.5(2)	C36-C34-Si1	114.8(2)
C38-C37-C39	110.3(2)	C38-C37-Si1	112.72(19)
C39-C37-Si1	114.68(19)	C41-C40-C42	110.9(3)
C41-C40-Si2	113.9(2)	C42-C40-Si2	112.4(2)
C44-C43-C45	111.0(3)	C44-C43-Si2	115.7(3)
C45-C43-Si2	111.6(2)	C47-C46-C48	110.1(2)
C47-C46-Si2	112.87(18)	C48-C46-Si2	111.13(19)
Cl1-C49-Cl2	110.3(2)		

Primed atoms (') correspond to those generated by the crystallographic center of inversion.

Table II-3-7. Anisotropic atomic displacement parameters ($Å^2$) for *anti*-**II-20b** ($C_{96}H_{120}O_8Si_4 \cdot 2CH_2Cl_2$). The anisotropic atomic displacement factor exponent takes the form: $-2\pi^2[h^2 a^{*2} U_{11} + ... + 2 h k a^* b^* U_{12}]$.

	U_{11}	U_{22}	U_{33}	U_{23}	U_{13}	U_{12}
Si1	0.0229(4)	0.0119(3)	0.0163(3)	0.0034(2)	-0.0031(3)	-0.0029(3)
Si2	0.0225(4)	0.0173(3)	0.0319(4)	0.0059(3)	-0.0072(3)	-0.0088(3)
O1	0.0224(9)	0.0153(8)	0.0249(10)	0.0078(7)	0.0025(8)	-0.0002(7)
O2	0.0205(9)	0.0177(8)	0.0275(10)	0.0092(7)	-0.0068(8)	-0.0073(7)
O3	0.0184(9)	0.0154(8)	0.0254(10)	-0.0022(7)	-0.0002(7)	0.0011(7)
O4	0.0184(9)	0.0177(8)	0.0233(9)	-0.0017(7)	0.0008(7)	0.0020(7)
C1	0.0196(12)	0.0098(10)	0.0205(12)	0.0032(9)	0.0030(10)	-0.0001(9)
C2	0.0212(13)	0.0160(12)	0.0234(13)	0.0047(10)	-0.0052(11)	0.0027(10)
C3	0.0168(12)	0.0182(12)	0.0288(14)	0.0019(10)	-0.0042(11)	-0.0028(10)
C4	0.0199(12)	0.0108(11)	0.0190(12)	0.0008(9)	0.0010(10)	-0.0016(9)
C5	0.0176(12)	0.0094(10)	0.0140(11)	-0.0019(9)	0.0008(9)	0.0001(9)
C6	0.0172(12)	0.0127(11)	0.0150(11)	0.0014(9)	-0.0004(9)	-0.0023(9)
C7	0.0228(13)	0.0161(11)	0.0167(12)	-0.0048(9)	-0.0019(10)	0.0003(10)
C8	0.0204(13)	0.0158(11)	0.0245(13)	-0.0072(10)	-0.0018(11)	-0.0043(10)
C9	0.0197(12)	0.0105(10)	0.0217(13)	0.0006(9)	-0.0003(10)	-0.0034(9)
C10	0.0167(12)	0.0096(10)	0.0173(12)	-0.0028(9)	0.0008(9)	0.0002(9)
C11	0.0170(12)	0.0116(10)	0.0166(12)	0.0030(9)	0.0013(9)	-0.0035(9)
C12	0.0207(12)	0.0178(11)	0.0163(12)	0.0013(9)	-0.0024(10)	-0.0069(9)
C13	0.0183(12)	0.0180(12)	0.0214(13)	0.0048(10)	-0.0057(10)	-0.0034(9)
C14	0.0183(12)	0.0121(11)	0.0226(13)	0.0033(10)	-0.0003(10)	-0.0026(9)
C15	0.0243(13)	0.0167(12)	0.0187(12)	-0.0020(10)	-0.0037(10)	-0.0014(10)
C16	0.0213(13)	0.0163(12)	0.0209(13)	-0.0001(10)	-0.0055(10)	0.0010(10)
C17	0.0185(12)	0.0136(11)	0.0240(13)	0.0008(10)	0.0000(10)	-0.0045(9)
C18	0.0226(14)	0.0257(13)	0.0255(14)	0.0023(11)	-0.0010(11)	-0.0026(11)
C19	0.0222(14)	0.0231(13)	0.0348(16)	0.0005(12)	0.0011(12)	0.0020(11)
C20	0.0178(13)	0.0134(11)	0.0322(15)	-0.0015(10)	0.0031(11)	0.0001(9)
C21	0.0154(12)	0.0147(11)	0.0325(15)	-0.0020(10)	0.0042(11)	-0.0022(9)
C22	0.0190(13)	0.0193(12)	0.0336(15)	0.0006(11)	0.0011(11)	0.0002(10)
C23	0.0221(13)	0.0231(13)	0.0284(15)	0.0005(11)	-0.0021(11)	-0.0019(11)
C24	0.0198(13)	0.0176(12)	0.0219(13)	0.0013(10)	-0.0005(10)	-0.0042(10)

	U_{11}	U_{22}	U_{33}	U_{23}	U_{13}	U_{12}
C25	0.0178(12)	0.0157(11)	0.0223(13)	0.0018(10)	0.0026(10)	-0.0042(9)
C26	0.0211(13)	0.0202(12)	0.0203(13)	0.0003(10)	0.0000(10)	-0.0016(10)
C27	0.0162(12)	0.0214(12)	0.0260(14)	0.0042(11)	-0.0014(10)	-0.0024(10)
C28	0.0179(12)	0.0134(11)	0.0211(13)	0.0008(9)	0.0016(10)	-0.0046(9)
C29	0.0203(13)	0.0223(12)	0.0178(12)	0.0017(10)	0.0006(10)	-0.0062(10)
C30	0.0185(12)	0.0184(12)	0.0218(13)	0.0024(10)	-0.0011(10)	-0.0004(10)
C31	0.0258(15)	0.0225(14)	0.0420(17)	0.0004(12)	0.0001(13)	-0.0063(11)
C32	0.044(2)	0.0366(19)	0.085(3)	-0.0021(19)	0.019(2)	-0.0112(16)
C33	0.0362(17)	0.0231(15)	0.062(2)	0.0063(15)	0.0026(16)	-0.0115(13)
C34	0.0344(15)	0.0240(13)	0.0190(13)	0.0060(11)	-0.0085(11)	-0.0082(11)
C35	0.056(2)	0.092(3)	0.0190(16)	-0.0116(17)	-0.0040(15)	-0.023(2)
C36	0.070(2)	0.0260(16)	0.060(2)	0.0166(15)	-0.0429(19)	-0.0065(16)
C37	0.0265(14)	0.0206(13)	0.0242(14)	-0.0024(11)	-0.0030(11)	-0.0013(11)
C38	0.0344(17)	0.0491(19)	0.0196(14)	-0.0086(13)	-0.0009(12)	-0.0108(14)
C39	0.0237(14)	0.0353(16)	0.0287(15)	-0.0074(12)	-0.0003(12)	-0.0007(12)
C40	0.0237(15)	0.0390(17)	0.0493(19)	0.0063(15)	-0.0099(14)	-0.0029(13)
C41	0.0341(18)	0.0420(19)	0.050(2)	-0.0007(16)	-0.0023(15)	0.0081(14)
C42	0.0228(16)	0.051(2)	0.063(2)	0.0018(18)	-0.0117(15)	-0.0069(14)
C43	0.061(2)	0.0309(16)	0.0426(19)	0.0010(14)	-0.0142(17)	-0.0209(15)
C44	0.074(3)	0.048(2)	0.043(2)	-0.0109(17)	0.0032(19)	-0.0230(19)
C45	0.055(2)	0.0292(16)	0.051(2)	0.0000(15)	-0.0173(17)	-0.0206(15)
C46	0.0210(13)	0.0174(12)	0.0321(15)	0.0066(11)	-0.0026(11)	-0.0077(10)
C47	0.0257(15)	0.0275(14)	0.0348(16)	0.0042(12)	-0.0044(12)	-0.0065(11)
C48	0.0247(14)	0.0228(13)	0.0400(17)	0.0076(12)	-0.0031(12)	-0.0044(11)
Cl1	0.0390(5)	0.0572(5)	0.0567(6)	0.0128(4)	0.0005(4)	-0.0098(4)
Cl2	0.1173(10)	0.0531(6)	0.0691(7)	-0.0088(5)	-0.0235(7)	-0.0215(6)
C49	0.048(2)	0.0377(18)	0.047(2)	0.0120(15)	-0.0074(16)	-0.0132(15)

Table II-3-8. Hydrogen atom coordinates and isotropic atomic displacement parameters ($Å^2$) for *anti*-**II-20b** ($C_{96}H_{120}O_8Si_4 \cdot 2CH_2Cl_2$).

	x/a	y/b	z/c	U(eq)
H2	1.1566	-0.0262	0.3431	0.025
H3	1.2267	0.1054	0.2458	0.025
H6	0.9935	0.1766	0.0234	0.018
H7	0.8712	0.0772	-0.0267	0.022
H8	0.8033	-0.0484	0.0691	0.024
H9	0.8501	-0.0810	0.2210	0.021
H12	0.7713	0.2671	0.0058	0.022
H13	0.6469	0.4051	0.0680	0.023
H15	0.8076	0.4076	0.2946	0.024
H16	0.9319	0.2694	0.2317	0.024
H18	0.5241	0.5674	0.1420	0.03
H19	0.4359	0.6807	0.2818	0.033
H22	0.6549	0.5283	0.5207	0.03
H23	0.5703	0.6309	0.6679	0.03
H26	0.3077	0.8488	0.5246	0.025
H27	0.4599	0.7737	0.7550	0.026
H29	0.6684	0.1104	0.1551	0.024
H30	0.8192	0.0342	0.3857	0.024
H31	0.8620	-0.2798	0.3227	0.036
H32A	0.7339	-0.2514	0.4501	0.086
H32B	0.7928	-0.1491	0.4284	0.086
H32C	0.8208	-0.2264	0.5151	0.086
H33A	0.9277	-0.4139	0.4706	0.061
H33B	0.9584	-0.4379	0.3599	0.061
H33C	0.8349	-0.4280	0.4077	0.061
H34	1.1588	-0.1858	0.4405	0.03
H35A	0.9864	-0.2486	0.5725	0.081
H35B	0.9982	-0.1294	0.5418	0.081
H35C	1.0858	-0.1961	0.5993	0.081
H36A	1.2170	-0.3405	0.5202	0.074

	x/a	y/b	z/c	U(eq)
H36B	1.2151	-0.3655	0.4112	0.074
H36C	1.1208	-0.3957	0.4905	0.074
H37	1.1236	-0.3656	0.2686	0.029
H38A	1.0170	-0.2170	0.1478	0.051
H38B	0.9773	-0.3259	0.1850	0.051
H38C	1.0869	-0.3254	0.1133	0.051
H39A	1.2574	-0.2943	0.1742	0.045
H39B	1.2480	-0.2416	0.2756	0.045
H39C	1.1969	-0.1774	0.1903	0.045
H40	1.3898	0.1596	0.1539	0.045
H41A	1.3667	0.0827	-0.0247	0.065
H41B	1.2995	0.0475	0.0724	0.065
H41C	1.4285	0.0214	0.0563	0.065
H42A	1.5399	0.1738	0.0387	0.068
H42B	1.4815	0.2884	0.0686	0.068
H42C	1.4646	0.2410	-0.0297	0.068
H43	1.2858	0.3084	0.2479	0.051
H44A	1.1407	0.4234	0.3136	0.082
H44B	1.1007	0.3212	0.2775	0.082
H44C	1.0886	0.4285	0.2168	0.082
H45A	1.2659	0.4960	0.1346	0.064
H45B	1.3776	0.4266	0.1511	0.064
H45C	1.3037	0.4876	0.2378	0.064
H46	1.2917	0.3977	-0.0255	0.028
H47A	1.1870	0.2398	-0.0968	0.044
H47B	1.3145	0.2440	-0.1135	0.044
H47C	1.2346	0.3323	-0.1603	0.044
H48A	1.1178	0.4661	-0.0651	0.044
H48B	1.1225	0.4743	0.0462	0.044
H48C	1.0647	0.3842	0.0082	0.044
H49A	0.4982	0.8909	0.4012	0.052
H49B	0.5626	0.9840	0.3563	0.052

Description of the X-ray Structural Analysis of II-2b ($C_{96}H_{116}O_8Si_4 \cdot 5CHCl_3$)

A light yellow irregular crystal of **II-2b** ($C_{96}H_{116}O_8Si_4 \cdot 5CHCl_3$) was covered in a polybutene oil (Sigma-Aldrich) and placed on the end of a MiTeGen loop. The sample was cooled to 140 K with an Oxford Cryostream 700 system and optically aligned on a Bruker AXS D8 Venture fixed-chi X-ray diffractometer equipped with a Triumph monochromator, a Mo Kα radiation source (λ = 0.71073 Å), and a PHOTON 100 CMOS detector. Two sets of 12 frames each were collected using the omega scan method with a 10 s exposure time. Integration of these frames followed by reflection indexing and least-squares refinement produced a crystal orientation matrix for the orthorhombic crystal lattice that was used for the structural analysis.

Data collection consisted of the measurement of a total of 372 frames in one run using omega scans with the detector held at 5.00 cm from the crystal. Frame scan parameters are summarized in Table II-4-1 below:

Table II-4-1. Data collection details for **II-2b** ($C_{96}H_{116}O_8Si_4 \cdot 5CHCl_3$).

Run	2θ	ω	φ	χ	Scan Width (°)	Frames	Exposure Time (sec)
1	12.11	-170.89	-122.25	54.79	0.50	372	80.00

The APEX2 software program (version 2014.1-1)[S3] was used for diffractometer control, preliminary frame scans, indexing, orientation matrix calculations, least-squares refinement of cell parameters, and the data collection. The frames were integrated with the Bruker SAINT software package using a narrow-frame algorithm. The integration of the data using an orthorhombic unit cell yielded a total of 24352 reflections to a maximum θ angle of 25.00° (0.84 Å resolution), of which 8361 were independent (average redundancy 2.913, completeness = 99.7%, R_{int} = 2.74%,

R_{sig} = 3.30%) and 7086 (84.75%) were greater than $2\sigma(F^2)$. The final cell constants of a = 32.8975(15) Å, b = 19.4563(9) Å, c = 17.0894(8) Å, volume = 10938.3(9) $Å^3$, are based upon the refinement of the XYZ-centroids of 9932 reflections above 20 σ(I) with 6.346° < 2θ < 53.45°. Data were corrected for absorption effects using the multi-scan method (SADABS). The ratio of minimum to maximum apparent transmission was 0.856. The calculated minimum and maximum transmission coefficients (based on crystal size) are 0.781 and 0.940.

The structure was solved by direct methods and difference Fourier analysis using the programs provided by SHELXL-2014.[S7] The molecular geometry of **II-2b** ($C_{96}H_{116}Si_4O_8$) is constrained by a crystallographic mirror plane. The crystallographic asymmetric unit consists of an independent half molecule of **II-2b** ($C_{96}H_{116}O_8Si_4$), an independent molecule of $CHCl_3$, a half molecule of $CHCl_3$ that lies on a mirror plane, and two independent molecules of $CHCl_3$ that lie within the void of the central ring of **II-2b** ($C_{96}H_{116}O_8Si_4$). These latter two $CHCl_3$ molecules are disordered across the same mirror that relates the two mirror-related half molecules of **II-2b** ($C_{96}H_{116}O_8Si_4$). Idealized positions for the hydrogen atoms were included as fixed contributions using a riding model with isotropic temperature factors set at 1.2 times (methane and aromatic hydrogens) or 1.5 times (methyl hydrogens) that of the adjacent carbon atom. The positions of the methyl hydrogen atoms were optimized by a rigid rotating group refinement with idealized angles. The two disordered molecules of $CHCl_3$ were treated as a diffuse electron density contribution with the aid of the SQUEEZE routine in the program PLATON.[S8] Although specific positions for the independent carbon, hydrogen, and chlorine atoms of these two $CHCl_3$ molecules were not determined, the calculated density, absorption coefficient, and empirical formula weight reflect their presence within the crystal lattice. Full-matrix least-squares refinement, based upon the minimization of $\Sigma w_i |F_o^2 - F_c^2|^2$, with weighting $w_i^{-1} = [\sigma^2(F_o^2) + (0.1251\ P)^2 + 26.1027\ P]$, where

P = (Max (F_o^2, 0) + 2 F_c^2)/3.[S7] The final anisotropic full-matrix least-squares refinement on F^2 with 556 variables converged at R1 = 6.86%, for the 7086 observed data and wR2 = 20.43% for all data. The goodness-of-fit was 1.056.[S5]

A correction for secondary extinction was not applied. The largest peak in the final difference electron density synthesis was 1.273 $e^-/Å^3$ and the largest hole was -0.560 $e^-/Å^3$ with an RMS deviation of 0.089 $e^-/Å^3$. The linear absorption coefficient, atomic scattering factors, and anomalous dispersion corrections were calculated from values found in the International Tables of X-ray Crystallography.[S6]

Table II-4-2. Crystal data for **II-2b** ($C_{96}H_{116}O_8Si_4 \cdot 5CHCl_3$).

Identification code	kw31cms
Empirical formula	$C_{50.50}H_{60.50}Cl_{7.50}O_4Si_2$
Empirical formula weight	1053.54 g/mol
Temperature	140(2) K
Wavelength	0.71073 Å
Crystal size	0.132 x 0.185 x 0.550 mm
Crystal system	orthorhombic
Space group	$Cmc2_1$ (No. 36)
Unit cell dimensions	a = 32.8975(15) Å α = 90°
	b = 19.4563(9) Å β = 90°
	c = 17.0894(8) Å γ = 90°
Volume	10938.3(9) $Å^3$
Z (empirical units)	8
Density (calculated)	1.280 g/cm^3
Absorption coefficient	0.472 mm^{-1}
F(000)	4408

Table II-4-3. Data collection and structure refinement for **II-2b** ($C_{96}H_{116}O_8Si_4 \cdot 5CHCl_3$).

Theta range for data used in the structural refinement	3.17 to 25.00°	
Index ranges	$-39 \leq h \leq 35$, $-23 \leq k \leq 22$, $-18 \leq l \leq 20$	
Reflections	24352	
Independent reflections	8361 [R(int) = 0.0274]	
Coverage of independent reflections	99.7%	
Absorption correction	multi-scan	
Max. and min. transmission	0.940 and 0.781	
Refinement method	Full-matrix least-squares on F^2	
Refinement program	SHELXL-2014 (Sheldrick, 2014)	
Data / restraints / parameters	8361 / 1 / 556	
Goodness-of-fit on F^2	1.056	
Final R indices	7086 data; $I>2\sigma(I)$	R1 = 0.0686, wR2 = 0.1897
	all data	R1 = 0.0817, wR2 = 0.2043
Largest diff. peak and hole	1.273 and -0.560 $e^-/Å^3$	
Flack parameter	0.09(2)	

Table II-4-4. Atomic coordinates and equivalent isotropic atomic displacement parameters ($Å^2$) for the atoms of the independent half-molecule of **II-2b** ($C_{96}H_{116}O_8Si_4$). U(eq) is defined as one third of the trace of the orthogonalized U_{ij} tensor.

	x/a	y/b	z/c	U(eq)
Si1	0.11791(4)	0.04525(6)	0.94418(8)	0.0354(3)
Si2	0.11886(4)	0.36433(7)	0.34545(8)	0.0341(3)
O1	0.19427(9)	0.42732(15)	0.71264(19)	0.0363(8)
O2	0.19390(8)	0.36368(16)	0.8428(2)	0.0365(8)
O3	0.08382(10)	0.10775(16)	0.9460(2)	0.0429(8)
O4	0.08420(9)	0.37104(15)	0.41538(18)	0.0346(8)
C1	0.08574(14)	0.2429(2)	0.9888(3)	0.0340(11)
C2	0.11433(15)	0.2612(2)	0.0428(3)	0.0373(12)

	x/a	y/b	z/c	U(eq)
C3	0.15192(15)	0.2884(2)	0.0203(3)	0.0365(12)
C4	0.16025(14)	0.2996(2)	0.9418(3)	0.0392(12)
C5	0.13132(16)	0.2809(3)	0.8855(3)	0.0441(13)
C6	0.09461(16)	0.2522(3)	0.9094(3)	0.0443(13)
C7	0.19754(15)	0.3331(2)	0.9150(3)	0.0383(12)
C8	0.23588(16)	0.3418(3)	0.9421(3)	0.0484(13)
C9	0.25727(15)	0.3809(3)	0.8828(3)	0.0494(15)
C10	0.23080(13)	0.3936(2)	0.8252(3)	0.0370(12)
C11	0.23030(13)	0.4319(2)	0.7526(3)	0.0365(12)
C12	0.25586(14)	0.4752(3)	0.7154(3)	0.0468(14)
C13	0.23367(16)	0.5006(3)	0.6478(3)	0.0517(14)
C14	0.19680(15)	0.4708(2)	0.6484(3)	0.0375(12)
C15	0.15932(14)	0.4730(2)	0.6021(3)	0.0354(11)
C16	0.15058(15)	0.5276(2)	0.5520(3)	0.0370(12)
C17	0.11406(15)	0.5308(2)	0.5126(3)	0.0355(11)
C18	0.08564(14)	0.4785(2)	0.5200(3)	0.0343(11)
C19	0.09518(15)	0.4219(2)	0.5682(3)	0.0336(11)
C20	0.13116(15)	0.4204(2)	0.6093(3)	0.0357(11)
C21	0.09693(17)	0.9652(3)	0.9927(3)	0.0468(14)
C22	0.0697(2)	0.9796(3)	0.0613(4)	0.0643(18)
C23	0.1296(2)	0.9142(3)	0.0141(4)	0.0694(19)
C24	0.16168(16)	0.0864(3)	0.9988(4)	0.0553(16)
C25	0.15319(19)	0.0943(3)	0.0847(4)	0.0588(16)
C26	0.2021(2)	0.0563(4)	0.9868(6)	0.086(2)
C27	0.1359(2)	0.0273(3)	0.8409(3)	0.0626(17)
C28	0.1098(3)	0.9842(5)	0.7931(4)	0.095(3)
C29	0.1463(5)	0.0937(5)	0.8003(5)	0.178(5)
C30	0.16720(15)	0.3901(3)	0.3980(3)	0.0423(13)
C31	0.18273(17)	0.3360(3)	0.4527(4)	0.0546(15)
C32	0.19973(17)	0.4172(4)	0.3434(4)	0.0624(17)
C33	0.11966(16)	0.2742(3)	0.3060(3)	0.0490(14)
C34	0.1177(2)	0.2176(3)	0.3668(5)	0.068(2)
C35	0.15545(19)	0.2620(4)	0.2505(4)	0.075(2)
C36	0.10661(17)	0.4277(3)	0.2659(3)	0.0517(15)

	x/a	y/b	z/c	U(eq)
C37	0.0708(2)	0.4086(4)	0.2154(4)	0.073(2)
C38	0.1028(2)	0.5003(3)	0.2984(4)	0.0598(16)
C39	0.04331(14)	0.2232(2)	0.0092(3)	0.0368(12)
C40	0.02167(15)	0.2670(2)	0.0552(3)	0.0391(12)
C41	0.02205(14)	0.1670(2)	0.9719(3)	0.0345(11)
C42	0.04251(14)	0.1108(2)	0.9376(3)	0.0363(11)
C43	0.02153(16)	0.0609(3)	0.8996(3)	0.0452(13)
C44	0.04298(14)	0.4827(2)	0.4896(3)	0.0344(11)
C45	0.02155(16)	0.5407(2)	0.5071(3)	0.0408(12)
C46	0.02179(14)	0.4255(2)	0.4542(2)	0.0300(10)
C47	0.04287(14)	0.3704(2)	0.4170(3)	0.0306(10)
C48	0.02081(15)	0.3182(2)	0.3825(3)	0.0397(12)

Table II-4-5. Interatomic distances (Å) for the non-hydrogen atoms of the independent half-molecule of **II-2b** ($C_{96}H_{116}O_8Si_4$).[a]

Si1-O3	1.655(3)	Si1-C24	1.893(6)
Si1-C27	1.895(6)	Si1-C21	1.896(5)
Si2-O4	1.657(3)	Si2-C36	1.878(6)
Si2-C33	1.879(5)	Si2-C30	1.893(5)
O1-C11	1.371(6)	O1-C14	1.389(6)
O2-C7	1.374(6)	O2-C10	1.380(5)
O3-C42	1.368(5)	O4-C47	1.360(5)
Cl1-C49	1.706(7)	Cl2-C49	1.713(7)
Cl3-C49	1.731(8)	Cl4-C50	1.740(5)
Cl5-C50	1.775(9)	C1-C2	1.365(7)
C1-C6	1.400(7)	C1-C39	1.489(7)
C2-C3	1.399(7)	C3-C4	1.387(7)
C4-C5	1.402(7)	C4-C7	1.463(7)
C5-C6	1.391(7)	C7-C8	1.354(7)
C8-C9	1.449(8)	C9-C10	1.338(7)
C10-C11	1.448(7)	C11-C12	1.349(7)

C12-C13	1.454(8)	C13-C14	1.344(7)
C14-C15	1.465(7)	C15-C20	1.386(7)
C15-C16	1.395(6)	C16-C17	1.379(7)
C17-C18	1.388(6)	C18-C19	1.410(6)
C18-C44	1.499(7)	C19-C20	1.376(7)
C21-C22	1.500(8)	C21-C23	1.508(8)
C24-C26	1.467(9)	C24-C25	1.503(9)
C27-C28	1.453(10)	C27-C29	1.505(11)
C30-C31	1.497(8)	C30-C32	1.514(8)
C33-C34	1.516(9)	C33-C35	1.531(9)
C36-C37	1.508(9)	C36-C38	1.523(9)
C39-C40	1.361(7)	C39-C41	1.447(6)
C40-C40'	1.426(10)	C41-C42	1.411(7)
C41-C41'	1.451(9)	C42-C43	1.357(7)
C43-C43'	1.417(10)	C44-C45	1.362(7)
C44-C46	1.447(6)	C45-C45'	1.418(10)
C46-C47	1.426(6)	C46-C46'	1.433(9)
C47-C48	1.380(6)	C48-C48'	1.369(10)

[a]The primed (') atoms are related by a crystallographic mirror plane.

Table II-4-6. Bond angles (°) for the atoms of the independent half-molecule of **II-2b (**$C_{96}H_{116}O_8Si_4$).

O3-Si1-C24	101.3(2)	O3-Si1-C27	111.4(2)
C24-Si1-C27	107.4(3)	O3-Si1-C21	110.4(2)
C24-Si1-C21	114.1(3)	C27-Si1-C21	111.7(3)
O4-Si2-C36	108.8(2)	O4-Si2-C33	110.0(2)
C36-Si2-C33	110.8(3)	O4-Si2-C30	102.4(2)
C36-Si2-C30	110.5(2)	C33-Si2-C30	113.9(2)
C11-O1-C14	107.6(4)	C7-O2-C10	107.6(4)
C42-O3-Si1	134.7(3)	C47-O4-Si2	134.6(3)
C2-C1-C6	118.6(4)	C2-C1-C39	123.7(4)
C6-C1-C39	117.1(4)	C1-C2-C3	121.5(4)
C4-C3-C2	120.0(4)	C3-C4-C5	119.3(5)
C3-C4-C7	122.6(5)	C5-C4-C7	118.0(5)

C6-C5-C4	119.5(5)	C5-C6-C1	121.1(5)
C8-C7-O2	109.5(4)	C8-C7-C4	136.8(5)
O2-C7-C4	113.6(4)	C7-C8-C9	106.2(5)
C10-C9-C8	107.2(4)	C9-C10-O2	109.5(4)
C9-C10-C11	137.2(4)	O2-C10-C11	113.2(4)
C12-C11-O1	110.2(4)	C12-C11-C10	135.9(5)
O1-C11-C10	113.8(4)	C11-C12-C13	105.9(4)
C14-C13-C12	107.4(5)	C13-C14-O1	108.8(4)
C13-C14-C15	137.9(5)	O1-C14-C15	113.2(4)
C20-C15-C16	118.6(4)	C20-C15-C14	119.6(4)
C16-C15-C14	121.8(4)	C17-C16-C15	120.9(4)
C16-C17-C18	120.7(4)	C17-C18-C19	118.4(4)
C17-C18-C44	123.9(4)	C19-C18-C44	117.0(4)
C20-C19-C18	120.4(4)	C19-C20-C15	120.9(4)
C22-C21-C23	111.1(5)	C22-C21-Si1	113.9(4)
C23-C21-Si1	112.7(4)	C26-C24-C25	110.2(6)
C26-C24-Si1	116.8(5)	C25-C24-Si1	112.5(4)
C28-C27-C29	111.8(7)	C28-C27-Si1	116.4(5)
C29-C27-Si1	110.0(5)	C31-C30-C32	112.8(5)
C31-C30-Si2	113.4(4)	C32-C30-Si2	113.2(4)
C34-C33-C35	110.2(5)	C34-C33-Si2	115.6(4)
C35-C33-Si2	112.2(4)	C37-C36-C38	112.0(5)
C37-C36-Si2	114.9(4)	C38-C36-Si2	111.3(4)
C40-C39-C41	118.4(4)	C40-C39-C1	117.6(4)
C41-C39-C1	123.1(4)	C39-C40-C40'	121.6(3)
C42-C41-C39	122.6(4)	C42-C41-C41	118.5(3)
C39-C41-C41'	118.9(3)	C43-C42-O3	121.6(4)
C43-C42-C41	120.7(4)	O3-C42-C41	117.6(4)
C42-C43-C43'	120.6(3)	C45-C44-C46	118.6(4)
C45-C44-C18	117.0(4)	C46-C44-C18	123.6(4)
C44-C45-C45'	121.2(3)	C47-C46-C46'	119.1(3)
C47-C46-C44	122.1(4)	C46'-C46-C44	118.8(3)
O4-C47-C48	121.6(4)	O4-C47-C46	119.2(4)
C48-C47-C46	119.2(4)	C48'-C48-C47	121.7(3)

[a]The primed (') atoms are related by a crystallographic mirror plane.

Table II-4-7. Anisotropic atomic displacement parameters ($Å^2$) for the atoms of the independent half-molecule of **II-2b** ($C_{96}H_{116}O_8Si_4$). The anisotropic atomic displacement factor exponent takes the form: $-2\pi^2[h^2 a^{*2} U_{11} + ... + 2 h k a^* b^* U_{12}]$.

	U_{11}	U_{22}	U_{33}	U_{23}	U_{13}	U_{12}
Si1	0.0425(6)	0.0370(6)	0.0267(5)	-0.0025(5)	0.0030(6)	0.0070(6)
Si2	0.0345(6)	0.0408(6)	0.0270(5)	-0.0016(5)	0.0002(6)	-0.0024(5)
O1	0.0343(15)	0.0363(15)	0.0384(17)	-0.0015(14)	-0.0016(15)	-0.0008(13)
O2	0.0279(14)	0.0414(15)	0.0401(16)	0.0031(15)	-0.0056(15)	0.0003(13)
O3	0.0358(16)	0.0370(15)	0.0558(19)	-0.0051(16)	-0.0065(17)	0.0056(14)
O4	0.0383(16)	0.0350(15)	0.0305(15)	-0.0010(13)	-0.0001(15)	-0.0032(13)
Cl1	0.0991(13)	0.1013(14)	0.0820(12)	-0.0061(11)	0.0061(12)	0.0096(11)
Cl2	0.207(2)	0.1517(15)	0.1223(16)	-0.0697(13)	0.0942(14)	-0.1194(13)
Cl3	0.0882(11)	0.0756(10)	0.0694(10)	-0.0009(8)	-0.0046(10)	-0.0062(9)
Cl4	0.1353(15)	0.0964(12)	0.1060(14)	0.0280(11)	-0.0536(12)	-0.0526(11)
Cl5	0.0647(12)	0.0545(10)	0.0631(12)	-0.0006(10)	0	0
C1	0.043(2)	0.0260(19)	0.033(2)	0.0085(18)	-0.008(2)	0.0002(18)
C2	0.048(3)	0.029(2)	0.034(2)	-0.0023(19)	-0.004(2)	0.001(2)
C3	0.041(2)	0.035(2)	0.034(2)	-0.0013(19)	-0.014(2)	0.006(2)
C4	0.036(2)	0.038(2)	0.044(3)	0.003(2)	-0.005(2)	0.000(2)
C5	0.044(3)	0.057(3)	0.032(2)	0.006(2)	-0.011(2)	-0.005(2)
C6	0.045(3)	0.051(3)	0.037(2)	0.009(2)	-0.012(2)	-0.005(2)
C7	0.043(2)	0.032(2)	0.039(2)	0.001(2)	-0.005(2)	0.004(2)
C8	0.041(3)	0.057(3)	0.047(3)	0.009(3)	-0.017(2)	-0.005(2)
C9	0.028(2)	0.061(3)	0.059(3)	0.003(3)	-0.006(2)	-0.004(2)
C10	0.027(2)	0.035(2)	0.049(3)	-0.002(2)	-0.005(2)	0.0022(18)
C11	0.029(2)	0.037(2)	0.043(3)	-0.007(2)	0.002(2)	0.0020(19)
C12	0.024(2)	0.058(3)	0.058(3)	-0.007(3)	0.003(2)	-0.009(2)
C13	0.049(3)	0.064(3)	0.042(3)	0.001(3)	0.009(3)	-0.017(3)
C14	0.045(3)	0.033(2)	0.034(2)	-0.004(2)	0.006(2)	-0.002(2)
C15	0.036(2)	0.037(2)	0.033(2)	-0.005(2)	0.006(2)	-0.0008(19)
C16	0.049(3)	0.030(2)	0.032(2)	-0.0001(19)	0.009(2)	-0.0142(19)
C17	0.051(3)	0.025(2)	0.030(2)	0.0037(18)	0.002(2)	-0.0084(19)
C18	0.046(2)	0.031(2)	0.026(2)	-0.0008(18)	-0.001(2)	-0.0031(19)
C19	0.044(2)	0.029(2)	0.027(2)	0.0022(18)	0.002(2)	-0.0077(19)

	U_{11}	U_{22}	U_{33}	U_{23}	U_{13}	U_{12}
C20	0.047(3)	0.033(2)	0.027(2)	-0.0025(19)	0.006(2)	-0.002(2)
C21	0.055(3)	0.048(3)	0.037(3)	-0.003(2)	0.000(3)	-0.003(2)
C22	0.090(4)	0.059(3)	0.044(3)	0.016(3)	0.011(3)	-0.009(3)
C23	0.096(4)	0.045(3)	0.067(4)	0.005(3)	-0.013(4)	0.015(3)
C24	0.041(3)	0.069(3)	0.056(3)	0.000(3)	-0.001(3)	0.003(3)
C25	0.059(3)	0.063(3)	0.054(3)	-0.006(3)	-0.017(3)	-0.004(3)
C26	0.056(4)	0.090(5)	0.113(6)	-0.026(5)	-0.016(4)	0.008(4)
C27	0.090(4)	0.058(3)	0.040(3)	-0.007(3)	0.011(3)	0.011(3)
C28	0.137(7)	0.105(5)	0.043(3)	-0.023(4)	0.020(4)	-0.012(5)
C29	0.381(16)	0.077(5)	0.076(4)	0.017(4)	0.121(6)	-0.004(8)
C30	0.040(2)	0.047(3)	0.040(3)	-0.006(2)	-0.005(2)	-0.008(2)
C31	0.043(3)	0.066(3)	0.055(3)	-0.004(3)	-0.015(3)	0.002(3)
C32	0.045(3)	0.083(4)	0.059(3)	0.002(3)	0.001(3)	-0.015(3)
C33	0.040(3)	0.052(3)	0.055(3)	-0.019(3)	-0.009(3)	0.002(2)
C34	0.072(4)	0.042(3)	0.091(5)	-0.008(3)	-0.020(4)	0.002(3)
C35	0.053(3)	0.102(5)	0.069(4)	-0.041(3)	-0.006(3)	0.007(3)
C36	0.054(3)	0.070(3)	0.031(2)	0.019(2)	0.006(3)	-0.002(3)
C37	0.074(4)	0.104(5)	0.041(3)	0.004(3)	-0.016(3)	0.005(4)
C38	0.071(4)	0.062(3)	0.046(3)	0.025(3)	0.006(3)	-0.007(3)
C39	0.039(2)	0.031(2)	0.040(2)	0.014(2)	-0.005(2)	-0.0014(19)
C40	0.043(2)	0.027(2)	0.047(3)	0.002(2)	-0.002(2)	0.0001(19)
C41	0.042(2)	0.029(2)	0.032(2)	0.0075(18)	-0.003(2)	-0.0052(18)
C42	0.031(2)	0.041(2)	0.037(2)	0.000(2)	-0.003(2)	0.0023(19)
C43	0.047(3)	0.045(2)	0.043(3)	-0.013(2)	0.002(2)	0.004(2)
C44	0.048(2)	0.032(2)	0.023(2)	0.0044(18)	0.004(2)	-0.005(2)
C45	0.054(3)	0.032(2)	0.037(2)	-0.001(2)	0.001(2)	-0.006(2)
C46	0.045(2)	0.0245(18)	0.0202(19)	0.0039(17)	0.0016(19)	0.0006(18)
C47	0.039(2)	0.0268(19)	0.026(2)	0.0026(17)	-0.001(2)	-0.0001(18)
C48	0.039(2)	0.037(2)	0.044(3)	-0.012(2)	0.002(2)	-0.002(2)

Table II-4-8. Hydrogen atom coordinates and isotropic atomic displacement parameters ($Å^2$) for the independent half-molecule of **II-2b** ($C_{96}H_{116}O_8Si_4$).

	x/a	y/b	z/c	U(eq)
H2	0.1086	0.2553	1.0969	0.045
H3	0.1717	0.2992	1.0588	0.044
H5	0.1367	0.2877	0.8315	0.053
H6	0.0752	0.2386	0.8712	0.053
H8	0.2466	0.3256	0.9903	0.058
H9	0.2849	0.3948	0.8846	0.059
H12	0.2828	0.4867	0.7303	0.056
H13	0.2434	0.5325	0.6101	0.062
H16	0.1700	0.5631	0.5449	0.044
H17	0.1083	0.5691	0.4800	0.043
H19	0.0767	0.3846	0.5724	0.04
H20	0.1368	0.3827	0.6430	0.043
H21	0.0795	-0.0580	0.9526	0.056
H22A	0.0580	-0.0636	1.0803	0.096
H22B	0.0478	0.0107	1.0451	0.096
H22C	0.0856	0.0012	1.1032	0.096
H23A	0.1464	-0.0670	1.0564	0.104
H23B	0.1468	-0.0948	0.9682	0.104
H23C	0.1170	-0.1289	1.0314	0.104
H24	0.1636	0.1343	0.9779	0.066
H25A	0.1529	0.0489	1.1095	0.088
H25B	0.1267	0.1164	1.0919	0.088
H25C	0.1744	0.1227	1.1087	0.088
H26A	0.2218	0.0793	1.0210	0.13
H26B	0.2102	0.0623	0.9321	0.13
H26C	0.2012	0.0072	0.9994	0.13
H27	0.1622	0.0017	0.8463	0.075
H28A	0.0840	0.0079	0.7836	0.143
H28B	0.1046	-0.0592	0.8204	0.143
H28C	0.1232	-0.0253	0.7430	0.143

	x/a	y/b	z/c	U(eq)
H29A	0.1633	0.0841	0.7545	0.267
H29B	0.1611	0.1237	0.8365	0.267
H29C	0.1212	0.1165	0.7835	0.267
H30	0.1595	0.4298	0.4319	0.051
H31A	0.1976	0.3010	0.4229	0.082
H31B	0.1598	0.3145	0.4799	0.082
H31C	0.2010	0.3571	0.4911	0.082
H32A	0.2240	0.4293	0.3738	0.094
H32B	0.1896	0.4581	0.3163	0.094
H32C	0.2067	0.3817	0.3050	0.094
H33	0.0946	0.2693	0.2735	0.059
H34A	0.1099	0.1743	0.3415	0.103
H34B	0.0974	0.2295	0.4066	0.103
H34C	0.1443	0.2123	0.3915	0.103
H35A	0.1809	0.2617	0.2804	0.112
H35B	0.1564	0.2987	0.2113	0.112
H35C	0.1520	0.2176	0.2242	0.112
H36	0.1308	0.4282	0.2304	0.062
H37A	0.0456	0.4138	0.2455	0.11
H37B	0.0735	0.3607	0.1983	0.11
H37C	0.0699	0.4387	0.1695	0.11
H38A	0.0960	0.5320	0.2559	0.09
H38B	0.1287	0.5140	0.3221	0.09
H38C	0.0813	0.5015	0.3381	0.09
H40	0.0358	0.2983	1.0881	0.047
H43	0.0358	0.0256	0.8728	0.054
H45	0.0357	0.5818	0.5195	0.049
H48	0.0349	0.2814	0.3581	0.048

UV-vis and Fluorescence Spectra.

a)

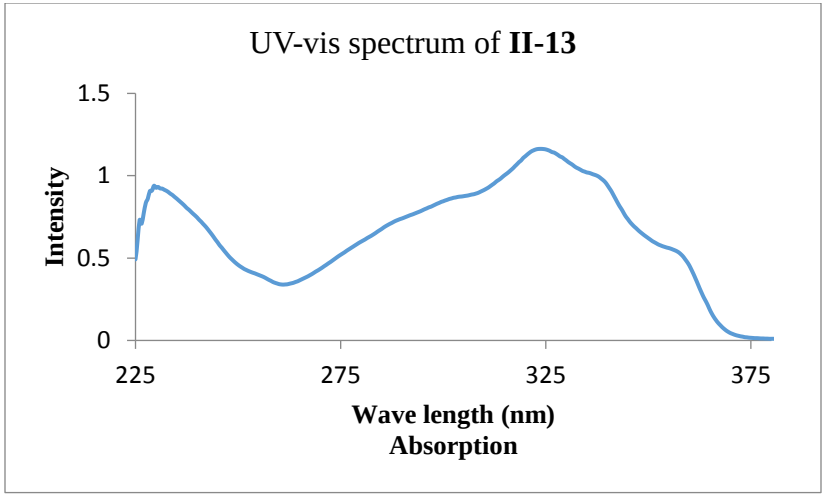

Spectrum a): UV-vis absorption spectrum of **II-13** (sample 2) at the concentration of 2.6×10^{-5} M in degassed CH_2Cl_2. At the absorption maximum λ_{abs} = 324 nm, $\varepsilon = 4.4 \times 10^4$ cm^{-1} M^{-1}.

b)

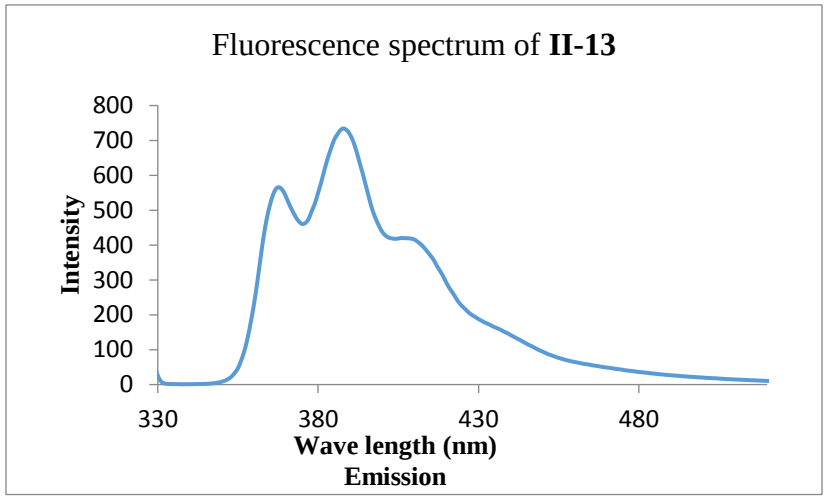

Spectrum b): Fluorescence spectrum of **II-13** (sample 2) at the concentration of 5.3×10^{-7} M in degassed CH_2Cl_2 upon excitation at 324 nm. Fluorescence maximum λ_{em} = 388 nm.

c)

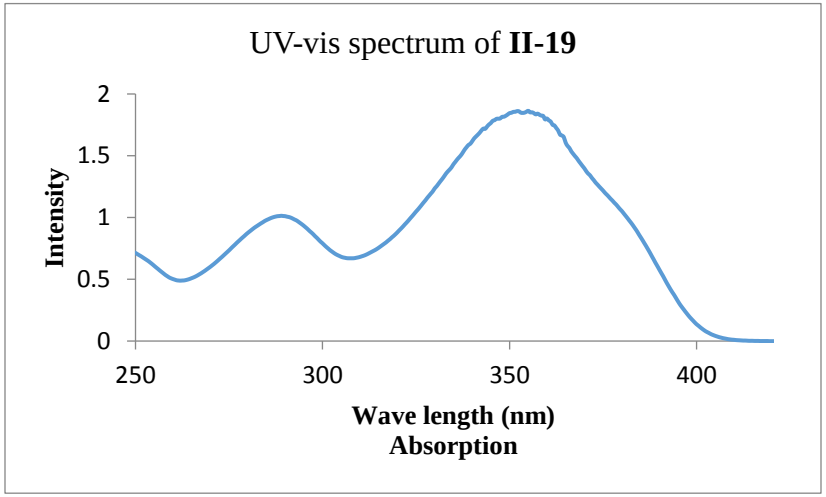

Spectrum c): UV-vis absorption spectrum of **II-19** at the concentration of 2.0×10^{-5} M in degassed CH_2Cl_2. At the absorption maximum λ_{abs} = 355 nm, $\varepsilon = 9.1 \times 10^4$ cm^{-1} M^{-1}.

d)

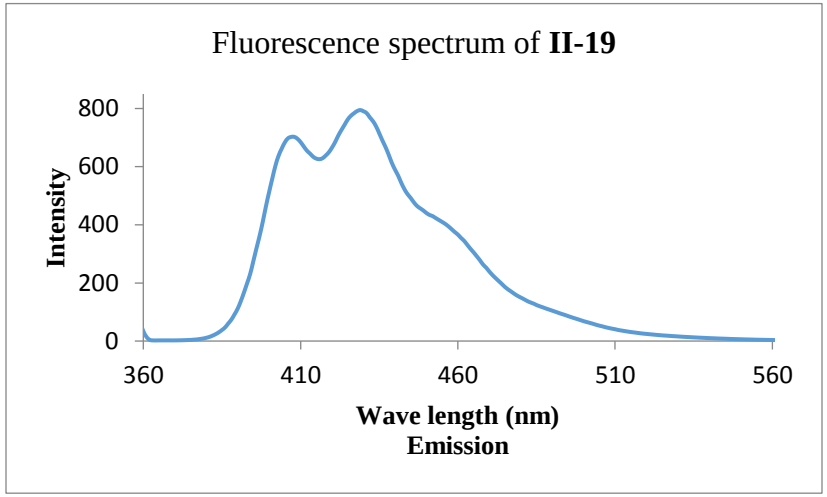

Spectrum d): Fluorescence spectrum of **II-19** at the concentration of 2.0×10^{-7} M in degassed CH_2Cl_2 upon excitation at 355 nm. Fluorescence maximum λ_{em} = 429 nm.

e)

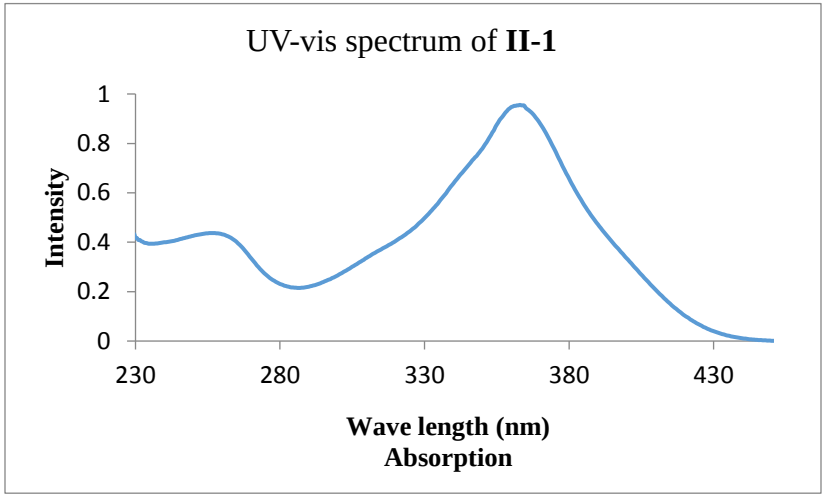

Spectrum e): UV-vis absorption spectrum of **II-1** at the concentration of 5.3×10^{-6} M in degassed CH_2Cl_2. At the absorption maximum λ_{abs} = 363 nm, $\varepsilon = 1.8 \times 10^5$ cm^{-1} M^{-1}.

f)

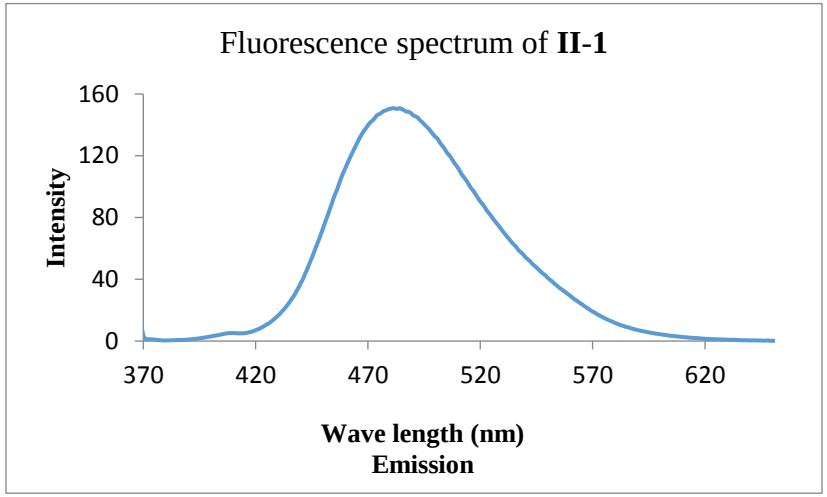

Spectrum f): Fluorescence spectrum of **II-1** at the concentration of 1.1×10^{-7} M in degassed CH_2Cl_2 upon excitation at 363 nm. Fluorescence maximum λ_{em} = 481 nm.

g)

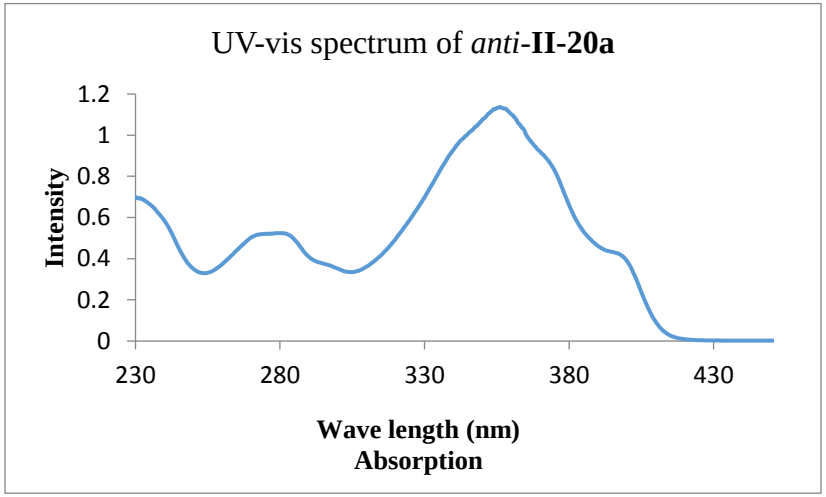

Spectrum g): UV-vis absorption spectrum of *anti*-**II-20a** at the concentration of 1.5×10^{-5} M in degassed CH_2Cl_2. At the absorption maximum λ_{abs} = 356 nm, $\varepsilon = 7.4 \times 10^4$ cm^{-1} M^{-1}.

h)

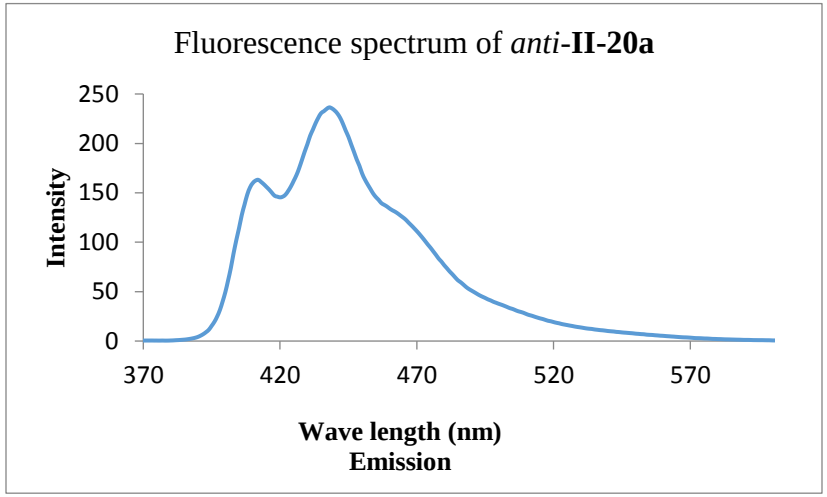

Spectrum h): Fluorescence spectrum of *anti*-**II-20a** at the concentration of 1.5×10^{-7} M in degassed CH_2Cl_2 upon excitation at 356 nm. Fluorescence maximum λ_{em} = 438 nm.

i)

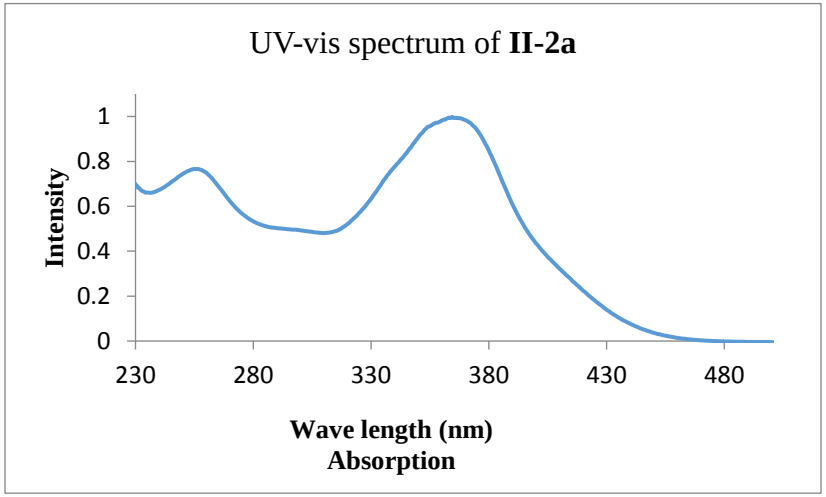

Spectrum i): UV-vis absorption spectrum of **II-2a** at the concentration of 1.6×10^{-5} M in degassed CH_2Cl_2. At the absorption maximum λ_{abs} = 364.5 nm, $\varepsilon = 6.0 \times 10^4$ cm^{-1} M^{-1}.

j)

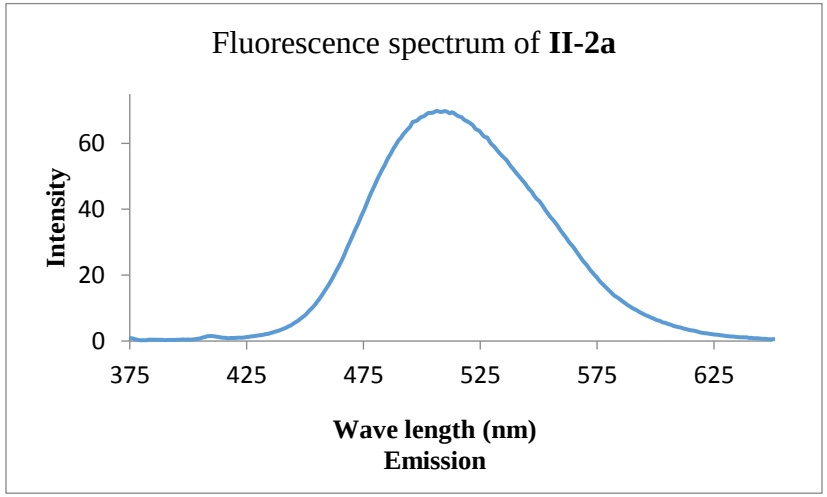

Spectrum j): Fluorescence spectrum of **II-2a** at the concentration of 3.3×10^{-7} M in degassed CH_2Cl_2 upon excitation at 364.5 nm. Fluorescence maximum λ_{em} = 510 nm.

k)

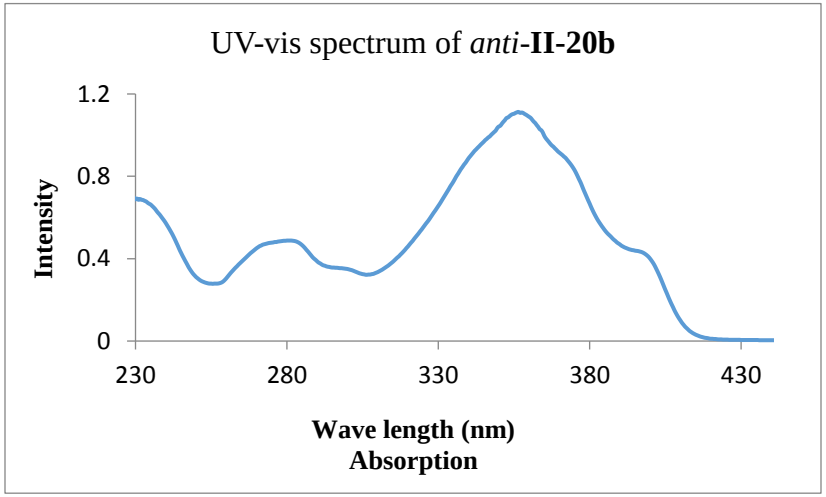

Spectrum k): UV-vis absorption spectrum of *anti*-**II-20b** at the concentration of 1.6×10^{-5} M in degassed CH_2Cl_2. At the absorption maximum λ_{abs} = 356.5 nm, $\varepsilon = 7.0 \times 10^4$ cm^{-1} M^{-1}.

l)

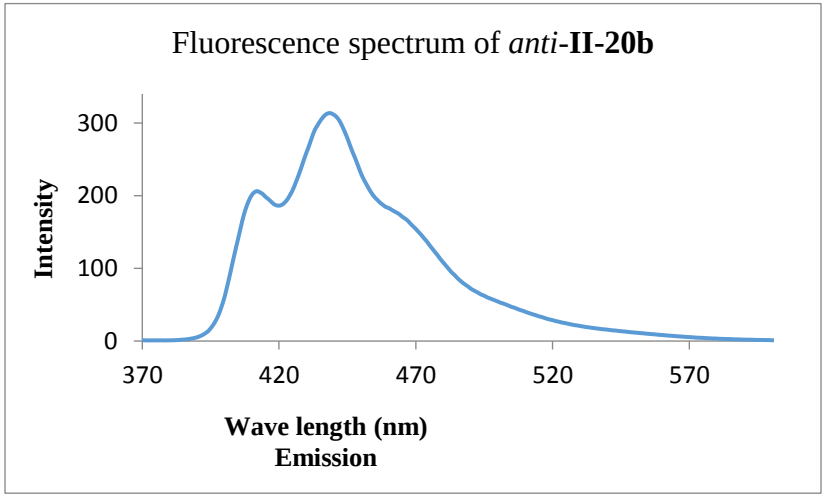

Spectrum l): Fluorescence spectrum of *anti*-**II-20b** at the concentration of 1.6×10^{-7} M in degassed CH_2Cl_2 upon excitation at 356.5 nm. Fluorescence maximum λ_{em} = 438 nm.

m)

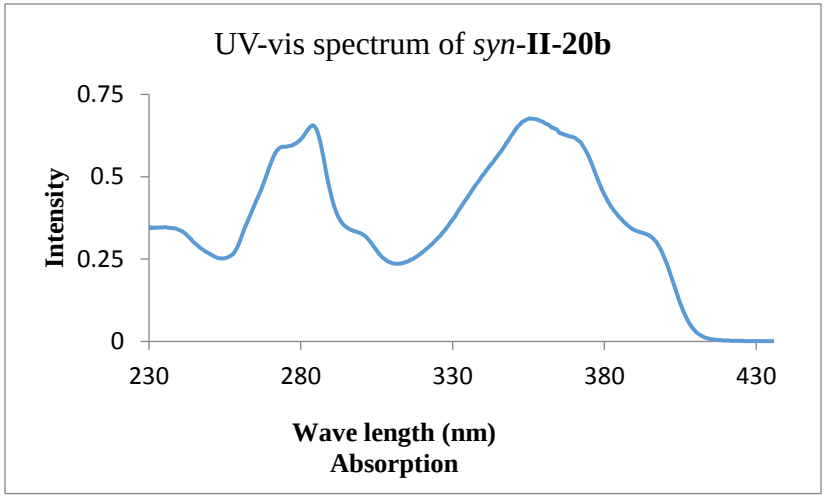

Spectrum m): UV-vis absorption spectrum of *syn*-**II-20b** at the concentration of 5.3×10^{-6} M in degassed CH_2Cl_2. At the absorption maximum λ_{abs} = 356 nm, $\varepsilon = 1.3 \times 10^5$ cm^{-1} M^{-1}.

n)

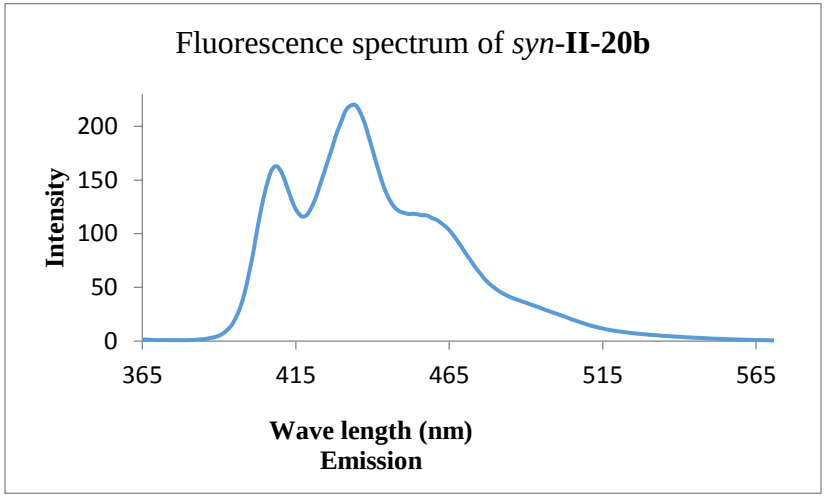

Spectrum n): Fluorescence spectrum of *syn*-**II-20b** at the concentration of 5.3×10^{-8} M in degassed CH_2Cl_2 upon excitation at 356 nm. Fluorescence maximum λ_{em} = 434 nm.

o)

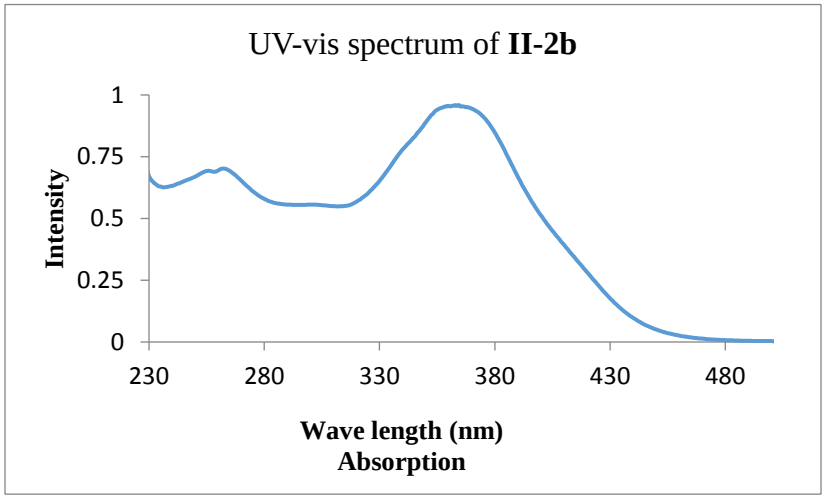

Spectrum o): UV-vis absorption spectrum of **II-2b** at the concentration of 2.0×10^{-5} M in degassed CH_2Cl_2. At the absorption maximum λ_{abs} = 364.5 nm, $\varepsilon = 4.8 \times 10^4$ cm^{-1} M^{-1}.

p)

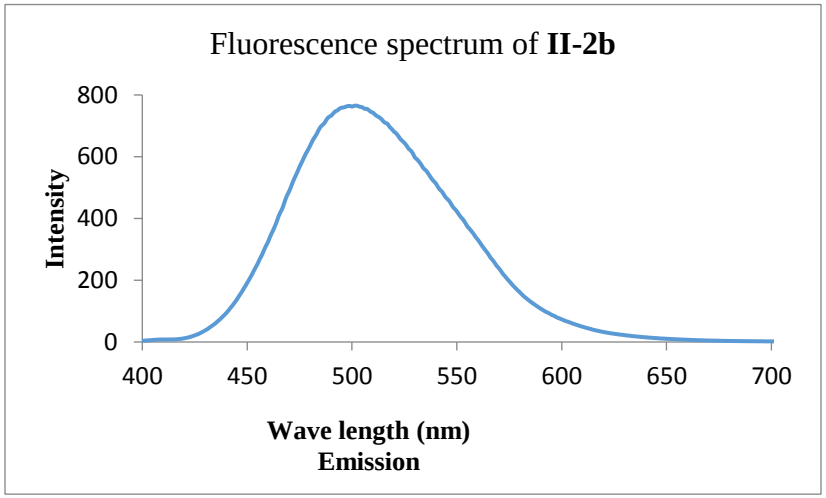

Spectrum p): Fluorescence spectrum of **II-2b** at the concentration of 2.0×10^{-5} M in degassed CH_2Cl_2 upon excitation at 364.5 nm. Fluorescence maximum λ_{em} = 502 nm.

q)

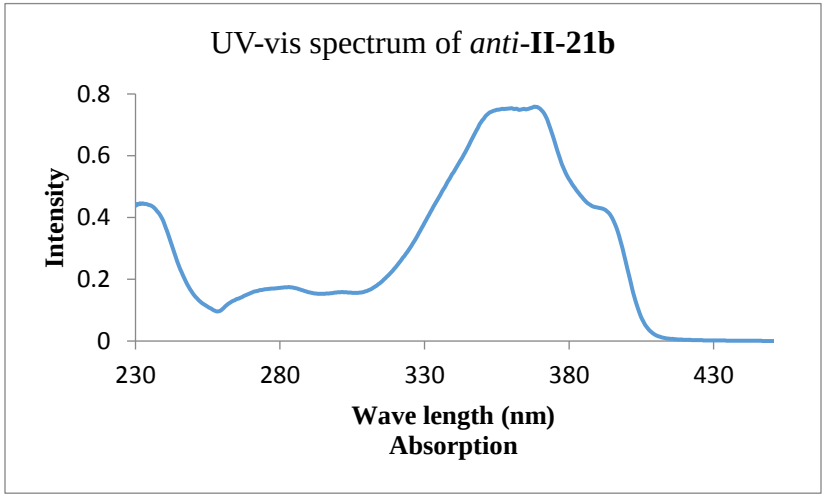

Spectrum q): UV-vis absorption spectrum of *anti*-**II-21b** at the concentration of 7.5×10^{-6} M in degassed CH_2Cl_2. At the absorption maximum λ_{abs} = 368 nm, $\varepsilon = 1.0 \times 10^5$ cm^{-1} M^{-1}.

r)

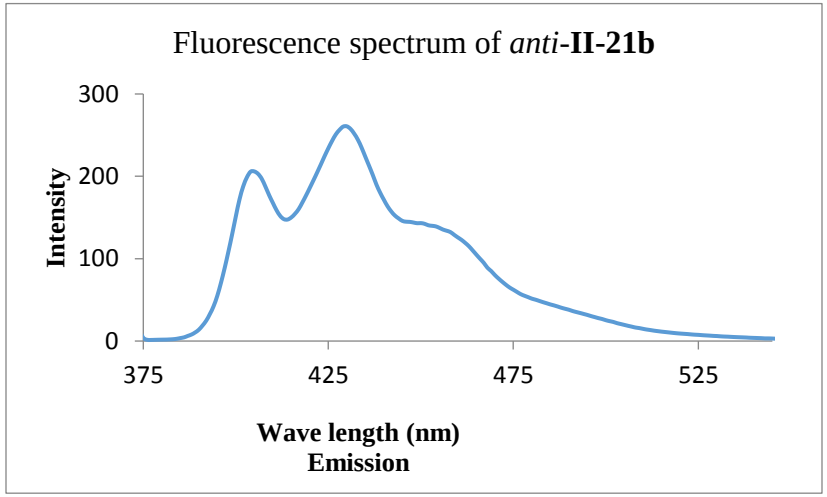

Spectrum r): Fluorescence spectrum of *anti*-**II-21b** at the concentration of 7.5×10^{-8} M in degassed CH_2Cl_2 upon excitation at 368 nm. Fluorescence maximum λ_{em} = 430 nm.

s)

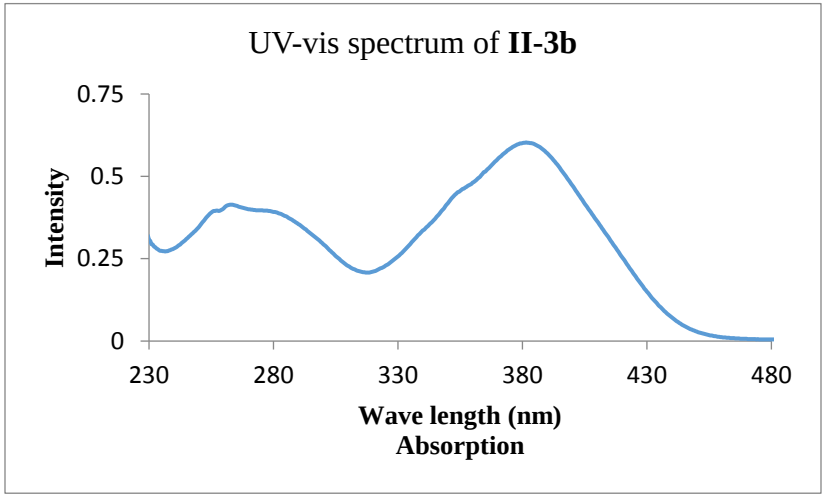

Spectrum s): UV-vis absorption spectrum of **II-3b** at the concentration of 4.8×10^{-6} M in degassed CH_2Cl_2. At the absorption maximum λ_{abs} = 381.5 nm, $\varepsilon = 1.2 \times 10^5$ cm^{-1} M^{-1}.

t)

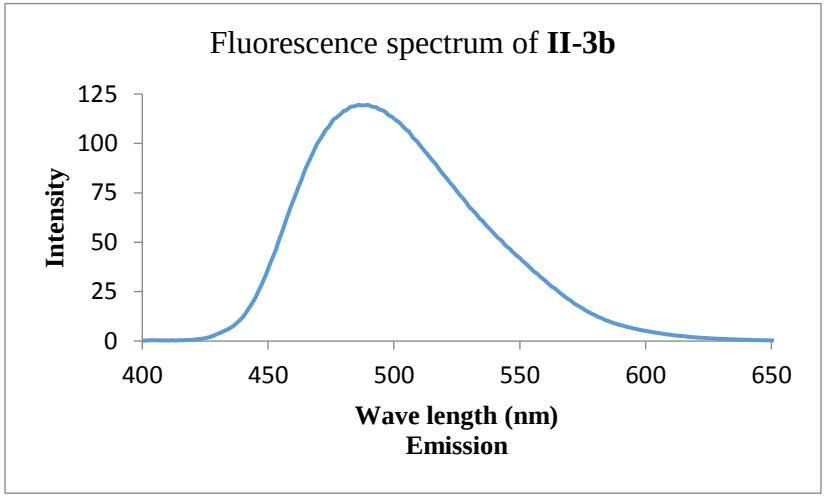

Spectrum t): Fluorescence spectrum of **II-3b** at the concentration of 9.2×10^{-8} M in degassed CH_2Cl_2 upon excitation at 381.5 nm. Fluorescence maximum λ_{em} = 486 nm.

u)

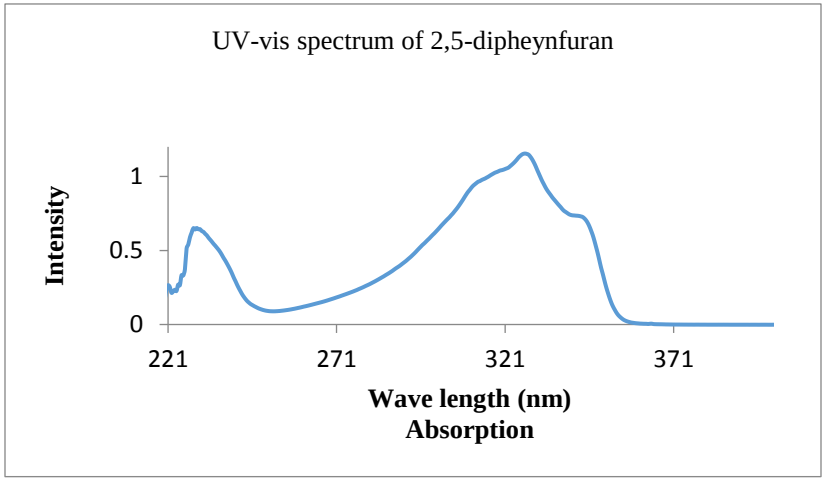

Spectrum u): UV-vis absorption spectrum of 2,5-diphenylfuran at the concentration of 5.9×10^{-5} M in degassed CH_2Cl_2. The absorption maximum λ_{abs} = 230 and 327 nm. At 327 nm, $\varepsilon = 2.3 \times 10^5$ cm^{-1} M^{-1}.

v)

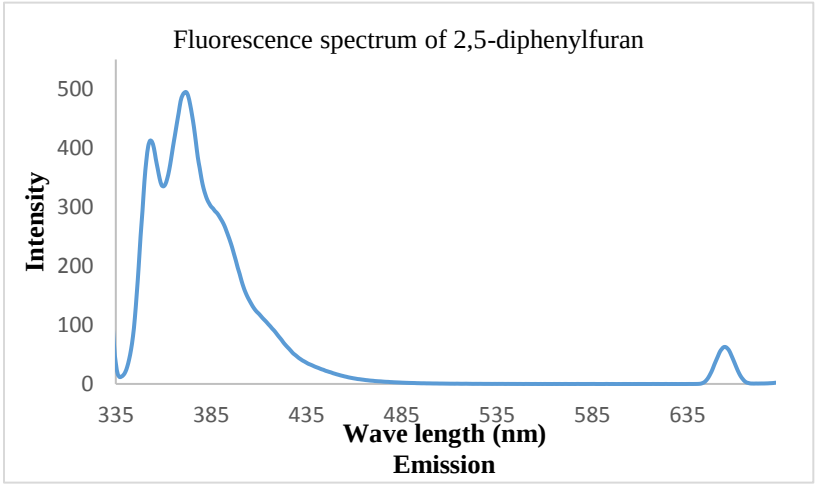

Spectrum v): Fluorescence spectrum of 2,5-diphenylfuran at the concentration of 5.9×10^{-8} in degassed CH_2Cl_2 upon excitation at 327 nm. Fluorescence maximum λ_{em} = 353, 372 nm.

w)

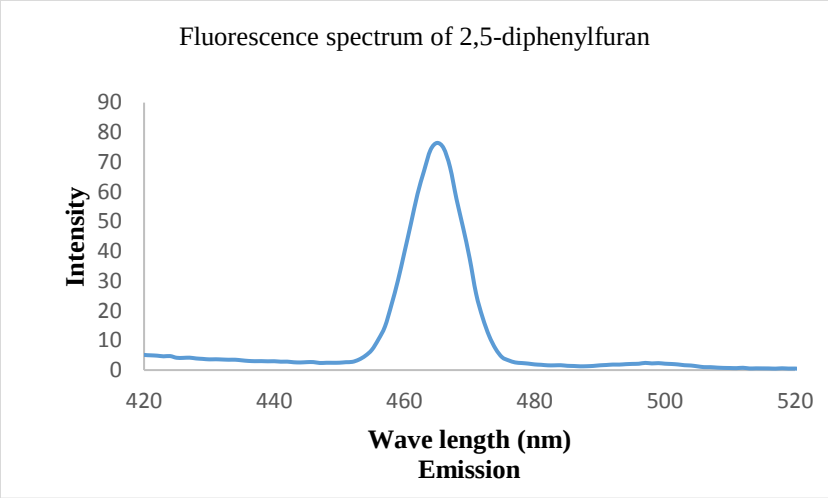

Spectrum w): Fluorescence spectrum of 2,5-diphenylfuran at the concentration of 5.9×10^{-8} in degassed CH_2Cl_2 upon excitation at 230 nm. Fluorescence maximum λ_{em} = 465 nm.

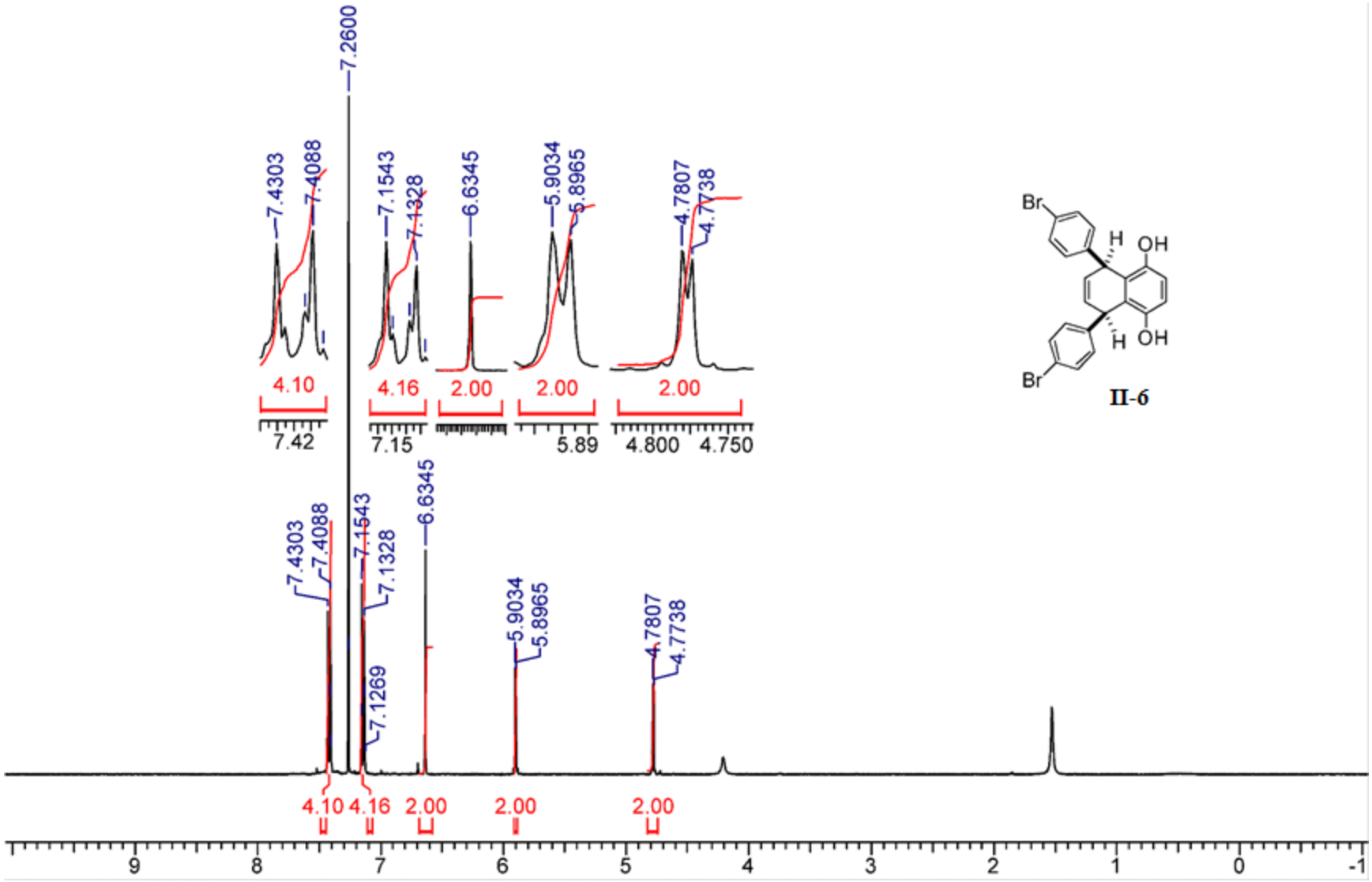
7.2600
7.4303
7.4088
7.1543
7.1328
6.6345
5.9034
5.8965
4.7807
4.7738
7.1269
4.10
4.16
2.00
2.00
2.00
7.42
7.15
5.89
4.800
4.750
Br
H
OH
H
OH
Br
II-6
9
8
7
6
5
4
3
2
1
0
-1

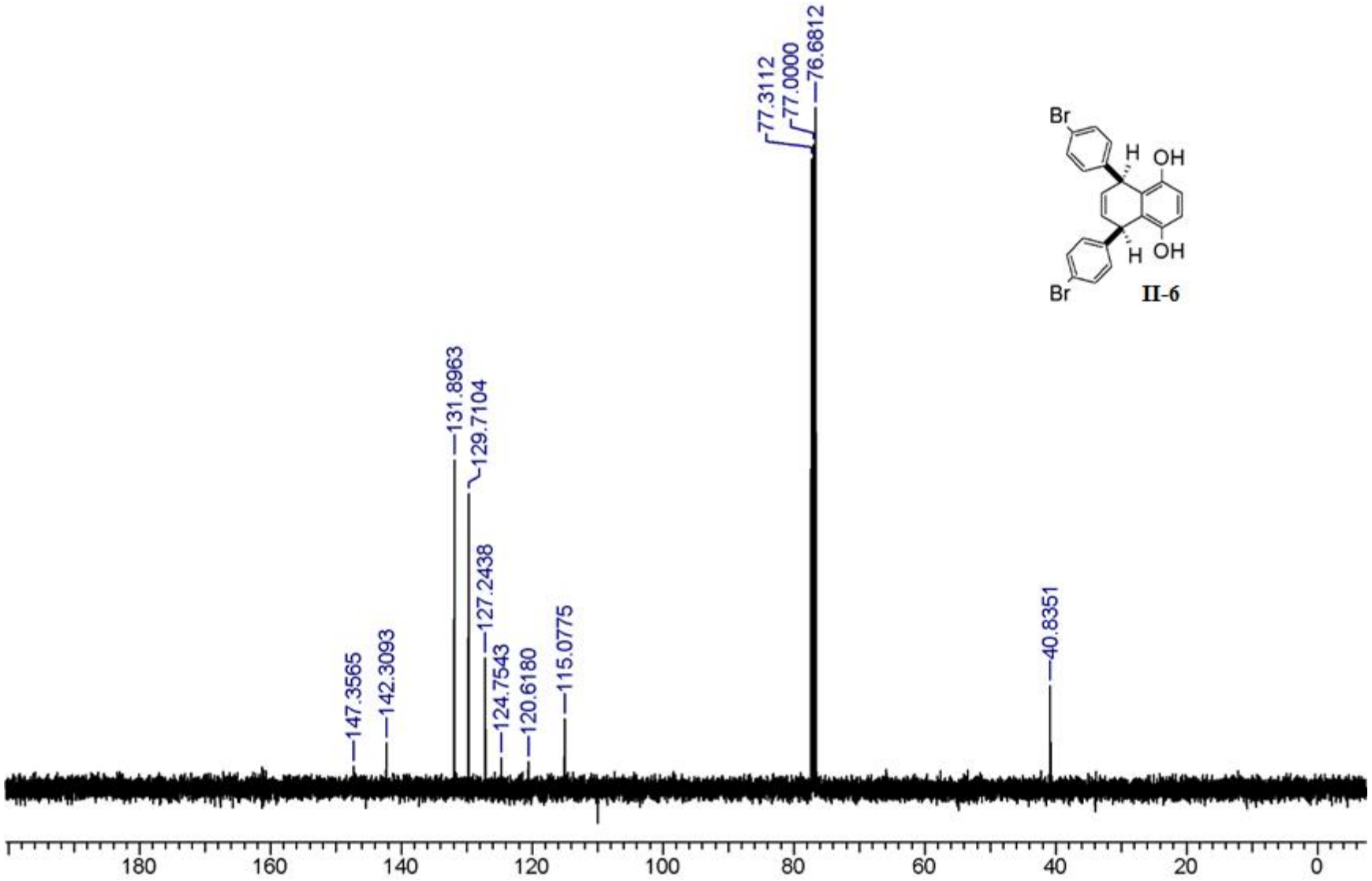
77.3112
77.0000
76.6812
131.8963
129.7104
127.2438
124.7543
120.6180
115.0775
147.3565
142.3093
40.8351
Br
H
OH
H
OH
Br
II-6
180
160
140
120
100
80
60
40
20
0

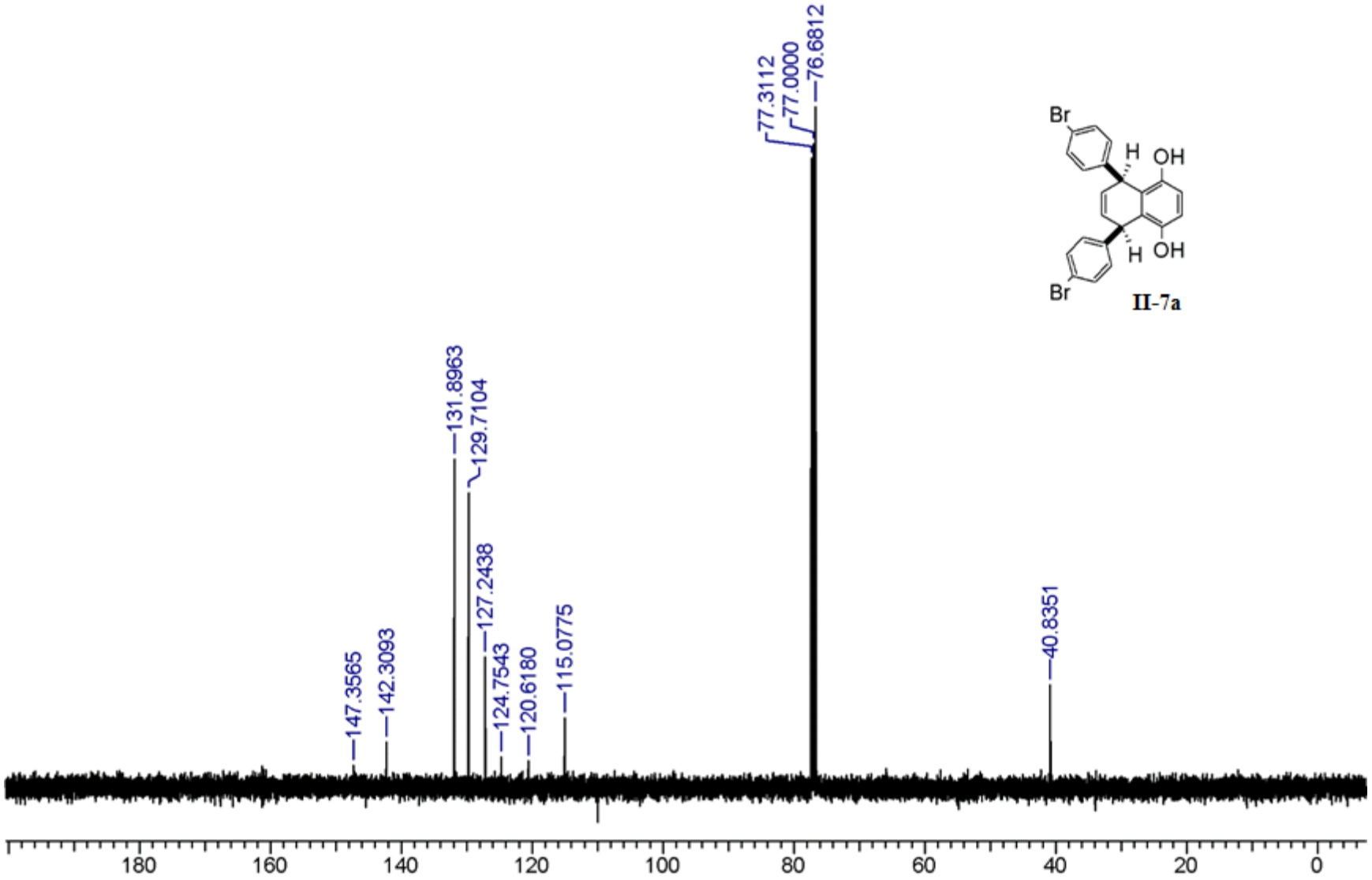
77.3112
77.0000
76.6812
131.8963
129.7104
127.2438
124.7543
120.6180
115.0775
147.3565
142.3093
40.8351
Br
H
OH
H
OH
Br
II-7a
180
160
140
120
100
80
60
40
20
0

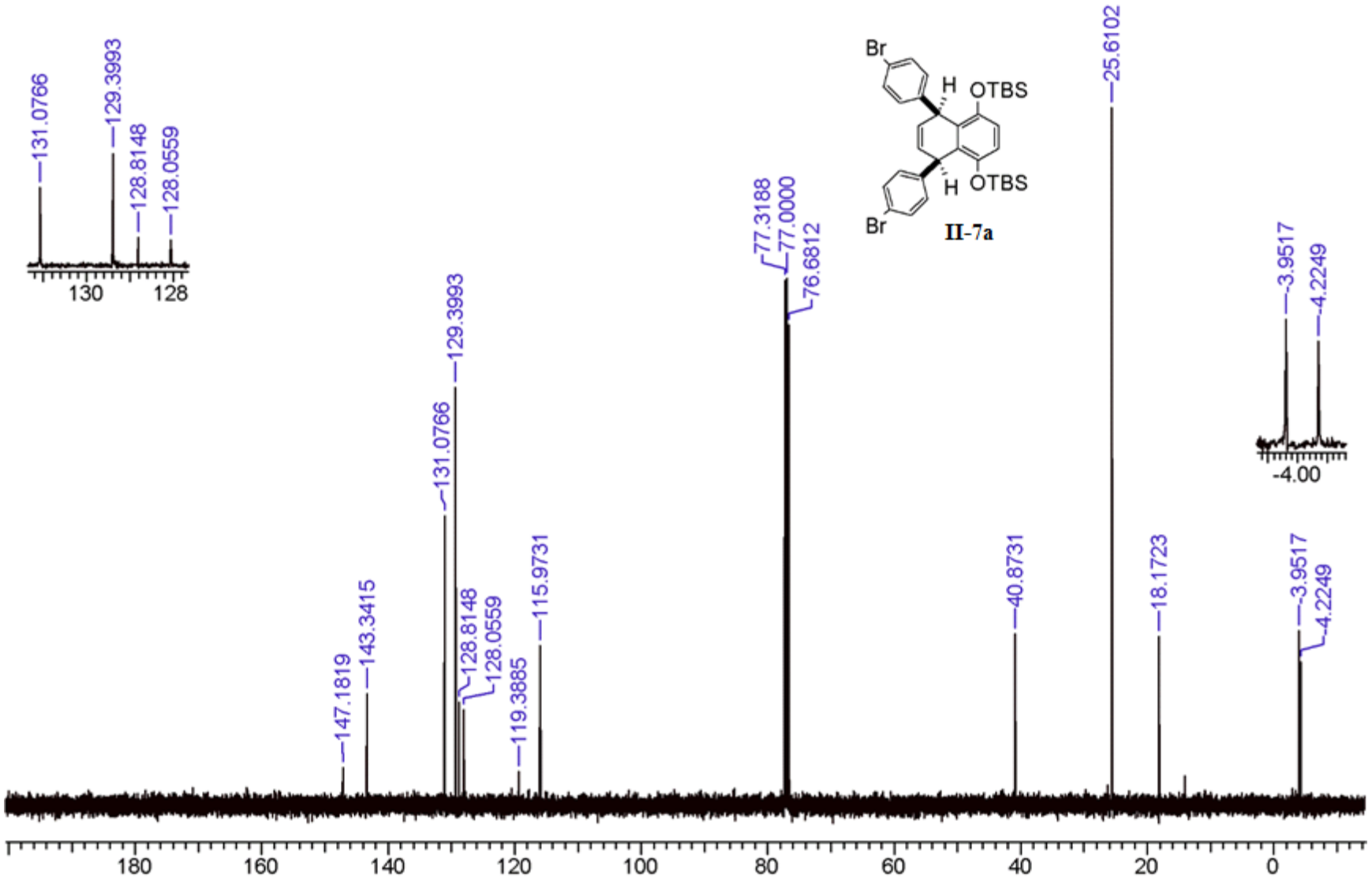
131.0766
129.3993
128.8148
128.0559
130
128
Br
H
OTBS
H
OTBS
Br
II-7a
25.6102
77.3188
77.0000
76.6812
129.3993
131.0766
128.8148
128.0559
147.1819
143.3415
119.3885
115.9731
40.8731
18.1723
3.9517
4.2249
-3.9517
-4.2249
-4.00
180
160
140
120
100
80
60
40
20
0

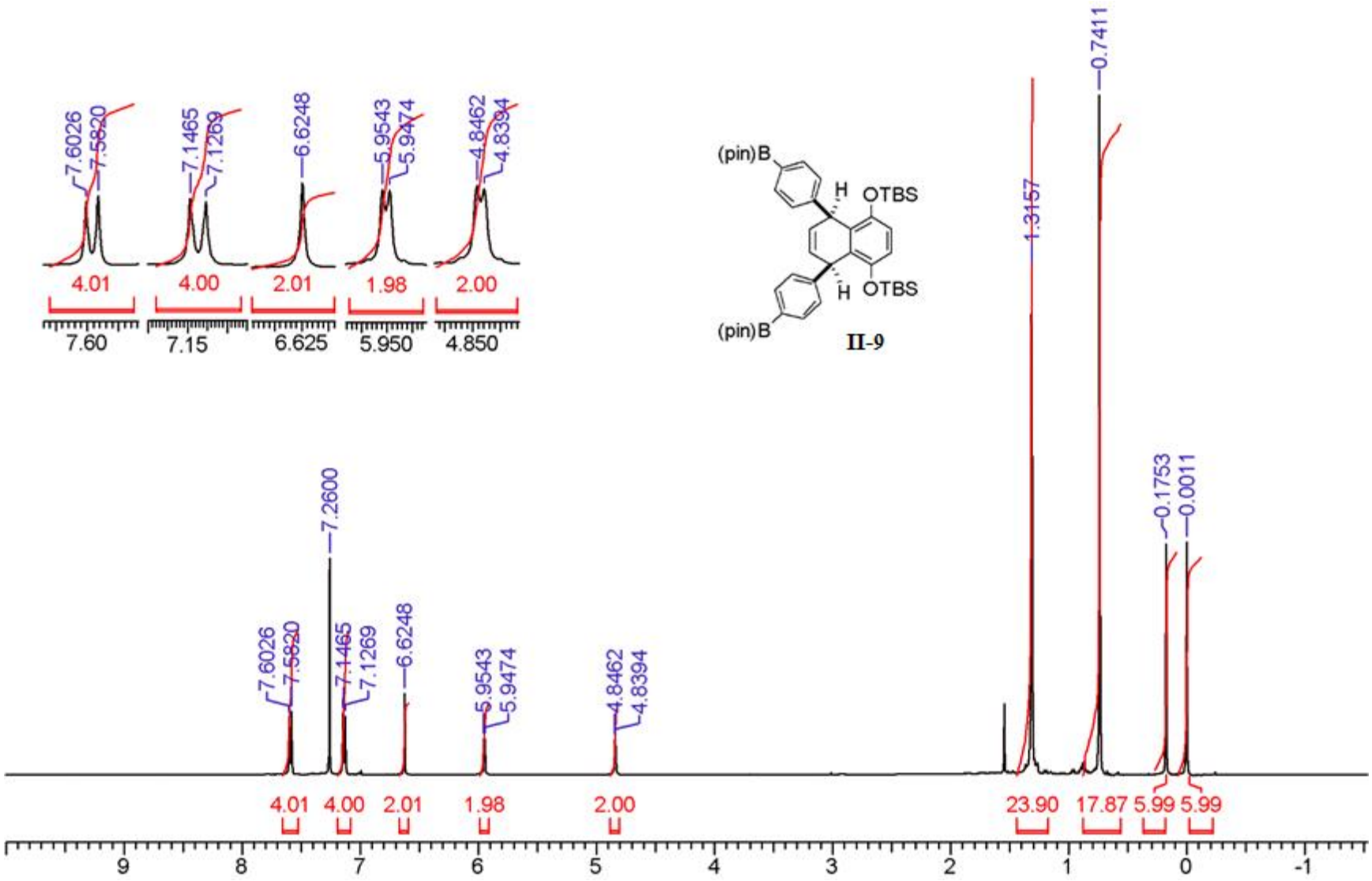
7.6026
7.5820
7.1465
7.1269
6.6248
5.9543
5.9474
4.8462
4.8394
4.01
4.00
2.01
1.98
2.00
7.60
7.15
6.625
5.950
4.850
(pin)B
H
OTBS
H
OTBS
(pin)B
II-9
1.3157
0.7411
0.1753
0.0011
23.90
17.87
5.99
5.99
9
8
7
6
5
4
3
2
1
0
-1

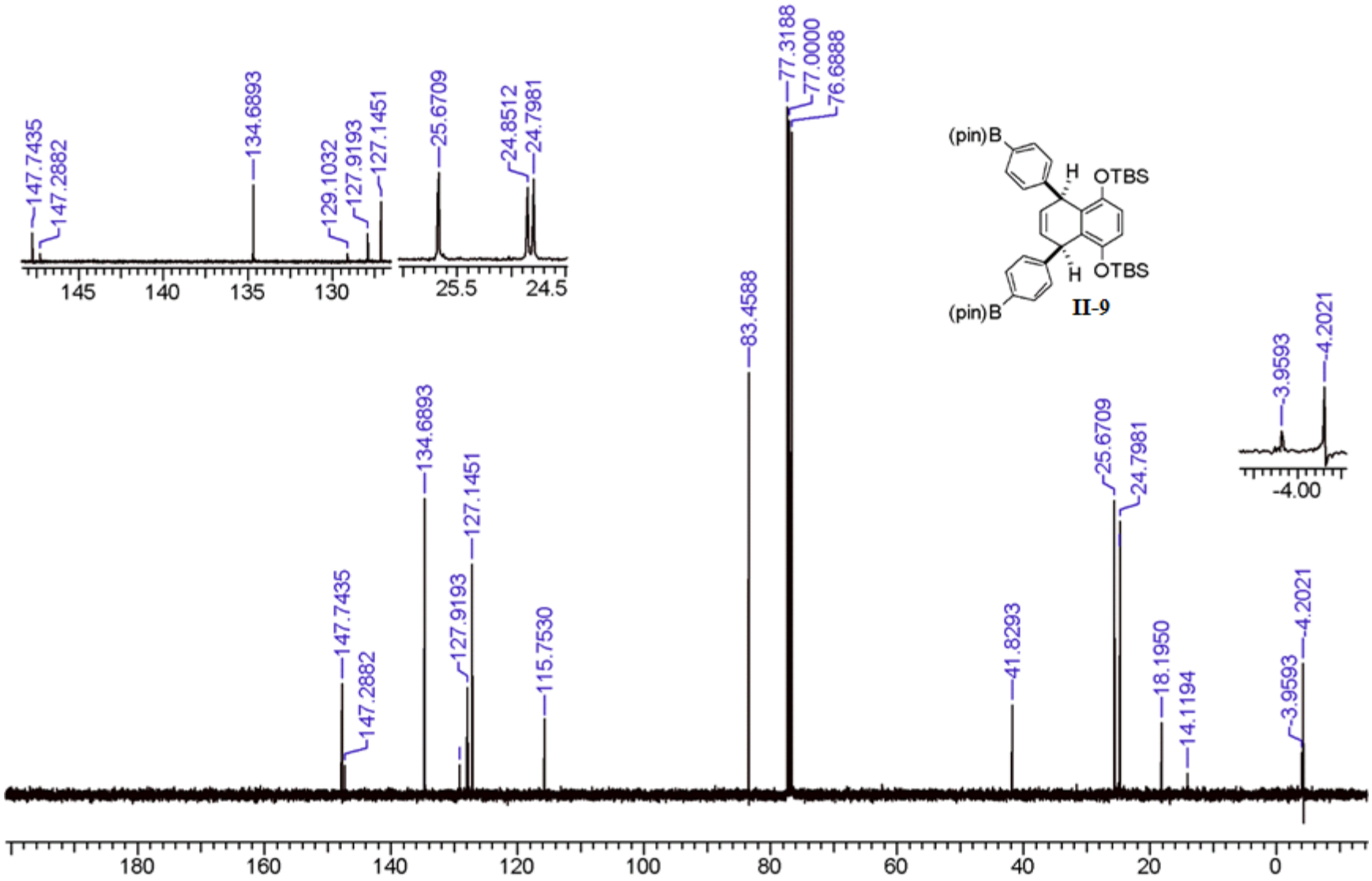
147.7435
147.2882
134.6893
129.1032
127.9193
127.1451
25.6709
24.8512
24.7981
77.3188
77.0000
76.6888
(pin)B
H
OTBS
OTBS
H
(pin)B
II-9
83.4588
3.9593
4.2021
-4.00
147.7435
147.2882
134.6893
127.9193
127.1451
115.7530
41.8293
25.6709
24.7981
18.1950
14.1194
3.9593
4.2021

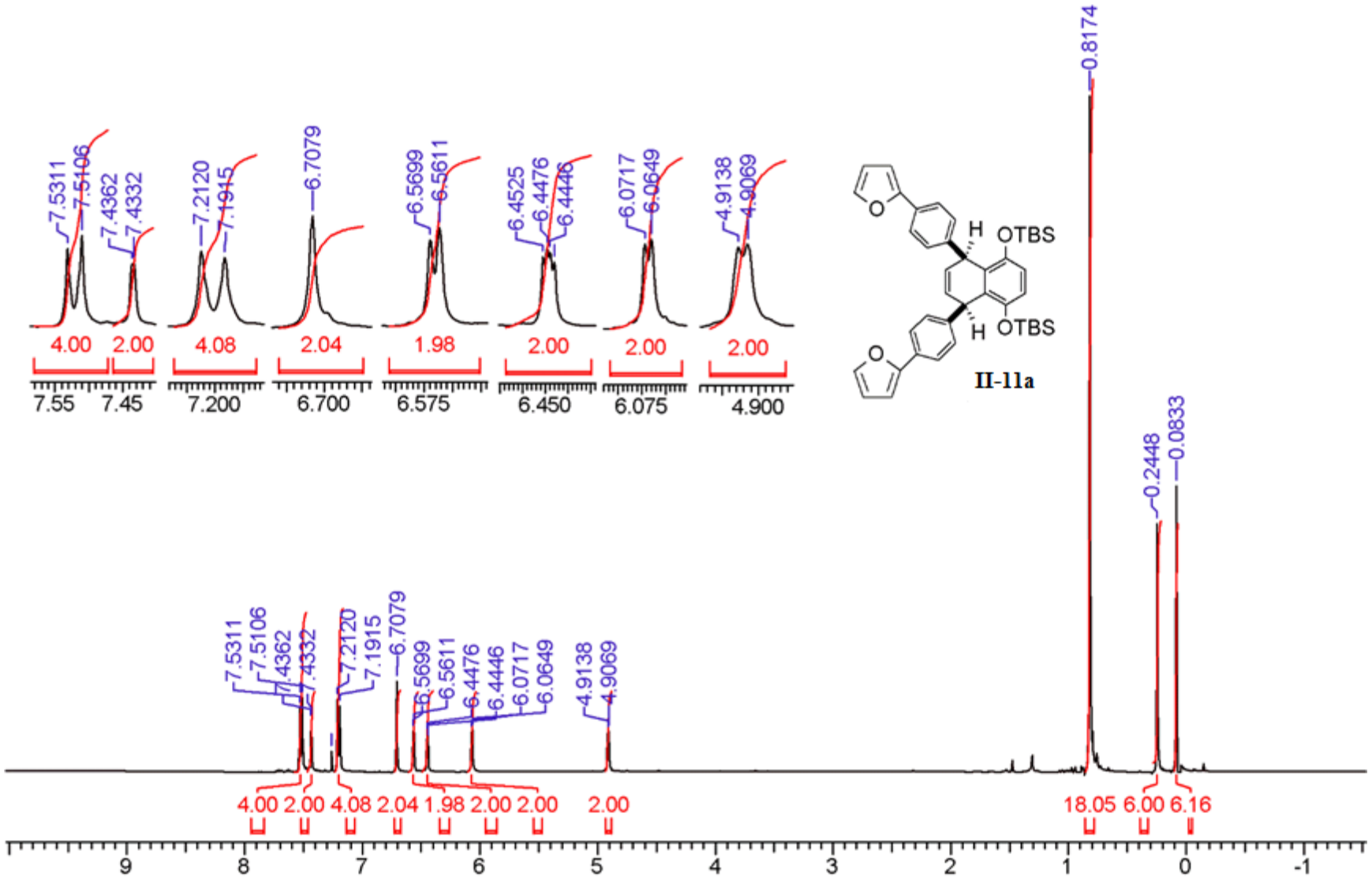
7.5311
7.5106
7.4362
7.4332
7.2120
7.1915
6.7079
6.5699
6.5611
6.4525
6.4476
6.4446
6.0717
6.0649
4.9138
4.9069
0.8174
0.2448
0.0833
H
OTBS
H
OTBS
O
O
II-11a
4.00 2.00 4.08 2.04 1.98 2.00 2.00 2.00
18.05 6.00 6.16
9 8 7 6 5 4 3 2 1 0 -1

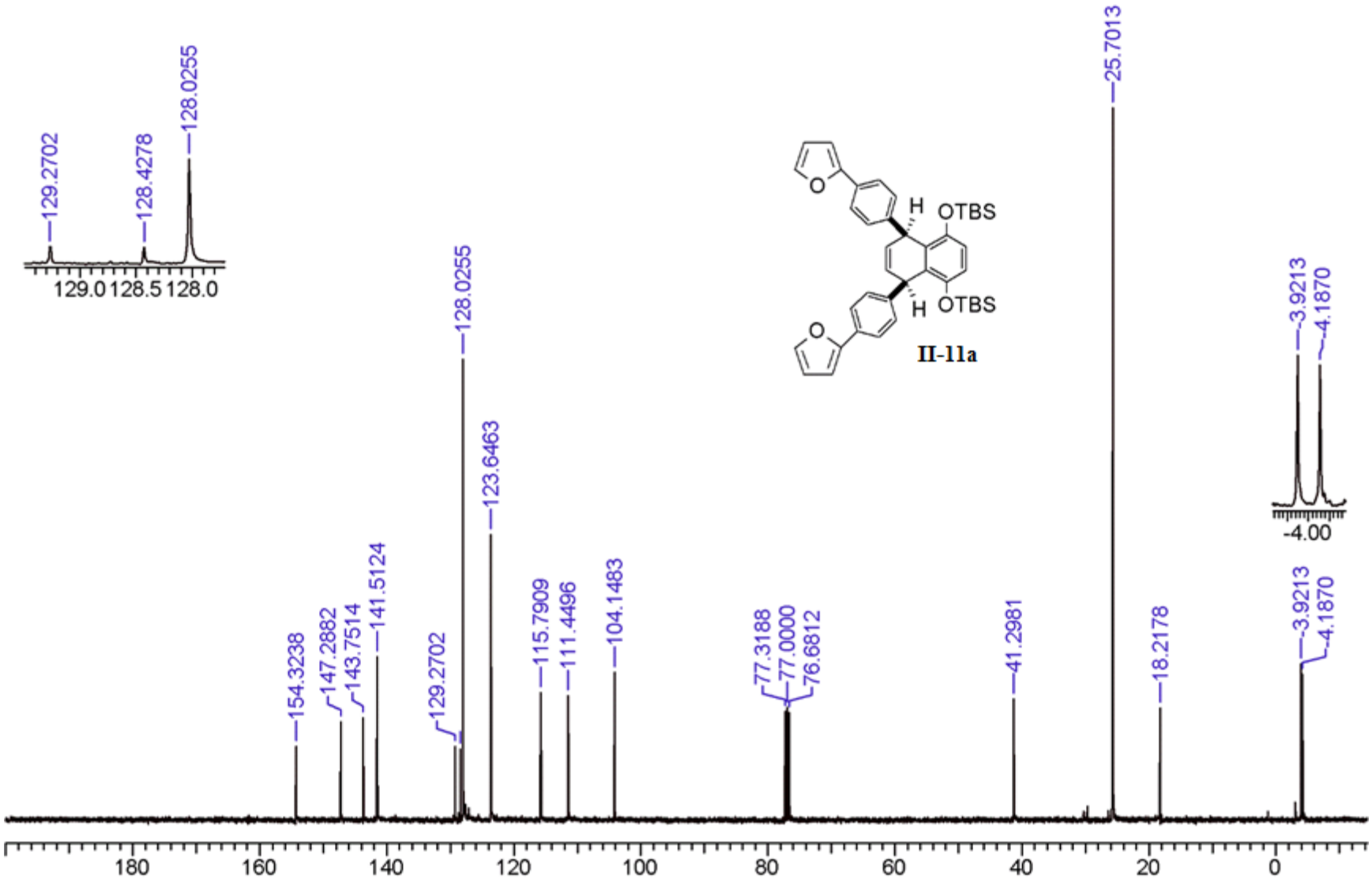
129.2702
128.4278
128.0255
129.0 128.5 128.0
H
OTBS
H
OTBS
O
O
II-11a
25.7013
3.9213
4.1870
-4.00
128.0255
123.6463
154.3238
147.2882
143.7514
141.5124
129.2702
115.7909
111.4496
104.1483
77.3188
77.0000
76.6812
41.2981
18.2178
3.9213
4.1870
180
160
140
120
100
80
60
40
20
0

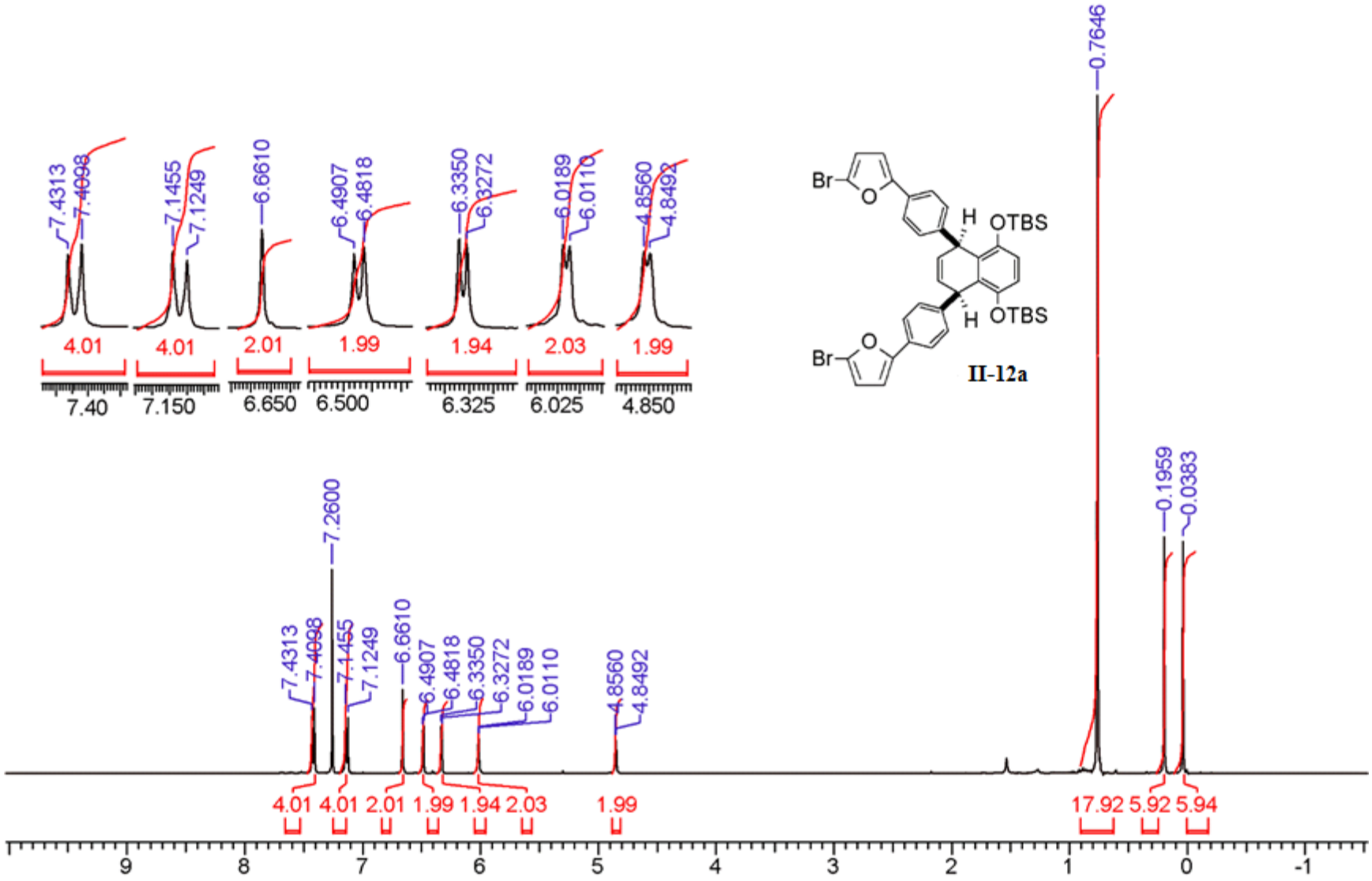
7.4313
7.4098
7.1455
7.1249
6.6610
6.4907
6.4818
6.3350
6.3272
6.0189
6.0110
4.8560
4.8492
4.01
4.01
2.01
1.99
1.94
2.03
1.99
7.40
7.150
6.650
6.500
6.325
6.025
4.850
Br
O
H
OTBS
H
OTBS
Br
O
II-12a
7.2600
0.7646
0.1959
0.0383
4.01 4.01 2.01 1.99 1.94 2.03
1.99
17.92 5.92 5.94
9
8
7
6
5
4
3
2
1
0
-1

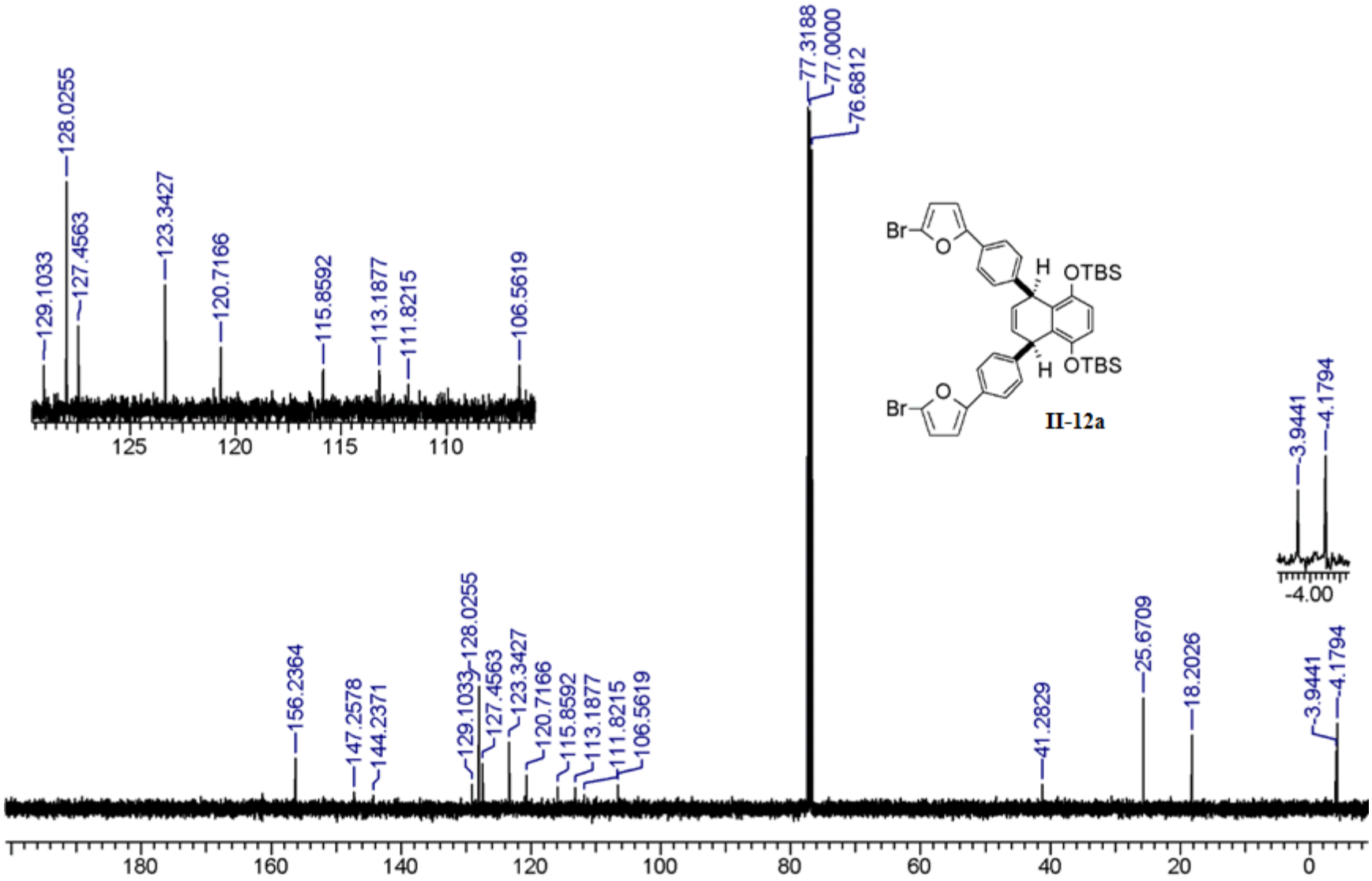
77.3188
77.0000
76.6812
128.0255
129.1033
127.4563
123.3427
120.7166
115.8592
113.1877
111.8215
106.5619
Br
O
H
OTBS
H
OTBS
Br
O
II-12a
3.9441
4.1794
-4.00
156.2364
147.2578
144.2371
129.1033
128.0255
127.4563
123.3427
120.7166
115.8592
113.1877
111.8215
106.5619
41.2829
25.6709
18.2026
3.9441
4.1794
180
160
140
120
100
80
60
40
20
0
125
120
115
110

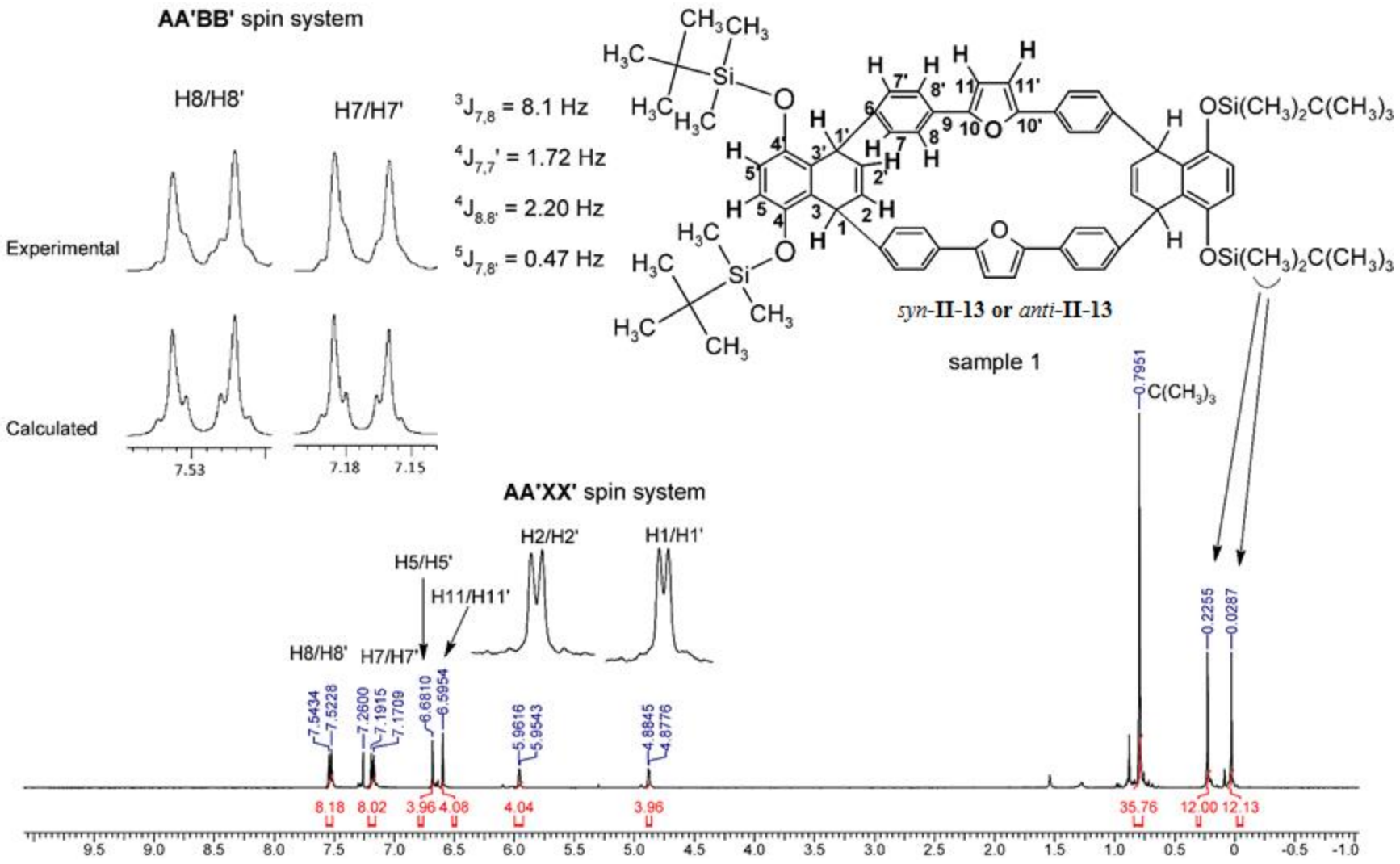
AA'BB' spin system
H8/H8'
H7/H7'
$^3J_{7,8}$ = 8.1 Hz
$^4J_{7,7'}$ = 1.72 Hz
$^4J_{8,8'}$ = 2.20 Hz
$^5J_{7,8'}$ = 0.47 Hz
Experimental
Calculated
7.53
7.18
7.15
OSi(CH3)2C(CH3)3
syn-II-13 or anti-II-13
sample 1
AA'XX' spin system
H2/H2'
H1/H1'
H5/H5'
H11/H11'
H8/H8'
H7/H7'
C(CH3)3
0.7951
0.2255
0.0287
7.5434
7.5228
7.2600
7.1915
7.1709
6.6810
6.5954
5.9616
5.9543
4.8845
4.8776
8.18
8.02
3.96
4.08
4.04
3.96
35.76
12.00
12.13

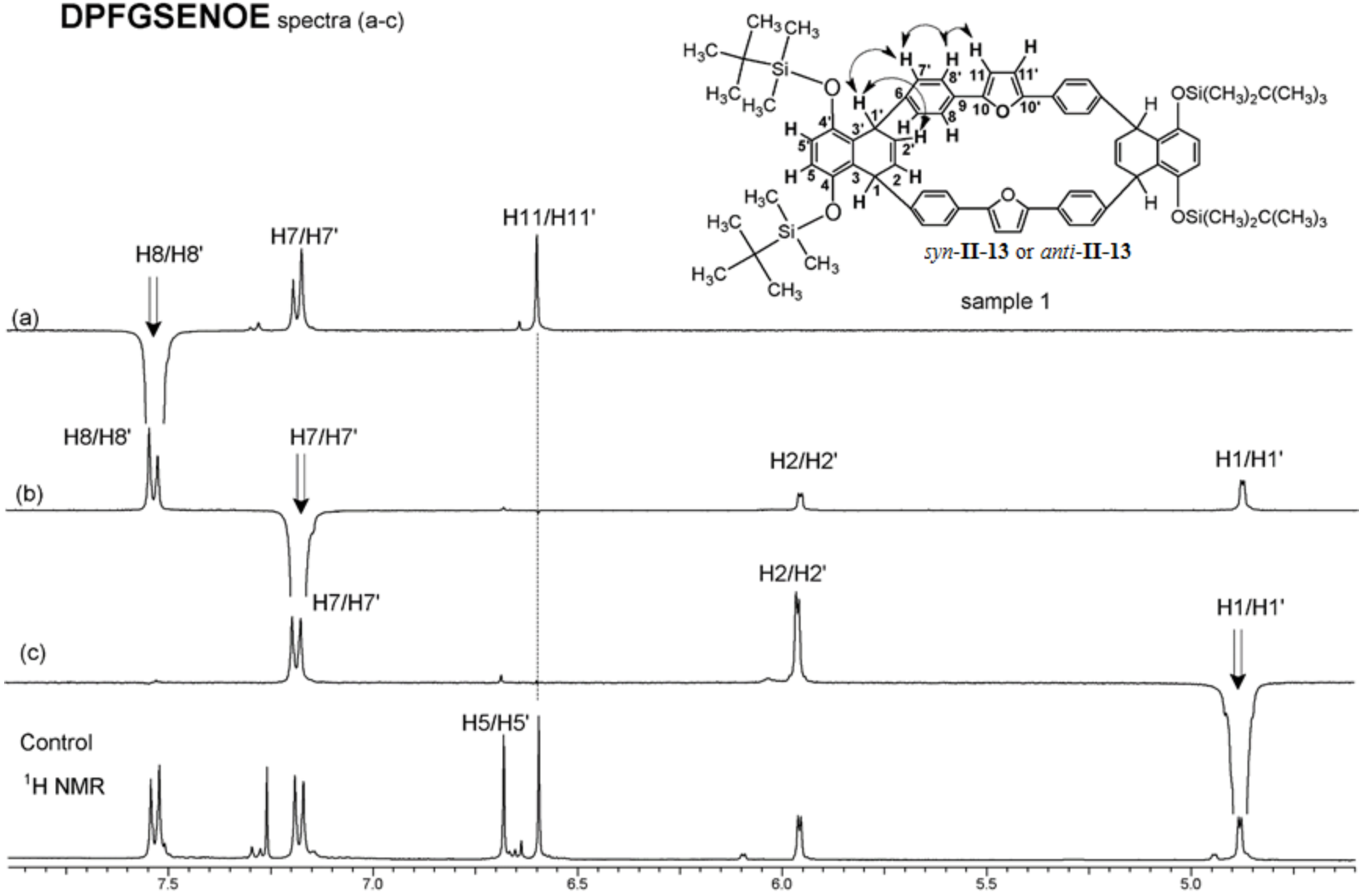
DPFGSENOE spectra (a-c)
H8/H8'
H7/H7'
H11/H11'
(a)
sample 1
H8/H8'
H7/H7'
H2/H2'
H1/H1'
(b)
H7/H7'
H2/H2'
H1/H1'
(c)
H5/H5'
Control
^{1}H NMR
7.5
7.0
6.5
6.0
5.5
5.0
OSi(CH3)2C(CH3)3
OSi(CH3)2C(CH3)3
syn-II-13 or anti-II-13

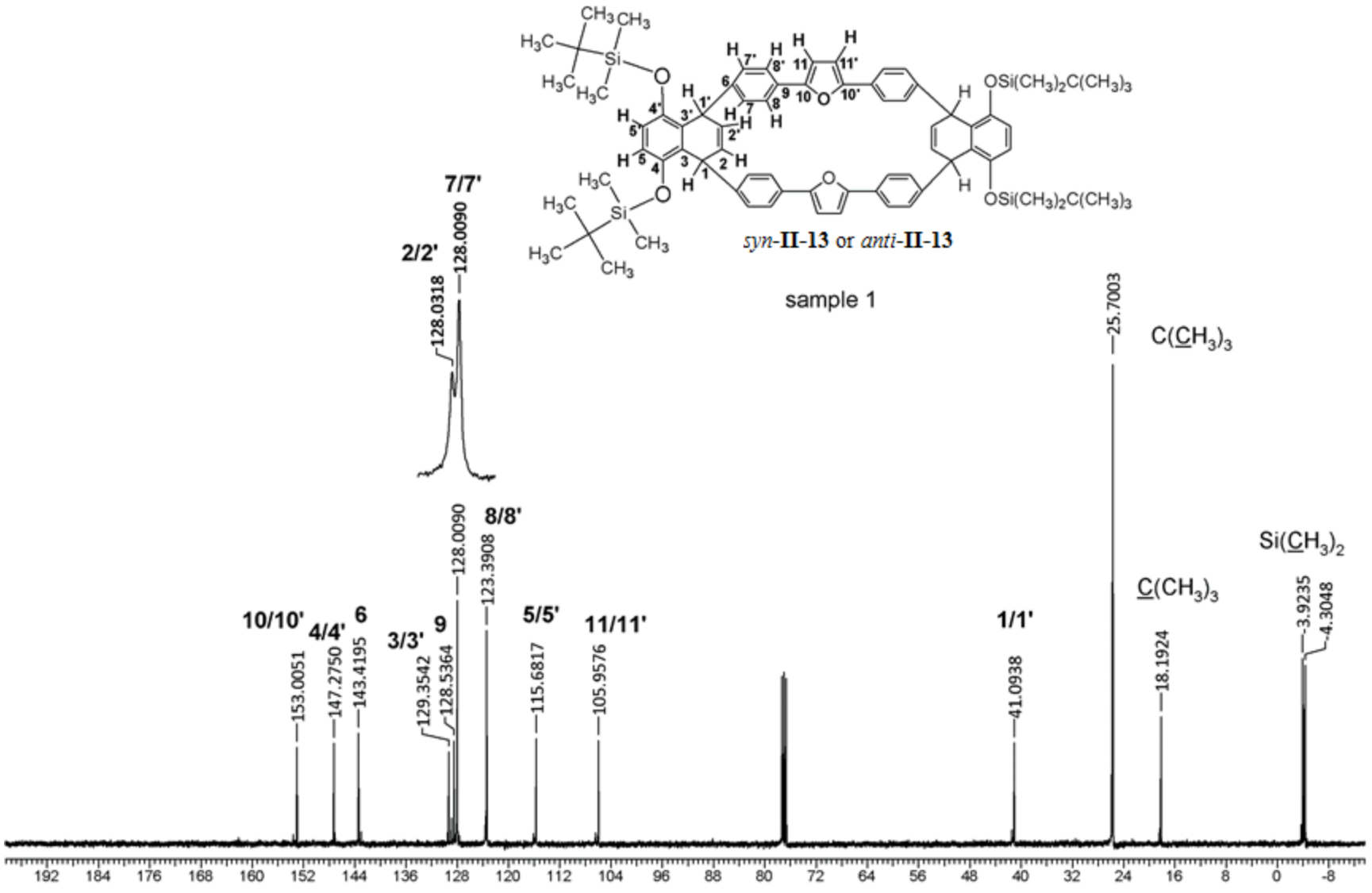
OSi(CH3)2C(CH3)3
OSi(CH3)2C(CH3)3
syn-II-13 or anti-II-13
sample 1
7/7'
2/2'
128.0318
128.0090
8/8'
10/10'
4/4'
6
3/3'
9
5/5'
11/11'
1/1'
C(CH3)3
C(CH3)3
Si(CH3)2
153.0051
147.2750
143.4195
129.3542
128.5364
128.0090
123.3908
115.6817
105.9576
41.0938
25.7003
18.1924
-3.9235
-4.3048

One-bond **gHSQC** correlations

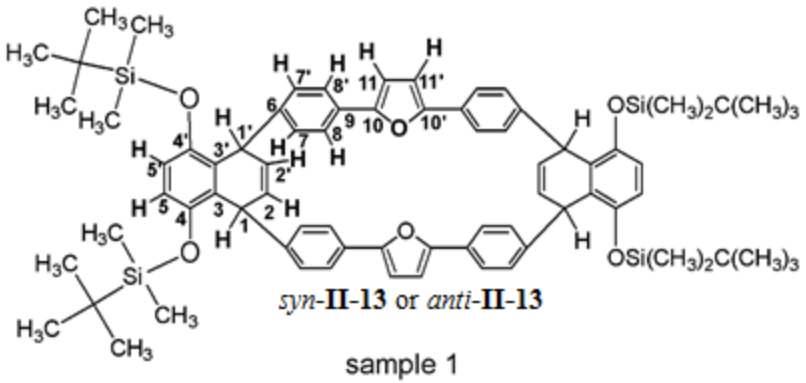

syn-**II-13** or *anti*-**II-13**

sample 1

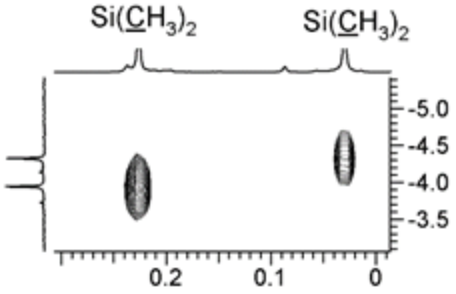

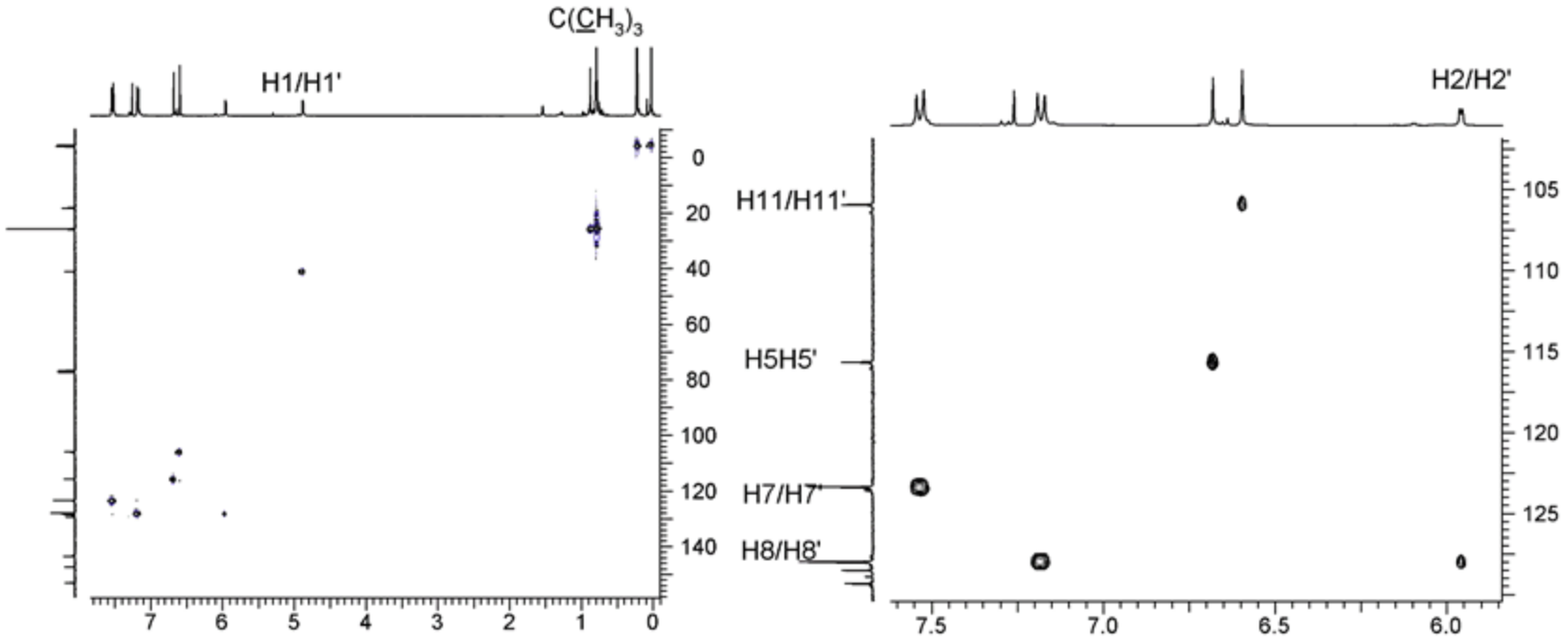

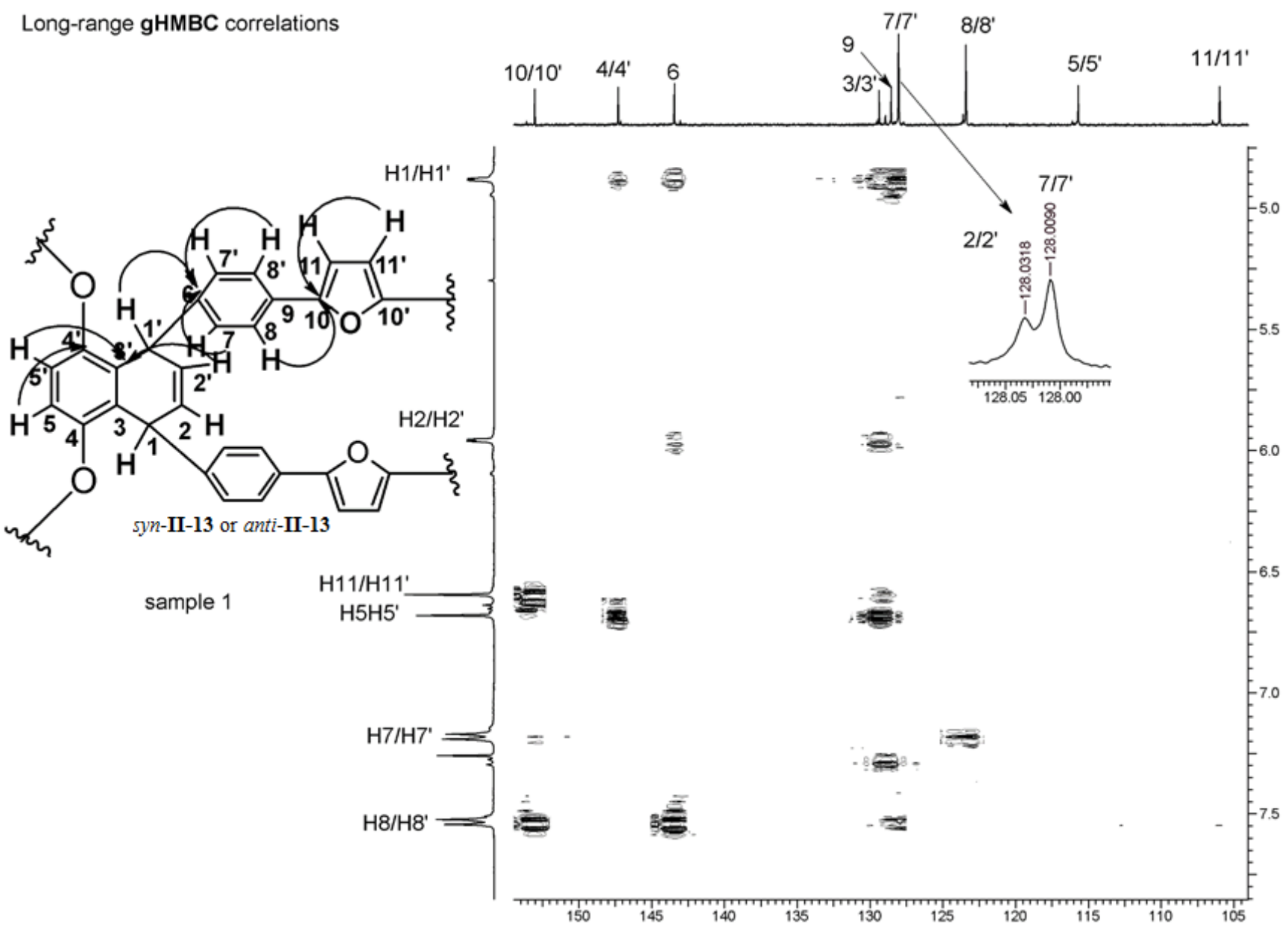
Long-range gHMBC correlations
10/10'
4/4'
6
9
3/3'
7/7'
8/8'
5/5'
11/11'
H1/H1'
H2/H2'
H11/H11'
H5H5'
H7/H7'
H8/H8'
7/7'
2/2'
128.0318
128.0090
128.05
128.00
syn-II-13 or anti-II-13
sample 1
150
145
140
135
130
125
120
115
110
105
5.0
5.5
6.0
6.5
7.0
7.5

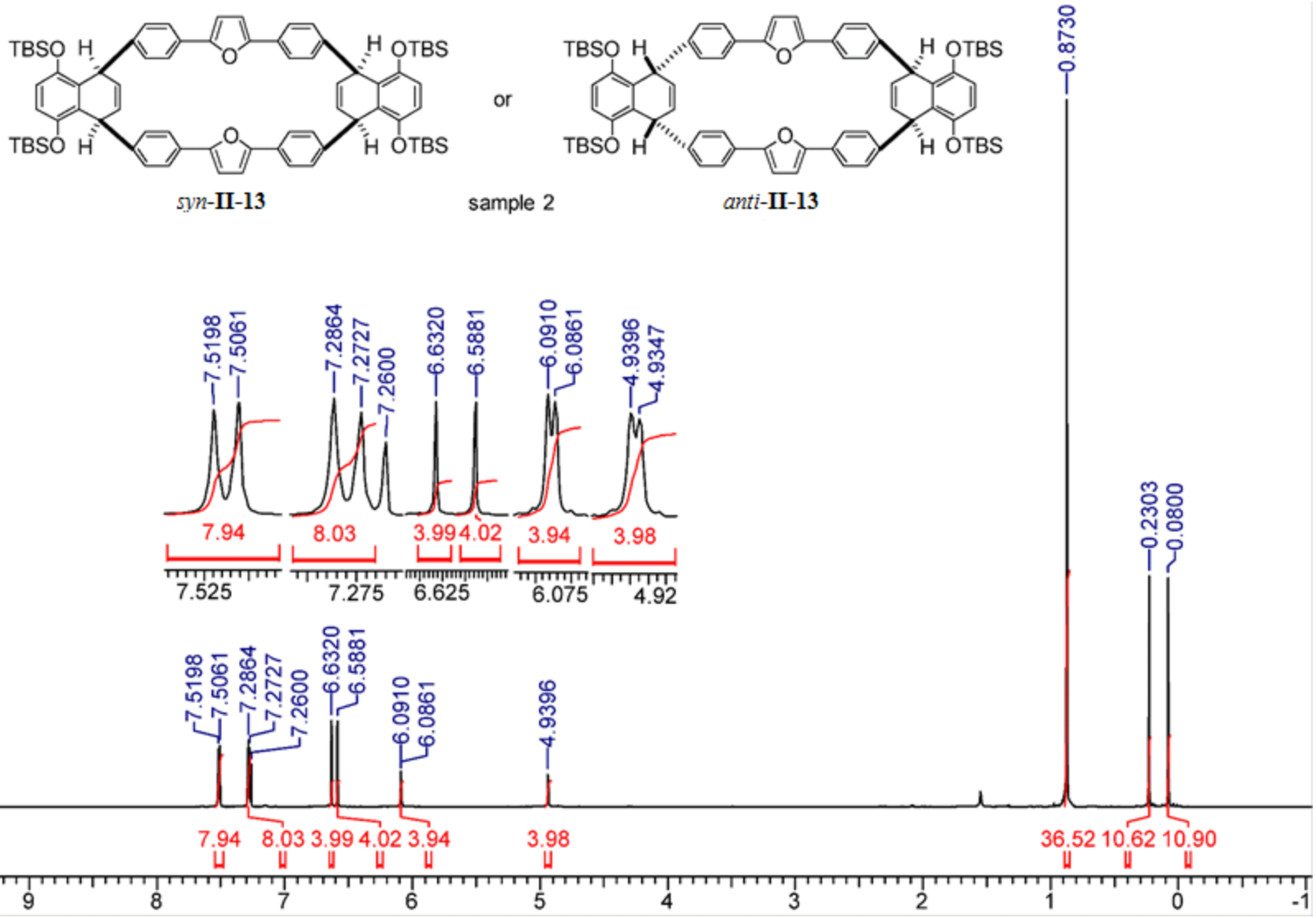
TBSO H
H OTBS
O
TBSO H
H OTBS
or
TBSO H
H OTBS
O
TBSO H
H OTBS
syn-II-13
sample 2
anti-II-13
7.5198
7.5061
7.2864
7.2727
7.2600
6.6320
6.5881
6.0910
6.0861
4.9396
4.9347
7.94
8.03
3.99
4.02
3.94
3.98
7.525
7.275
6.625
6.075
4.92
0.8730
0.2303
0.0800
36.52
10.62
10.90
9
8
7
6
5
4
3
2
1
0
-1

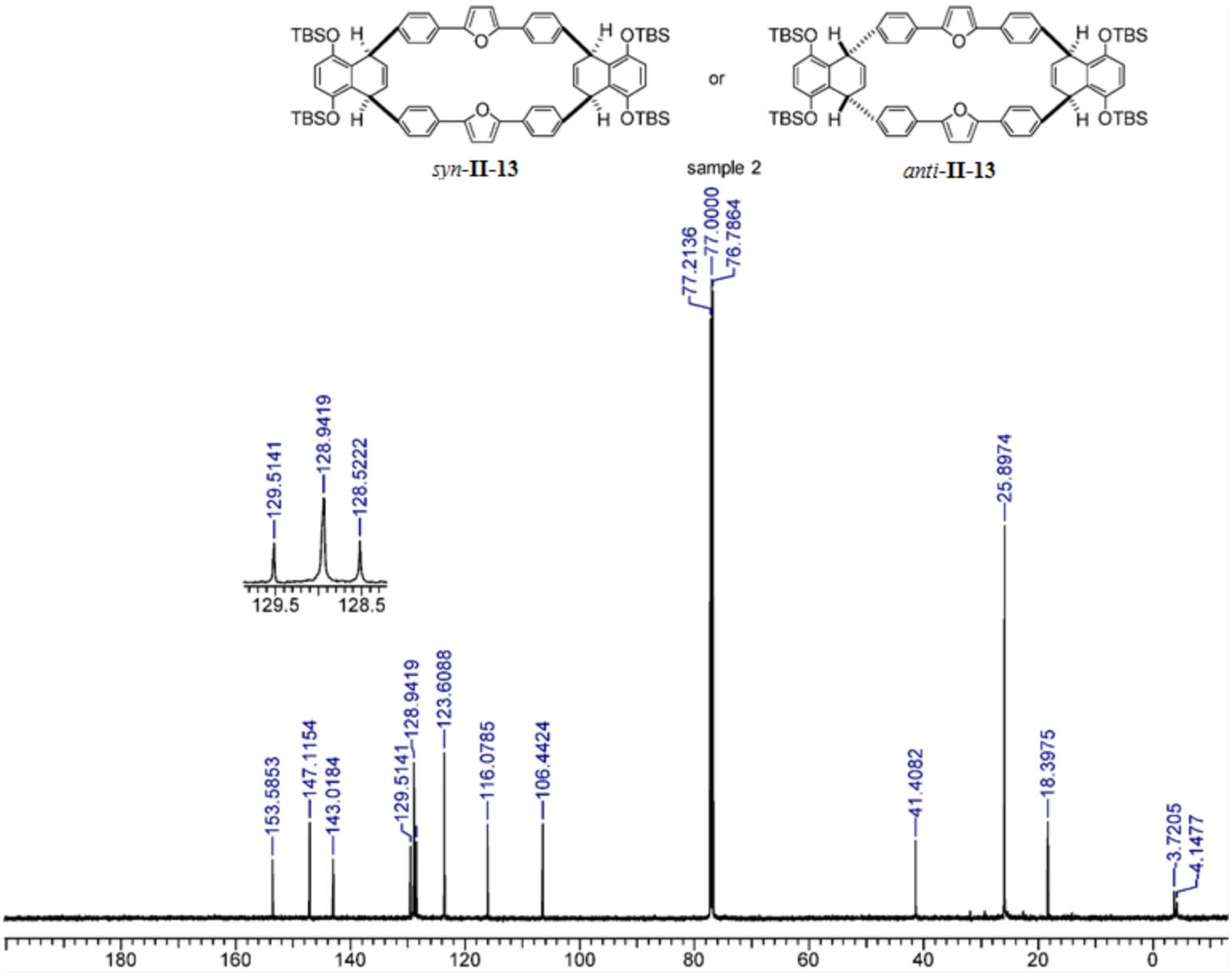

syn-**II-13** *anti*-**II-13**

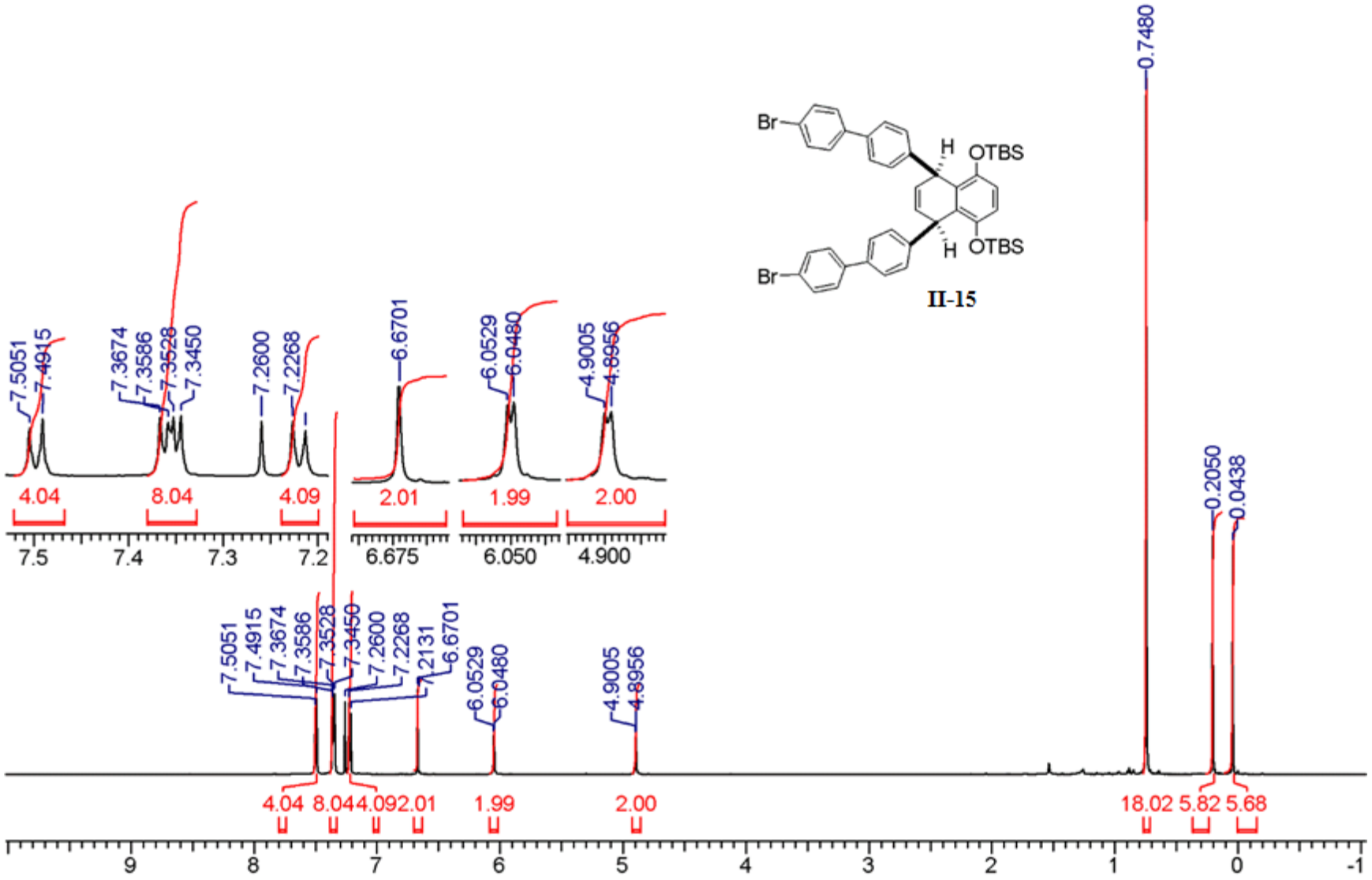
Br
H
OTBS
H
OTBS
Br
II-15
0.7480
0.2050
0.0438
7.5051
7.4915
7.3674
7.3586
7.3528
7.3450
7.2600
7.2268
7.2131
6.6701
6.0529
6.0480
4.9005
4.8956
4.04
8.04
4.09
2.01
1.99
2.00
18.02
5.82
5.68

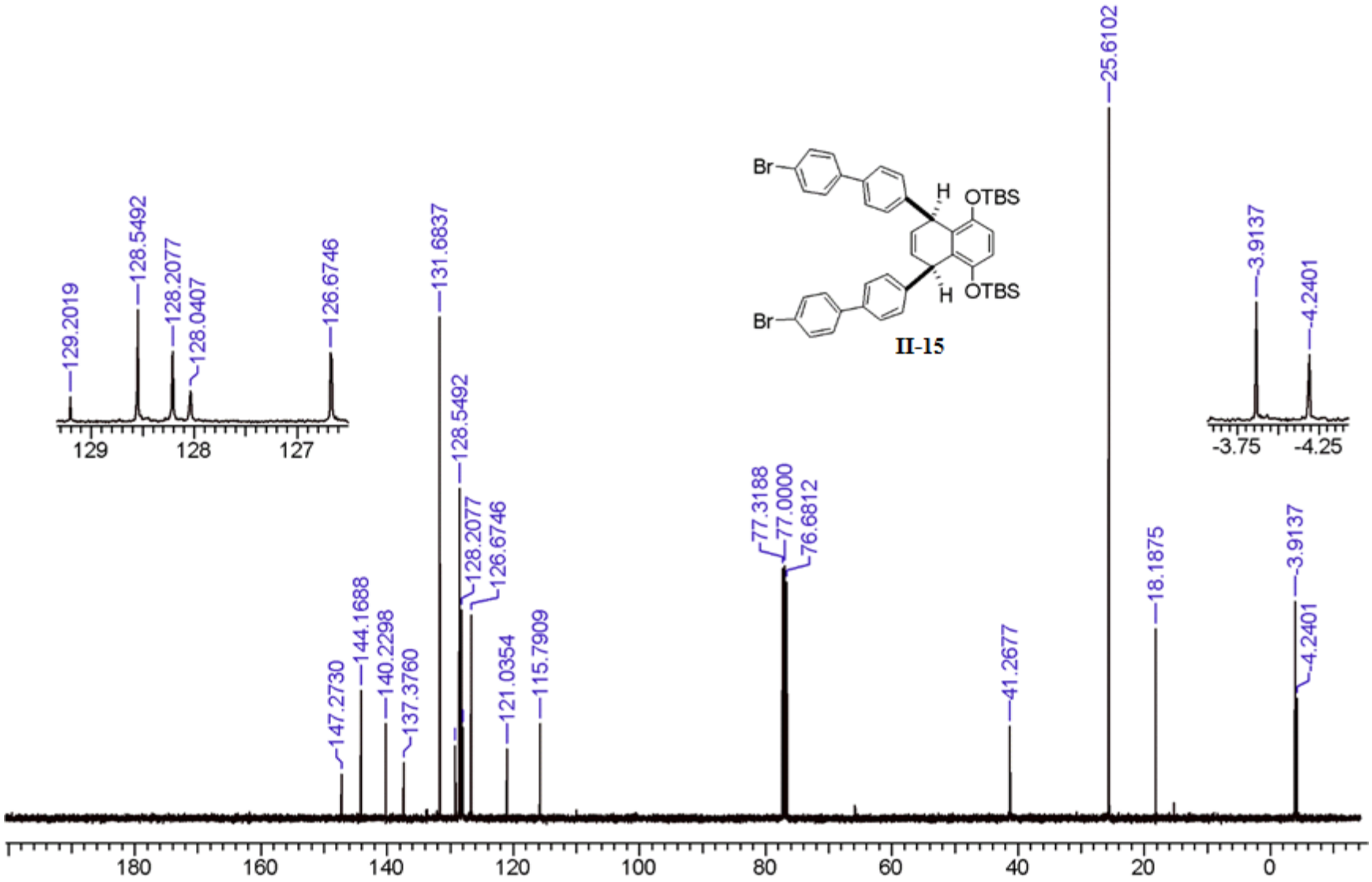
Br
H
OTBS
H
OTBS
Br
II-15
129.2019
128.5492
128.2077
128.0407
126.6746
131.6837
128.5492
128.2077
126.6746
121.0354
115.7909
147.2730
144.1688
140.2298
137.3760
77.3188
77.0000
76.6812
41.2677
25.6102
18.1875
3.9137
4.2401
3.9137
4.2401
129
128
127
-3.75
-4.25
180
160
140
120
100
80
60
40
20
0

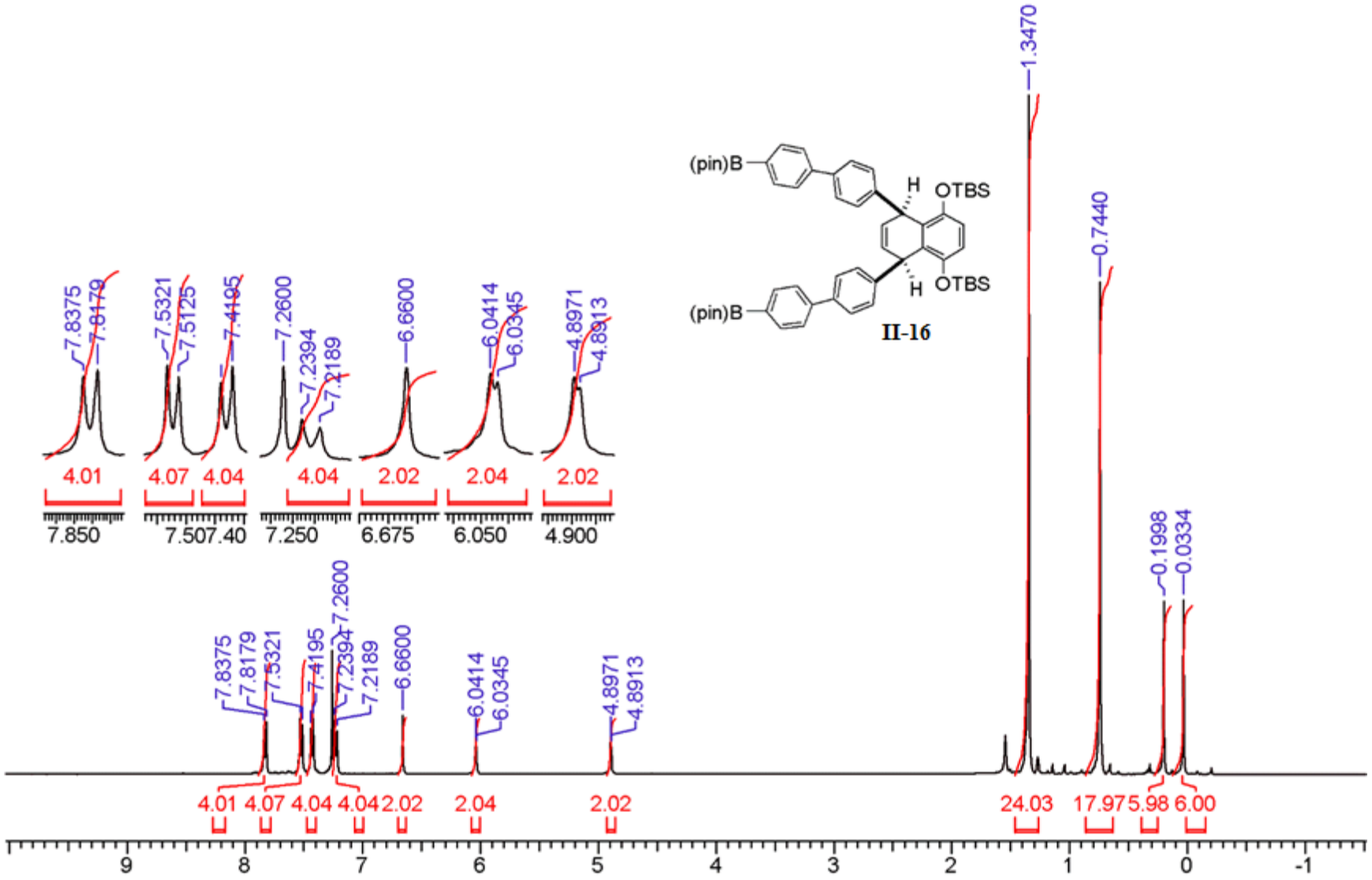
(pin)B
H
OTBS
H
OTBS
(pin)B
II-16
7.8375
7.8179
7.5321
7.5125
7.4195
7.2600
7.2394
7.2189
6.6600
6.0414
6.0345
4.8971
4.8913
1.3470
0.7440
0.1998
0.0334
4.01
4.07
4.04
4.04
2.02
2.04
2.02
24.03
17.97
5.98
6.00

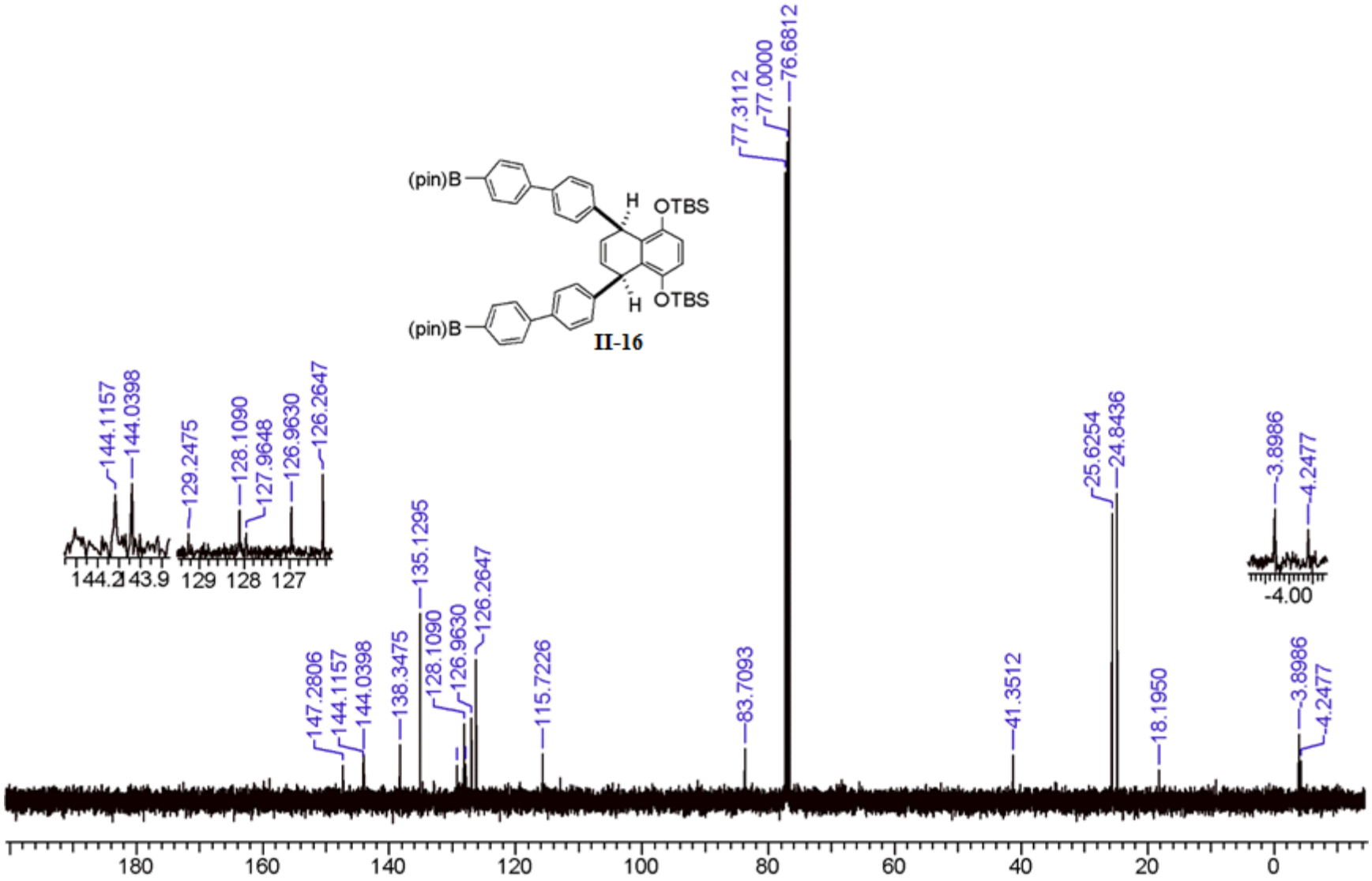
(pin)B
H
OTBS
H
OTBS
(pin)B
II-16
77.3112
77.0000
76.6812
144.1157
144.0398
129.2475
128.1090
127.9648
126.9630
126.2647
144.2
143.9
129
128
127
147.2806
144.1157
144.0398
138.3475
135.1295
128.1090
126.9630
126.2647
115.7226
83.7093
41.3512
25.6254
24.8436
18.1950
3.8986
4.2477
-4.00
180
160
140
120
100
80
60
40
20
0

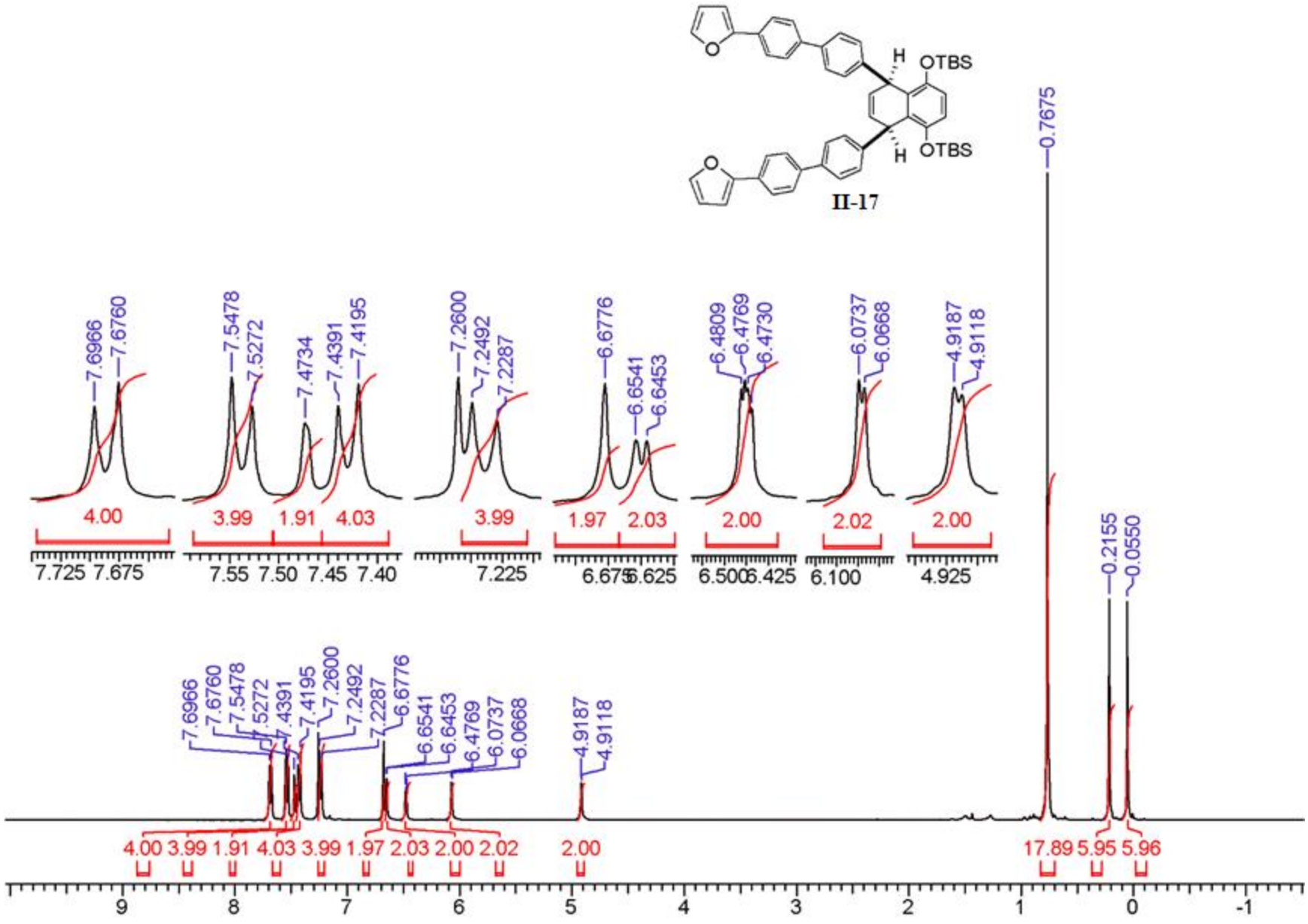
OTBS
H
H
OTBS
II-17
7.6966
7.6760
7.5478
7.5272
7.4734
7.4391
7.4195
7.2600
7.2492
7.2287
6.6776
6.6541
6.6453
6.4809
6.4769
6.4730
6.0737
6.0668
4.9187
4.9118
0.7675
0.2155
0.0550
4.00
3.99
1.91
4.03
3.99
1.97
2.03
2.00
2.02
2.00
17.89
5.95
5.96

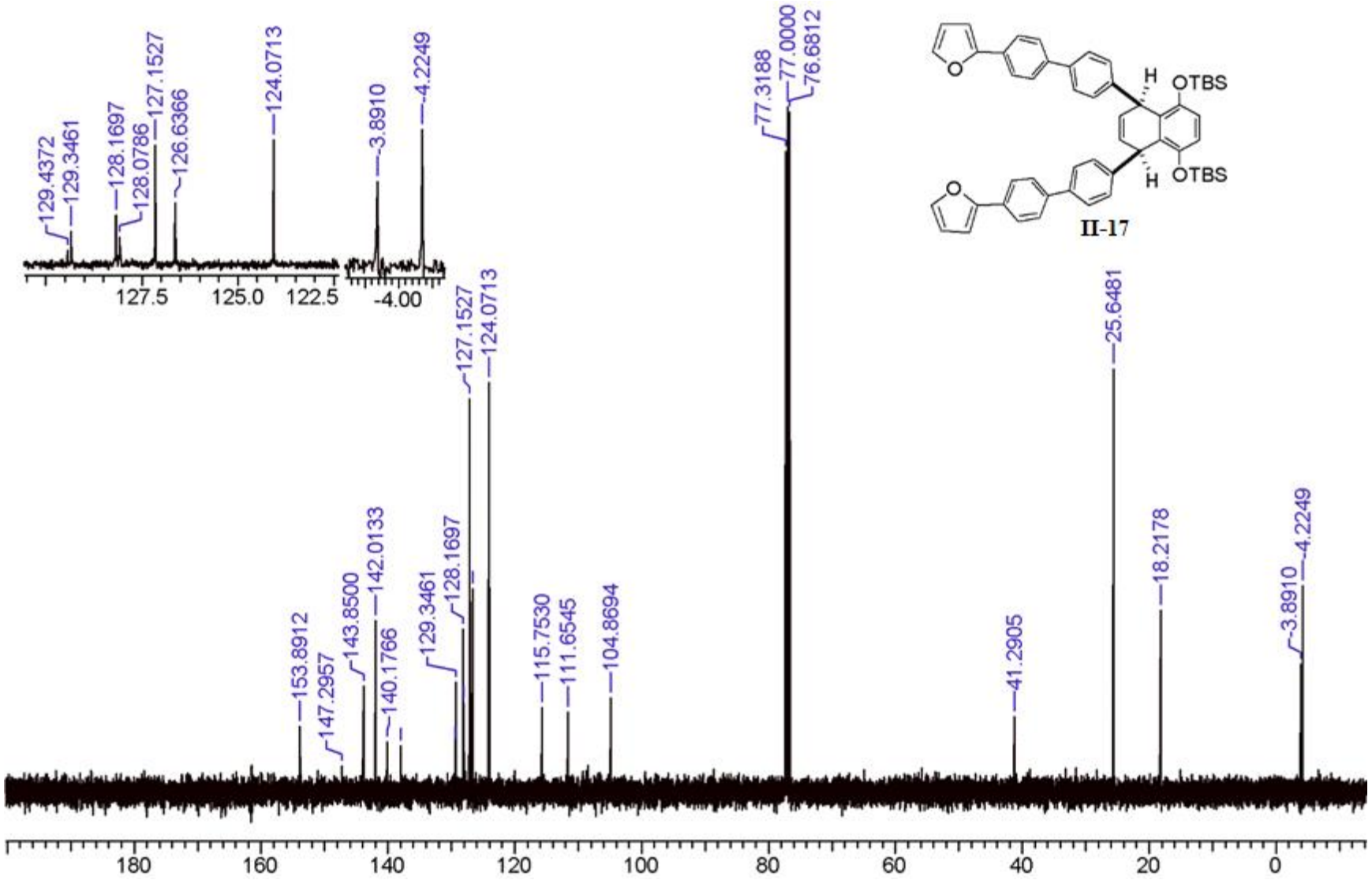
129.4372
129.3461
128.1697
128.0786
127.1527
126.6366
124.0713
3.8910
4.2249
127.5
125.0
122.5
-4.00
77.3188
77.0000
76.6812
H
OTBS
H
OTBS
O
O
II-17
153.8912
147.2957
143.8500
142.0133
140.1766
129.3461
128.1697
127.1527
124.0713
115.7530
111.6545
104.8694
41.2905
25.6481
18.2178
3.8910
4.2249
180
160
140
120
100
80
60
40
20
0

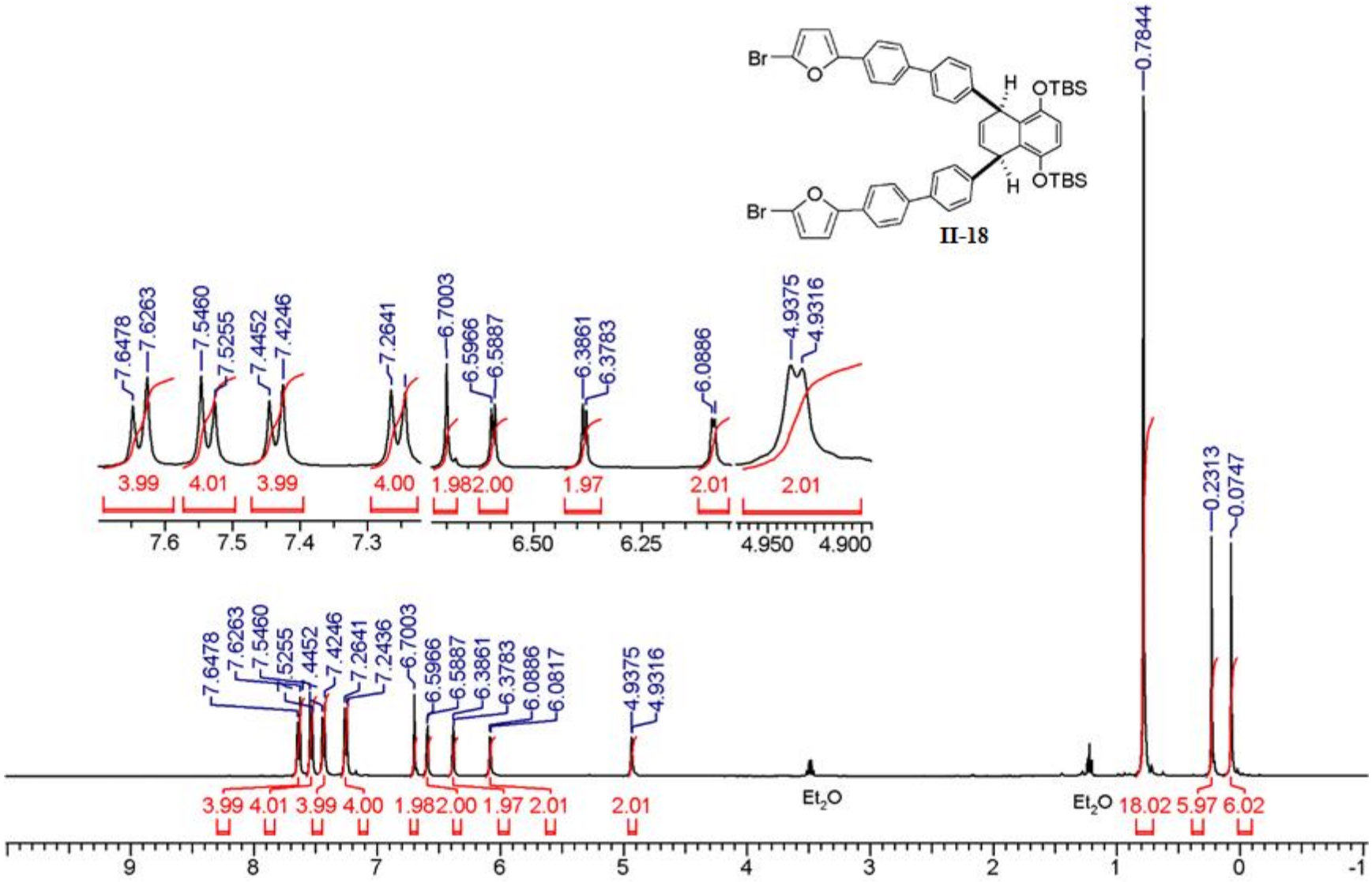
Br
O
H
OTBS
H
OTBS
Br
O
II-18
7.6478
7.6263
7.5460
7.5255
7.4452
7.4246
7.2641
6.7003
6.5966
6.5887
6.3861
6.3783
6.0886
4.9375
4.9316
3.99
4.01
3.99
4.00
1.98
2.00
1.97
2.01
2.01
7.6
7.5
7.4
7.3
6.50
6.25
4.950
4.900
7.6478
7.6263
7.5460
7.5255
7.4452
7.4246
7.2641
7.2436
6.7003
6.5966
6.5887
6.3861
6.3783
6.0886
6.0817
4.9375
4.9316
0.7844
0.2313
0.0747
3.99
4.01
3.99
4.00
1.98
2.00
1.97
2.01
2.01
Et2O
Et2O
18.02
5.97
6.02
9
8
7
6
5
4
3
2
1
0
-1

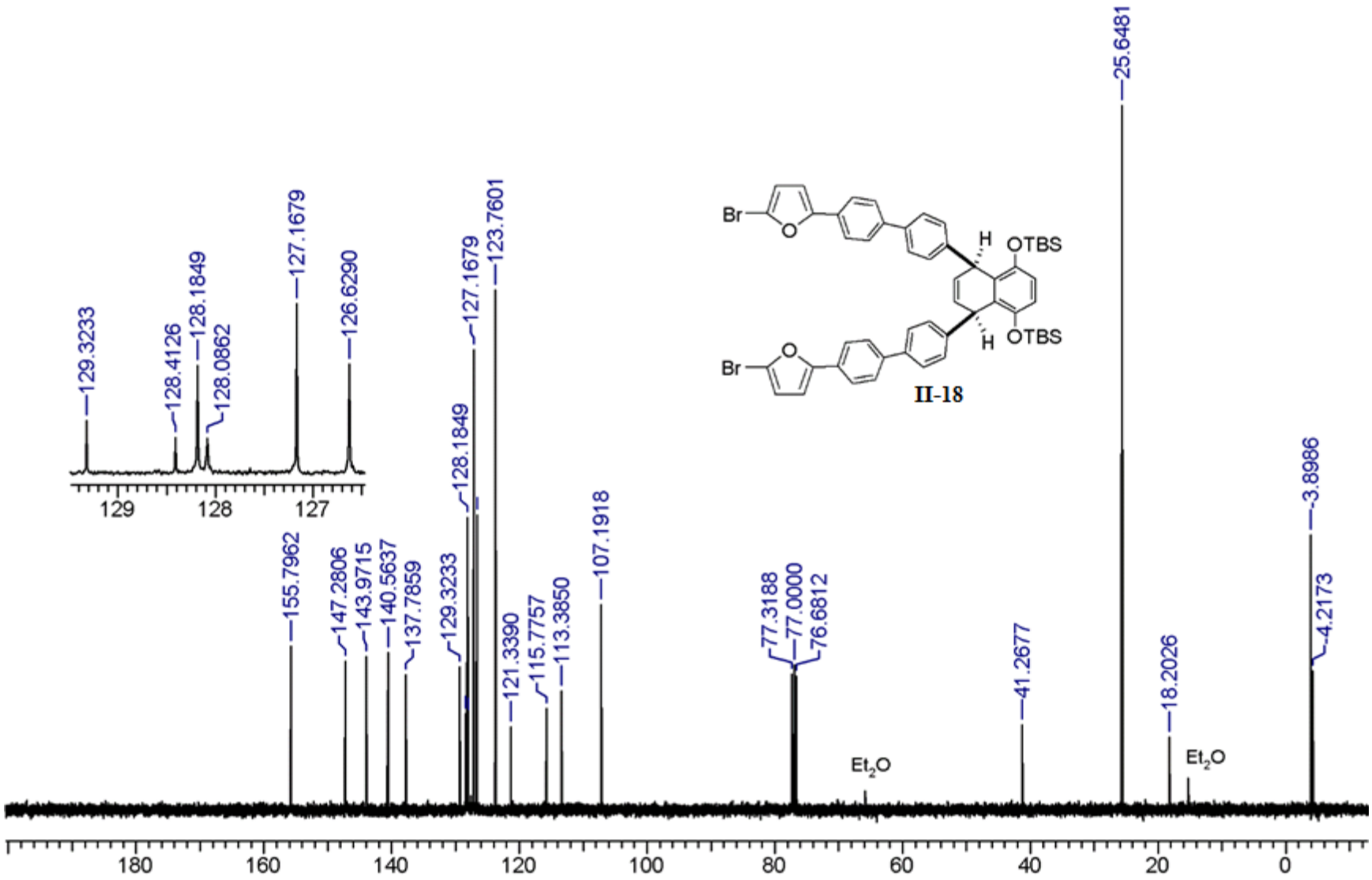
Br
O
H
OTBS
H
OTBS
Br
O
II-18
25.6481
3.8986
4.2173
18.2026
41.2677
77.3188
77.0000
76.6812
Et2O
Et2O
155.7962
147.2806
143.9715
140.5637
137.7859
129.3233
128.1849
127.1679
123.7601
121.3390
115.7757
113.3850
107.1918
129.3233
128.4126
128.1849
128.0862
127.1679
126.6290
129
128
127
180
160
140
120
100
80
60
40
20
0

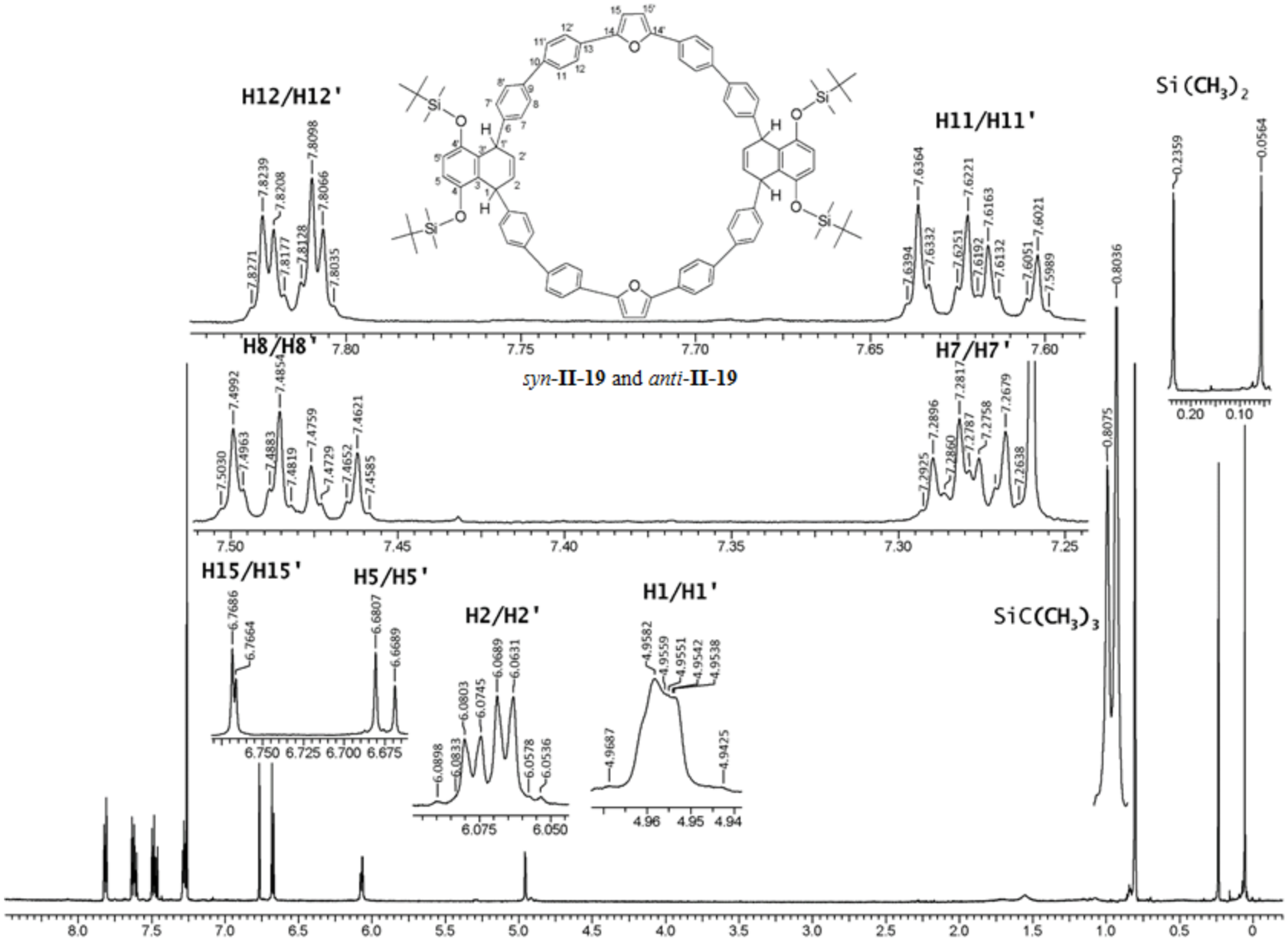
H12/H12'
H11/H11'
Si(CH3)2
H8/H8'
H7/H7'
syn-II-19 and anti-II-19
H15/H15'
H5/H5'
H2/H2'
H1/H1'
SiC(CH3)3

gCOSY

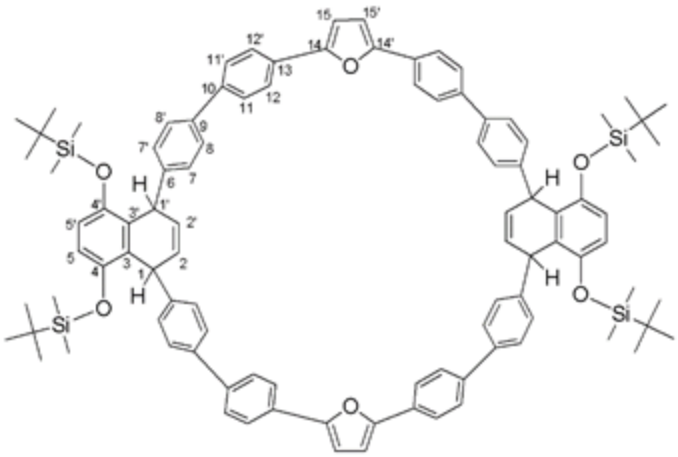

syn-**II-19** and *anti*-**II-19**

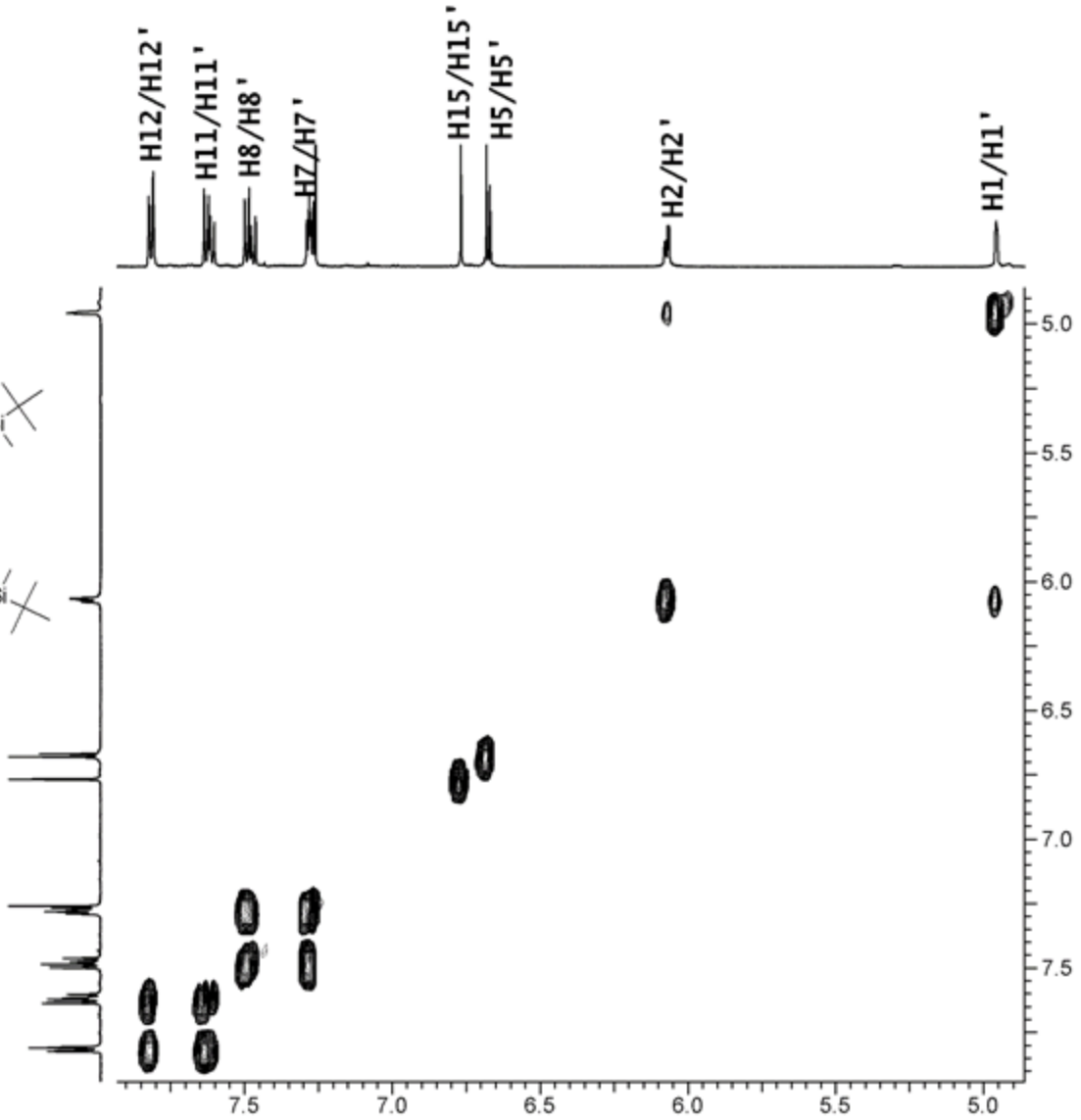

DPFGSENOE subspectra

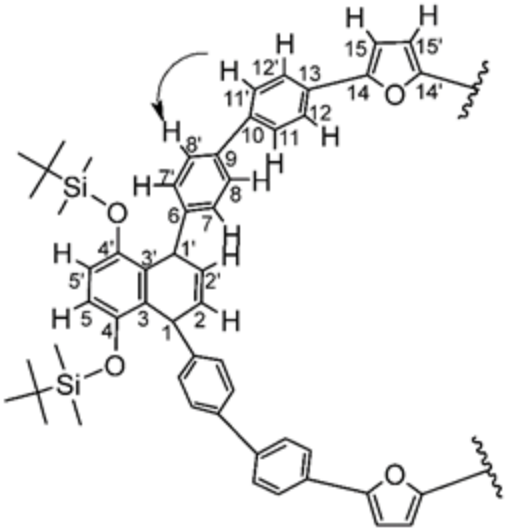

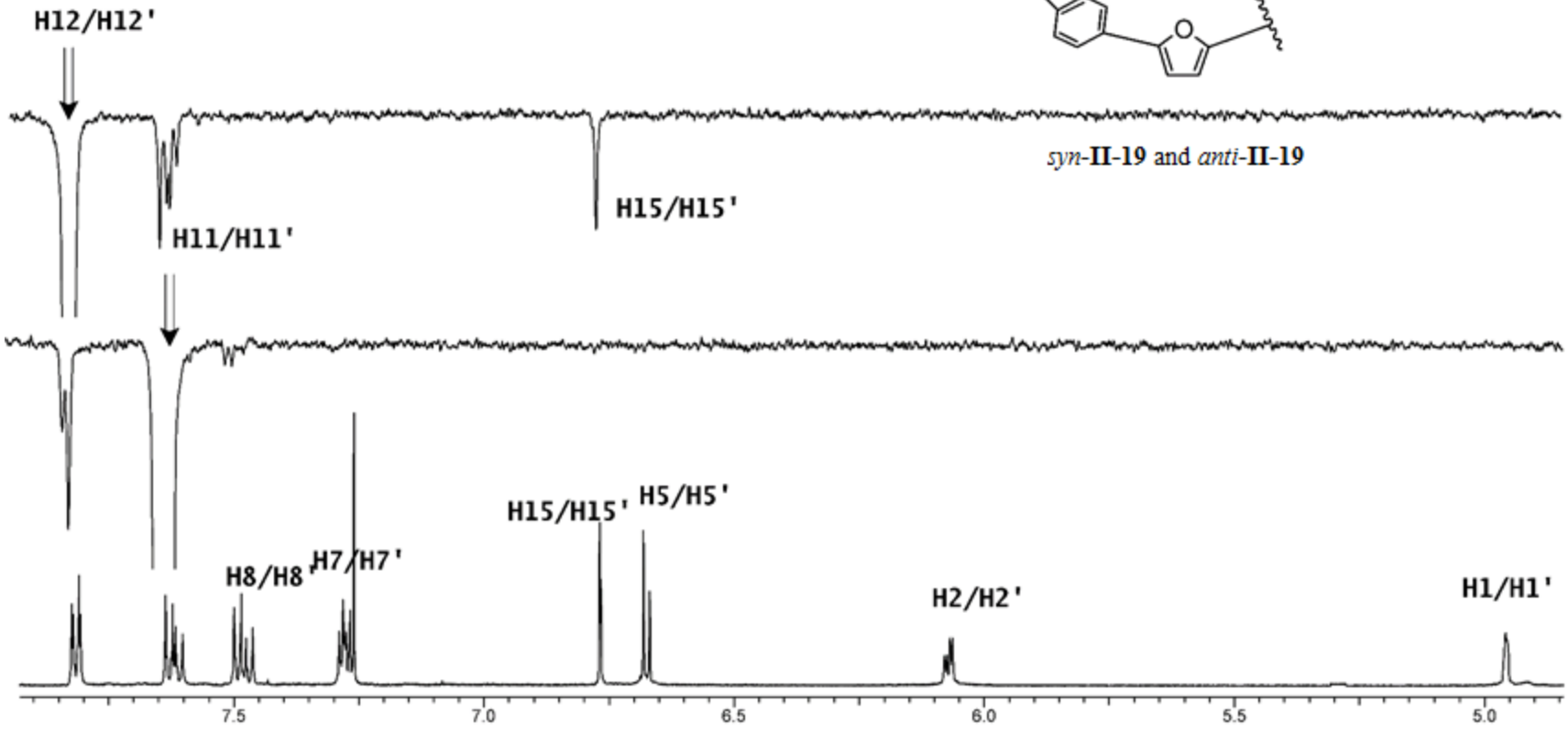

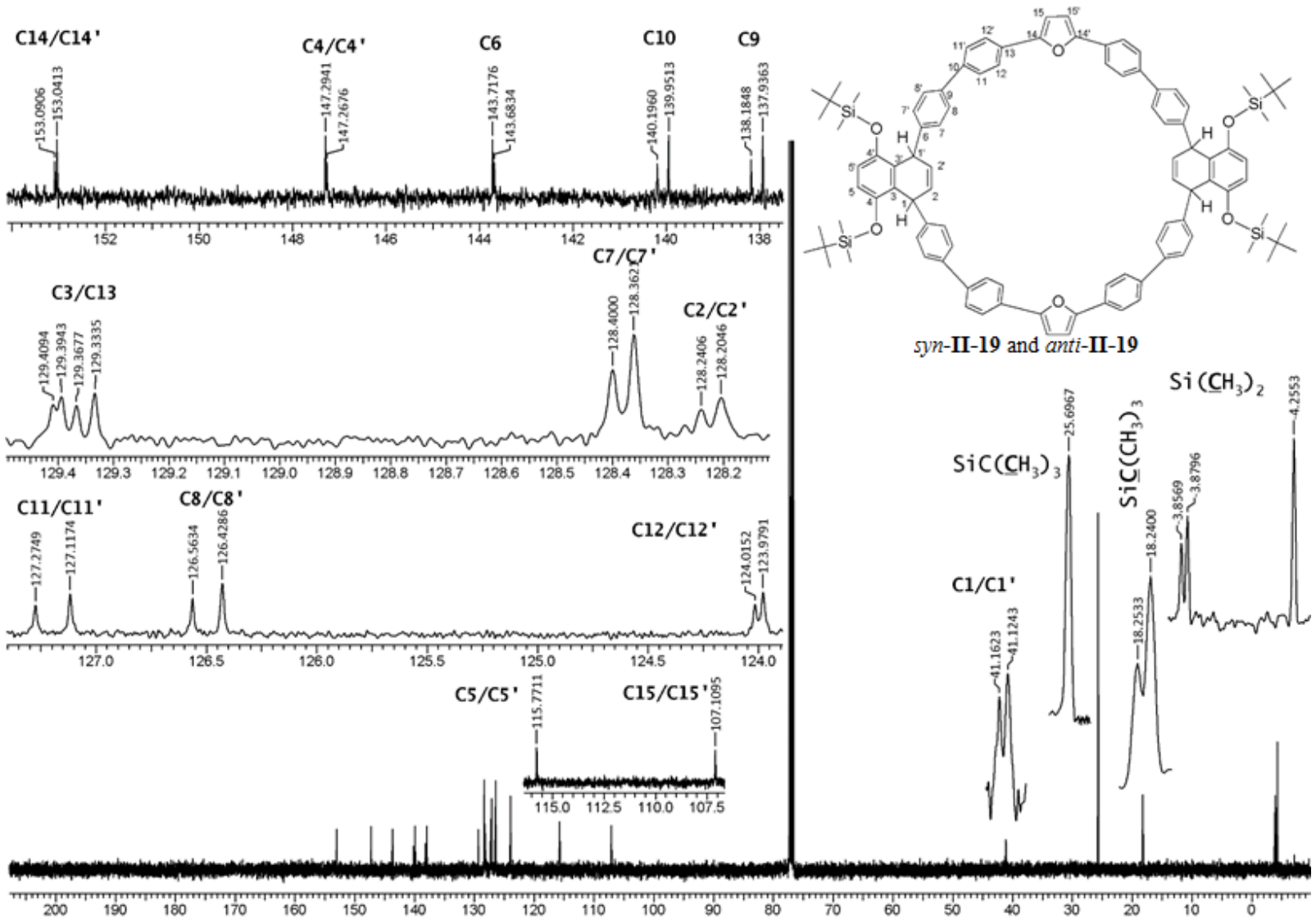

syn-**II-19** and *anti*-**II-19**

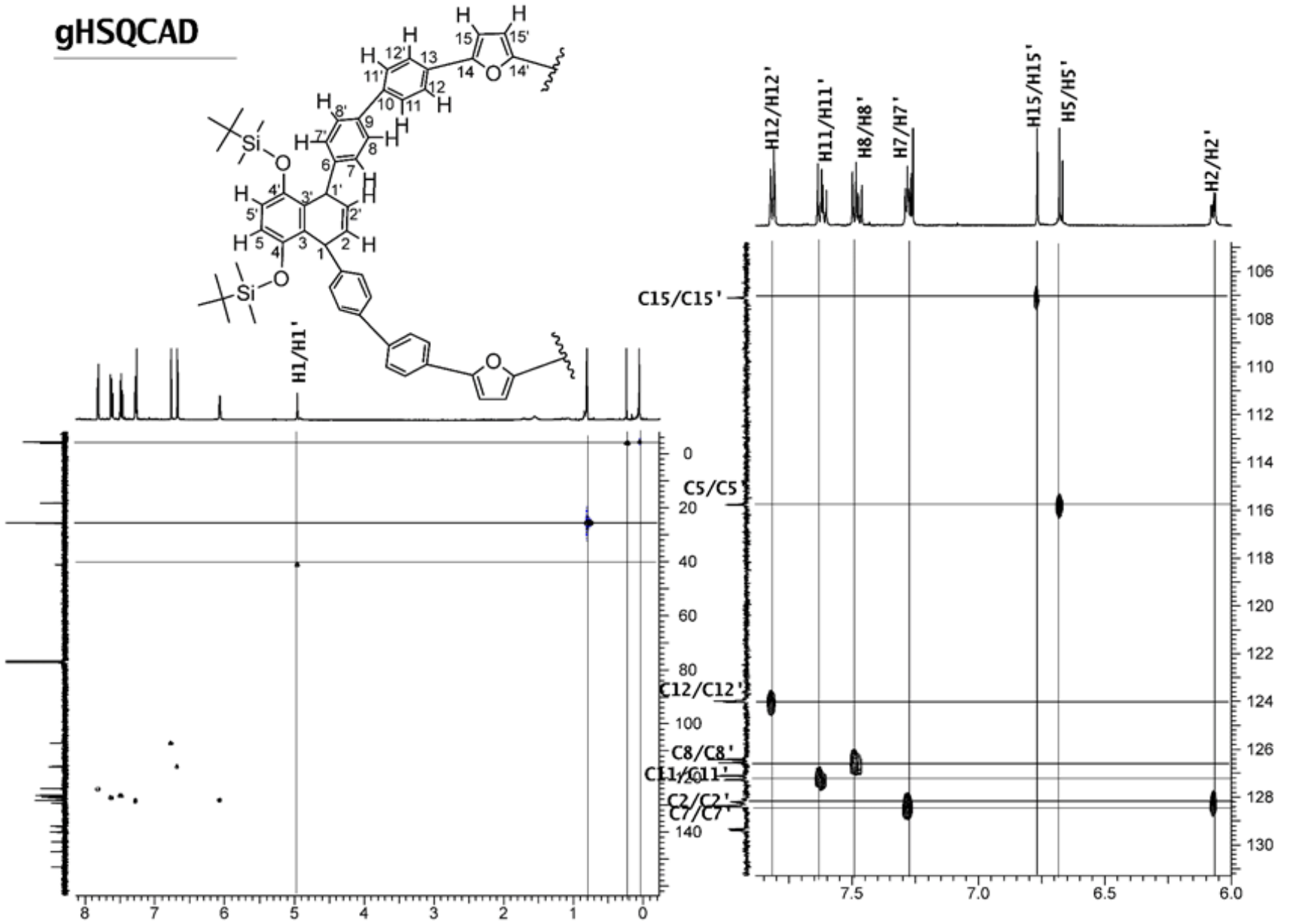
gHSQCAD
H1/H1'
H12/H12'
H11/H11'
H8/H8'
H7/H7'
H15/H15'
H5/H5'
H2/H2'
C15/C15'
C5/C5'
C12/C12'
C8/C8'
C11/C11'
C2/C2'
C7/C7'

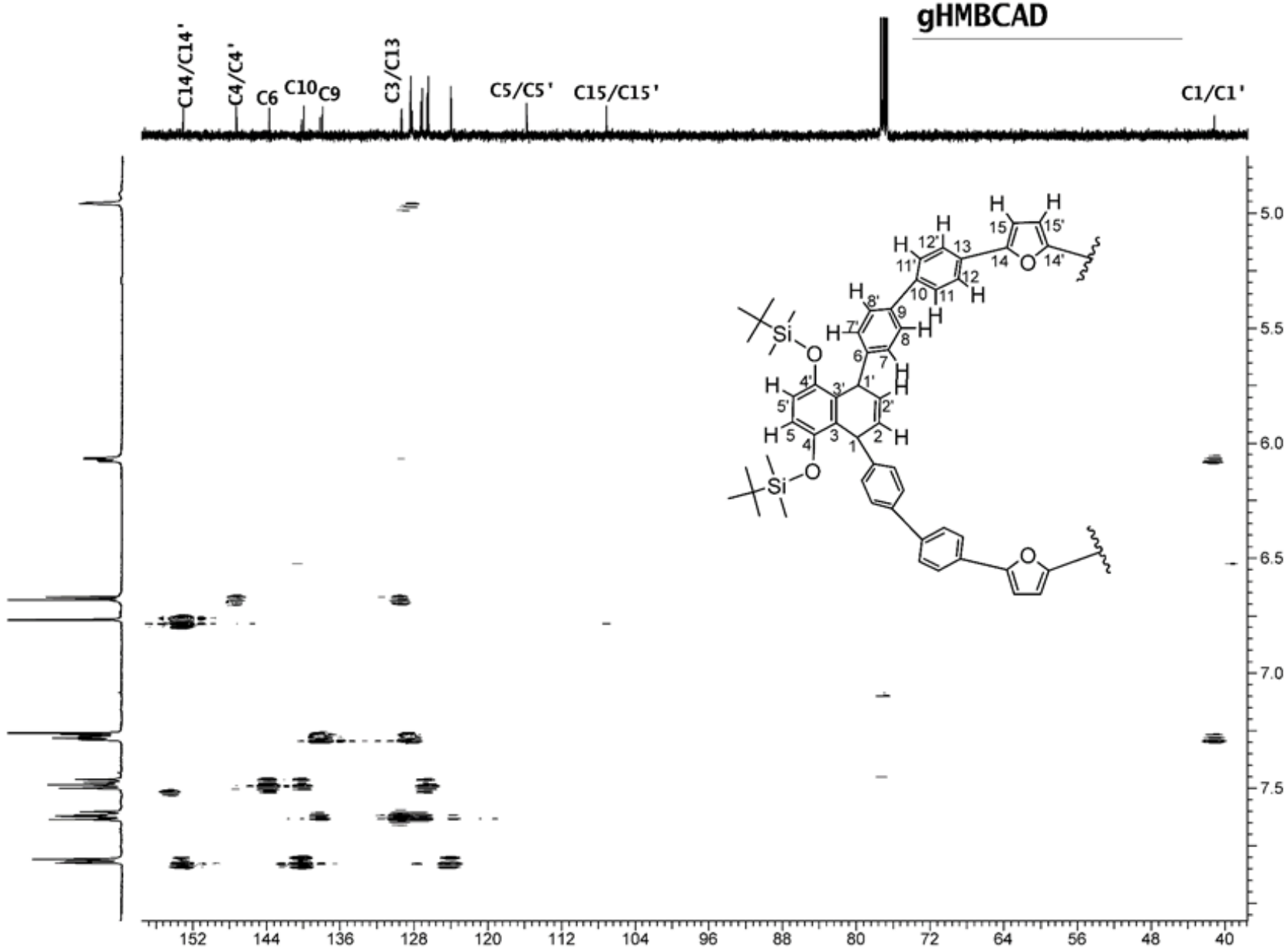
gHMBCAD
C14/C14'
C4/C4'
C6
C10
C9
C3/C13
C5/C5'
C15/C15'
C1/C1'
152
144
136
128
120
112
104
96
88
80
72
64
56
48
40
5.0
5.5
6.0
6.5
7.0
7.5

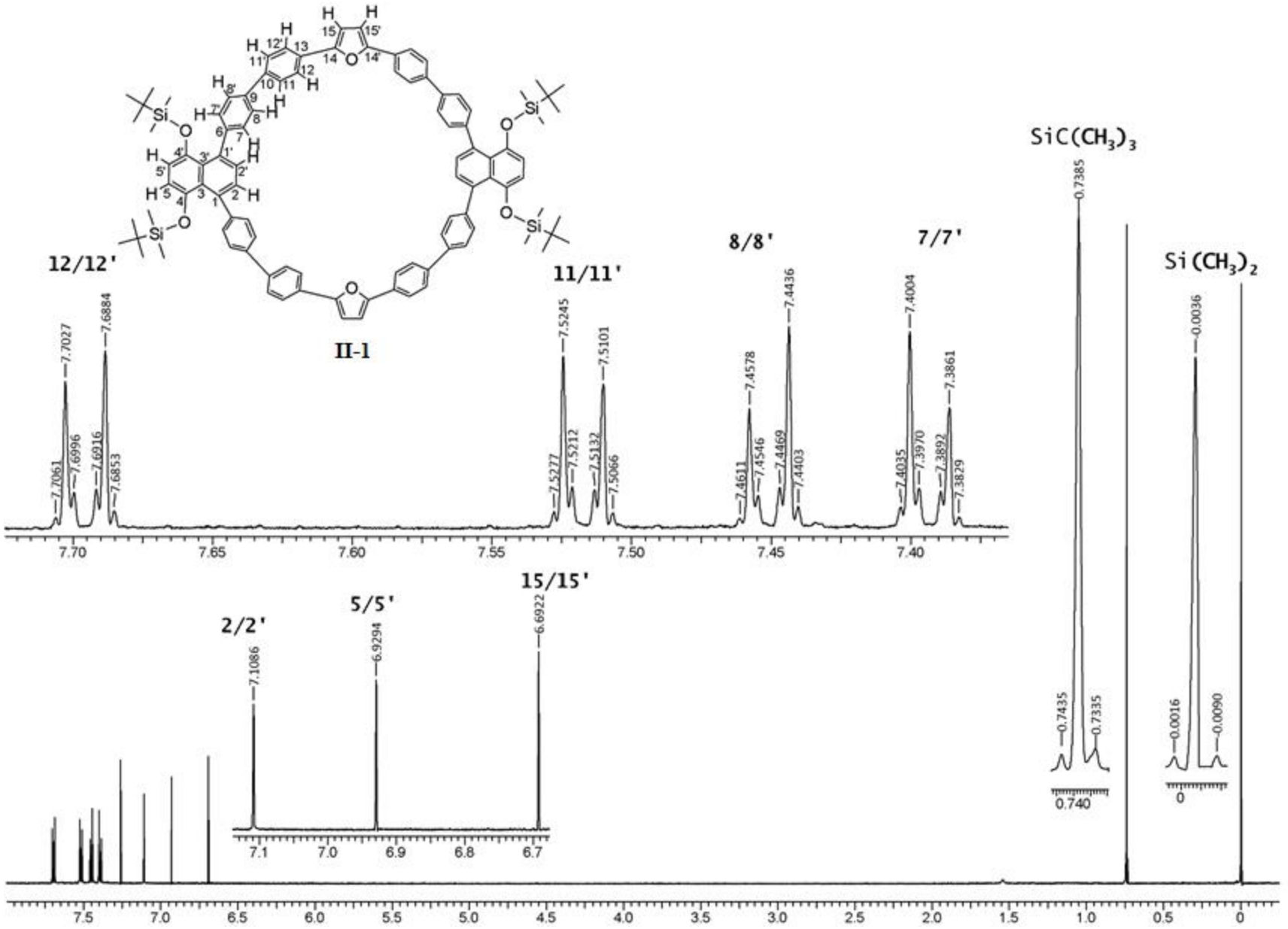
II-1
12/12'
11/11'
8/8'
7/7'
15/15'
5/5'
2/2'
SiC(CH3)3
Si(CH3)2
7.7061
7.7027
7.6996
7.6916
7.6884
7.6853
7.5277
7.5245
7.5212
7.5132
7.5101
7.5066
7.4611
7.4578
7.4546
7.4469
7.4436
7.4403
7.4035
7.4004
7.3970
7.3892
7.3861
7.3829
7.1086
6.9294
6.6922
0.7435
0.7385
0.7335
0.740
0.0016
0.0036
0.0090
0

gCOSY

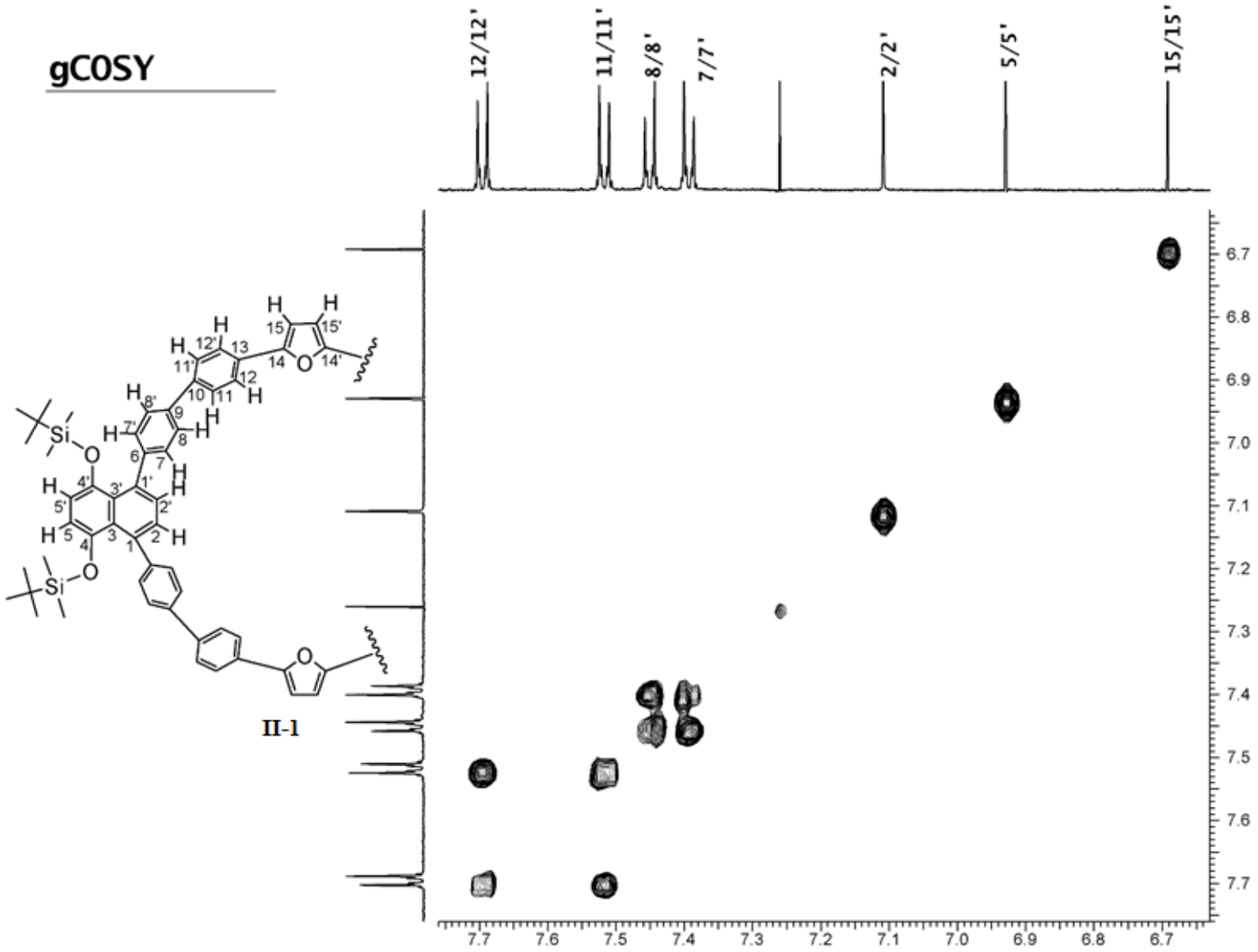
12/12'
11/11'
8/8'
7/7'
2/2'
5/5'
15/15'
6.7
6.8
6.9
7.0
7.1
7.2
7.3
7.4
7.5
7.6
7.7
7.7
7.6
7.5
7.4
7.3
7.2
7.1
7.0
6.9
6.8
6.7

II-1

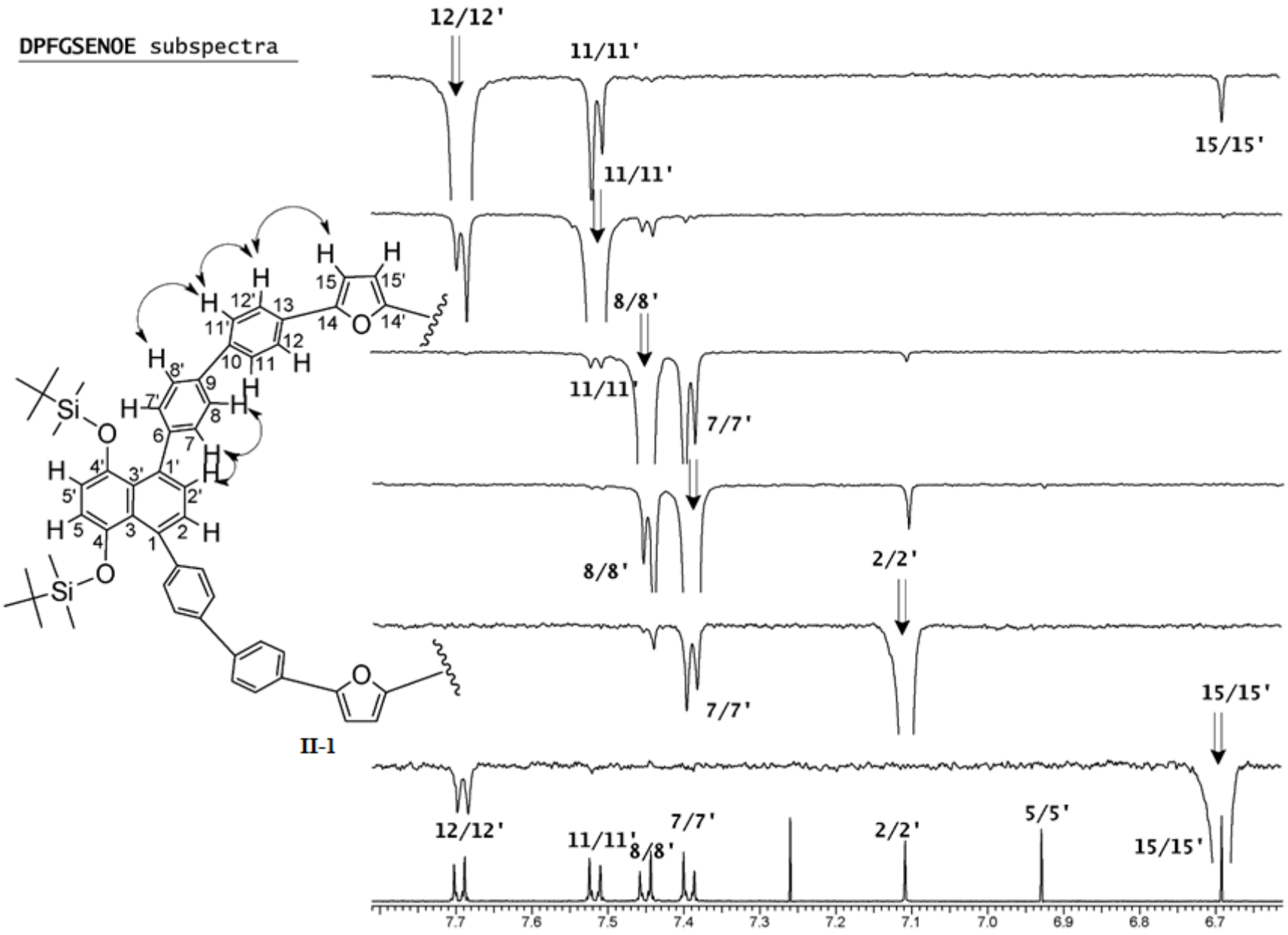
DPFGSENOE subspectra
12/12'
11/11'
15/15'
11/11'
8/8'
11/11'
7/7'
8/8'
2/2'
7/7'
15/15'
12/12'
11/11'
8/8'
7/7'
2/2'
5/5'
15/15'
7.7
7.6
7.5
7.4
7.3
7.2
7.1
7.0
6.9
6.8
6.7

II-1

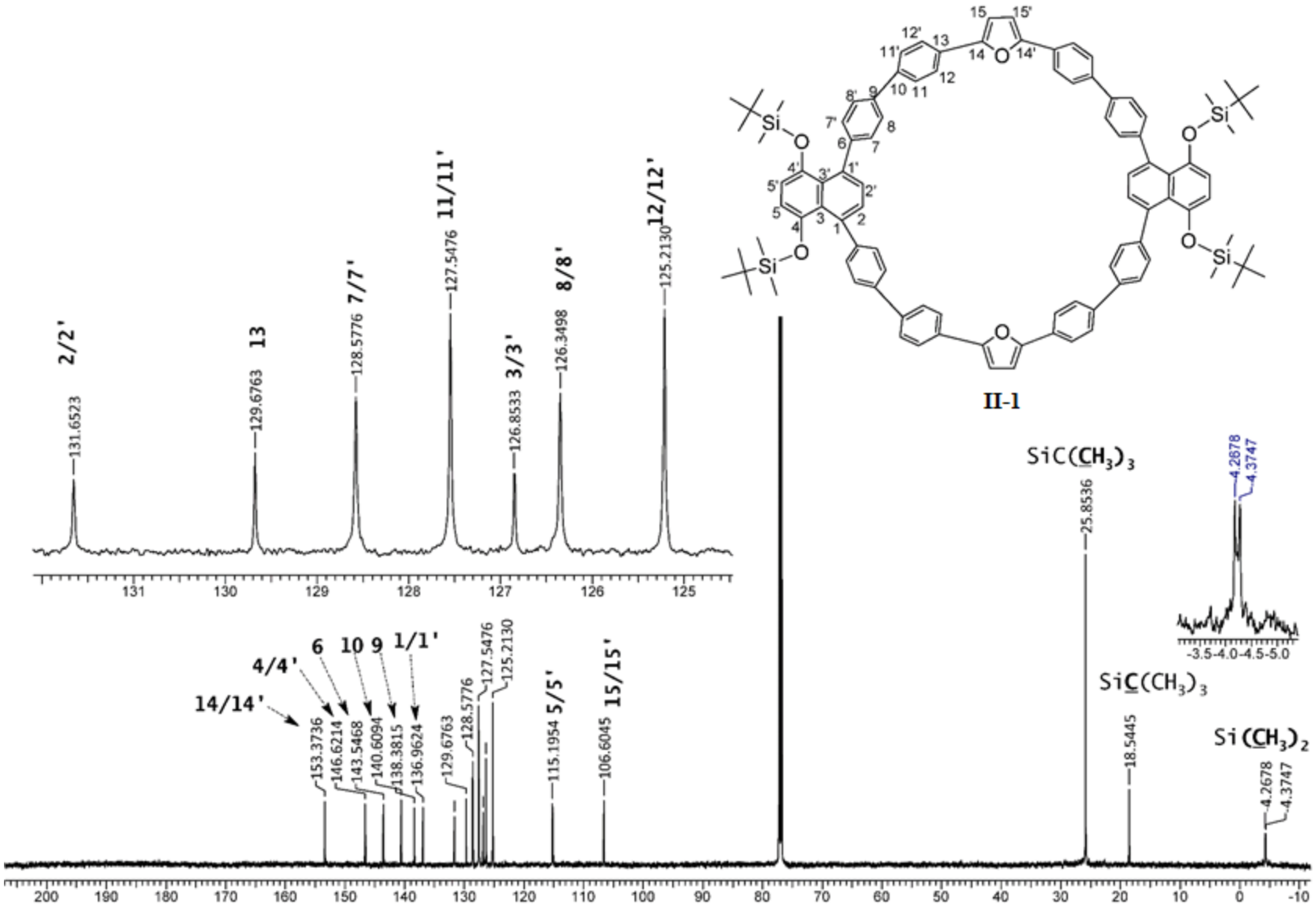
II-1
2/2'
13
7/7'
11/11'
3/3'
8/8'
12/12'
131.6523
129.6763
128.5776
127.5476
126.8533
126.3498
125.2130
14/14'
4/4'
6
10
9
1/1'
5/5'
15/15'
153.3736
146.6214
143.5468
140.6094
138.3815
136.9624
129.6763
128.5776
127.5476
125.2130
115.1954
106.6045
SiC(CH3)3
SiC(CH3)3
Si(CH3)2
25.8536
18.5445
4.2678
4.3747
-3.5-4.0-4.5-5.0

gHSQCAD

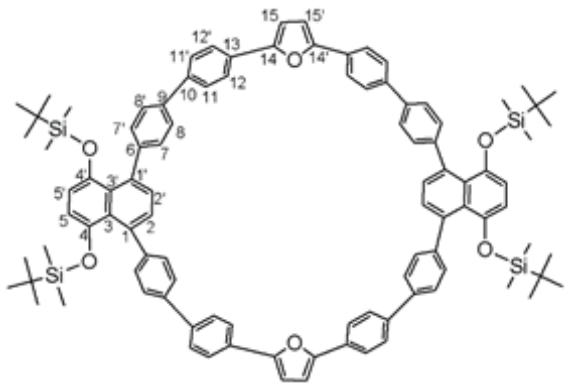

II-1

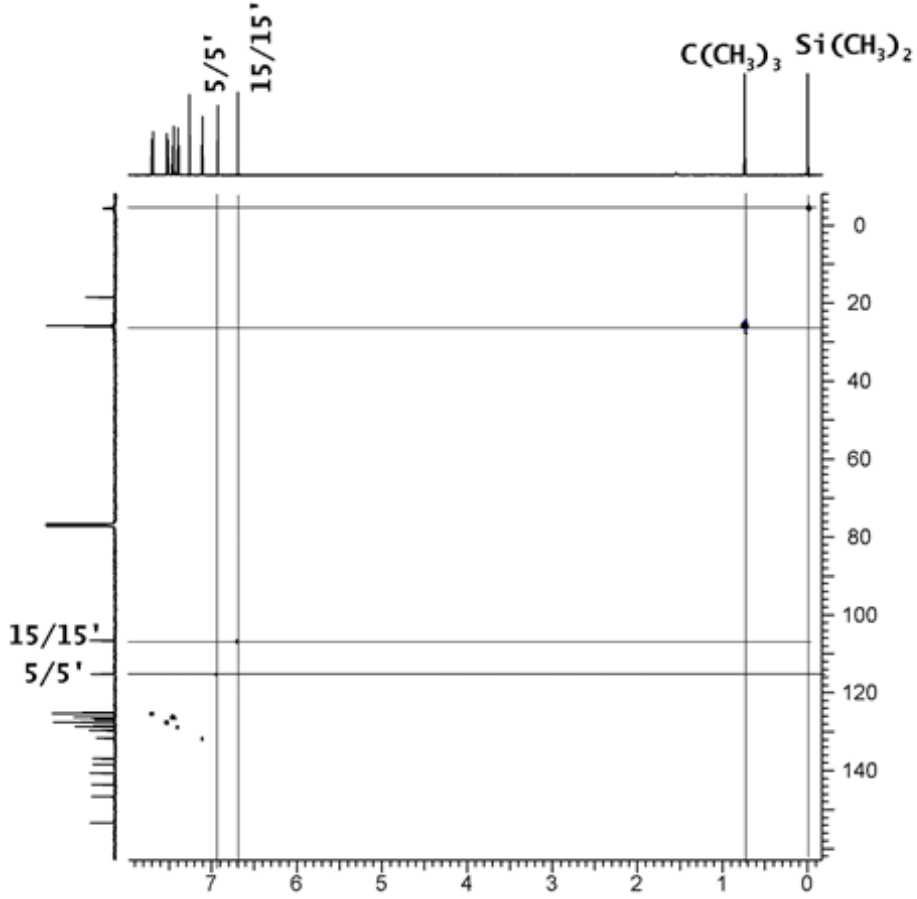
5/5'
15/15'
C(CH3)3
Si(CH3)2
15/15'
5/5'
0
20
40
60
80
100
120
140
7
6
5
4
3
2
1
0

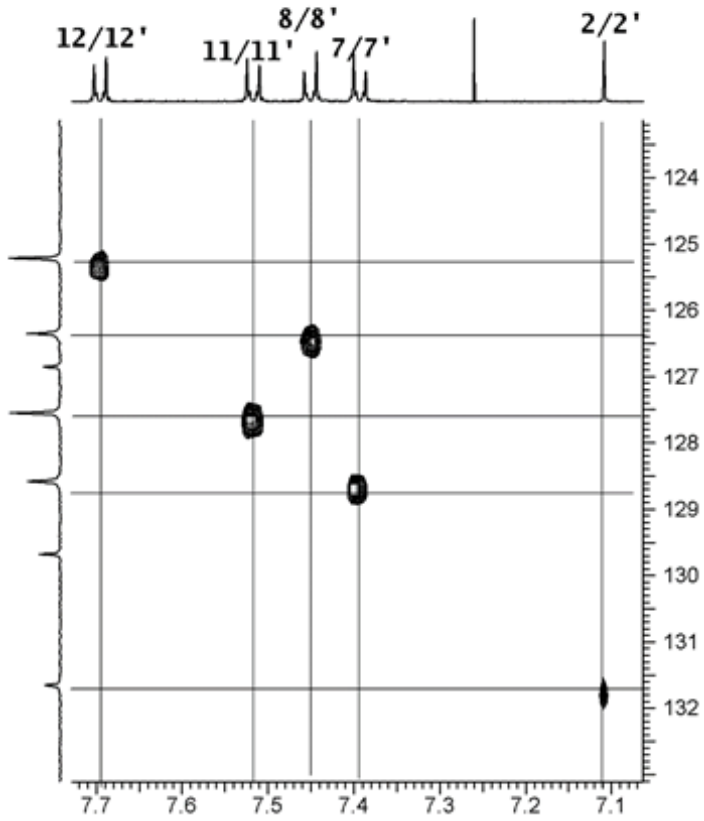
12/12'
11/11'
8/8'
7/7'
2/2'
124
125
126
127
128
129
130
131
132
7.7
7.6
7.5
7.4
7.3
7.2
7.1

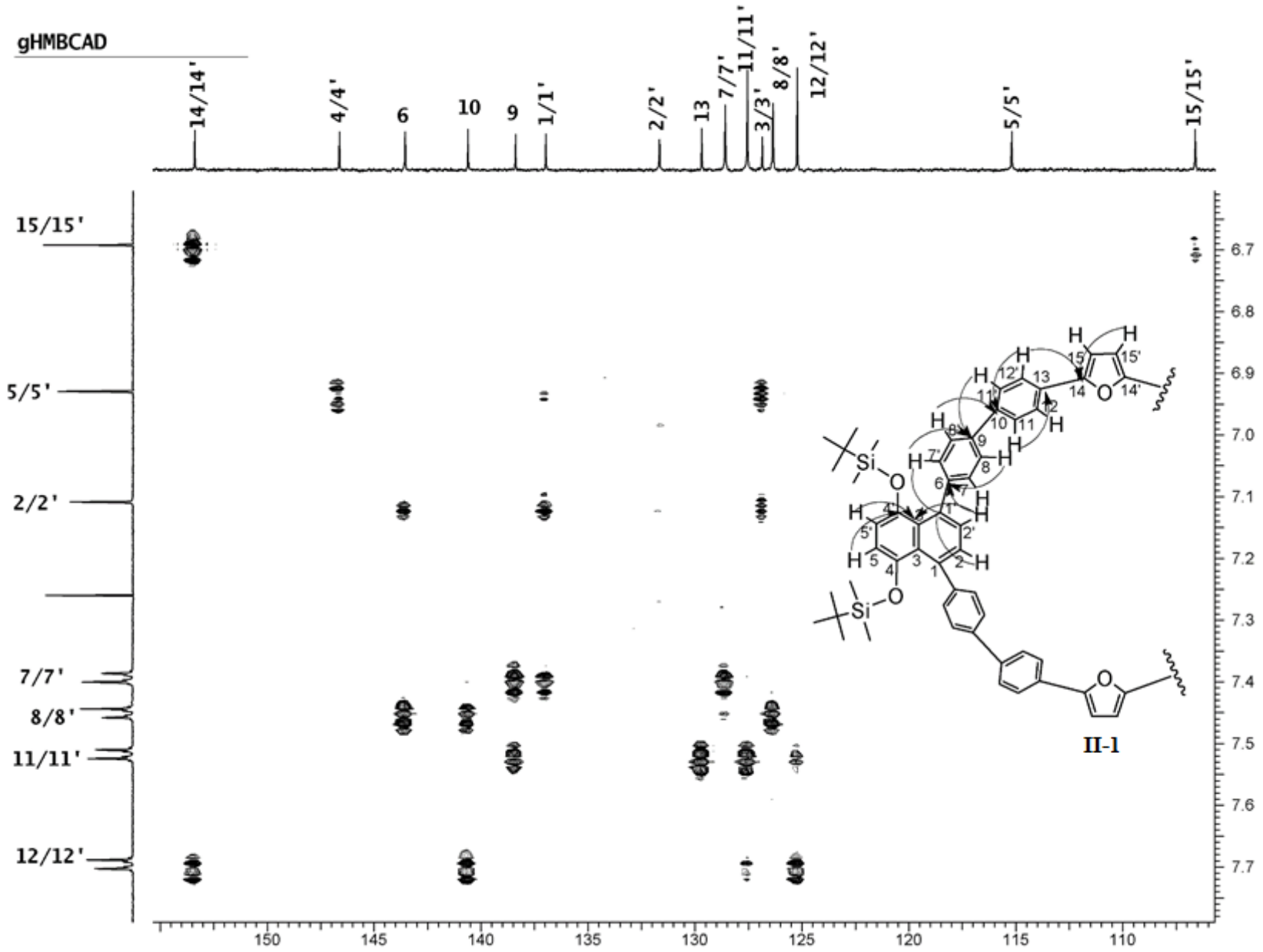
gHMBCAD
14/14'
4/4'
6
10
9
1/1'
2/2'
13
7/7'
11/11'
3/3'
8/8'
12/12'
5/5'
15/15'
15/15'
5/5'
2/2'
7/7'
8/8'
11/11'
12/12'
150
145
140
135
130
125
120
115
110
6.7
6.8
6.9
7.0
7.1
7.2
7.3
7.4
7.5
7.6
7.7
II-1

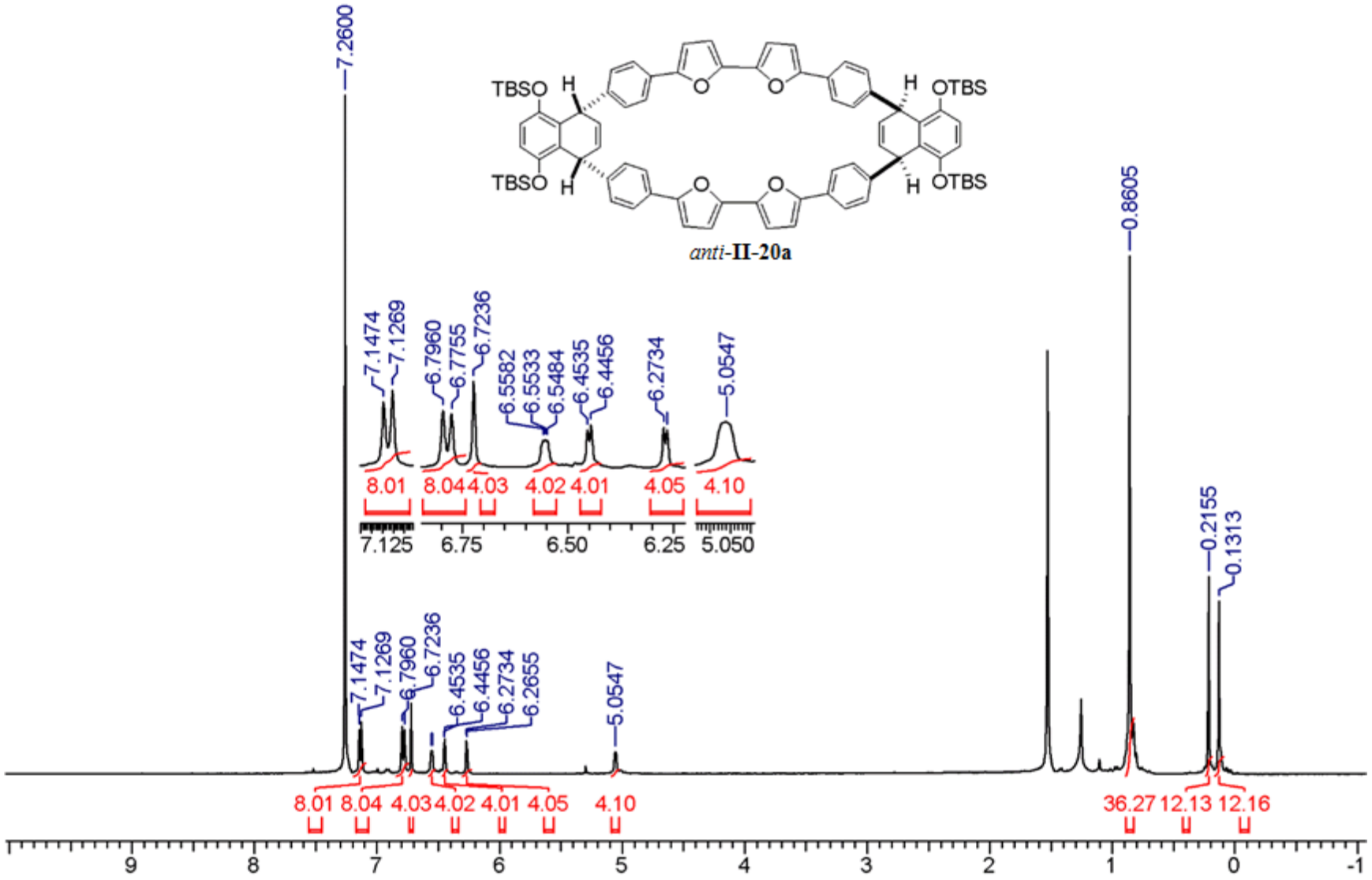
TBSO
H
TBSO
H
O
O
H
OTBS
H
OTBS
anti-II-20a
7.2600
0.8605
0.2155
0.1313
5.0547
8.01
8.04
4.03
4.02
4.01
4.05
4.10
36.27
12.13
12.16

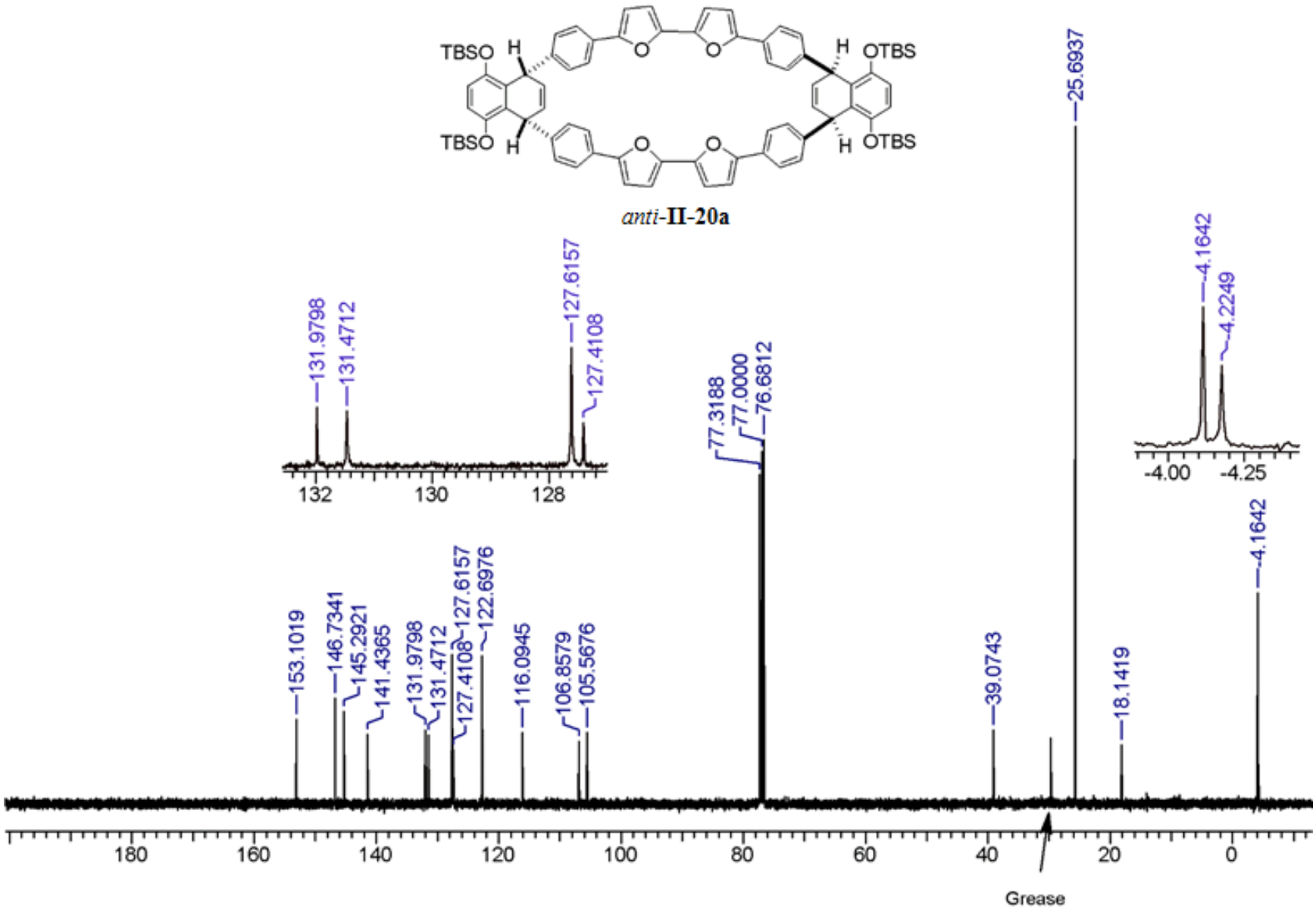
TBSO
H
TBSO
H
O
O
O
O
H
OTBS
H
OTBS
anti-II-20a
153.1019
146.7341
145.2921
141.4365
131.9798
131.4712
127.4108
127.6157
122.6976
116.0945
106.8579
105.5676
77.3188
77.0000
76.6812
39.0743
25.6937
18.1419
4.1642
4.2249
Grease

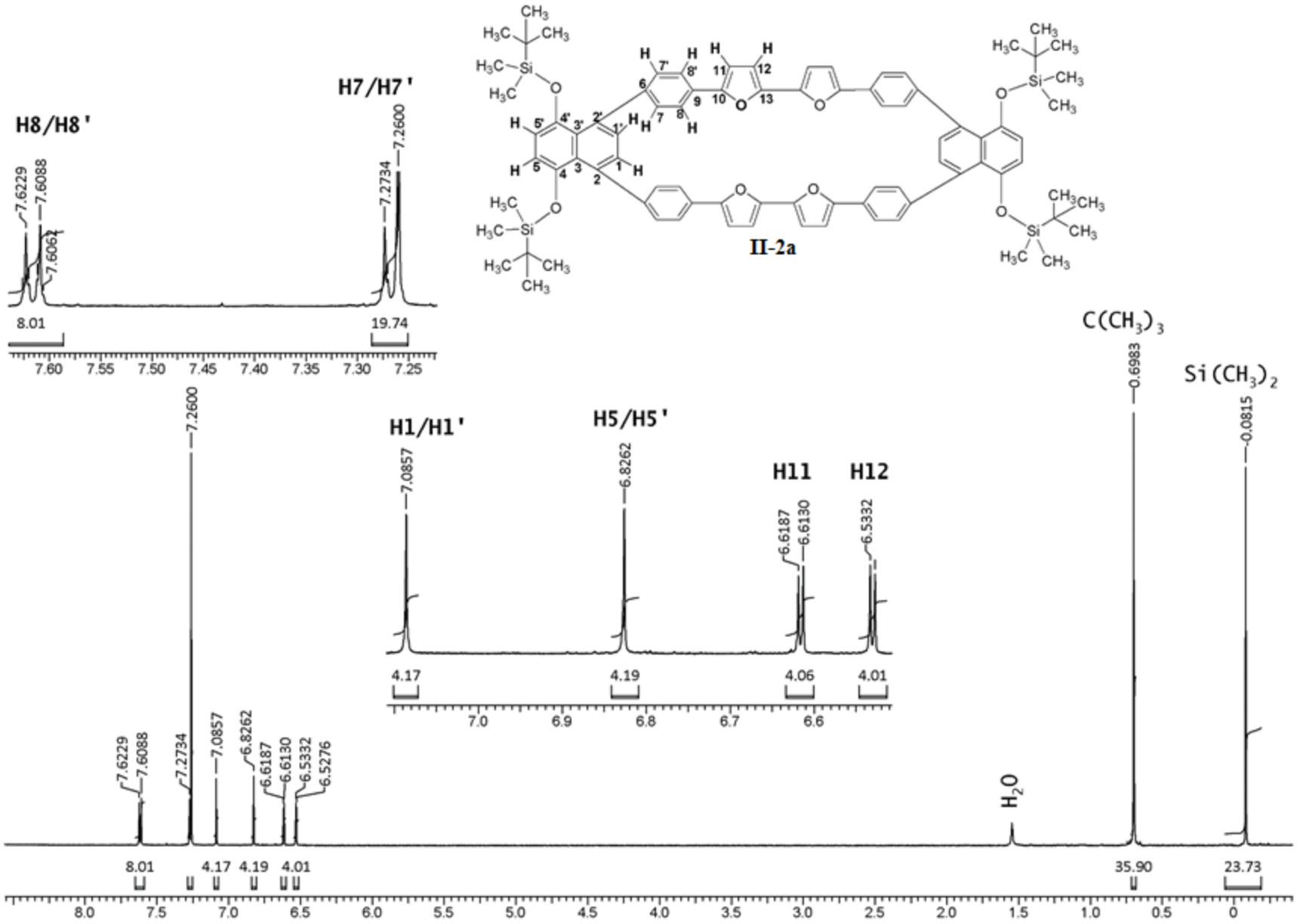
H8/H8'
H7/H7'
7.6229
7.6088
7.6062
7.2734
7.2600
8.01
19.74
7.60 7.55 7.50 7.45 7.40 7.35 7.30 7.25
II-2a
H1/H1'
H5/H5'
H11
H12
7.0857
6.8262
6.6187
6.6130
6.5332
4.17
4.19
4.06
4.01
7.0 6.9 6.8 6.7 6.6
C(CH3)3
Si(CH3)2
0.6983
0.0815
7.6229
7.6088
7.2734
7.2600
7.0857
6.8262
6.6187
6.6130
6.5332
6.5276
H2O
8.01
4.17
4.19
4.01
35.90
23.73
8.0 7.5 7.0 6.5 6.0 5.5 5.0 4.5 4.0 3.5 3.0 2.5 2.0 1.5 1.0 0.5 0

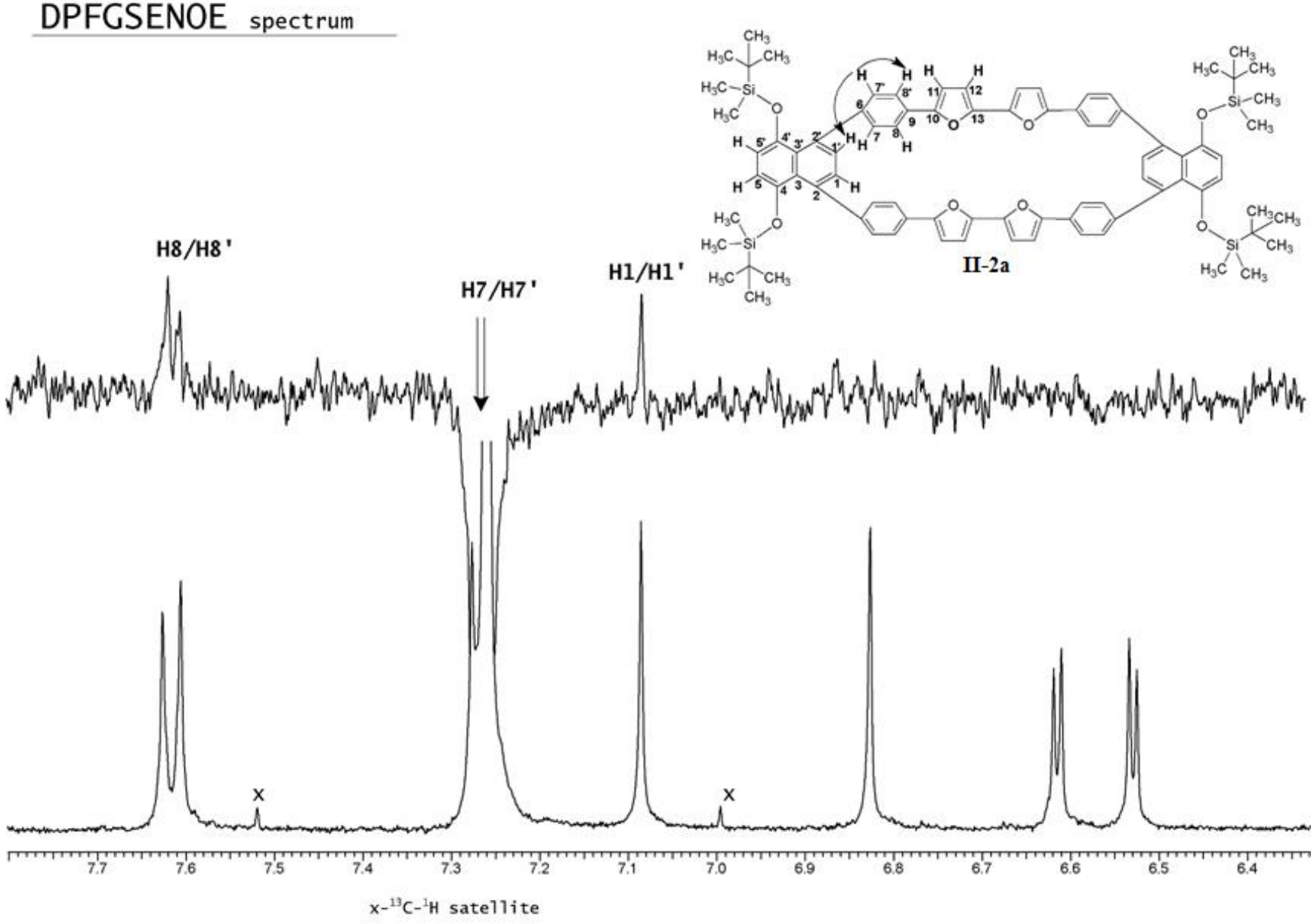
DPFGSENOE spectrum
H8/H8'
H7/H7'
H1/H1'
II-2a
X
X
7.7
7.6
7.5
7.4
7.3
7.2
7.1
7.0
6.9
6.8
6.7
6.6
6.5
6.4
x-13C-1H satellite

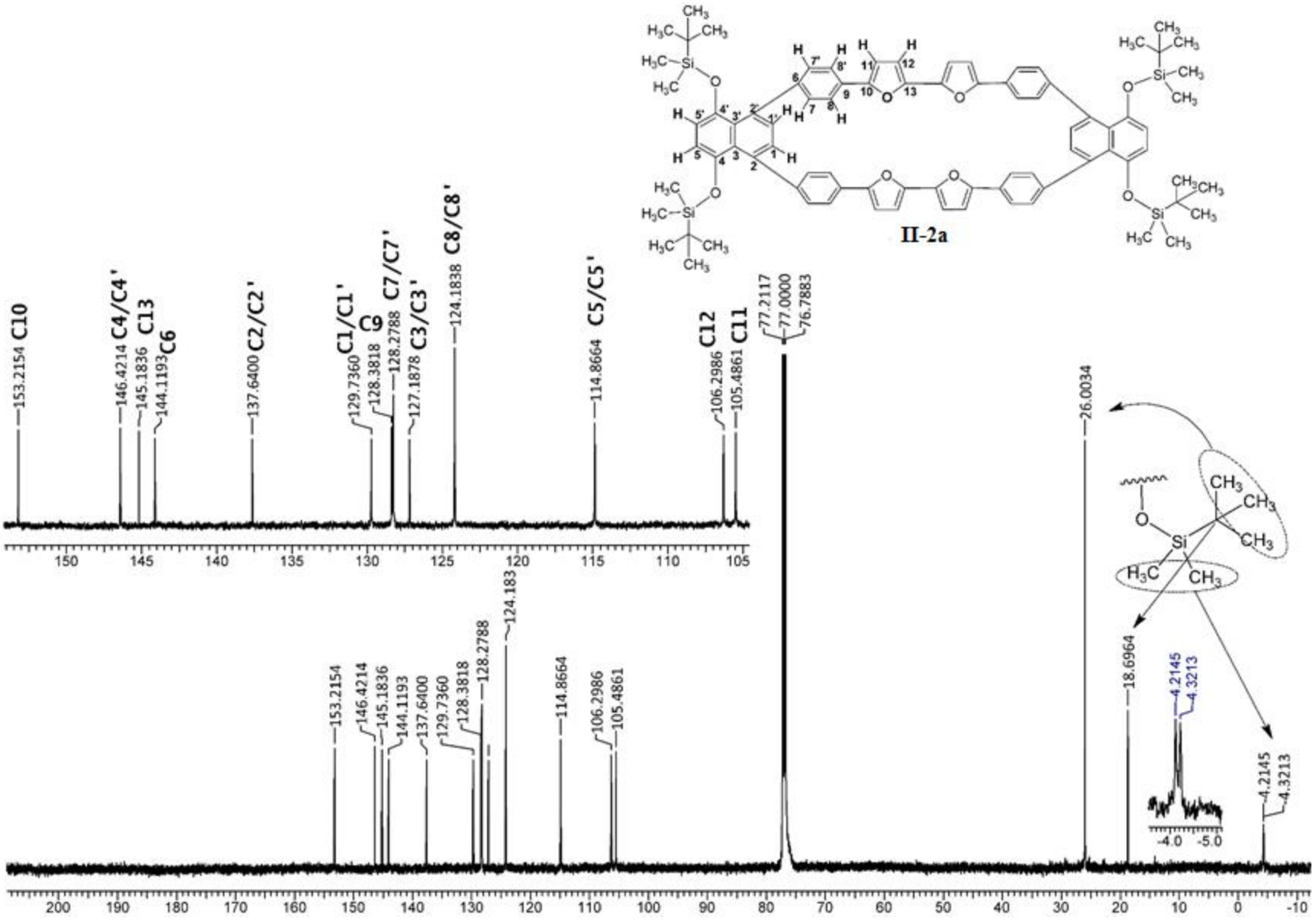
II-2a
153.2154 C10
146.4214 C4/C4'
145.1836 C13
144.1193 C6
137.6400 C2/C2'
129.7360 C1/C1'
128.3818 C9
128.2788 C7/C7'
127.1878 C3/C3'
124.1838 C8/C8'
114.8664 C5/C5'
106.2986 C12
105.4861 C11
77.2117
77.0000
76.7883
26.0034
18.6964
4.2145
4.3213

gHSQCAD

One-bond correlations

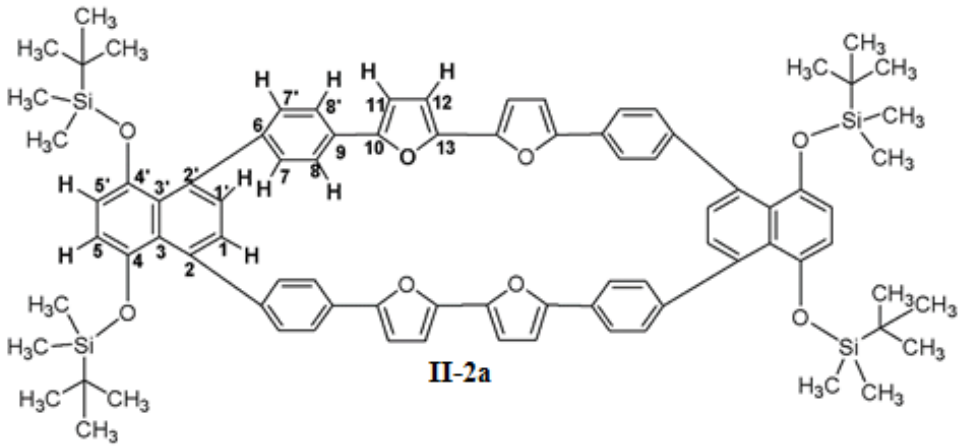

II-2a

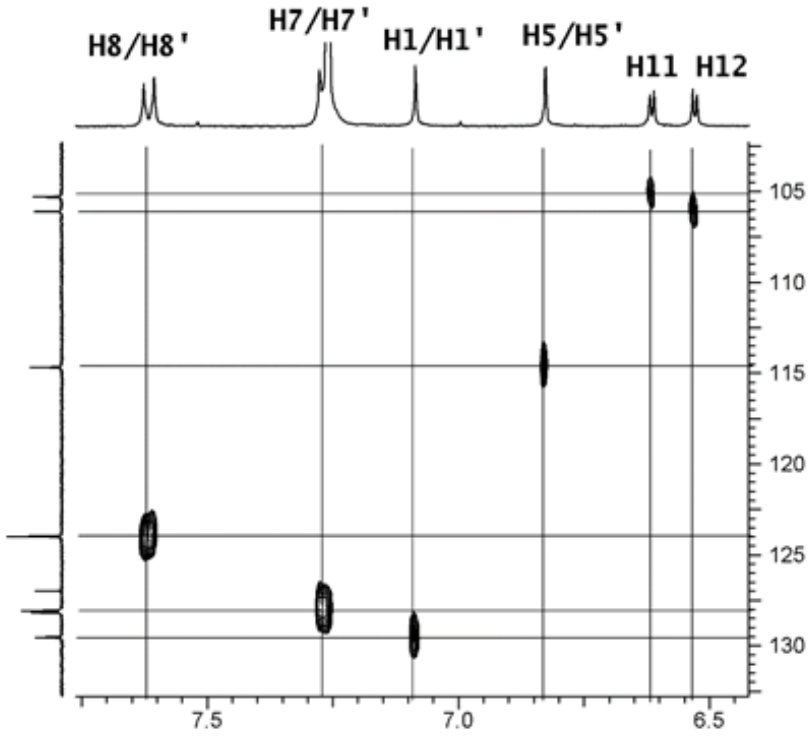

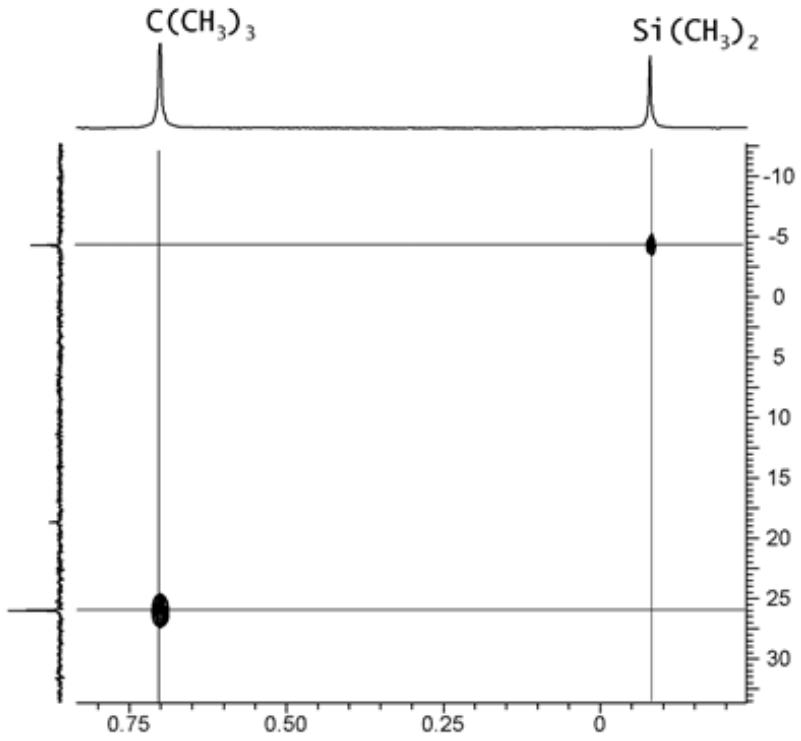

Long-range HMBC correlations

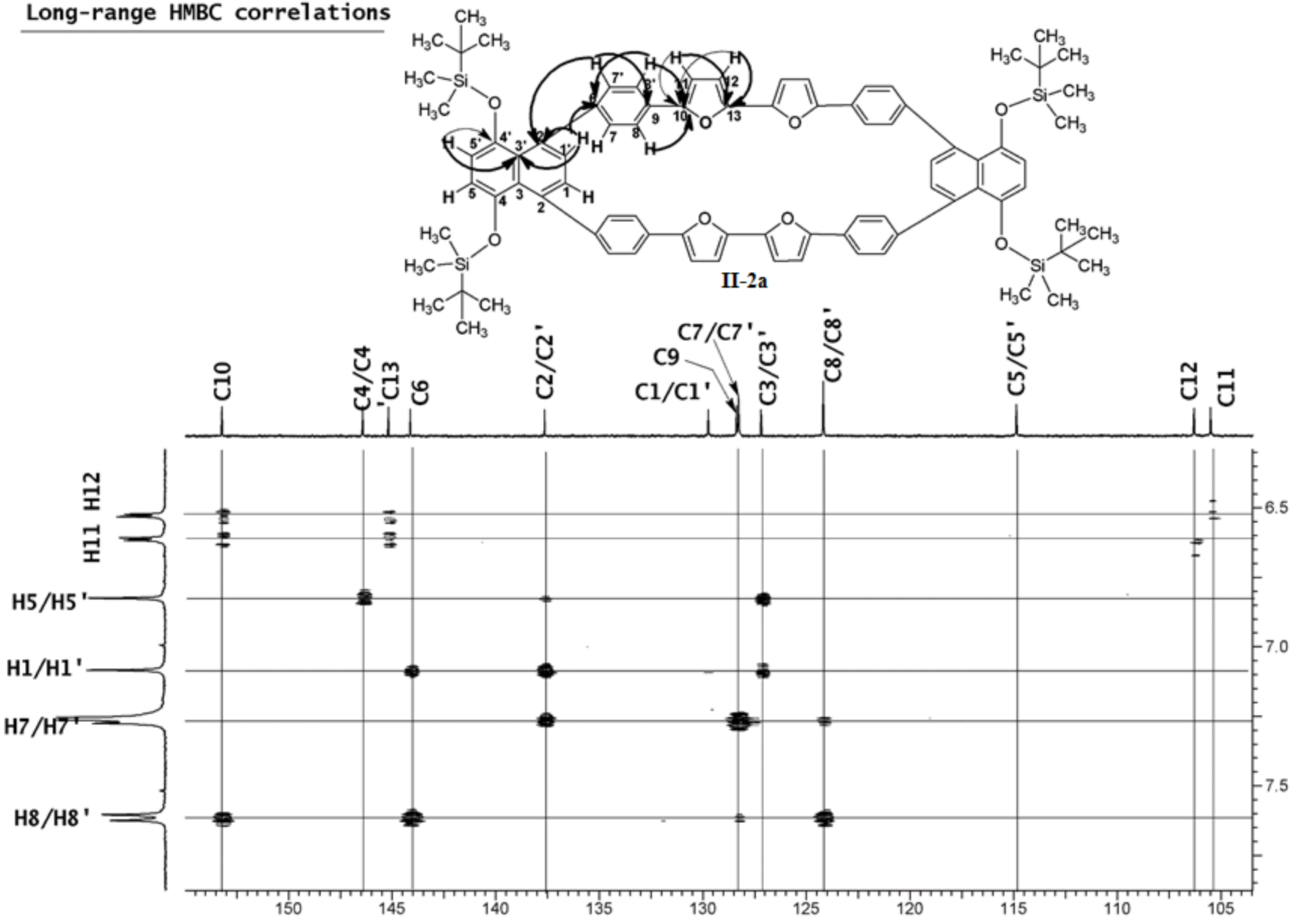

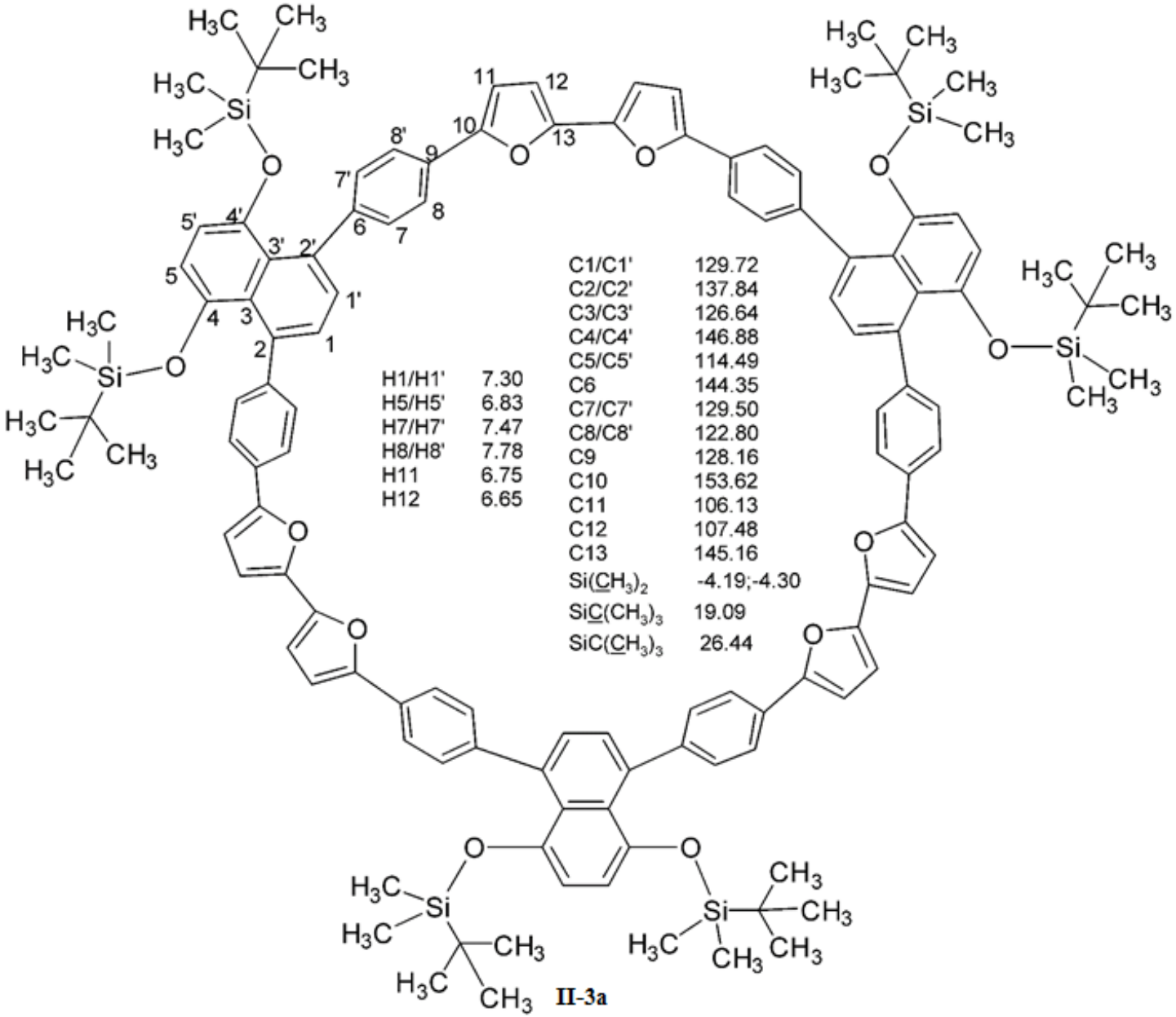
H1/H1' 7.30
H5/H5' 6.83
H7/H7' 7.47
H8/H8' 7.78
H11 6.75
H12 6.65
C1/C1' 129.72
C2/C2' 137.84
C3/C3' 126.64
C4/C4' 146.88
C5/C5' 114.49
C6 144.35
C7/C7' 129.50
C8/C8' 122.80
C9 128.16
C10 153.62
C11 106.13
C12 107.48
C13 145.16
Si(CH3)2 -4.19;-4.30
SiC(CH3)3 19.09
SiC(CH3)3 26.44

II-3a

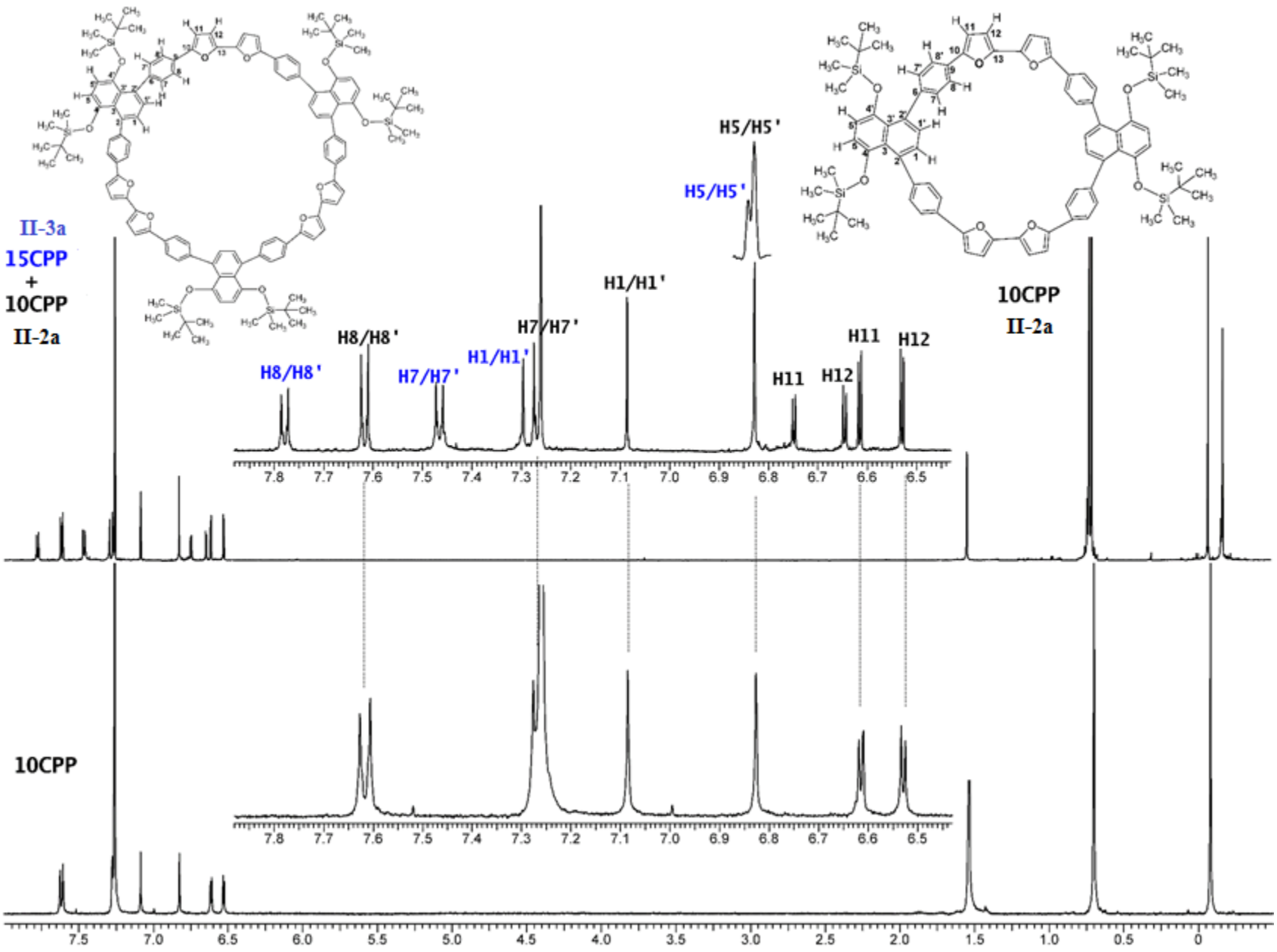
II-3a
15CPP
+
10CPP
II-2a
10CPP
10CPP
II-2a
H5/H5'
H5/H5'
H1/H1'
H8/H8'
H8/H8'
H7/H7'
H1/H1'
H7/H7'
H11
H12
H11
H12
7.8 7.7 7.6 7.5 7.4 7.3 7.2 7.1 7.0 6.9 6.8 6.7 6.6 6.5
7.8 7.7 7.6 7.5 7.4 7.3 7.2 7.1 7.0 6.9 6.8 6.7 6.6 6.5
7.5 7.0 6.5 6.0 5.5 5.0 4.5 4.0 3.5 3.0 2.5 2.0 1.5 1.0 0.5 0

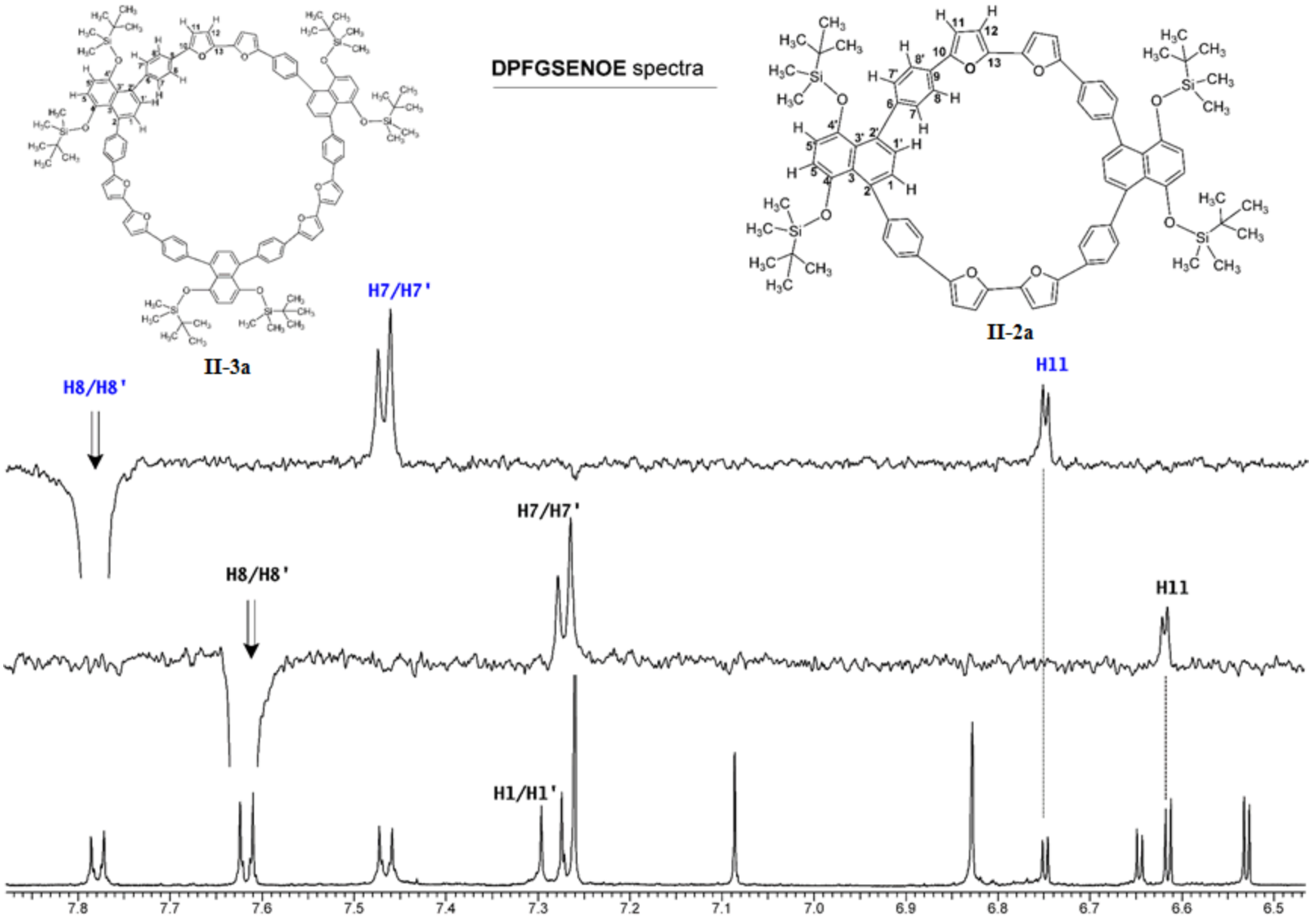
DPFGSENOE spectra
II-3a
II-2a
H7/H7'
H8/H8'
H11
H7/H7'
H8/H8'
H11
H1/H1'
7.8
7.7
7.6
7.5
7.4
7.3
7.2
7.1
7.0
6.9
6.8
6.7
6.6
6.5

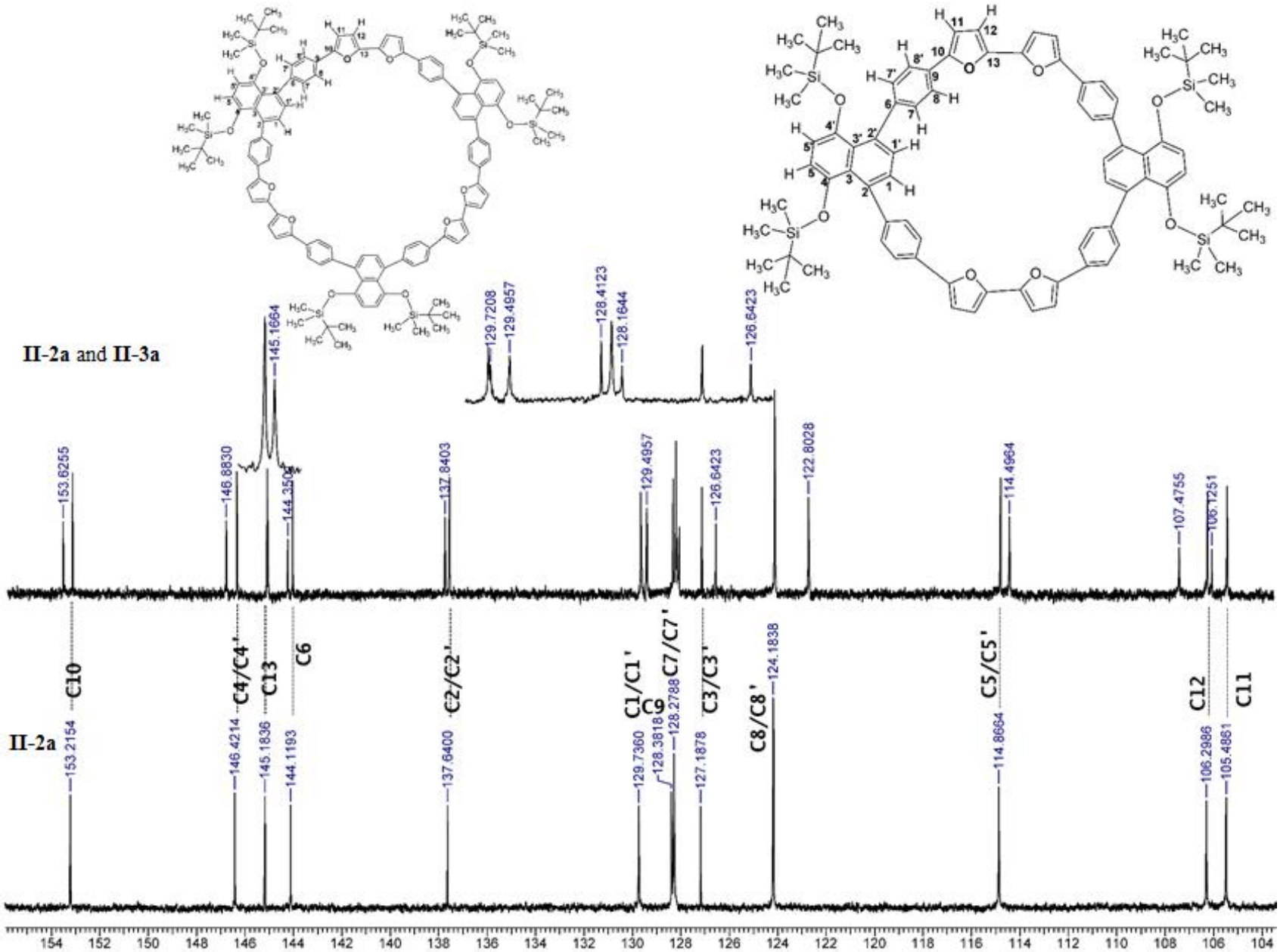
II-2a and II-3a
153.6255
146.8830
145.1664
144.3506
137.8403
129.7208
129.4957
128.4123
128.1644
126.6423
129.4957
126.6423
122.8028
114.4964
107.4755
106.1251
II-2a
153.2154
146.4214
145.1836
144.1193
137.6400
129.7360
128.3818
128.2788
127.1878
124.1838
114.8664
106.2986
105.4861
C10
C4/C4'
C13
C6
C2/C2'
C1/C1'
C9
C7/C7'
C3/C3'
C8/C8'
C5/C5'
C12
C11
154 152 150 148 146 144 142 140 138 136 134 132 130 128 126 124 122 120 118 116 114 112 110 108 106 104

gHSQCAD

One-bond correlations

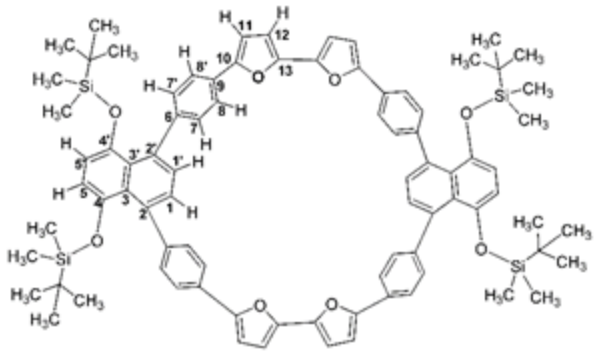

II-2a

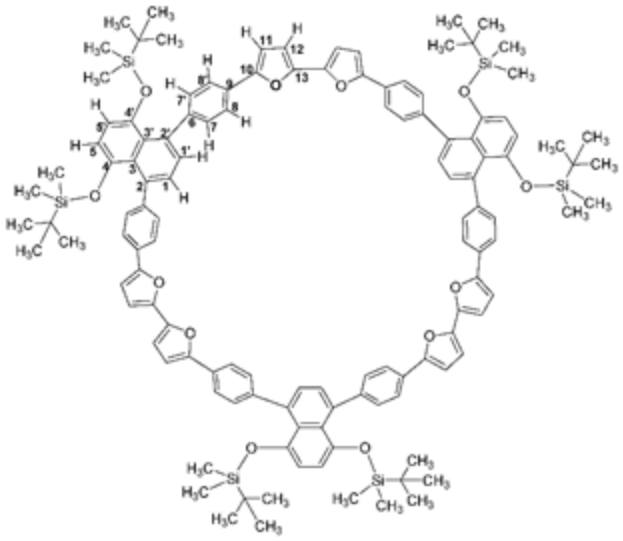

II-3a

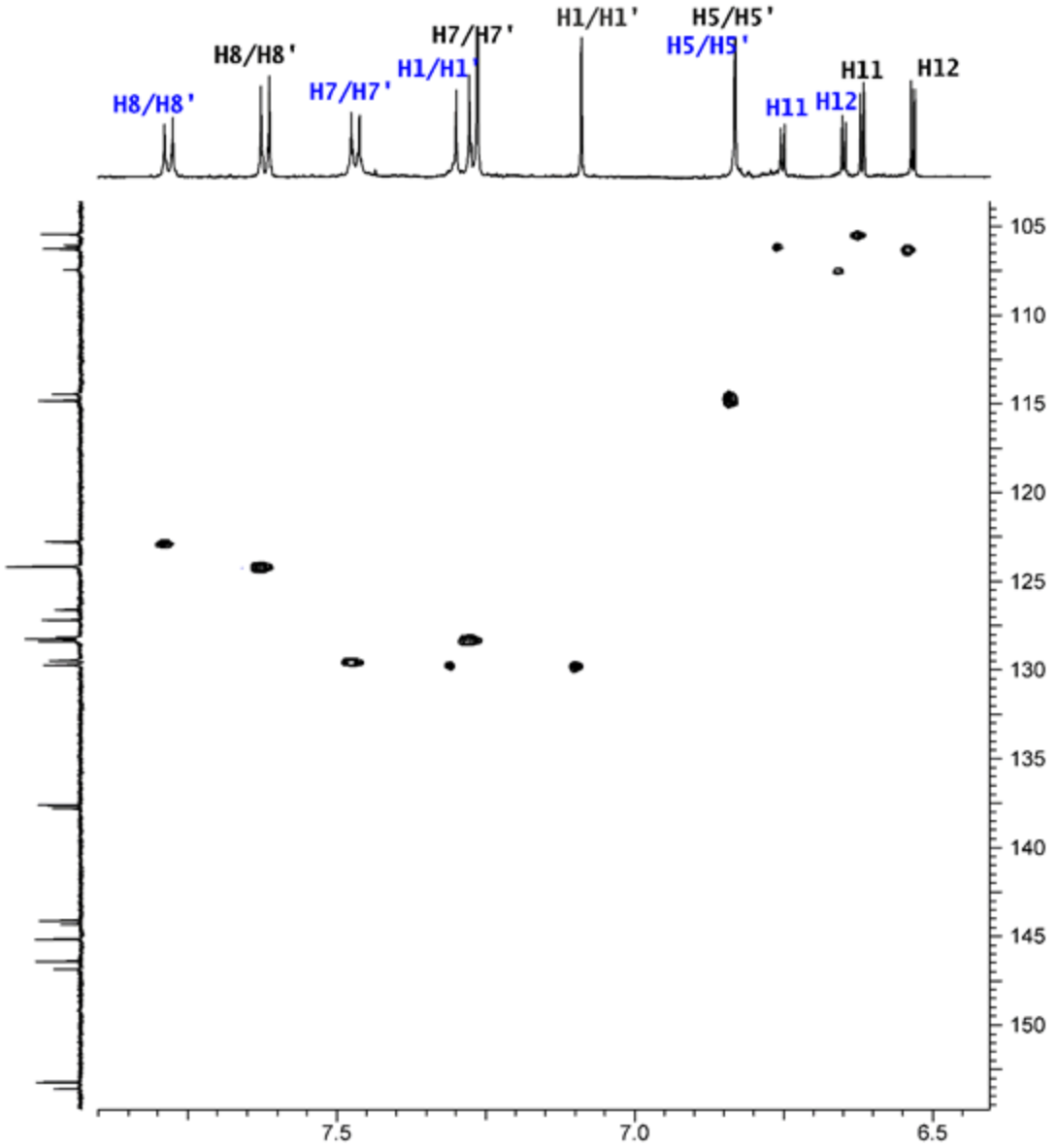

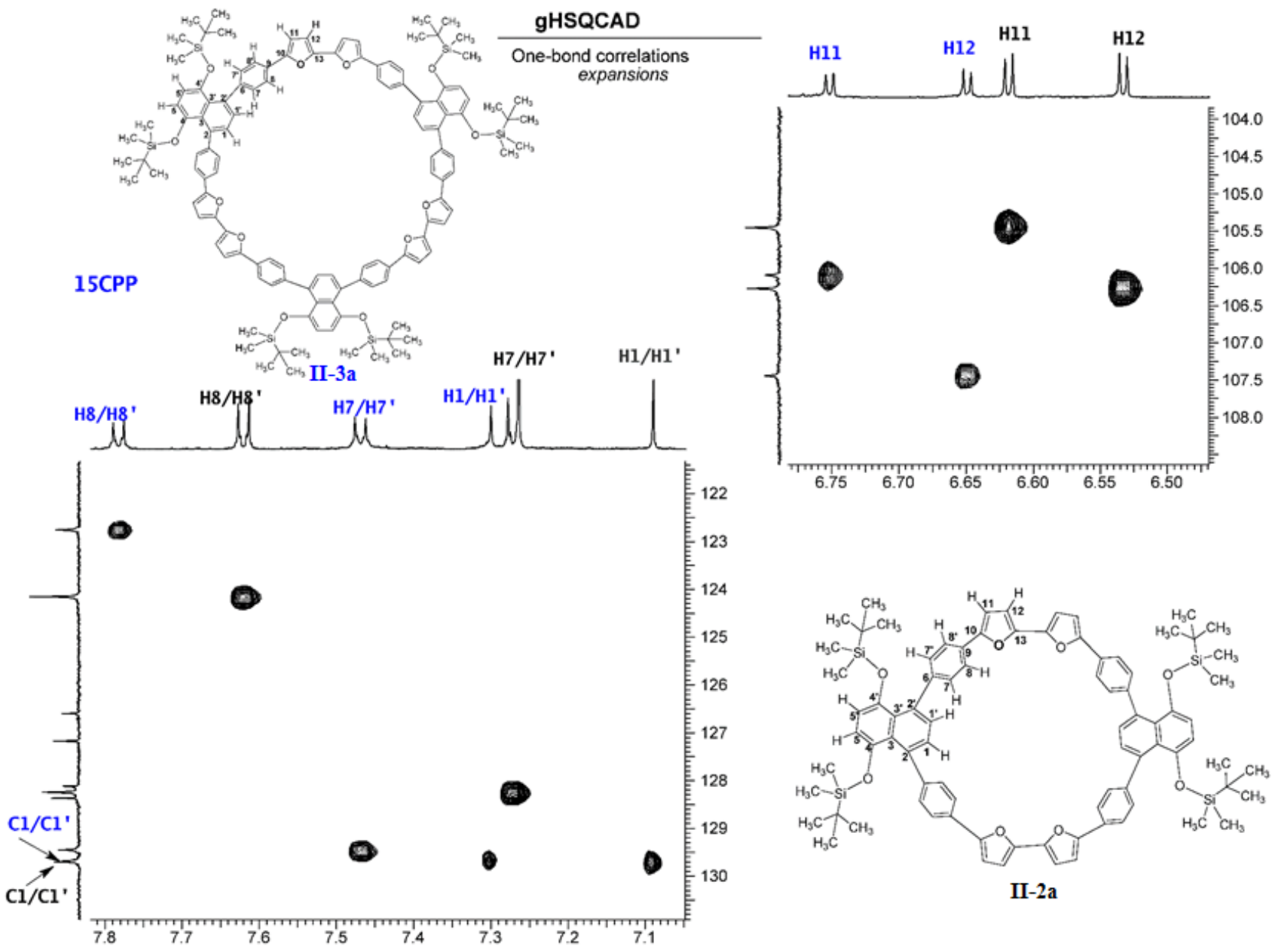
gHSQCAD
One-bond correlations
expansions
15CPP
II-3a
H8/H8'
H8/H8'
H7/H7'
H1/H1'
H7/H7'
H1/H1'
C1/C1'
C1/C1'
H11
H12
H11
H12
II-2a

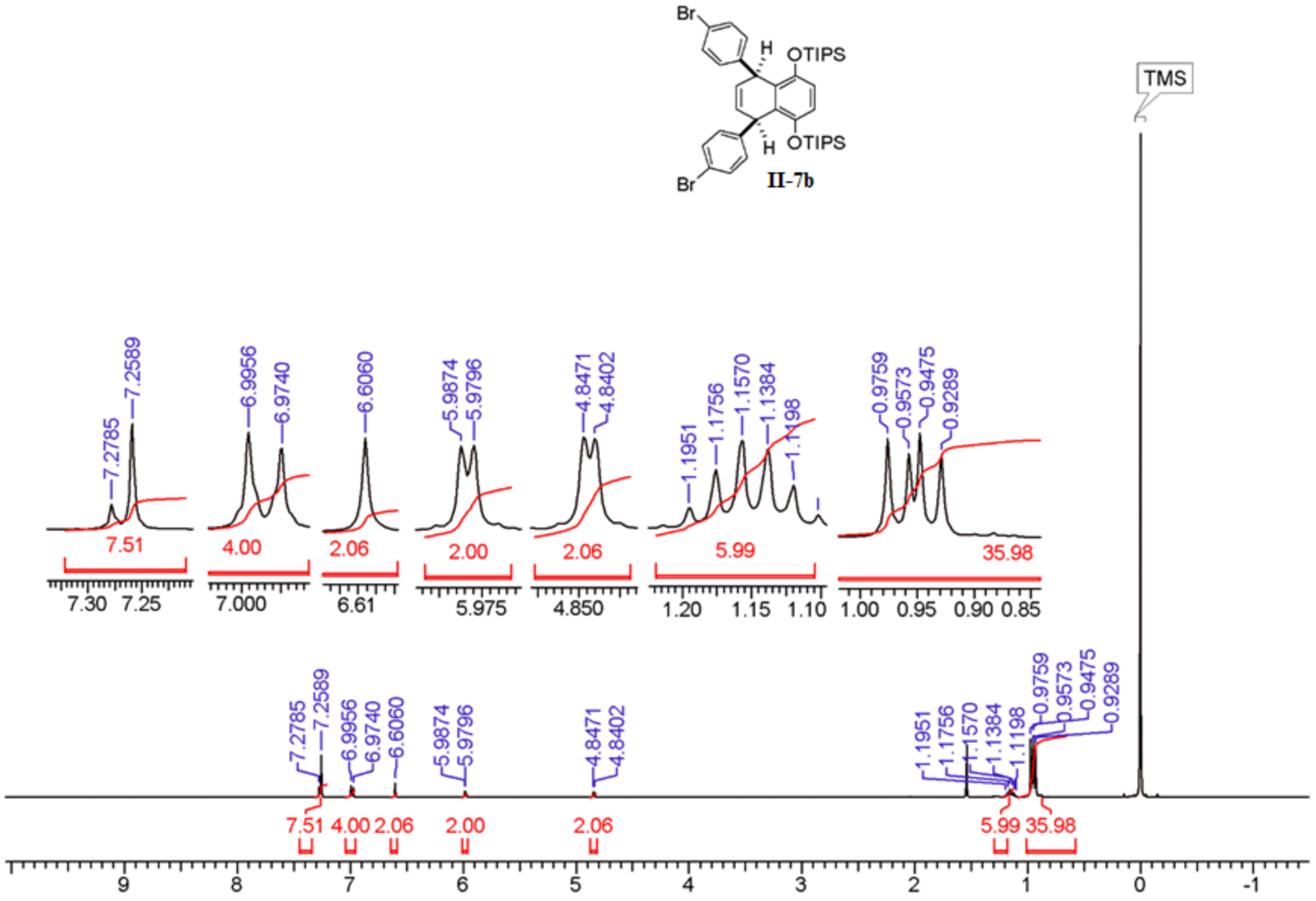
Br
H
OTIPS
H
OTIPS
Br
II-7b
TMS
7.2785
7.2589
6.9956
6.9740
6.6060
5.9874
5.9796
4.8471
4.8402
1.1951
1.1756
1.1570
1.1384
1.1198
0.9759
0.9573
0.9475
0.9289
7.51
4.00
2.06
2.00
2.06
5.99
35.98
7.30 7.25
7.000
6.61
5.975
4.850
1.20 1.15 1.10
1.00 0.95 0.90 0.85
9 8 7 6 5 4 3 2 1 0 -1

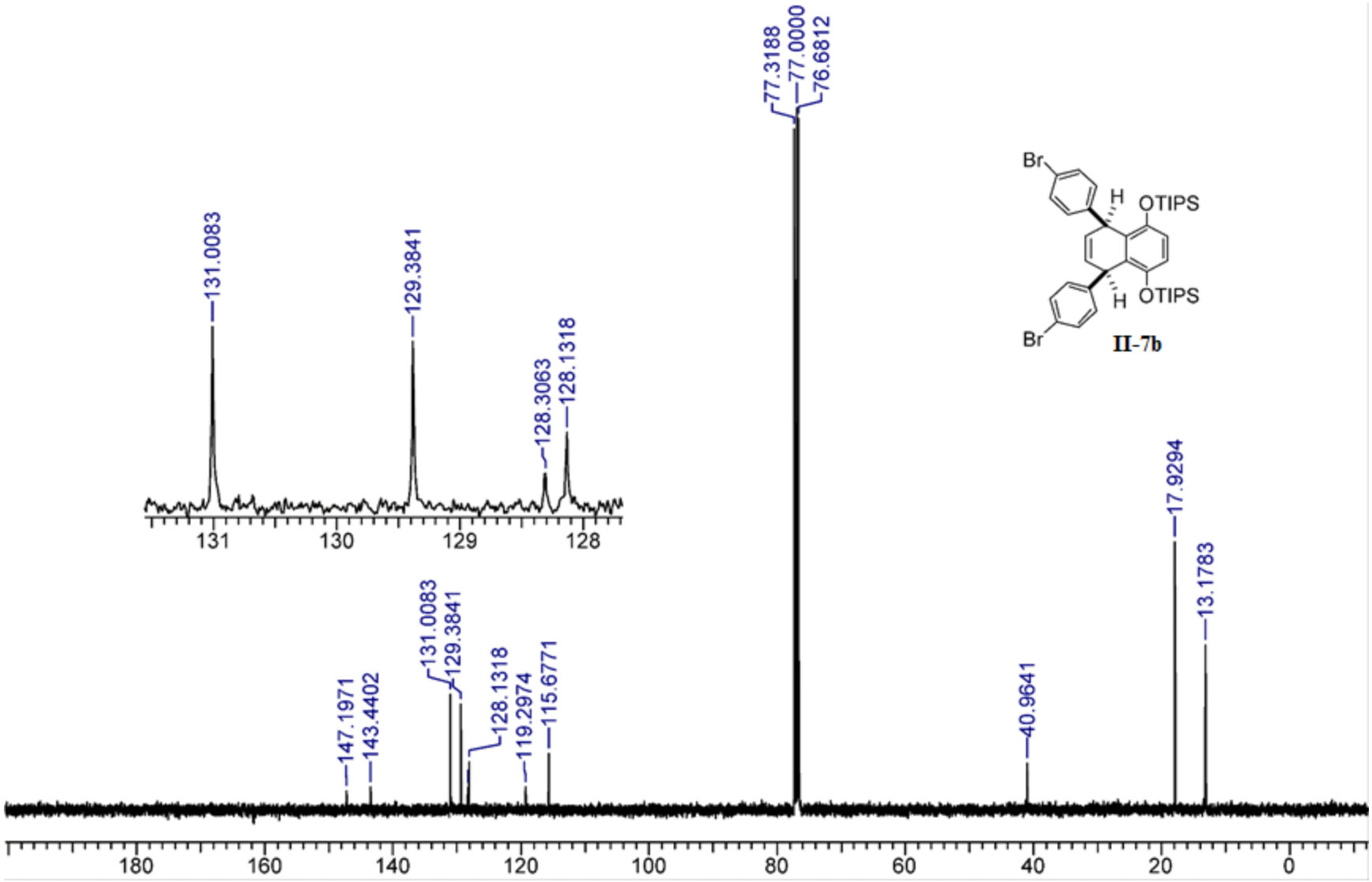
77.3188
77.0000
76.6812
131.0083
129.3841
128.3063
128.1318
147.1971
143.4402
131.0083
129.3841
128.1318
119.2974
115.6771
40.9641
17.9294
13.1783
Br
H
OTIPS
H
OTIPS
Br
II-7b
131
130
129
128
180
160
140
120
100
80
60
40
20
0

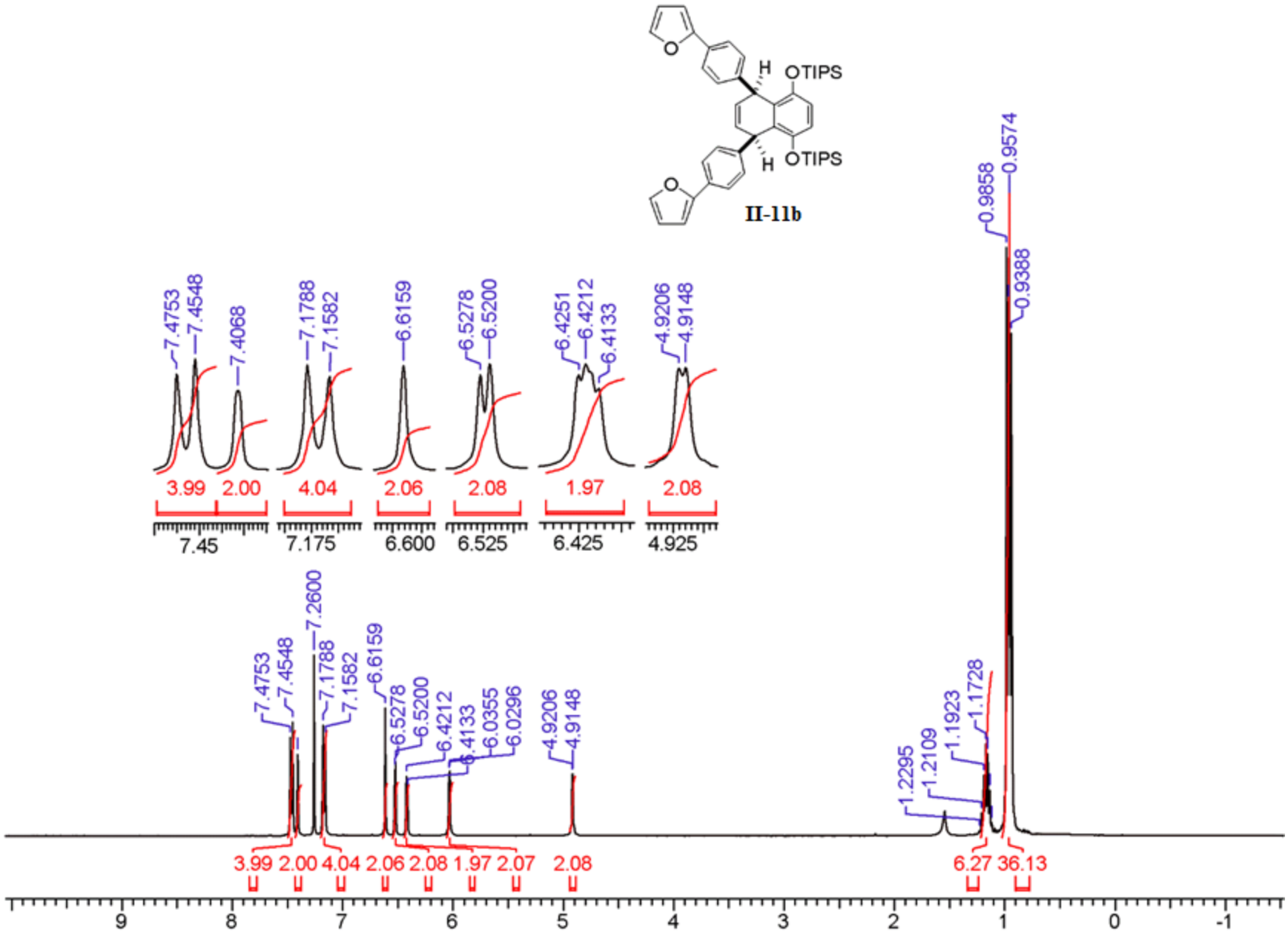
OTIPS
H
OTIPS
H
II-11b
7.4753
7.4548
7.4068
7.1788
7.1582
6.6159
6.5278
6.5200
6.4251
6.4212
6.4133
4.9206
4.9148
3.99
2.00
4.04
2.06
2.08
1.97
2.08
7.45
7.175
6.600
6.525
6.425
4.925
7.2600
6.0355
6.0296
1.2295
1.2109
1.1923
1.1728
0.9858
0.9574
0.9388
3.99
2.00
4.04
2.06
2.08
1.97
2.07
2.08
6.27
36.13
9
8
7
6
5
4
3
2
1
0
-1

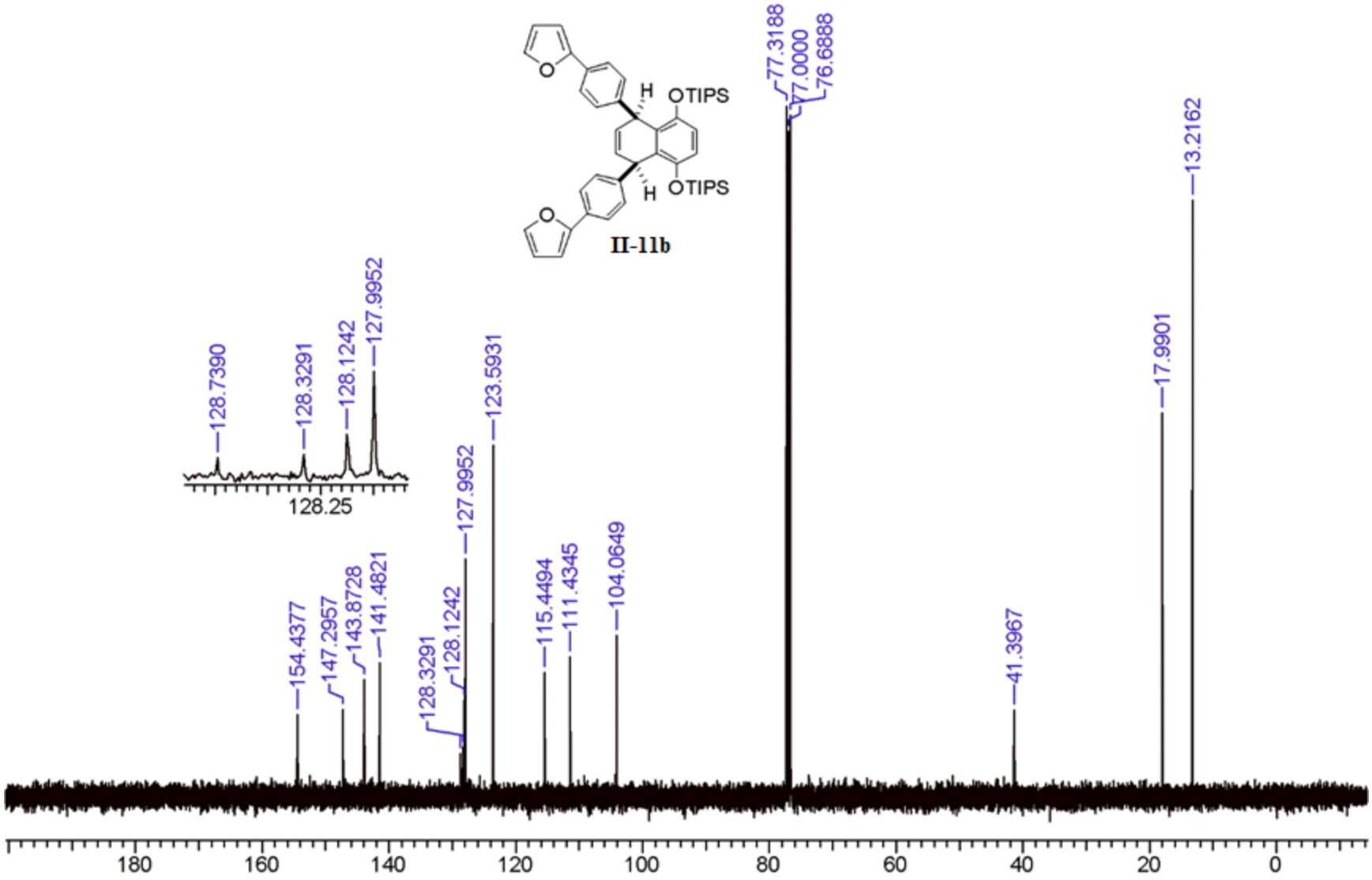
OTIPS
H
OTIPS
H
II-11b
77.3188
77.0000
76.6888
13.2162
17.9901
123.5931
127.9952
128.1242
128.3291
128.7390
154.4377
147.2957
143.8728
141.4821
115.4494
111.4345
104.0649
41.3967
128.25
180
160
140
120
100
80
60
40
20
0

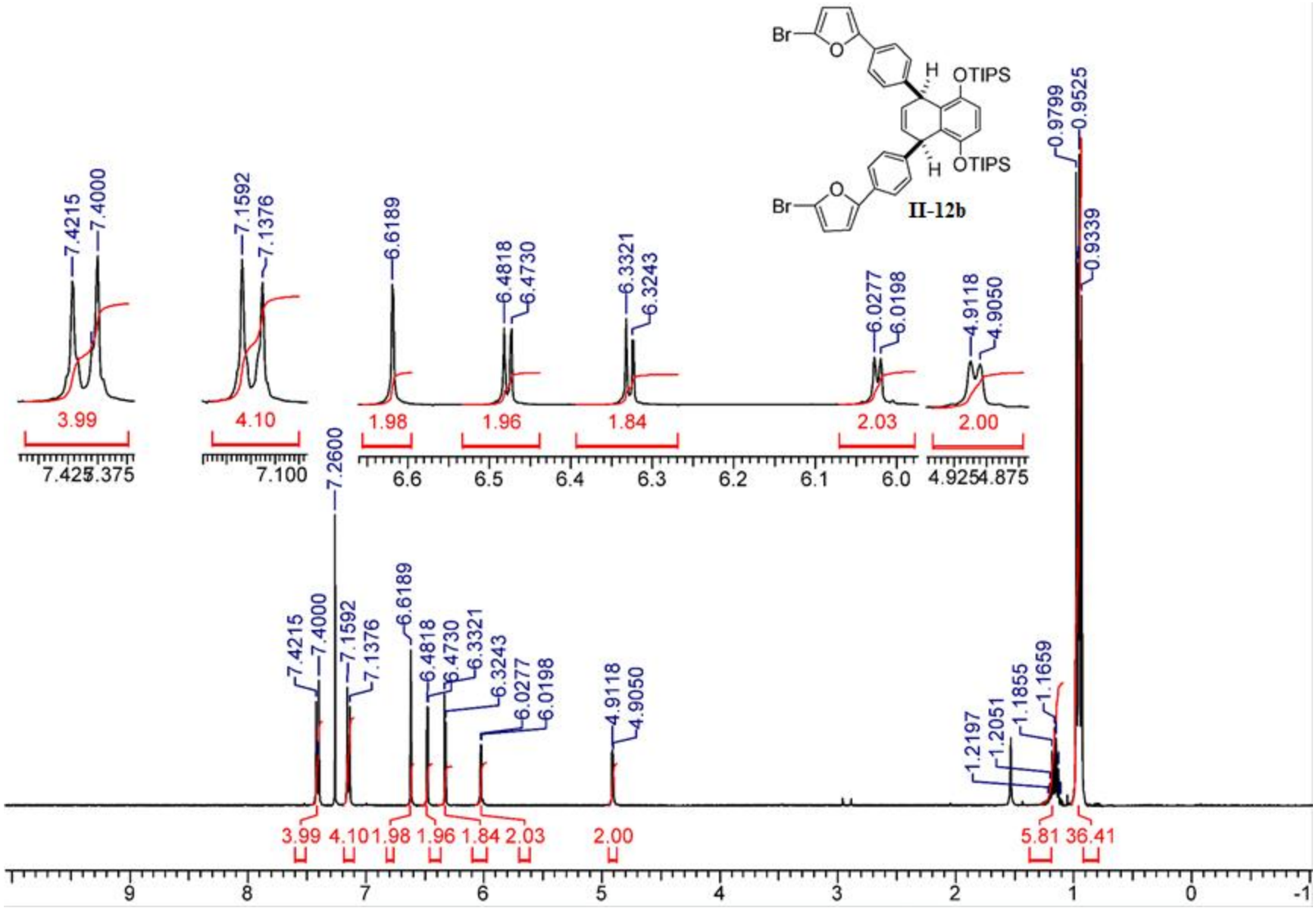
Br
O
H
OTIPS
H
OTIPS
Br
O
II-12b
7.4215
7.4000
7.1592
7.1376
6.6189
6.4818
6.4730
6.3321
6.3243
6.0277
6.0198
4.9118
4.9050
0.9799
0.9525
0.9339
7.2600
1.2197
1.2051
1.1855
1.1659
3.99
4.10
1.98
1.96
1.84
2.03
2.00
5.81
36.41

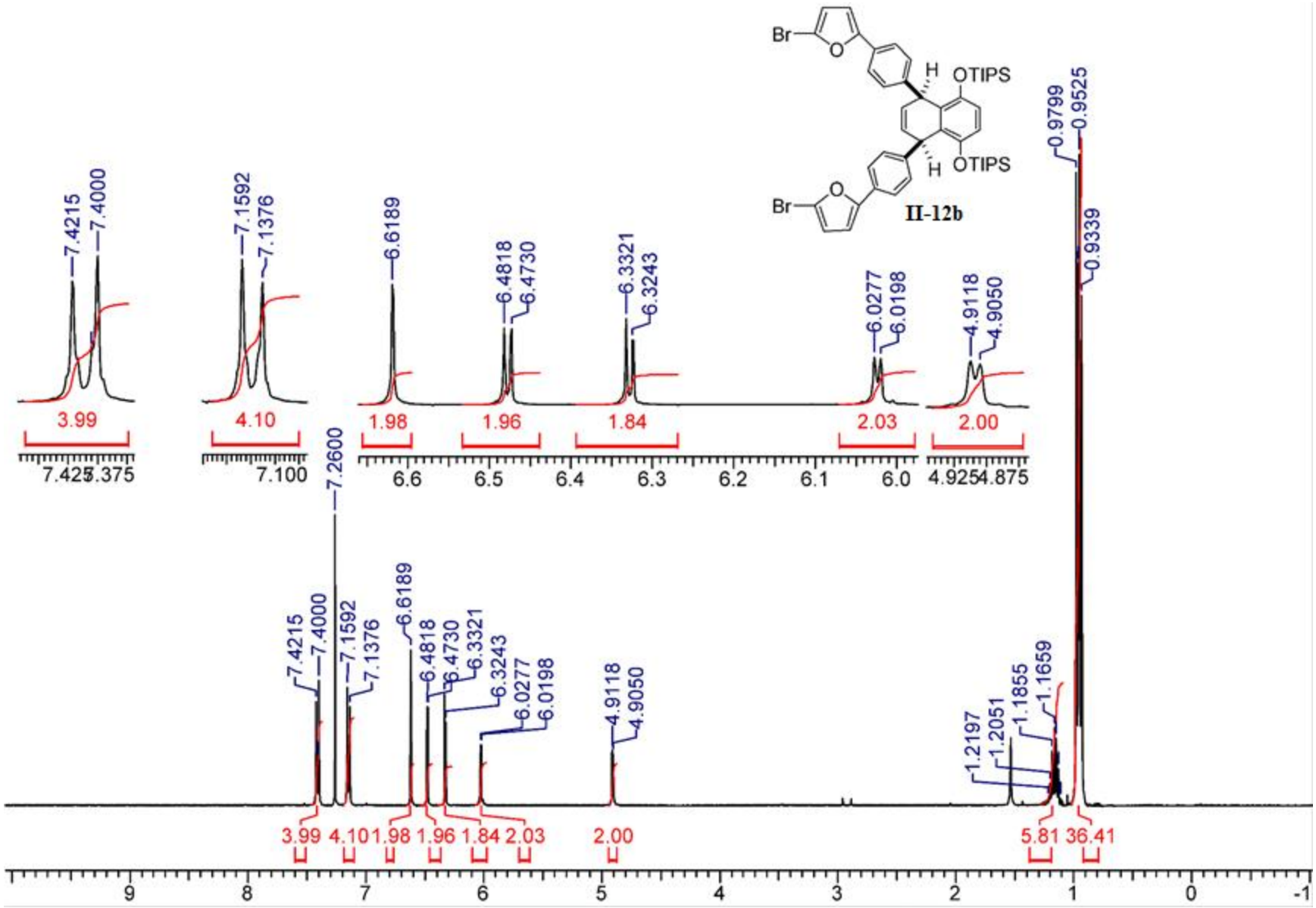
Br
O
H
OTIPS
H
OTIPS
Br
O
II-12b
7.4215
7.4000
7.1592
7.1376
6.6189
6.4818
6.4730
6.3321
6.3243
6.0277
6.0198
4.9118
4.9050
0.9799
0.9525
0.9339
7.2600
1.2197
1.2051
1.1855
1.1659
3.99
4.10
1.98
1.96
1.84
2.03
2.00
5.81
36.41

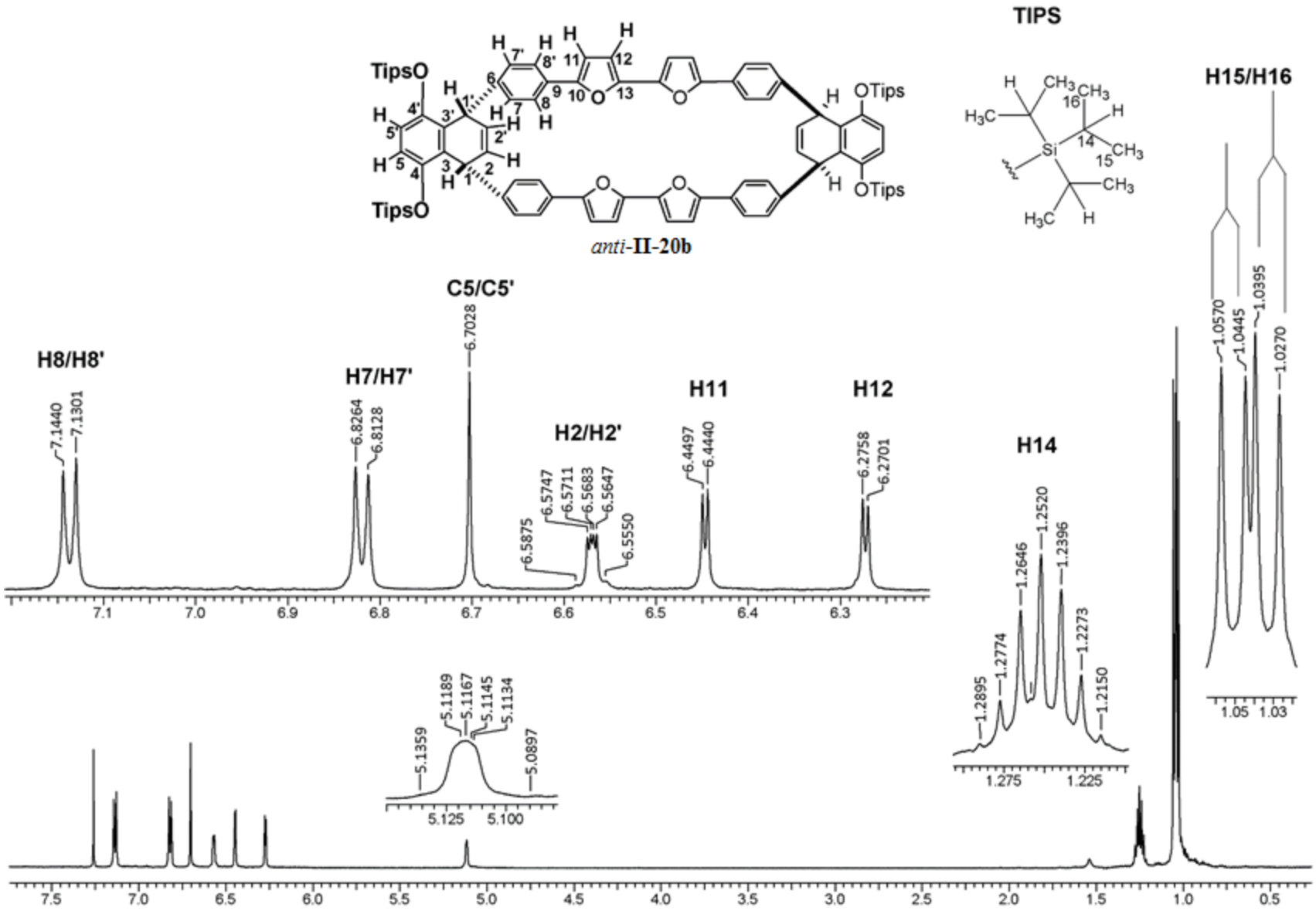
TIPS
H15/H16
C5/C5'
H8/H8'
H7/H7'
H11
H12
H2/H2'
H14
TipsO
OTips
7.1440
7.1301
6.8264
6.8128
6.7028
6.5875
6.5747
6.5711
6.5683
6.5647
6.5550
6.4497
6.4440
6.2758
6.2701
5.1359
5.1189
5.1167
5.1145
5.1134
5.0897
1.2895
1.2774
1.2646
1.2520
1.2396
1.2273
1.2150
1.0570
1.0445
1.0395
1.0270

anti-**II-20b**

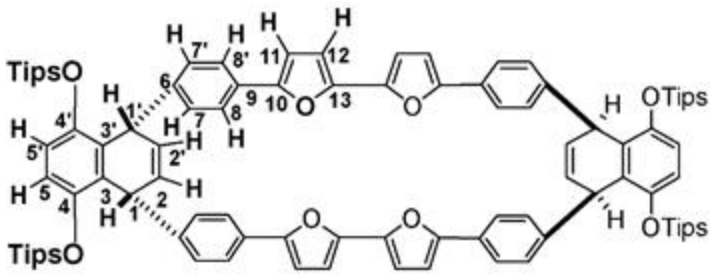
TipsO
TipsO
OTips
OTips

anti-**II-20b**

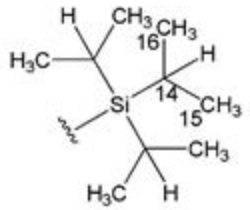

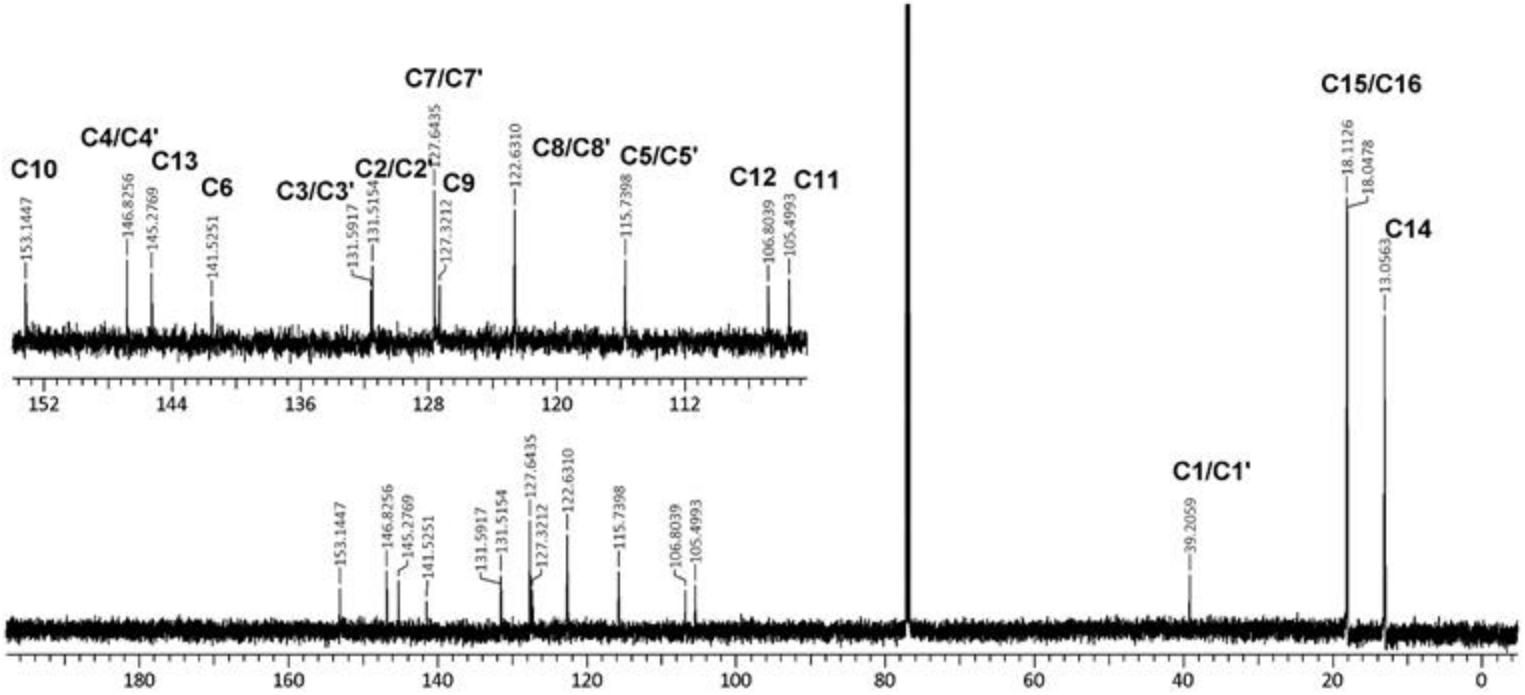
C10
C4/C4'
C13
C6
C3/C3'
C2/C2'
C7/C7'
C9
C8/C8'
C5/C5'
C12
C11
C15/C16
C14
C1/C1'
153.1447
146.8256
145.2769
141.5251
131.5917
131.5154
127.6435
127.3212
122.6310
115.7398
106.8039
105.4993
39.2059
18.1126
18.0478
13.0563

gHSQCAD

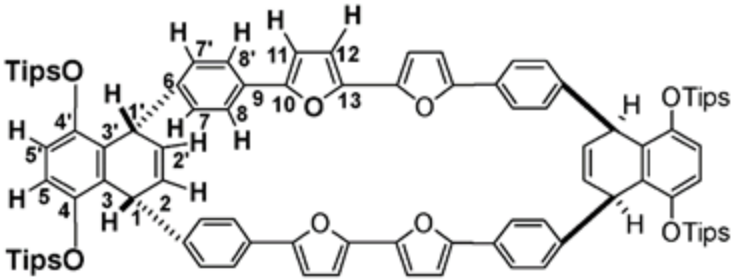

anti-**II-20b**

Tips

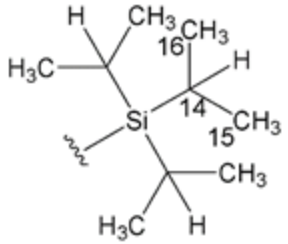

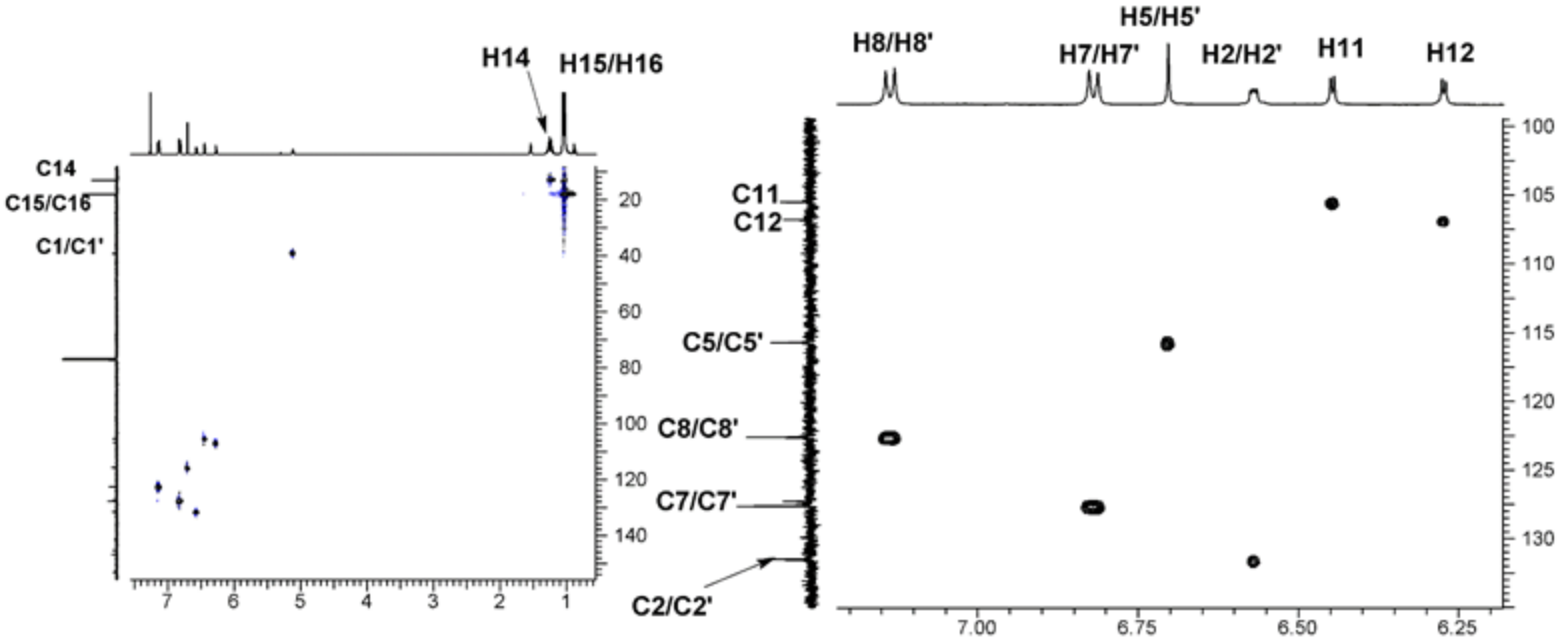

gHMBCAD

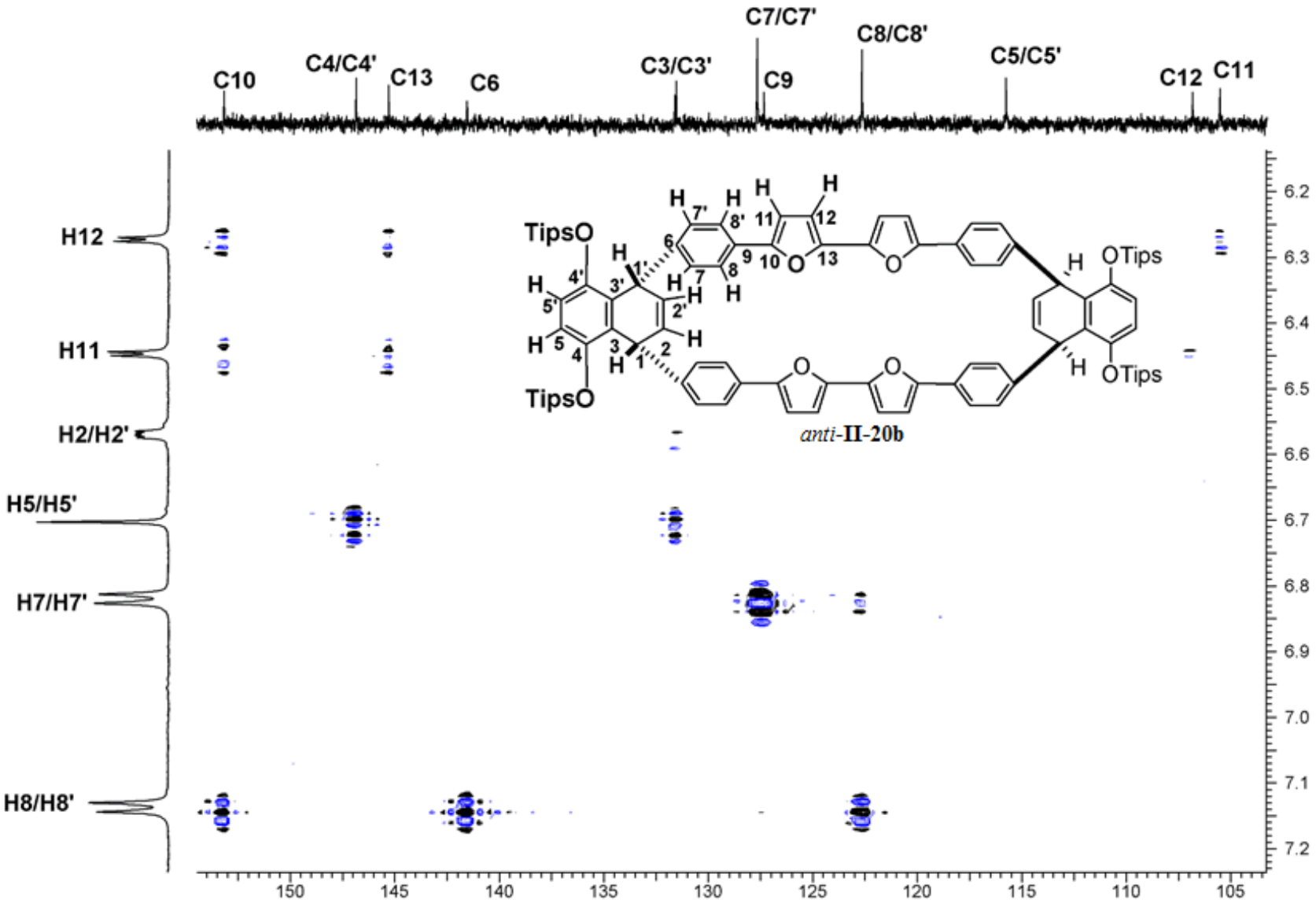
C10
C4/C4'
C13
C6
C3/C3'
C7/C7'
C9
C8/C8'
C5/C5'
C12
C11
H12
H11
H2/H2'
H5/H5'
H7/H7'
H8/H8'
TipsO
OTips
anti-II-20b
150
145
140
135
130
125
120
115
110
105
6.2
6.3
6.4
6.5
6.6
6.7
6.8
6.9
7.0
7.1
7.2

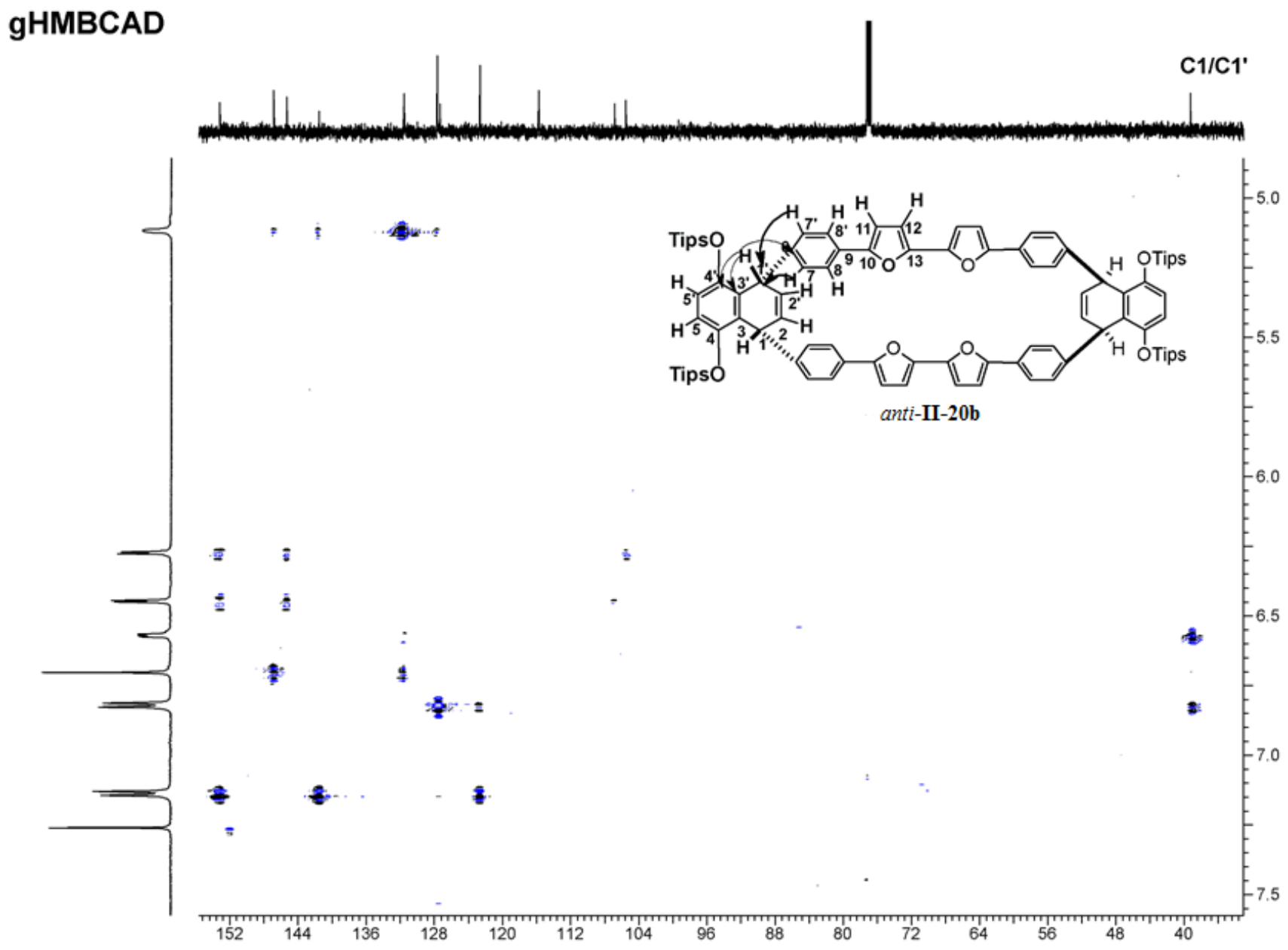
gHMBCAD
C1/C1'
TipsO
OTips
TipsO
OTips
anti-II-20b
5.0
5.5
6.0
6.5
7.0
7.5
152
144
136
128
120
112
104
96
88
80
72
64
56
48
40

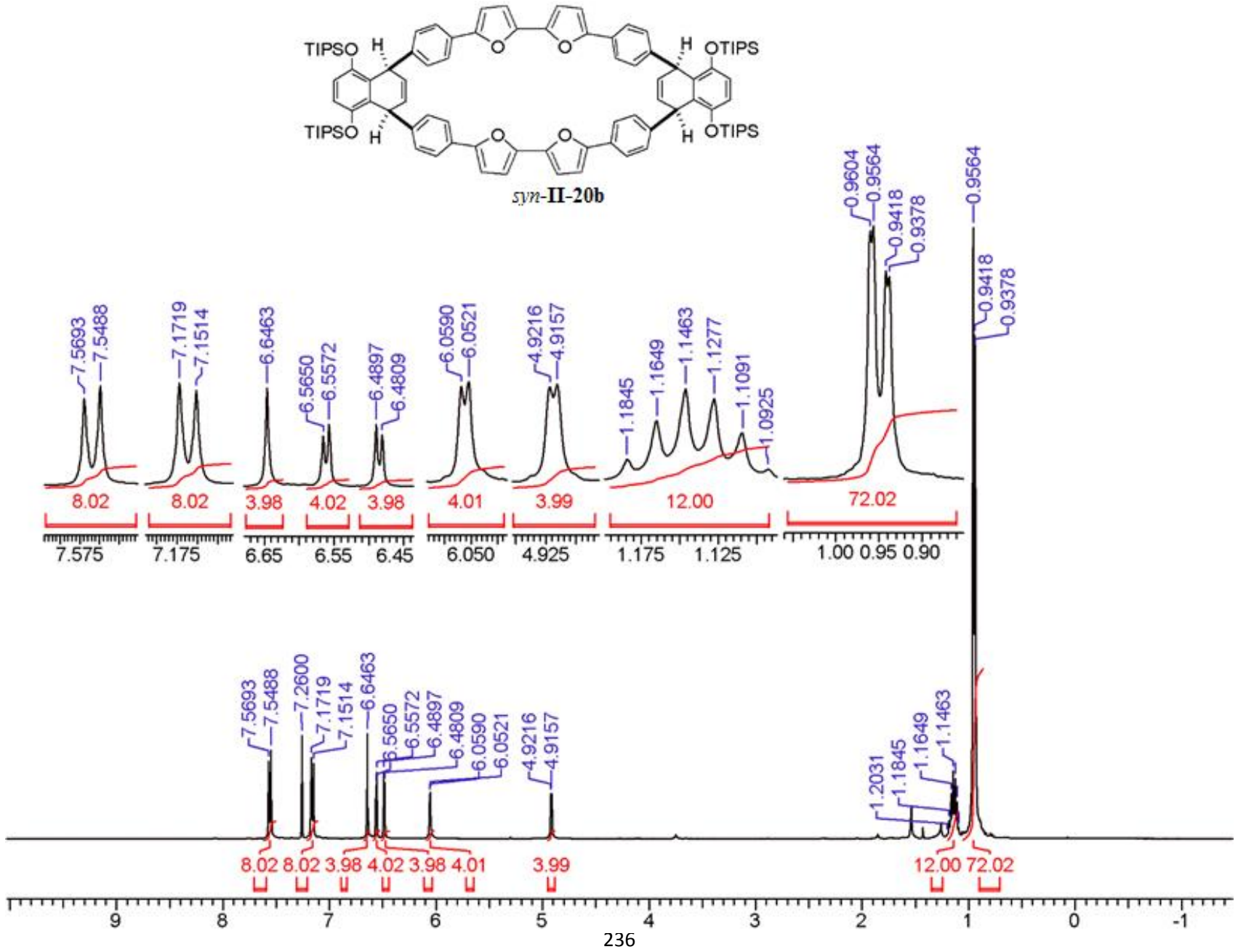
TIPSO
H
OTIPS
TIPSO
H
H
OTIPS
H
O
O
O
O
O
O
syn-II-20b
7.5693
7.5488
7.1719
7.1514
6.6463
6.5650
6.5572
6.4897
6.4809
6.0590
6.0521
4.9216
4.9157
1.1845
1.1649
1.1463
1.1277
1.1091
1.0925
0.9604
0.9564
0.9418
0.9378
8.02
8.02
3.98
4.02
3.98
4.01
3.99
12.00
72.02
7.575
7.175
6.65
6.55
6.45
6.050
4.925
1.175
1.125
1.00 0.95 0.90
7.2600
1.2031
9
8
7
6
5
4
3
2
1
0
-1

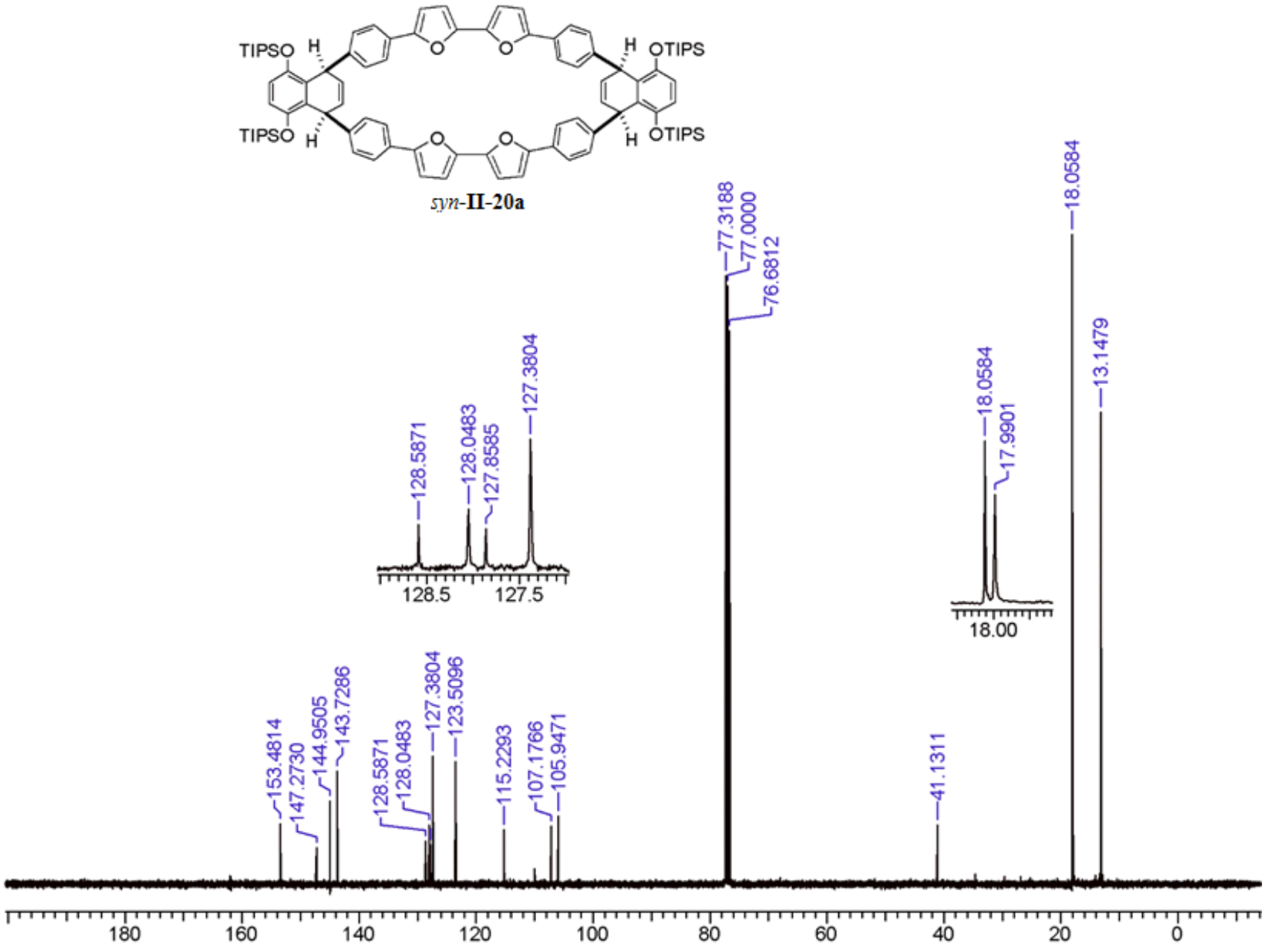
TIPSO
H
OTIPS
TIPSO
H
H
OTIPS
H
O
O
O

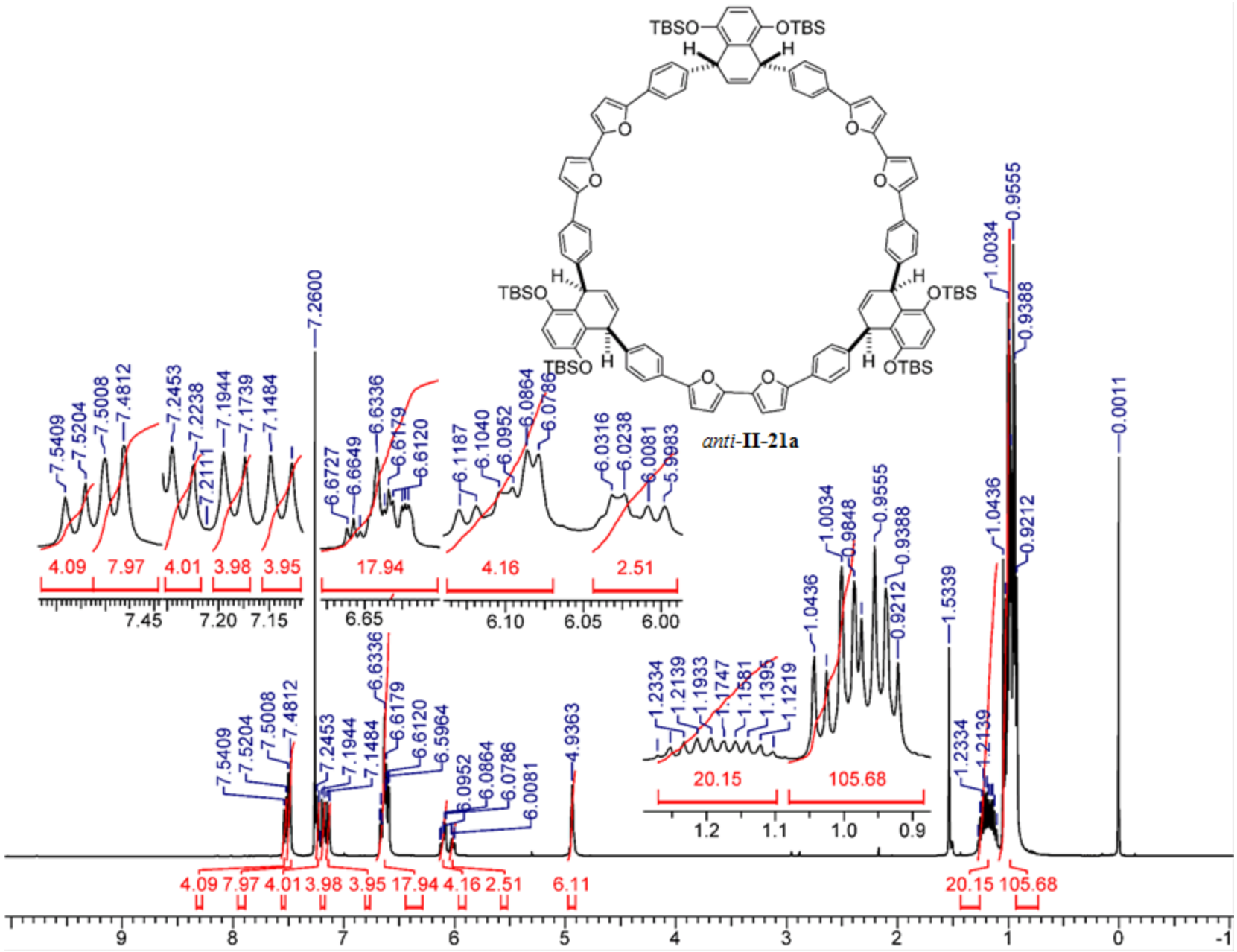
TBSO
OTBS
H
O
anti-II-21a
7.2600
4.09
7.97
4.01
3.98
3.95
17.94
4.16
2.51
6.11
20.15
105.68
0.0011

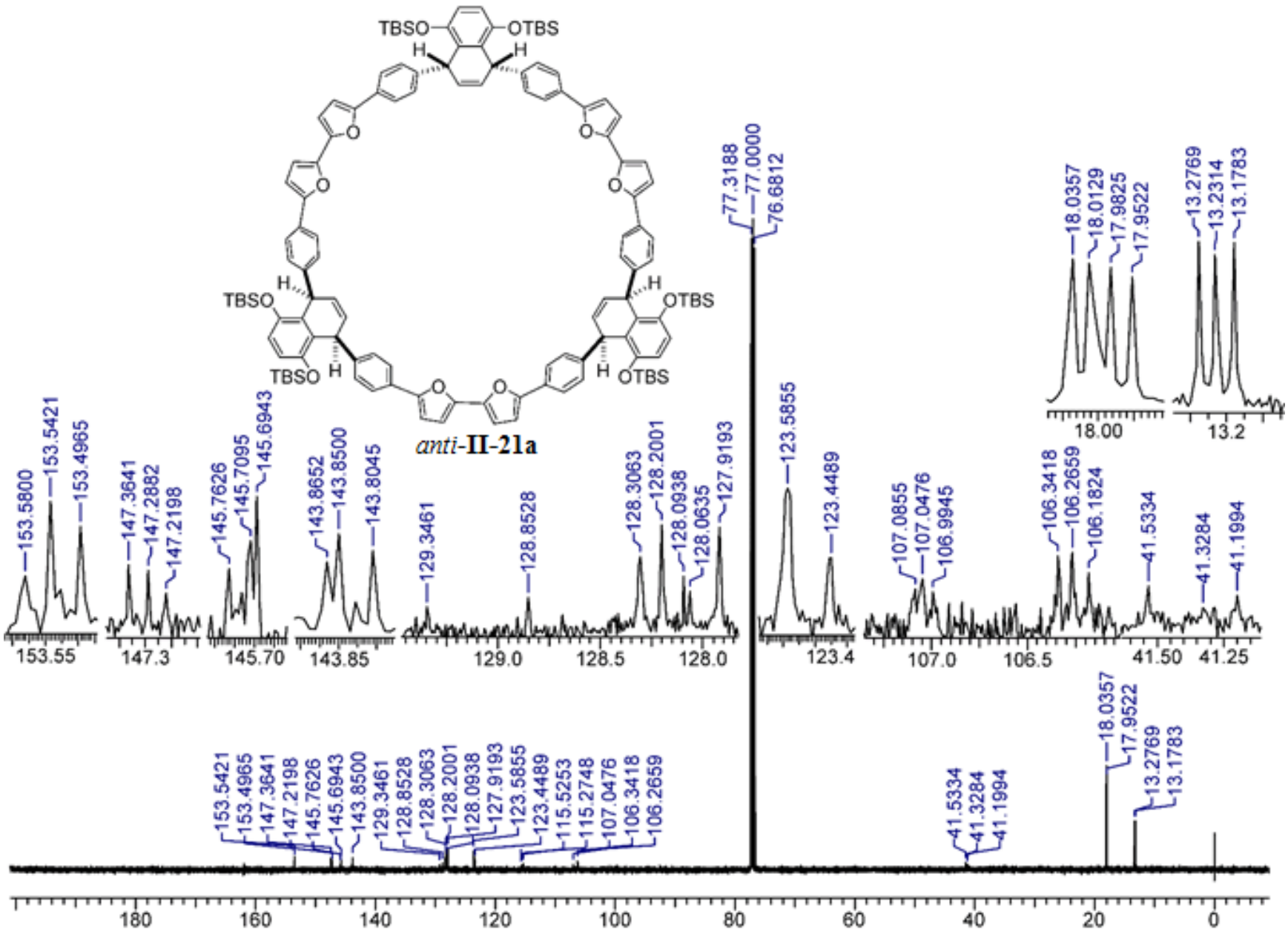
TBSO
OTBS
H
O
anti-II-21a
153.5800
153.5421
153.4965
147.3641
147.2882
147.2198
145.7626
145.7095
145.6943
143.8652
143.8500
143.8045
129.3461
128.8528
128.3063
128.2001
128.0938
128.0635
127.9193
123.5855
123.4489
107.0855
107.0476
106.9945
106.3418
106.2659
106.1824
41.5334
41.3284
41.1994
77.3188
77.0000
76.6812
18.0357
18.0129
17.9825
17.9522
13.2769
13.2314
13.1783
153.55
147.3
145.70
143.85
129.0
128.5
128.0
123.4
107.0
106.5
41.50
41.25
18.00
13.2
180
160
140
120
100
80
60
40
20
0

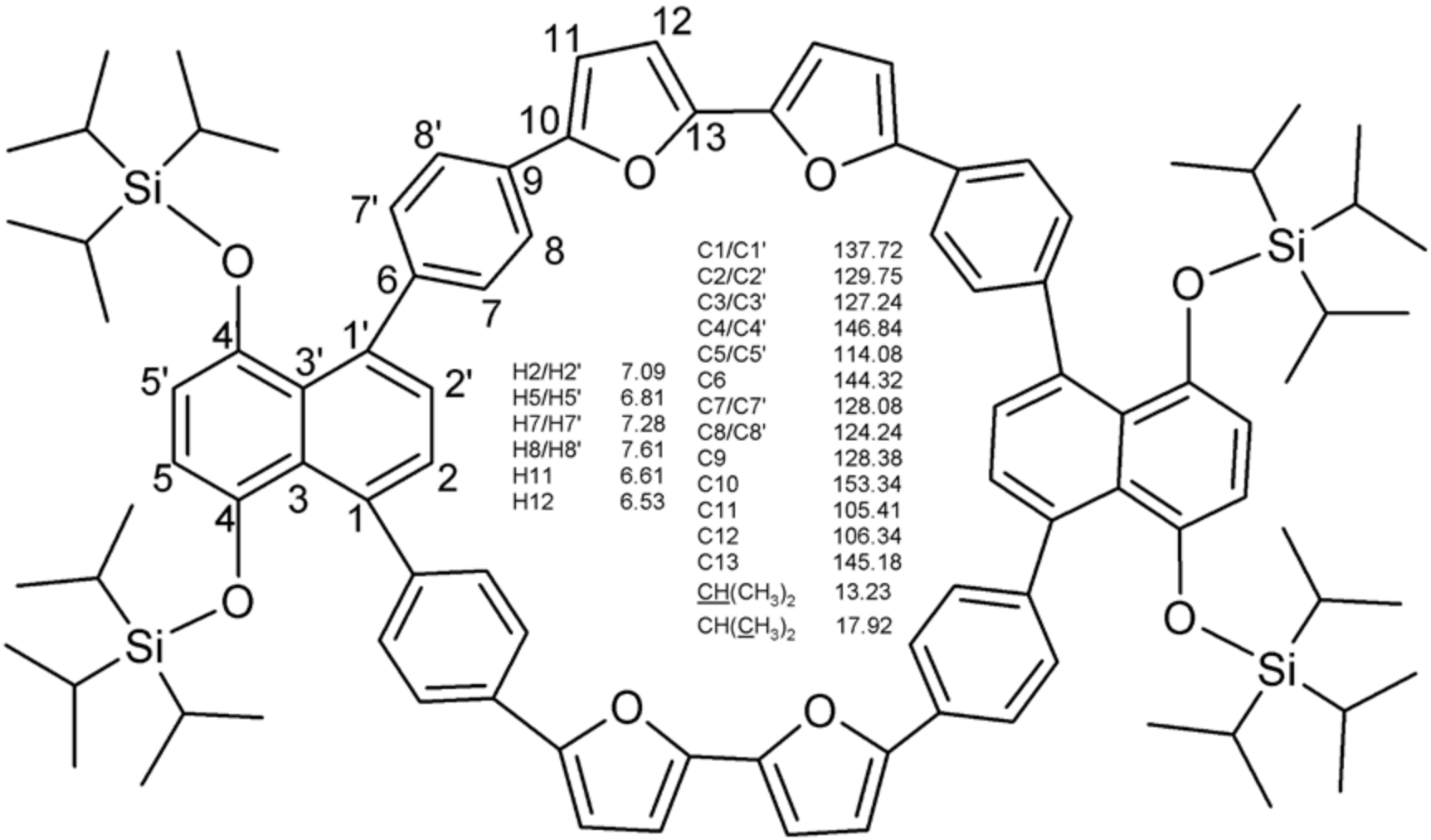
H2/H2' 7.09
H5/H5' 6.81
H7/H7' 7.28
H8/H8' 7.61
H11 6.61
H12 6.53
C1/C1' 137.72
C2/C2' 129.75
C3/C3' 127.24
C4/C4' 146.84
C5/C5' 114.08
C6 144.32
C7/C7' 128.08
C8/C8' 124.24
C9 128.38
C10 153.34
C11 105.41
C12 106.34
C13 145.18
CH(CH3)2 13.23
CH(CH3)2 17.92

II-2b

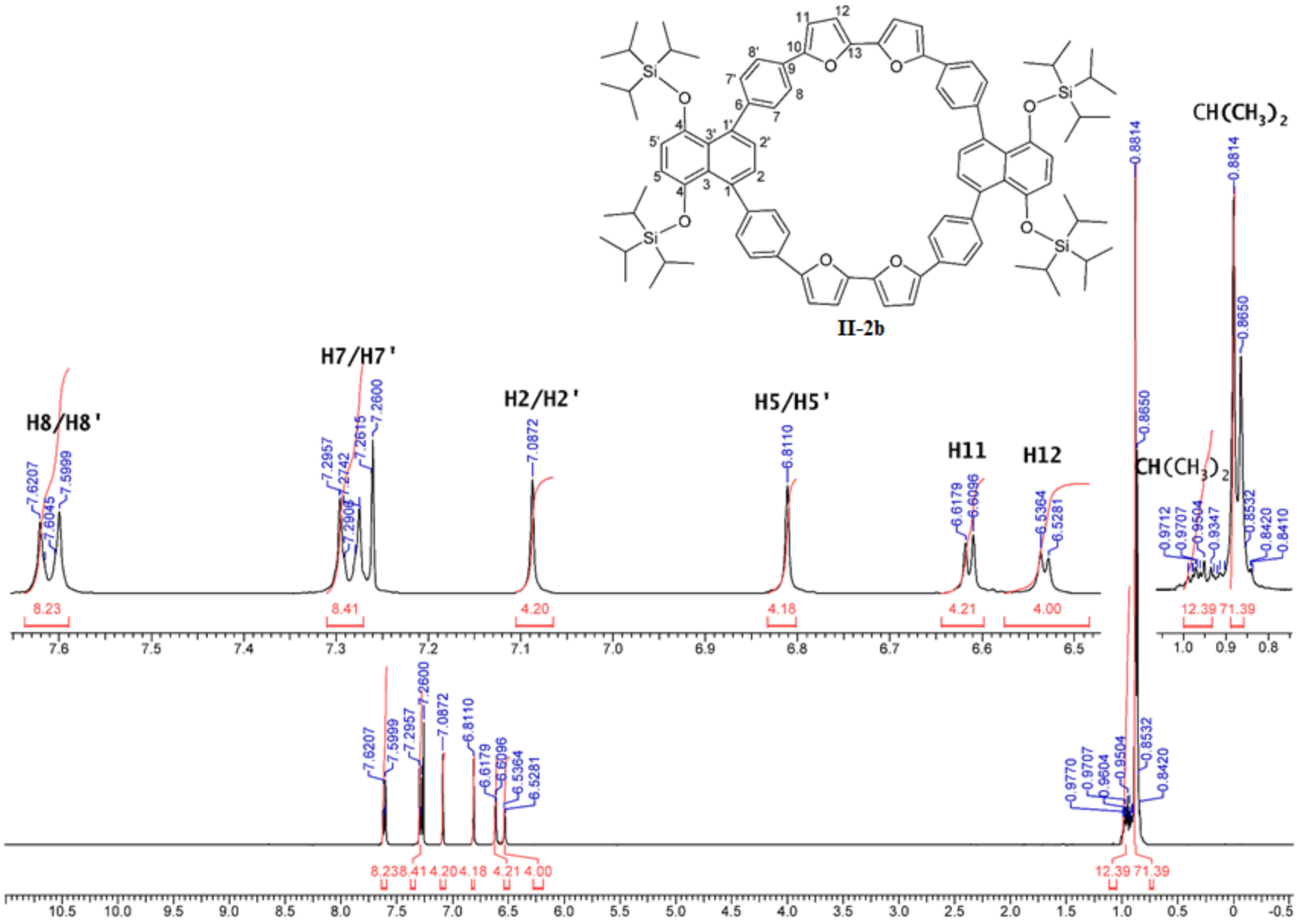
II-2b
H8/H8'
H7/H7'
H2/H2'
H5/H5'
H11
H12
CH(CH3)2
CH(CH3)2
7.6207
7.6045
7.5999
7.2957
7.2742
7.2615
7.2600
7.0872
6.8110
6.6179
6.6096
6.5364
6.5281
0.8814
0.8650
0.8532
0.8420
0.8410
0.9712
0.9707
0.9504
0.9347
0.9770
0.9604
8.23
8.41
4.20
4.18
4.21
4.00
12.39
71.39

Expanded portion of the **NOESY** spectrum

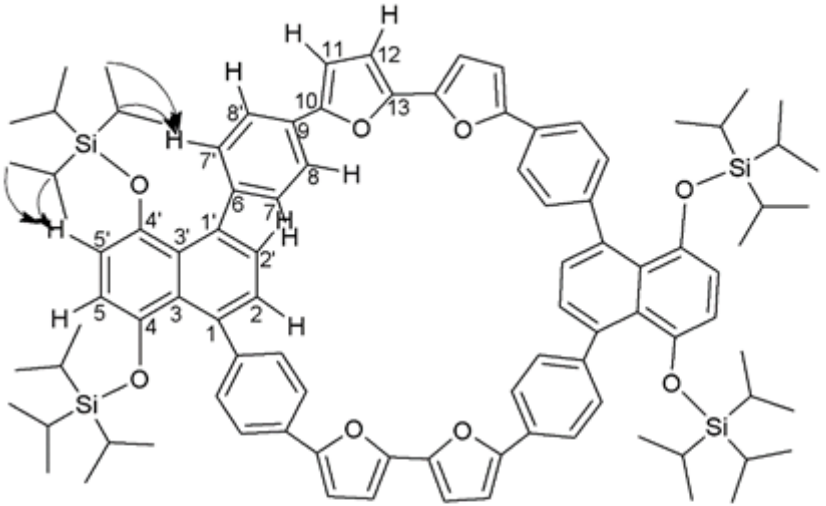

II-2b

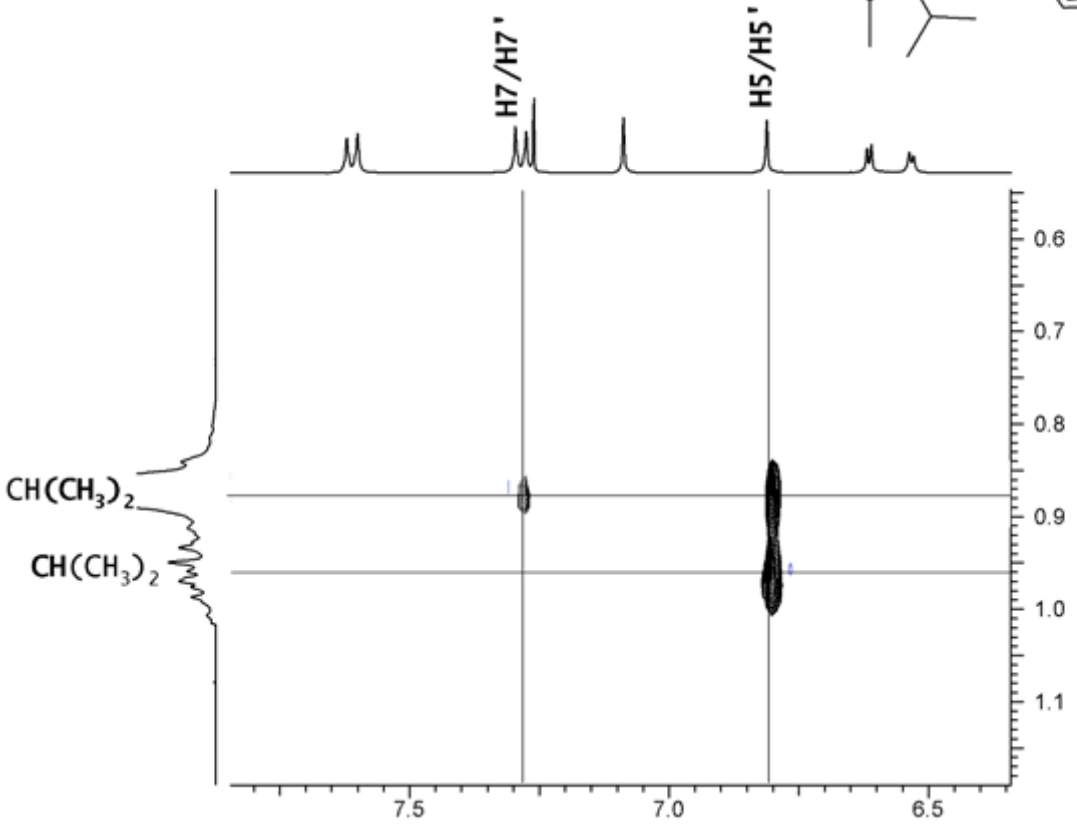

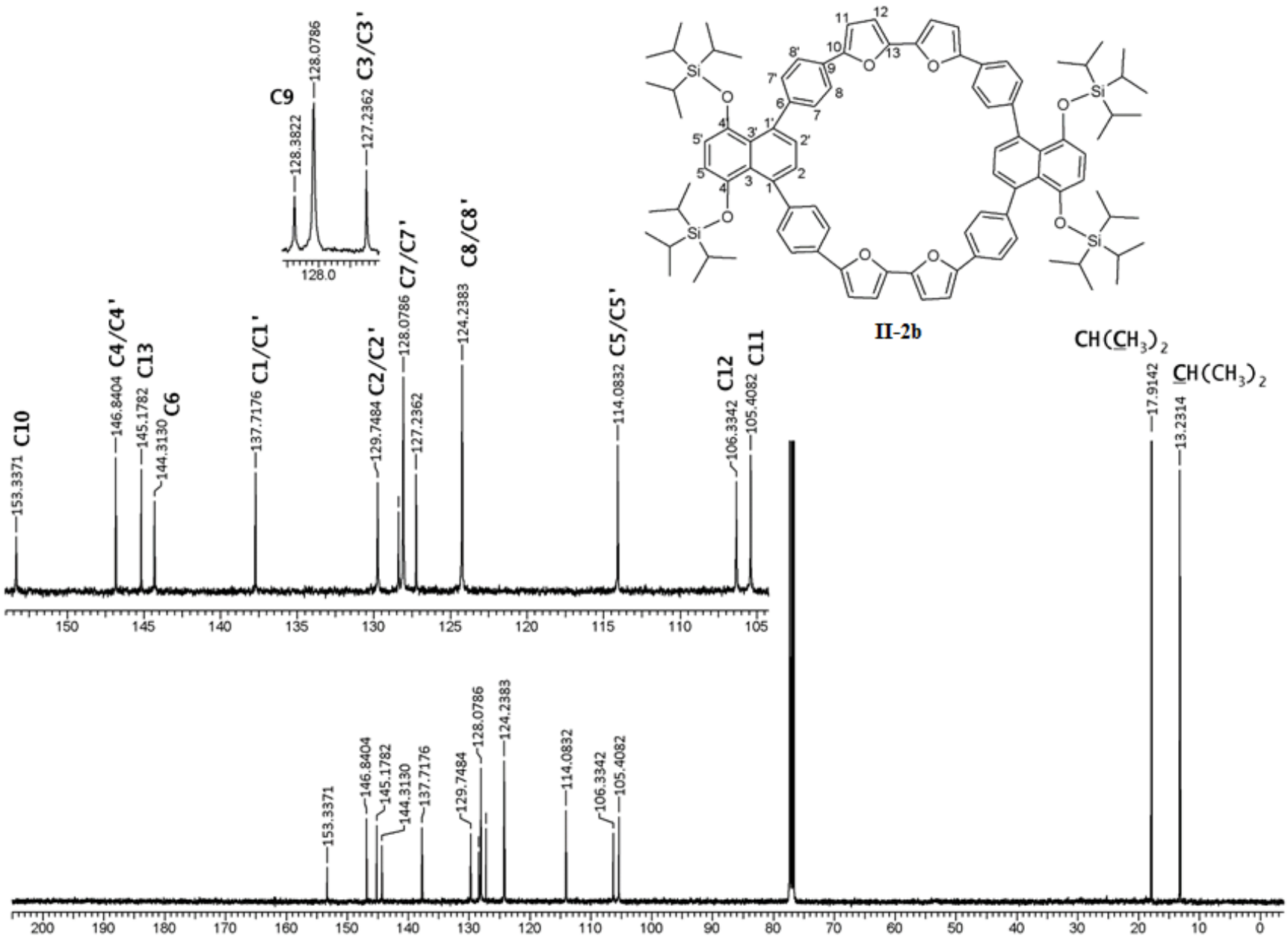
C9
128.3822
128.0786
127.2362
C3/C3'
128.0
153.3371 C10
146.8404 C4/C4'
145.1782 C13
144.3130 C6
137.7176 C1/C1'
129.7484 C2/C2'
128.0786 C7/C7'
127.2362
124.2383 C8/C8'
114.0832 C5/C5'
106.3342 C12
105.4082 C11
II-2b
CH(CH3)2
17.9142
CH(CH3)2
13.2314
153.3371
146.8404
145.1782
144.3130
137.7176
129.7484
128.0786
124.2383
114.0832
106.3342
105.4082

gHSQCAD

One-bond correlations

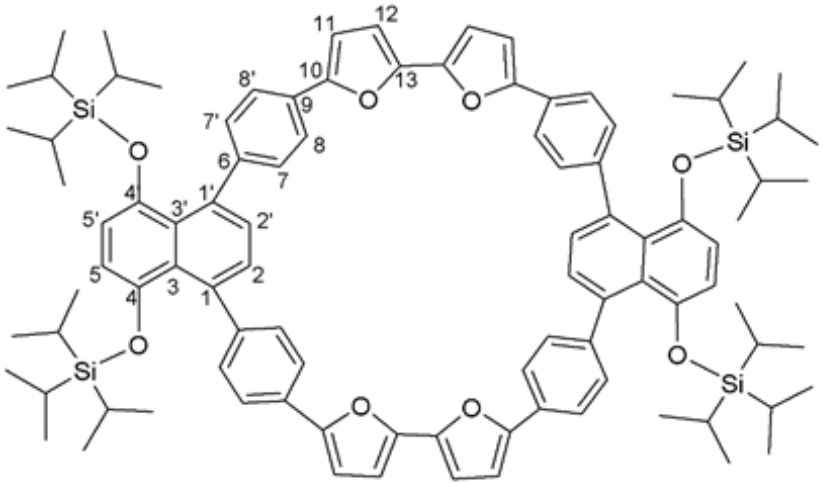

II-2b

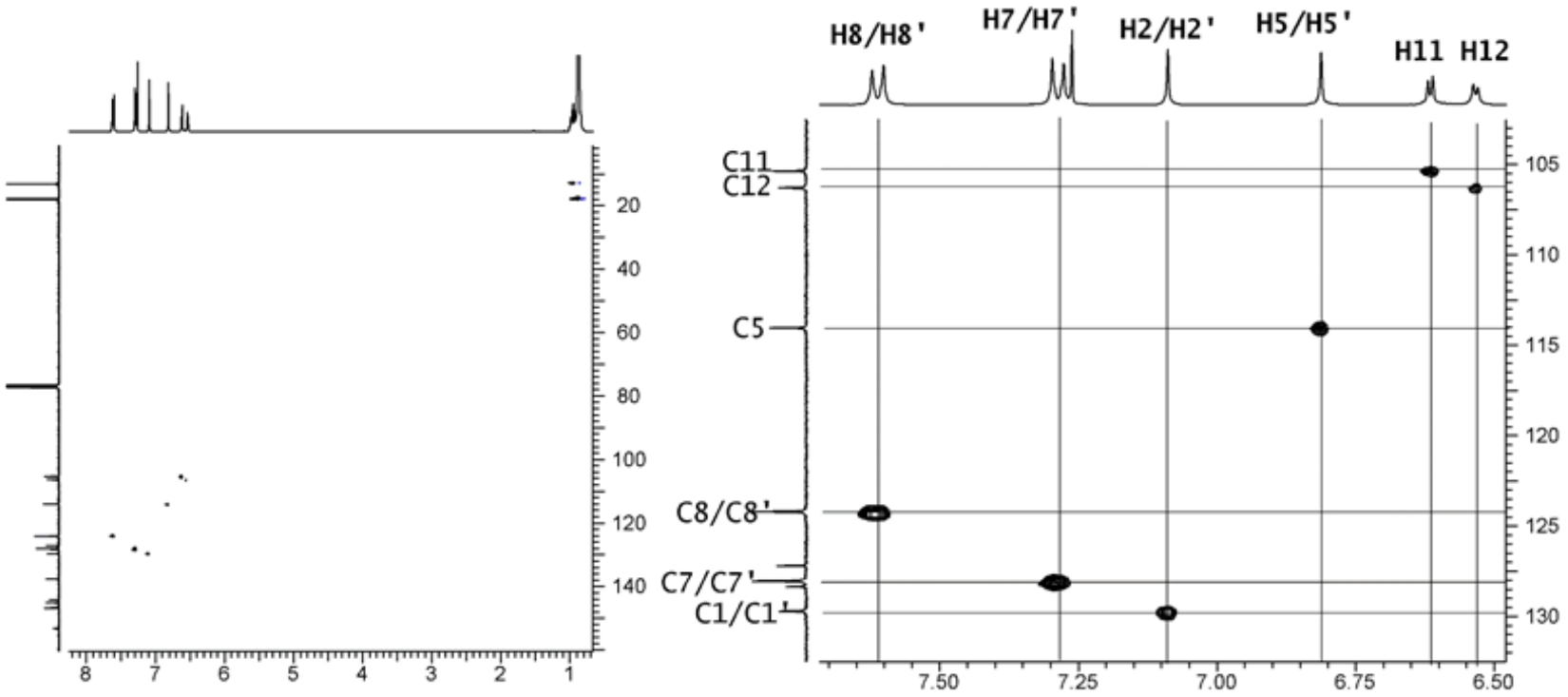

Long-range **HMBC** correlations

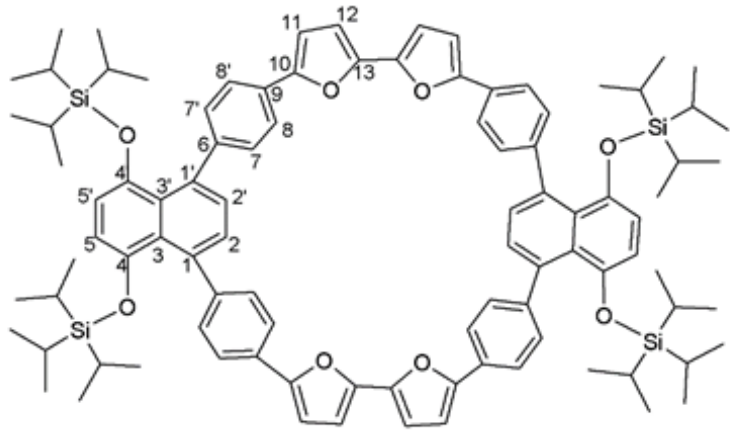

II-2b

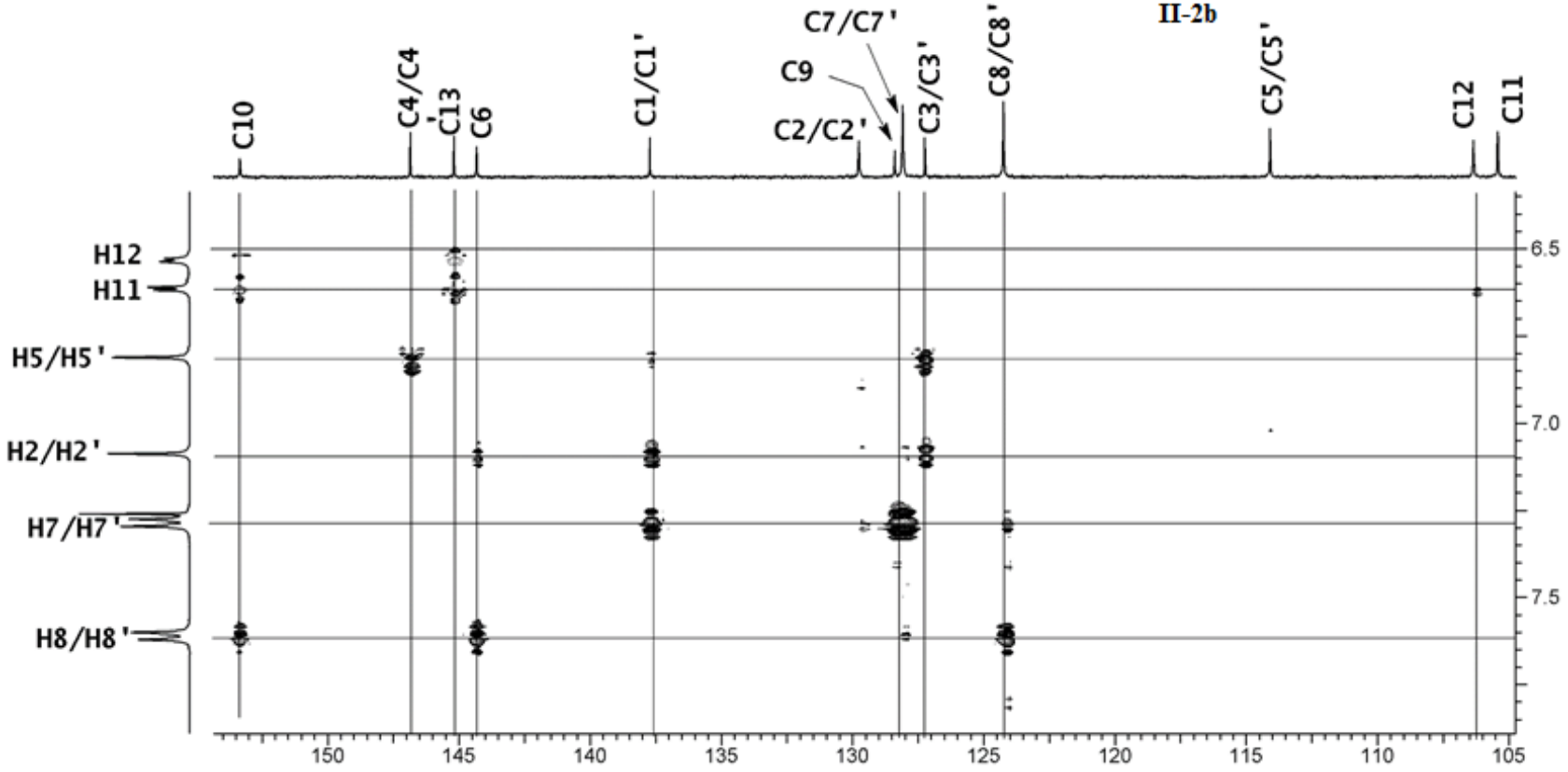

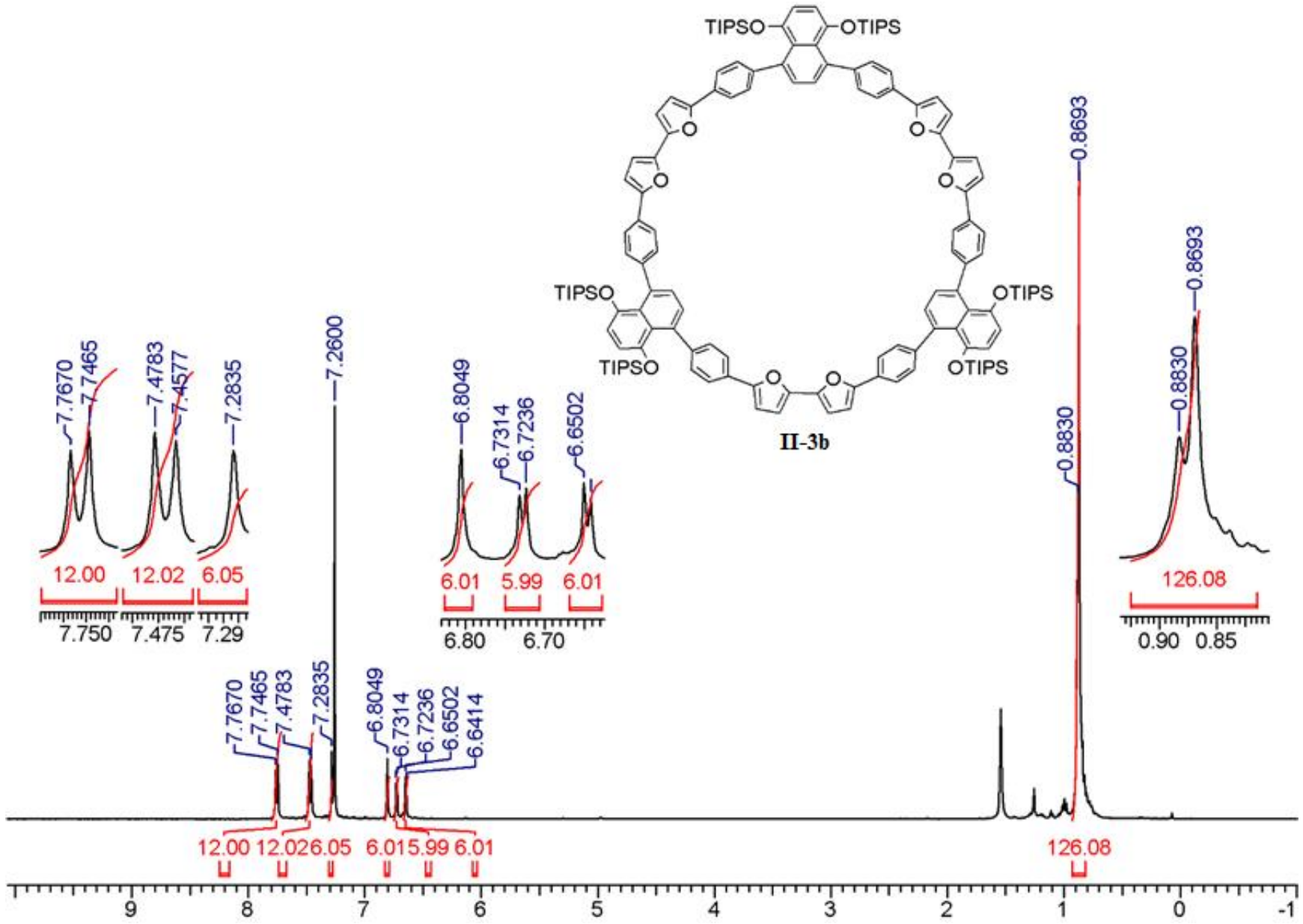
TIPSO
OTIPS
TIPSO
OTIPS
TIPSO
OTIPS
II-3b
7.7670
7.7465
7.4783
7.4577
7.2835
7.2600
6.8049
6.7314
6.7236
6.6502
6.6414
0.8693
0.8830
12.00
12.02
6.05
6.01
5.99
6.01
126.08
7.750
7.475
7.29
6.80
6.70
0.90
0.85

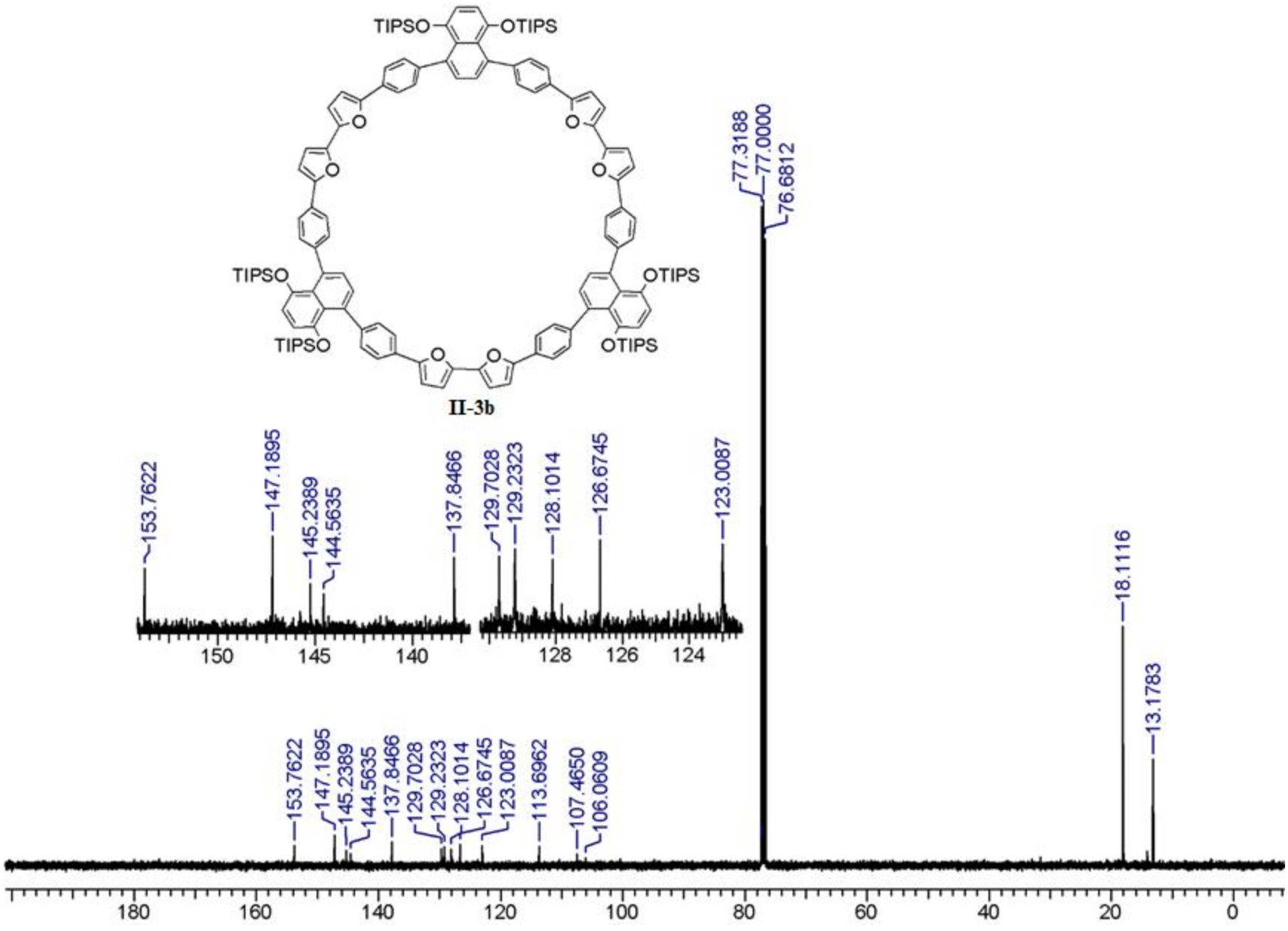
TIPSO
OTIPS
TIPSO
OTIPS
TIPSO
OTIPS
II-3b
153.7622
147.1895
145.2389
144.5635
137.8466
129.7028
129.2323
128.1014
126.6745
123.0087
77.3188
77.0000
76.6812
18.1116
13.1783
153.7622
147.1895
145.2389
144.5635
137.8466
129.7028
129.2323
128.1014
126.6745
123.0087
113.6962
107.4650
106.0609
150
145
140
128
126
124
180
160
140
120
100
80
60
40
20
0

Electrochemical Characterization Methods

Electrochemical experiments were recorded using the Pine WaveNow USB potentiostat and BAS electrodes in anhydrous dichloromethane under an argon atmosphere with 100 mM tetrabutylammonium hexafluorophosphate as supporting electrolyte. All samples were analyzed between 0.50-0.90 mM depending on their solubility in dichloromethane. Cyclic voltammograms were recorded with a glassy carbon working electrode, platinum wire counter electrode, and a silver coil wire quasi-reference electrode. Differential pulse voltammetry measurements were recorded under the same conditions with the exception that a gold working electrode was used. All of the recorded data are presented versus the ferrocene/ferrocenium (Fc/Fc^{+}) redox couple.

2,5-diphenylfuran: CV at 0.1 V/s (**A**), CV scan-dependence (0.80 mM) (**B**), i_{pa} vs. (scan rate)$^{1/2}$ dependence for the first redox couple (**C**), and DPV scan (**D**).

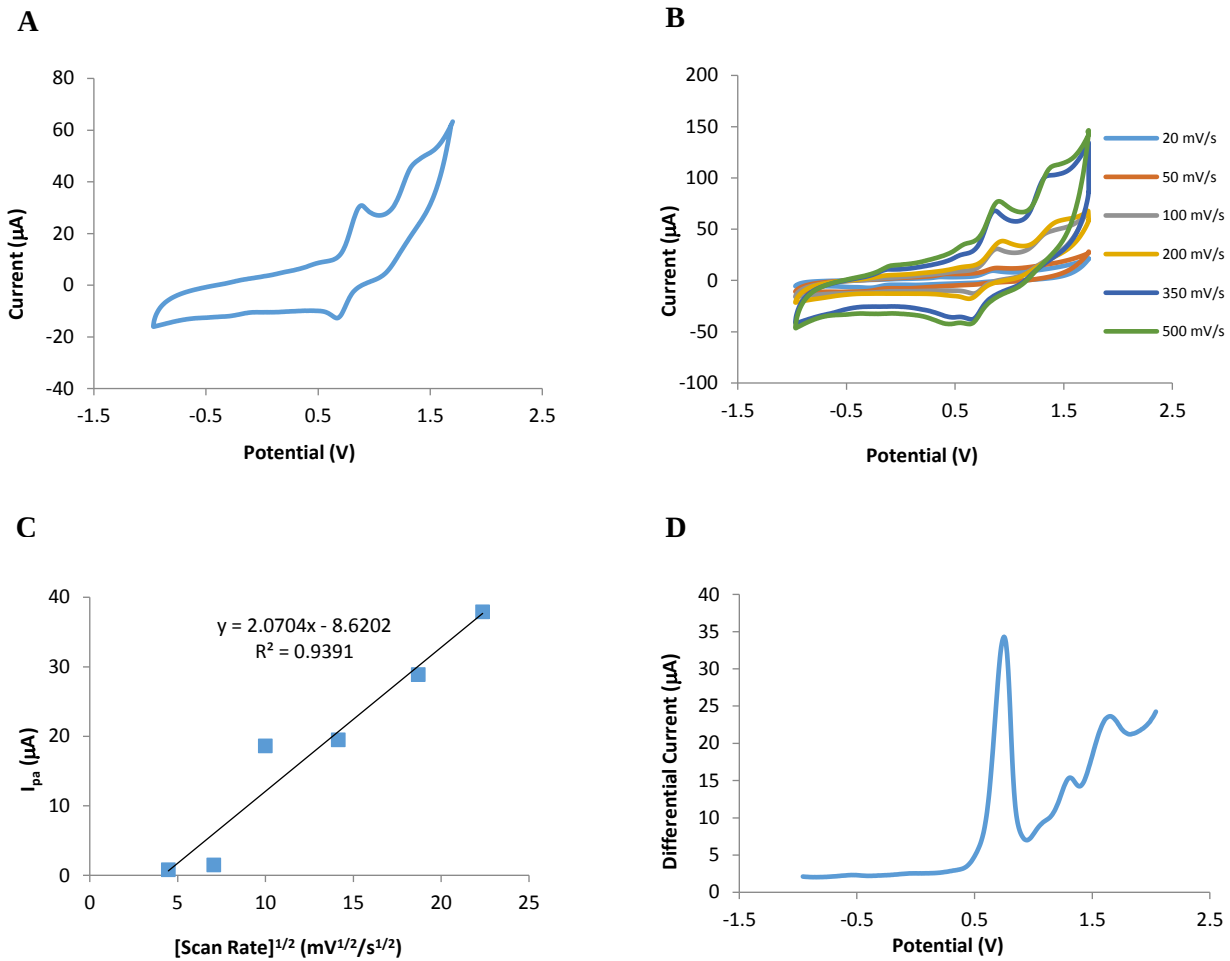

***syn*-II-20b:** CV at 0.1 V/s (**A**), CV scan-dependence (0.50 mM) (**B**), i_{pa} vs. (scan rate)$^{1/2}$ dependence for the first redox couple (**C**), and DPV scan (**D**).

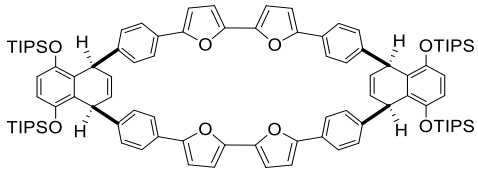

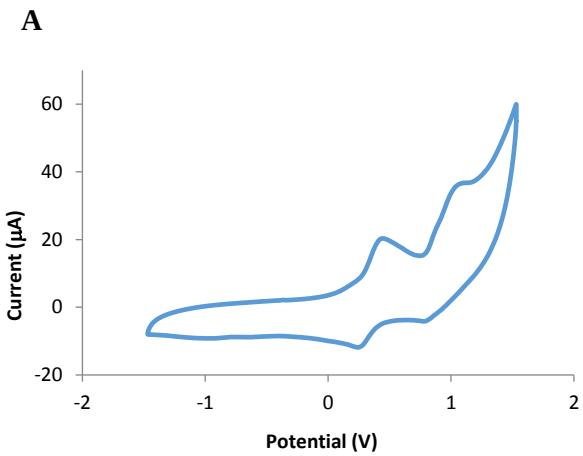

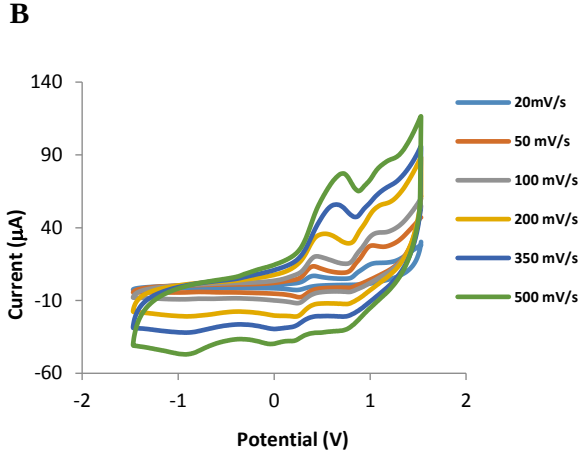

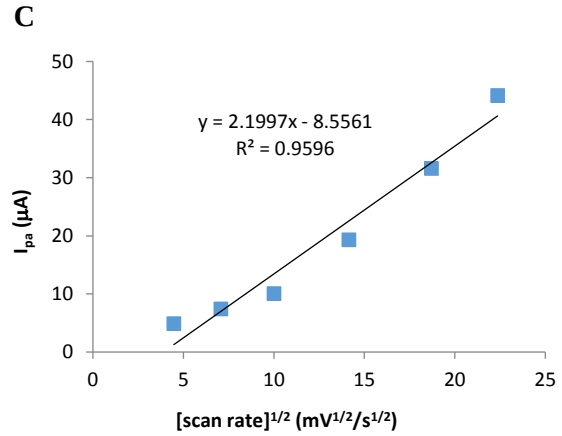

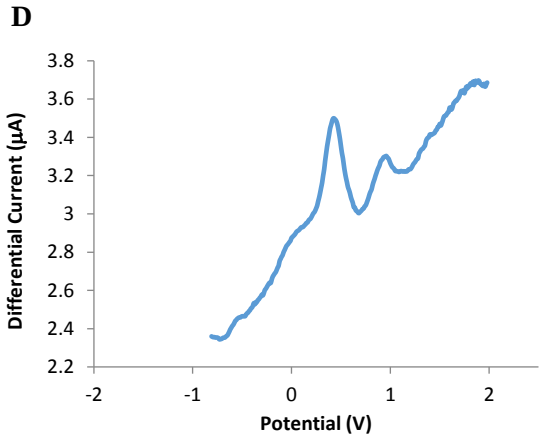

***anti*-II-20b:** CV at 0.1 V/s (**A**), CV scan-dependence (0.50 mM) (**B**), i_{pa} vs. (scan rate)$^{1/2}$ dependence for the first redox couple (**C**), and DPV scan (**D**).

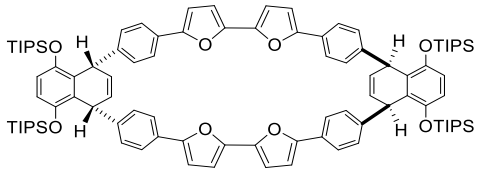

A

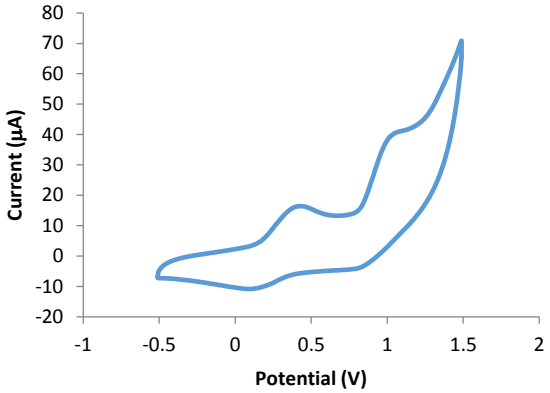

B

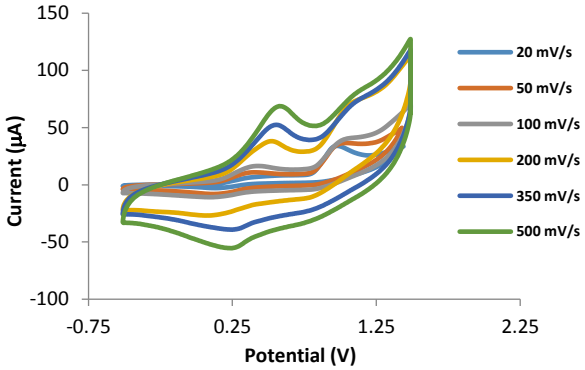

C

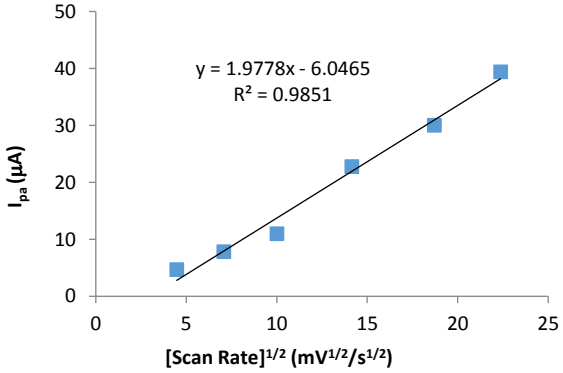

D

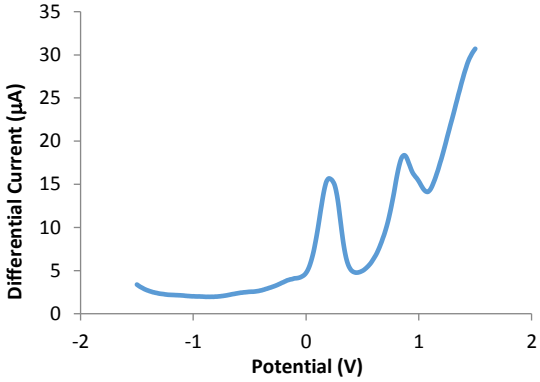

***anti*-II-21b:** CV at 0.1 V/s (**A**), CV scan-dependence (0.63 mM) (**B**), i_{pa} vs. $(\text{scan rate})^{1/2}$ dependence for the first redox couple (**C**), and DPV scan (**D**).

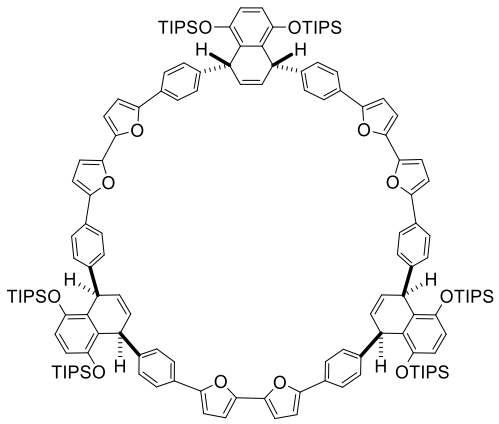
TIPSO
OTIPS
H
H
O
O
O
O
H
TIPSO
OTIPS
TIPSO
H
H
OTIPS
O
O

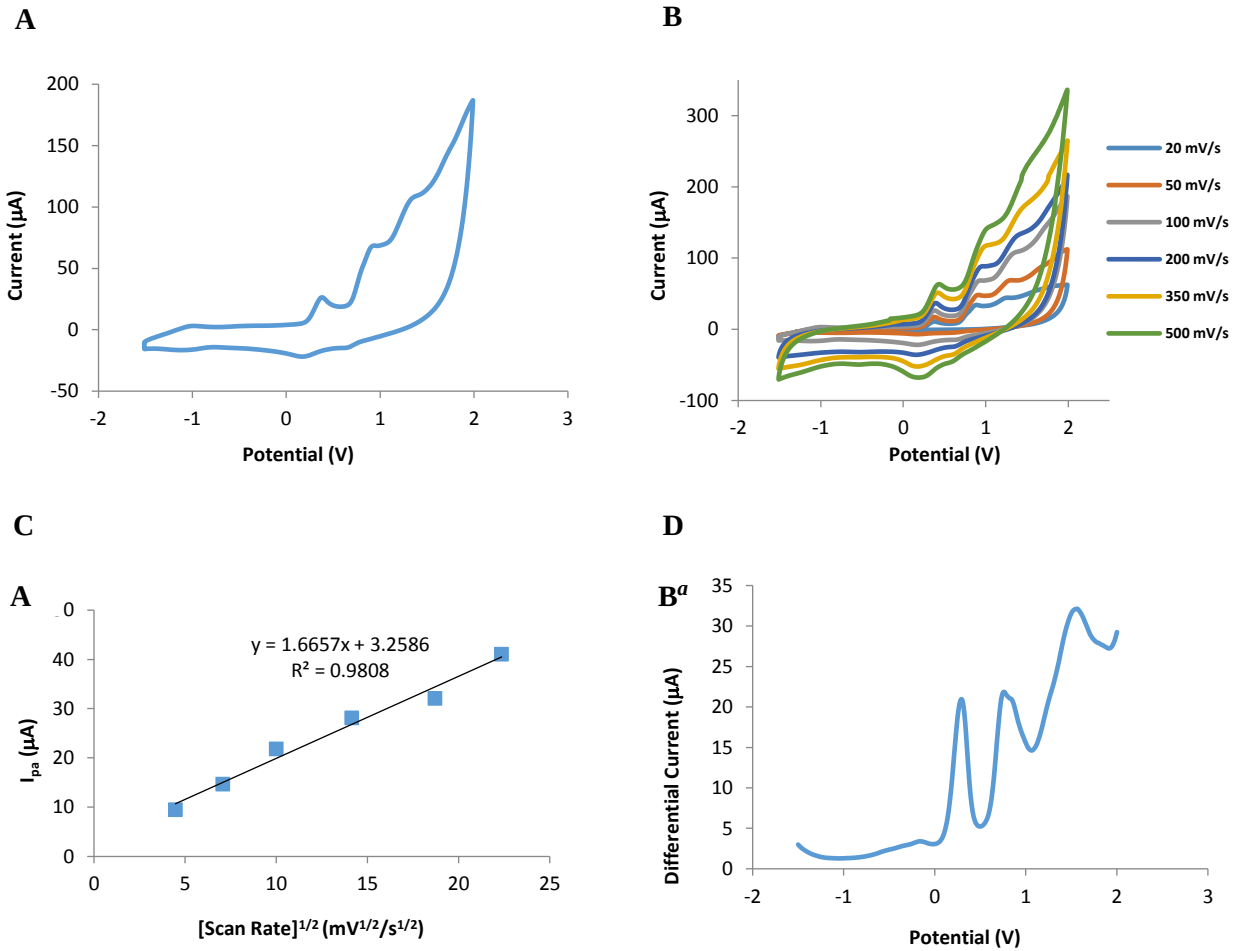

Compound II-19: CV at 0.1 V/s (**A**), CV scan-dependence (0.50 mM) (**B**), i_{pa} vs. (scan rate)$^{1/2}$ dependence for the first redox couple (**C**), and DPV scan (**D**).

C

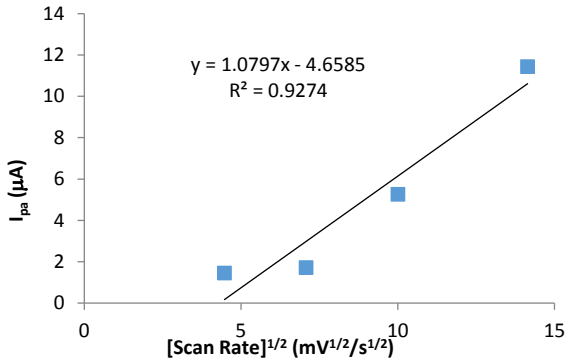

D

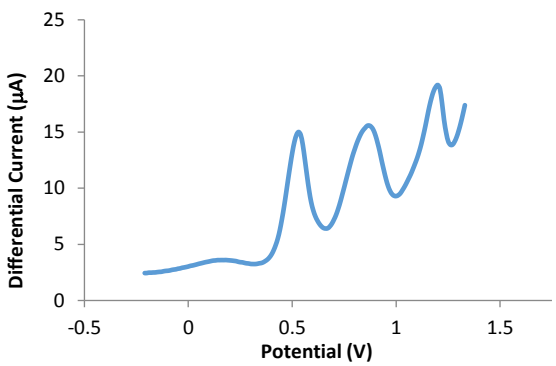

[a] Redox behavior was convoluted in cyclic voltammograms collected above 200 mV/s.

Description of the X-ray Structural Analysis of III-7 ($C_{32}H_{26}O_4$)

An irregular colorless crystal of **III-7** ($C_{32}H_{26}O_4$) was covered in a polybutene oil (Sigma-Aldrich) and placed on the end of a MiTeGen loop. The sample was cooled to 100 K with an Oxford Cryostream 700 system and optically aligned on a Bruker AXS D8 Venture fixed-chi X-ray diffractometer equipped with a Triumph monochromator, a Mo Kα radiation source (λ = 0.71073 Å), and a PHOTON 100 CMOS detector. Two sets of 12 frames each were collected using the omega scan method with a 10 s exposure time. Integration of these frames followed by reflection indexing and least-squares refinement produced a crystal orientation matrix for the monoclinic crystal lattice that was used for the structural analysis.

Data collection consisted of the measurement of a total of 1104 frames in three runs using omega scans with the detector held at 5.00 cm from the crystal. Frame scan parameters are summarized in Table III-S1 below:

Table III-S1. Data collection details for **III-7** ($C_{32}H_{26}O_4$).

Run	2θ	ω	φ	χ	Scan Width (º)	Frames	Exposure Time (sec)
1	16.35	-165.65	-180.00	54.74	0.50	368	10.00
2	16.35	-165.65	-60.00	54.74	0.50	368	10.00
3	16.35	-165.65	60.00	54.74	0.50	368	10.00

The APEX2 software program (version 2014.1-1)[S1] was used for diffractometer control, preliminary frame scans, indexing, orientation matrix calculations, least-squares refinement of cell parameters, and the data collection. The frames were integrated with the Bruker SAINT software package using a narrow-frame algorithm. The integration of the data using a monoclinic unit cell yielded a total of 33075 reflections to a maximum θ angle of 27.50° (0.77 Å resolution), of which 5470 were independent (average redundancy 6.047, completeness = 99.9%, R_{int} = 2.85%, R_{sig} = 1.79%) and 4678 (85.52%) were greater than $2\sigma(F^2)$. The final cell constants of $\underline{a}$ = 25.5180(10) Å, $\underline{b}$ = 8.0088(3) Å, $\underline{c}$ = 23.3552(9) Å, β = 93.9449(12)°, volume = 4761.8(3) $Å^3$, are based upon the refinement of the XYZ-centroids of 9990 reflections above 20 σ(I) with 6.317° < 2θ < 60.11°. Data were corrected for absorption effects using the multi-scan method (SADABS). The ratio of minimum to maximum apparent transmission was 0.912. The calculated minimum and maximum transmission coefficients are 0.954 and 0.964.

The structure of **7** ($C_{32}H_{26}O_4$) was solved by direct methods and difference Fourier analysis using the programs provided by SHELXL-2014.[S2] Idealized positions for the hydrogen atoms were included as fixed contributions using a riding model with isotropic temperature factors set at 1.2 (methine and aromatic hydrogens) or 1.5 (methyl hydrogens) times that of the adjacent carbon atom. The positions of the methyl hydrogen atoms were optimized by a rigid rotating group refinement with idealized angles. Full-matrix least-squares refinement, based upon the minimization of $\Sigma w_i |F_o^2 - F_c^2|^2$, with weighting $w_i^{-1} = [\sigma^2(F_o^2) + (0.0607\ P)^2 + 3.9782\ P]$, where $P = (\text{Max}\ (F_o^2, 0) + 2\ F_c^2)/3$.[S2] The final anisotropic full-matrix least-squares refinement on F^2 with 327 variables converged at R1 = 4.25%, for the 4678 observed data with $I > 2\sigma(I)$ and wR2 = 11.87% for all data. The goodness-of-fit was 1.028.[S3]

A correction for secondary extinction was not applied. The largest peak in the final difference electron density synthesis was 0.318 $e^-/Å^3$ and the largest hole was -0.216 $e^-/Å^3$ with an RMS deviation of 0.046 $e^-/Å^3$. The linear absorption coefficient, atomic scattering factors, and anomalous dispersion corrections were calculated from values found in the International Tables of X-ray Crystallography.[S4]

Table III-S2. Crystal data for **III-7** ($C_{32}H_{26}O_4$).

Identification code	Compd **III-7** - kw36cms	
Chemical formula	$C_{32}H_{26}O_4$	
Formula weight	474.53 g/mol	
Temperature	100(2) K	
Wavelength	0.71073 Å	
Crystal size	0.429 x 0.493 x 0.551 mm	
Crystal system	monoclinic	
Space group	C 2/c (No. 15)	
Unit cell dimensions	a = 25.5180(10) Å	α = 90°
	b = 8.0088(3) Å	β = 93.9449(12)°
	c = 23.3552(9) Å	γ = 90°
Volume	4761.8(3) $Å^3$	
Z (empirical units)	8	
Density (calculated)	1.324 g/cm^3	
Absorption coefficient	0.086 mm^{-1}	
F(000)	2000	

Table III-S3. Data collection and structure refinement for **III-7** ($C_{32}H_{26}O_4$).

Theta range for data used in the structural refinement	2.82 to 27.50°	
Index ranges	$-33 \leq h \leq 33$, $-10 \leq k \leq 10$, $-30 \leq l \leq 30$	
Reflections	33075	
Independent reflections	5470 [R(int) = 0.0285]	
Coverage of independent reflections	99.9%	
Absorption correction	multi-scan	
Max. and min. transmission	0.964 and 0.954	
Refinement method	Full-matrix least-squares on F^2	
Refinement program	SHELXL-2014 (Sheldrick, 2014)	
Data / restraints / parameters	5470 / 0 / 327	
Goodness-of-fit on F^2	1.028	
Final R indices	4678 data; $I>2\sigma(I)$	R1 = 0.0425, wR2 = 0.1099
	all data	R1 = 0.0503, wR2 = 0.1187
Largest diff. peak and hole	0.318 and -0.216 $e^-/Å^3$	

Table III-S4. Atomic coordinates and equivalent isotropic atomic displacement parameters ($Å^2$) for the atoms of **III-7** ($C_{32}H_{26}O_4$). U(eq) is defined as one third of the trace of the orthogonalized U_{ij} tensor.

	x/a	y/b	z/c	U(eq)
O1	0.17956(4)	0.36578(11)	0.01860(4)	0.0318(2)
O2	0.16899(4)	0.30007(11)	0.25239(4)	0.0336(2)
O3	0.99644(3)	0.78412(12)	0.92493(4)	0.0320(2)
O4	0.01856(4)	0.70789(14)	0.33185(5)	0.0389(3)
C1	0.17519(5)	0.36000(15)	0.07680(6)	0.0279(3)
C2	0.19013(4)	0.20674(14)	0.10364(6)	0.0243(3)
C3	0.20876(4)	0.06724(14)	0.06591(5)	0.0231(2)
C4	0.23086(4)	0.92172(14)	0.10056(5)	0.0235(2)
C5	0.23068(4)	0.90849(15)	0.15686(5)	0.0241(3)
C6	0.20960(4)	0.03923(15)	0.19557(5)	0.0236(2)
C7	0.18801(4)	0.19082(14)	0.16266(6)	0.0247(3)
C8	0.16953(5)	0.32662(15)	0.19449(6)	0.0281(3)
C9	0.15501(5)	0.47495(16)	0.16770(7)	0.0318(3)
C10	0.15836(5)	0.49241(15)	0.10886(7)	0.0320(3)
C11	0.16379(6)	0.51785(17)	0.99041(7)	0.0369(3)
C12	0.14528(5)	0.42698(18)	0.28492(7)	0.0380(3)
C13	0.16545(4)	0.00138(14)	0.02328(5)	0.0227(2)
C14	0.17589(5)	0.96115(15)	0.96731(5)	0.0243(3)
C15	0.13711(5)	0.89629(15)	0.92902(5)	0.0249(3)
C16	0.08592(5)	0.87375(14)	0.94565(5)	0.0239(3)
C17	0.07563(5)	0.91113(16)	0.00208(6)	0.0269(3)
C18	0.11495(5)	0.97202(16)	0.04034(6)	0.0266(3)
C19	0.04394(5)	0.82227(15)	0.90374(6)	0.0262(3)
C20	0.03948(6)	0.81419(18)	0.84581(6)	0.0343(3)
C21	0.98635(6)	0.76812(18)	0.82974(7)	0.0365(3)

	x/a	y/b	z/c	U(eq)
C22	0.96243(5)	0.75154(18)	0.87845(7)	0.0354(3)
C23	0.17203(4)	0.95806(14)	0.23533(5)	0.0240(3)
C24	0.11953(5)	0.92709(16)	0.21805(6)	0.0265(3)
C25	0.08590(5)	0.85554(16)	0.25533(6)	0.0276(3)
C26	0.10400(5)	0.81135(15)	0.31115(6)	0.0263(3)
C27	0.15727(5)	0.83623(16)	0.32765(6)	0.0266(3)
C28	0.19029(5)	0.90941(15)	0.29029(6)	0.0259(3)
C29	0.06884(5)	0.74565(16)	0.35240(6)	0.0285(3)
C30	0.07444(6)	0.72153(16)	0.40958(6)	0.0315(3)
C31	0.02453(6)	0.66322(18)	0.42619(7)	0.0397(3)
C32	0.99274(6)	0.6583(2)	0.37838(7)	0.0439(4)

Table III-S5. Interatomic distances (Å) for the non-hydrogen atoms of **III-7** ($C_{32}H_{26}O_4$).

O1-C1	1.3722(17)	O1-C11	1.4291(15)
O2-C8	1.3700(17)	O2-C12	1.4281(15)
O3-C22	1.3675(16)	O3-C19	1.3746(15)
O4-C32	1.3681(19)	O4-C29	1.3723(16)
C1-C10	1.3835(18)	C1-C2	1.4185(17)
C2-C7	1.3892(19)	C2-C3	1.5192(16)
C3-C4	1.5060(16)	C3-C13	1.5296(16)
C4-C5	1.3196(18)	C5-C6	1.5066(16)
C6-C7	1.5198(17)	C6-C23	1.5252(17)
C7-C8	1.4163(17)	C8-C9	1.3813(19)

C9-C10	1.390(2)	C13-C14	1.3898(18)
C13-C18	1.3947(16)	C14-C15	1.3883(17)
C15-C16	1.3999(17)	C16-C17	1.3939(18)
C16-C19	1.4599(17)	C17-C18	1.3854(17)
C19-C20	1.3516(19)	C20-C21	1.4302(19)
C21-C22	1.334(2)	C23-C28	1.3908(18)
C23-C24	1.3946(16)	C24-C25	1.3877(19)
C25-C26	1.3984(18)	C26-C27	1.4014(17)
C26-C29	1.4591(19)	C27-C28	1.3842(19)
C29-C30	1.347(2)	C30-C31	1.435(2)
C31-C32	1.335(2)		

Table III-S6. Bond angles (°) for the atoms of **III-7** ($C_{32}H_{26}O_4$).

C1-O1-C11	116.46(11)	C8-O2-C12	116.61(11)
C22-O3-C19	106.48(11)	C32-O4-C29	106.02(12)
O1-C1-C10	124.03(12)	O1-C1-C2	115.42(11)
C10-C1-C2	120.54(13)	C7-C2-C1	119.36(11)
C7-C2-C3	122.90(11)	C1-C2-C3	117.74(12)
C4-C3-C2	112.21(10)	C4-C3-C13	108.06(9)
C2-C3-C13	112.97(9)	C5-C4-C3	124.80(11)
C4-C5-C6	124.61(11)	C5-C6-C7	112.57(10)
C5-C6-C23	109.54(10)	C7-C6-C23	115.29(10)
C2-C7-C8	119.17(12)	C2-C7-C6	122.52(10)
C8-C7-C6	118.05(12)	O2-C8-C9	124.05(12)
O2-C8-C7	115.16(11)	C9-C8-C7	120.75(13)
C8-C9-C10	120.10(12)	C1-C10-C9	120.03(12)

C14-C13-C18	118.06(11)	C14-C13-C3	121.03(10)
C18-C13-C3	120.83(11)	C15-C14-C13	121.22(11)
C14-C15-C16	120.46(12)	C17-C16-C15	118.34(11)
C17-C16-C19	121.15(11)	C15-C16-C19	120.40(12)
C18-C17-C16	120.68(11)	C17-C18-C13	121.16(12)
C20-C19-O3	109.52(11)	C20-C19-C16	133.79(12)
O3-C19-C16	116.48(11)	C19-C20-C21	106.74(13)
C22-C21-C20	106.43(13)	C21-C22-O3	110.82(12)
C28-C23-C24	118.13(12)	C28-C23-C6	119.78(10)
C24-C23-C6	122.08(11)	C25-C24-C23	121.00(12)
C24-C25-C26	120.71(11)	C25-C26-C27	118.18(12)
C25-C26-C29	121.88(11)	C27-C26-C29	119.91(12)
C28-C27-C26	120.53(12)	C27-C28-C23	121.37(11)
C30-C29-O4	110.37(12)	C30-C29-C26	132.69(12)
O4-C29-C26	116.82(12)	C29-C30-C31	106.20(13)
C32-C31-C30	106.45(14)	C31-C32-O4	110.96(13)

Table III-S7. Anisotropic atomic displacement parameters ($Å^2$) for the atoms of **III-7** ($C_{32}H_{26}O_4$). The anisotropic atomic displacement factor exponent takes the form: $-2\pi^2[h^2 a^{*2} U_{11} + ... + 2 h k a^* b^* U_{12}]$.

	U_{11}	U_{22}	U_{33}	U_{23}	U_{13}	U_{12}
O1	0.0263(5)	0.0180(4)	0.0517(6)	0.0082(4)	0.0061(4)	0.0039(3)
O2	0.0309(5)	0.0237(5)	0.0451(6)	-0.0161(4)	-0.0059(4)	0.0061(4)
O3	0.0206(4)	0.0320(5)	0.0432(5)	-0.0074(4)	0.0014(4)	-0.0035(4)

	U_{11}	U_{22}	U_{33}	U_{23}	U_{13}	U_{12}
O4	0.0242(5)	0.0434(6)	0.0487(6)	-0.0017(5)	-0.0003(4)	-0.0031(4)
C1	0.0163(5)	0.0168(6)	0.0506(8)	0.0021(5)	0.0025(5)	-0.0010(4)
C2	0.0132(5)	0.0140(5)	0.0456(7)	-0.0024(5)	0.0000(5)	-0.0002(4)
C3	0.0162(5)	0.0158(5)	0.0371(6)	0.0002(5)	0.0012(4)	0.0015(4)
C4	0.0170(5)	0.0155(5)	0.0377(7)	-0.0031(5)	-0.0006(5)	0.0032(4)
C5	0.0167(5)	0.0162(5)	0.0388(7)	-0.0030(5)	-0.0028(5)	0.0039(4)
C6	0.0159(5)	0.0180(5)	0.0363(6)	-0.0067(5)	-0.0035(4)	0.0018(4)
C7	0.0134(5)	0.0152(5)	0.0447(7)	-0.0064(5)	-0.0028(5)	-0.0007(4)
C8	0.0161(5)	0.0191(6)	0.0482(8)	-0.0097(5)	-0.0029(5)	-0.0010(4)
C9	0.0183(6)	0.0159(6)	0.0609(9)	-0.0096(6)	0.0008(5)	0.0009(4)
C10	0.0202(6)	0.0134(5)	0.0625(9)	0.0009(5)	0.0032(6)	0.0006(4)
C11	0.0303(7)	0.0197(6)	0.0606(9)	0.0108(6)	0.0010(6)	0.0032(5)
C12	0.0268(6)	0.0306(7)	0.0558(9)	-0.0214(6)	-0.0029(6)	0.0053(5)
C13	0.0183(5)	0.0137(5)	0.0357(6)	0.0030(4)	-0.0009(5)	0.0024(4)
C14	0.0187(5)	0.0186(5)	0.0358(6)	0.0074(5)	0.0027(5)	0.0017(4)
C15	0.0240(6)	0.0204(6)	0.0304(6)	0.0064(5)	0.0017(5)	0.0014(5)
C16	0.0208(5)	0.0153(5)	0.0351(6)	0.0044(5)	-0.0010(5)	0.0008(4)
C17	0.0182(5)	0.0231(6)	0.0396(7)	0.0000(5)	0.0028(5)	-0.0009(5)
C18	0.0214(6)	0.0226(6)	0.0360(7)	-0.0020(5)	0.0040(5)	0.0001(5)
C19	0.0211(6)	0.0181(5)	0.0393(7)	0.0034(5)	0.0004(5)	0.0001(4)
C20	0.0300(7)	0.0341(7)	0.0380(7)	0.0076(6)	-0.0033(5)	-0.0057(6)
C21	0.0315(7)	0.0334(7)	0.0430(8)	0.0029(6)	-0.0088(6)	-0.0031(6)
C22	0.0228(6)	0.0313(7)	0.0508(8)	-0.0072(6)	-0.0060(6)	-0.0016(5)
C23	0.0187(5)	0.0159(5)	0.0370(6)	-0.0087(5)	-0.0004(5)	0.0035(4)
C24	0.0204(6)	0.0246(6)	0.0339(6)	-0.0067(5)	-0.0033(5)	0.0025(5)
C25	0.0181(5)	0.0250(6)	0.0392(7)	-0.0070(5)	-0.0024(5)	0.0020(5)

	U_{11}	U_{22}	U_{33}	U_{23}	U_{13}	U_{12}
C26	0.0220(6)	0.0185(6)	0.0381(7)	-0.0088(5)	0.0007(5)	0.0033(4)
C27	0.0235(6)	0.0215(6)	0.0342(6)	-0.0086(5)	-0.0029(5)	0.0050(5)
C28	0.0184(5)	0.0207(6)	0.0378(7)	-0.0094(5)	-0.0035(5)	0.0035(4)
C29	0.0231(6)	0.0199(6)	0.0421(7)	-0.0060(5)	-0.0004(5)	0.0024(5)
C30	0.0315(7)	0.0227(6)	0.0401(7)	-0.0027(5)	0.0010(5)	0.0026(5)
C31	0.0430(8)	0.0275(7)	0.0498(9)	0.0041(6)	0.0116(7)	0.0026(6)
C32	0.0303(7)	0.0419(8)	0.0603(10)	0.0024(7)	0.0082(7)	-0.0061(6)

Table III-S8. Hydrogen atom coordinates and isotropic atomic displacement parameters ($Å^2$) of **III-7** ($C_{32}H_{26}O_4$).

	x/a	y/b	z/c	U(eq)
H3	0.2374	0.1130	0.0434	0.028
H4	0.2460	-0.1671	0.0804	0.028
H5	0.2448	-0.1904	0.1742	0.029
H6	0.2403	0.0797	0.2207	0.028
H9	0.1427	0.5652	0.1895	0.038
H10	0.1491	0.5953	0.0906	0.038
H11A	0.1271	0.5419	-0.0027	0.055
H11B	0.1673	0.5065	-0.0509	0.055
H11C	0.1862	0.6094	0.0055	0.055
H12A	0.1650	0.5313	0.2821	0.057
H12B	0.1456	0.3925	0.3252	0.057
H12C	0.1089	0.4442	0.2697	0.057
H14	0.2102	-0.0217	-0.0450	0.029
H15	0.1454	-0.1330	-0.1087	0.03
H17	0.0413	-0.1053	0.0144	0.032

	x/a	y/b	z/c	U(eq)
H18	0.1074	-0.0058	0.0789	0.032
H20	0.0664	-0.1649	-0.1794	0.041
H21	-0.0289	-0.2476	-0.2081	0.044
H22	-0.0734	-0.2788	-0.1194	0.042
H24	0.1066	-0.0446	0.1802	0.032
H25	0.0502	-0.1636	0.2428	0.033
H27	0.1708	-0.1974	0.3648	0.032
H28	0.2262	-0.0732	0.3024	0.031
H30	0.1053	-0.2605	0.4340	0.038
H31	0.0158	-0.3661	0.4638	0.048
H32	-0.0430	-0.3752	0.3769	0.053

Description of the X-ray Structural Analysis of III-14 ($C_{36}H_{28}Br_2O_2$)

A colorless crystal of **III-14** ($C_{36}H_{28}Br_2O_2$) was covered in a polybutene oil (Sigma-Aldrich) and placed on the end of a MiTeGen loop. The sample was cooled to 100 K with an Oxford Cryostream 700 system and optically aligned on a Bruker AXS D8 Venture fixed-chi X-ray diffractometer equipped with a Triumph monochromator, a Mo Kα radiation source (λ = 0.71073 Å), and a PHOTON 100 CMOS detector. Two sets of 12 frames each were collected using the omega scan method with a 10 s exposure time. Integration of these frames followed by reflection indexing and least-squares refinement produced a crystal orientation matrix for the orthorhombic crystal lattice.

Data collection consisted of the measurement of a total of 372 frames in one run using omega scans with the detector held at 5.00 cm from the crystal. Frame scan parameters are summarized in Table S9 below:

Table III-S9. Data collection details for **III-14** ($C_{36}H_{28}Br_2O_2$).

Run	2θ	ω	φ	χ	Scan Width (°)	Frames	Exposure Time (sec)
1	22.76	-160.24	-59.09	54.79	0.50	372	10.00

The APEX2 software program (version 2014.1-7)[S1] was used for diffractometer control, preliminary frame scans, indexing, orientation matrix calculations, least-squares refinement of cell parameters, and the data collection. The frames were integrated with the Bruker SAINT software package using a narrow-frame algorithm. The integration of the data using an orthorhombic unit cell yielded a total of 23622 reflections to a maximum θ angle of 27.50° (0.77 Å resolution), of which 6338 were independent (average redundancy 3.727, completeness = 99.7%, R_{int} = 2.53%, R_{sig} = 2.40%) and 5528 (87.22%) were greater than $2\sigma(F^2)$. The final cell constants of $\underline{a}$ = 10.6995(4) Å, $\underline{b}$ = 15.0959(6) Å, $\underline{c}$ = 34.2987(13) Å, volume = 5539.9(4) $Å^3$, are based upon the refinement of the XYZ-centroids of 9954 reflections above 20 σ(I) with 5.872° < 2θ < 65.10°. Data were corrected for absorption effects using the multi-scan method (SADABS). The ratio of minimum to maximum apparent transmission was 0.752. The calculated minimum and maximum transmission coefficients (based on crystal size) are 0.399 and 0.493.

The structure was solved by direct methods and difference Fourier analysis using the programs provided by SHELXL-2013.[S5] Idealized positions for the hydrogen atoms were included as fixed contributions using a riding model with isotropic temperature factors set at 1.2 times (aromatic and methine hydrogens) or 1.5 (methyl hydrogens) times that of the adjacent carbon atom. The positions of the methyl hydrogen atoms were optimized by a rigid rotating group refinement with idealized angles. Full-matrix least-squares refinement, based upon the minimization of $\Sigma w_i |F_o^2 - F_c^2|^2$, with weighting $w_i^{-1} = [\sigma^2(F_o^2) + (0.0365\ P)^2 + 7.8371\ P]$, where $P = (\text{Max}(F_o^2, 0) + 2\ F_c^2)/3$.[S5] The final anisotropic full-matrix least-squares refinement on F^2 with 363 variables converged at R1 = 3.27% for 5528 observed data with $I>2\sigma(I)$ and wR2 = 8.13% for all data. The goodness-of-fit was 1.068.[S3]

A correction for secondary extinction was not applied. The largest peak in the final difference electron density synthesis was 0.657 $e^-/Å^3$ and the largest hole was -0.564 $e^-/Å^3$ with an RMS deviation of 0.080 $e^-/Å^3$. The linear absorption coefficient, atomic scattering factors, and anomalous dispersion corrections were calculated from values found in the International Tables of X-ray Crystallography.[S4]

Table III-S10. Crystal data for **III-14** ($C_{36}H_{28}Br_2O_2$).

Identification code	Compd **III-14** - kw14cms
Chemical formula	$C_{36}H_{28}Br_2O_2$
Formula weight	652.40 g/mol

Temperature	100(2) K	
Wavelength	0.71073 Å	
Crystal size	0.278 x 0.371 x 0.380 mm	
Crystal system	orthorhombic	
Space group	Pbca (No. 61)	
Unit cell dimensions	a = 10.6995(4) Å	α = 90°
	b = 15.0959(6) Å	β = 90°
	c = 34.2987(13) Å	γ = 90°
Volume	5539.9(4) $Å^3$	
Z	8	
Density (calculated)	1.564 g/cm^3	
Absorption coefficient	2.960 mm^{-1}	
F(000)	2640	

Table III-S11. Data collection and structure refinement for **III-14** ($C_{36}H_{28}Br_2O_2$).

Theta range used for refinement	2.94 to 27.50°
Index ranges	$-13 \leq h \leq 13$, $-19 \leq k \leq 15$, $-44 \leq l \leq 30$
Reflections collected	23622
Independent reflections	6338 [R(int) = 0.0253]
Coverage of independent reflections	99.7%
Absorption correction	multi-scan
Max. and min. trans.	0.493 and 0.399
Refinement method	Full-matrix least-squares on F^2
Refinement program	SHELXL-2013 (Sheldrick, 2013)
Data / restraints / parameters	6338 / 0 / 363
Goodness-of-fit on F^2	1.068

Final R indices	5528 data; I>2σ(I)	R1 = 0.0327, wR2 = 0.0781
	all data	R1 = 0.0399, wR2 = 0.0813
Largest diff. peak and hole	0.657 and -0.564 $e^-/Å^3$	

Table III-S12. Atomic coordinates and equivalent isotropic atomic displacement parameters ($Å^2$) for **III-14 (**$C_{36}H_{28}Br_2O_2$). U(eq) is defined as one third of the trace of the orthogonalized U_{ij} tensor.

	x/a	y/b	z/c	U(eq)
Br1	0.62328(2)	0.03660(2)	0.19541(2)	0.01714(7)
Br2	0.42232(3)	0.98451(2)	0.91169(2)	0.02373(8)
O1	0.21117(16)	0.63375(10)	0.17700(5)	0.0189(3)
O2	0.57739(17)	0.56480(12)	0.06801(5)	0.0229(4)
C1	0.2988(2)	0.62161(14)	0.14848(7)	0.0152(4)
C2	0.3815(2)	0.54962(14)	0.15445(6)	0.0132(4)
C3	0.3681(2)	0.49498(15)	0.19116(6)	0.0140(4)
C4	0.4818(2)	0.43794(15)	0.19826(7)	0.0156(4)
C5	0.5682(2)	0.42074(15)	0.17188(7)	0.0152(4)
C6	0.5675(2)	0.45824(14)	0.13131(7)	0.0140(4)
C7	0.4744(2)	0.53333(14)	0.12689(7)	0.0140(4)
C8	0.4835(2)	0.58715(15)	0.09366(7)	0.0167(4)
C9	0.4022(2)	0.65696(15)	0.08820(7)	0.0185(5)
C10	0.3096(2)	0.67416(15)	0.11578(7)	0.0183(5)
C11	0.2529(2)	0.43452(14)	0.19193(6)	0.0130(4)
C12	0.1720(2)	0.42397(14)	0.16070(6)	0.0146(4)
C13	0.0750(2)	0.36323(15)	0.16197(6)	0.0154(4)
C14	0.0536(2)	0.31035(14)	0.19454(6)	0.0126(4)

	x/a	y/b	z/c	U(eq)
C15	0.1338(2)	0.32200(15)	0.22636(6)	0.0152(4)
C16	0.2309(2)	0.38248(15)	0.22514(6)	0.0153(4)
C17	0.9495(2)	0.24526(14)	0.19549(6)	0.0140(4)
C18	0.8502(2)	0.25056(18)	0.16962(8)	0.0280(6)
C19	0.7533(3)	0.18913(18)	0.16939(8)	0.0282(6)
C20	0.7545(2)	0.12197(15)	0.19657(6)	0.0156(4)
C21	0.8488(2)	0.11526(16)	0.22364(7)	0.0199(5)
C22	0.9463(2)	0.17632(16)	0.22269(7)	0.0182(5)
C23	0.5451(2)	0.38445(14)	0.10166(6)	0.0142(4)
C24	0.6435(2)	0.33151(16)	0.08916(7)	0.0188(5)
C25	0.6250(2)	0.26351(16)	0.06271(7)	0.0195(5)
C26	0.5072(2)	0.24682(15)	0.04689(6)	0.0156(4)
C27	0.4083(2)	0.29975(15)	0.05971(7)	0.0172(5)
C28	0.4266(2)	0.36662(15)	0.08674(7)	0.0164(4)
C29	0.4874(2)	0.17949(15)	0.01601(7)	0.0165(4)
C30	0.5829(2)	0.15983(16)	0.98964(7)	0.0196(5)
C31	0.5654(2)	0.10127(16)	0.95890(7)	0.0208(5)
C32	0.4495(2)	0.06130(15)	0.95448(7)	0.0188(5)
C33	0.3525(2)	0.07923(16)	0.98034(7)	0.0201(5)
C34	0.3722(2)	0.13699(16)	0.01098(7)	0.0199(5)
C35	0.1231(2)	0.70329(16)	0.17058(8)	0.0209(5)
C36	0.5769(3)	0.60848(18)	0.03136(8)	0.0272(6)

Table III-S13. Interatomic distances (Å) for **III-14** ($C_{36}H_{28}Br_2O_2$).

Br1-C20	1.906(2)	Br2-C32	1.893(2)
O1-C1	1.368(3)	O1-C35	1.428(3)
O2-C8	1.378(3)	O2-C36	1.420(3)
C1-C10	1.379(3)	C1-C2	1.416(3)
C2-C7	1.394(3)	C2-C3	1.512(3)
C3-C4	1.510(3)	C3-C11	1.534(3)
C4-C5	1.319(3)	C5-C6	1.502(3)
C6-C7	1.516(3)	C6-C23	1.527(3)
C7-C8	1.403(3)	C8-C9	1.379(3)
C9-C10	1.394(3)	C11-C12	1.386(3)
C11-C16	1.404(3)	C12-C13	1.385(3)
C13-C14	1.392(3)	C14-C15	1.399(3)
C14-C17	1.486(3)	C15-C16	1.384(3)
C17-C18	1.386(3)	C17-C22	1.398(3)
C18-C19	1.391(4)	C19-C20	1.377(3)
C20-C21	1.375(3)	C21-C22	1.392(3)
C23-C24	1.389(3)	C23-C28	1.393(3)
C24-C25	1.384(3)	C25-C26	1.395(3)
C26-C27	1.397(3)	C26-C29	1.483(3)
C27-C28	1.385(3)	C29-C30	1.396(3)
C29-C34	1.399(3)	C30-C31	1.389(3)
C31-C32	1.388(4)	C32-C33	1.392(3)
C33-C34	1.382(3)		

Table III-S14. Bond angles (°) for **III-14** ($C_{36}H_{28}Br_2O_2$).

C1-O1-C35	116.15(18)	C8-O2-C36	116.68(19)
O1-C1-C10	124.2(2)	O1-C1-C2	115.32(19)
C10-C1-C2	120.5(2)	C7-C2-C1	118.9(2)
C7-C2-C3	122.40(19)	C1-C2-C3	118.7(2)
C4-C3-C2	111.65(19)	C4-C3-C11	107.77(18)
C2-C3-C11	114.52(18)	C5-C4-C3	124.5(2)
C4-C5-C6	123.9(2)	C5-C6-C7	112.18(19)
C5-C6-C23	110.04(18)	C7-C6-C23	112.07(18)
C2-C7-C8	119.8(2)	C2-C7-C6	122.2(2)
C8-C7-C6	118.0(2)	O2-C8-C9	124.1(2)
O2-C8-C7	115.3(2)	C9-C8-C7	120.6(2)
C8-C9-C10	119.9(2)	C1-C10-C9	120.3(2)
C12-C11-C16	117.3(2)	C12-C11-C3	123.83(19)
C16-C11-C3	118.81(19)	C13-C12-C11	121.3(2)
C12-C13-C14	121.9(2)	C13-C14-C15	117.0(2)
C13-C14-C17	121.3(2)	C15-C14-C17	121.7(2)
C16-C15-C14	121.3(2)	C15-C16-C11	121.3(2)
C18-C17-C22	116.8(2)	C18-C17-C14	121.5(2)
C22-C17-C14	121.7(2)	C17-C18-C19	122.4(2)
C20-C19-C18	118.7(2)	C21-C20-C19	121.2(2)
C21-C20-Br1	120.33(17)	C19-C20-Br1	118.50(18)
C20-C21-C22	119.0(2)	C21-C22-C17	121.8(2)
C24-C23-C28	117.7(2)	C24-C23-C6	120.4(2)
C28-C23-C6	121.9(2)	C25-C24-C23	121.4(2)
C24-C25-C26	121.2(2)	C25-C26-C27	117.3(2)
C25-C26-C29	122.0(2)	C27-C26-C29	120.6(2)

C28-C27-C26	121.4(2)	C27-C28-C23	121.0(2)
C30-C29-C34	117.8(2)	C30-C29-C26	120.2(2)
C34-C29-C26	121.9(2)	C31-C30-C29	121.9(2)
C32-C31-C30	118.7(2)	C31-C32-C33	120.8(2)
C31-C32-Br2	119.25(18)	C33-C32-Br2	119.90(18)
C34-C33-C32	119.6(2)	C33-C34-C29	121.2(2)

Table III-S15. Anisotropic atomic displacement parameters ($Å^2$) for **III-14** ($C_{36}H_{28}Br_2O_2$). The anisotropic atomic displacement factor exponent takes the form: $-2\pi^2[h^2 a^{*2} U_{11} + ... + 2 h k a^* b^* U_{12}]$.

	U_{11}	U_{22}	U_{33}	U_{23}	U_{13}	U_{12}
Br1	0.01770(11)	0.01705(11)	0.01668(12)	0.00090(9)	-0.0002(1)	-0.0034(1)
Br2	0.03306(15)	0.02126(12)	0.01689(12)	-0.0031(1)	-0.0018(1)	-0.0019(1)
O1	0.0229(9)	0.0130(8)	0.0208(8)	0.0011(7)	0.0028(7)	0.0047(7)
O2	0.0225(9)	0.0239(9)	0.0222(9)	0.0113(7)	0.0069(7)	0.0048(7)
C1	0.0152(10)	0.0124(10)	0.0181(11)	-0.0022(9)	-0.0021(9)	-0.0013(8)
C2	0.0158(10)	0.0096(9)	0.0141(10)	-0.0006(8)	-0.0041(8)	-0.0025(8)
C3	0.0170(11)	0.0117(9)	0.0133(10)	-0.0001(8)	-0.0022(8)	0.0008(8)
C4	0.0182(11)	0.0140(10)	0.0147(10)	0.0029(8)	-0.0064(9)	-0.0009(8)
C5	0.0154(11)	0.0135(10)	0.0168(11)	0.0031(8)	-0.0062(9)	-0.0003(8)
C6	0.0131(10)	0.0135(10)	0.0153(10)	0.0016(9)	-0.0016(8)	0.0001(8)
C7	0.0139(10)	0.0099(9)	0.0183(11)	0.0002(8)	-0.0039(9)	-0.0016(8)
C8	0.0157(11)	0.0156(10)	0.0188(11)	0.0020(9)	-0.0008(9)	-0.0013(9)
C9	0.0217(12)	0.0144(10)	0.0194(11)	0.0072(9)	-0.0027(9)	-0.0024(9)
C10	0.0190(12)	0.0123(10)	0.0236(12)	0.0025(9)	-0.0040(9)	0.0010(9)

	U_{11}	U_{22}	U_{33}	U_{23}	U_{13}	U_{12}
C11	0.0144(10)	0.0095(9)	0.0150(10)	-0.0012(8)	-0.0001(8)	0.0030(8)
C12	0.0183(11)	0.0123(10)	0.0133(10)	0.0015(8)	-0.0006(9)	0.0005(9)
C13	0.0167(11)	0.0161(10)	0.0135(10)	0.0009(9)	-0.0028(8)	0.0023(9)
C14	0.0135(10)	0.0099(9)	0.0144(10)	-0.0008(8)	0.0024(8)	0.0034(8)
C15	0.0197(11)	0.0148(10)	0.0111(10)	0.0016(8)	0.0007(8)	0.0012(9)
C16	0.0189(11)	0.0151(10)	0.0119(10)	-0.0015(8)	-0.0018(8)	0.0017(9)
C17	0.0150(10)	0.0119(10)	0.0152(10)	0.0002(8)	0.0022(8)	0.0025(8)
C18	0.0262(14)	0.0270(13)	0.0308(14)	0.0183(11)	-0.010(1)	-0.007(1)
C19	0.0235(13)	0.0309(14)	0.0301(14)	0.0127(12)	-0.011(1)	-0.006(1)
C20	0.0133(10)	0.0139(10)	0.0195(11)	-0.0012(9)	0.0033(9)	-0.0007(8)
C21	0.0249(12)	0.0168(11)	0.0180(11)	0.0037(9)	-0.0013(9)	-0.0026(9)
C22	0.0202(12)	0.0200(11)	0.0143(11)	0.0020(9)	-0.0022(9)	-0.0011(9)
C23	0.0171(10)	0.0132(10)	0.0122(10)	0.0030(8)	-0.0017(8)	-0.0006(8)
C24	0.0151(11)	0.0225(11)	0.0187(11)	0.0024(10)	-0.0040(9)	0.0028(9)
C25	0.0169(11)	0.0211(11)	0.0207(12)	0.0001(10)	-0.0005(9)	0.0042(9)
C26	0.0180(11)	0.0160(10)	0.0129(10)	0.0049(9)	0.0010(8)	-0.0003(9)
C27	0.0144(11)	0.0205(11)	0.0167(11)	0.0021(9)	-0.0009(9)	-0.0019(9)
C28	0.0130(10)	0.0182(11)	0.0179(11)	0.0006(9)	0.0016(9)	0.0018(9)
C29	0.0213(12)	0.0145(10)	0.0136(10)	0.0030(8)	-0.0011(9)	0.0015(9)
C30	0.0190(11)	0.0211(11)	0.0188(11)	-0.0001(9)	0.0002(9)	-0.0013(9)
C31	0.0255(13)	0.0207(12)	0.0162(11)	-0.0011(9)	0.0025(9)	0.0018(10)
C32	0.0284(13)	0.0156(11)	0.0124(10)	-0.0010(9)	-0.0026(9)	0.0005(9)
C33	0.0198(12)	0.0198(11)	0.0209(12)	0.0018(10)	-0.0023(9)	-0.0044(9)
C34	0.0199(12)	0.0208(11)	0.0189(11)	0.0006(9)	0.0038(9)	0.0002(9)
C35	0.0191(12)	0.0154(11)	0.0281(13)	0.0001(10)	0.0022(10)	0.0049(9)
C36	0.0279(13)	0.0304(14)	0.0235(13)	0.0129(11)	0.0072(11)	0.0032(11)

Table III-S16. Hydrogen atom coordinates and isotropic atomic displacement parameters ($Å^2$) for **III-14** ($C_{36}H_{28}Br_2O_2$).

	x/a	y/b	z/c	U(eq)
H3	0.3607	0.5370	0.2136	0.017
H4	0.4918	0.4127	0.2234	0.019
H5	0.6348	0.3824	0.1790	0.018
H6	0.6526	0.4831	0.1262	0.017
H9	0.4092	0.6933	0.0657	0.022
H10	0.2537	0.7223	0.1120	0.022
H12	0.1833	0.4591	0.1380	0.018
H13	0.0216	0.3575	0.1400	0.019
H15	0.1213	0.2877	0.2493	0.018
H16	0.2837	0.3889	0.2472	0.018
H18	-0.1517	0.2979	0.1514	0.034
H19	-0.3123	0.1934	0.1509	0.034
H21	-0.1525	0.0696	0.2427	0.024
H22	0.0125	0.1710	0.2410	0.022
H24	0.7251	0.3422	0.0990	0.023
H25	0.6937	0.2276	0.0552	0.023
H27	0.3268	0.2897	0.0497	0.021
H28	0.3573	0.4009	0.0953	0.02
H30	0.6621	0.1873	-0.0072	0.024
H31	0.6316	0.0888	-0.0587	0.025
H33	0.2732	0.0519	-0.0231	0.024
H34	0.3065	0.1480	0.0290	0.024

	x/a	y/b	z/c	U(eq)
H35A	0.1675	0.7597	0.1680	0.031
H35B	0.0653	0.7065	0.1927	0.031
H35C	0.0759	0.6913	0.1467	0.031
H36A	0.4967	0.5982	0.0183	0.041
H36B	0.6448	0.5852	0.0151	0.041
H36C	0.5888	0.6722	0.0353	0.041

Computational Details.

Spin-restricted density functional theory (RDFT) calculations were performed with the Gaussian 09 (G09) program.[S6] Geometry optimization and normal mode analyses were performed using the M06 functional and the 6-31G* basis set to identify all ground state and transition state geometries.[S7] The identified stationary points met or exceeded all default G09 convergence criteria. Using the same functional-basis set, normal-modes were calculated for each optimized structure to confirm the absence of negative eigenvalues and determine thermochemical corrections.[4a,b]

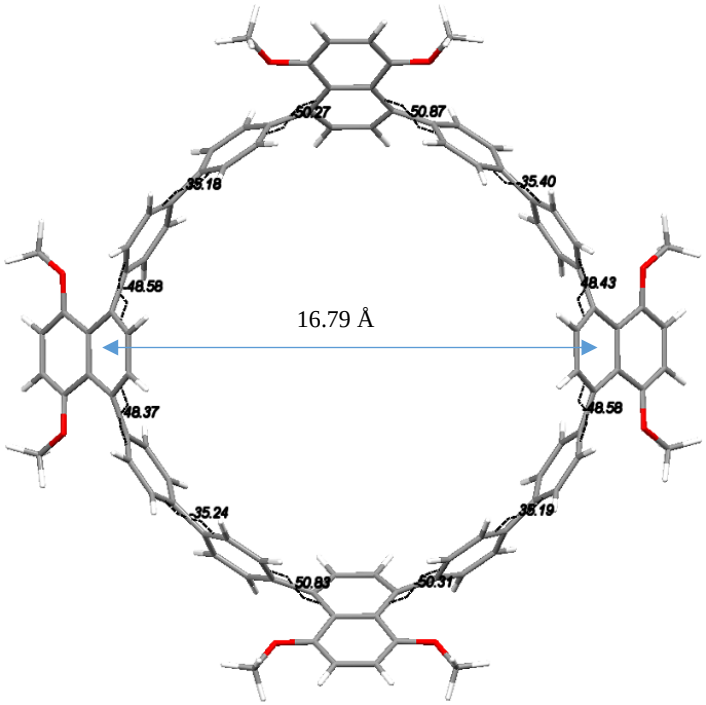

perspective view

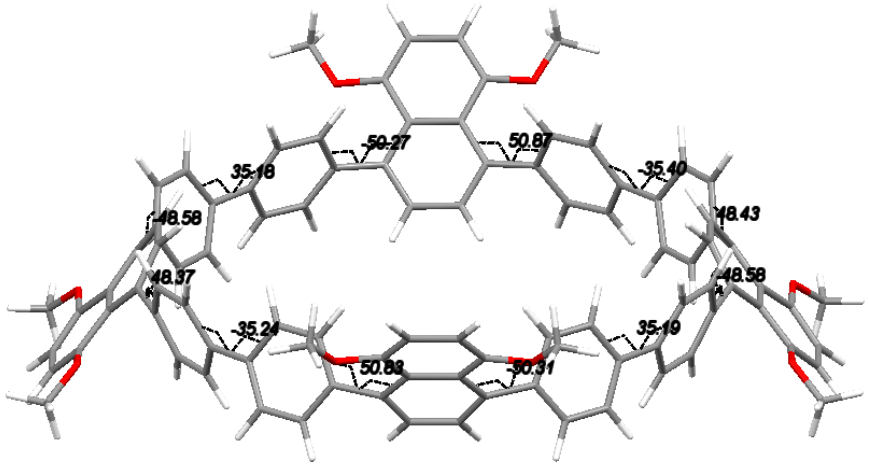

aerial view

Figure III-S1. Analysis of the Molecular Structure of the Functionalized [12]CPP **III-23**

The capped-stick molecular structure for the functionalized [12]CPP **III-23** is derived from the DFT calculation with the four 5,8-dimethoxynaphthyl-1,4-diyl units alternating above and below the plane of the [12]CPP circle. The phenyl-phenyl and the phenyl-5,8-dimethoxynaphthyl-1,4-diyl torsions on the top face are noted. The four biphenyl units have torsional angles of –35.4°, 35.2°, –35.2°, and 35.2° between the phenyl groups. The torsional angles between the phenyl and the 5,8-dimethoxynaphthyl-1,4-diyl groups are –50.3°, 50.9°, 48.4°, –48.6°, –50.3°, 50.8°, 48.4°, and –48.6°. The 5,8-dimethoxynaphthyl-1,4-diyl units cant away from the inner plan of the [12]CPP circle at an angle of 124.9° on average.

Computational Coordinates and Energetic Details.

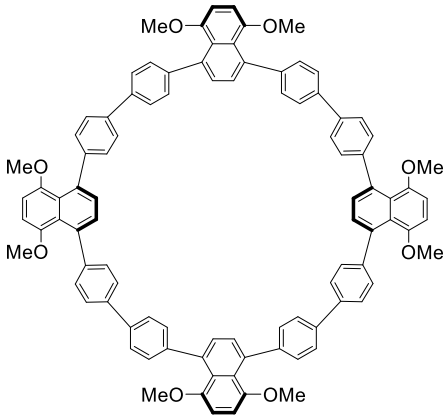

Calculation results at DFT-optimized geometry:

Total Energy: -4300.09486583 AU

SCF Convergence: 0.60E-08

Enthalpy Correction: 1.502798 AU

Free Energy Correction: 1.287820 AU

Three lowest frequencies (cm^{-1}): 8.01, 10.16, 11.77

H 2.19400 6.85800 -1.96900
C 1.76500 7.53200 -1.22800
C 2.57100 7.99900 -0.20800
C -0.24900 8.39600 -0.18600
C 1.99100 8.89600 0.74700
C 0.38200 7.72800 -1.21800
C 0.56900 9.09400 0.76000
C 2.79800 9.64400 1.66500
H -0.22700 7.20100 -1.95200
C 2.21600 10.48700 2.58000
H 2.82500 11.05300 3.27900
C 0.82200 10.67800 2.59400
H 0.40400 11.38600 3.30500
C 0.01500 10.02800 1.69400
C -1.69800 8.11300 -0.04800
C -4.24700 6.87600 0.03000
C -2.18000 7.52400 1.12800
C -2.55800 8.16100 -1.14900
C -3.80900 7.55800 -1.11000
C -3.42400 6.91800 1.16400
H -1.52900 7.46900 2.00000
H -2.22300 8.65000 -2.06400
H -4.44800 7.59100 -1.99400
H -3.72700 6.38100 2.06300
C -5.42600 5.98900 0.01400
C -7.32300 3.88400 0.08100
C -5.70400 5.22400 -1.12700
C -6.19400 5.74400 1.15700
C -7.12100 4.71000 1.19100
C -6.63200 4.19700 -1.09600
H -5.11000 5.37500 -2.02800
H -6.04000 6.35500 2.04700
H -7.67700 4.51300 2.10800
H -6.76600 3.56600 -1.97400
O 4.14000 9.49800 1.53000
O -1.31900 10.25100 1.59100
C 4.97500 10.23600 2.37800
H 4.82400 11.32000 2.25200
H 4.81400 9.97700 3.43700
H 6.00000 9.97900 2.09900
C -1.90200 11.18400 2.46000
H -1.78400 10.88900 3.51400
H -2.96700 11.20900 2.21300
H -1.47300 12.18900 2.32200
H -6.85200 2.19200 1.96300
C -7.52800 1.76400 1.22400
C -7.99800 2.57000 0.20500
C -8.39500 -0.25000 0.18300
C -8.89700 1.99000 -0.74800
C -7.72400 0.38000 1.21300
C -9.09500 0.56800 -0.76100
C -9.64800 2.79700 -1.66400
H -7.19700 -0.22900 1.94600
C -10.49500 2.21600 -2.57500
H -11.06400 2.82500 -3.27200
C -10.68600 0.82200 -2.58900
H -11.39700 0.40400 -3.29700
C -10.03200 0.01400 -1.69200
C -8.11400 -1.70000 0.04500
C -6.87800 -4.24800 -0.03200
C -8.16100 -2.55900 1.14700
C -7.52600 -2.18200 -1.13100
C -6.92000 -3.42600 -1.16700
C -7.55900 -3.81000 1.10800
H -8.65000 -2.22300 2.06200
H -7.47100 -1.53100 -2.00300
H -6.38400 -3.73000 -2.06500
H -7.59100 -4.44800 1.99200
C -5.99000 -5.42700 -0.01500
C -3.88600 -7.32400 -0.08300
C -5.22300 -5.70300 1.12500
C -5.74700 -6.19700 -1.15800
C -4.71300 -7.12400 -1.19200
C -4.19600 -6.63100 1.09300
H -5.37300 -5.10700 2.02500
H -6.36000 -6.04500 -2.04700
H -4.51800 -7.68200 -2.10800
H -3.56400 -6.76300 1.97100
O -9.50000 4.13900 -1.53100
O -10.25200 -1.32100 -1.59000
C -10.23800 4.97400 -2.38100
H -11.32200 4.82800 -2.25000
H -9.98300 4.80700 -3.43900
H -9.97600 5.99900 -2.10700
C -11.20100 -1.90100 -2.44300
H -12.20200 -1.47000 -2.28600
H -11.22400 -2.96600 -2.19700
H -10.92500 -1.78200 -3.50200
H -2.19600 -6.85900 -1.96900
C -1.76700 -7.53300 -1.22800
C -2.57100 -8.00000 -0.20700
C 0.24900 -8.39500 -0.18700
C -1.99100 -8.89500 0.74800
C -0.38300 -7.72800 -1.21900
C -0.56800 -9.09300 0.75900
C -2.79600 -9.64200 1.66800
H 0.22500 -7.20200 -1.95300
C -2.21400 -10.48300 2.58400
H -2.82200 -11.04700 3.28600
C -0.81900 -10.67500 2.59700
H -0.40000 -11.38200 3.30800
C -0.01400 -10.02700 1.69300
C 1.69800 -8.11200 -0.05000
C 4.24700 -6.87700 0.02800
C 2.18000 -7.52400 1.12600
C 2.55700 -8.16100 -1.15100

C 3.80900 -7.55800 -1.11300
C 3.42400 -6.91800 1.16200
H 1.52900 -7.46800 1.99800
H 2.22200 -8.65000 -2.06600
H 4.44700 -7.59100 -1.99600
H 3.72700 -6.38100 2.06000
C 5.42600 -5.99000 0.01100
C 7.32400 -3.88600 0.08000
C 5.70400 -5.22400 -1.12900
C 6.19400 -5.74600 1.15500
C 7.12200 -4.71200 1.18900
C 6.63300 -4.19700 -1.09700
H 5.11000 -5.37500 -2.03000
H 6.04100 -6.35800 2.04400
H 7.67800 -4.51600 2.10700
H 6.76700 -3.56600 -1.97500
O -4.13800 -9.49600 1.53500
O 1.32000 -10.25200 1.58700
C -4.97300 -10.23500 2.38300
H -4.81300 -9.97500 3.44200
H -4.82200 -11.31800 2.25800
H -5.99900 -9.97800 2.10400
C 1.90600 -11.17600 2.46300
H 1.78600 -10.87300 3.51500
H 2.97100 -11.19900 2.21700
H 1.48000 -12.18300 2.33200
H 6.85300 -2.19500 1.96300
C 7.52900 -1.76700 1.22400
C 7.99900 -2.57200 0.20500
C 8.39500 0.24900 0.18500
C 8.89800 -1.99100 -0.74700
C 7.72400 -0.38300 1.21500
C 9.09500 -0.56900 -0.75900
C 9.64900 -2.79700 -1.66400
H 7.19600 0.22600 1.94800
C 10.49600 -2.21500 -2.57400
H 11.06500 -2.82300 -3.27200
C 10.68800 -0.82100 -2.58700
H 11.39800 -0.40300 -3.29400
C 10.03300 -0.01400 -1.68900
C 8.11200 1.69800 0.04800
C 6.87500 4.24600 -0.03100
C 8.16000 2.55800 1.14900
C 7.52300 2.17900 -1.12800
C 6.91700 3.42300 -1.16500
C 7.55700 3.80900 1.11000
H 8.64900 2.22200 2.06400
H 7.46800 1.52700 -2.00000
H 6.38000 3.72600 -2.06400
H 7.59000 4.44700 1.99300
C 5.98900 5.42600 -0.01500
C 3.88500 7.32400 -0.08400
C 5.22300 5.70300 1.12500
C 5.74500 6.19400 -1.15900
C 4.71100 7.12200 -1.19300
C 4.19600 6.63200 1.09300
H 5.37300 5.10900 2.02600
H 6.35700 6.04000 -2.04800
H 4.51600 7.67800 -2.11000
H 3.56500 6.76600 1.97100
O 9.50100 -4.13900 -1.53200
O 10.25400 1.32000 -1.58600
C 10.24100 -4.97300 -2.38200
H 9.98700 -4.80400 -3.44000
H 9.97800 -5.99800 -2.11100
H 11.32400 -4.82700 -2.25000
C 11.19200 1.90400 -2.44800
H 10.90700 1.78100 -3.50500
H 12.19700 1.47800 -2.30000
H 11.21300 2.96900 -2.20400

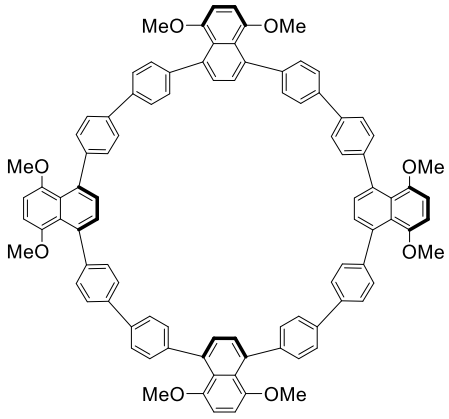

Calculation results at DFT-optimized geometry:
Total Energy: -4300.09071907 AU

SCF Convergence: 0.40E-08

Enthalpy Correction: 1.503300 AU

Free Energy Correction: 1.288822 AU

Three lowest frequencies (cm^{-1}): 9.40, 10.24, 11.20

H -1.19600 -6.67600 -2.19800
C -0.56200 -7.37300 -1.65100
C -1.13600 -8.17200 -0.68000
C 1.69100 -8.03200 -1.02900
C -0.29300 -9.09500 0.01500
C 0.82200 -7.29400 -1.81000
C 1.13000 -9.04300 -0.18200
C -0.83200 -10.11500 0.86500
H 1.22700 -6.52300 -2.46400
C -0.00500 -11.01200 1.49400
H -0.41300 -11.78600 2.13800
C 1.38500 -10.98200 1.27500
H 2.00000 -11.74100 1.75100
C 1.94300 -10.04600 0.43900
C 3.08500 -7.53000 -0.99600
C 5.39400 -5.87400 -0.89600
C 3.71900 -7.09500 -2.16500
C 3.70100 -7.21500 0.22200
C 4.83100 -6.41700 0.26900
C 4.84200 -6.28200 -2.11600
H 3.28600 -7.35200 -3.13200
H 3.24600 -7.55400 1.15200
H 5.26100 -6.17300 1.24000
H 5.24600 -5.89000 -3.04900
C 6.39900 -4.79300 -0.84300
C 7.93200 -2.40500 -0.87700
C 7.19500 -4.45400 -1.94400
C 6.47000 -3.95400 0.27900
C 7.22600 -2.79500 0.26700
C 7.93400 -3.27700 -1.96800
H 7.21400 -5.10600 -2.81700
H 5.85300 -4.16600 1.15000
H 7.21100 -2.13100 1.13100
H 8.50200 -3.01200 -2.86000
O -2.18500 -10.15200 0.96200
O 3.25800 -10.03300 0.10500
C -2.76600 -11.17200 1.72800
H -2.50700 -12.16800 1.33800
H -2.46000 -11.11400 2.78400
H -3.84800 -11.02700 1.66100

C 4.09600 -11.00700 0.66400
H 4.13100 -10.93400 1.76200
H 5.09500 -10.82100 0.26100
H 3.77600 -12.02400 0.38600
H 7.19300 -0.77400 -2.73000
C 7.78900 -0.25600 -1.97900
C 8.39100 -0.99900 -0.98200
C 8.30300 1.84100 -0.87200
C 9.19300 -0.30700 -0.02000
C 7.73600 1.14000 -1.91800
C 9.16500 1.12700 0.02200
C 10.06300 -1.00600 0.87800
H 7.08800 1.67000 -2.61600
C 10.84000 -0.31500 1.77600
H 11.50600 -0.84200 2.45400
C 10.83100 1.09200 1.80100
H 11.49600 1.60200 2.49200
C 10.03800 1.80400 0.93500
C 7.74900 3.19300 -0.62500
C 6.05100 5.43400 -0.25100
C 7.18700 3.47500 0.62600
C 7.52200 4.10700 -1.65800
C 6.69200 5.20700 -1.47400
C 6.35700 4.56700 0.80800
H 7.33800 2.77300 1.44500
H 7.98000 3.93500 -2.63300
H 6.51700 5.89100 -2.30600
H 5.86000 4.70000 1.76800
C 4.96200 6.41600 -0.08900
C 2.54100 7.82000 0.35300
C 4.04000 6.62100 -1.12600
C 4.69700 7.03100 1.14000
C 3.50600 7.71200 1.35800
C 2.85800 7.31100 -0.91200
H 4.20900 6.14500 -2.09200
H 5.41900 6.94200 1.95100
H 3.29700 8.13400 2.34100
H 2.12300 7.38800 -1.71300
O 10.09500 -2.35500 0.74400
O 10.05700 3.15800 0.84300
C 10.95300 -3.08400 1.57800
H 10.70400 -2.94300 2.64200
H 12.00600 -2.80200 1.42100
H 10.81700 -4.13600 1.31500
C 10.90100 3.87000 1.70600
H 10.64900 3.68800 2.76300
H 10.74800 4.92800 1.47900
H 11.95900 3.61100 1.54300
H 1.19600 6.67700 2.19800
C 0.56200 7.37400 1.65100
C 1.13600 8.17200 0.68000
C -1.69100 8.03300 1.02900
C 0.29300 9.09400 -0.01600
C -0.82200 7.29500 1.81100
C -1.13000 9.04300 0.18100
C 0.83200 10.11400 -0.86600
H -1.22800 6.52400 2.46400
C 0.00500 11.01100 -1.49500
H 0.41300 11.78600 -2.13900
C -1.38500 10.98200 -1.27600
H -2.00000 11.74100 -1.75200
C -1.94300 10.04600 -0.44000
C -3.08500 7.53000 0.99600
C -5.39400 5.87400 0.89600
C -3.71900 7.09600 2.16500
C -3.70100 7.21500 -0.22200
C -4.83100 6.41700 -0.26900
C -4.84200 6.28200 2.11600
H -3.28600 7.35300 3.13200
H -3.24600 7.55300 -1.15200
H -5.26100 6.17300 -1.24000
H -5.24600 5.89100 3.04900
C -6.39900 4.79300 0.84400
C -7.93100 2.40400 0.87700
C -6.47000 3.95300 -0.27800
C -7.19500 4.45400 1.94500
C -7.93400 3.27700 1.96800
C -7.22600 2.79500 -0.26600
H -5.85300 4.16500 -1.15000
H -7.21400 5.10600 2.81800
H -8.50200 3.01100 2.86000
H -7.21100 2.13100 -1.13100
O 2.18500 10.15200 -0.96300
O -3.25800 10.03300 -0.10600
C 2.76600 11.17100 -1.72900
H 2.50700 12.16800 -1.33900
H 2.46000 11.11400 -2.78500
H 3.84800 11.02700 -1.66100
C -4.09500 11.00800 -0.66400
H -3.77500 12.02500 -0.38600
H -5.09400 10.82300 -0.26000
H -4.13100 10.93600 -1.76200
H -7.19300 0.77400 2.73100
C -7.78900 0.25600 1.97900
C -8.39100 0.99800 0.98300
C -8.30300 -1.84100 0.87200
C -9.19300 0.30700 0.02000
C -7.73600 -1.14100 1.91900
C -9.16500 -1.12700 -0.02200
C -10.06300 1.00600 -0.87800
H -7.08800 -1.67000 2.61600
C -10.84000 0.31500 -1.77600
H -11.50600 0.84200 -2.45400
C -10.83100 -1.09200 -1.80000
H -11.49600 -1.60100 -2.49200
C -10.03800 -1.80400 -0.93500
C -7.74900 -3.19300 0.62500
C -6.05200 -5.43400 0.25100
C -7.52200 -4.10700 1.65800
C -7.18700 -3.47500 -0.62600
C -6.35700 -4.56700 -0.80800
C -6.69200 -5.20800 1.47400
H -7.98000 -3.93600 2.63300
H -7.33800 -2.77300 -1.44500
H -5.86000 -4.70000 -1.76800
H -6.51700 -5.89100 2.30600
C -4.96200 -6.41600 0.08900
C -2.54100 -7.82000 -0.35300
C -4.04000 -6.62100 1.12600
C -4.69700 -7.03100 -1.14000
C -3.50600 -7.71200 -1.35800
C -2.85800 -7.31100 0.91200
H -4.21000 -6.14600 2.09200
H -5.41900 -6.94200 -1.95100
H -3.29700 -8.13400 -2.34200
H -2.12300 -7.38900 1.71300
O -10.09500 2.35500 -0.74400
O -10.05800 -3.15800 -0.84200
C -10.95300 3.08400 -1.57800
H -10.70300 2.94300 -2.64100
H -10.81600 4.13600 -1.31500
H -12.00600 2.80200 -1.42100
C -10.90100 -3.87000 -1.70600
H -10.64900 -3.68800 -2.76300
H -11.95900 -3.61100 -1.54300
H -10.74800 -4.92800 -1.47900

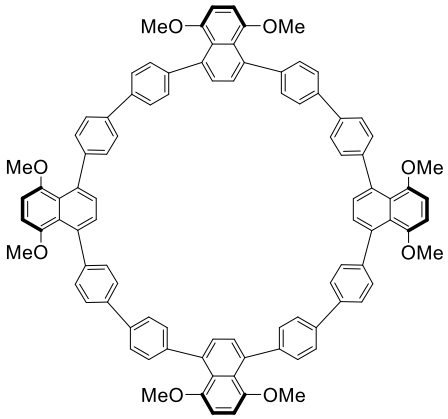

Calculation results at DFT-optimized geometry:
Total Energy: -4300.09055550 AU

SCF Convergence: 0.69E-08

Enthalpy Correction: 1.501879 AU

Free Energy Correction: 1.285748 AU

Three lowest frequencies (cm^{-1}): 3.81, 9.14, 11.32

H -6.19000 -1.79200 -2.66000
C -7.05500 -1.37000 -2.15000
C -7.84100 -2.19900 -1.37200
C -8.17100 0.63500 -1.35700
C -8.97700 -1.62200 -0.71800
C -7.21600 0.01600 -2.14200
C -9.14300 -0.19400 -0.71000
C -9.99100 -2.43300 -0.11100
H -6.47300 0.63100 -2.64700
C -11.06500 -1.85600 0.52000
H -11.83200 -2.47000 0.98300
C -11.22500 -0.45800 0.53100
H -12.11100 -0.04200 1.00300
C -10.31200 0.35700 -0.09200
C -7.92500 2.07700 -1.11500
C -6.67100 4.57800 -0.63700
C -7.73700 2.55500 0.18900
C -7.58600 2.93100 -2.16900
C -6.97100 4.15400 -1.93600
C -7.12900 3.77700 0.42000
H -8.01200 1.92400 1.03300
H -7.74900 2.59800 -3.19400
H -6.63700 4.74700 -2.78700
H -6.96200 4.09900 1.44800
C -5.75000 5.70800 -0.40700
C -3.60900 7.55400 -0.17800
C -4.85300 5.65600 0.67000
C -5.60500 6.76600 -1.31200
C -4.54900 7.66500 -1.20600
C -3.81300 6.56100 0.78600
H -4.91800 4.83400 1.38200
H -6.31400 6.87300 -2.13300
H -4.43200 8.45100 -1.95200
H -3.08800 6.44800 1.59300
O -9.83600 -3.77400 -0.24600
O -10.46500 1.70000 -0.20700
C -10.80600 -4.61500 0.31400
H -10.88100 -4.48100 1.40500
H -11.79800 -4.44400 -0.13300
H -10.48500 -5.63700 0.10000
C -11.60600 2.29000 0.35400
H -12.53000 1.89500 -0.09600
H -11.53200 3.36000 0.14400
H -11.64900 2.13900 1.44400
H -2.05500 7.60900 -2.24800
C -1.56100 8.04400 -1.38000
C -2.29200 8.23300 -0.22300
C 0.53700 8.50300 -0.25000
C -1.63100 8.82400 0.90000
C -0.16700 8.17600 -1.39300
C -0.20400 8.96200 0.88600
C -2.35900 9.32100 2.02900
H 0.38400 7.84100 -2.27100
C -1.69700 9.87400 3.09900
H -2.24600 10.25300 3.95600
C -0.29700 10.01200 3.08300
H 0.18600 10.49400 3.92900
C 0.43700 9.59600 1.99900
C 1.95800 8.08300 -0.22600
C 4.41000 6.67500 -0.46300
C 2.36600 7.16900 0.75300
C 2.84100 8.34500 -1.27700
C 4.04800 7.66200 -1.38700
C 3.55700 6.47800 0.63300
H 1.69200 6.94100 1.57800
H 2.56400 9.07700 -2.03500
H 4.70800 7.88200 -2.22600
H 3.79000 5.70100 1.36000
C 5.53400 5.74400 -0.68800
C 7.27900 3.55300 -1.14600
C 6.15700 5.07400 0.37400
C 5.89800 5.36600 -1.98500
C 6.75500 4.29500 -2.20800
C 7.00400 4.00100 0.15300
H 5.93800 5.37200 1.39900
H 5.43600 5.86000 -2.83900
H 6.97500 3.98900 -3.23100
H 7.41300 3.45600 1.00300
O -3.71100 9.25300 1.93900
O 1.77400 9.79400 1.88000
C -4.47100 9.73900 3.01100
H -4.29800 10.81400 3.17600
H -4.25200 9.19700 3.94500
H -5.51800 9.57900 2.74300
C 2.44100 10.44700 2.92600
H 2.04400 11.46100 3.08800
H 3.49000 10.51200 2.62800
H 2.36900 9.88300 3.87000
H 6.19100 1.79300 -2.66100
C 7.05500 1.37100 -2.15000
C 7.84200 2.19900 -1.37200
C 8.17100 -0.63500 -1.35800
C 8.97700 1.62200 -0.71800
C 7.21700 -0.01500 -2.14300
C 9.14300 0.19400 -0.71000
C 9.99100 2.43200 -0.11000
H 6.47300 -0.63000 -2.64800
C 11.06500 1.85500 0.52100
H 11.83300 2.46900 0.98400
C 11.22600 0.45700 0.53100
H 12.11100 0.04000 1.00300
C 10.31200 -0.35800 -0.09200
C 7.92500 -2.07700 -1.11500
C 6.67100 -4.57800 -0.63700
C 7.58600 -2.93000 -2.17000
C 7.73700 -2.55500 0.18800
C 7.12900 -3.77700 0.42000
C 6.97000 -4.15400 -1.93600
H 7.74900 -2.59800 -3.19500

H 8.01300 -1.92400 1.03200
H 6.96200 -4.09900 1.44800
H 6.63600 -4.74700 -2.78700
C 5.75000 -5.70800 -0.40700
C 3.60800 -7.55300 -0.17800
C 4.85300 -5.65500 0.67000
C 5.60500 -6.76600 -1.31100
C 4.54900 -7.66500 -1.20400
C 3.81300 -6.56000 0.78700
H 4.91800 -4.83200 1.38100
H 6.31400 -6.87400 -2.13200
H 4.43200 -8.45200 -1.95100
H 3.08800 -6.44700 1.59200
O 9.83700 3.77300 -0.24500
O 10.46500 -1.70100 -0.20900
C 10.80800 4.61300 0.31500
H 11.80000 4.44200 -0.13200
H 10.88300 4.48000 1.40600
H 10.48700 5.63600 0.10100
C 11.60600 -2.29100 0.35200
H 12.53000 -1.89600 -0.09800
H 11.53100 -3.36200 0.14100
H 11.64900 -2.14100 1.44200
H 2.05600 -7.60900 -2.24800
C 1.56100 -8.04400 -1.38000
C 2.29200 -8.23300 -0.22300
C -0.53700 -8.50300 -0.25100
C 1.63000 -8.82400 0.90100
C 0.16800 -8.17600 -1.39300
C 0.20300 -8.96200 0.88600
C 2.35800 -9.32100 2.03000
H -0.38300 -7.84100 -2.27200
C 1.69600 -9.87300 3.09900
H 2.24500 -10.25200 3.95700
C 0.29600 -10.01100 3.08300
H -0.18800 -10.49200 3.92900
C -0.43800 -9.59600 1.99900
C -1.95800 -8.08300 -0.22700
C -4.41000 -6.67500 -0.46400
C -2.84000 -8.34400 -1.27800
C -2.36600 -7.16900 0.75300
C -3.55800 -6.47800 0.63300
C -4.04700 -7.66200 -1.38900
H -2.56300 -9.07700 -2.03600
H -1.69200 -6.94200 1.57800
H -3.79100 -5.70200 1.36000
H -4.70800 -7.88200 -2.22700
C -5.53400 -5.74500 -0.68900
C -7.27900 -3.55300 -1.14700
C -5.89700 -5.36500 -1.98600
C -6.15800 -5.07500 0.37300
C -7.00500 -4.00200 0.15200
C -6.75400 -4.29400 -2.20900
H -5.43500 -5.85900 -2.84000
H -5.94000 -5.37400 1.39800
H -7.41400 -3.45700 1.00200
H -6.97400 -3.98700 -3.23200
O 3.71000 -9.25300 1.94000
O -1.77500 -9.79400 1.88000
C 4.47000 -9.74000 3.01300
H 4.25000 -9.19700 3.94600
H 5.51700 -9.58000 2.74400
H 4.29600 -10.81500 3.17800
C -2.44200 -10.44600 2.92600
H -2.37000 -9.88300 3.86900
H -2.04500 -11.46000 3.08700
H -3.49100 -10.51100 2.62700

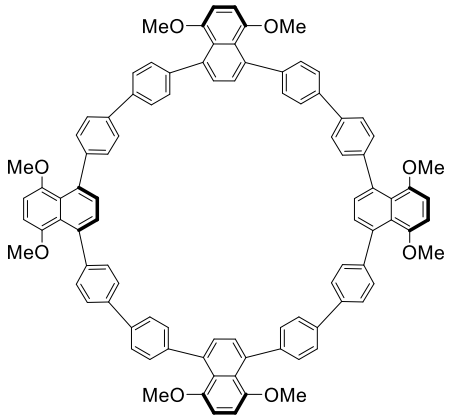

Calculation results at DFT-optimized geometry:
Total Energy: -4300.09195457 AU

SCF Convergence: 0.68E-08

Enthalpy Correction: 1.503142 AU

Free Energy Correction: 1.288753 AU

Three lowest frequencies (cm^{-1}): 9.01, 10.13, 12.28

H 6.76500 0.08100 2.47700
C 7.41500 0.63700 1.80300
C 8.28700 -0.06100 0.98900
C 7.82500 2.73100 0.65000
C 9.13500 0.69600 0.11500
C 7.19900 2.00800 1.64600
C 8.88500 2.09900 -0.07400
C 10.26100 0.10700 -0.54500
H 6.39900 2.48300 2.21400
C 11.03200 0.84500 -1.40900
H 11.88300 0.39800 -1.91500
C 10.77000 2.21300 -1.61600
H 11.42400 2.77100 -2.28000
C 9.74600 2.83800 -0.94900
C 7.16500 4.01700 0.31400
C 5.26400 6.06400 -0.15700
C 6.59000 4.18900 -0.95000
C 6.85400 4.95200 1.30400
C 5.92900 5.96200 1.07000
C 5.65500 5.18600 -1.17800
H 6.82000 3.47400 -1.73900
H 7.31700 4.86000 2.28700
H 5.69300 6.66500 1.86900
H 5.14800 5.22600 -2.14200
C 4.07400 6.92100 -0.33200
C 1.52300 8.10000 -0.70800
C 3.68500 7.42300 -1.57900
C 3.19500 7.11500 0.74300
C 1.95200 7.69500 0.56200
C 2.43100 7.99400 -1.76500
H 4.36400 7.33900 -2.42800
H 3.45400 6.71700 1.72400
H 1.26100 7.76100 1.40100
H 2.13500 8.33700 -2.75700
O 10.53100 -1.18200 -0.22000
O 9.50500 4.17100 -1.02900
C 11.62500 -1.80700 -0.83400
H 11.51100 -1.84400 -1.92900
H 12.57100 -1.29700 -0.59400
H 11.65500 -2.82700 -0.44200
C 10.36000 4.95200 -1.81800

H 11.40100 4.89700 -1.46300
H 10.00200 5.98100 -1.73000
H 10.33000 4.65000 -2.87700
H 0.10400 6.91500 -2.51100
C -0.52400 7.53100 -1.86900
C 0.07900 8.34800 -0.93200
C -2.73000 7.89600 -0.92500
C -0.76400 9.16200 -0.11000
C -1.90500 7.30900 -1.86500
C -2.18100 8.93400 -0.10500
C -0.23800 10.23500 0.68000
H -2.31100 6.52600 -2.50500
C -1.06700 10.99100 1.47200
H -0.67200 11.80600 2.07300
C -2.45600 10.76500 1.47900
H -3.08400 11.41100 2.08700
C -3.01100 9.78600 0.69200
C -4.02500 7.20900 -0.69800
C -6.07600 5.28700 -0.32500
C -4.30700 6.68900 0.57100
C -4.85200 6.82200 -1.75600
C -5.86200 5.88500 -1.57200
C -5.30500 5.74800 0.75200
H -3.67400 6.96900 1.41200
H -4.67900 7.24100 -2.74800
H -6.47700 5.58900 -2.42200
H -5.42800 5.29000 1.73300
C -6.93400 4.09800 -0.15400
C -8.08800 1.55200 0.31200
C -7.01000 3.13600 -1.17100
C -7.54900 3.79400 1.06600
C -8.10600 2.54200 1.29700
C -7.58000 1.89400 -0.94700
H -6.52800 3.33100 -2.12900
H -7.56000 4.53800 1.86200
H -8.53100 2.31200 2.27400
H -7.55900 1.13800 -1.73200
O 1.09200 10.47000 0.55100
O -4.34900 9.58800 0.57600
C 1.65000 11.53500 1.27100
H 1.53700 11.39600 2.35800
H 1.19500 12.49700 0.98800
H 2.71400 11.55000 1.02100
C -5.20600 10.39700 1.33500
H -5.02600 10.27800 2.41500
H -6.22200 10.06800 1.10300
H -5.10000 11.46100 1.07200
H -6.88800 0.34800 2.22600
C -7.48900 -0.35900 1.65400
C -8.30600 0.12300 0.65100
C -7.85000 -2.66800 0.99800
C -9.10300 -0.81700 -0.07600
C -7.25500 -1.72600 1.81600
C -8.89200 -2.22500 0.11900
C -10.15100 -0.39500 -0.95700
H -6.46500 -2.04300 2.49500
C -10.92300 -1.31800 -1.61900
H -11.72000 -1.00100 -2.28600
C -10.73600 -2.69700 -1.40400
H -11.40200 -3.39500 -1.90400
C -9.76900 -3.14600 -0.54000
C -7.17400 -3.98600 0.95400
C -5.23800 -6.06200 0.83600
C -6.68700 -4.59100 2.11700
C -6.75800 -4.52200 -0.27200
C -5.82100 -5.53900 -0.32800
C -5.73700 -5.60200 2.06100
H -7.01800 -4.22000 3.08800
H -7.13400 -4.08700 -1.19700
H -5.50000 -5.90800 -1.30100
H -5.31600 -5.98200 2.99100
C -4.03800 -6.91900 0.77700
C -1.49000 -8.16800 0.80600
C -3.14600 -6.78600 -0.29800
C -3.65500 -7.76500 1.82500
C -2.40200 -8.36800 1.84600
C -1.90800 -7.40200 -0.28800
H -3.39300 -6.11500 -1.12000
H -4.34000 -7.93700 2.65600
H -2.11300 -8.98600 2.69600
H -1.21200 -7.22800 -1.10800
O -10.34400 0.94400 -1.05000
O -9.61100 -4.45300 -0.21100
C -11.38900 1.40900 -1.86000
H -12.36600 1.03800 -1.51400
H -11.25100 1.11400 -2.91200
H -11.37100 2.49900 -1.78900
C -10.43800 -5.39900 -0.83100
H -11.49900 -5.23500 -0.58600
H -10.12600 -6.37500 -0.45000
H -10.32100 -5.38600 -1.92700
H -0.00200 -7.56200 2.84100
C 0.59700 -7.97700 2.03000
C -0.05000 -8.49400 0.92500
C 2.75700 -8.05800 0.93000
C 0.75100 -9.05400 -0.12200
C 1.98000 -7.76100 2.03300
C 2.16800 -8.83600 -0.11700
C 0.18300 -9.86200 -1.15900
H 2.42100 -7.18200 2.84400
C 0.97500 -10.37500 -2.15700
H 0.54700 -10.98900 -2.94500
C 2.36600 -10.16300 -2.15100
H 2.96400 -10.62100 -2.93400
C 2.96000 -9.43800 -1.14700
C 4.02700 -7.30400 0.81000
C 6.05000 -5.31400 0.77500
C 4.94800 -7.19500 1.85400
C 4.19100 -6.45700 -0.29300
C 5.17100 -5.48200 -0.30500
C 5.94700 -6.22700 1.83100
H 4.86400 -7.86500 2.71100
H 3.48000 -6.51800 -1.11700
H 5.19900 -4.77700 -1.13400
H 6.64500 -6.16600 2.66700
C 6.91400 -4.11800 0.83300
C 8.07300 -1.52700 0.94600
C 7.23200 -3.51600 2.05600
C 7.30400 -3.44000 -0.33200
C 7.86000 -2.17400 -0.27900
C 7.80400 -2.25200 2.11000
H 6.95100 -4.00800 2.98700
H 7.12600 -3.89700 -1.30500
H 8.07700 -1.64400 -1.20500
H 7.99200 -1.79200 3.08000
O -1.14600 -10.11300 -1.05400
O 4.30300 -9.28200 -1.02900
C -1.74900 -10.90700 -2.03900
H -1.65200 -10.45700 -3.04000
H -2.80800 -10.97100 -1.77600
H -1.31900 -11.92100 -2.06300
C 5.12500 -9.86400 -2.00300
H 4.91500 -9.46200 -3.00600
H 5.01200 -10.95900 -2.02800
H 6.15300 -9.61400 -1.72600

References Cited

III-S1. APEX2 is a Bruker AXS crystallographic software package for single crystal data collection, reduction and preparation.

III-S2. Sheldrick, G. M., SHELXL-2014, Crystallographic software package, Bruker AXS, Inc., Madison, Wisconsin, USA.

III-S3. $R_1 = \sum(||F_o| - |F_c||) / \sum|F_o|$, $wR_2 = [\sum[w(F_o^2 - F_c^2)^2] / \sum[w(F_o^2)^2]]^{1/2}$, $R_{int.} = \sum|F_o^2 - F_o^2(mean)|^2 / \sum[F_o^2]$, and GOF = $[\sum[w(F_o^2 - F_c^2)^2] / (n-p)]^{1/2}$, where n is the number of reflections and p is the total number of parameters which were varied during the last refinement cycle.

III-S4. *International Tables for X-ray Crystallography*; Ibers, J. A.; Hamilton, W. C., Eds; Kynoch Press: Birmingham, 1974; Vol *4*, p 55.

III-S5. Sheldrick, G. M., SHELXL-2013, Crystallographic software package, Bruker AXS, Inc., Madison, Wisconsin, USA.

III-S6. Frisch, M. J.; Trucks, G. W.; Schlegel, H. B.; Scuseria, G. E.; Robb, M. A.; Cheeseman, J. R.; MontgomeryJr., J. A.; Vreven, T.; Kudin, K. N.; Burant, J. C.;Millam, J. M.; Iyengar, S. S.; Tomasi, J.; Barone, V.; Mennucci, B.; Cossi, M.; Scalmani, G.; Rega, N.; Petersson, G. A.; Nakatsuji, H.; Hada, M.; Ehara, M.; K. Toyota; Fukuda, R.; Hasegawa, J.; Ishida, M.; Nakajima, T.; Honda, Y.; Kitao, O.; Nakai, H.; Klene, M.; Li, X.; Knox, J. E.; Hratchian, H. P.; Cross, J. B.; Bakken, V.; Adamo, C.; Jaramillo, J.; Gomperts, R.; Stratmann, R. E.; Yazyev, O.; Austin, A. J.; Cammi, R.; Pomelli, C.; Ochterski, J. W.; Ayala, P. Y.; Morokuma, K.; Voth, G. A.; Salvador, P.; Dannenberg, J. J.; Zakrzewski, V. G.; Dapprich, S.; Daniels, A. D.; Strain, M. C.; Farkas, O.; Malick, D. K.; Rabuck, A. D.; Raghavachari, K.; Foresman, J. B.; Ortiz, J. V.; Cui, Q.; Baboul, A. G.; Clifford, S.; Cioslowski, J.; Stefanov, B. B.; Liu, G.; Liashenko, A.; Piskorz, P.; Komaromi, I.; Martin, R. L.; Fox, D. J.; Keith, T.; Al-Laham, M. A.; Peng, C. Y.; Nanayakkara, A.; Challacombe, M.; Gill, P. M. W.; Johnson, B.; Chen, W.; Wong, M. W.; Gonzalez, C.; Pople, J. A.; Gaussian, Inc.: Wallingford CT, 2004.

III-S7. Zhao, Y.; Truhlar, D. G. *Theor. Chem. Acc.* **2008**, *120*, 215–241.

UV-vis and Fluorescence Spectra.

a)

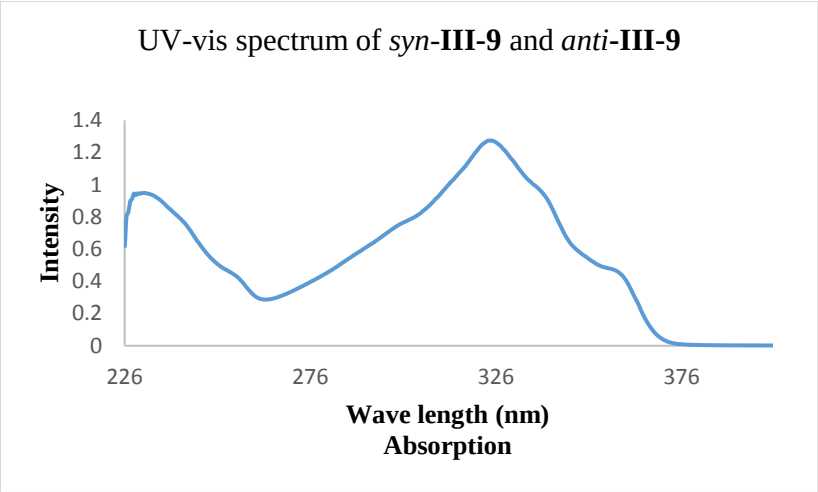

Spectrum a): UV-vis absorption spectrum of *syn*-**III-9** and *anti*-**III-9** at the concentration of 1.8×10^{-5} M in degassed CH_2Cl_2. At the absorption maximum λ_{abs} = 325 nm, $\varepsilon = 7.2 \times 10^4$ cm^{-1} M^{-1}.

b)

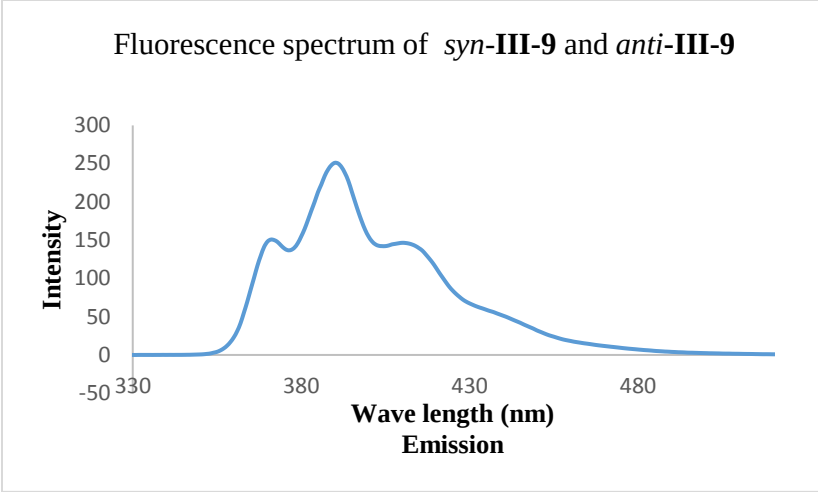

Spectrum b): Fluorescence spectrum of *syn*-**III-9** and *anti*-**III-9** at the concentration of 1.8×10^{-8} M in degassed CH_2Cl_2 upon excitation at 325 nm. Fluorescence maximum λ_{em} = 390 nm.

c)

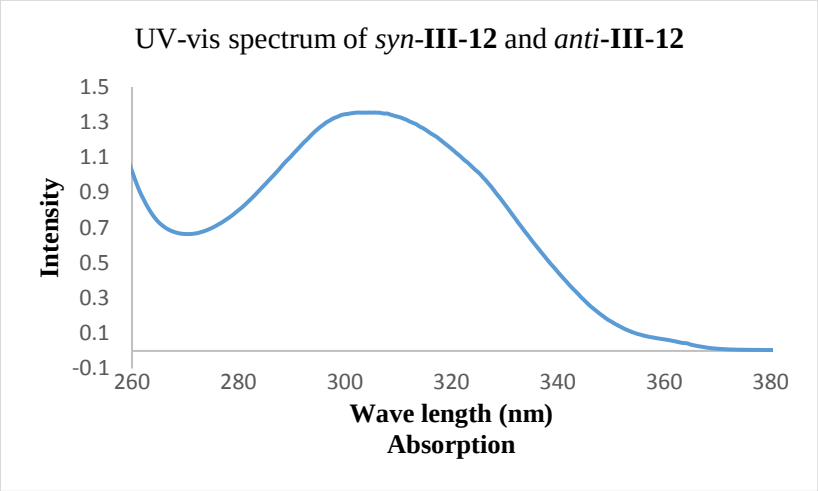

Spectrum c): UV-vis absorption spectrum of *syn*-**III-12** and *anti*-**III-12** at the concentration of 4.2×10^{-5} M in degassed CH_2Cl_2. At the absorption maximum $\lambda_{abs} = 306$ nm, $\varepsilon = 3.2 \times 10^4$ cm^{-1} M^{-1}.

d)

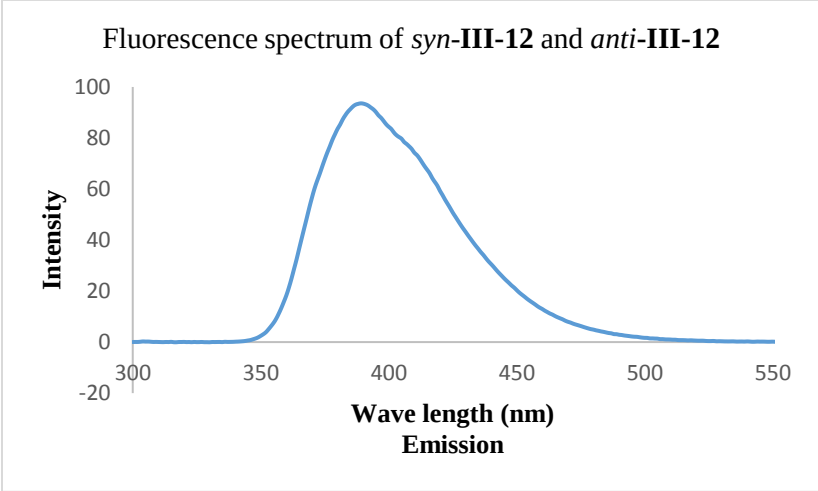

Spectrum d): Fluorescence spectrum of *syn*-**III-12** and *anti*-**III-12** at the concentration of 4.2×10^{-5} M in degassed CH_2Cl_2 upon excitation at 306 nm. Fluorescence maximum $\lambda_{em} = 389$ nm.

e)

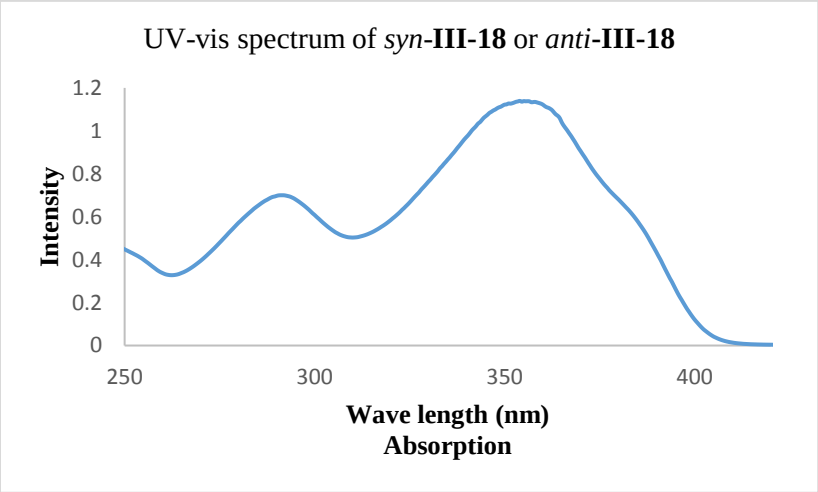

Spectrum e): UV-vis absorption spectrum of ***syn*-III-18** or ***anti*-III-18** at the concentration of 1.3×10^{-5} M in degassed CH_2Cl_2. At the absorption maximum λ_{abs} = 358 nm, $\varepsilon = 9.1 \times 10^4$ cm^{-1} M^{-1}.

f)

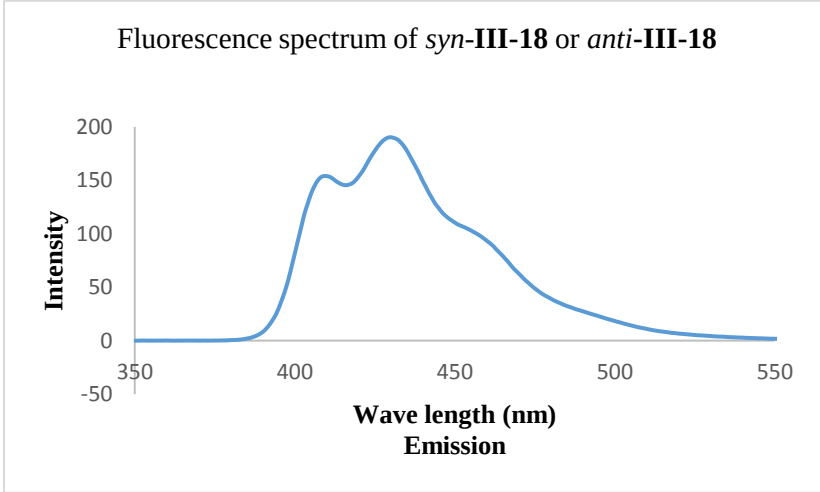

Spectrum f): Fluorescence spectrum of ***syn*-III-18** or ***anti*-III-18** at the concentration of 1.3×10^{-5} M in degassed CH_2Cl_2 upon excitation at 358 nm. Fluorescence maximum λ_{em} = 430 nm.

g)

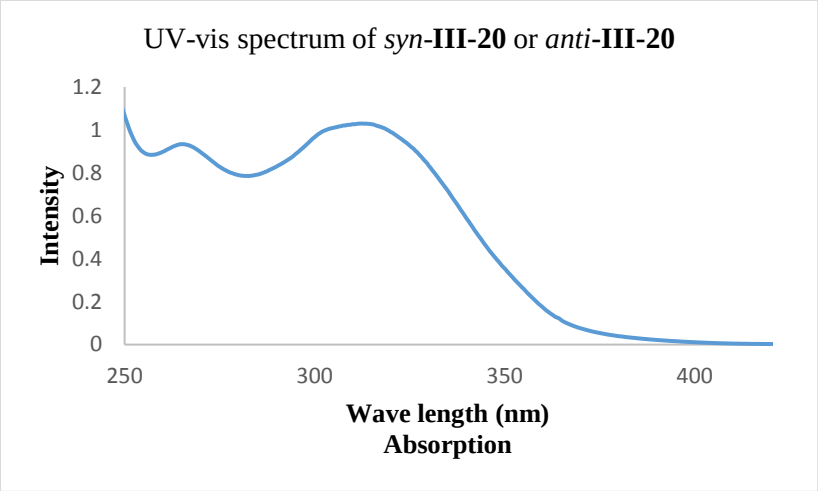

Spectrum g): UV-vis absorption spectrum of *syn*-**III-20** or *anti*-**III-20** at the concentration of 2.9×10^{-5} M in degassed CH_2Cl_2. At the absorption maximum λ_{abs} = 313 nm, $\varepsilon = 3.5 \times 10^4$ cm^{-1} M^{-1}.

h)

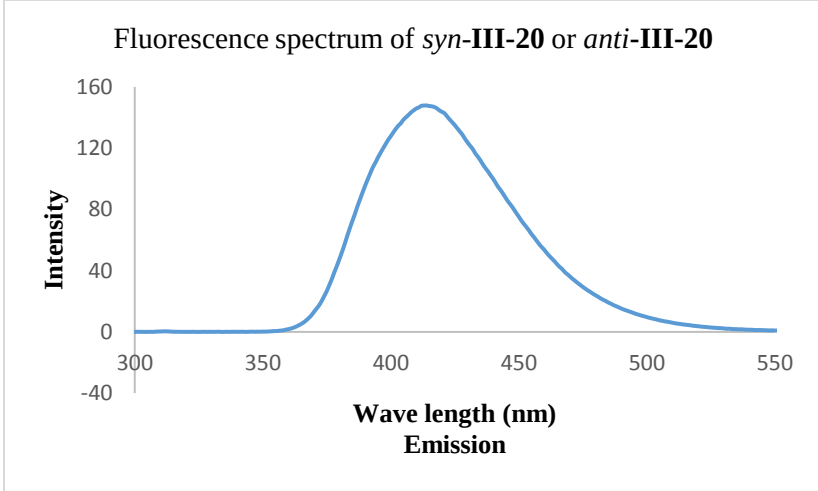

Spectrum h): Fluorescence spectrum of *syn*-**III-20** or *anti*-**III-20** at the concentration of 2.9×10^{-5} M in degassed CH_2Cl_2 upon excitation at 313 nm. Fluorescence maximum λ_{em} = 414 nm.

i)

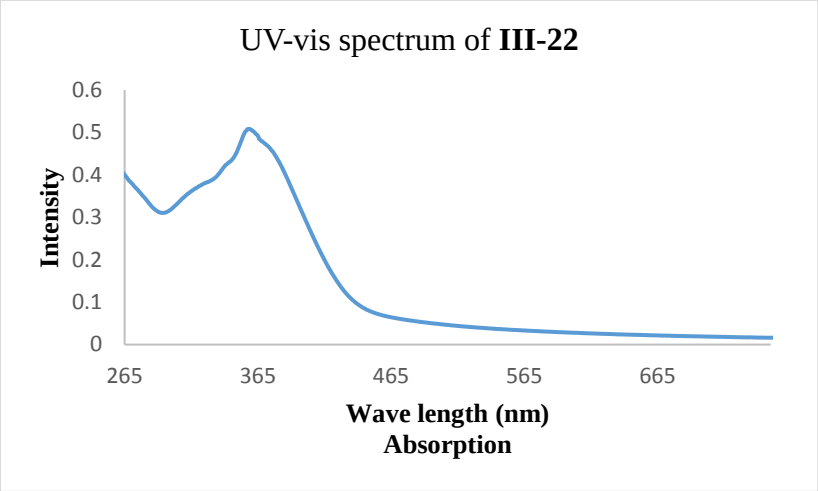

Spectrum i): UV-vis absorption spectrum of **III-22** in degassed CH_2Cl_2. At the absorption maximum λ_{abs} = 358 nm.

j)

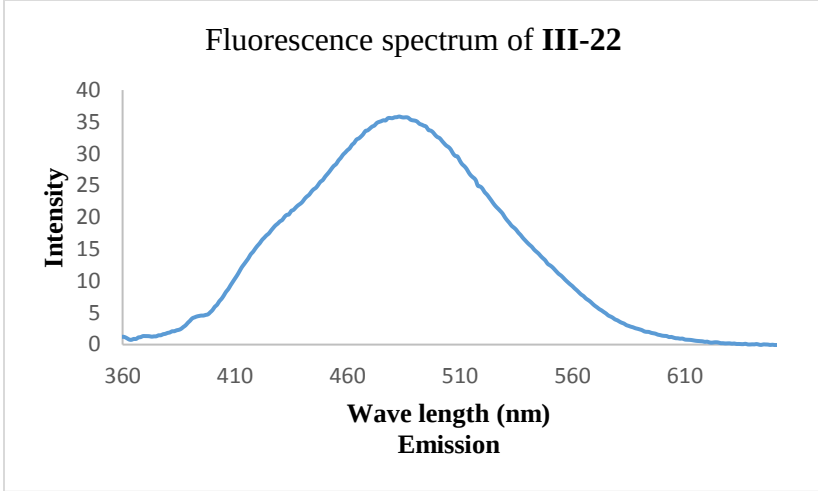

Spectrum j): Fluorescence spectrum of **III-22** in degassed CH_2Cl_2 upon excitation at 358 nm. Fluorescence maximum λ_{em} = 483 nm.

k)

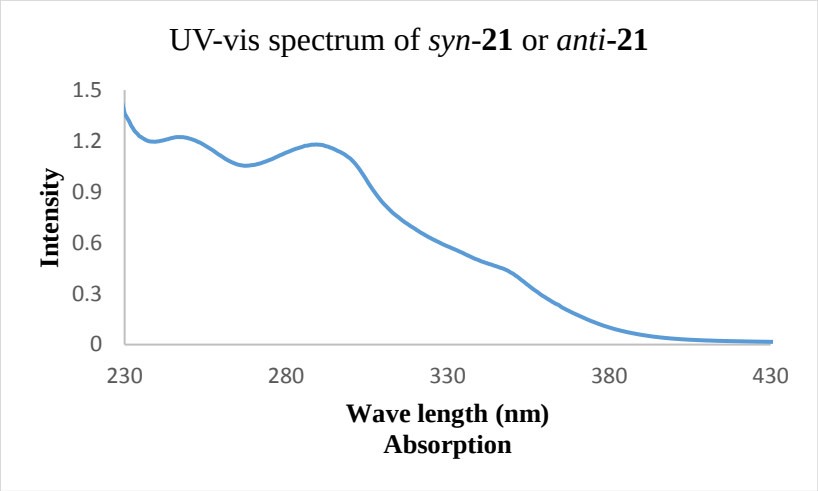

Spectrum k): UV-vis absorption spectrum of *syn*-**21** or *anti*-**21** at the concentration of 4.9×10^{-5} M in degassed CH_2Cl_2. At the absorption maximum λ_{abs} = 290 nm, $\varepsilon = 2.4 \times 10^4$ cm^{-1} M^{-1}.

l)

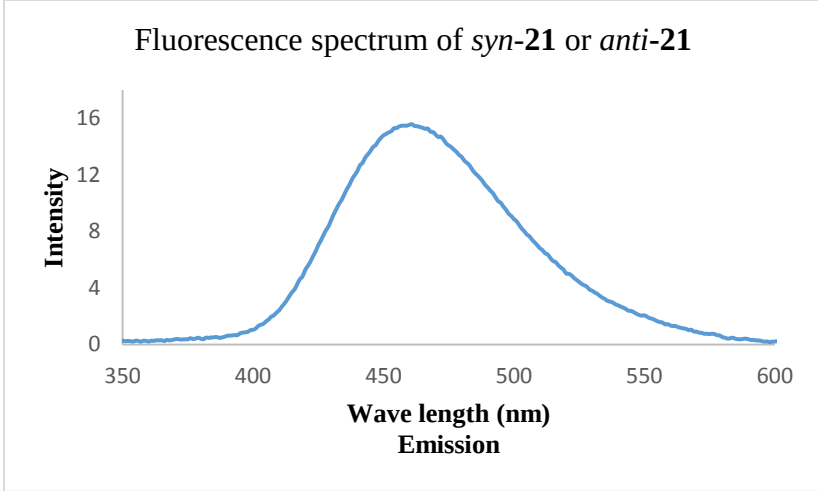

Spectrum l): Fluorescence spectrum of *syn*-**21** or *anti*-**21** at the concentration of 4.9×10^{-5} M in degassed CH_2Cl_2 upon excitation at 290 nm. Fluorescence maximum λ_{em} = 461 nm.

m)

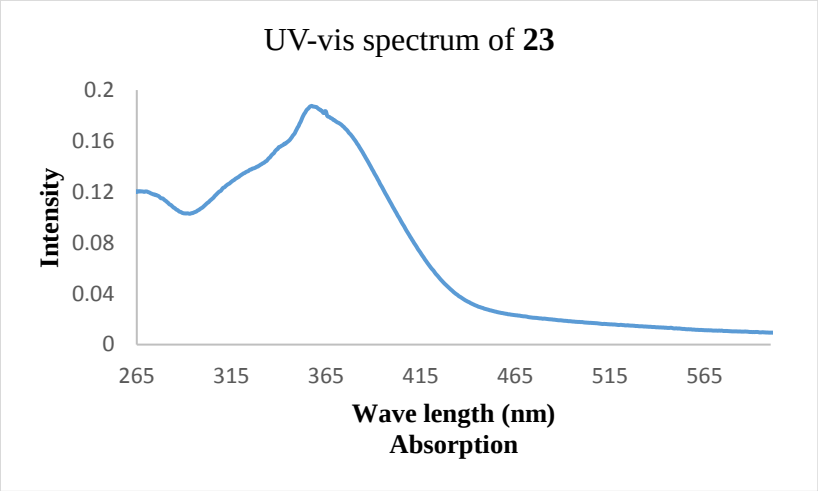

Spectrum m): UV-vis absorption spectrum of **23** in degassed CH_2Cl_2. At the absorption maximum λ_{abs} = 358 nm.

n)

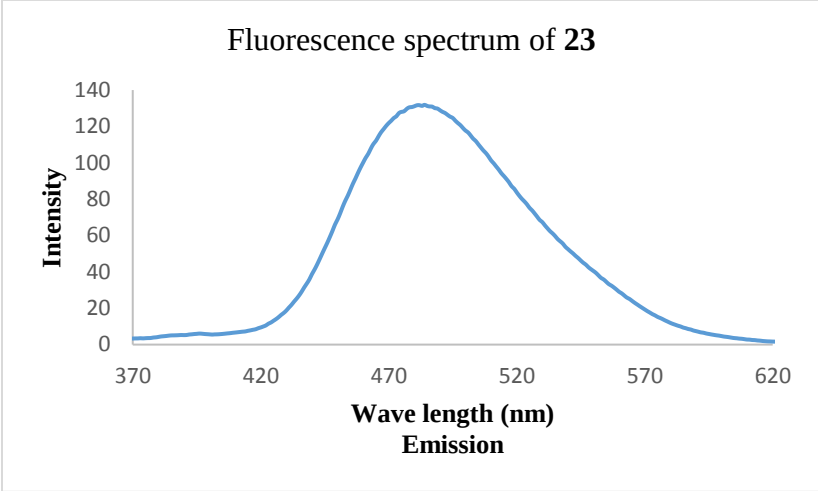

Spectrum n): Fluorescence spectrum of **23** in degassed CH_2Cl_2 upon excitation at 358 nm. Fluorescence maximum λ_{em} = 484 nm.

o)

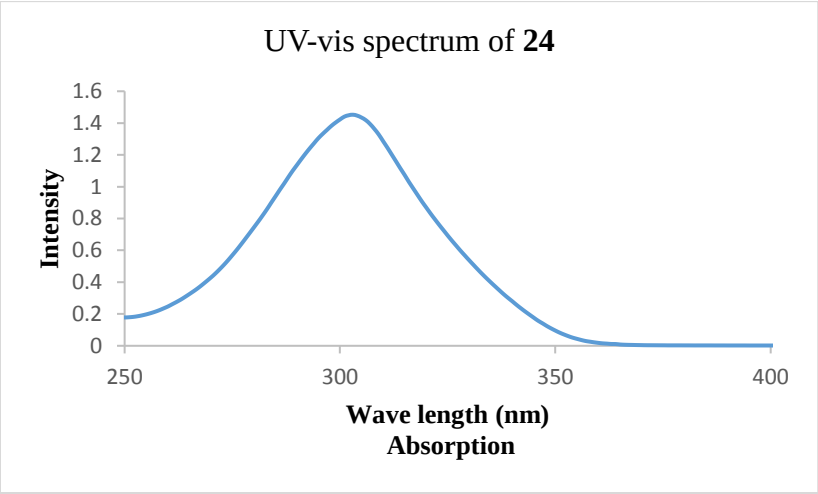

Spectrum o): UV-vis absorption spectrum of **24** in degassed CH_2Cl_2. At the absorption maximum λ_{abs} = 303 nm.

p)

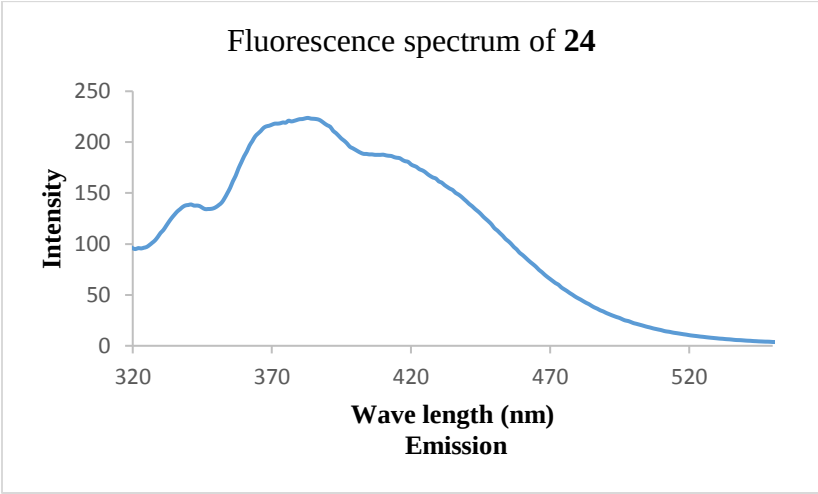

Spectrum p): Fluorescence spectrum of **24** in degassed CH_2Cl_2 upon excitation at 303 nm. Fluorescence maximum λ_{em} = 383 nm.

q)

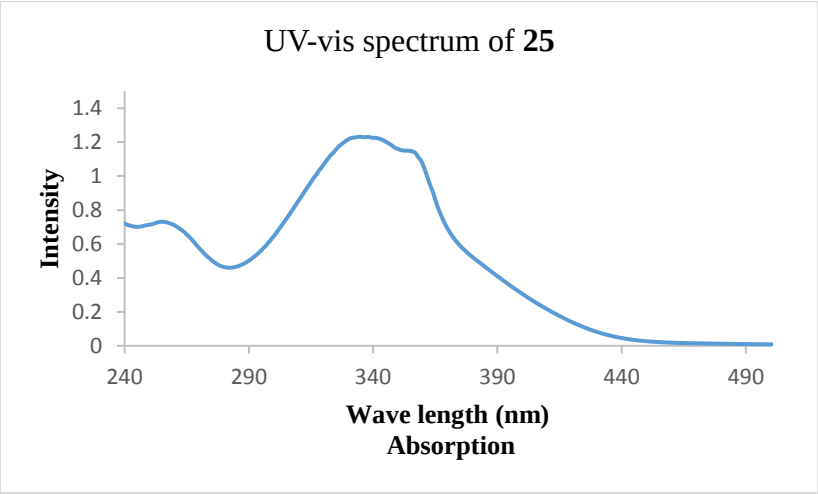

Spectrum q): UV-vis absorption spectrum of **25** in degassed CH_2Cl_2. At the absorption maximum λ_{abs} = 336 nm.

r)

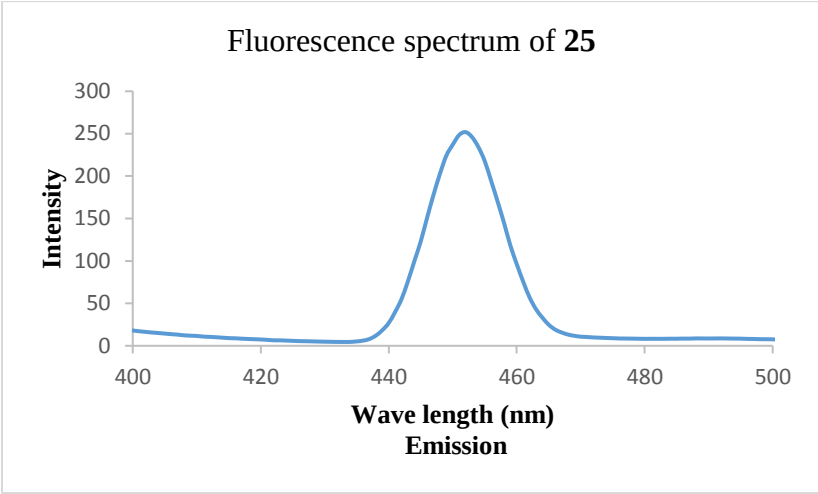

Spectrum r): Fluorescence spectrum of **25** in degassed CH_2Cl_2 upon excitation at 336 nm. Fluorescence maximum λ_{em} = 453 nm.

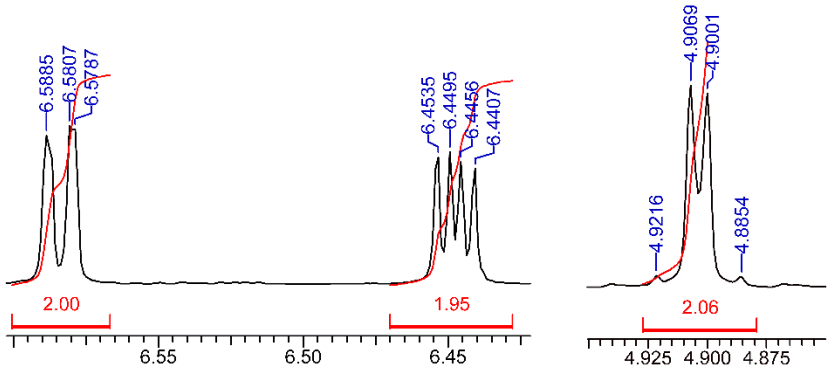
6.5885
6.5807
6.5787
6.4535
6.4495
6.4456
6.4407
2.00
1.95
6.55
6.50
6.45

4.9069
4.9001
4.9216
4.8854
2.06
4.925
4.900
4.875

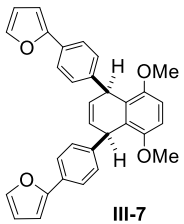
O
H
OMe
H
OMe
O

III-7

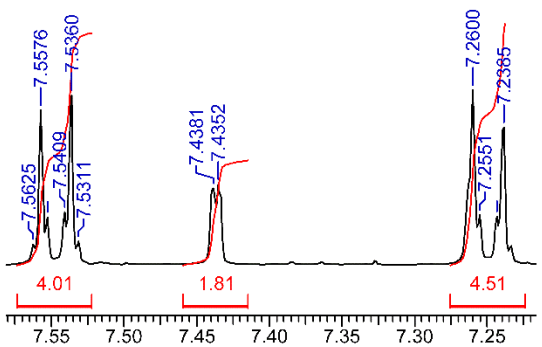
7.5576
7.5360
7.5625
7.5409
7.5311
7.4381
7.4352
7.2600
7.2385
7.2551
4.01
1.81
4.51
7.55
7.50
7.45
7.40
7.35
7.30
7.25

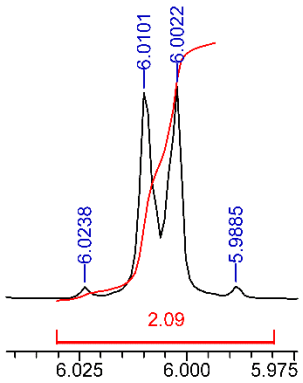
6.0101
6.0022
6.0238
5.9885
2.09
6.025
6.000
5.975

3.6100
7.6461
7.5576
7.5360
7.2600
7.2385
7.4352
7.5625
6.5885
6.5807
6.4495
6.4456
6.4407
6.0101
6.0022
4.9069
4.9001
4.01
1.81
4.51
2.05
2.00
1.95
2.09
2.06
6.00
10.0
9.5
9.0
8.5
8.0
7.5
7.0
6.5
6.0
5.5
5.0
4.5
4.0
3.5
3.0
2.5
2.0
1.5
1.0
0.5
0
-0.5

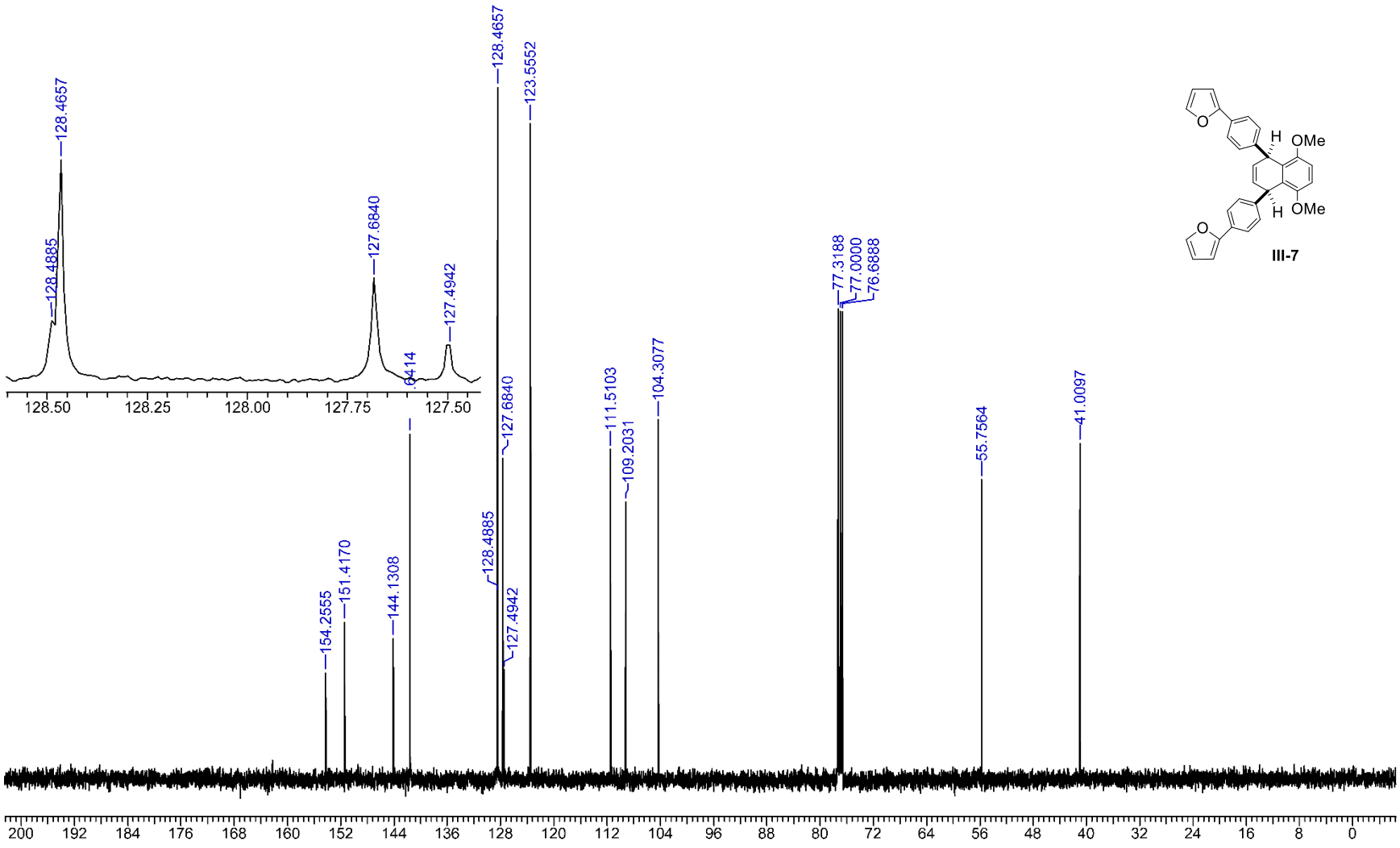
128.4657
128.4885
127.6840
127.4942
6414
128.50
128.25
128.00
127.75
127.50
128.4657
123.5552
127.6840
128.4885
127.4942
154.2555
151.4170
144.1308
111.5103
109.2031
104.3077
77.3188
77.0000
76.6888
55.7564
41.0097
200
192
184
176
168
160
152
144
136
128
120
112
104
96
88
80
72
64
56
48
40
32
24
16
8
0
O
H
OMe
H
OMe
O
III-7

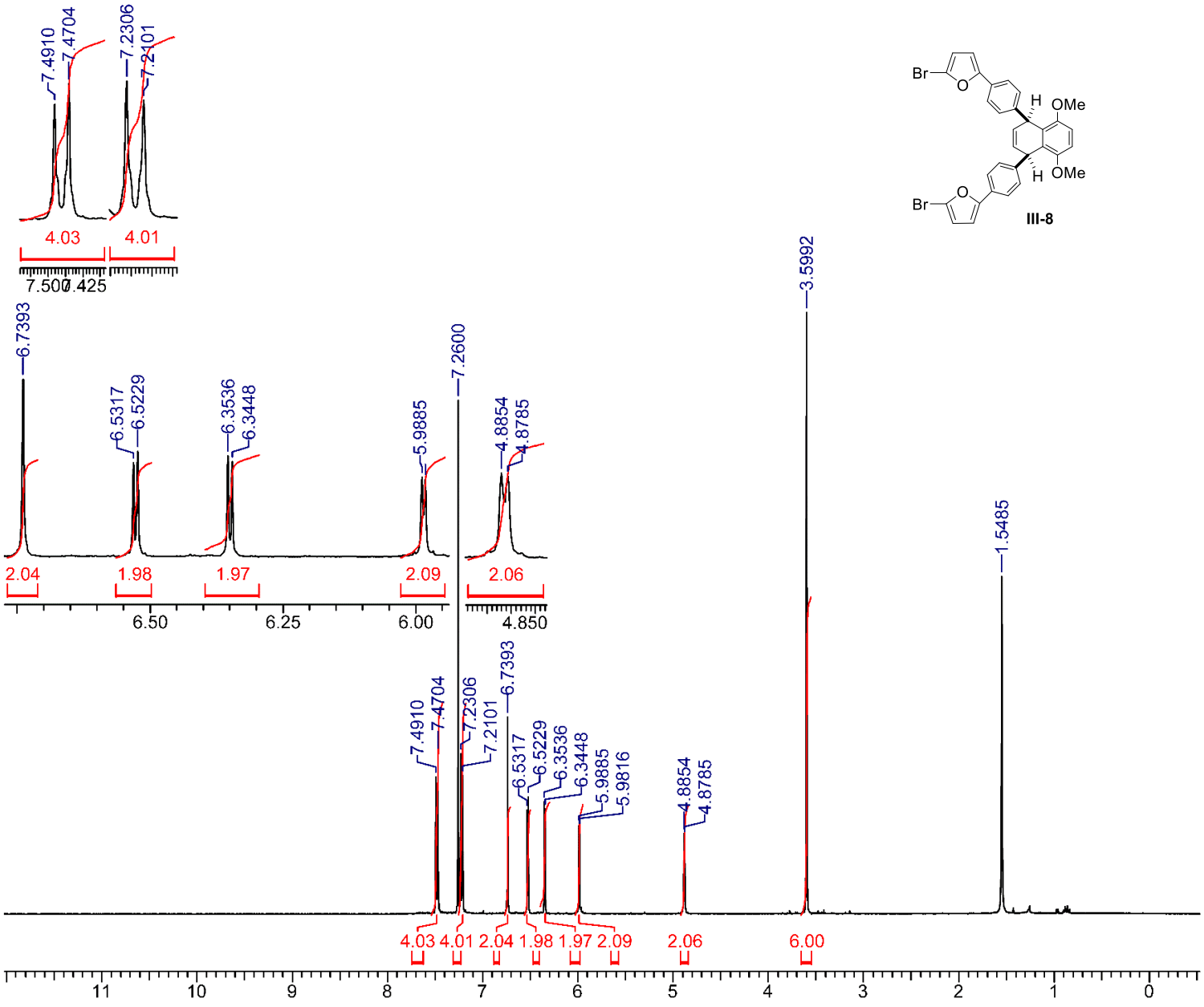
7.4910
7.4704
7.2306
7.2101
4.03
4.01
7.500
7.425
6.7393
6.5317
6.5229
6.3536
6.3448
5.9885
7.2600
4.8854
4.8785
2.04
1.98
1.97
2.09
2.06
6.50
6.25
6.00
4.850
3.5992
1.5485
5.9816
4.03 4.01 2.04 1.98 1.97 2.09
2.06
6.00
11
10
9
8
7
6
5
4
3
2
1
0
Br
O
H
OMe
III-8

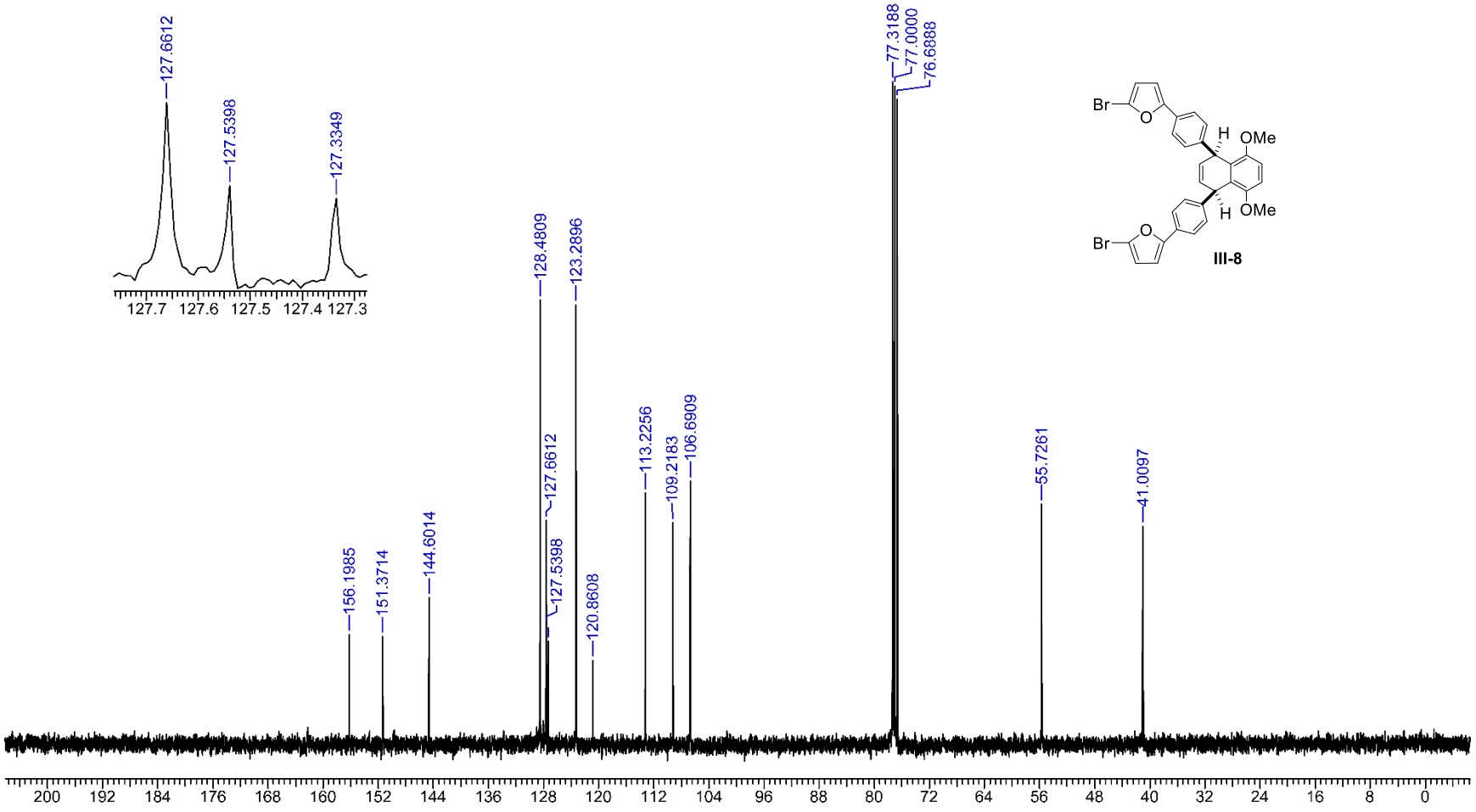
127.6612
127.5398
127.3349
127.7 127.6 127.5 127.4 127.3
77.3188
77.0000
76.6888
128.4809
123.2896
127.6612
127.5398
120.8608
156.1985
151.3714
144.6014
113.2256
109.2183
106.6909
55.7261
41.0097
Br
O
H
OMe
H
OMe
Br
O
III-8
200 192 184 176 168 160 152 144 136 128 120 112 104 96 88 80 72 64 56 48 40 32 24 16 8 0

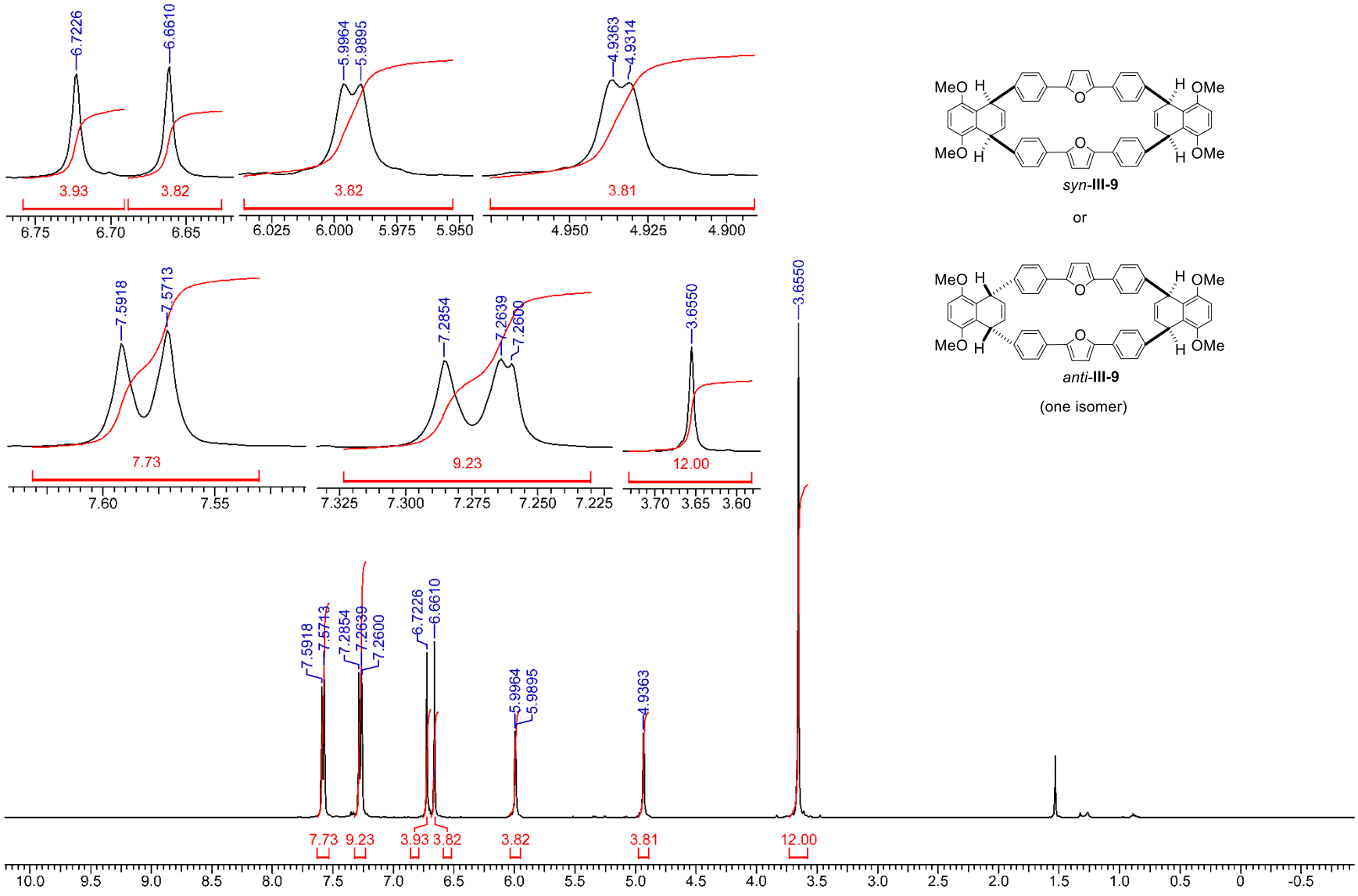

syn-**III-9**

or

anti-**III-9**

(one isomer)

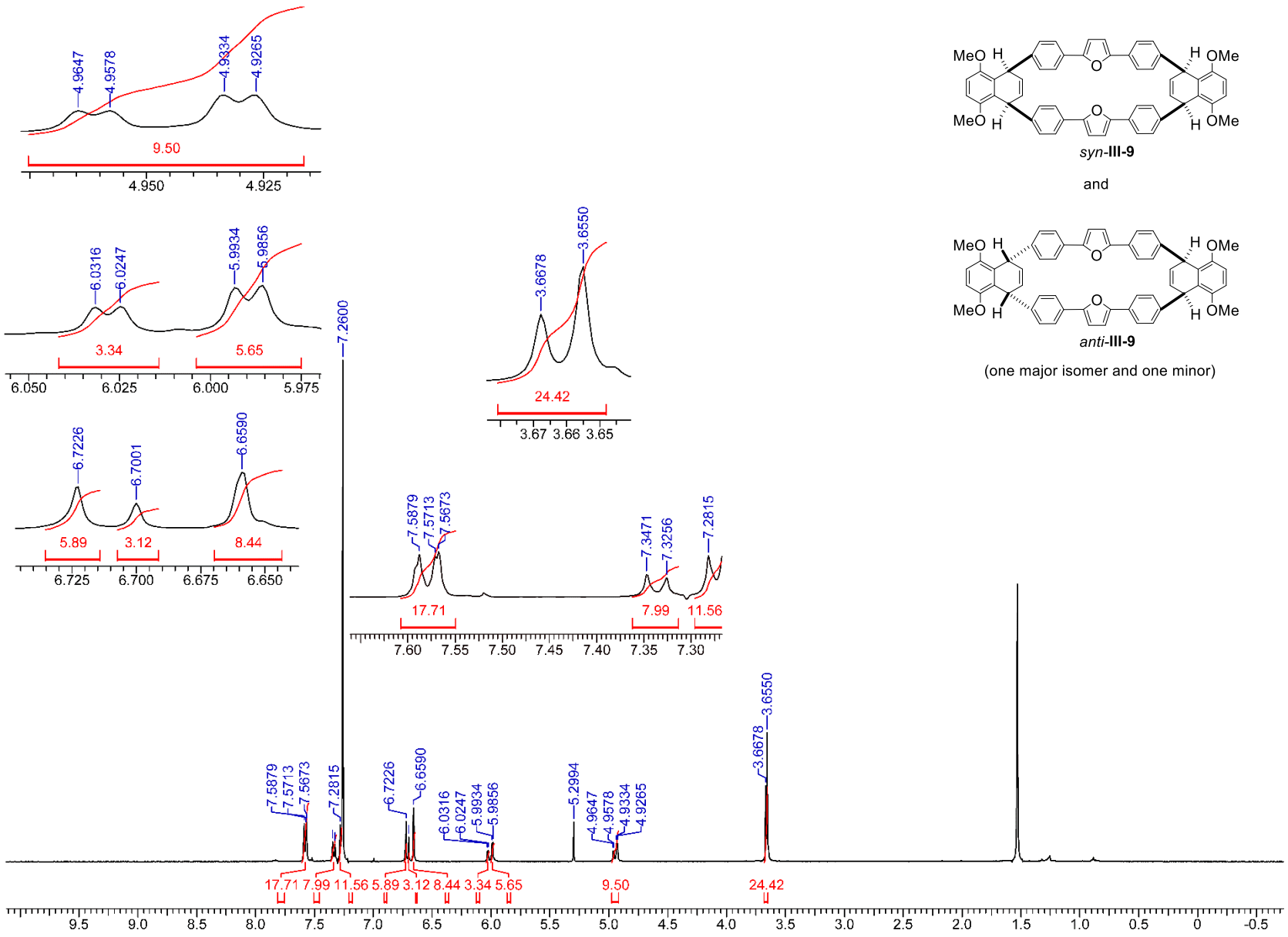

syn-**III-9**

and

anti-**III-9**

(one major isomer and one minor)

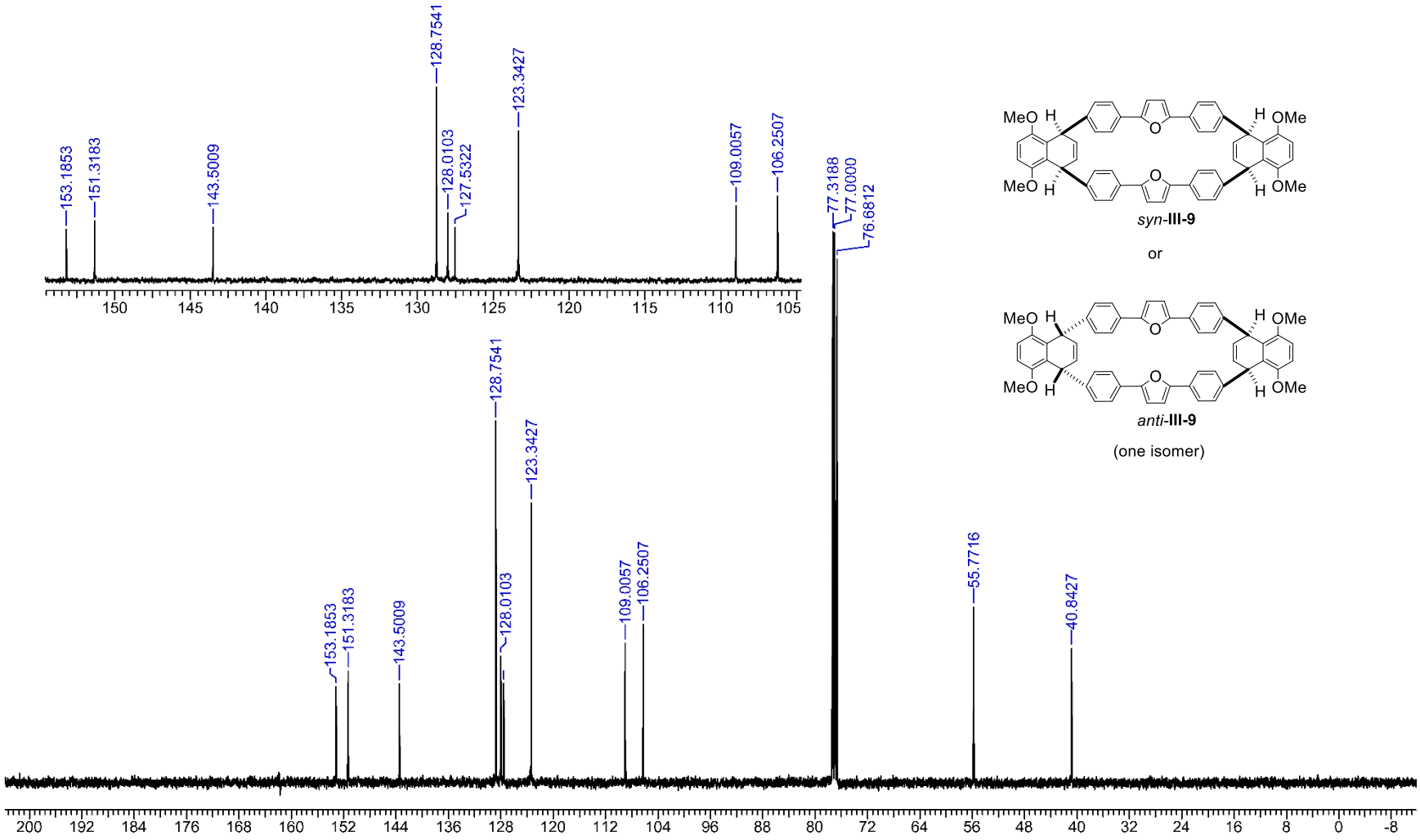
153.1853
151.3183
143.5009
128.7541
128.0103
127.5322
123.3427
109.0057
106.2507
77.3188
77.0000
76.6812
55.7716
40.8427
MeO
H
OMe
O
syn-III-9
or
anti-III-9
(one isomer)

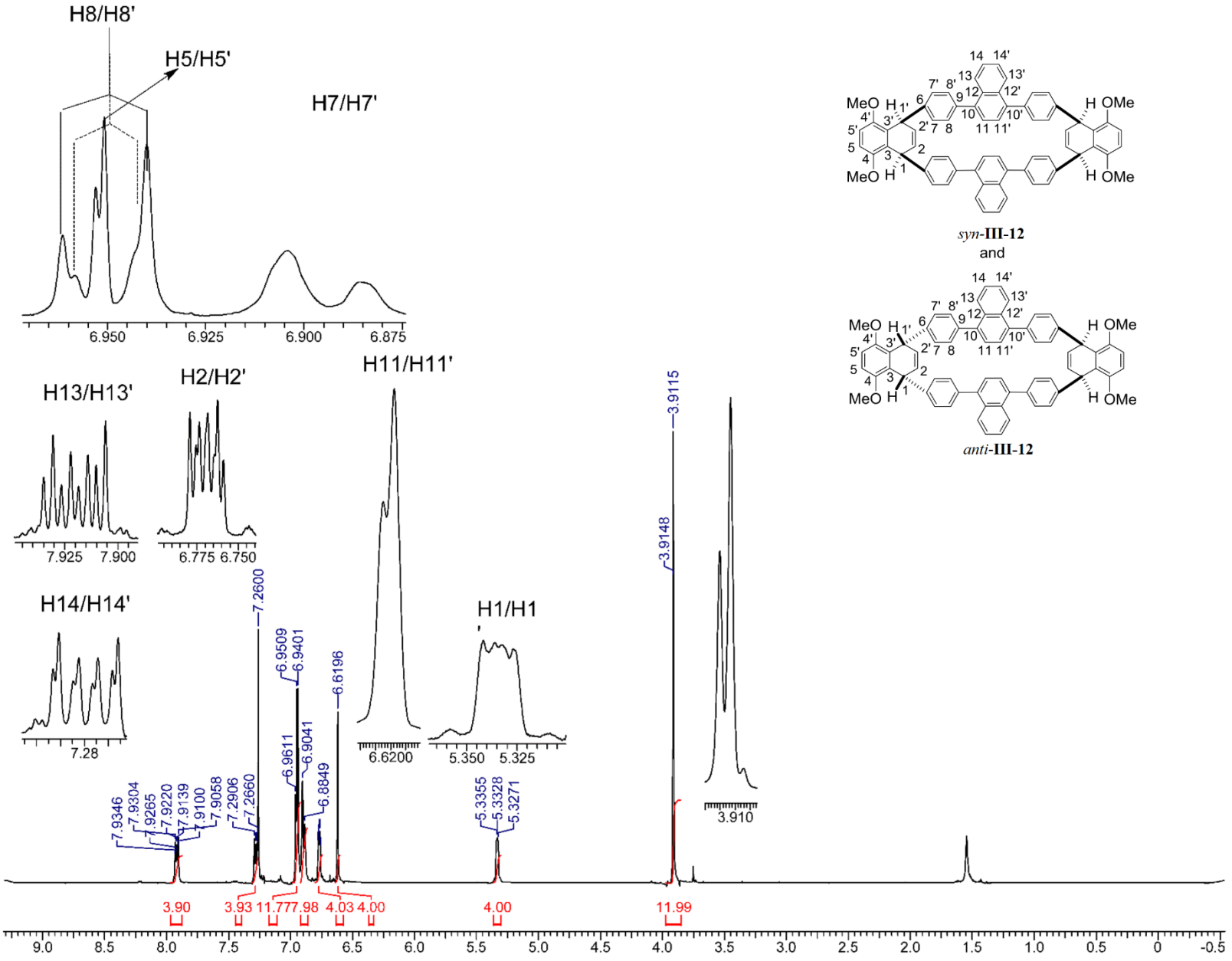

syn-**III-12**

and

anti-**III-12**

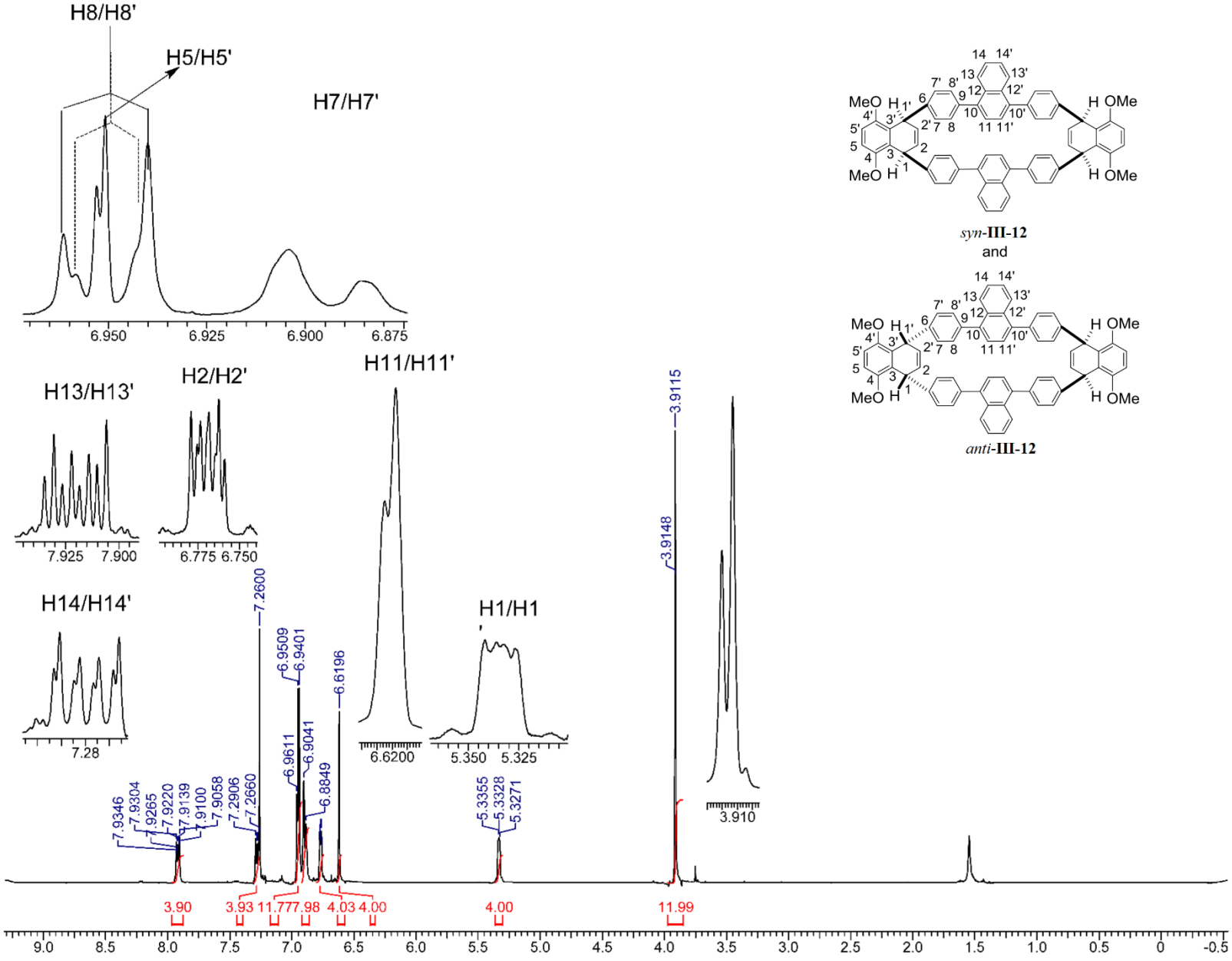

syn-**III-12**

and

anti-**III-12**

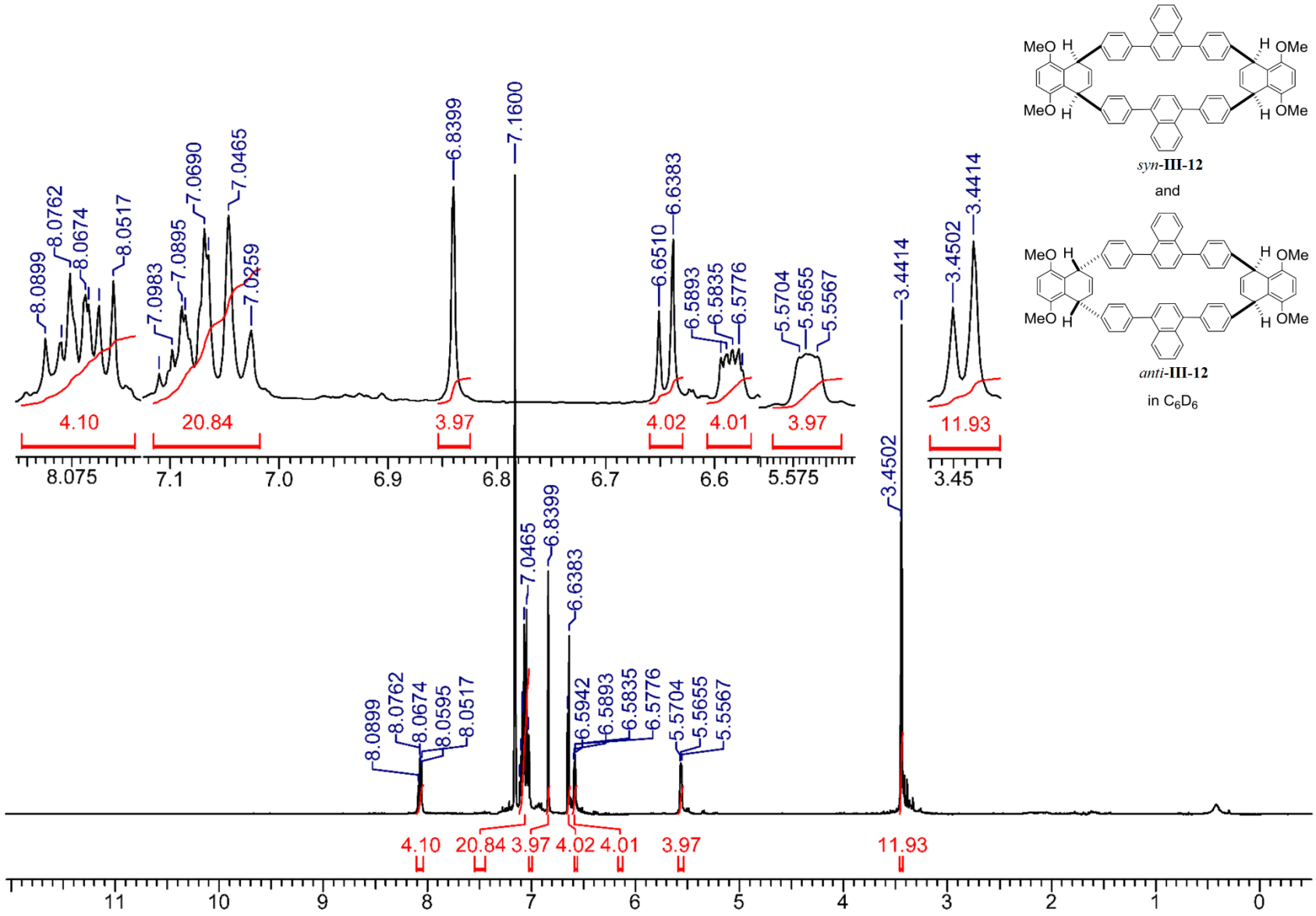
MeO H
H OMe
MeO H
H OMe
syn-III-12
and
MeO H
H OMe
MeO H
H OMe
anti-III-12
in C6D6
8.0899
8.0762
8.0674
8.0595
8.0517
7.0983
7.0895
7.0690
7.0465
7.0259
6.8399
7.1600
6.6510
6.6383
6.5942
6.5893
6.5835
6.5776
5.5704
5.5655
5.5567
3.4502
3.4414
4.10
20.84
3.97
4.02
4.01
3.97
11.93

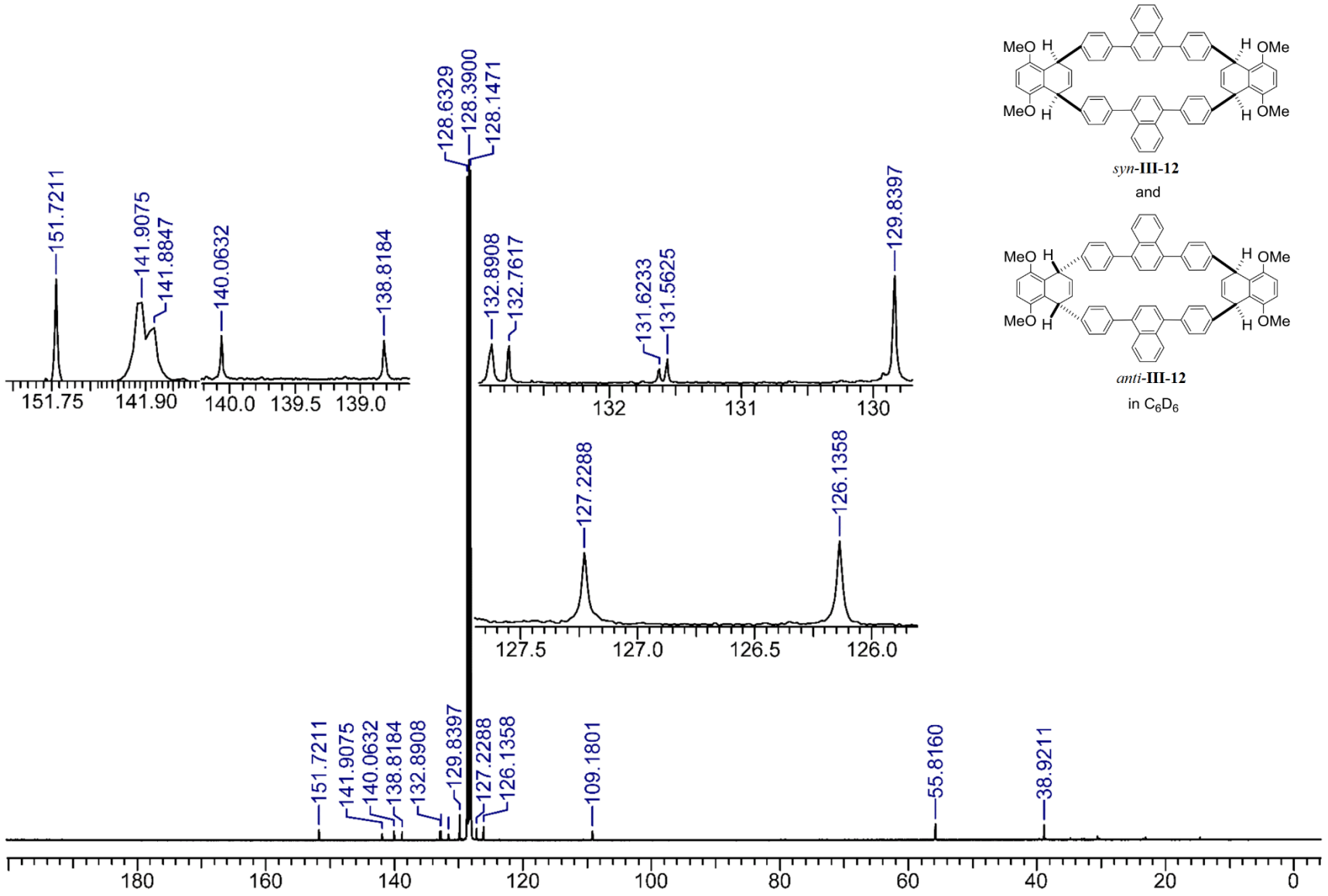
151.7211
141.9075
141.8847
140.0632
138.8184
128.6329
128.3900
128.1471
132.8908
132.7617
131.6233
131.5625
129.8397
127.2288
126.1358
151.75
141.90
140.0
139.5
139.0
132
131
130
127.5
127.0
126.5
126.0
180
160
140
120
100
80
60
40
20
0
109.1801
55.8160
38.9211
MeO
H
OMe
syn-III-12
and
anti-III-12
in C6D6

DPFGSENOE spectra

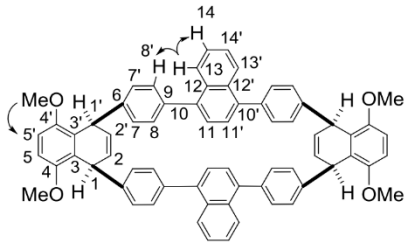

syn-**III-12**

and

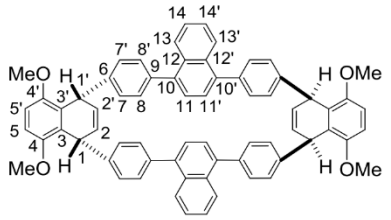

anti-**III-12**

One bond **gHSQC** correlations

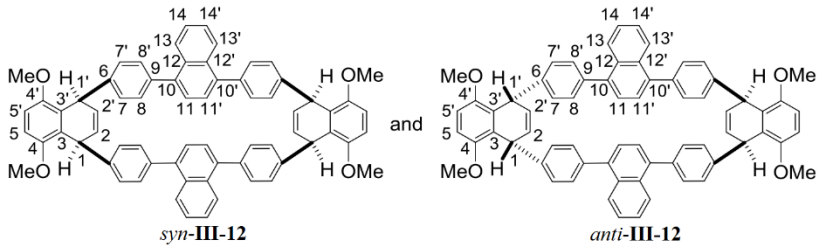

syn-**III-12** *anti*-**III-12**

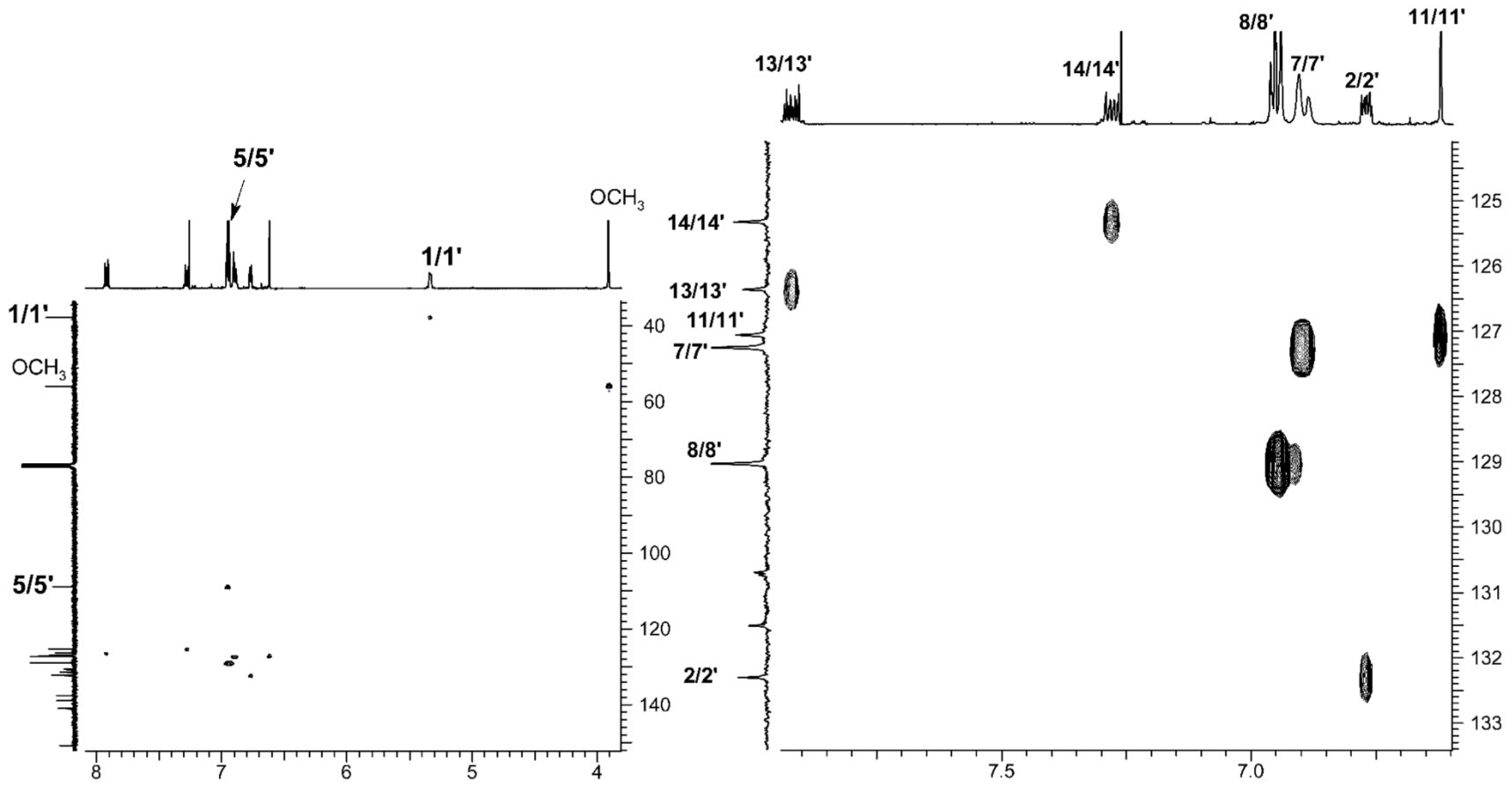

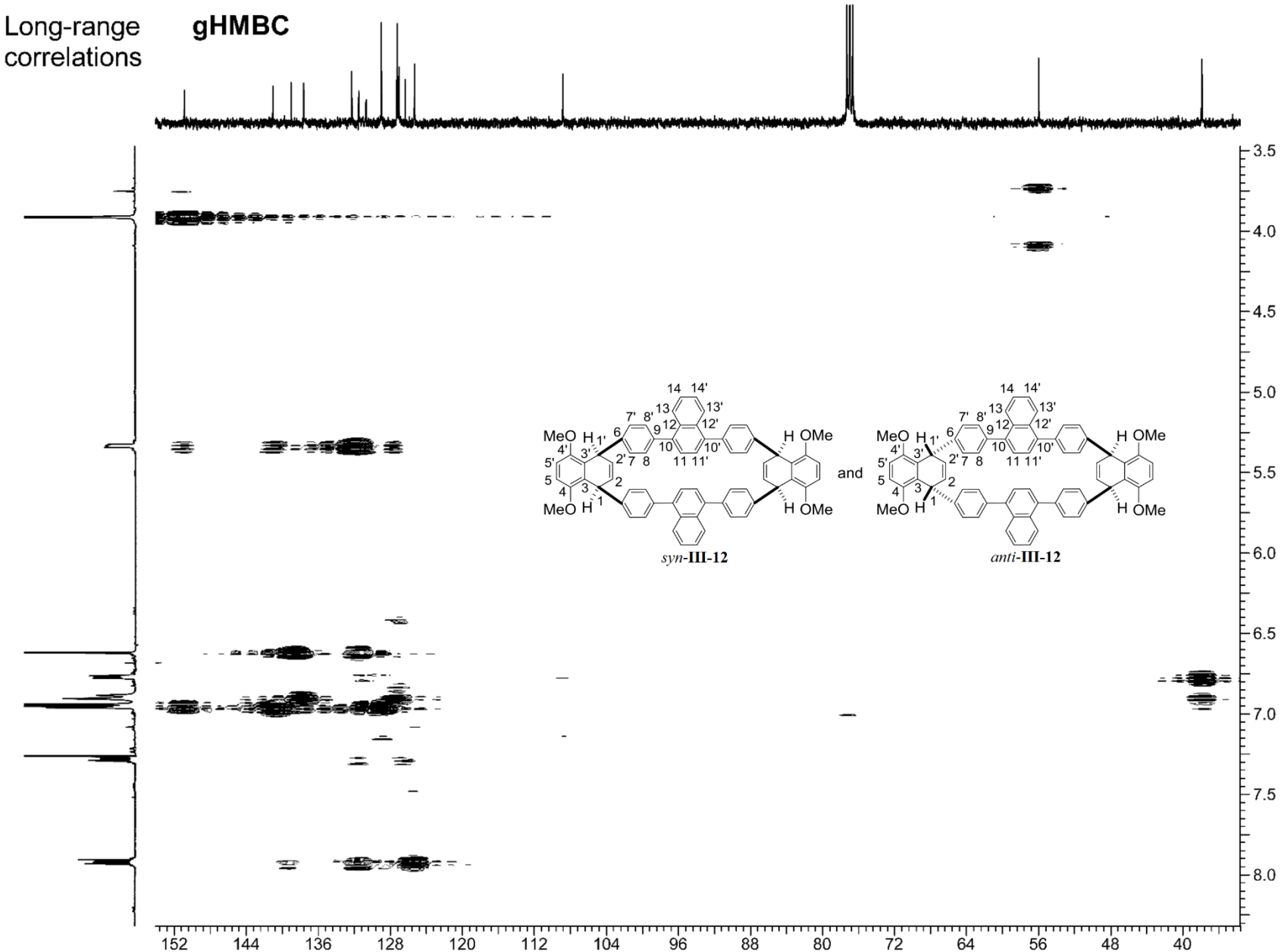

syn-**III-12**

anti-**III-12**

Long-range correlations **gHMBC**

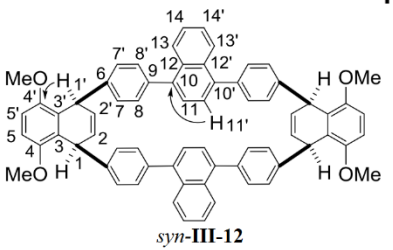

syn-**III-12**

and

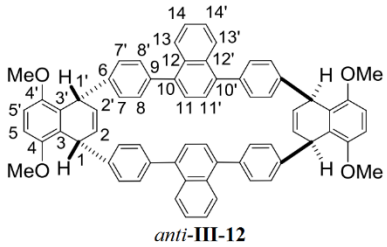

anti-**III-12**

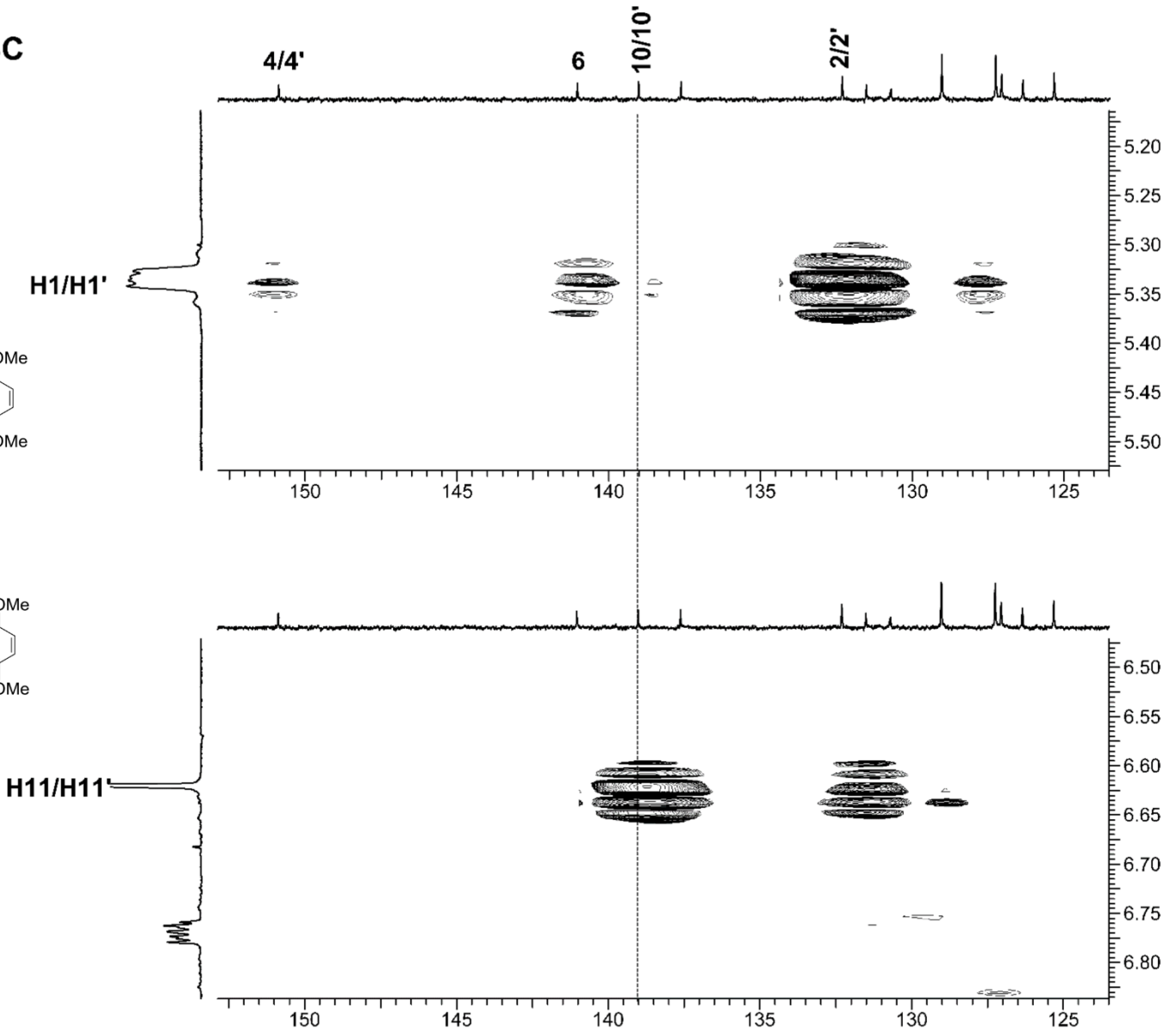

Long-range correlations **gHMBC**

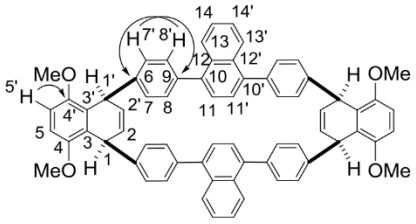

syn-**III-12**

and

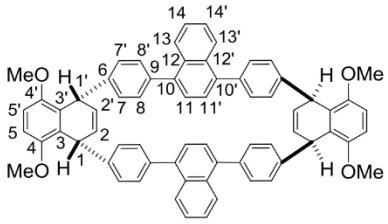

anti-**III-12**

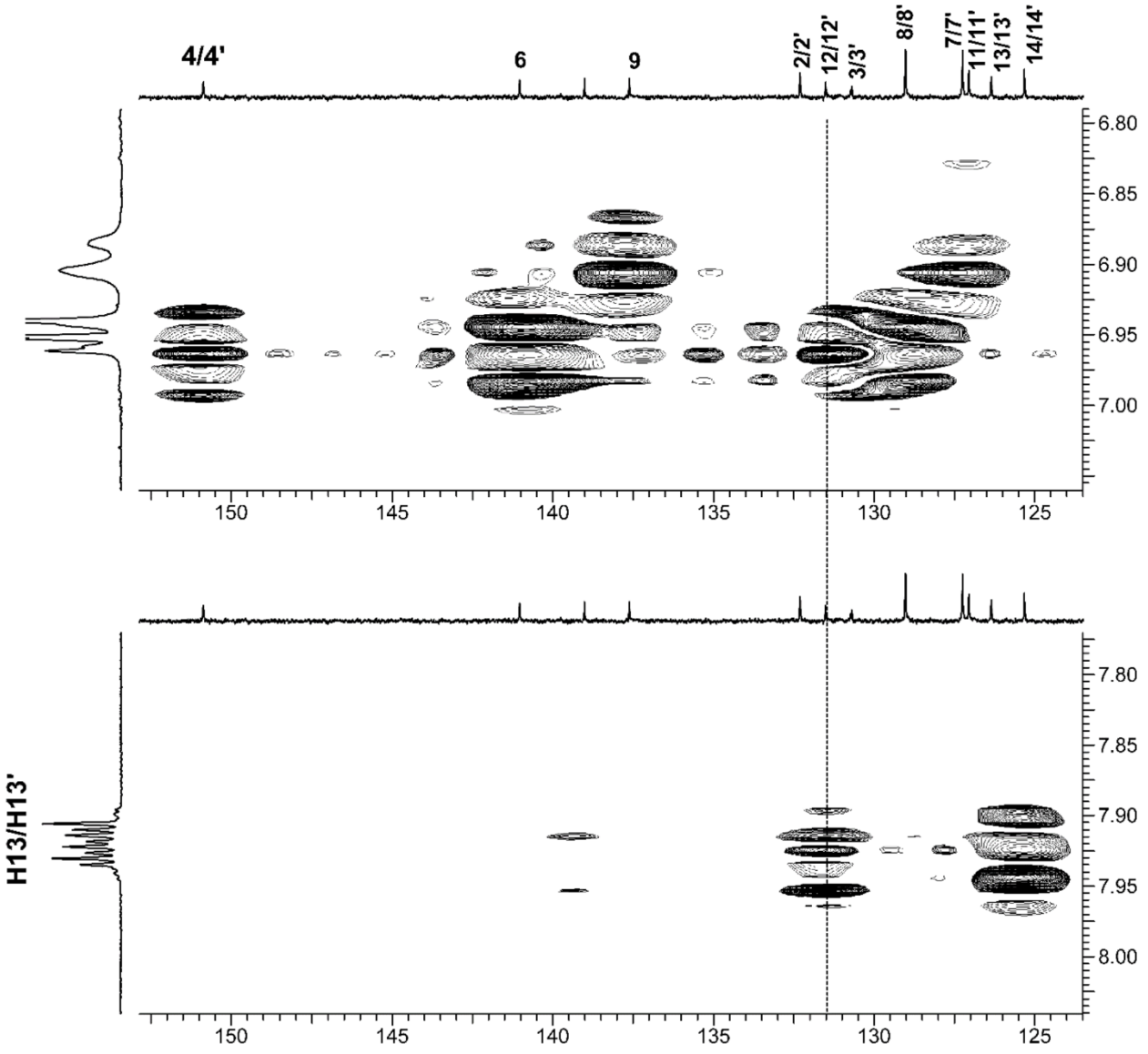

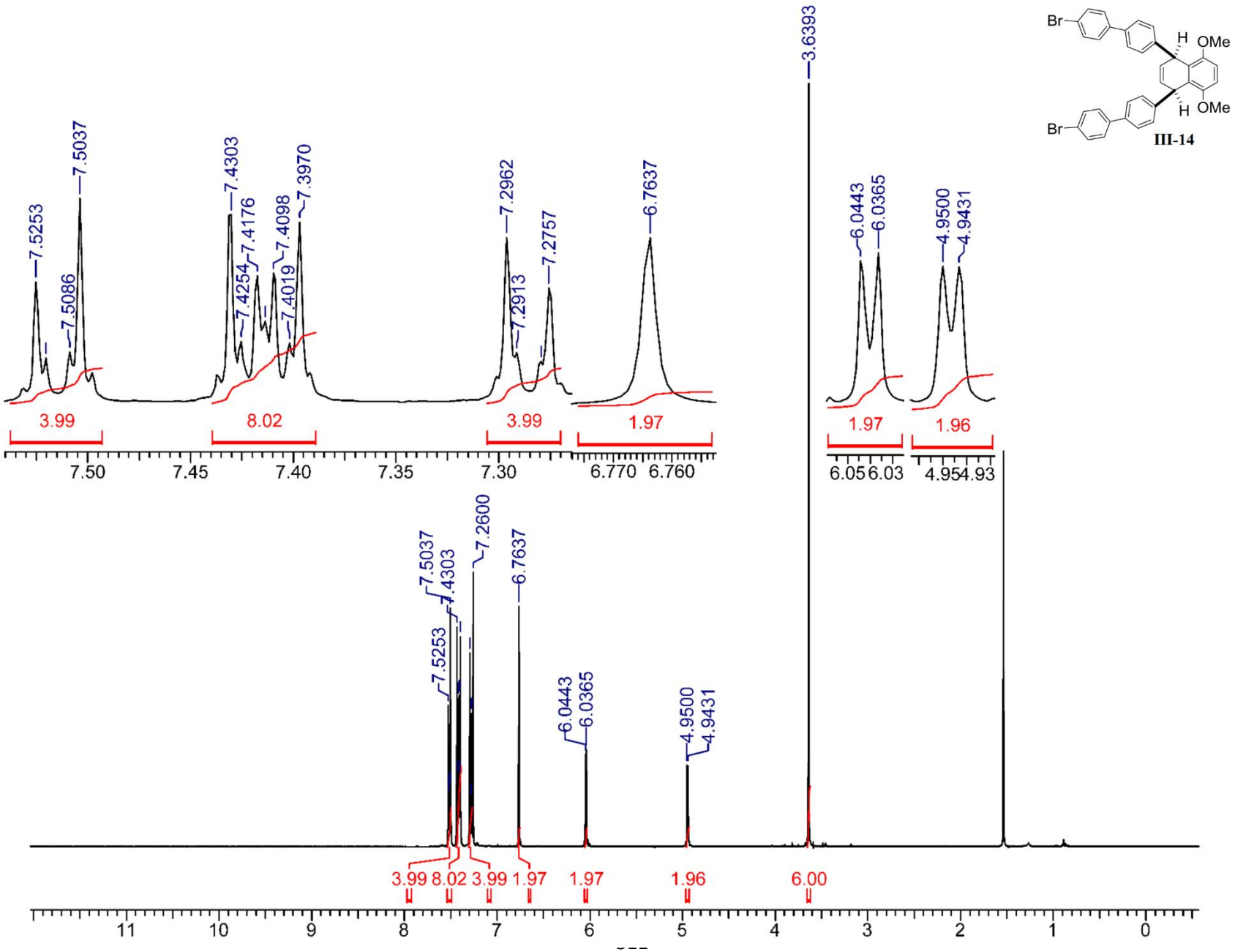
Br
H
OMe
H
OMe
Br
III-14
7.5253
7.5086
7.5037
7.4303
7.4254
7.4176
7.4098
7.4019
7.3970
7.2962
7.2913
7.2757
6.7637
6.0443
6.0365
4.9500
4.9431
3.6393
3.99
8.02
3.99
1.97
1.97
1.96
6.00
7.50
7.45
7.40
7.35
7.30
6.770
6.760
6.05
6.03
4.95
4.93
11
10
9
8
7
6
5
4
3
2
1
0

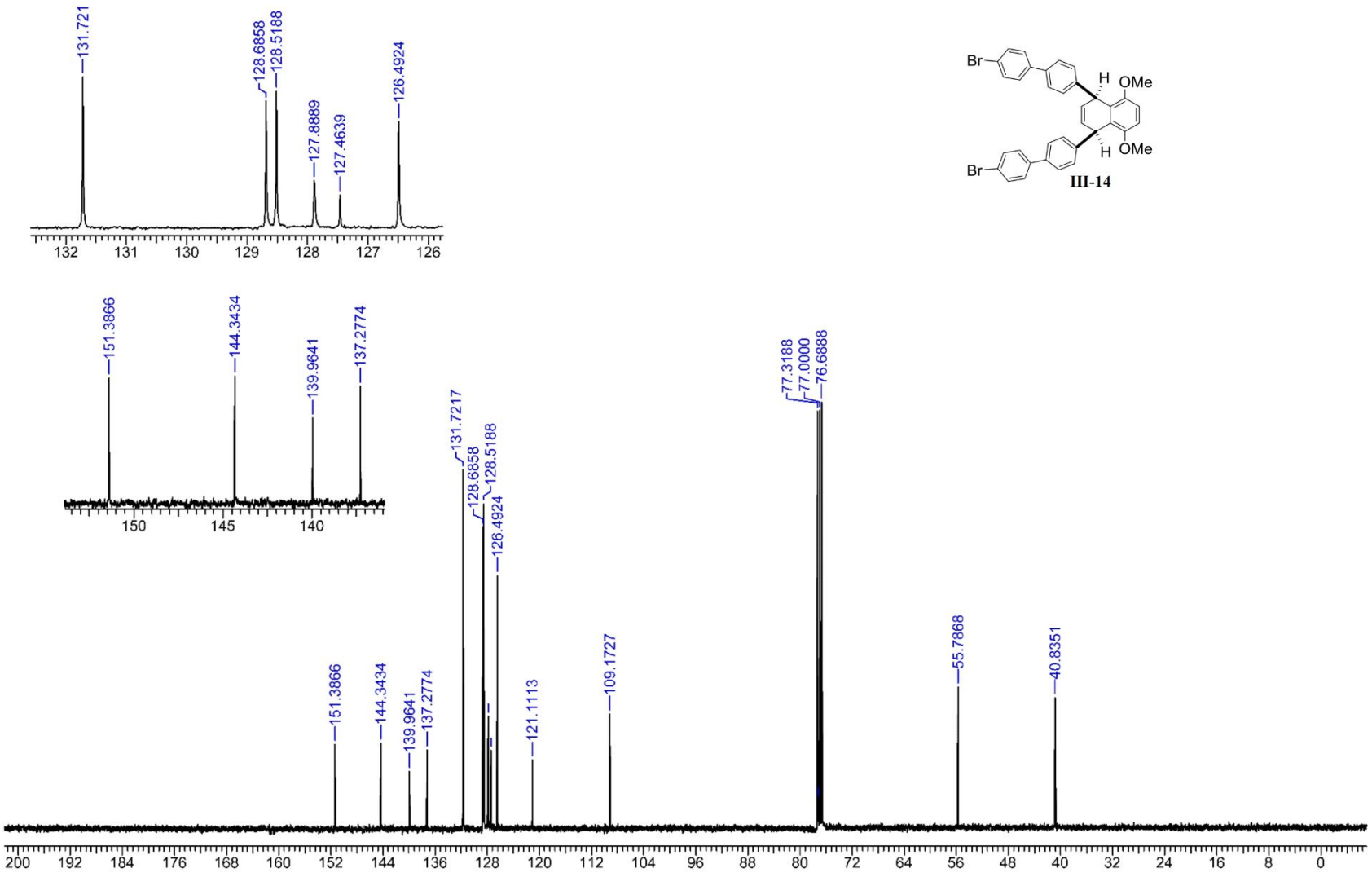
131.721
128.6858
128.5188
127.8889
127.4639
126.4924
132
131
130
129
128
127
126
151.3866
144.3434
139.9641
137.2774
150
145
140
131.7217
128.6858
128.5188
126.4924
77.3188
77.0000
76.6888
151.3866
144.3434
139.9641
137.2774
121.1113
109.1727
55.7868
40.8351
200
192
184
176
168
160
152
144
136
128
120
112
104
96
88
80
72
64
56
48
40
32
24
16
8
0

Br
H
OMe
H
OMe
Br

III-14

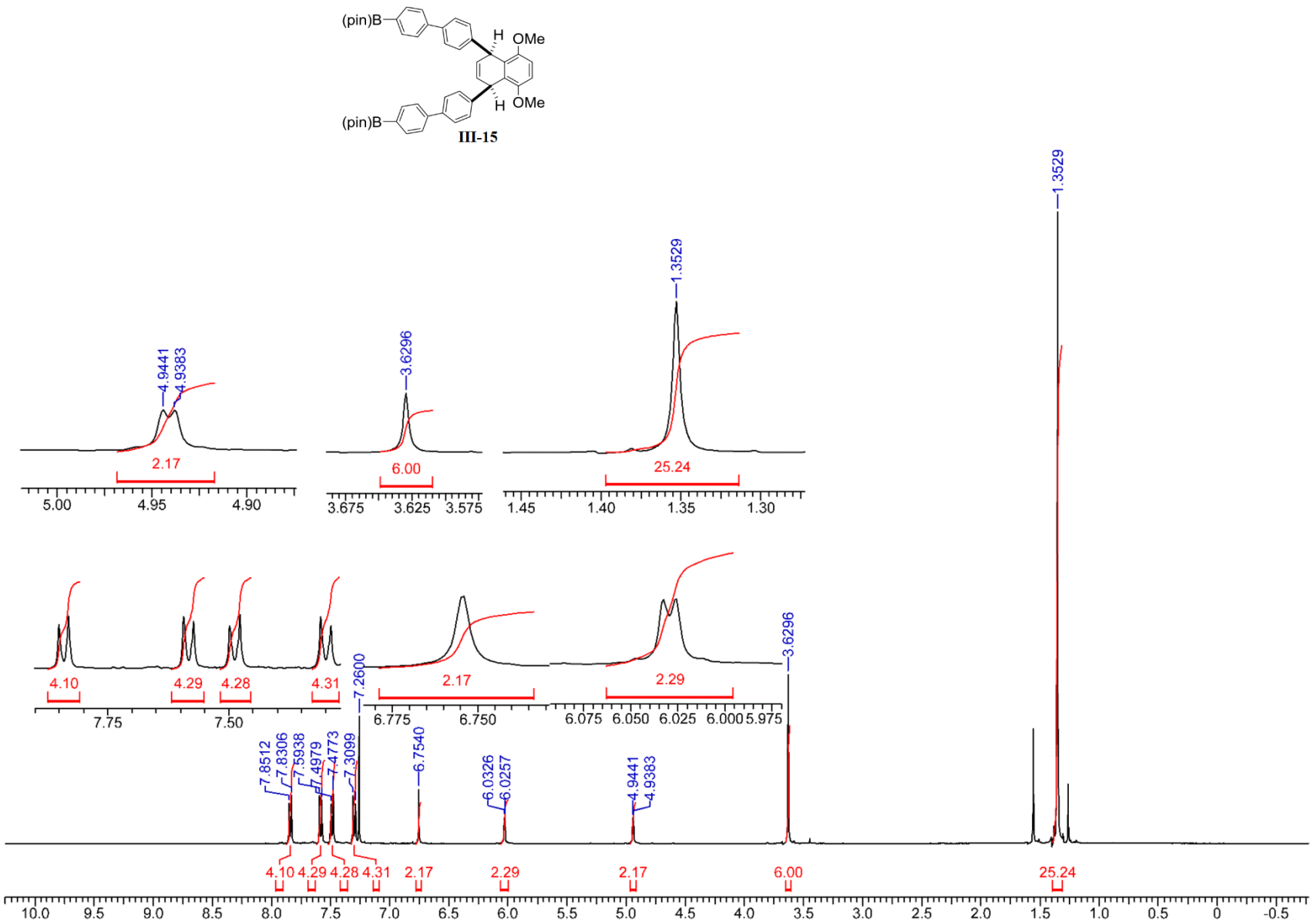
(pin)B
H
OMe
H
OMe
(pin)B
III-15
4.9441
4.9383
2.17
3.6296
6.00
1.3529
25.24
4.10
4.29
4.28
4.31
7.2600
2.17
2.29
3.6296
7.8512
7.8306
7.5938
7.4979
7.4773
7.3099
6.7540
6.0326
6.0257
4.9441
4.9383
1.3529
4.10 4.29 4.28 4.31
2.17
2.29
2.17
6.00
25.24

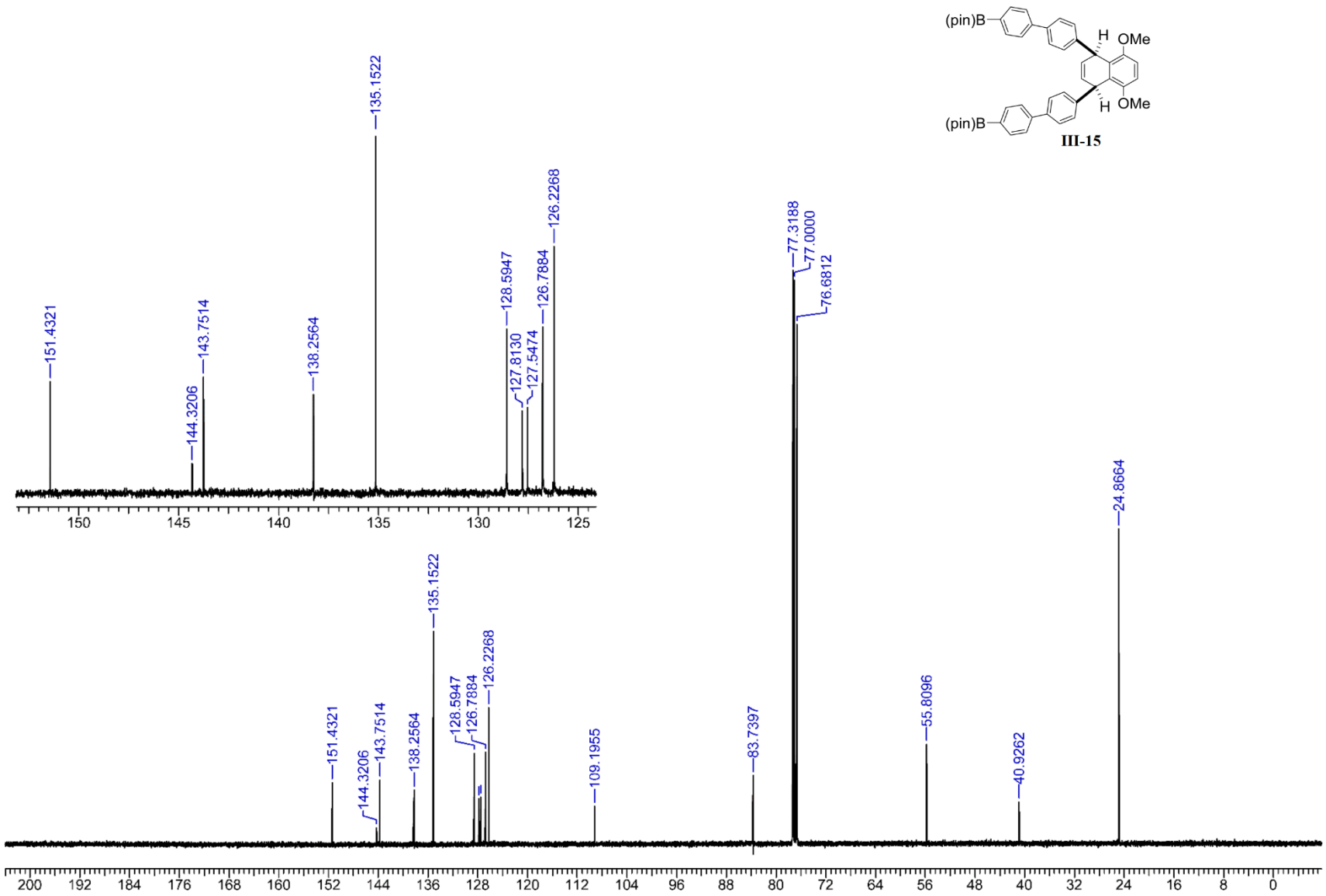
(pin)B
H
OMe
H
OMe
(pin)B
III-15
151.4321
144.3206
143.7514
138.2564
135.1522
128.5947
127.8130
127.5474
126.7884
126.2268
77.3188
77.0000
76.6812
24.8664
55.8096
40.9262
83.7397
109.1955

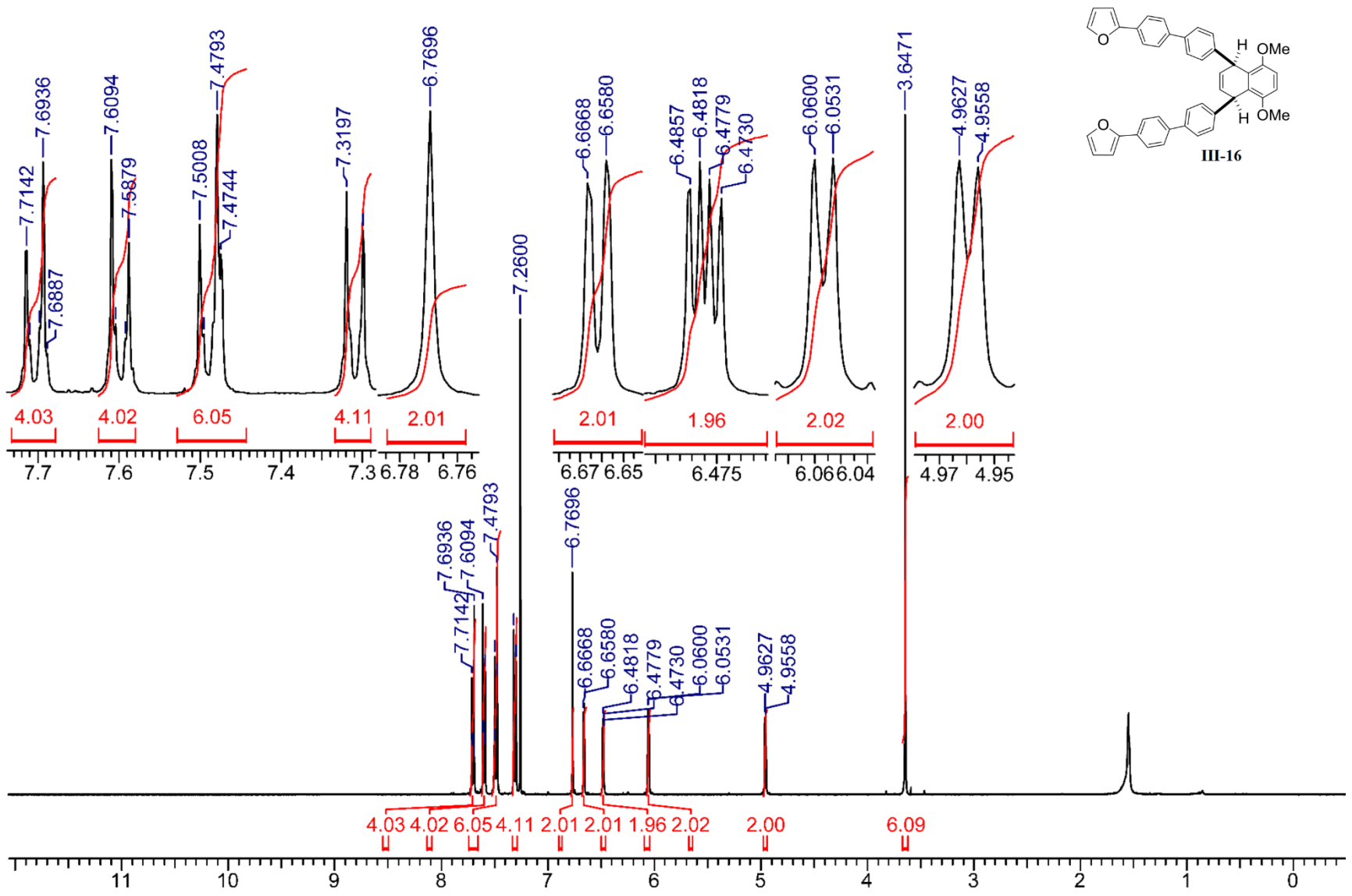
7.7142
7.6936
7.6887
7.6094
7.5879
7.5008
7.4793
7.4744
7.3197
6.7696
7.2600
6.6668
6.6580
6.4857
6.4818
6.4779
6.4730
6.0600
6.0531
3.6471
4.9627
4.9558
4.03
4.02
6.05
4.11
2.01
2.01
1.96
2.02
2.00
6.09
OMe
OMe
H
H
O
O
III-16

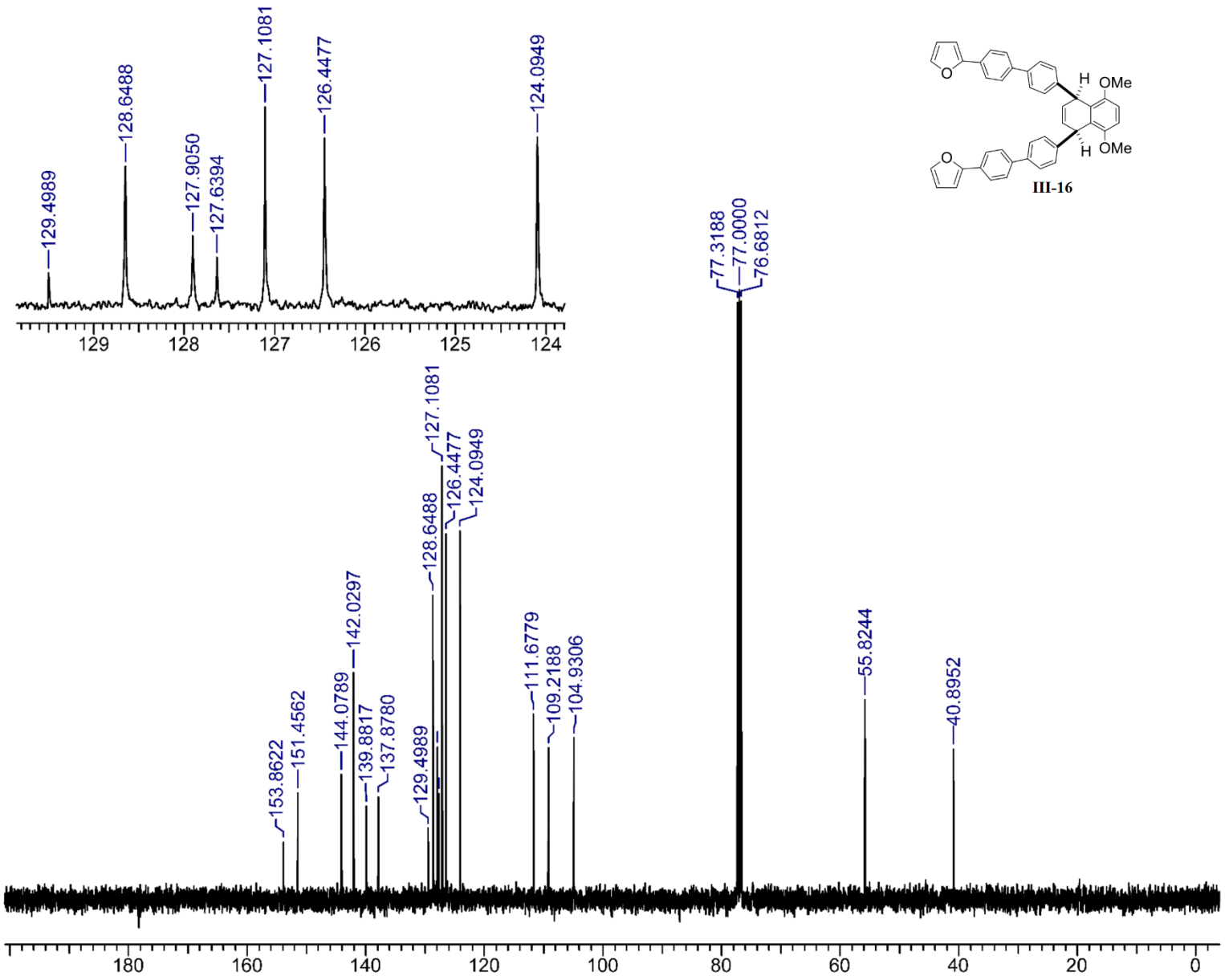
129.4989
128.6488
127.9050
127.6394
127.1081
126.4477
124.0949
129
128
127
126
125
124
77.3188
77.0000
76.6812
153.8622
151.4562
144.0789
142.0297
139.8817
137.8780
129.4989
128.6488
127.1081
126.4477
124.0949
111.6779
109.2188
104.9306
55.8244
40.8952
180
160
140
120
100
80
60
40
20
0
O
H
OMe
H
OMe
O

III-16

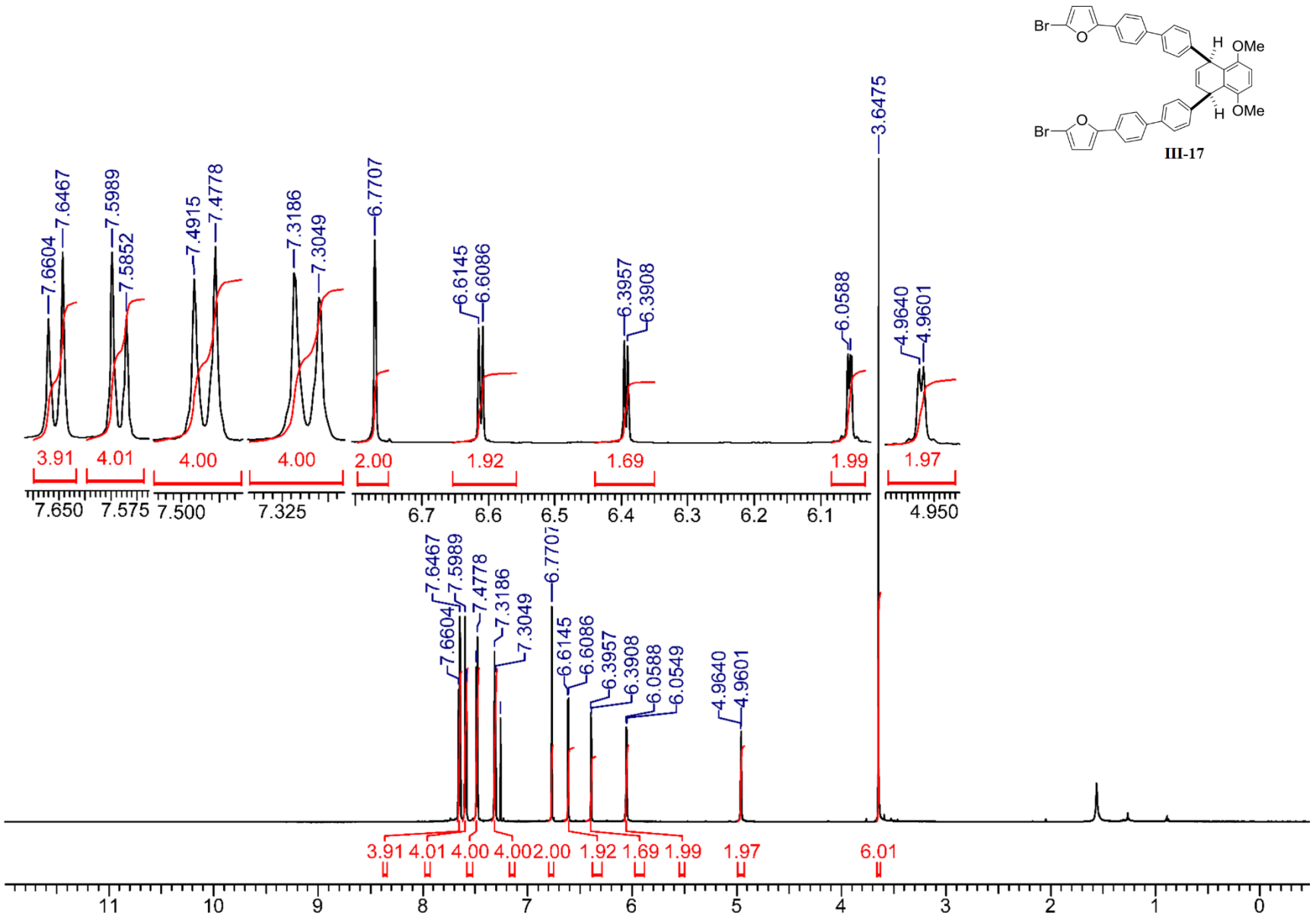
Br
O
H
OMe
H
OMe
Br
O
III-17
7.6604
7.6467
7.5989
7.5852
7.4915
7.4778
7.3186
7.3049
6.7707
6.6145
6.6086
6.3957
6.3908
6.0588
4.9640
4.9601
3.6475
3.91
4.01
4.00
4.00
2.00
1.92
1.69
1.99
1.97
7.650
7.575
7.500
7.325
6.7
6.6
6.5
6.4
6.3
6.2
6.1
4.950
7.6467
7.5989
7.6604
7.4778
7.3186
7.3049
6.7707
6.6145
6.6086
6.3957
6.3908
6.0588
6.0549
4.9640
4.9601
3.91
4.01
4.00
4.00
2.00
1.92
1.69
1.99
1.97
6.01
11
10
9
8
7
6
5
4
3
2
1
0

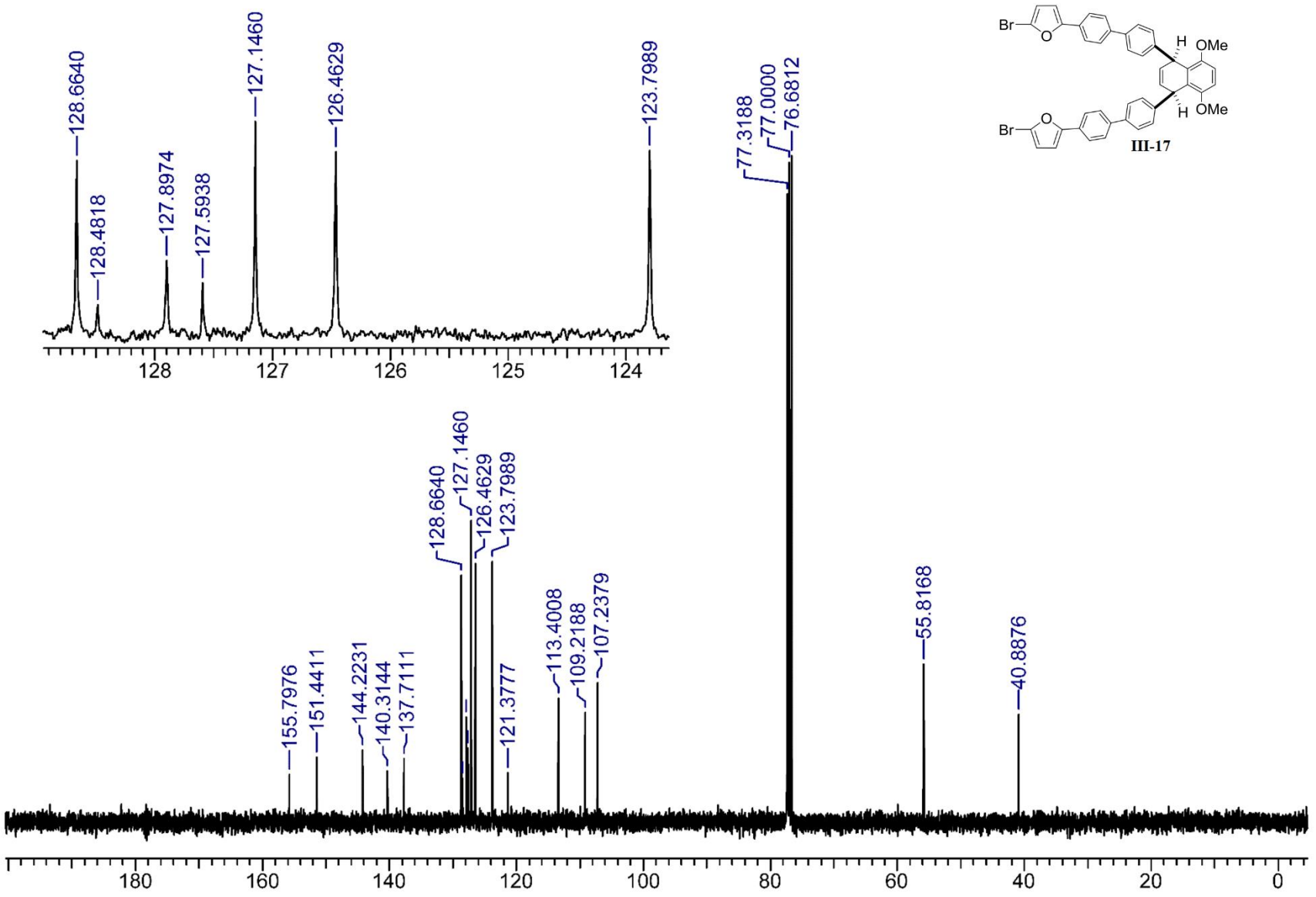
128.6640
128.4818
127.8974
127.5938
127.1460
126.4629
123.7989
128
127
126
125
124
77.3188
77.0000
76.6812
128.6640
127.1460
126.4629
123.7989
155.7976
151.4411
144.2231
140.3144
137.7111
121.3777
113.4008
109.2188
107.2379
55.8168
40.8876
180
160
140
120
100
80
60
40
20
0
Br
O
H
OMe
H
OMe
Br
O
III-17

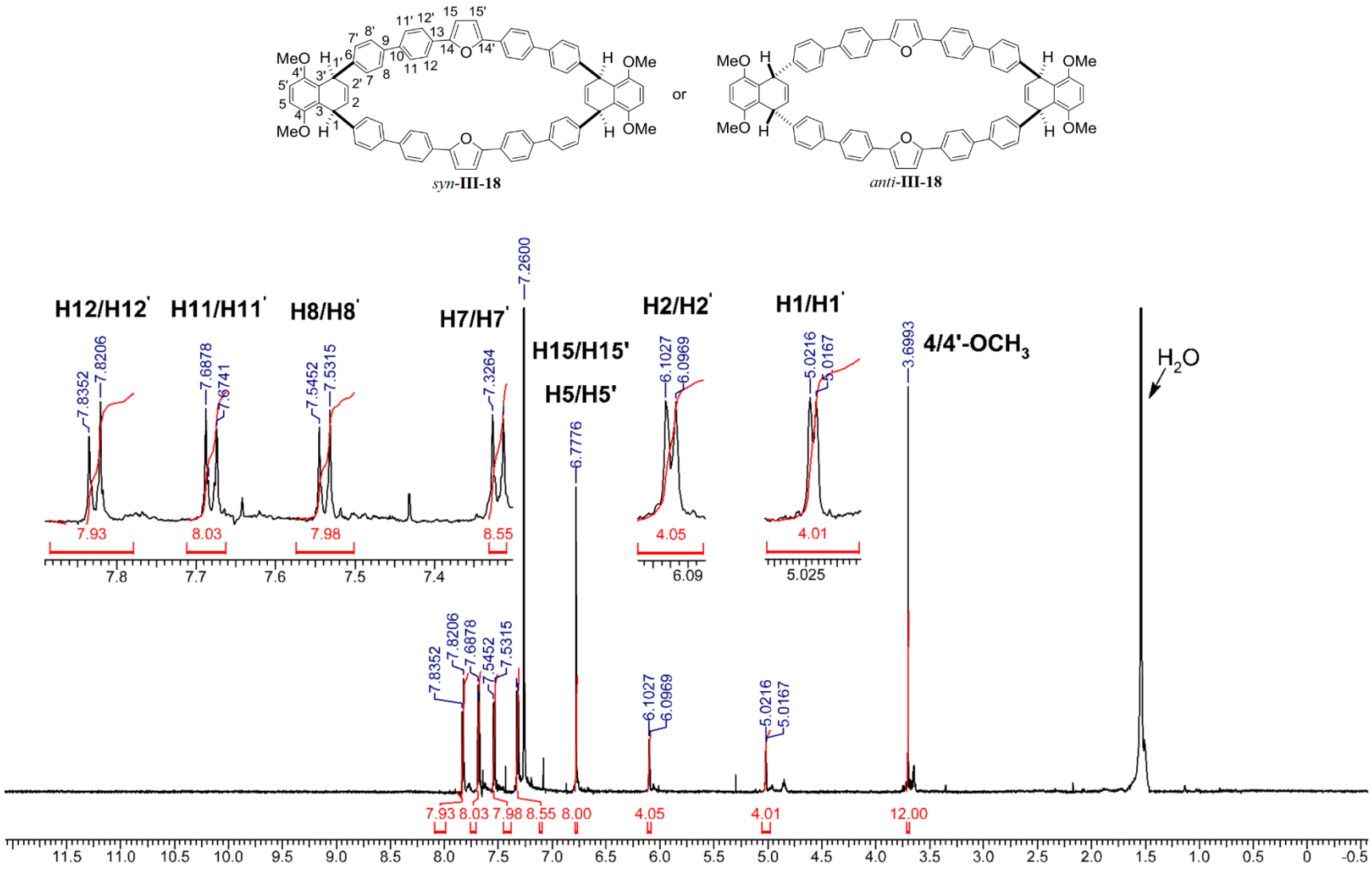
syn-III-18
or
anti-III-18
H12/H12'
H11/H11'
H8/H8'
H7/H7'
H15/H15'
H5/H5'
H2/H2'
H1/H1'
4/4'-OCH3
H2O
7.2600
7.8352
7.8206
7.6878
7.6741
7.5452
7.5315
7.3264
6.7776
6.1027
6.0969
5.0216
5.0167
3.6993
7.93
8.03
7.98
8.55
8.00
4.05
4.01
12.00

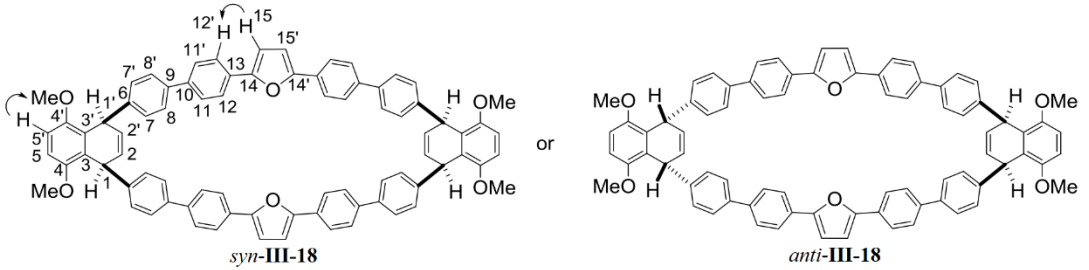

syn-**III-18** *anti*-**III-18**

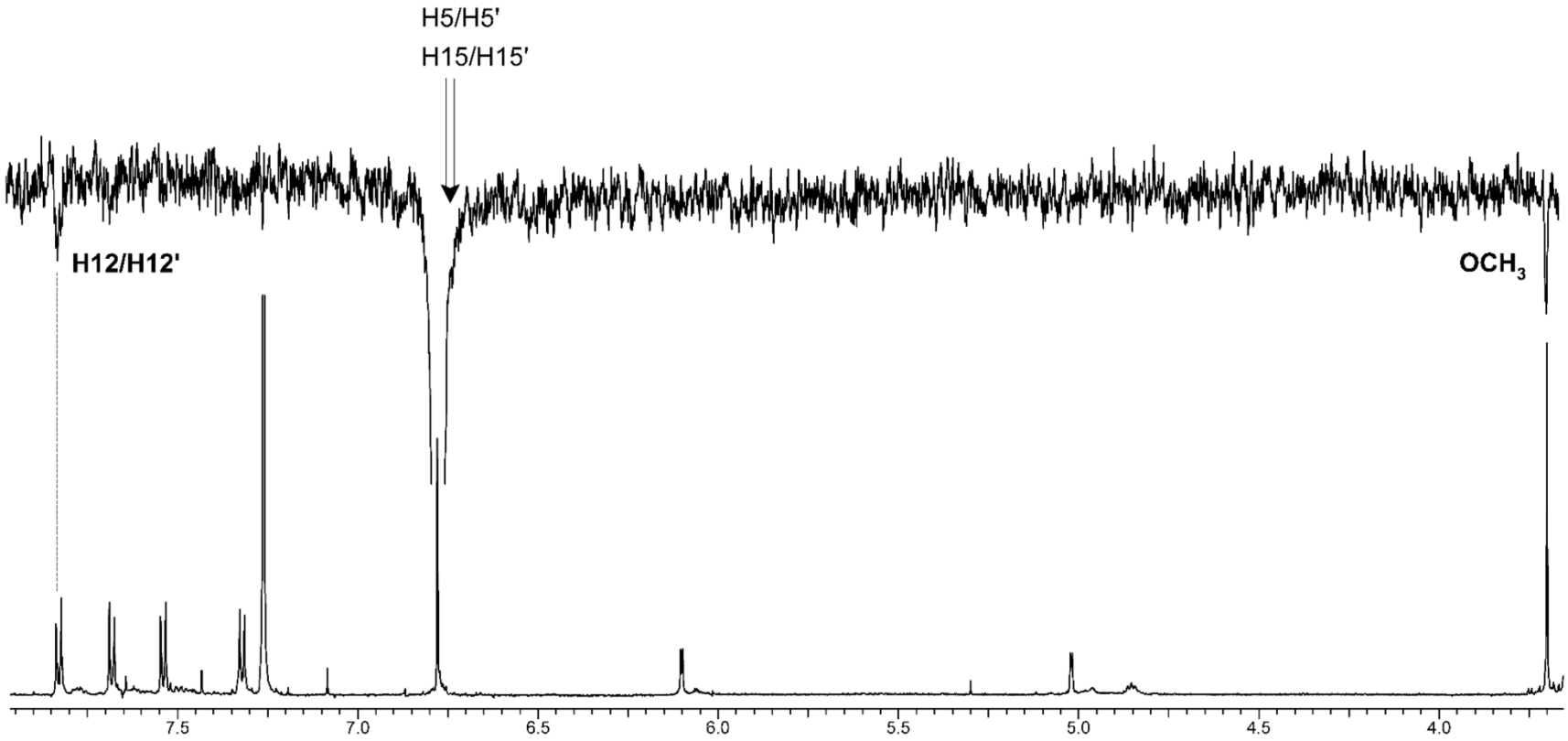

gCOSY

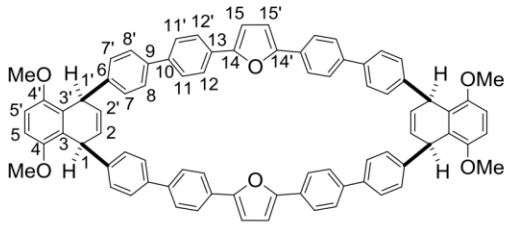

syn-**III-18**

or

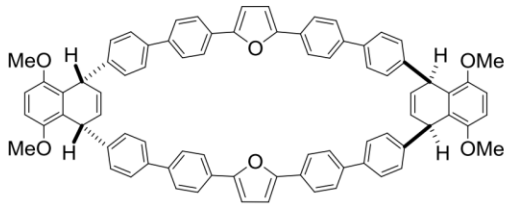

anti-**III-18**

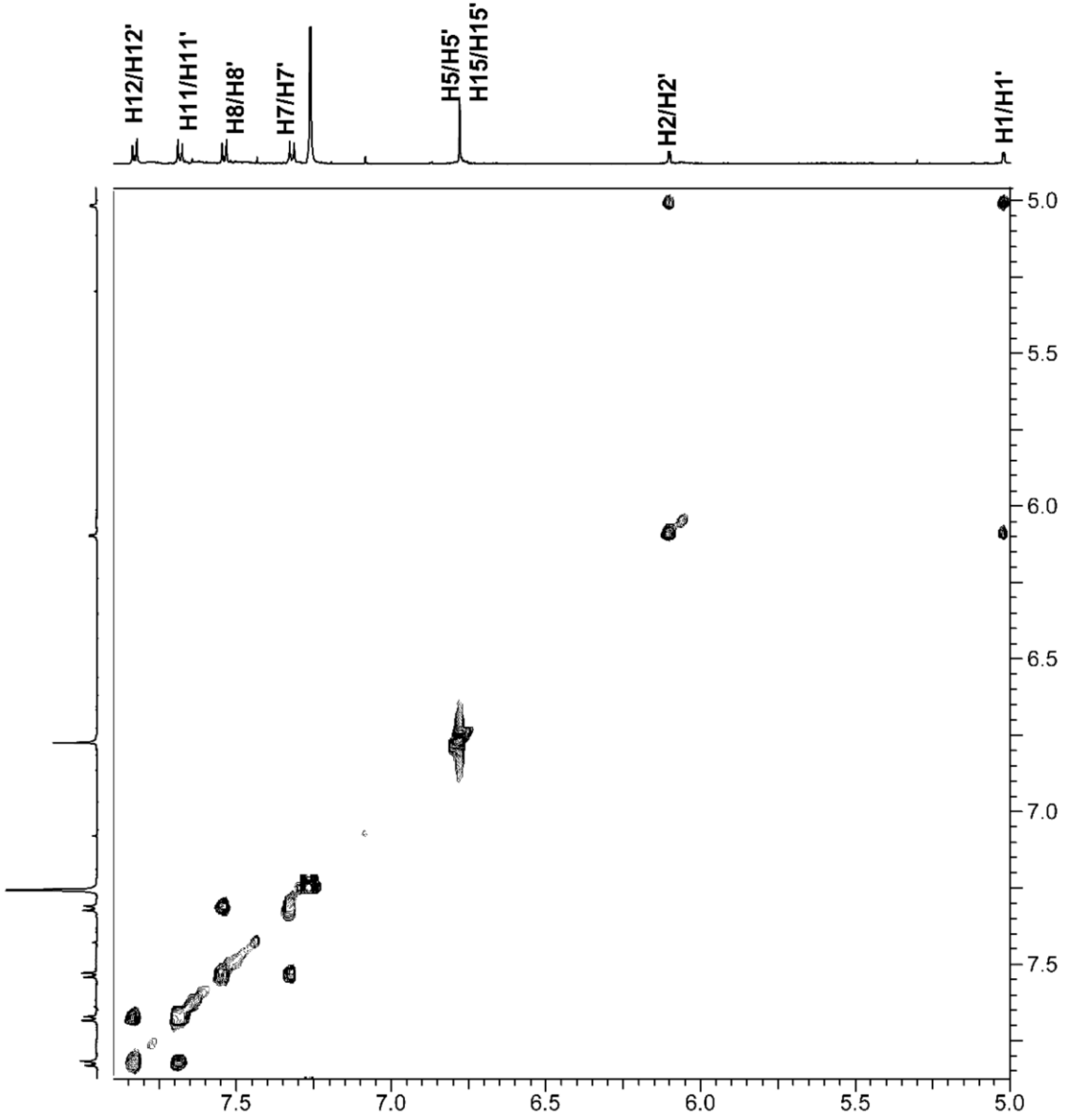

2D NOESY

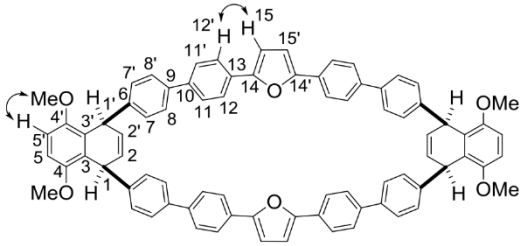

syn-III-18 or *anti*-III-18

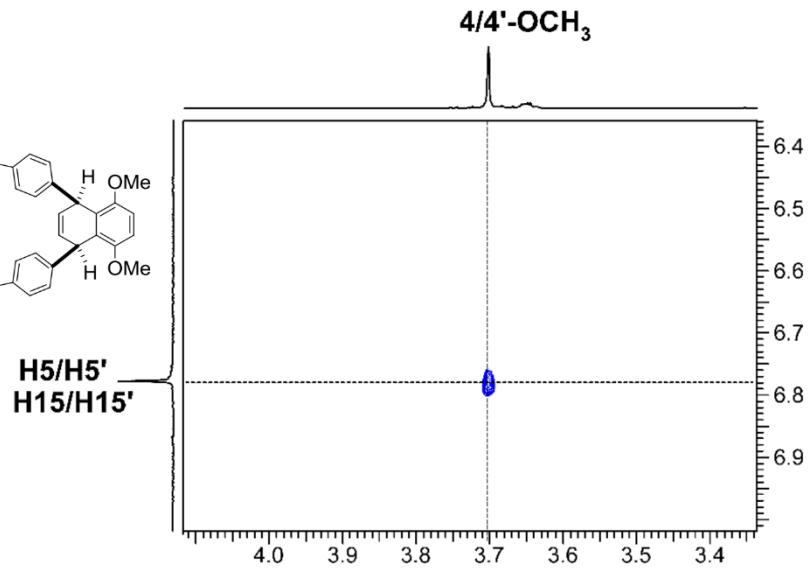

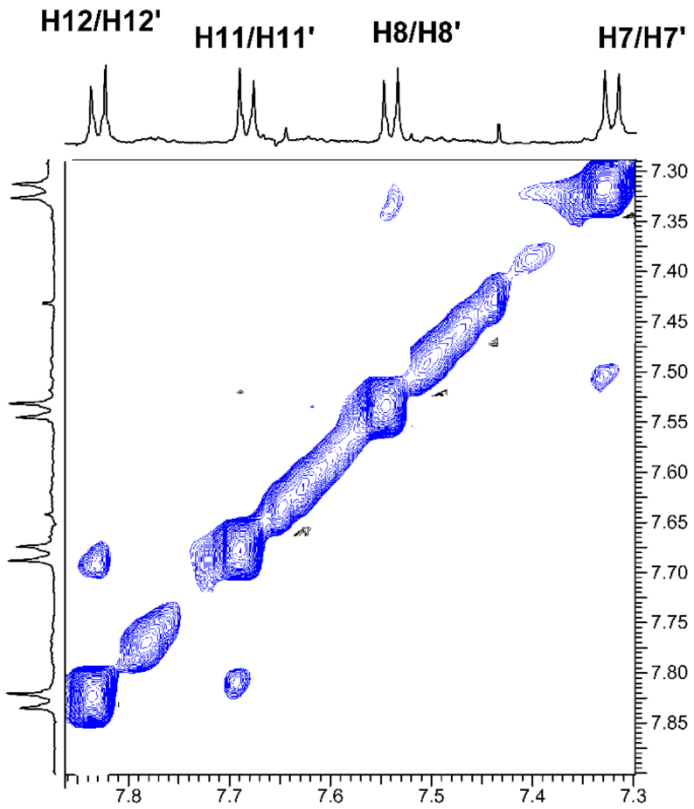

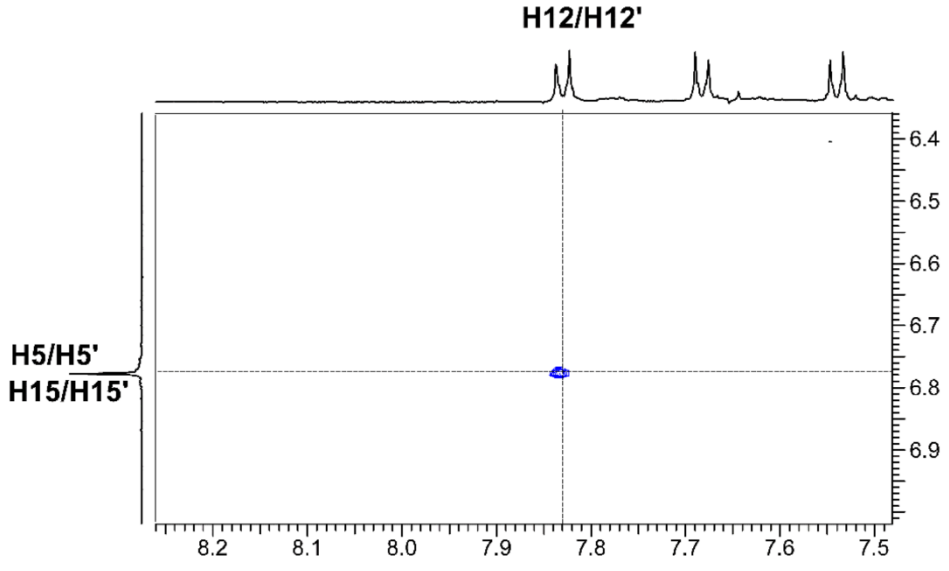

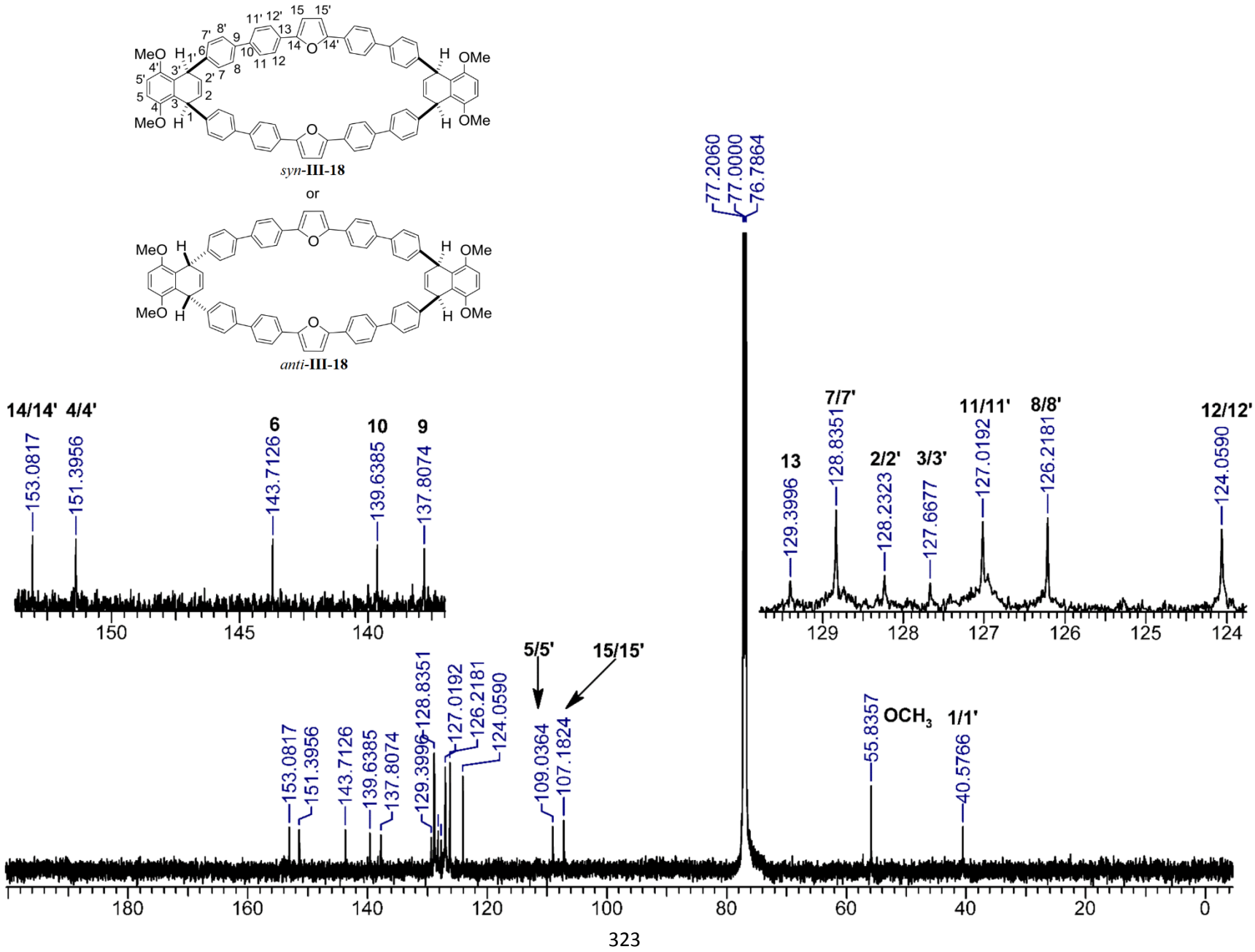
MeO
H
OMe
O
syn-III-18
or
anti-III-18
14/14'
4/4'
6
10
9
153.0817
151.3956
143.7126
139.6385
137.8074
7/7'
11/11'
8/8'
12/12'
13
2/2'
3/3'
129.3996
128.8351
128.2323
127.6677
127.0192
126.2181
124.0590
77.2060
77.0000
76.7864
5/5'
15/15'
109.0364
107.1824
55.8357
OCH3
1/1'
40.5766
180
160
140
120
100
80
60
40
20
0
150
145
140
129
128
127
126
125
124

gHSQC

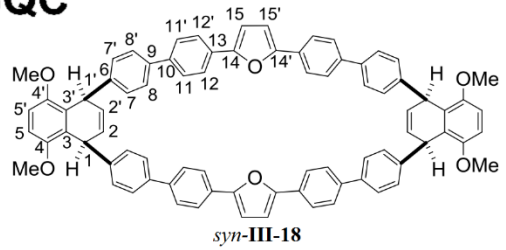

syn-**III-18**

or

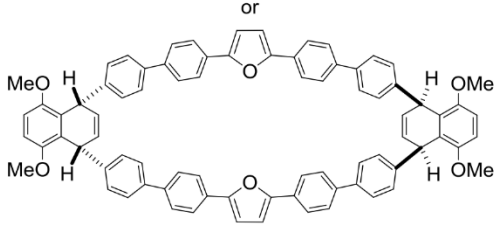

anti-**III-18**

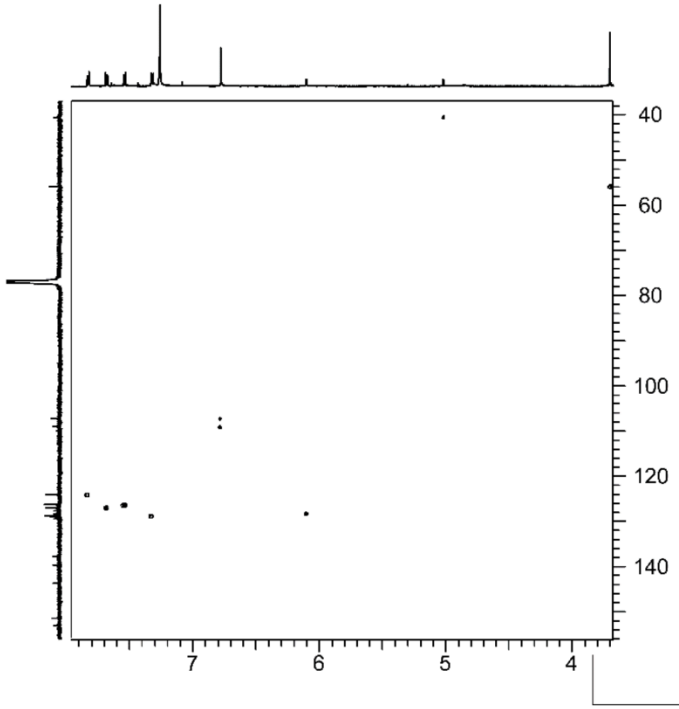

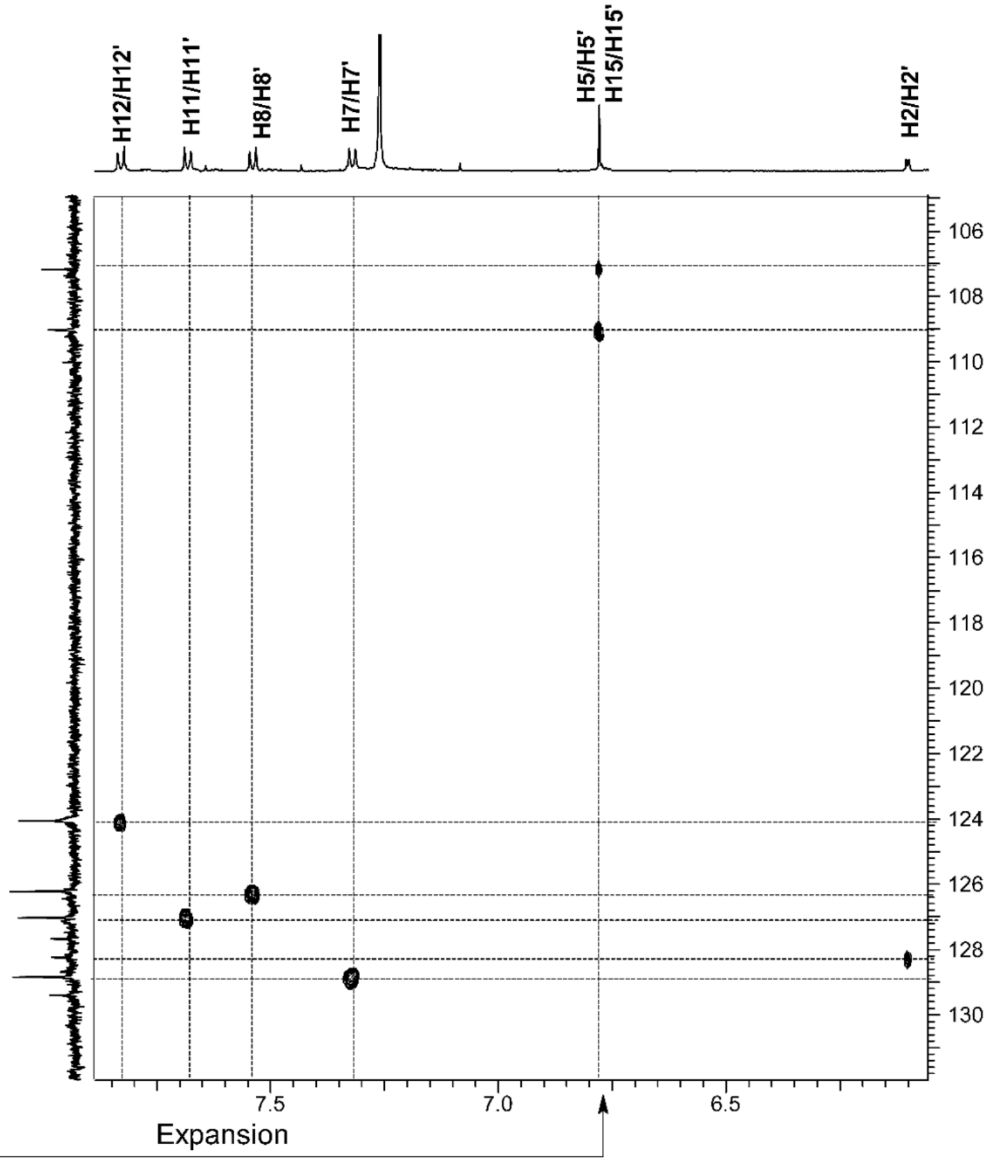

Three bond ($^3J_{HC}$) gHMBC correlations

confirm linkage between rings

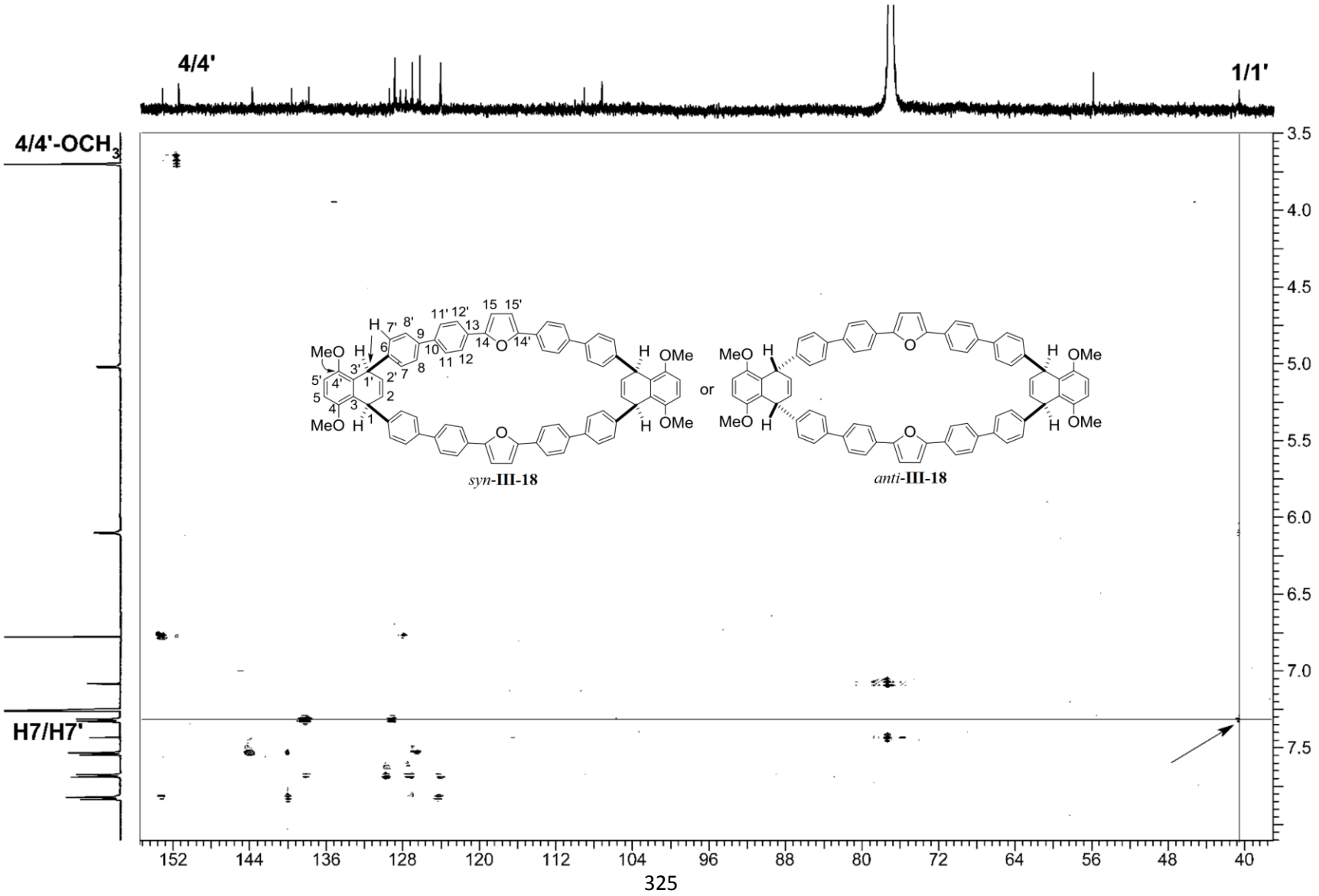

Three bond ($^3J_{HC}$) gHMBC correlations

confirm linkage between rings

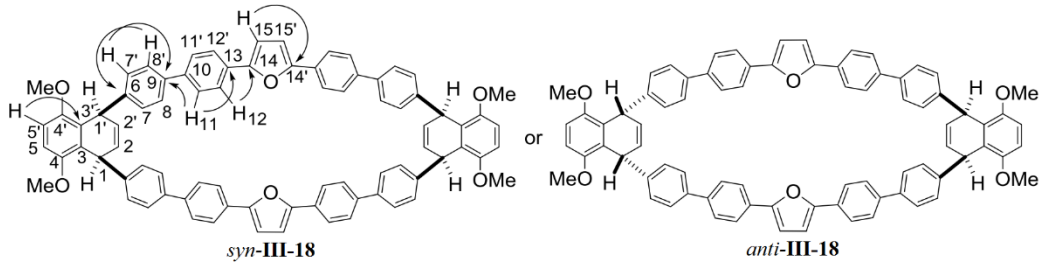

syn-**III-18** *anti*-**III-18**

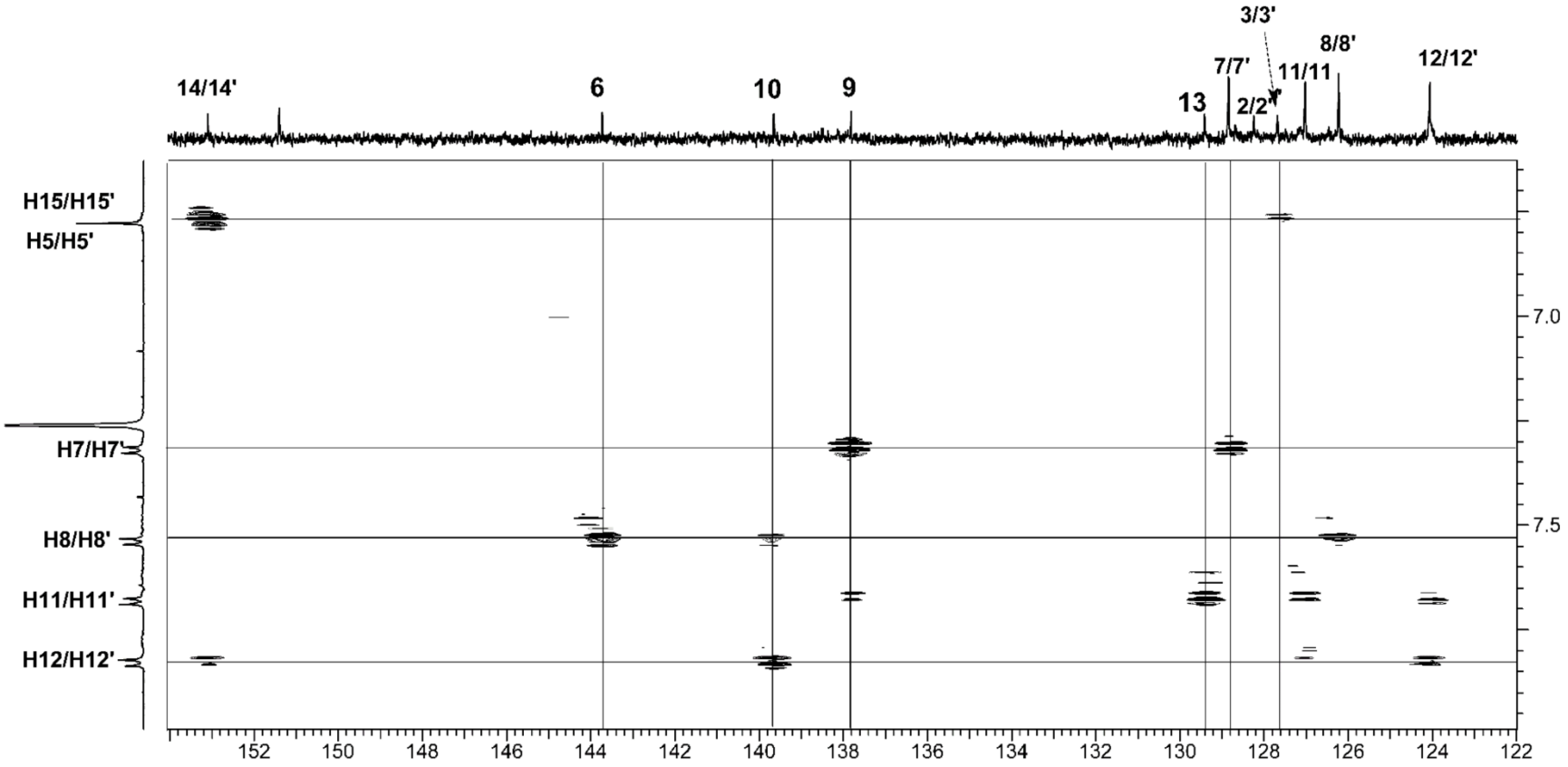

NMR parameters (chemical shifts and coupling constants) and experimental/calculated multiplicity patterns

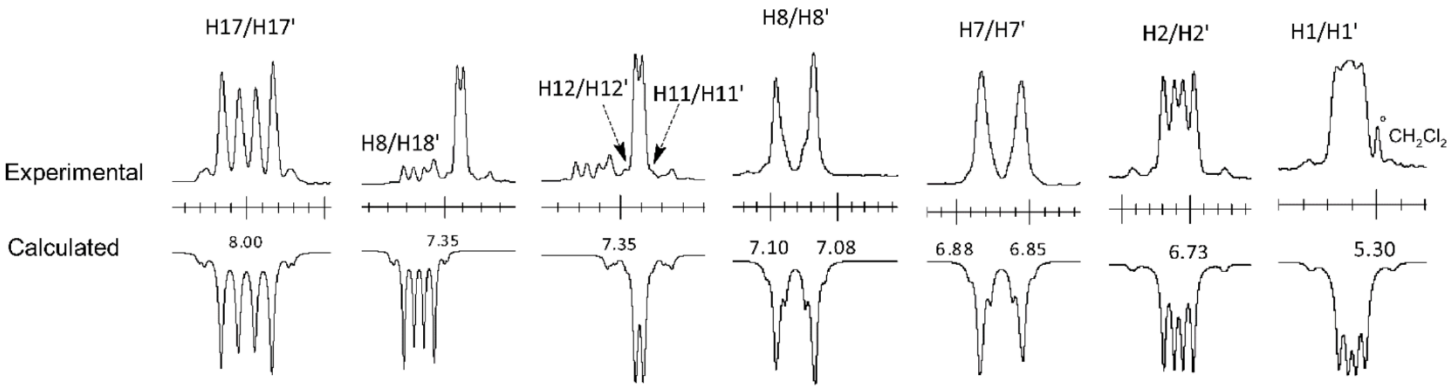

Proton	δ_H/ppm
H1/H1'	5.31
H2/H2'	6.73
H5/H5'	6.94
H7/H7'	6.86
H8/H8'	7.09
H11/11'	7.34
H12/H12'	7.35
H15/H15'	7.19
H17/H17'	8.00
H18/H18'	7.38
OCH_3	3.90

Carbon	δ_C/ppm
C1/C1'	37.93
C2/C2'	132.25
C3/C3'	130.74
C4/C4'	150.80
C5/C5'	108.88
C6	141.30
C7/C7'	126.92
C8/C8'	127.84
C9	137.63
C10	140.17
C11/C11'	130.30
C12/C12'	126.16
C13	139.08
C14/C14'	139.26
C15/C15'	126.50
C16/C16'	131.78
C17/C17'	126.35
C18/C18'	125.79
4/4-OCH_3	56.00

Coupling constants amd Spin systems

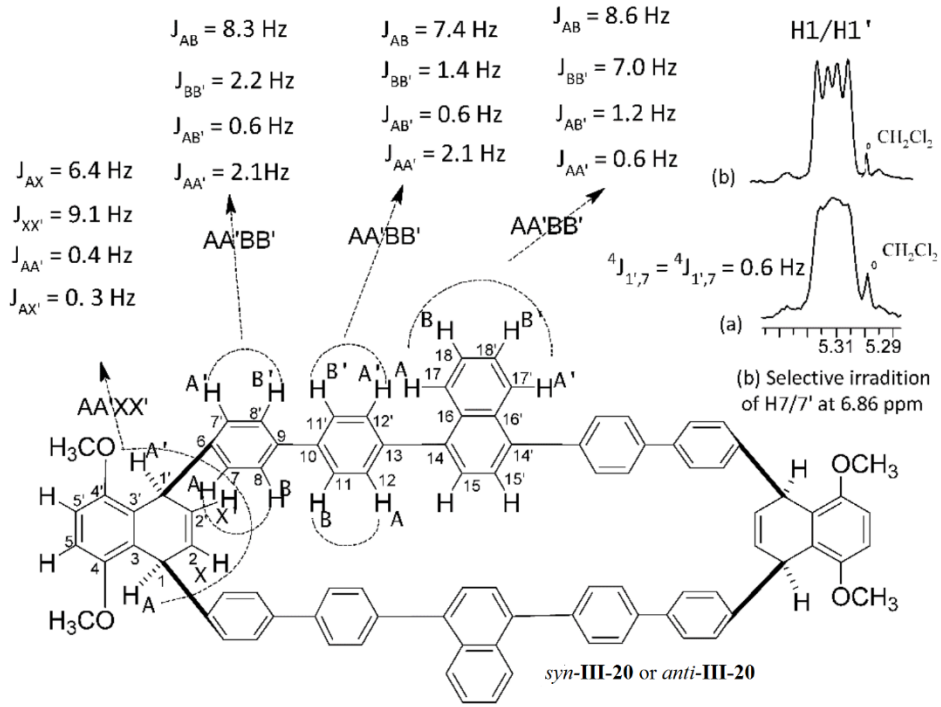

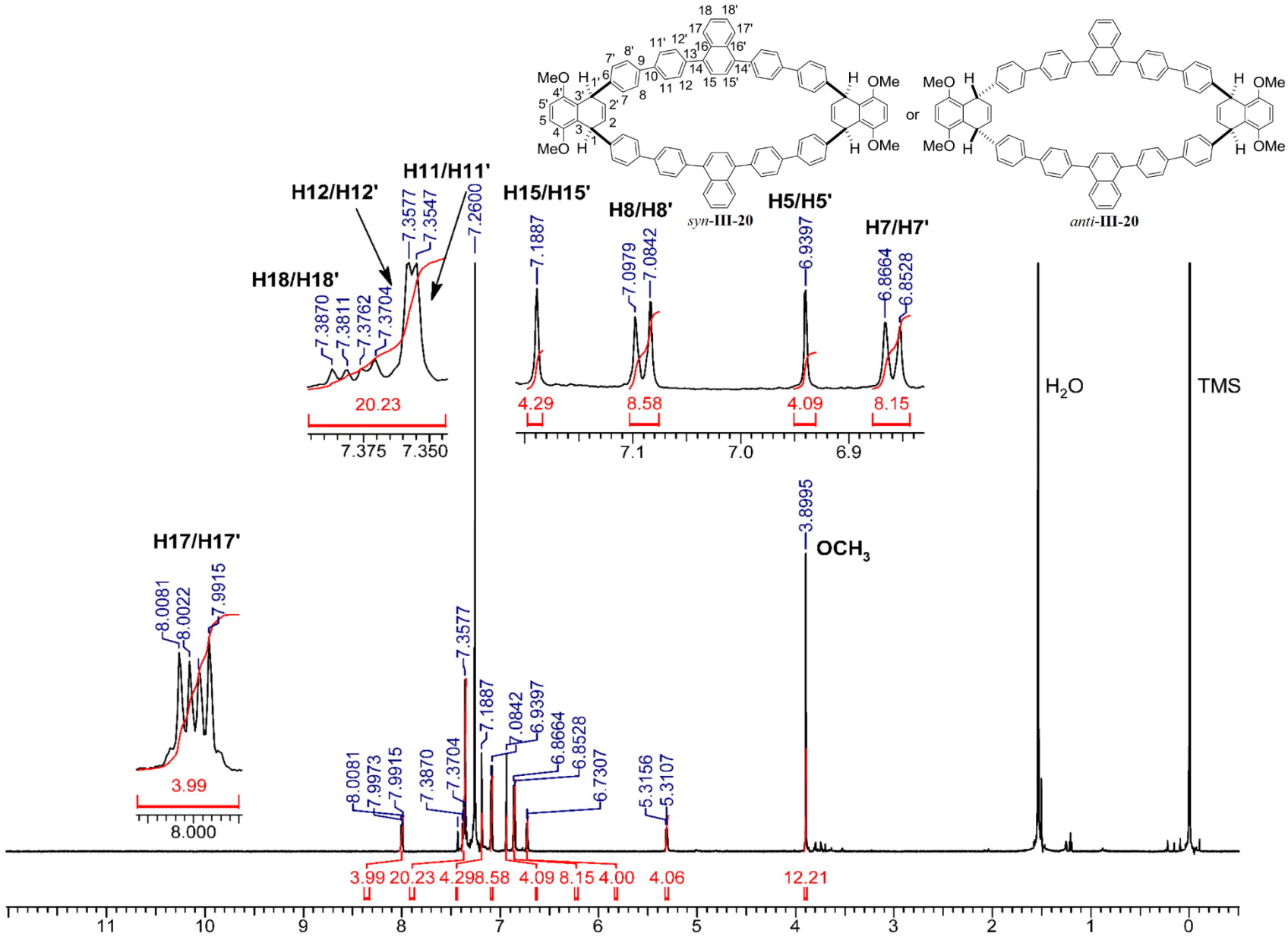
syn-III-20
or
anti-III-20
H12/H12'
H11/H11'
H18/H18'
H15/H15'
H8/H8'
H5/H5'
H7/H7'
H17/H17'
OCH3
H2O
TMS
3.99 20.23 4.29 8.58 4.09 8.15 4.00 4.06 12.21

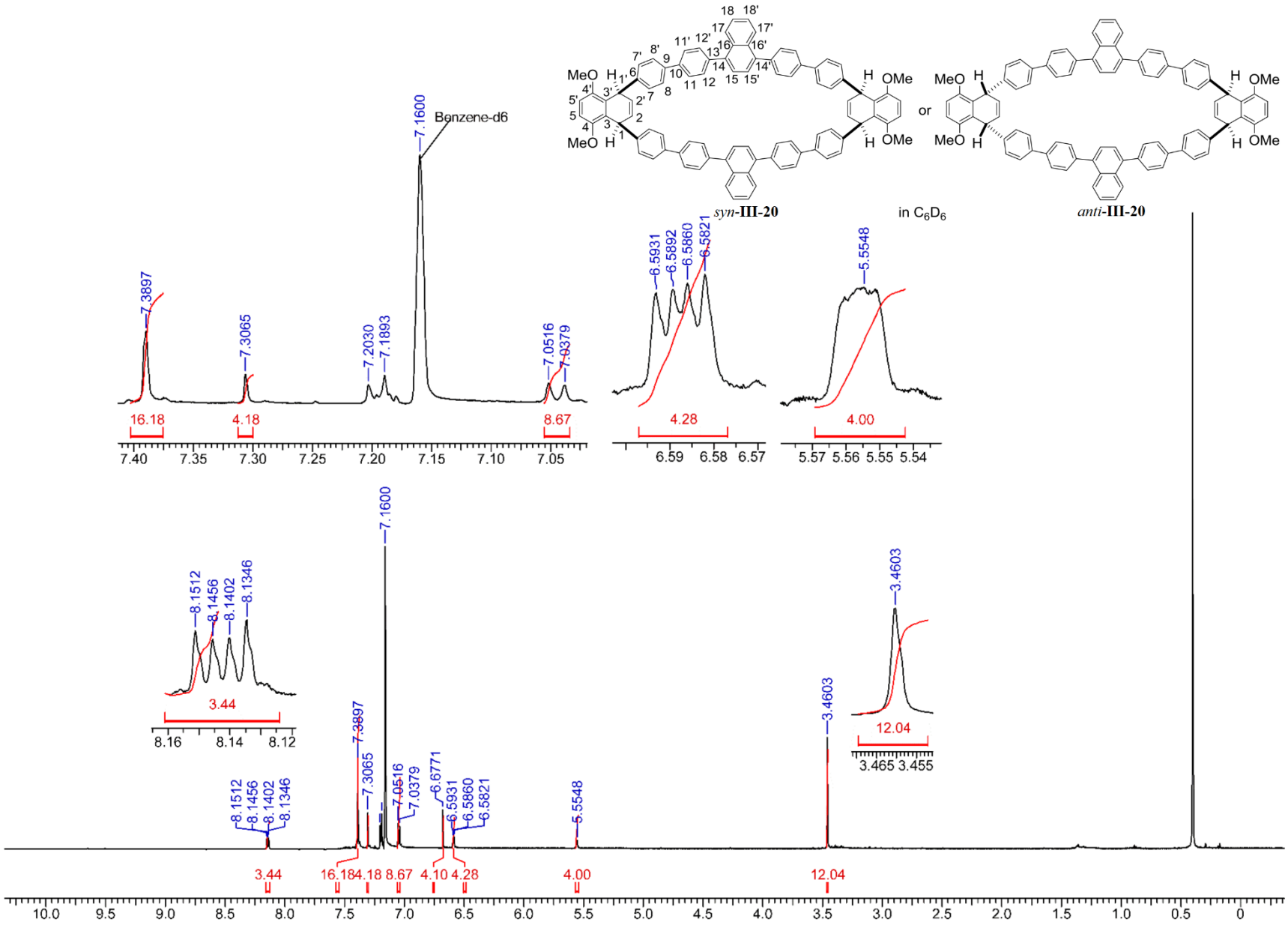
Benzene-d6
7.1600
7.3897
7.3065
7.2030
7.1893
7.0516
7.0379
16.18
4.18
8.67
6.5931
6.5892
6.5860
6.5821
4.28
5.5548
4.00
8.1512
8.1456
8.1402
8.1346
3.44
3.4603
12.04
6.6771
4.10
syn-III-20
in C6D6
anti-III-20
or

Expanded regions of the **2D NOESY** spectrum

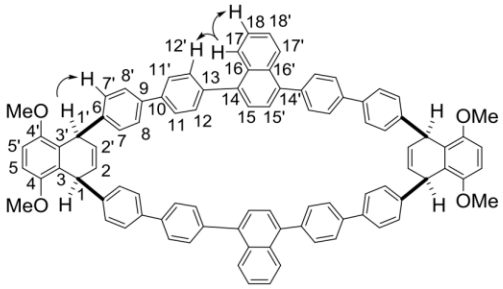

syn-**III-20**

or

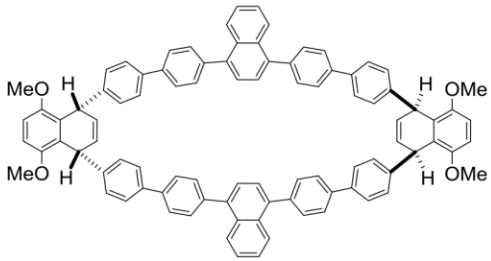

anti-**III-20**

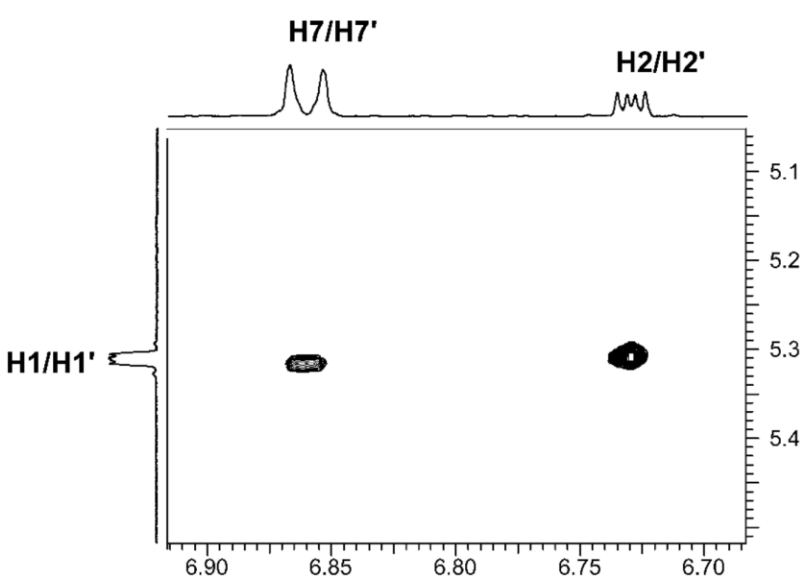

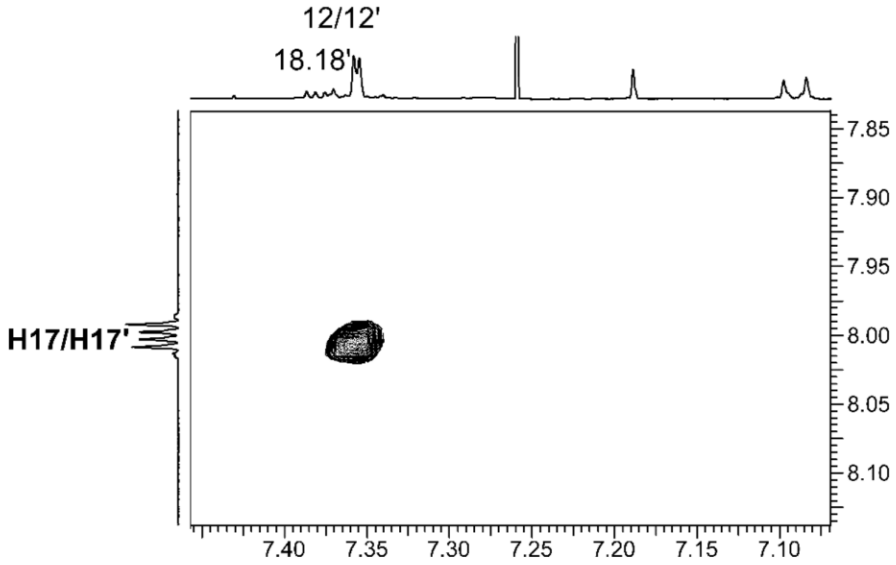

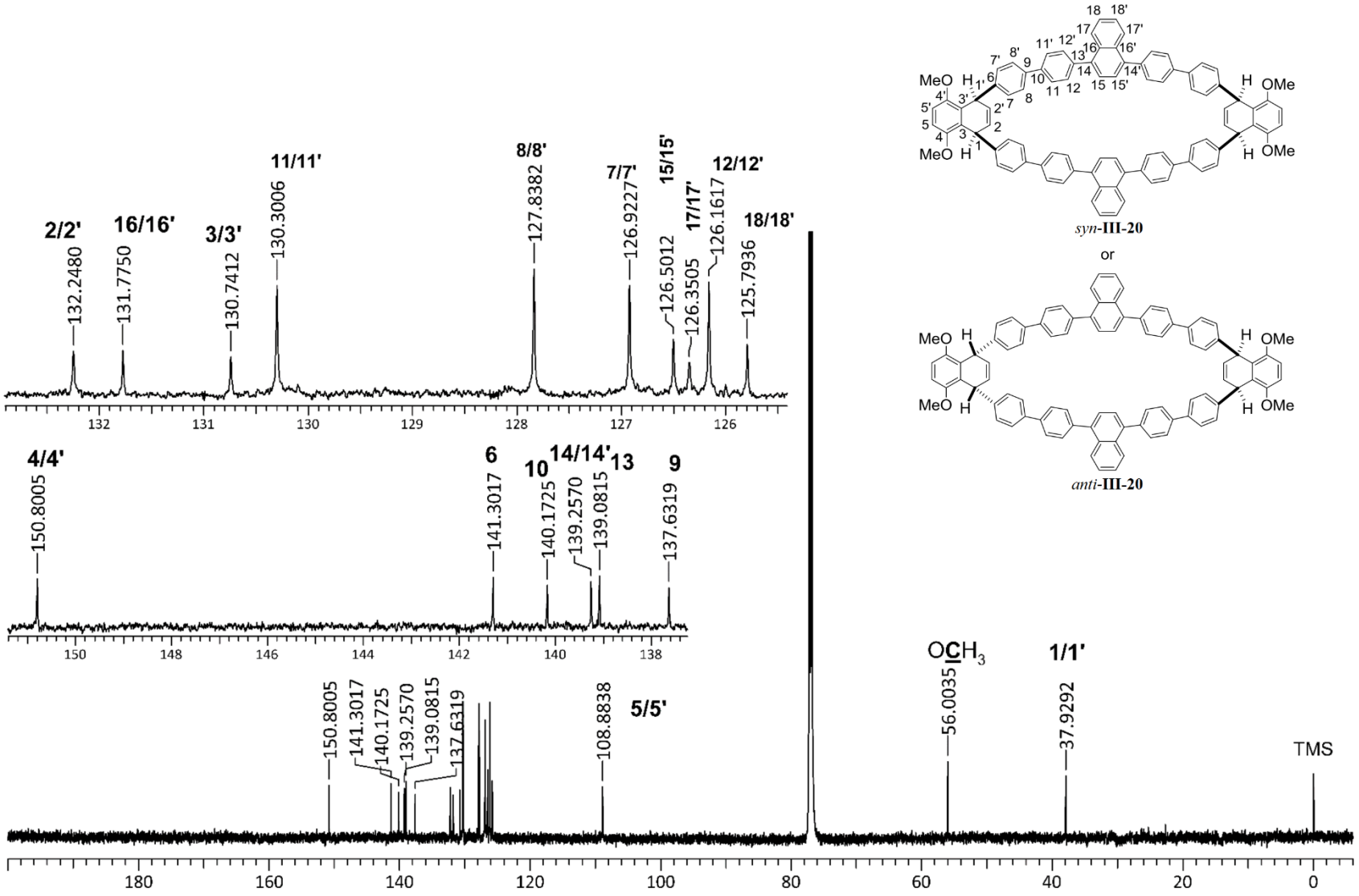
2/2'
16/16'
3/3'
11/11'
8/8'
7/7'
15/15'
17/17'
12/12'
18/18'
132.2480
131.7750
130.7412
130.3006
127.8382
126.9227
126.5012
126.3505
126.1617
125.7936
4/4'
6
10
14/14'
13
9
150.8005
141.3017
140.1725
139.2570
139.0815
137.6319
5/5'
108.8838
OCH3
1/1'
56.0035
37.9292
TMS
syn-III-20
or
anti-III-20

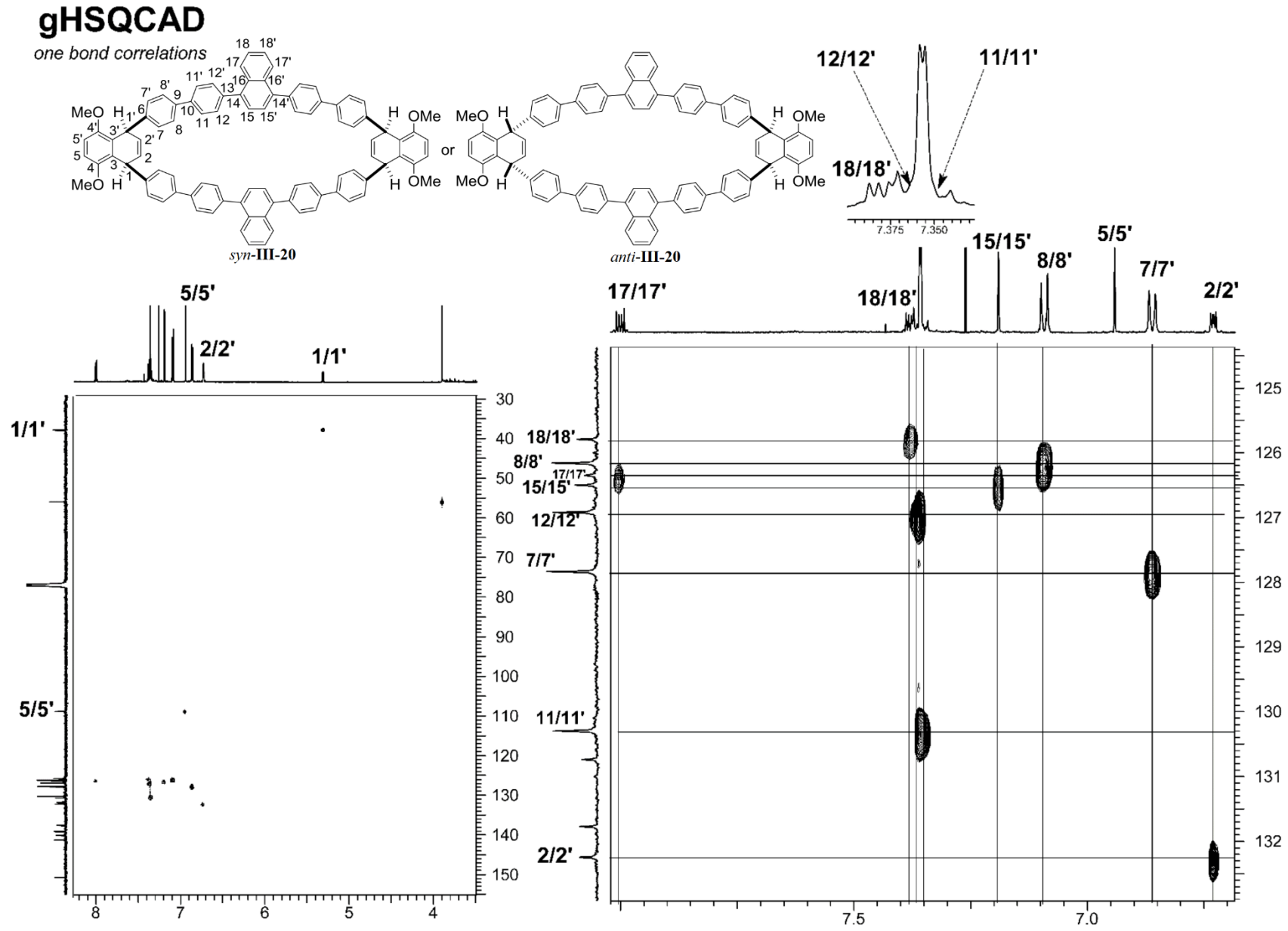
gHSQCAD
one bond correlations
syn-III-20
or
anti-III-20
12/12'
11/11'
18/18'
7.375
7.350
17/17'
18/18'
15/15'
8/8'
5/5'
7/7'
2/2'
1/1'
5/5'
2/2'
1/1'
18/18'
8/8'
17/17'
15/15'
12/12'
7/7'
11/11'
2/2'
7.5
7.0

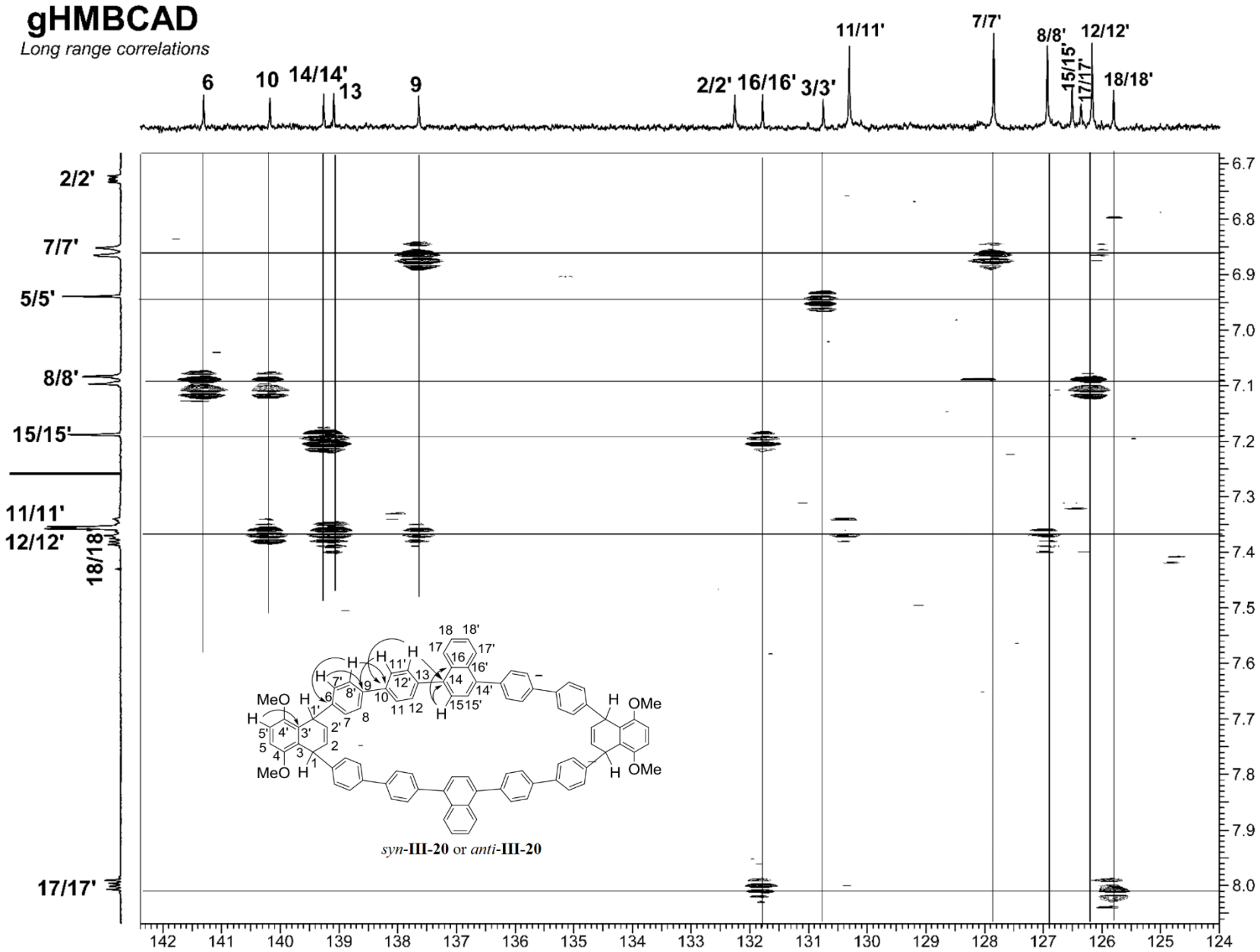
gHMBCAD
Long range correlations
6
10
14/14'
13
9
2/2'
16/16'
3/3'
11/11'
7/7'
8/8'
15/15'
17/17'
12/12'
18/18'
2/2'
7/7'
5/5'
8/8'
15/15'
11/11'
12/12'
18/18'
17/17'
6.7
6.8
6.9
7.0
7.1
7.2
7.3
7.4
7.5
7.6
7.7
7.8
7.9
8.0
142
141
140
139
138
137
136
135
134
133
132
131
130
129
128
127
126
125
124
MeO
OMe
syn-III-20 or anti-III-20

gHMBCAD

Long range correlations

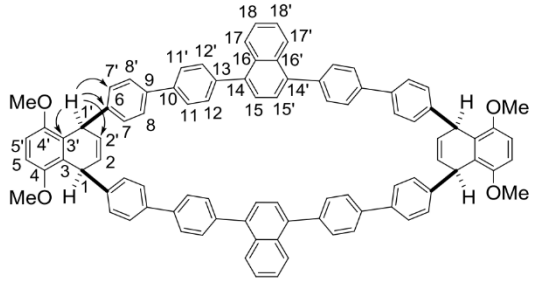

syn-**III-20**

or

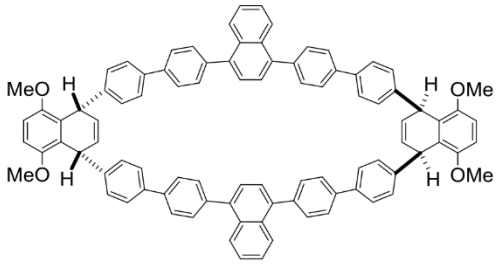

anti-**III-20**

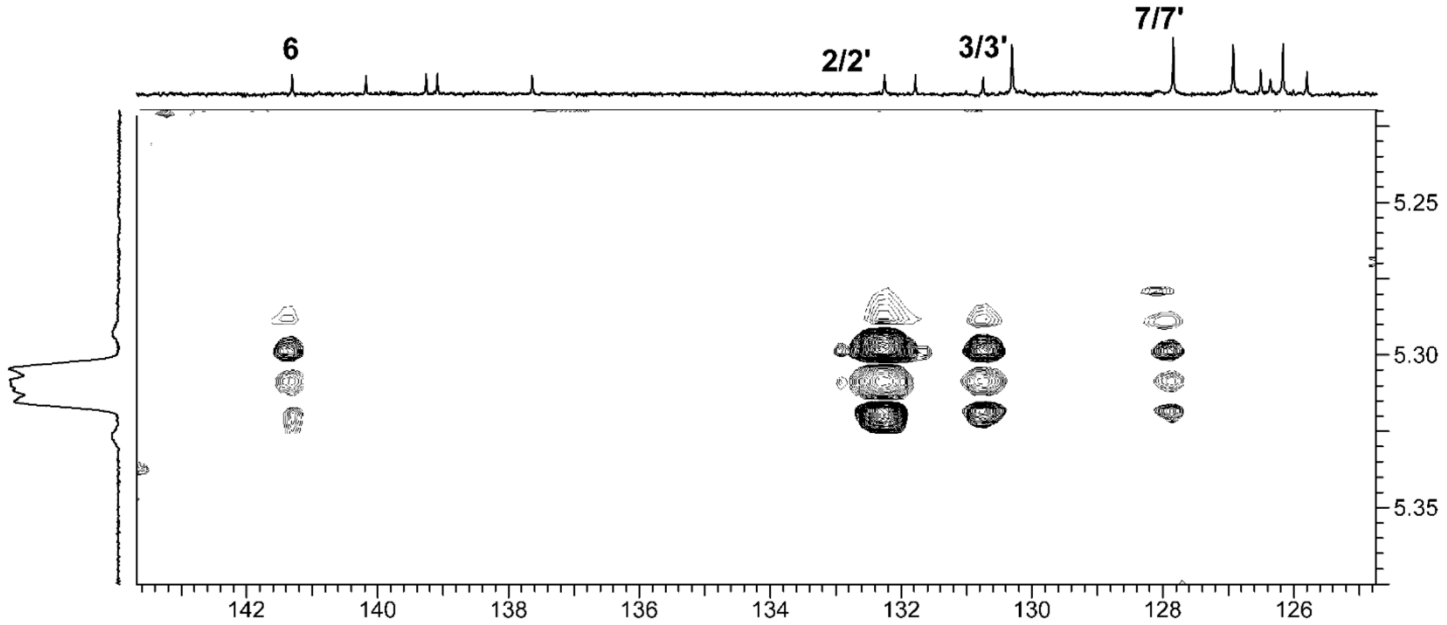

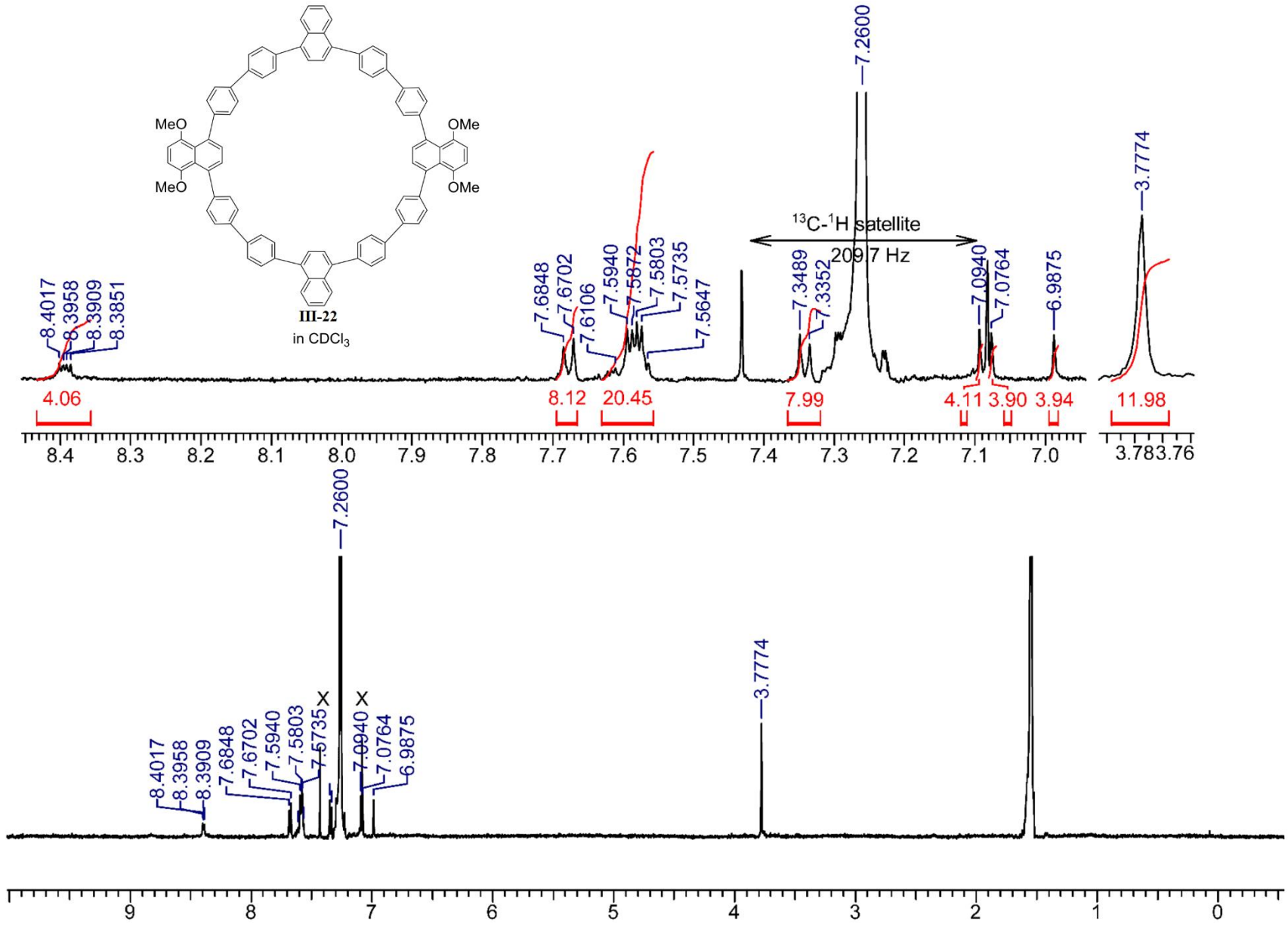
MeO
MeO
OMe
OMe
III-22
in CDCl3
8.4017
8.3958
8.3909
8.3851
7.6848
7.6702
7.6106
7.5940
7.5872
7.5803
7.5735
7.5647
7.3489
7.3352
7.2600
7.0940
7.0764
6.9875
3.7774
13C-1H satellite
209.7 Hz
4.06
8.12
20.45
7.99
4.11
3.90
3.94
11.98
8.4
8.3
8.2
8.1
8.0
7.9
7.8
7.7
7.6
7.5
7.4
7.3
7.2
7.1
7.0
3.783.76
X
X
9
8
7
6
5
4
3
2
1
0

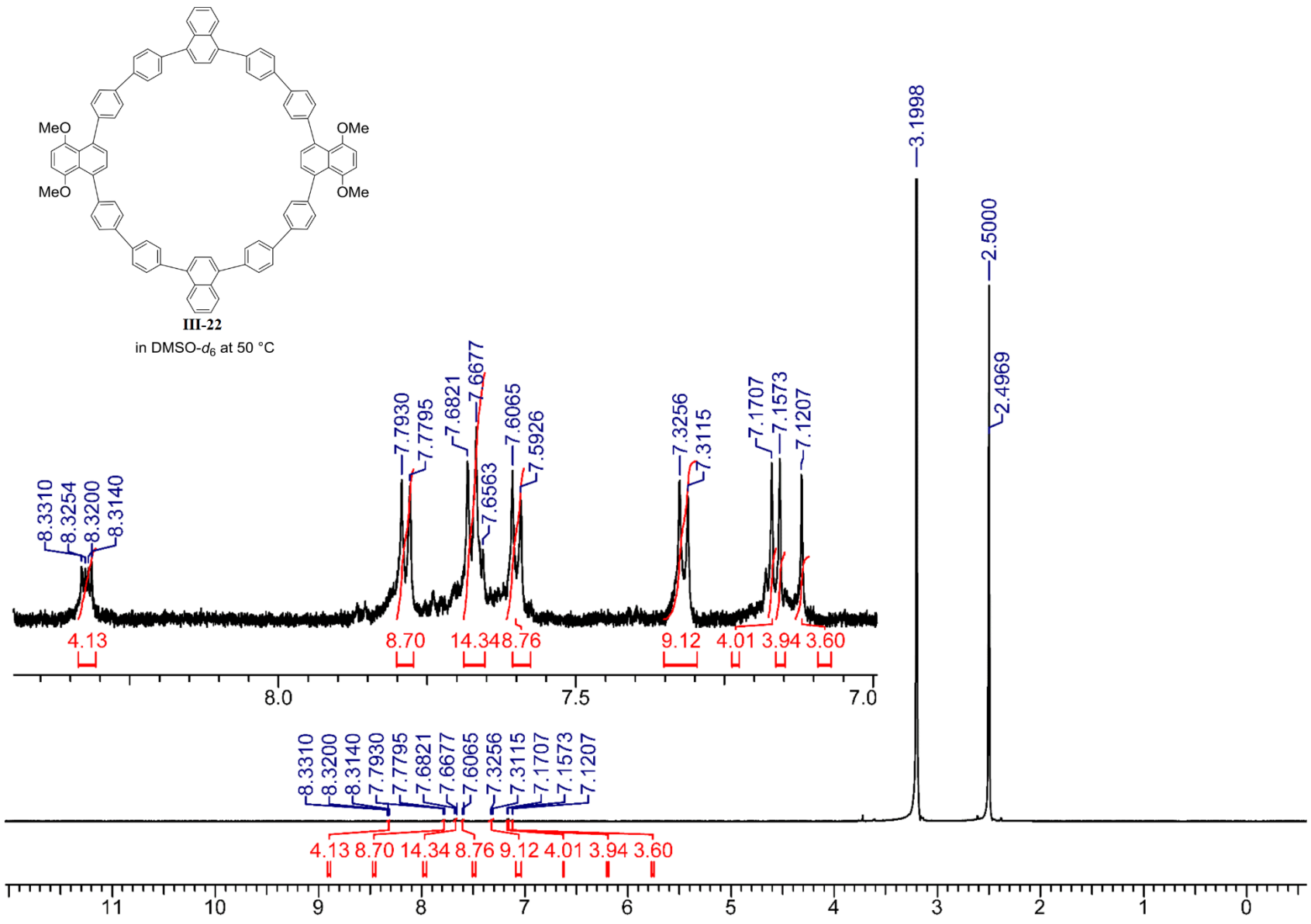
MeO
MeO
OMe
OMe
III-22
in DMSO-d_6 at 50 °C
8.3310
8.3254
8.3200
8.3140
7.7930
7.7795
7.6821
7.6677
7.6563
7.6065
7.5926
7.3256
7.3115
7.1707
7.1573
7.1207
3.1998
2.5000
2.4969
4.13
8.70
14.34
8.76
9.12
4.01
3.94
3.60
8.0
7.5
7.0
11
10
9
8
7
6
5
4
3
2
1
0

gCOSY spectrum

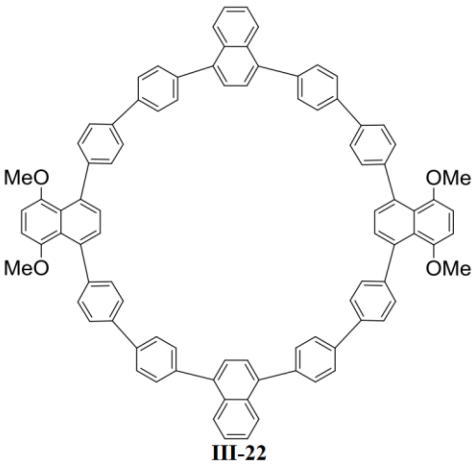

III-22

in DMSO-d_6 at 50 °C

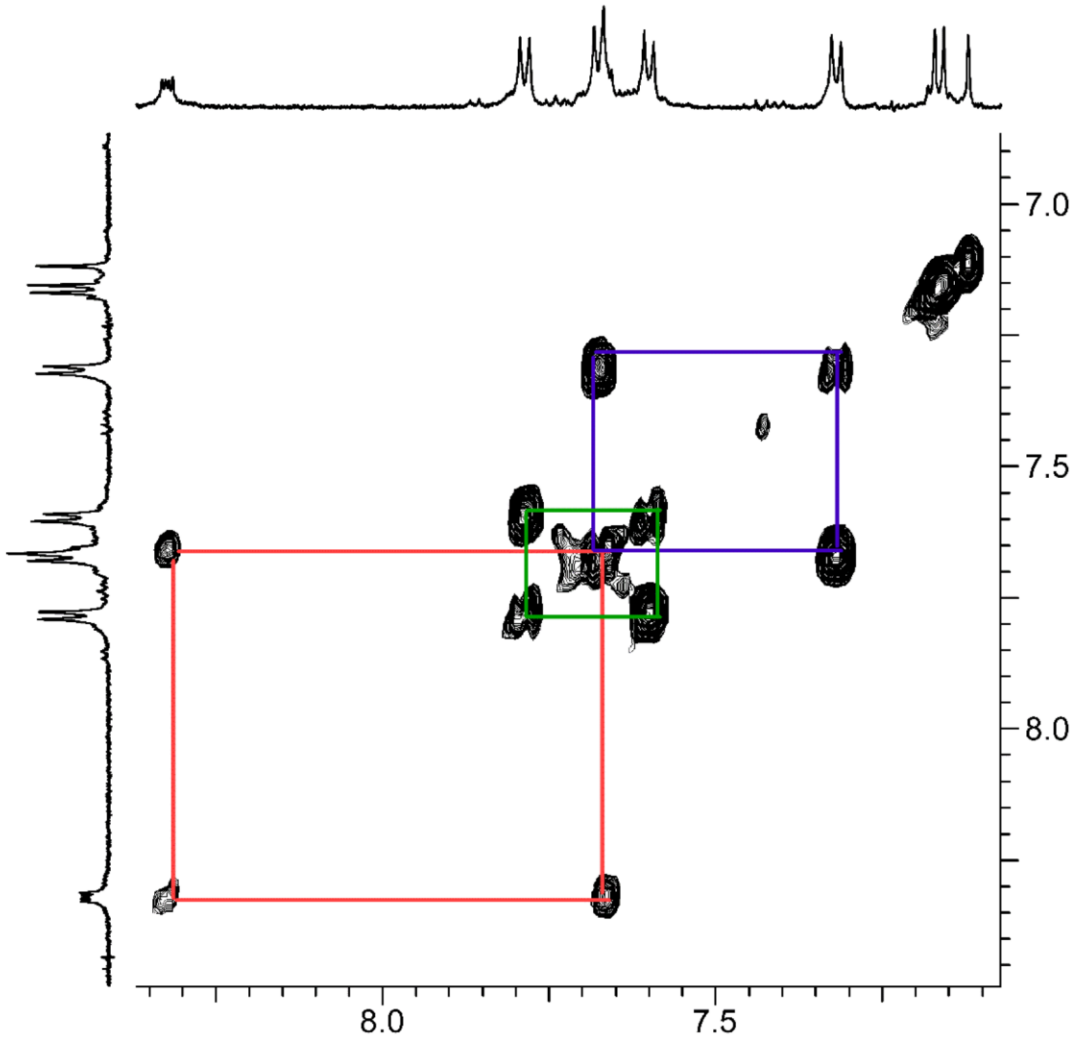

NMR parameters (chemical shifts and coupling constants)

AA'XX'

spin system

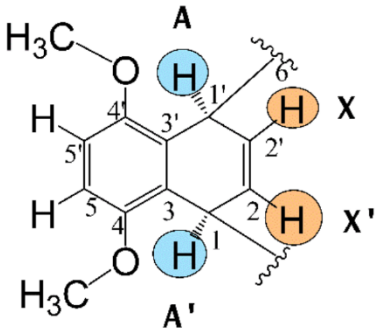

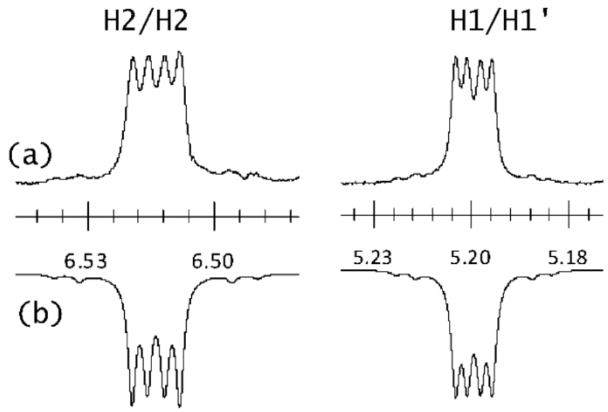

$J_{AA'}$ = **1.7 Hz**

J_{AX} = **6.1 Hz**

$J_{AX'}$ = **-0.4 Hz**

$J_{XX'}$ = **9.5 Hz**

(a) -experimental; (b)-calculated

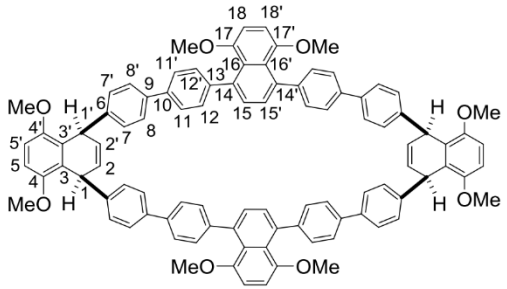

syn-**III-21**
or
anti-**III-21**

δ_H/ppm

7.36 (br d, J = 8.1 Hz, H11/H11')

7.23 (br d, J = 8.1 Hz, H8/H8')

7.23 (d, J = 8.3 Hz, H12/H12')

7.13 (s, H15/H15')

6.99 (d, J = 8.3 Hz, H7/H7')

6.89 (s, H5/H5')

6.76 (s, H18/H18')

6.52 (H2/H2', XX' part of the AA'XX' spin system)

5.20 (H1/H1', AA' part of the AA'XX' spin system)

3.84 (s, 4/4'-OCH_3)

3.41 (s, 17/17'-OCH_3)

Carbon	δ_C/ppm
C1/C1'	38.80
C2/C2'	130.74
C3/C3'	129.58
C4/C4'	151.05
4/4'-OCH_3	55.91
C5/C5	108.79
C6	141.60
C7/C7'	128.12
C8/C8'	126.33
C9	138.53
C10	138.36
C11/C11'	125.35
C12/C12'	128.54
C13	144.29
C14	137.73
C15/C15'	129.28
C16/C16'	125.43
C17/C17'	151.24
17/17'-OCH_3	56.05
C18/C18'	107.18

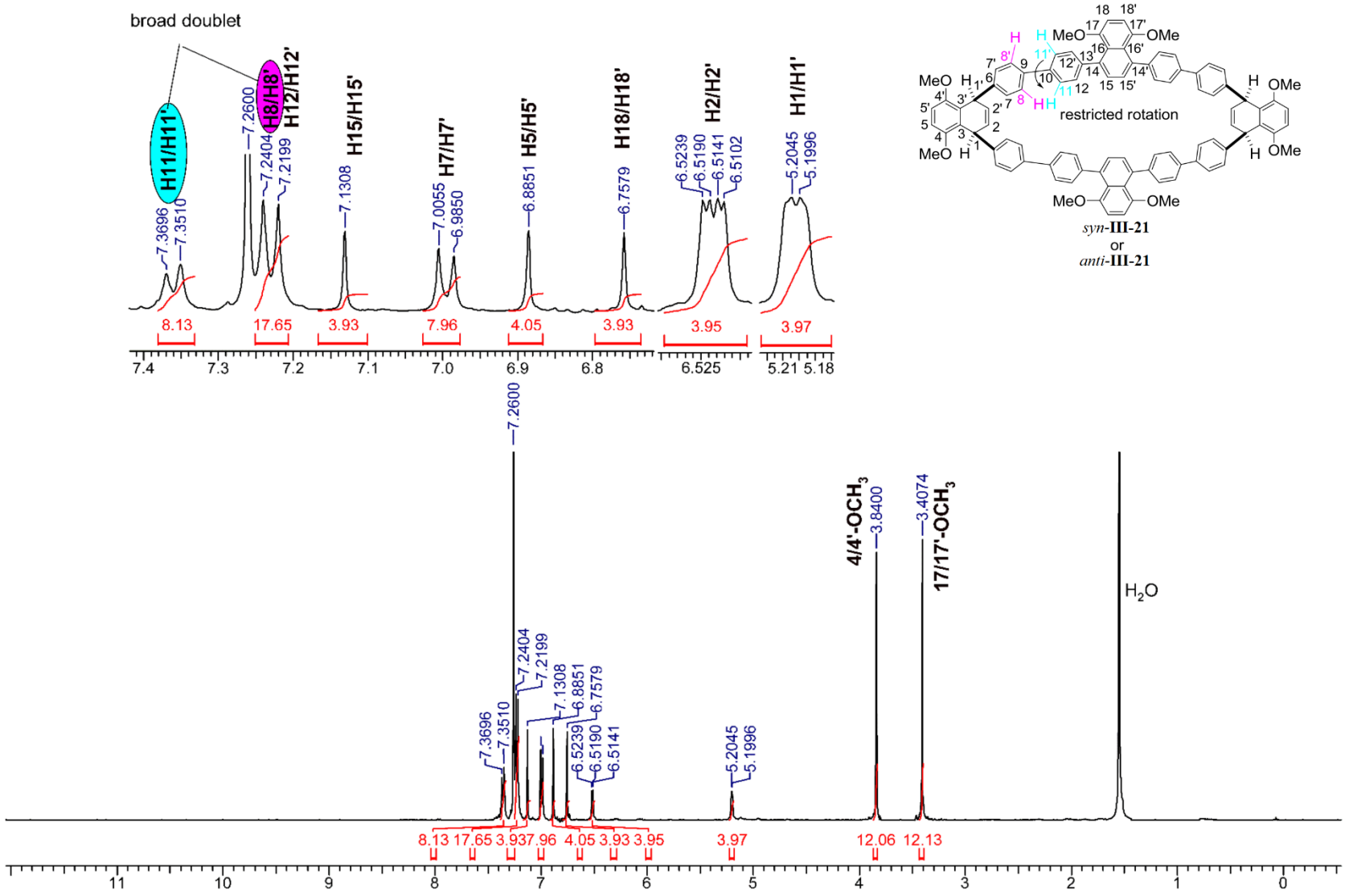
broad doublet
H11/H11'
H8/H8'
H12/H12'
H15/H15'
H7/H7'
H5/H5'
H18/H18'
H2/H2'
H1/H1'
7.3696
7.3510
7.2600
7.2404
7.2199
7.1308
7.0055
6.9850
6.8851
6.7579
6.5239
6.5190
6.5141
6.5102
5.2045
5.1996
8.13
17.65
3.93
7.96
4.05
3.93
3.95
3.97
restricted rotation
syn-III-21
or
anti-III-21
4/4'-OCH3
3.8400
17/17'-OCH3
3.4074
H2O
12.06
12.13

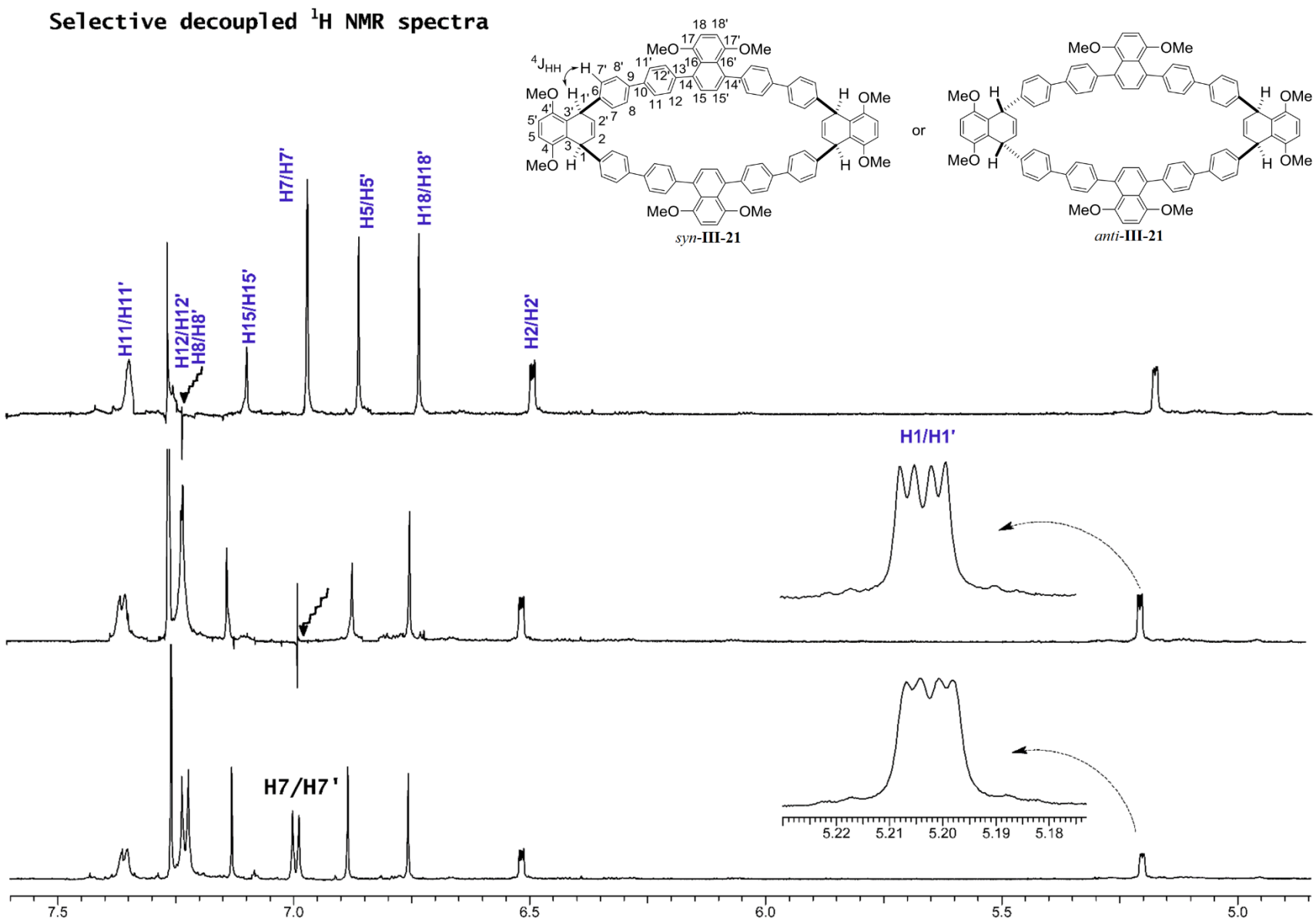
Selective decoupled ^{1}H NMR spectra
$^4J_{HH}$
MeO
OMe
H
or
syn-III-21
anti-III-21
H11/H11'
H12/H12'
H8/H8'
H15/H15'
H7/H7'
H5/H5'
H18/H18'
H2/H2'
H1/H1'
H7/H7'
5.22
5.21
5.20
5.19
5.18
7.5
7.0
6.5
6.0
5.5
5.0

ROESYAD

Through space correlations

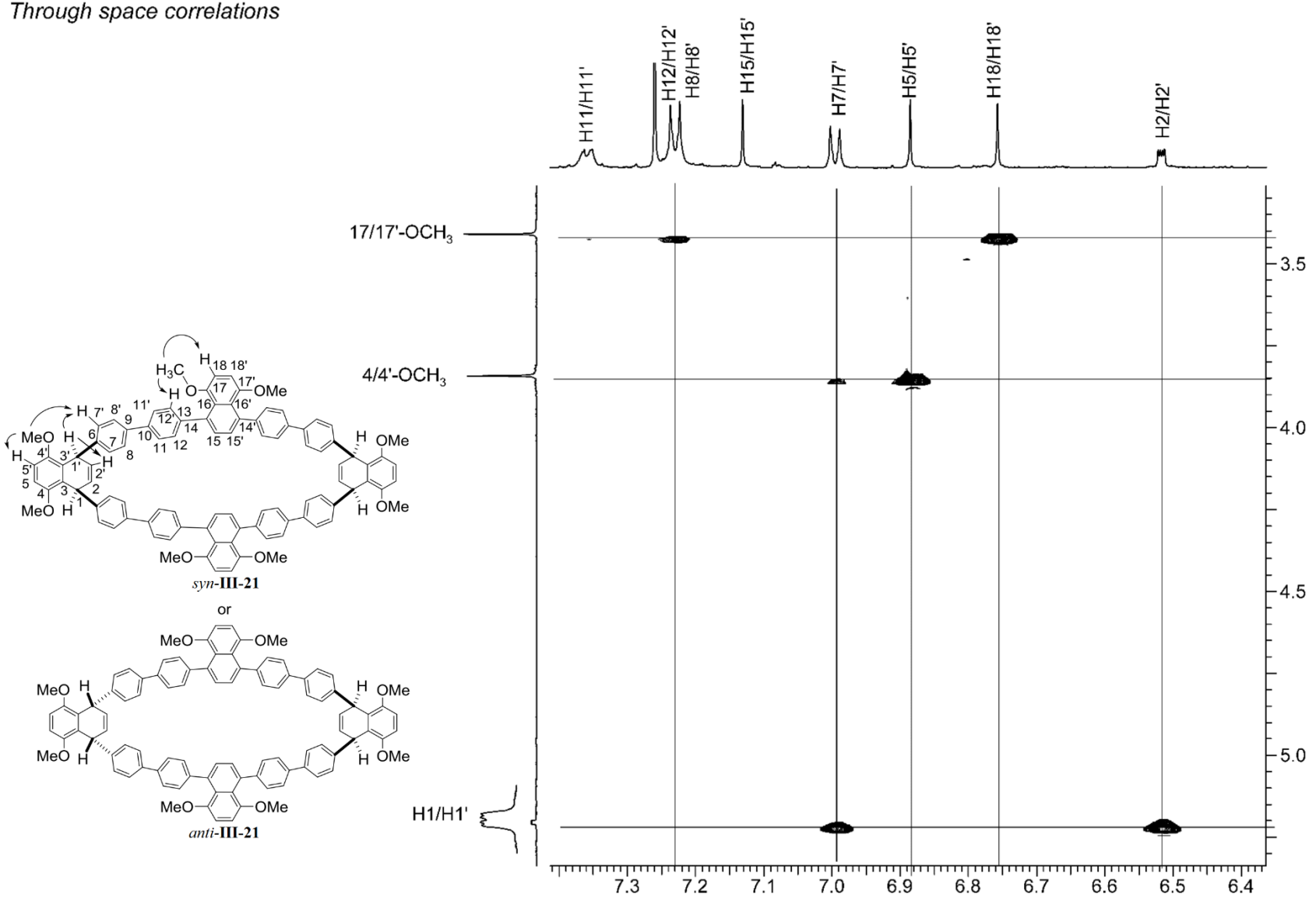

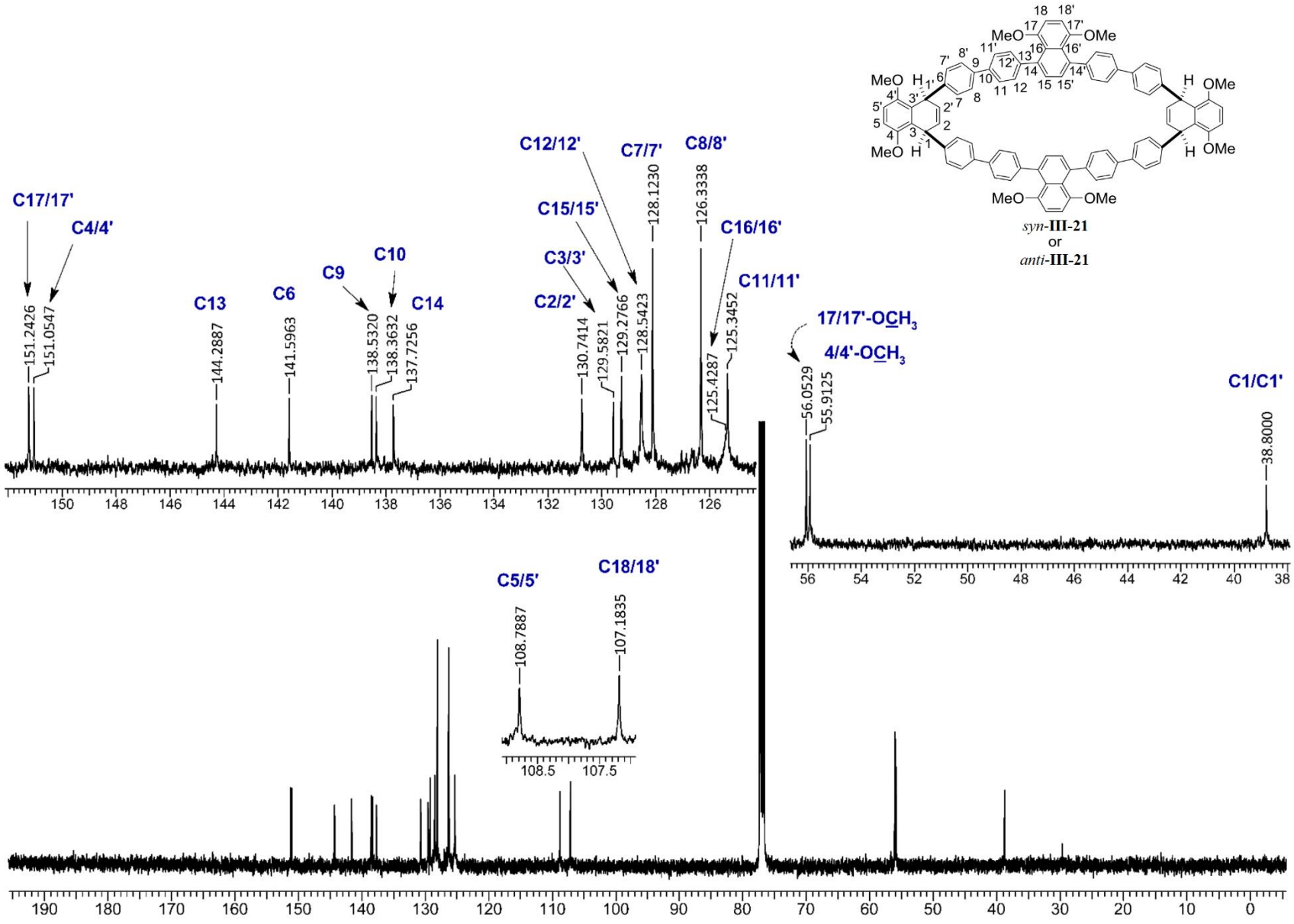

syn-**III-21**
or
anti-**III-21**

gHSQCAD

One-bond correlations

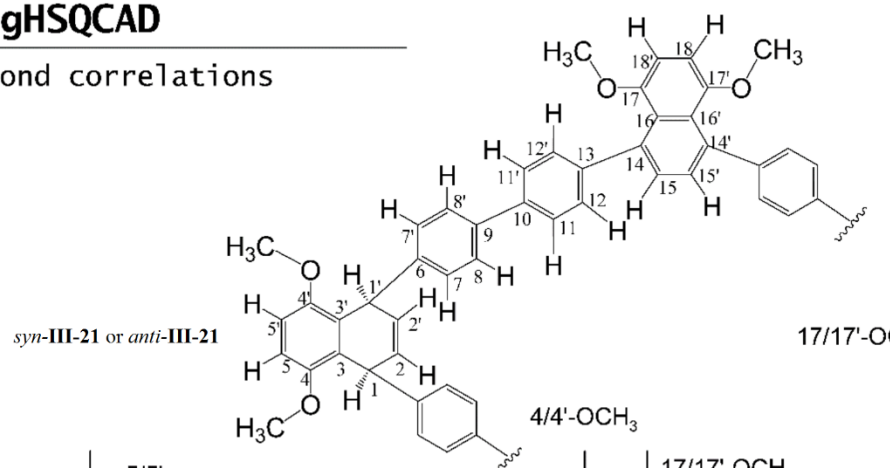

syn-**III-21** or *anti*-**III-21**

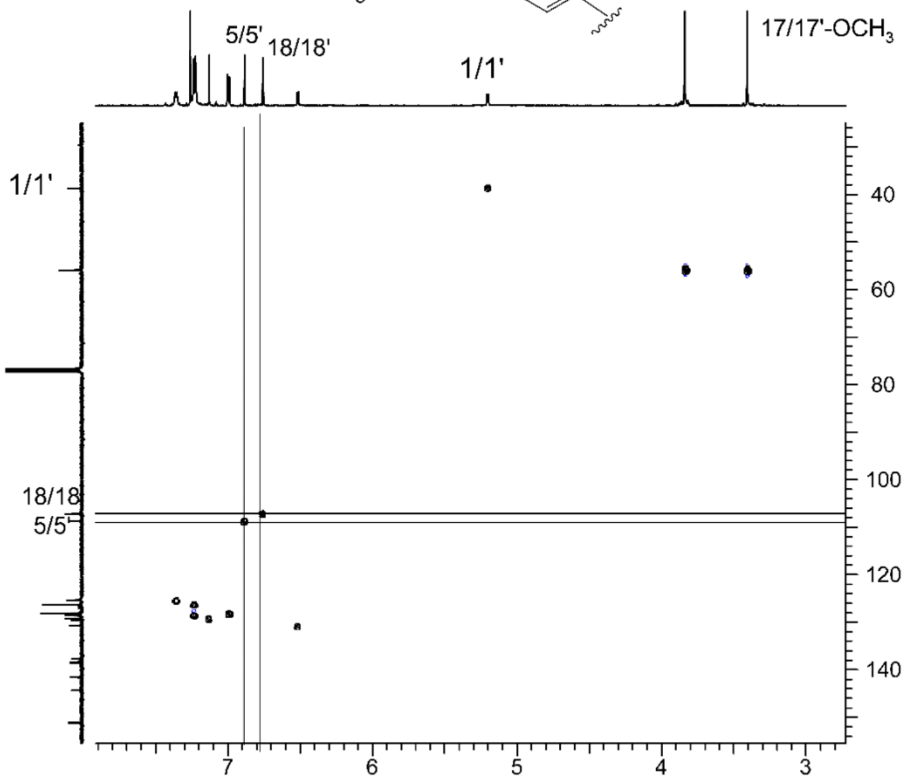

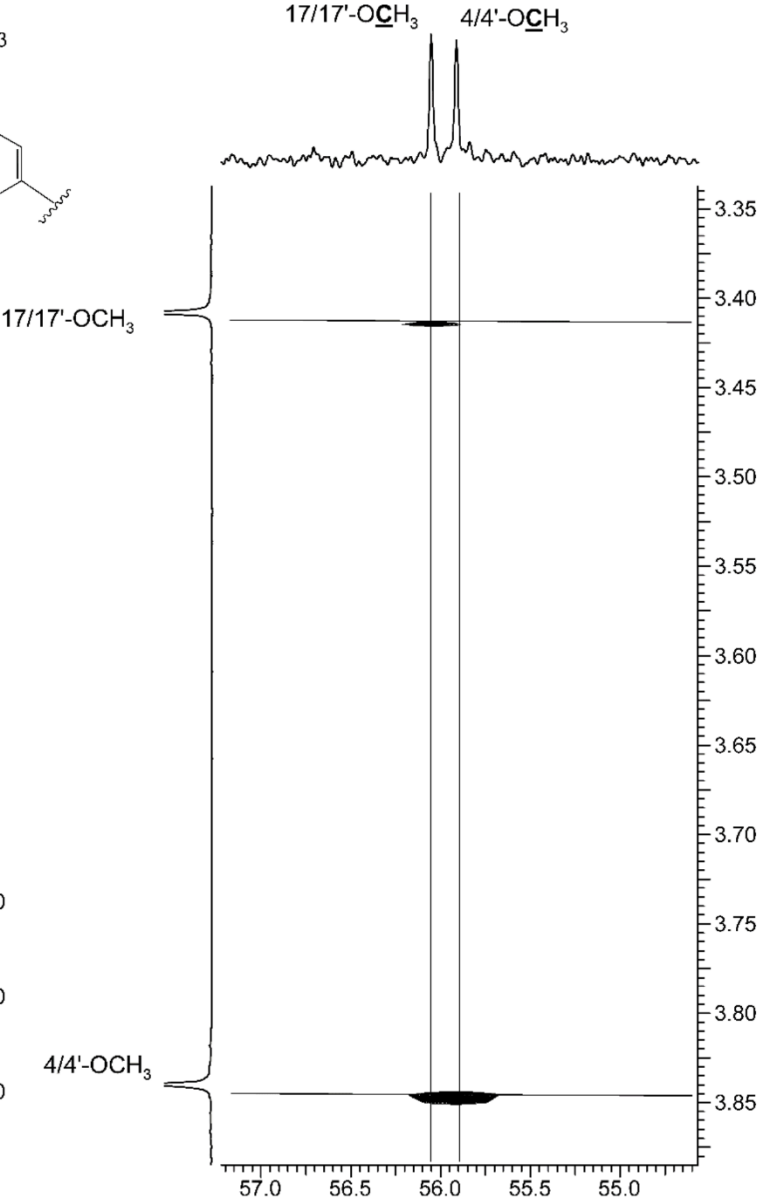

gHSQCAD

One-bond correlations

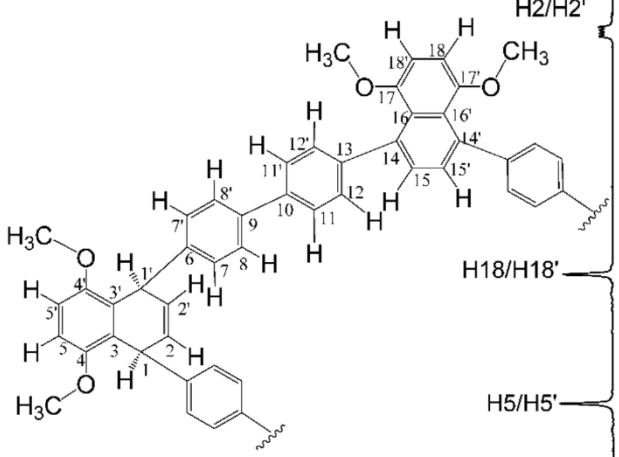

syn-**III-2**1 or *anti*-**III-21**

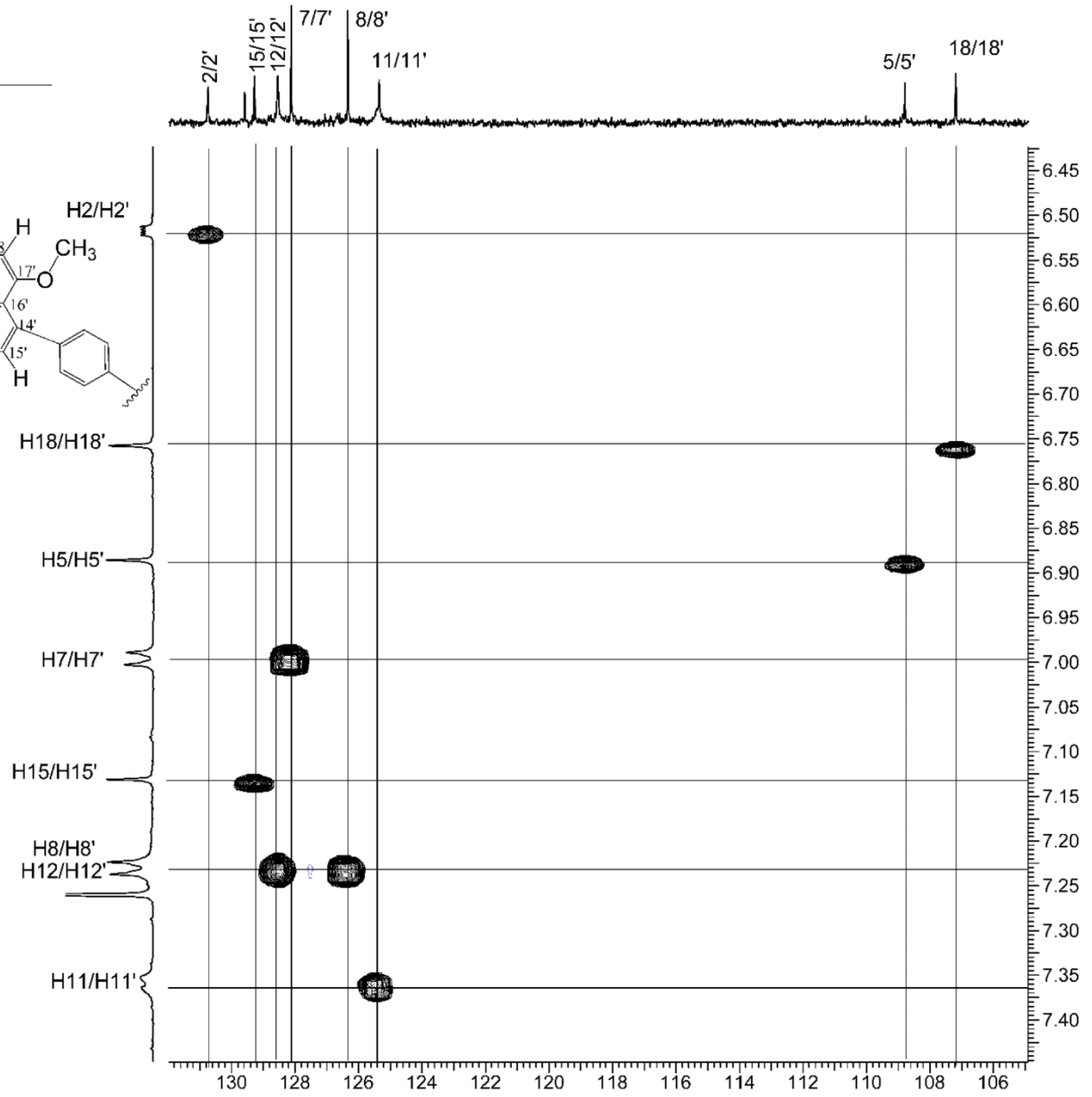

Expanded regions of the **gHMBCAD** spectrum

$^2J_{HC}$ and $^3J_{HC}$ correlations

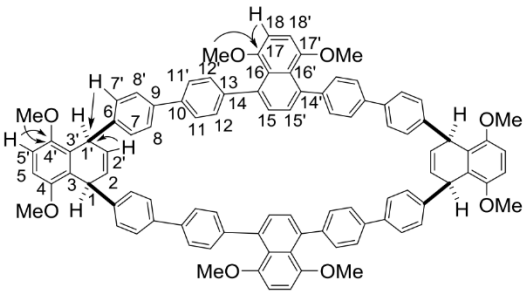

syn-**III-21**

or

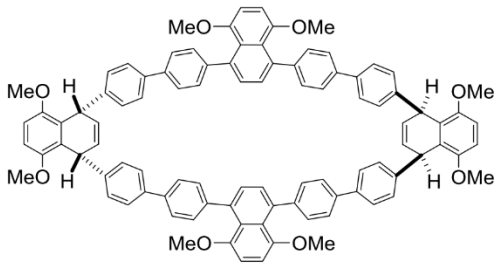

anti-**III-21**

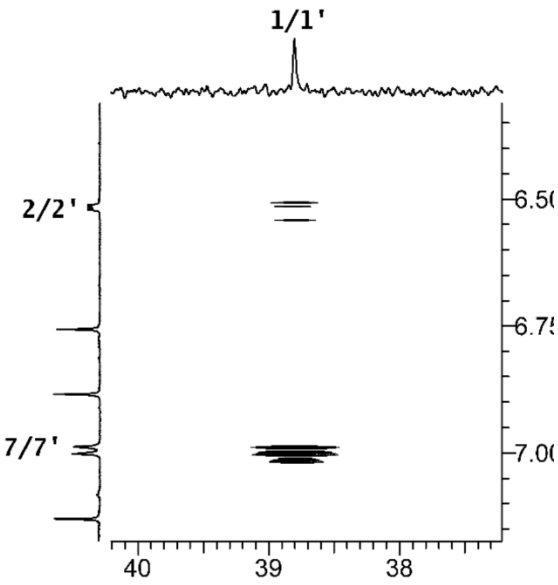

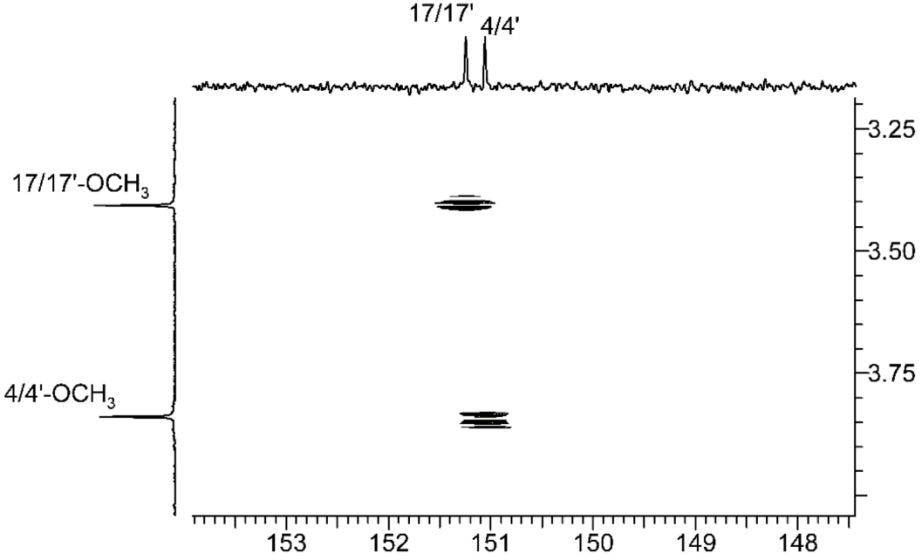

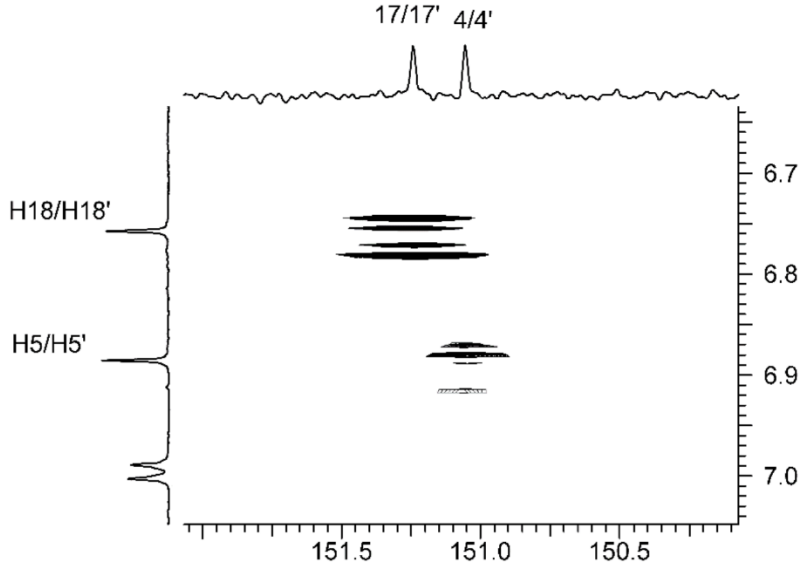

Expanded regions of the **gHMBCAD** spectrum

$^{2}J_{HC}$ and $^{3}J_{HC}$ correlations

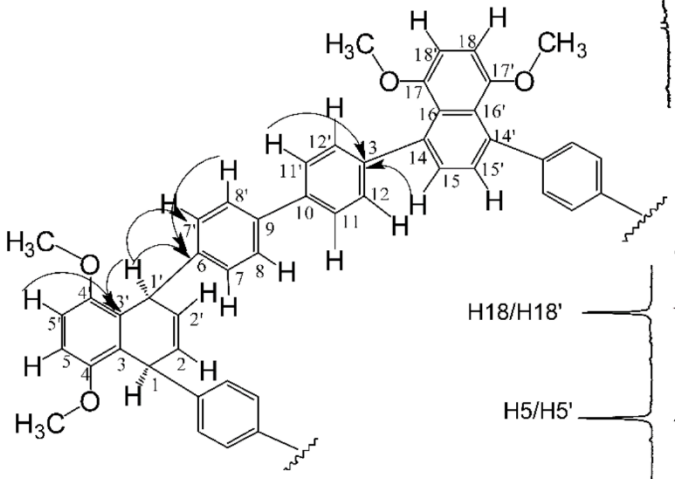

syn-**III-21** or *anti*-**III-21**

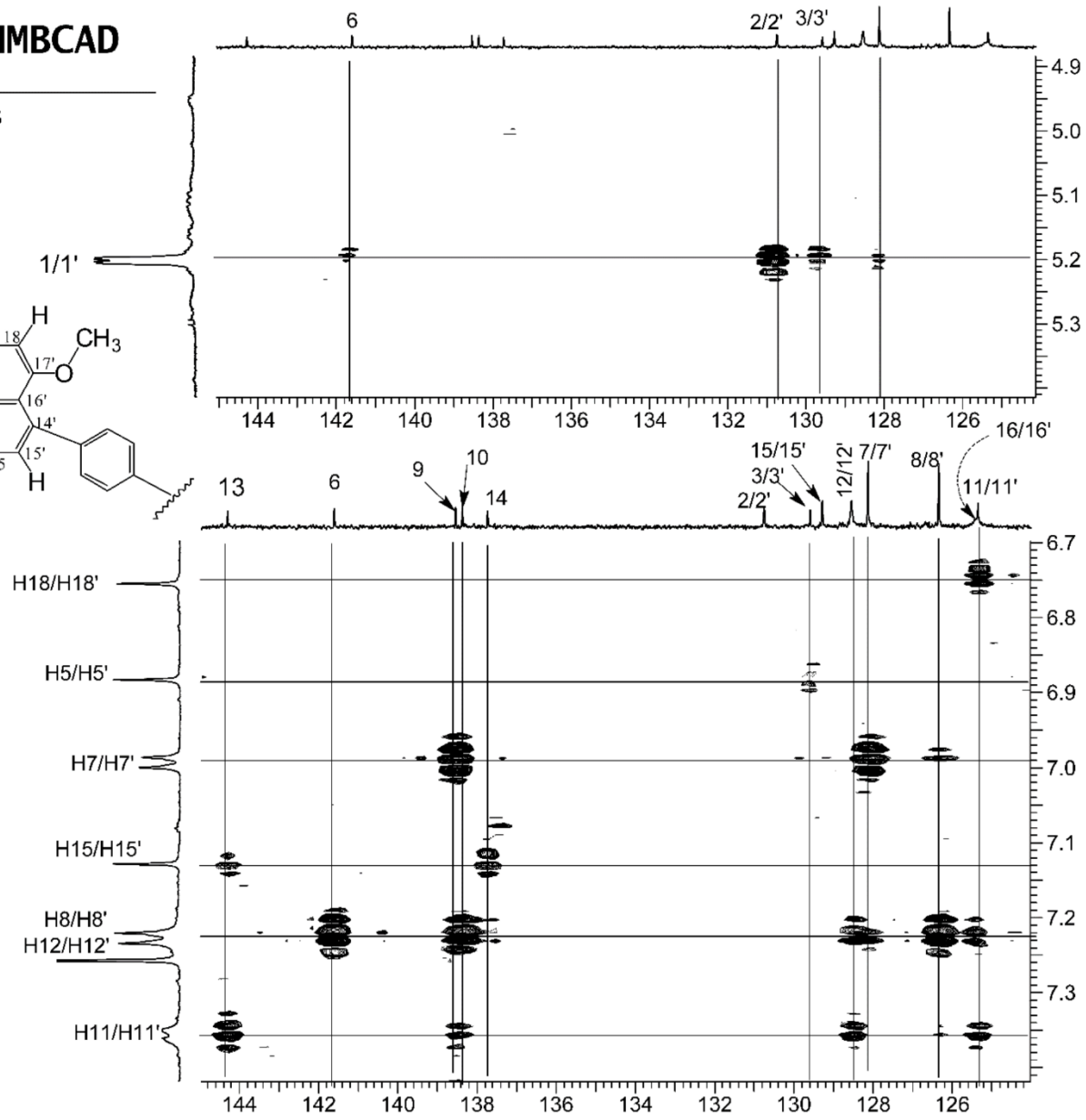

NMR parameters (chemical shifts and coupling constants)

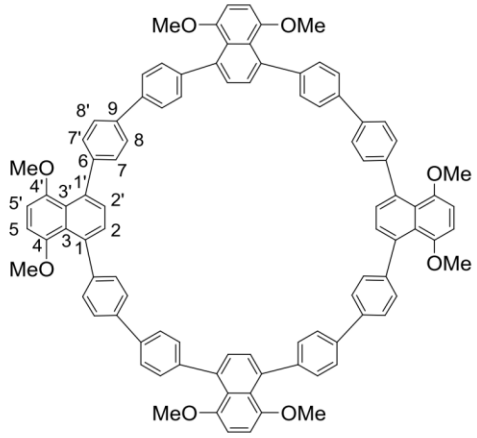

III-23
in DMSO-d_6 at 50 °C

δ_H/ppm	Multiplicity and coupling constants
7.64	(d, J = 8.5 Hz, H8/H8')
7.29	(d, J = 8.5 Hz, H7/H7')
7.13	(s, H/5/H5'/)
7.09	(s, H2/H2')
3.68	(s, H4/H4'-OCH_3)

Carbon	δ_C/ppm
C1/C1'	135.82
C2/C2'	131.01
C3/C3'	123.77
C4/C4'	150.17
4/4'-OCH_3	55.60
C5/C5'	107.77
C6	142.91
C7/C7'	127.69
C8/C8'	125.15
C9	136.47

+50°C

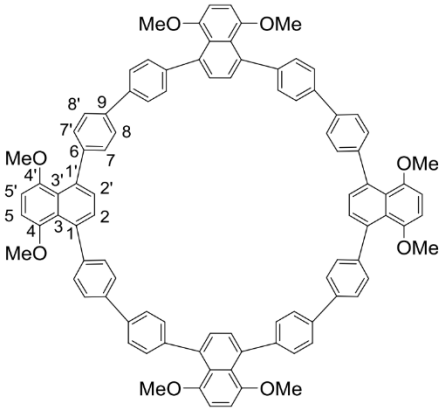

III-23

in DMSO-d_6 at 50 °C

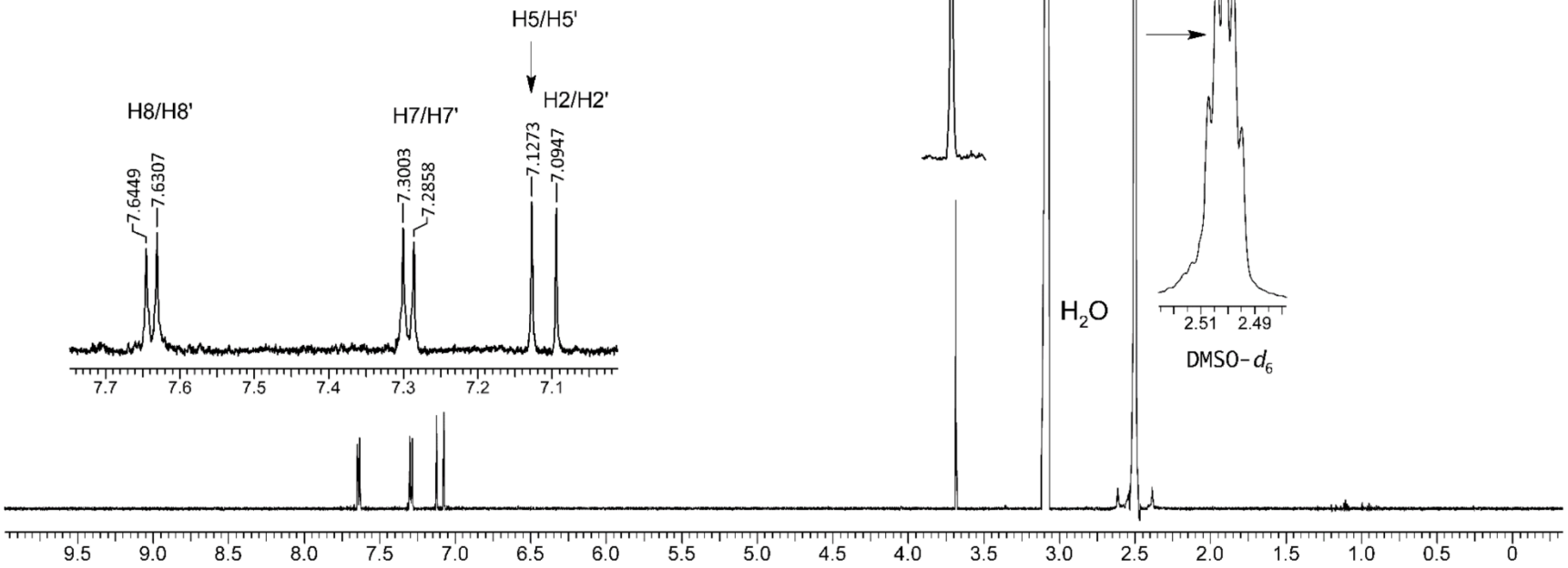

2D NOESY spectrum

Reveals long-range correlations between OCH_3 and H5/H5'

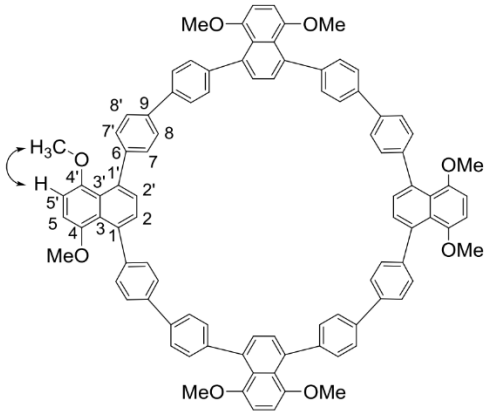

III-23

in DMSO-d_6 at 50 °C

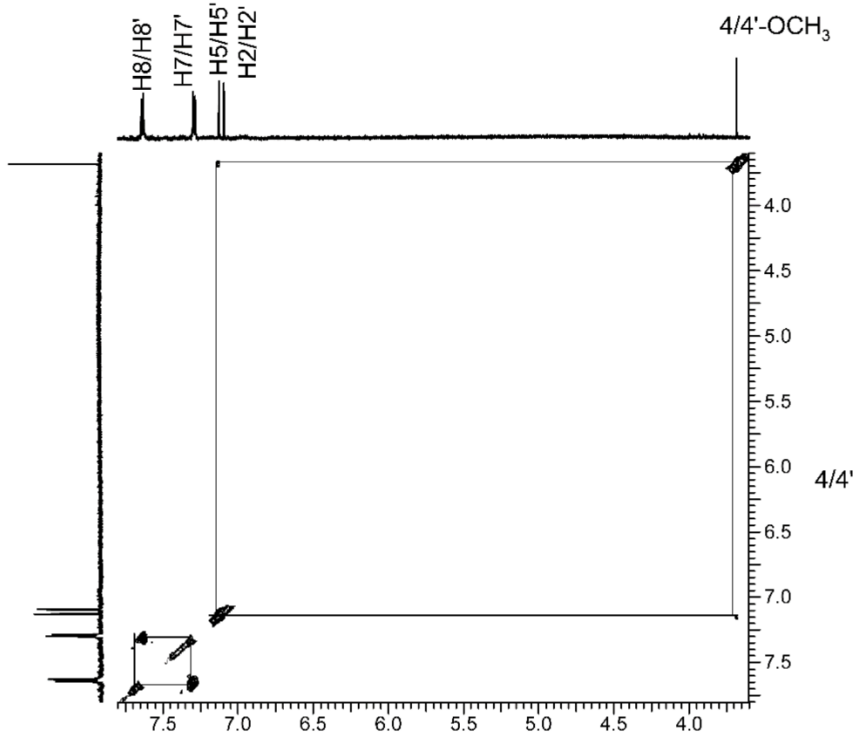

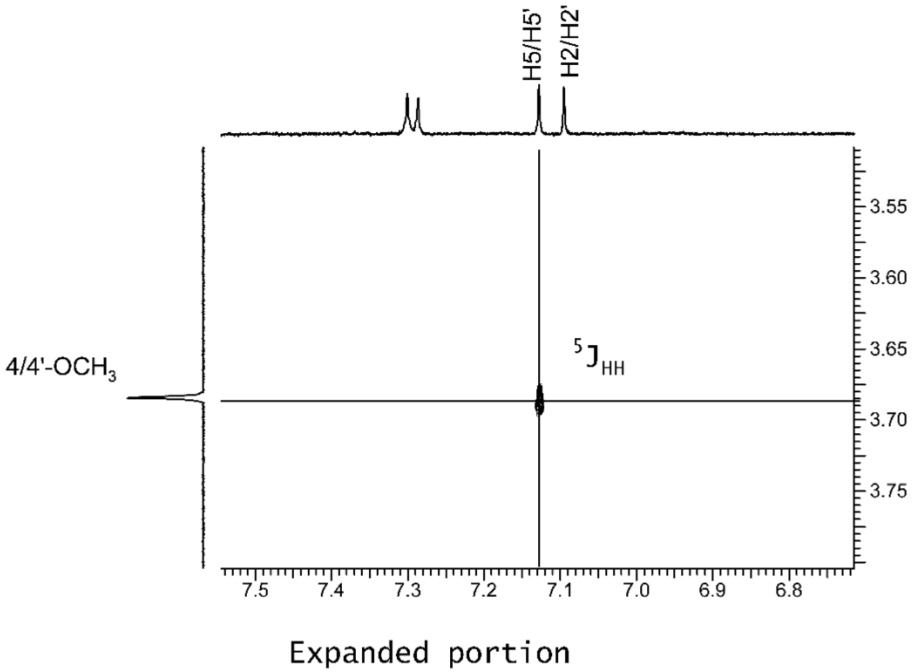

Expanded portion

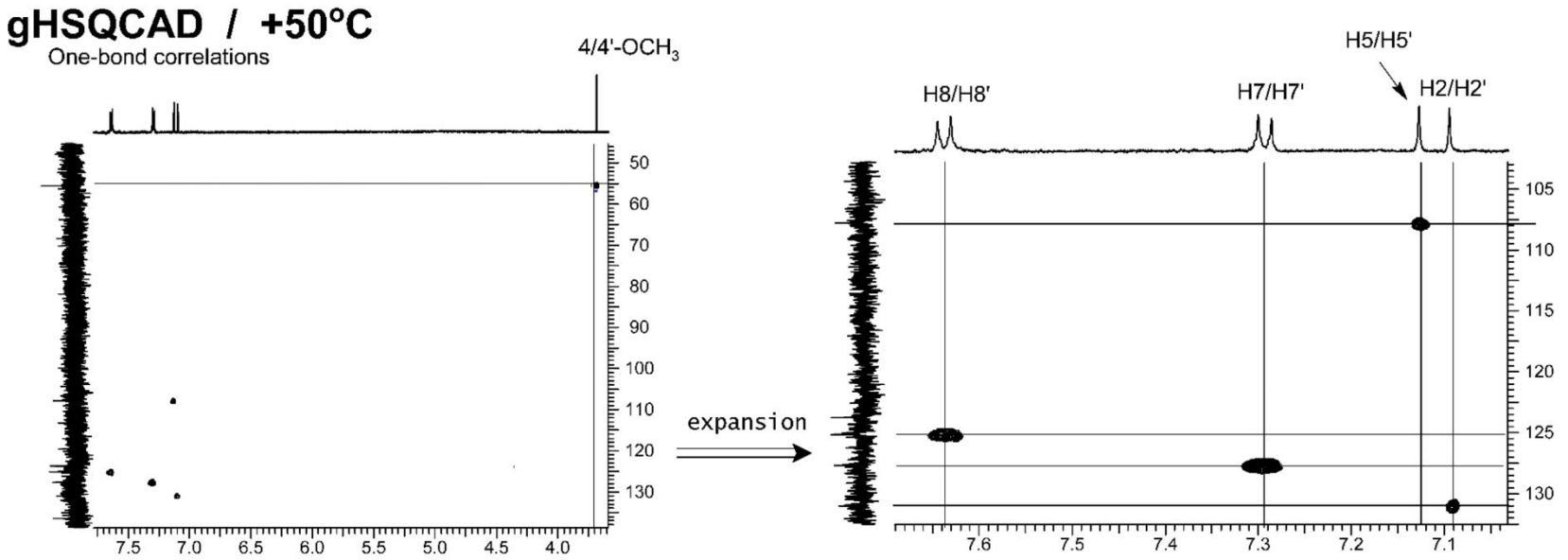
gHSQCAD / +50°C
One-bond correlations
4/4'-OCH3
H8/H8'
H7/H7'
H5/H5'
H2/H2'
expansion

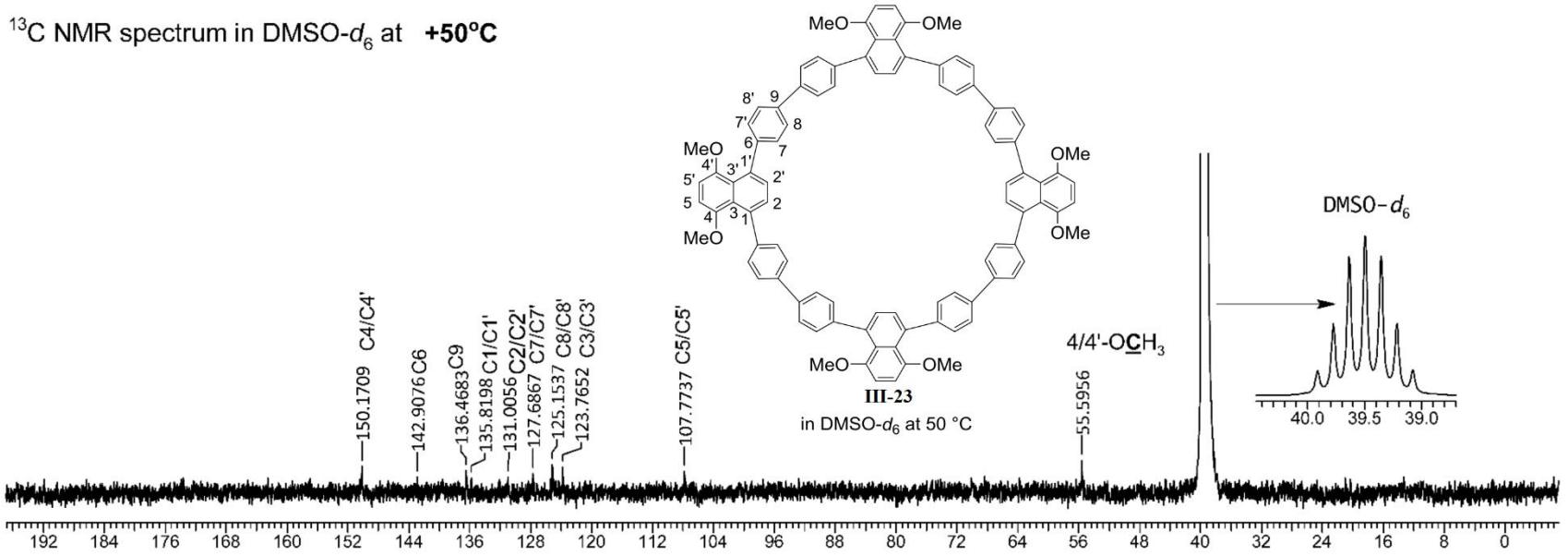
13C NMR spectrum in DMSO-d6 at +50°C
150.1709 C4/C4'
142.9076 C6
136.4683 C9
135.8198 C1/C1'
131.0056 C2/C2'
127.6867 C7/C7'
125.1537 C8/C8'
123.7652 C3/C3'
107.7737 C5/C5'
55.5956
4/4'-OCH3
DMSO-d6
III-23
in DMSO-d6 at 50 °C

gHMBCAD

Long-range correlations

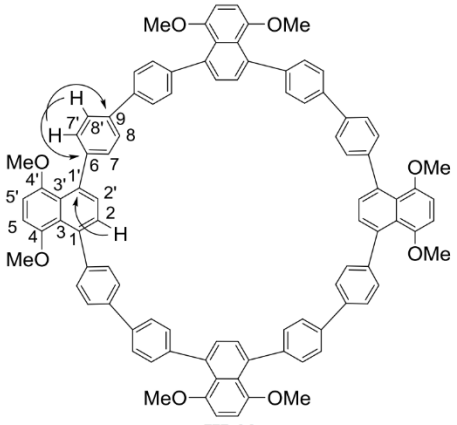

III-23

in DMSO-d_6 at 50 °C

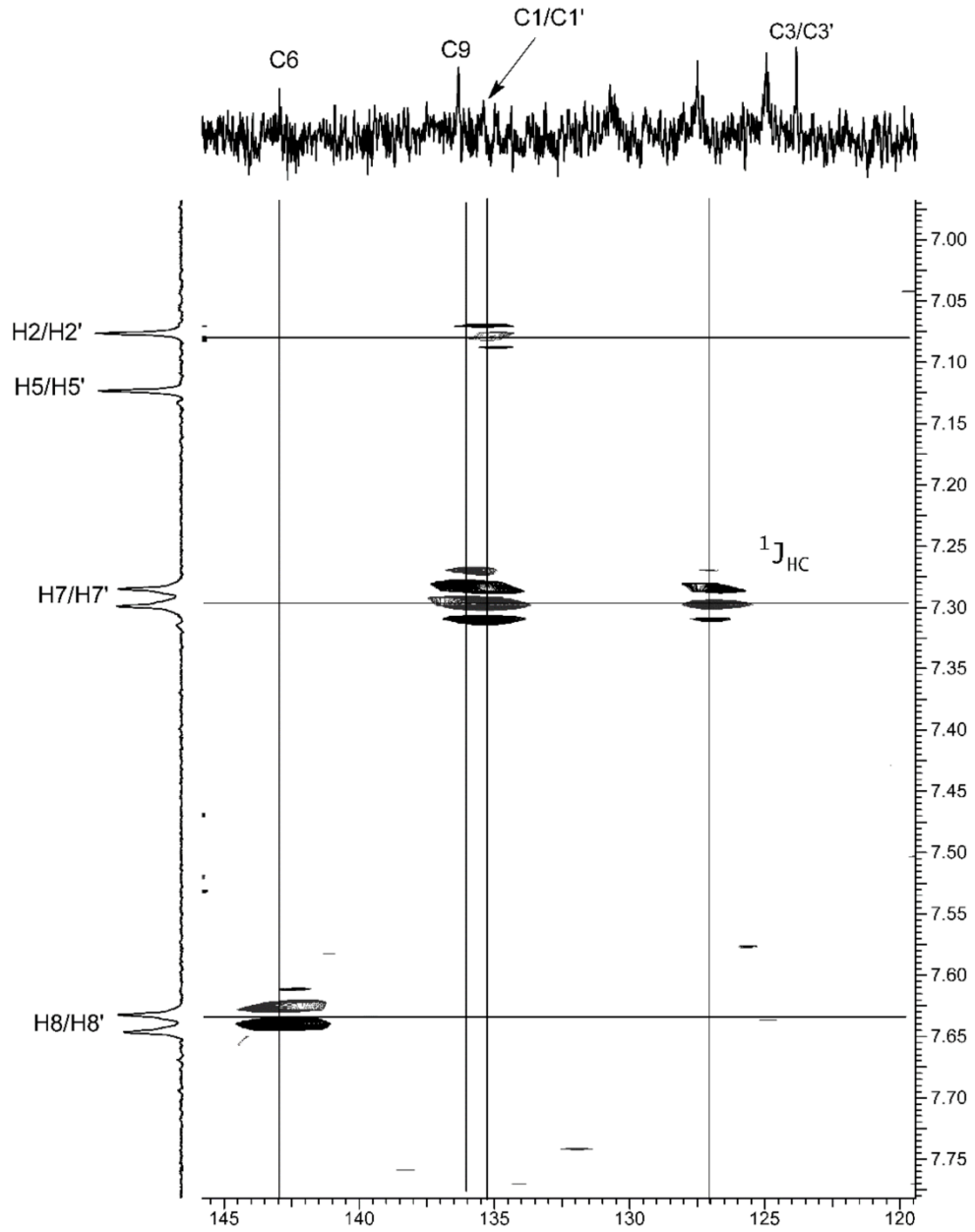

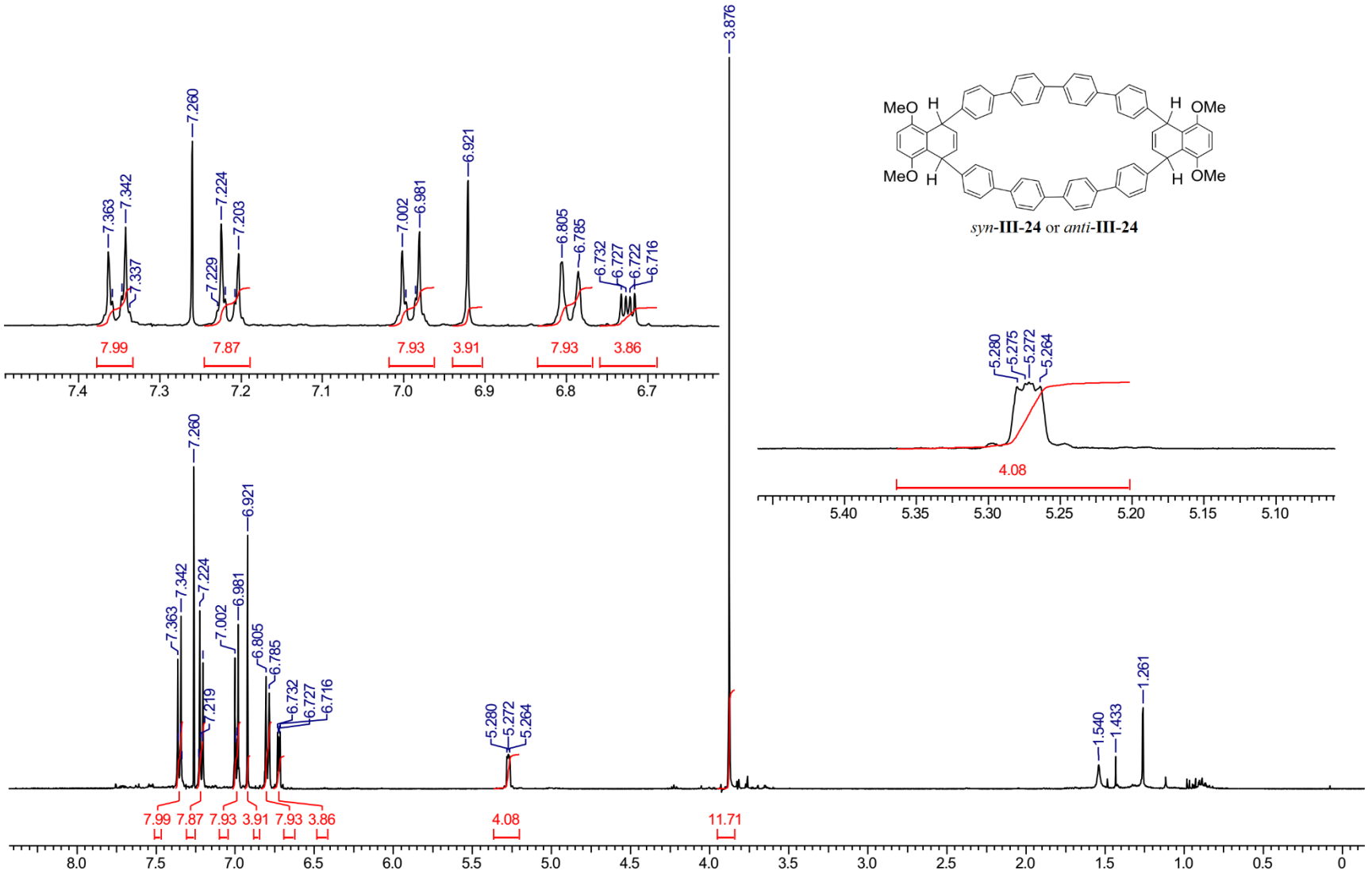
3.876
7.260
7.363
7.342
7.224
7.203
7.229
7.337
7.002
6.981
6.921
6.805
6.785
6.732
6.727
6.722
6.716
7.99
7.87
7.93
3.91
7.93
3.86
MeO
H
H
OMe
MeO
H
H
OMe
syn-III-24 or anti-III-24
5.280
5.275
5.272
5.264
4.08
7.260
6.921
7.342
7.363
7.224
7.002
6.981
6.805
6.785
7.219
6.732
6.727
6.716
5.280
5.272
5.264
1.540
1.433
1.261
7.99
7.87
7.93
3.91
7.93
3.86
4.08
11.71

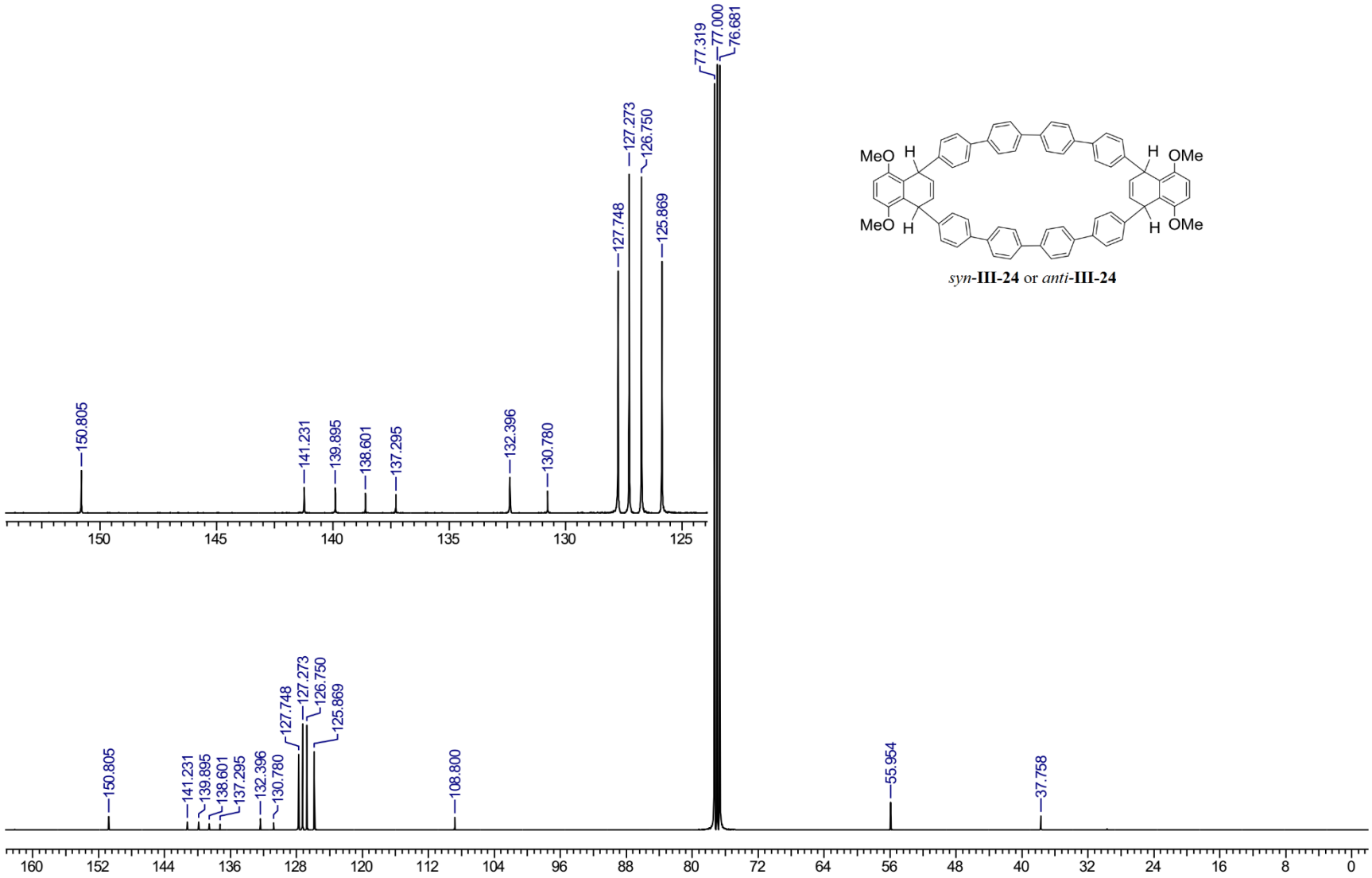

syn-**III-24** or *anti*-**III-24**

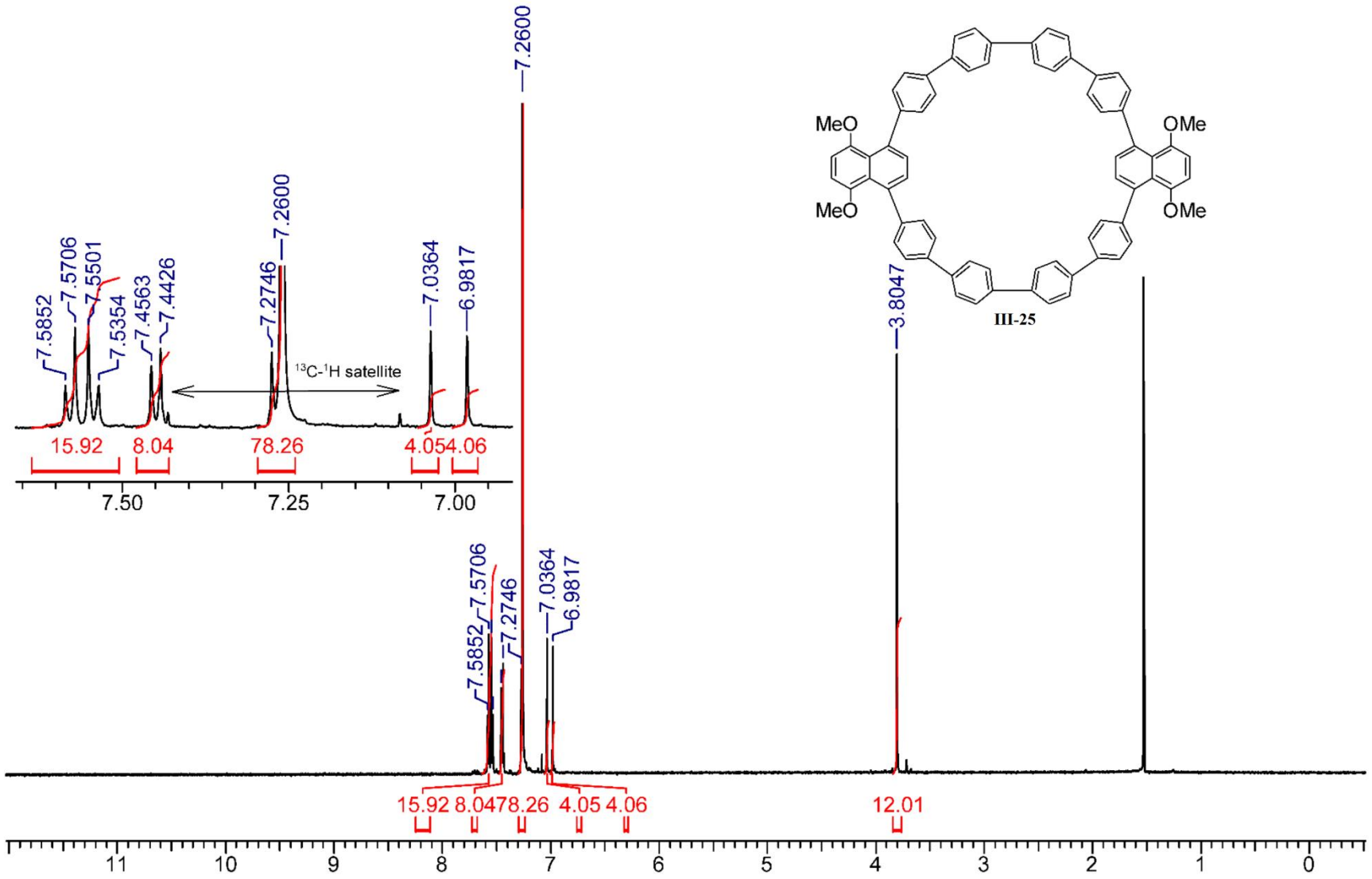
7.2600
7.5852
7.5706
7.5501
7.5354
7.4563
7.4426
7.2746
7.2600
7.0364
6.9817
13C-1H satellite
15.92
8.04
78.26
4.05
4.06
7.50
7.25
7.00
MeO
MeO
OMe
OMe
III-25
3.8047
12.01
11
10
9
8
7
6
5
4
3
2
1
0

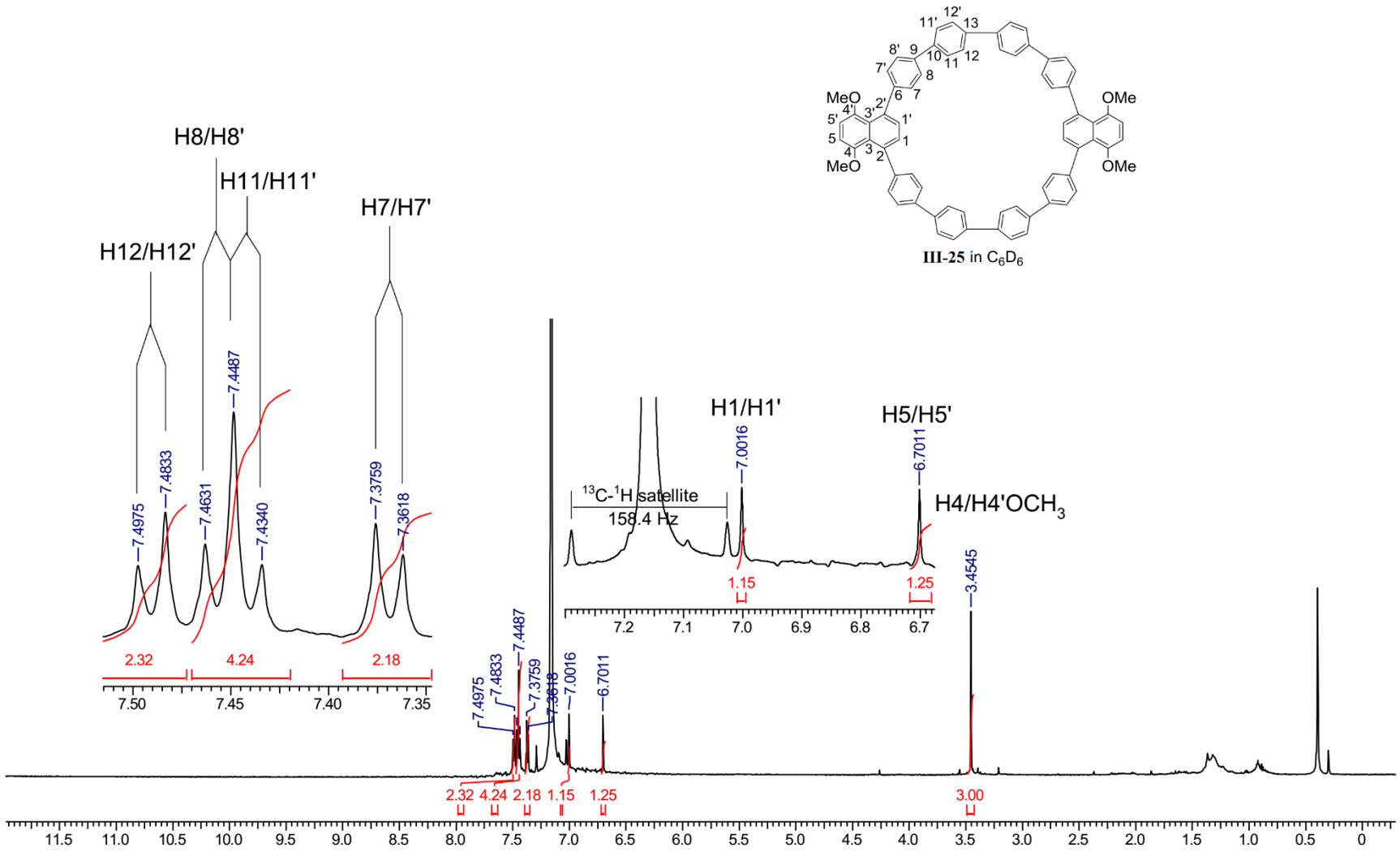
H8/H8'
H11/H11'
H7/H7'
H12/H12'
7.4975
7.4833
7.4631
7.4487
7.4340
7.3759
7.3618
2.32
4.24
2.18
7.50
7.45
7.40
7.35
H1/H1'
H5/H5'
7.0016
6.7011
^{13}C-^{1}H satellite
158.4 Hz
H4/H4'OCH$_3$
1.15
1.25
7.2
7.1
7.0
6.9
6.8
6.7
3.4545
3.00
MeO
MeO
OMe
OMe
III-25 in C_6D_6

1D NOESY spectra (b-c)

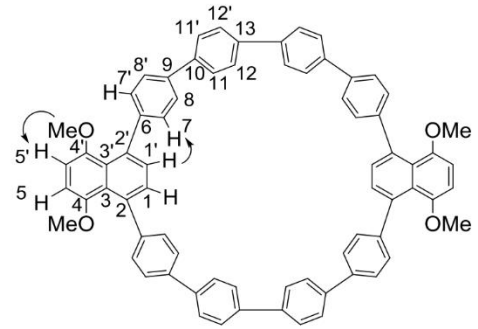

III-25 in C_6D_6

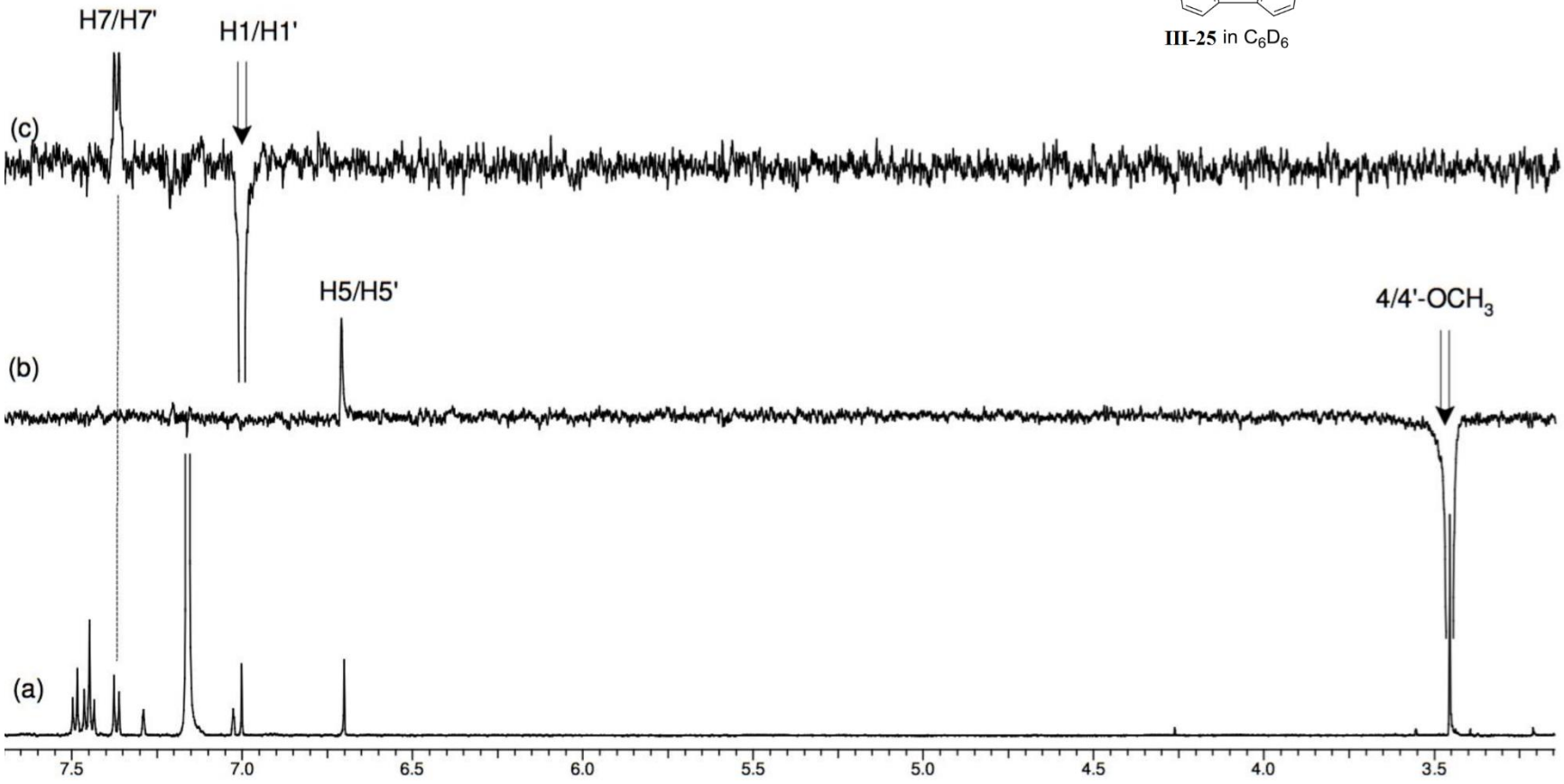

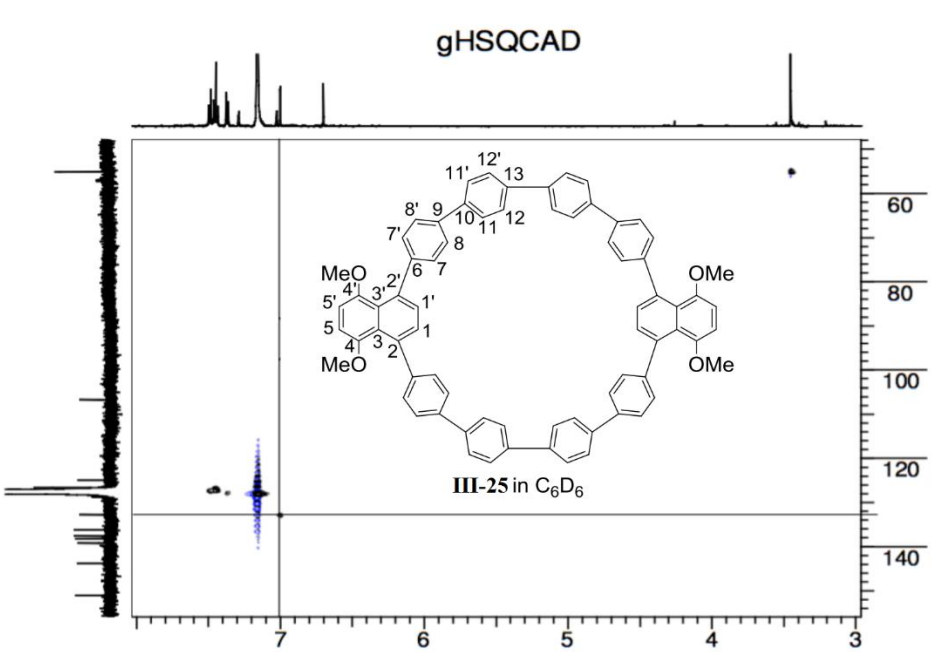

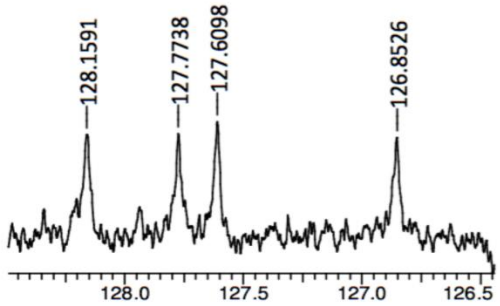

Expanded portion of the ^{13}C NMR spectrum in CD_2Cl_2

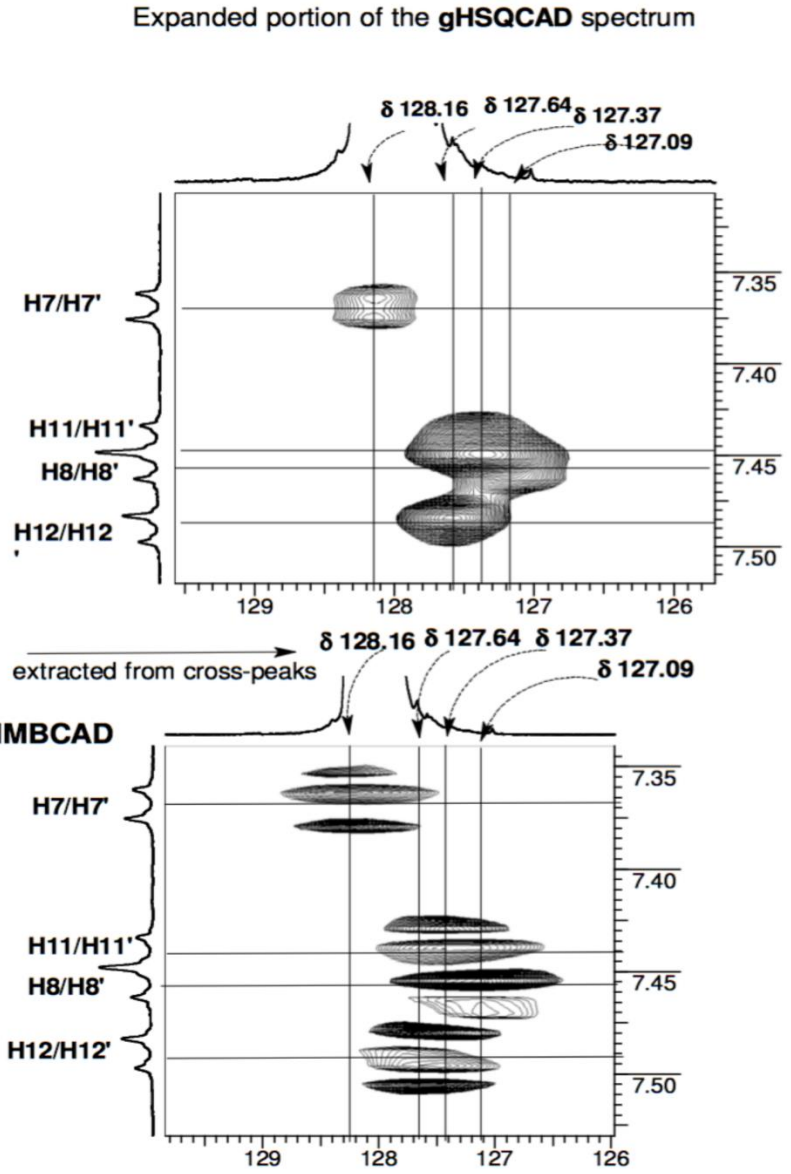

Long-range gHMBCAD correlations

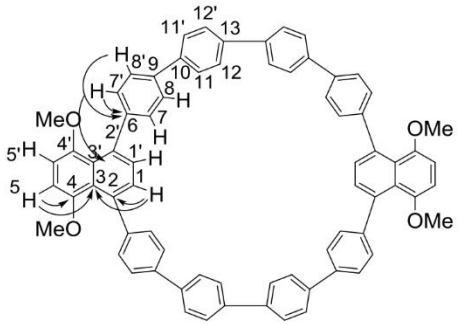

III-25 in C_6D_6

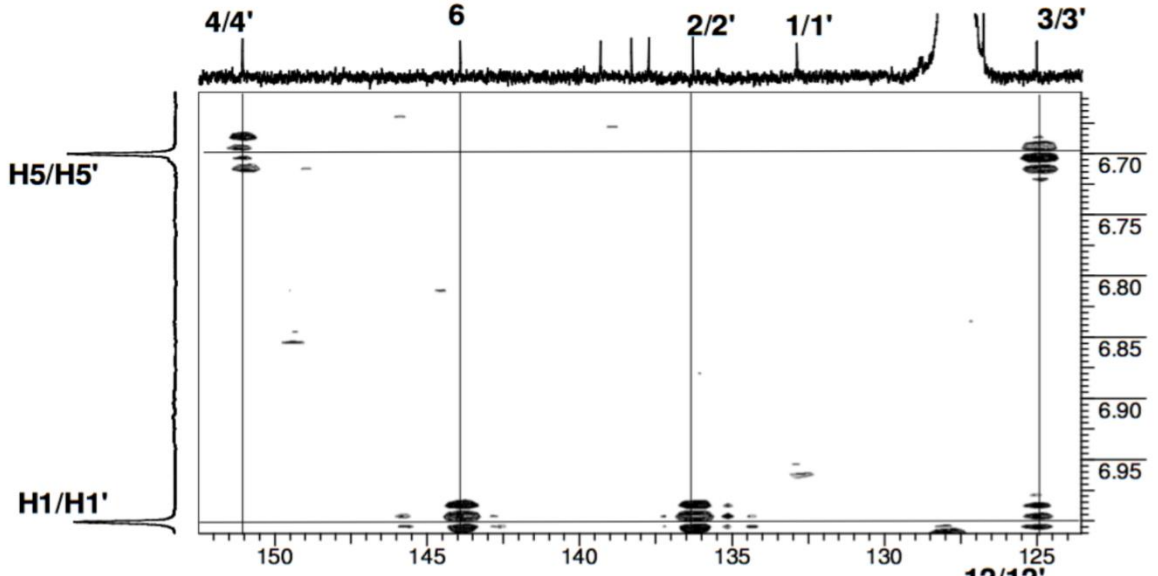

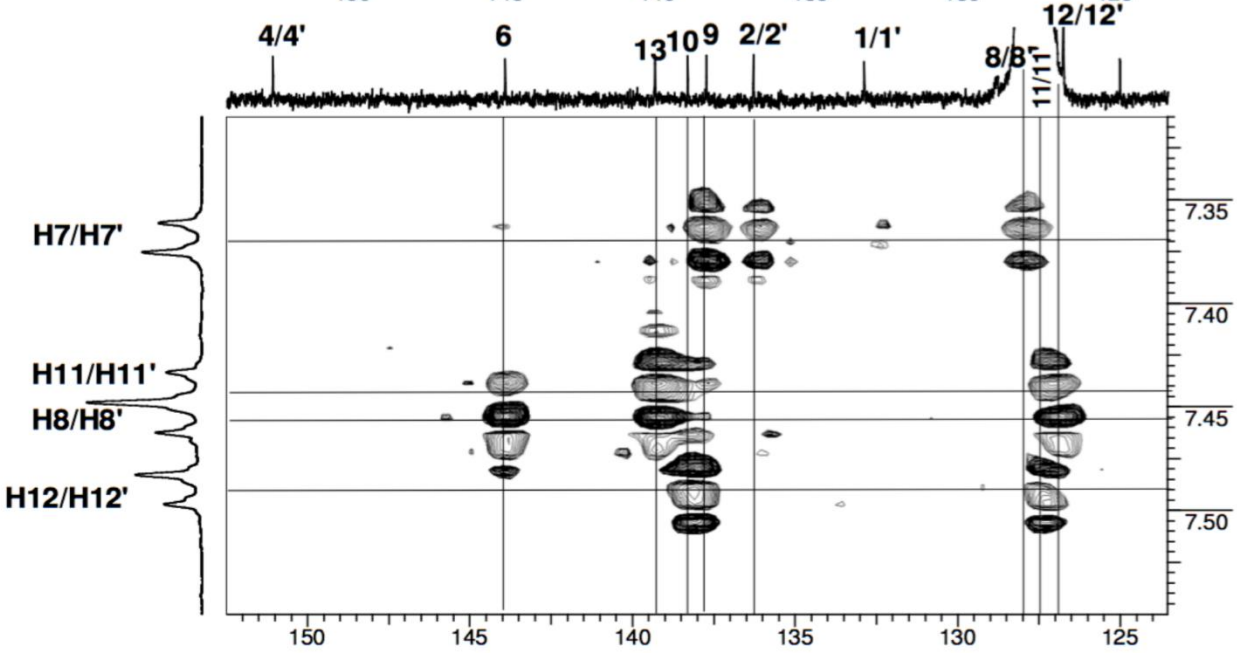

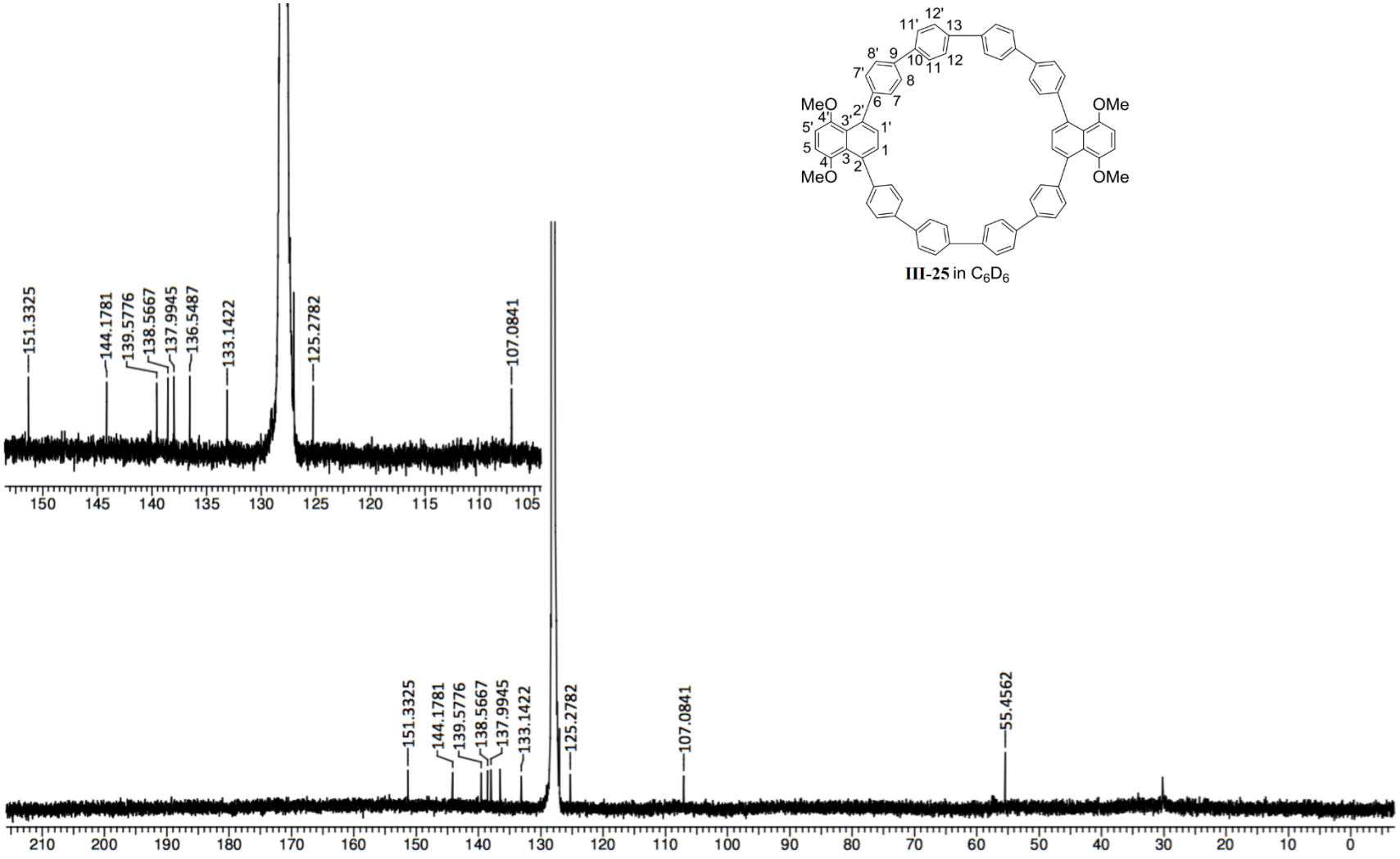

III-25 in C_6D_6

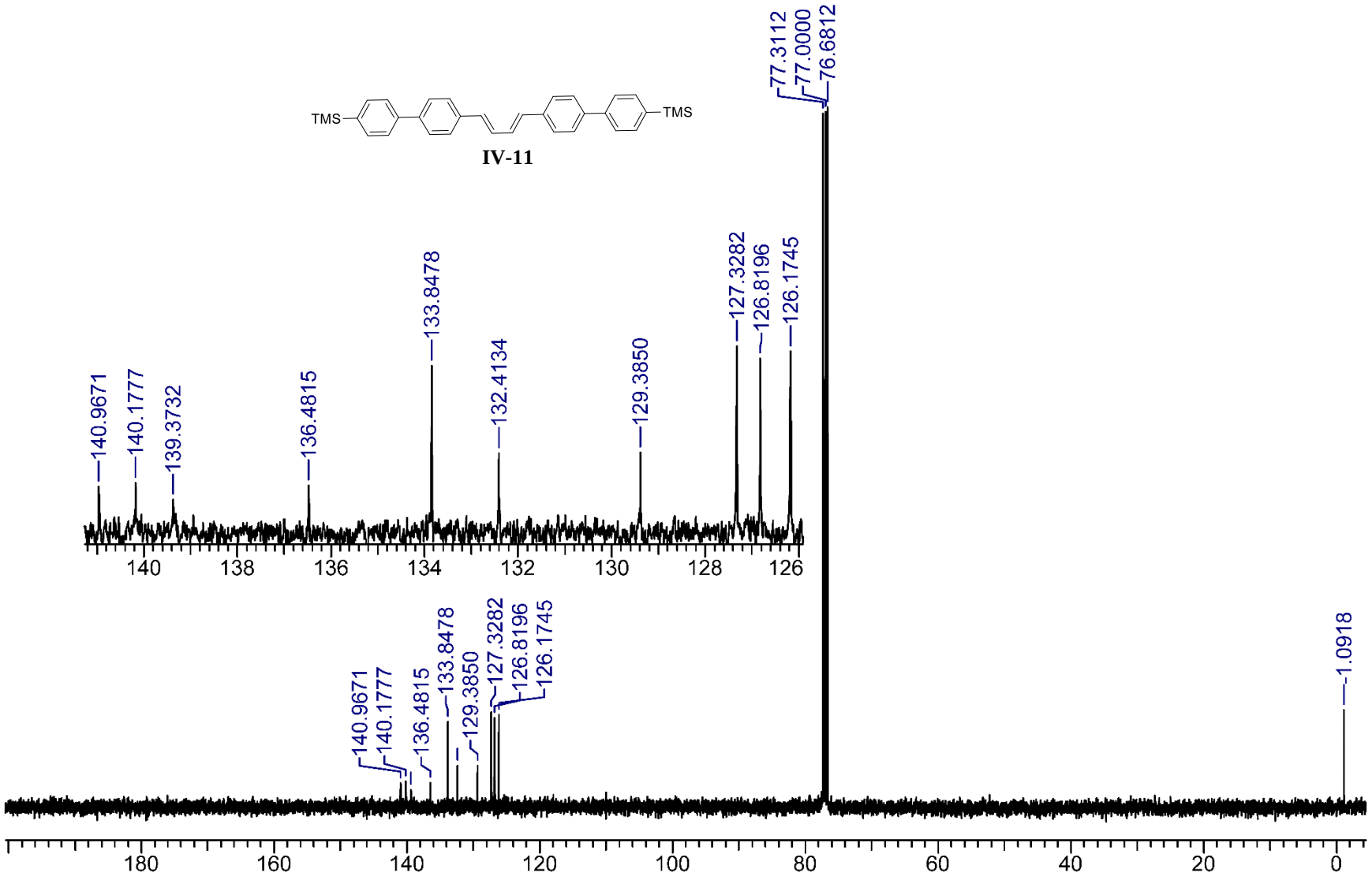
TMS
TMS
IV-11
77.3112
77.0000
76.6812
140.9671
140.1777
139.3732
136.4815
133.8478
132.4134
129.3850
127.3282
126.8196
126.1745
1.0918
180
160
140
120
100
80
60
40
20
0
140
138
136
134
132
130
128
126

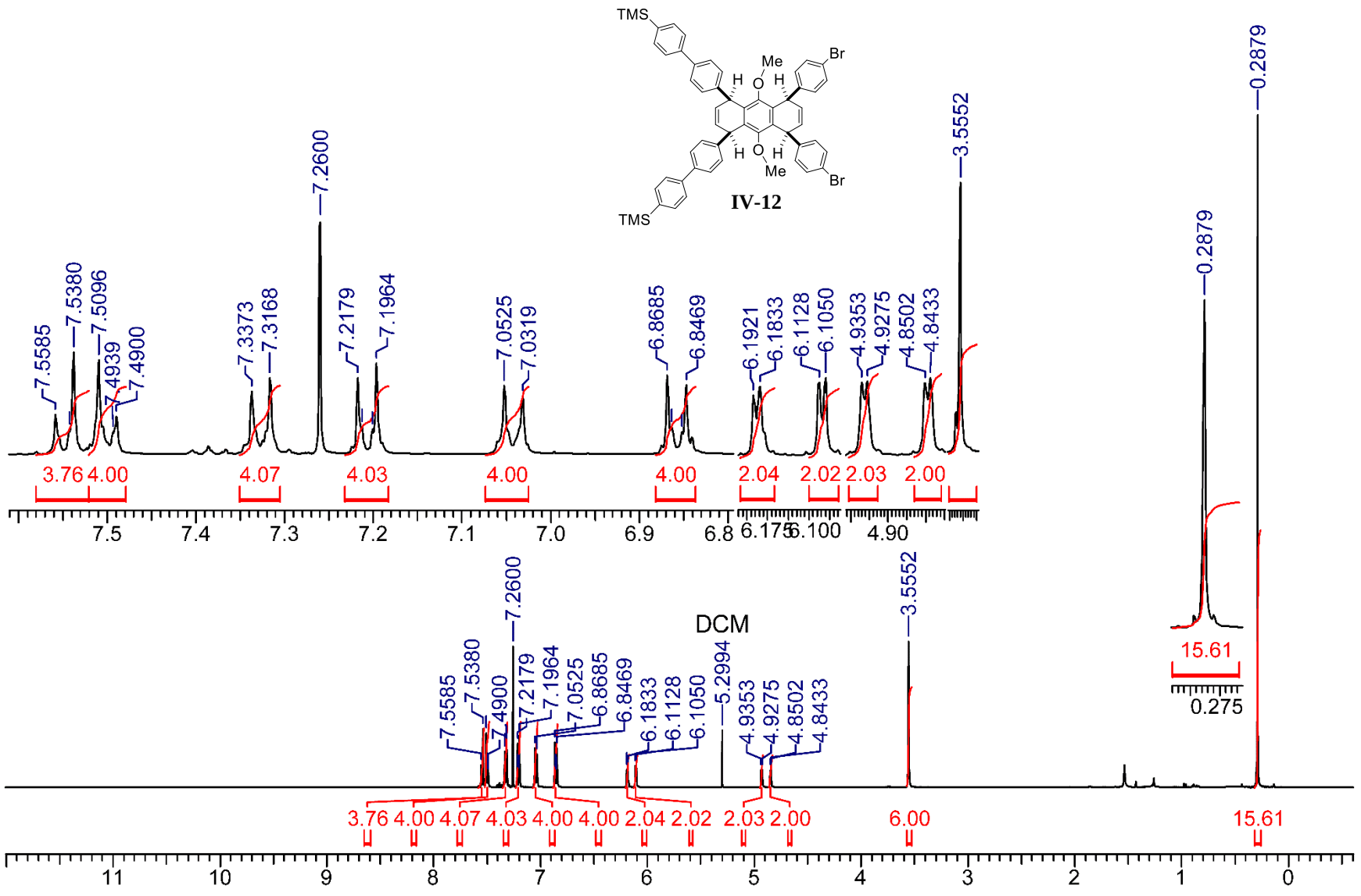
TMS
Me
Br
H
O
H
H
O
H
Me
Br
TMS
IV-12
7.5585
7.5380
7.5096
7.4939
7.4900
7.3373
7.3168
7.2600
7.2179
7.1964
7.0525
7.0319
6.8685
6.8469
6.1921
6.1833
6.1128
6.1050
4.9353
4.9275
4.8502
4.8433
3.5552
0.2879
3.76 4.00
4.07
4.03
4.00
4.00
2.04
2.02
2.03
2.00
DCM
5.2994
6.00
15.61
0.275

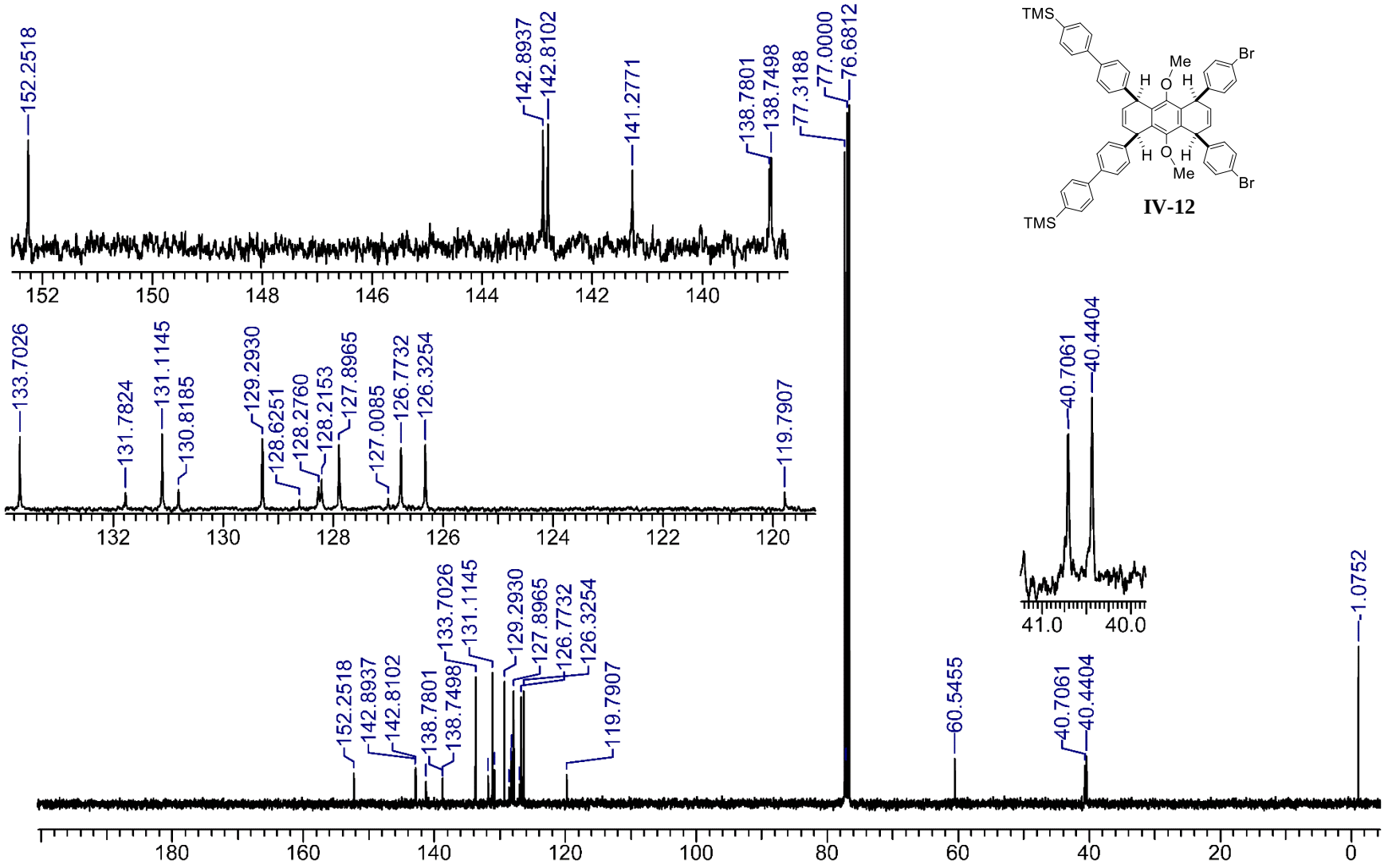
TMS
Br
Me
H
O
H
H
O
H
Me
Br
TMS
IV-12

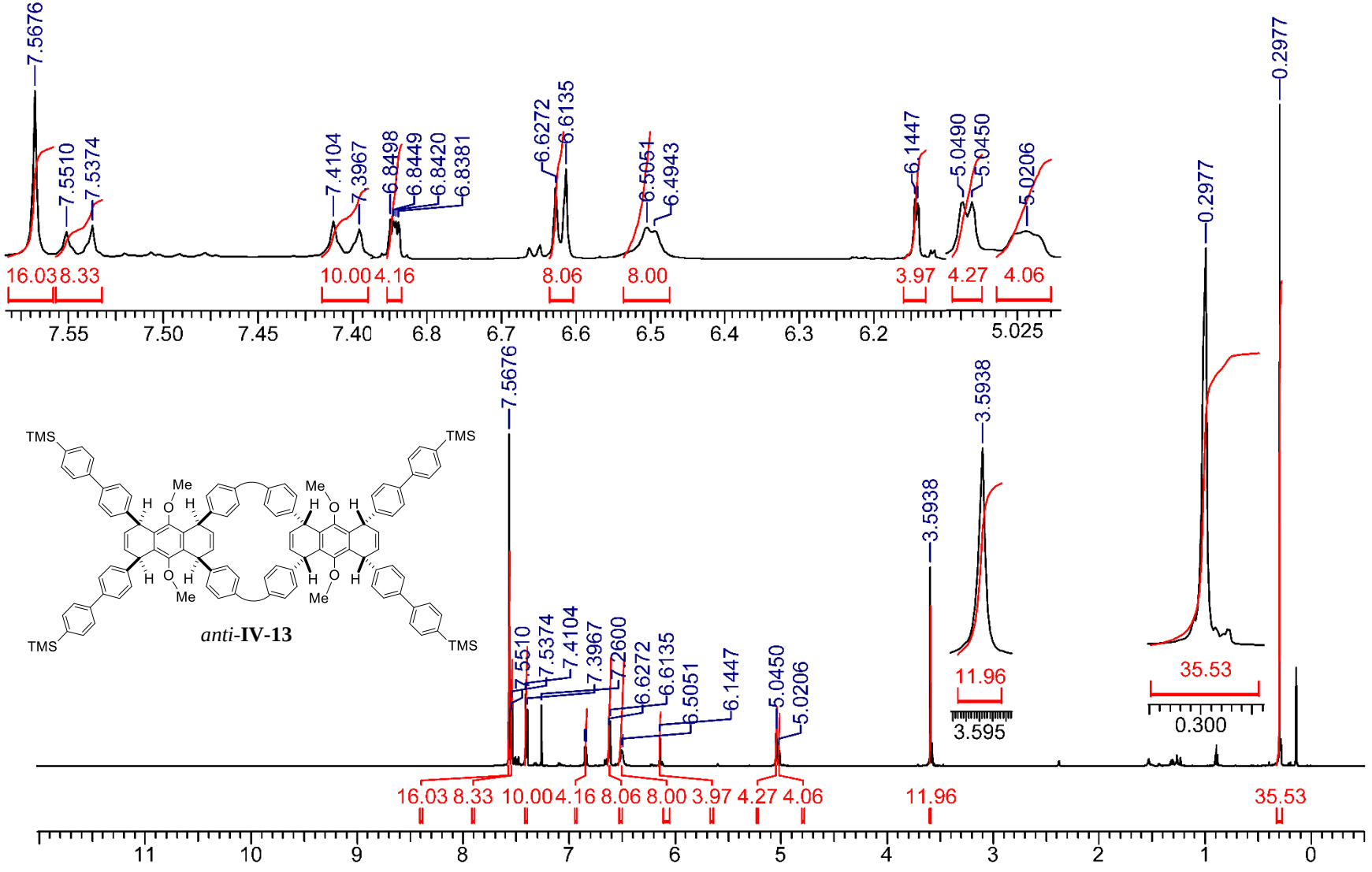
7.5676
7.5510
7.5374
7.4104
7.3967
6.8498
6.8449
6.8420
6.8381
6.6272
6.6135
6.5051
6.4943
6.1447
5.0490
5.0450
5.0206
0.2977
16.03 8.33 10.00 4.16 8.06 8.00 3.97 4.27 4.06
11.96
35.53
TMS
Me
H
O
anti-IV-13

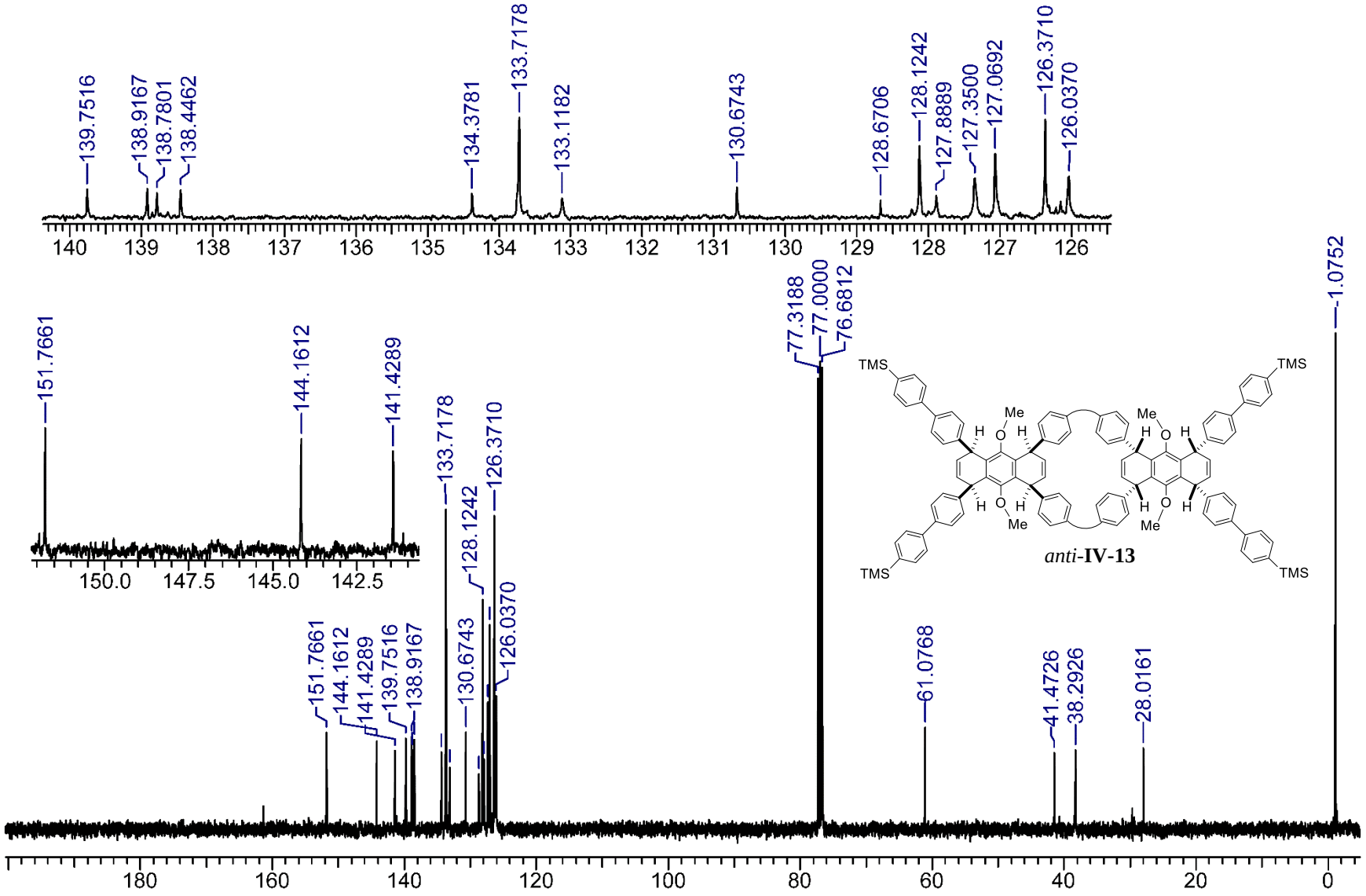
139.7516
138.9167
138.7801
138.4462
134.3781
133.7178
133.1182
130.6743
128.6706
128.1242
127.8889
127.3500
127.0692
126.3710
126.0370
140
139
138
137
136
135
134
133
132
131
130
129
128
127
126
151.7661
144.1612
141.4289
150.0
147.5
145.0
142.5
77.3188
77.0000
76.6812
1.0752
TMS
Me
H
O
anti-IV-13
151.7661
144.1612
141.4289
139.7516
138.9167
133.7178
130.6743
128.1242
126.3710
126.0370
61.0768
41.4726
38.2926
28.0161
180
160
140
120
100
80
60
40
20
0

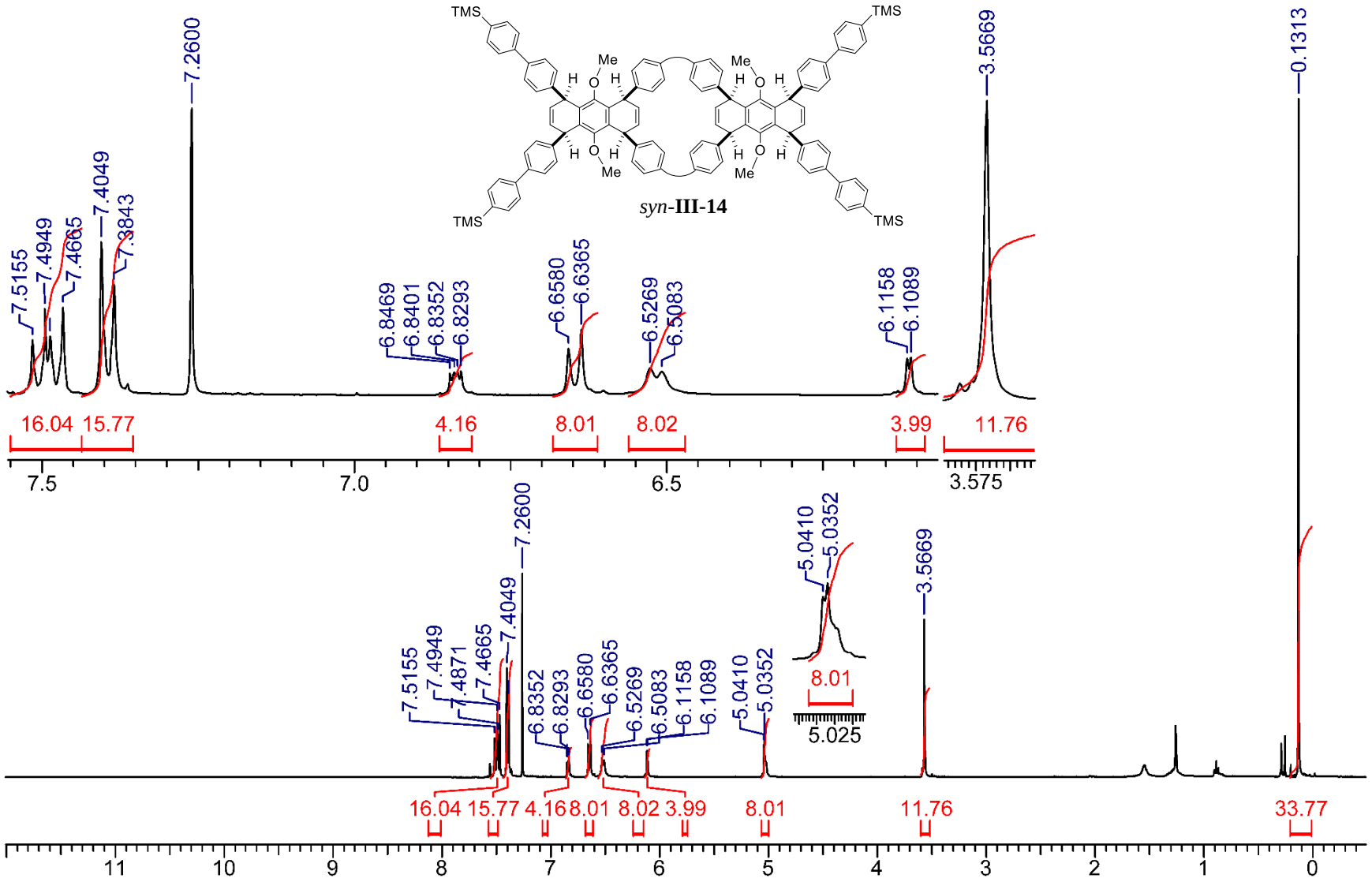
TMS
Me
H
O
syn-III-14
7.5155
7.4949
7.4665
7.4049
7.3843
7.2600
6.8469
6.8401
6.8352
6.8293
6.6580
6.6365
6.5269
6.5083
6.1158
6.1089
3.5669
0.1313
16.04
15.77
4.16
8.01
8.02
3.99
11.76
33.77
5.0410
5.0352
7.4871
6.5269
6.5083
6.1158
6.1089
5.025

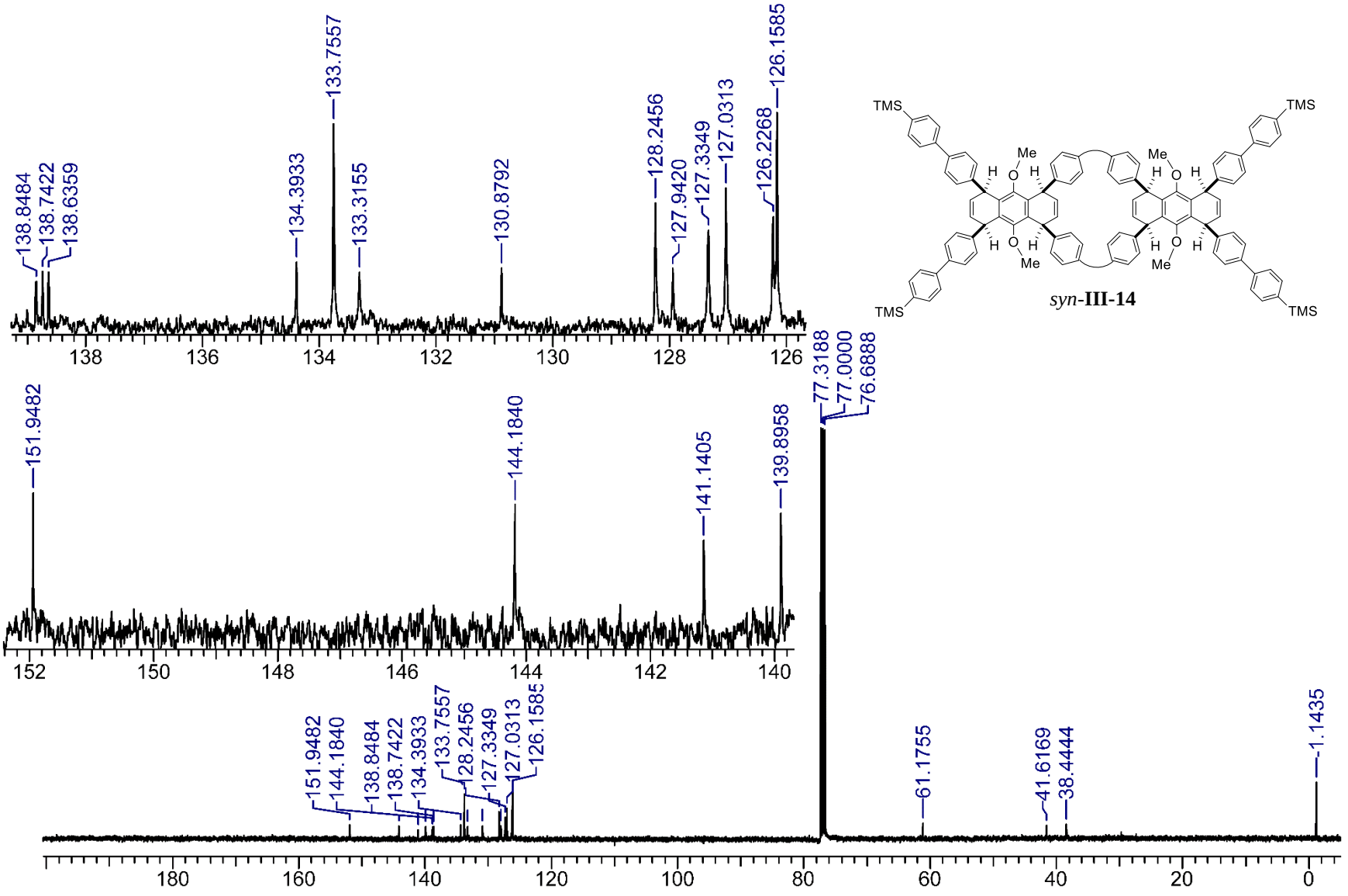
138.8484
138.7422
138.6359
134.3933
133.7557
133.3155
130.8792
128.2456
127.9420
127.3349
127.0313
126.2268
126.1585
151.9482
144.1840
141.1405
139.8958
77.3188
77.0000
76.6888
61.1755
41.6169
38.4444
1.1435
TMS
Me
H
O
syn-III-14

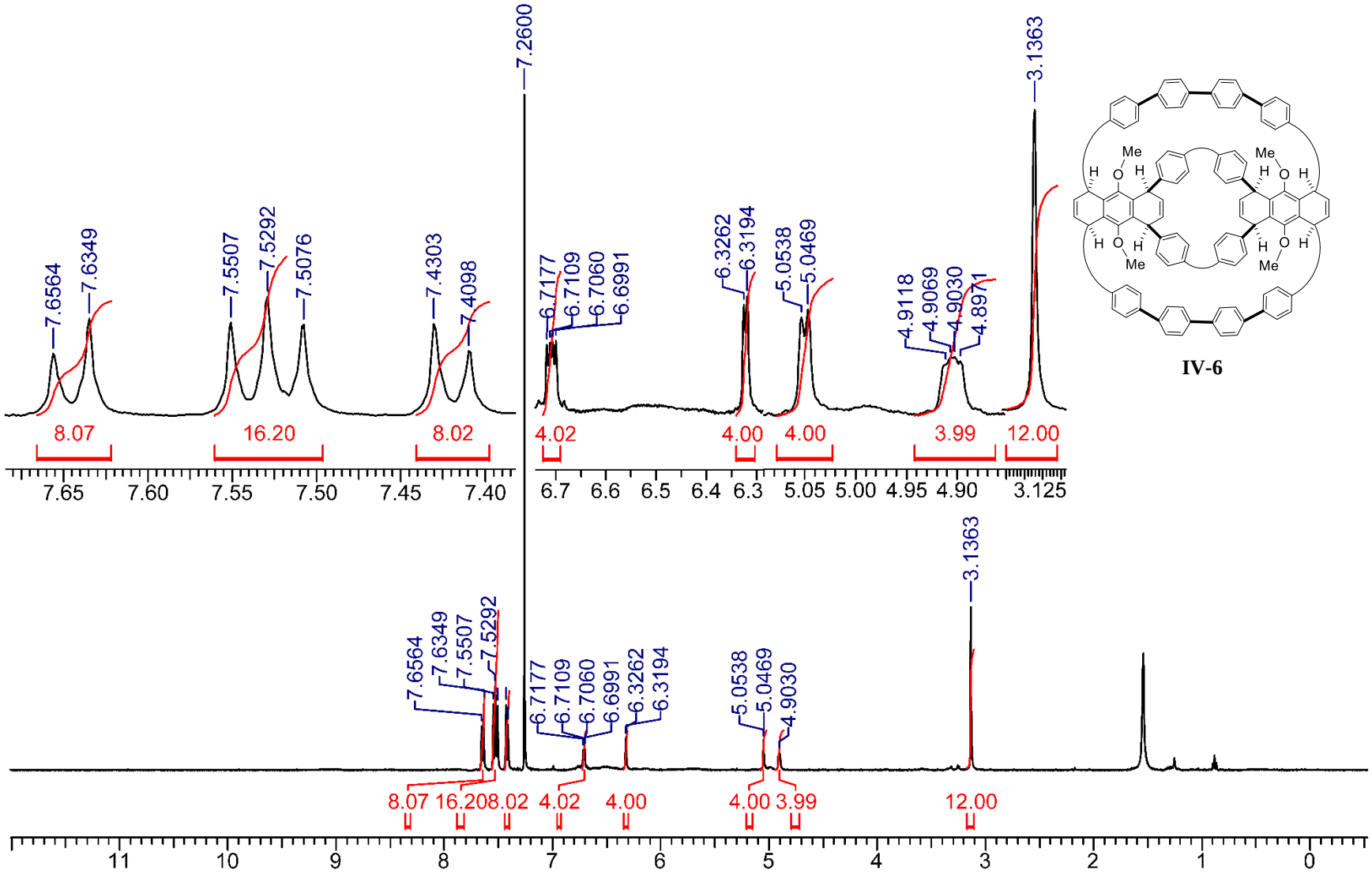
7.6564
7.6349
7.5507
7.5292
7.5076
7.4303
7.4098
7.2600
6.7177
6.7109
6.7060
6.6991
6.3262
6.3194
5.0538
5.0469
4.9118
4.9069
4.9030
4.8971
3.1363
8.07
16.20
8.02
4.02
4.00
4.00
3.99
12.00
IV-6

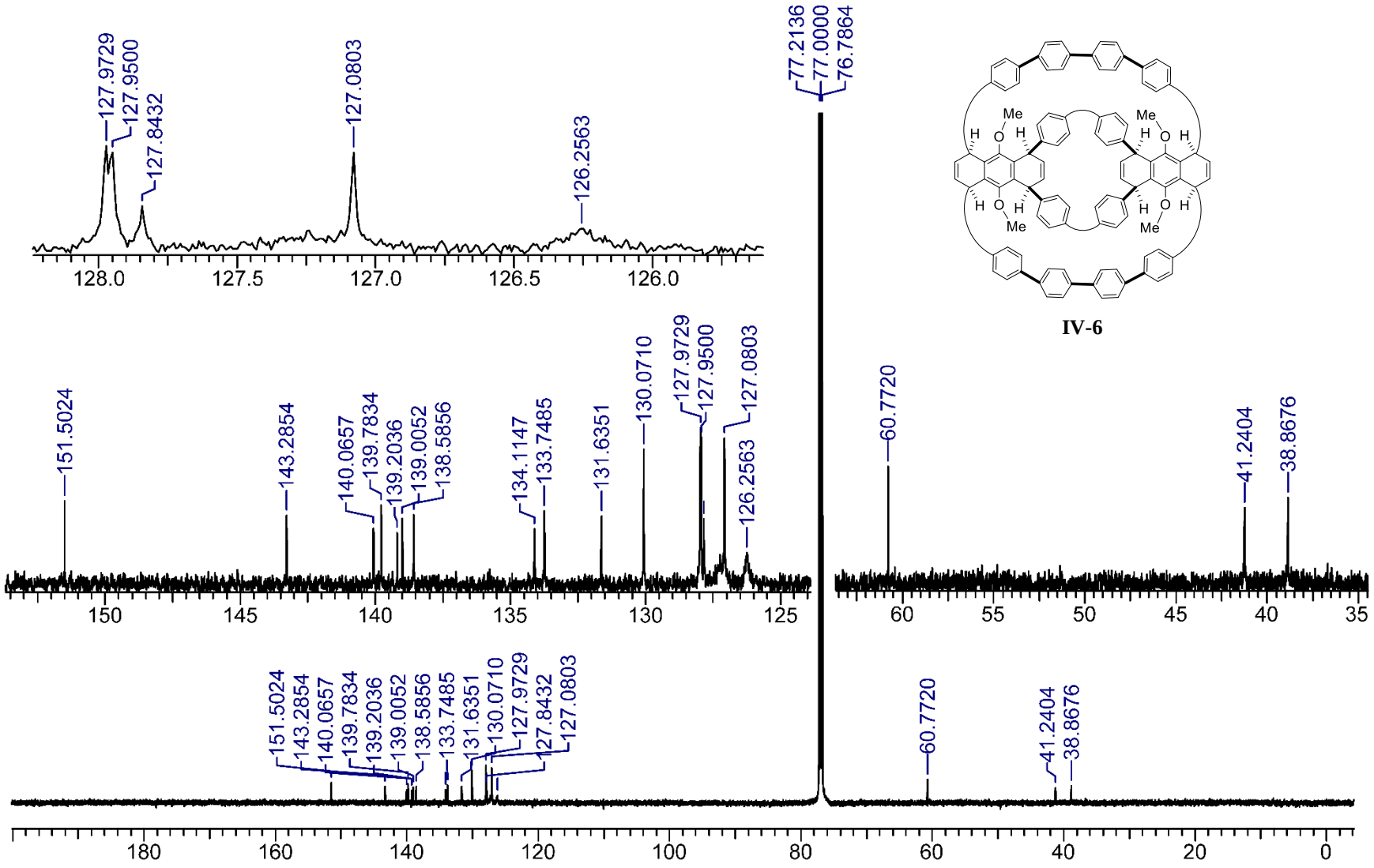
127.9729
127.9500
127.8432
127.0803
126.2563
77.2136
77.0000
76.7864
Me
H
O
H
IV-6
151.5024
143.2854
140.0657
139.7834
139.2036
139.0052
138.5856
134.1147
133.7485
131.6351
130.0710
127.9729
127.9500
127.0803
126.2563
60.7720
41.2404
38.8676

A Dynamic NMR study of restricted rotation of internal aromatic group in 6-10-CPP

Calculation of activation parameters ($\Delta G^{\ddagger}$, $\Delta H^{\ddagger}$, and $\Delta S^{\ddagger}$)

IV-6

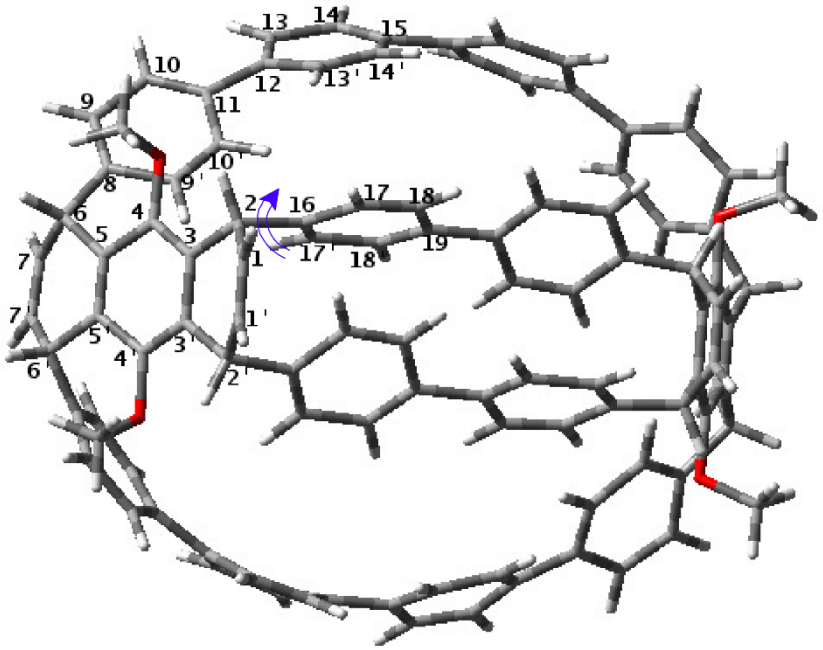

^{13}C NMR chemical Shifts

Carbon	δ_C/ppm	
	+25°C	-12°C
C1/C1'	133.75	133.60
C2/C2'	38.86	38.59
C3/C3'	134.13	133.82
C4/C4'	151.50	151.28
C5/C5'	131.63	131.18
C6/C6'	41.24	41.24
C7/C7'	127.84	127.30
C8	143.28	143.25
C9/C9'	130.07	130.13
C10/C10'	127.08	127.03
C11	139.20	139.27
C12	139.78	139.47
C13/C13'	134.11	128.31
C14/C14'	127.92	128.31
C15	139.00	139.09
C16	140.06	139.83
C17/C17'	127.23	127.19/126.80
C18/C18'	126.26	125.97/126.35
C19	138.58	138.38
OCH3	60.77	60.66

^{1}H NMR chemical Shifts

AA'BB' *spin system*

Pople *notation*	Proton	δ_H/ppm	**Pople** *notation*	Proton	δ_H/ppm
AA'	H9/H9'	7.42	AA'	H13/H13'	7.54
BB'	H10/H10'	7.34	BB'	H14/H14'	7.69

Coupling constants (*J*/Hz)

J(AB) = J(9,10) = 8.40	J(AB) = J(13,14) = 8.60
J(AB') = J(9,10') = 0.43	J(AB') = J(13,14')= 0.42
J(AA') = J(9,9') = 2.24	J(AA') = J(13,13') = 2.22
J(BB') = J(10,10') = 1.98	J(BB') = J(14,14') = 1.96

AA'XX' *spin system*

Pople *notation*	Proton	δ_H/ppm	**Pople** *notation*	Proton	δ_H/ppm
AA'	H2/H2'	4.90	AA'	H6/H6'	5.05
XX'	H1/H1'	6.71	XX'	H7/H7'	6.32

Coupling constants (*J*/Hz)

J(AA)' = J(2,2') = 0.22	J(AA') = J(6,6') = 0.23
J(AX) = J(1,2) = 6.85	J(AX) = J(6,7) = 4.32
J(AX') = J(2,1') = 0.35	J(AX') = J(6,7') = 1.11
J(XX') = J(10,10') = 8.92	J(XX") = J(10,10') = 6.65

Note: Experimental ^{1}H NMR spectrum was acquired at +50°C with a selective irradiation of the broad peaks centered at 6.39 ppm (H17/H17'/H18/H18').

Calculation of Activation parametres

Eyring equation

$$k = k\,\frac{k_B T}{h}\,e^{\left(-\Delta G^{\ddagger}/RT\right)} \qquad \text{(i)}$$

$$\frac{k}{T} = \frac{k_B}{h}\,e^{\left(-\Delta G^{\ddagger}/RT\right)} \qquad (k = 1)$$

$$\ln\left(\frac{k}{T}\right) = \ln\left[\frac{k_B}{h}\,e^{\left(-\Delta G^{\ddagger}/RT\right)}\right]$$

$$\ln\left(\frac{k}{T}\right) = \ln\left(\frac{k_B}{h}\right) + \left(\frac{-\Delta G^{\ddagger}}{RT}\right) \qquad \text{(ii)}$$

Equation **(ii)** can be written in terms of enthalpies and entropies, since

$$\Delta G^{\ddagger} = \Delta H^{\ddagger} - T\Delta S^{\ddagger}$$

thus taking the form of

$$\ln\left(\frac{k}{T}\right) = \ln\left(\frac{k_B}{h}\right) + \left(\frac{-\Delta H^{\ddagger} + T\Delta S^{\ddagger}}{RT}\right)$$

which can be linearized to the following form

$$\ln\left(\frac{k}{T}\right) = \ln\left(\frac{k_B}{h}\right) - \frac{\Delta H^{\ddagger}}{R}\left(\frac{1}{T}\right) + \frac{\Delta S^{\ddagger}}{R} \qquad \text{(iii)}$$

$$\ln\left(\frac{k_B}{h}\right) = \ln\left(\frac{1.3806 \times 10^{-23}}{6.6261 \times 10^{-34}}\right) = 23.76$$

$$\ln\left(\frac{k}{T}\right) = 23.76 - \frac{\Delta H^{\ddagger}}{R}\left(\frac{1}{T}\right) + \frac{\Delta S^{\ddagger}}{R} \qquad \text{(iii)}$$

Where **k** is the so called transmission coefficient, which is usually set equal to 1, k_B is the Boltzmann constant, **T** the absolute temperature, **R** the ideal gas constant and **h** the Planck's constant, and $\Delta G^{\ddagger}$ is the free energy of activation

T = 273.15 K

R = 1.987 cal K^{-1} mol^{-1}

h = 6.6261 × 10^{-34} J s

k_B = 1.3806 × 10^{-23} J K^{-1}

Plot **ln(k/T)** *vs.* **(1/T)**

Slope is $-\Delta H^{\ddagger}/R$

Intercept is $23.76 + \Delta S^{\ddagger}/R$

$$\Delta G^{\ddagger} = RT\left[23.76 - \ln\left(\frac{k}{T}\right)\right]$$

$$\Delta G^{\ddagger} = \Delta H^{\ddagger} - T\Delta S^{\ddagger}$$

Calculation of activation parameters

for the restricted rotation of the internal aromatic benzene ring.

T/°C	T/K	k/s	ln(k/T)	1/T
30	303.15	32	-2.24849	0.0033
25	298.15	20.2	-2.69191	0.00335
20	293.15	11.1	-3.27374	0.00341
15	288.15	5.91	-3.88684	0.00347
10	283.15	3.34	-4.44001	0.00353
5	278.15	1.95	-4.96033	0.0036
0	273.15	1	-5.61002	0.00366
-5	268.15	0.5	-6.28469	0.00373

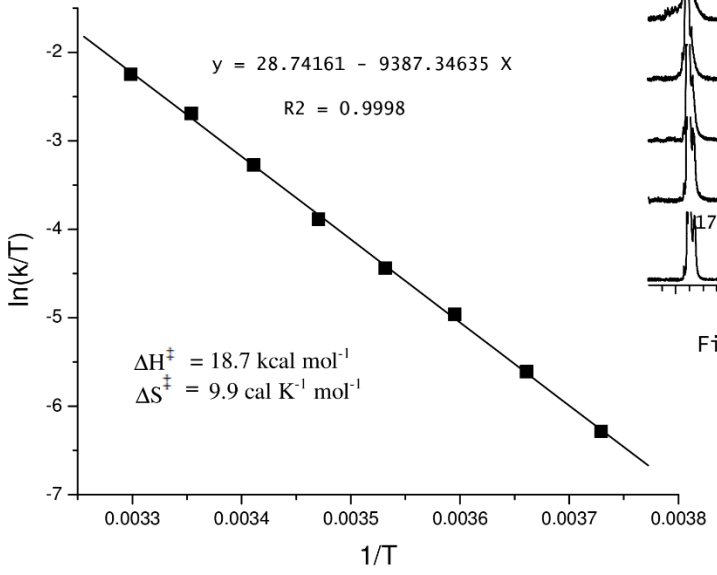

Fig. 2. Eyring plot of ln(k/T) *vs.* 1/T for rate constants obtained by simulation of ^{1}H NMR spectra at temperatures between 268 K and 303 K

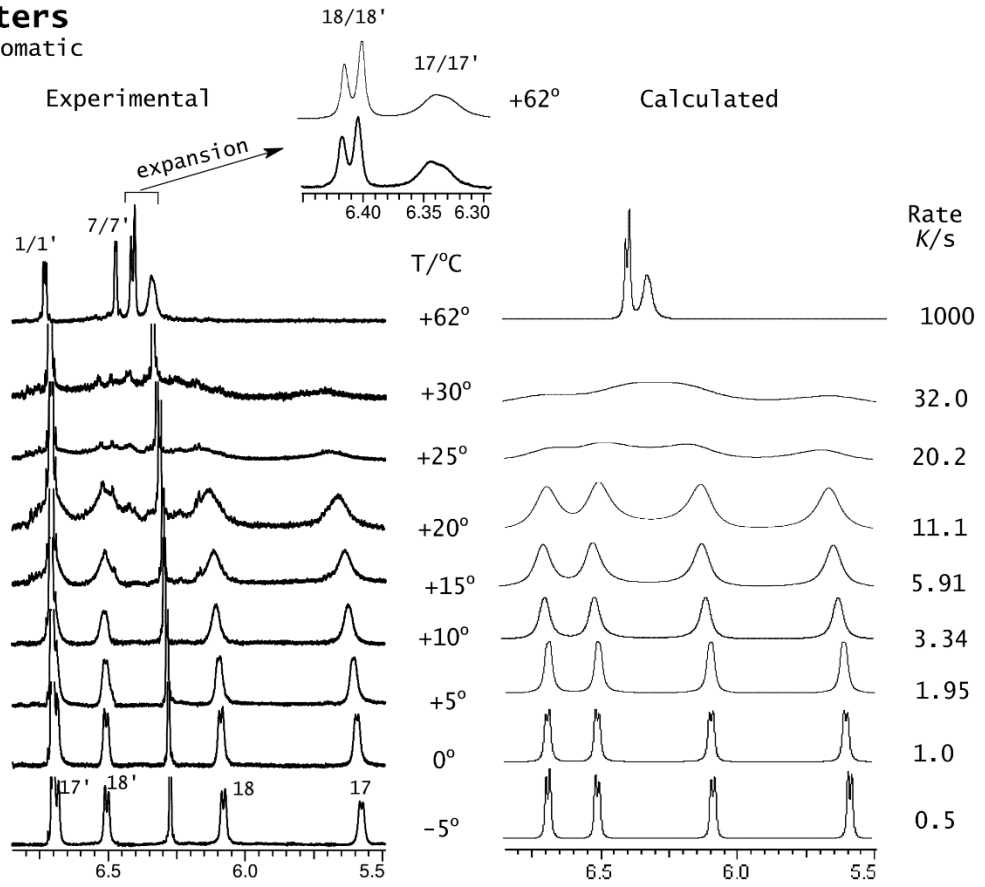

Fig. 1. Experimental and calculated portion of the variable temperature ^{1}H NMR spectrum;

B: Slope is $\frac{-\Delta H^{\ddagger}}{R}$ $\qquad \frac{\Delta S^{\ddagger}}{R} + 23.76 = 28.74161$

A: Intercept is $\frac{\Delta S^{\ddagger}}{R} + 23.76$ $\qquad \Delta S^{\ddagger} = 9.9$ cal K^{-1} mol^{-1}

$\frac{-\Delta H^{\ddagger}}{R} = -9387.34635$ $\qquad \Delta G^{\ddagger} = \Delta H^{\ddagger} - T\Delta S^{\ddagger}$ (T = 273.15 K)

R = 1.987 cal K^{-1} mol^{-1} $\qquad \Delta G^{\ddagger} = 19.7 - 273.15\ (9.9\text{x}10^{-3}) = 16$ kcal mol^{-1}

$\Delta H^{\ddagger} = 18.7$ kcal mol^{-1} $\qquad$ **$\Delta G^{\ddagger} = 16$ kcal mol^{-1}**

Non 1st order splitting patterns

(**AA'XX' and AA'BB'** spin systems)

Experimental (a) and calculated (b) multiplicity patterns

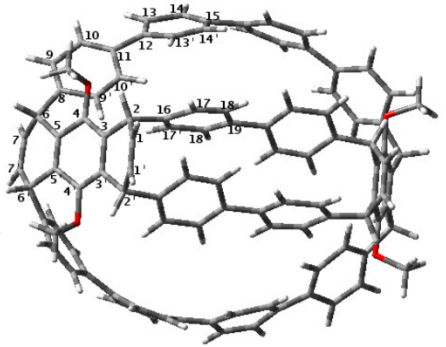

IV-6

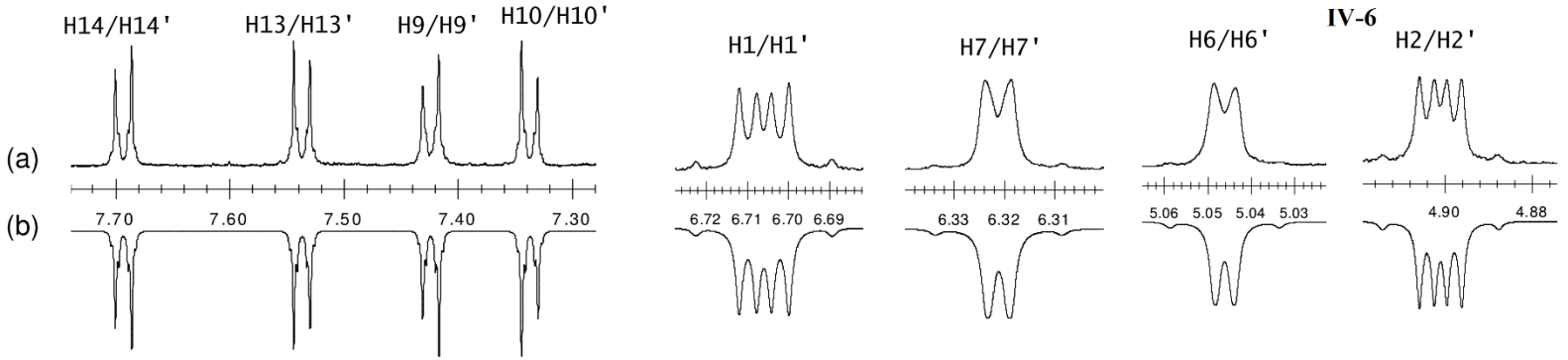

AA'BB' spin system

Pople *notation*	Proton	δ_H/ppm	**Pople** *notation*	Proton	δ_H/ppm
AA'	H9/H9'	7.42	AA'	H13/H13'	7.54
BB'	H10/H10'	7.34	BB'	H14/H14'	7.69

Coupling constants (*J*/Hz)

$J_{AB} = J_{9,10} = 8.40$	$J_{AB} = J_{13,14} = 8.60$
$J_{AB'} = J_{9,10'} = 0.43$	$J_{AB'} = J_{13,14'} = 0.42$
$J_{AA'} = J_{9,9'} = 2.24$	$J_{AA'} = J_{13,13'} = 2.22$
$J_{BB'} = J_{10,10'} = 1.98$	$J_{BB'} = J_{14,14'} = 1.96$

AA'XX' spin system

Pople *notation*	Proton	δ_H/ppm	**Pople** *notation*	Proton	δ_H/ppm
AA'	H2/H2'	4.90	AA'	H6/H6'	5.05
XX'	H1/H1'	6.71	XX'	H7/H7'	6.32

Coupling constants (*J*/Hz)

$J_{AA'} = J_{2,2'} = 0.22$	$J_{AA'} = J_{6,6'} = 0.23$
$J_{AX} = J_{1,2} = 6.85$	$J_{AX} = J_{6,7} = 4.32$
$J_{AX'} = J_{2,1'} = 0.35$	$J_{AX'} = J_{6,7'} = 1.11$
$J_{XX''} = J_{10,10'} = 8.92$	$J_{XX''} = J_{10,10'} = 6.65$

Note: Experimental ^{1}H NMR spectrum was acquired at +50°C with a selective irradiation of the broad peaks centered at 6.39 ppm (H17/H17'/H18/H18').

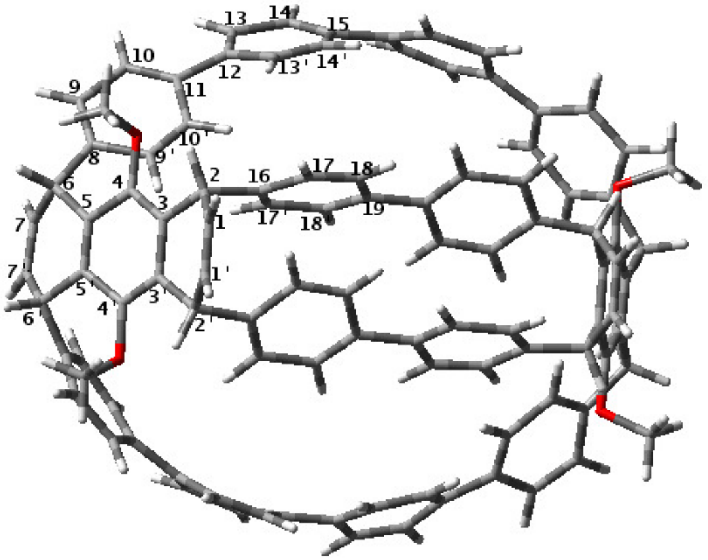

IV-6

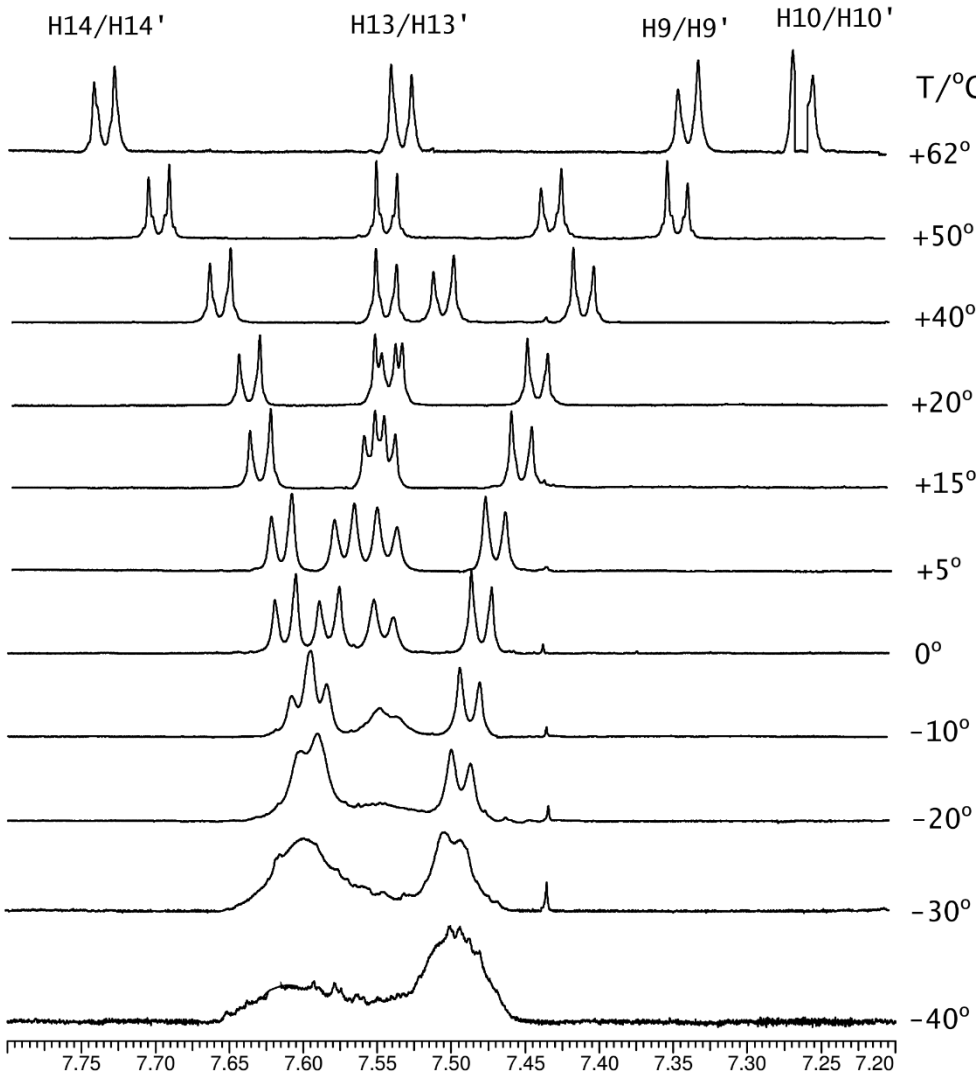

Fig.3. Portion of the variable temperature dependent ^{1}H NMR spectrum

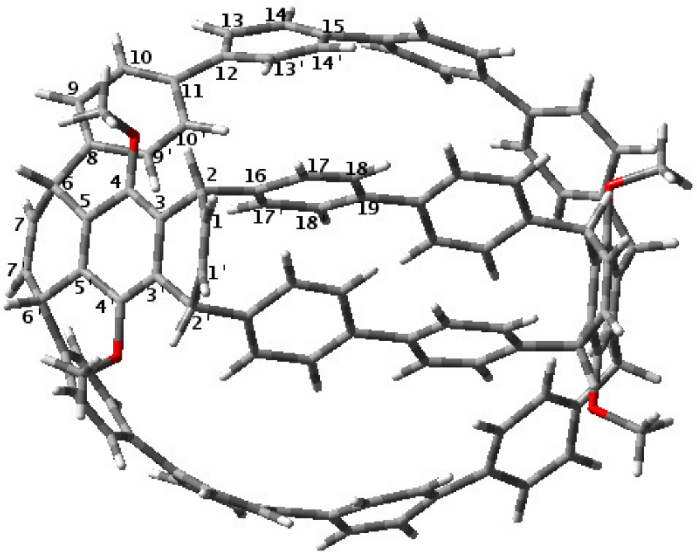

IV-6

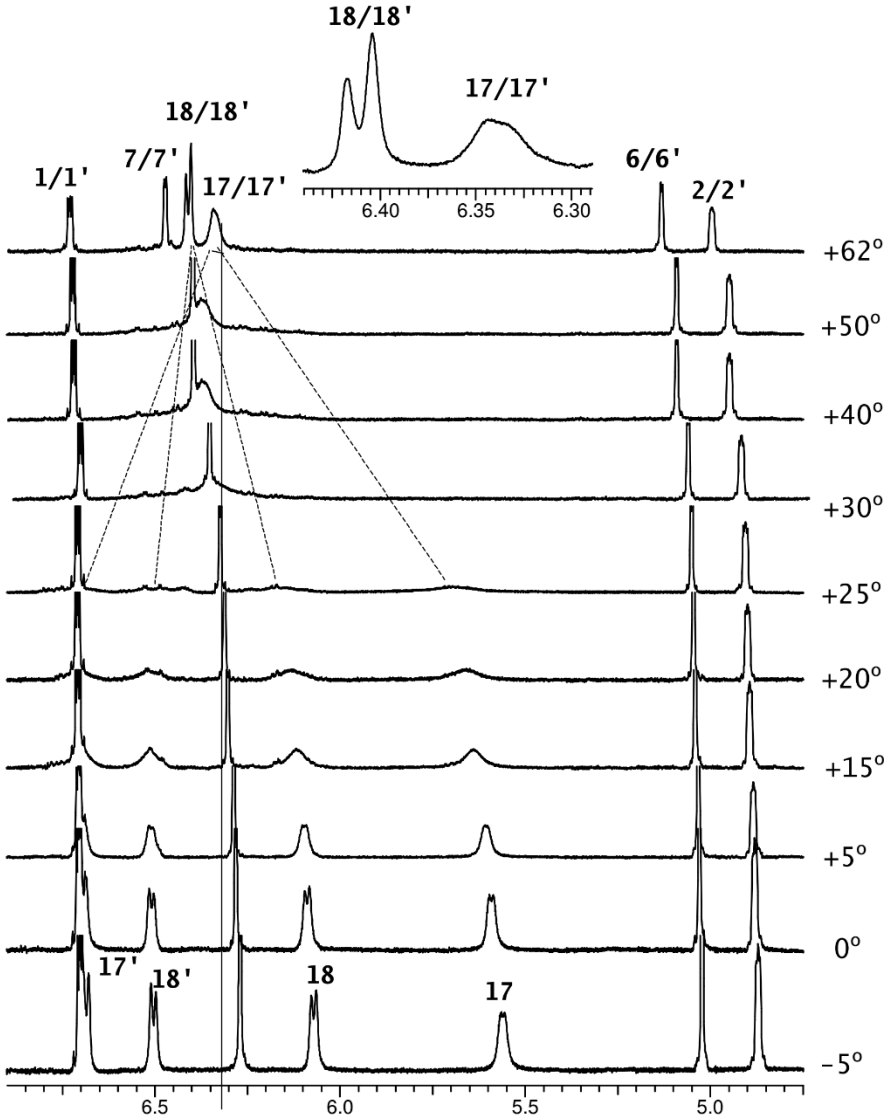

Fig.4. Portion of the variable temperature dependent ^{1}H NMR spectrum

^{1}H NMR spectrum (a) at +25°C and at -5°C (b)

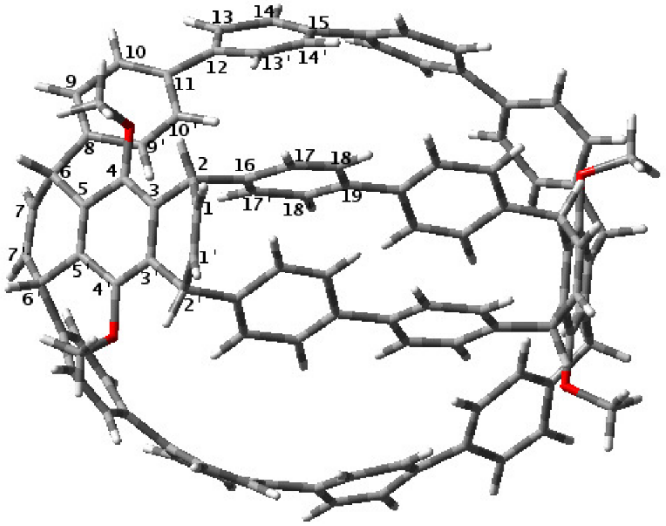

IV-6

-5°C

+25°C

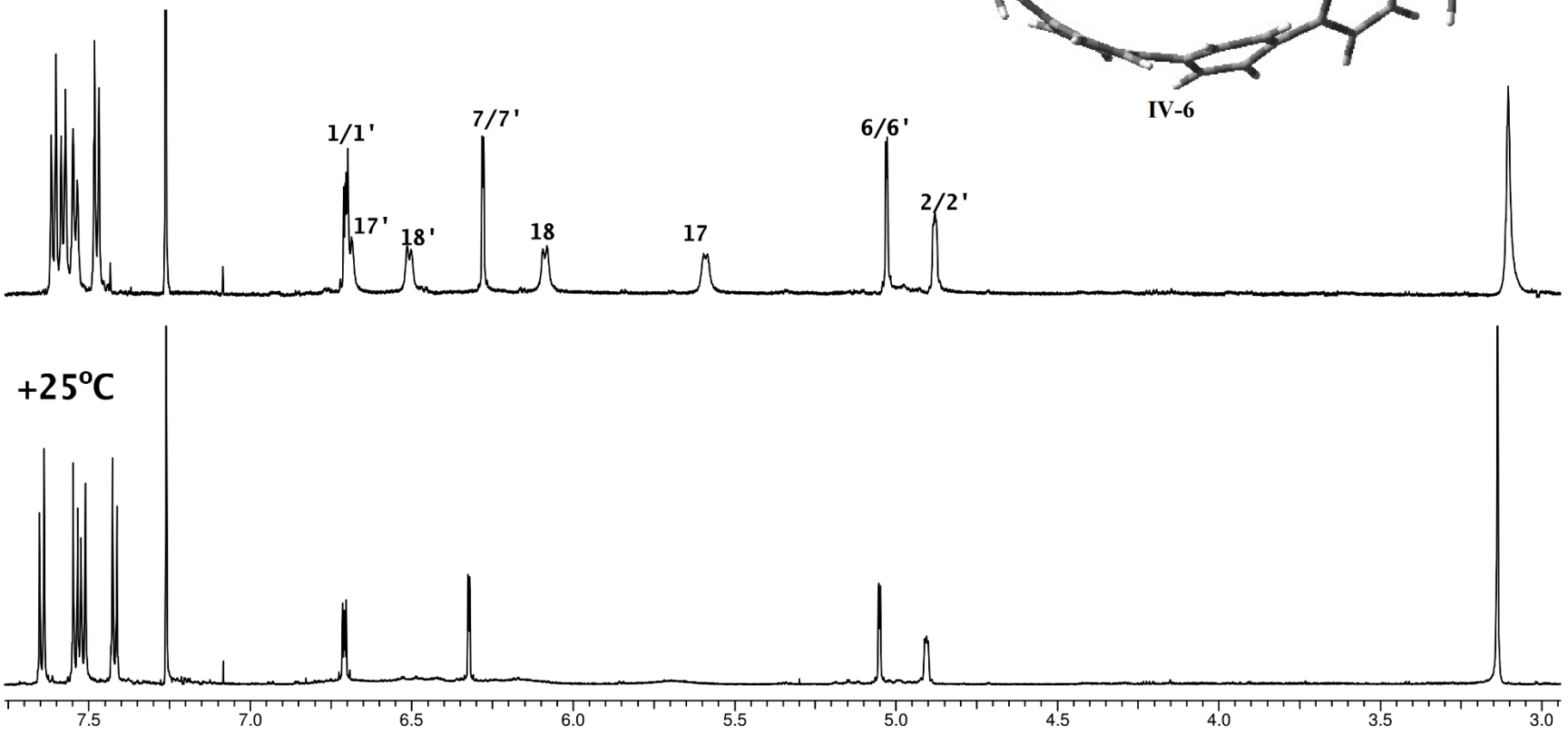

Selective decoupled ^{1}H NMR spectra at -20°C (b-e); Control ^{1}H NMR spectrum (a).

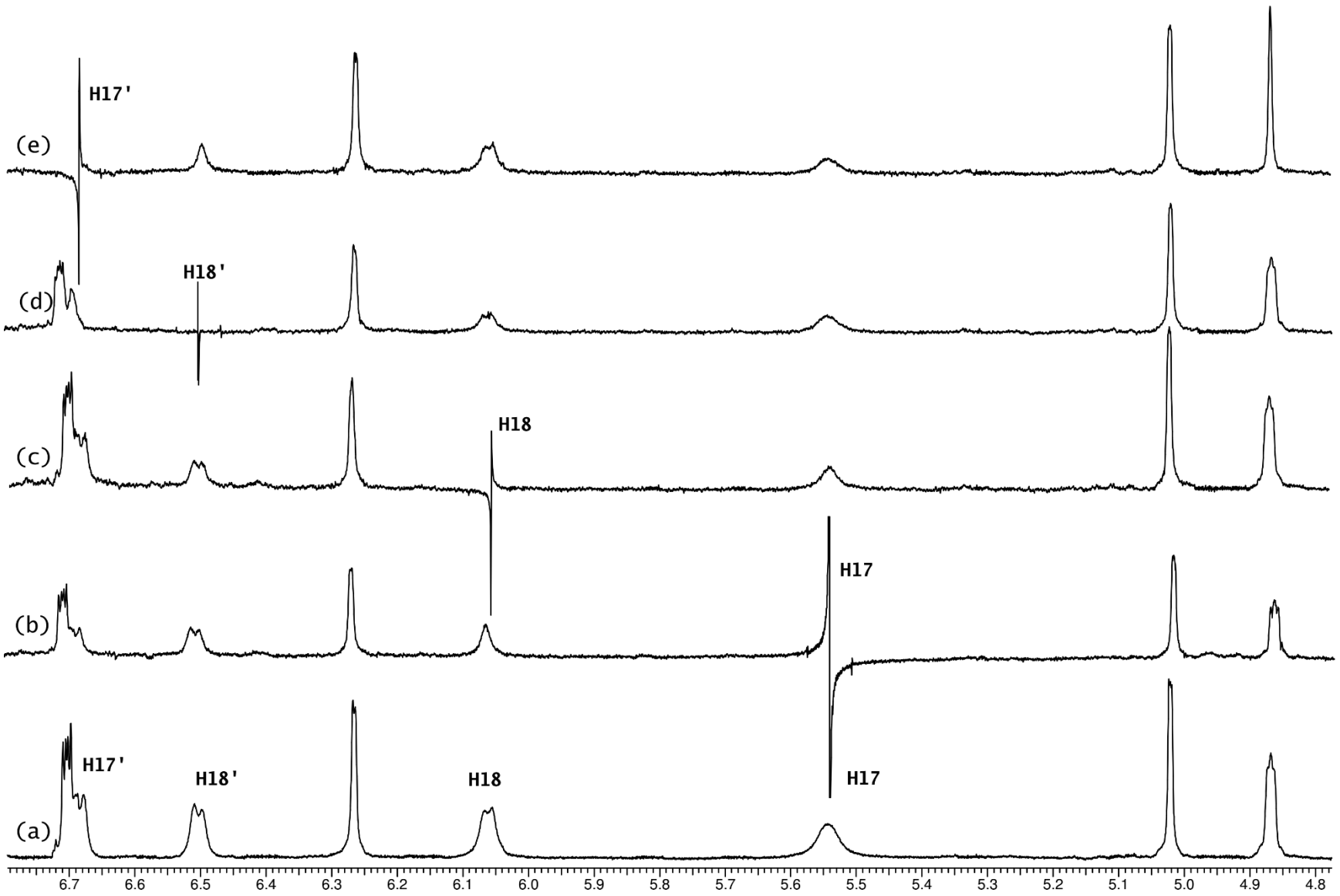

Selective decoupled ^{1}H NMR spectrum at **+25°C** (b) and Control ^{1}H NMR spectrum (a) at **+50°C**

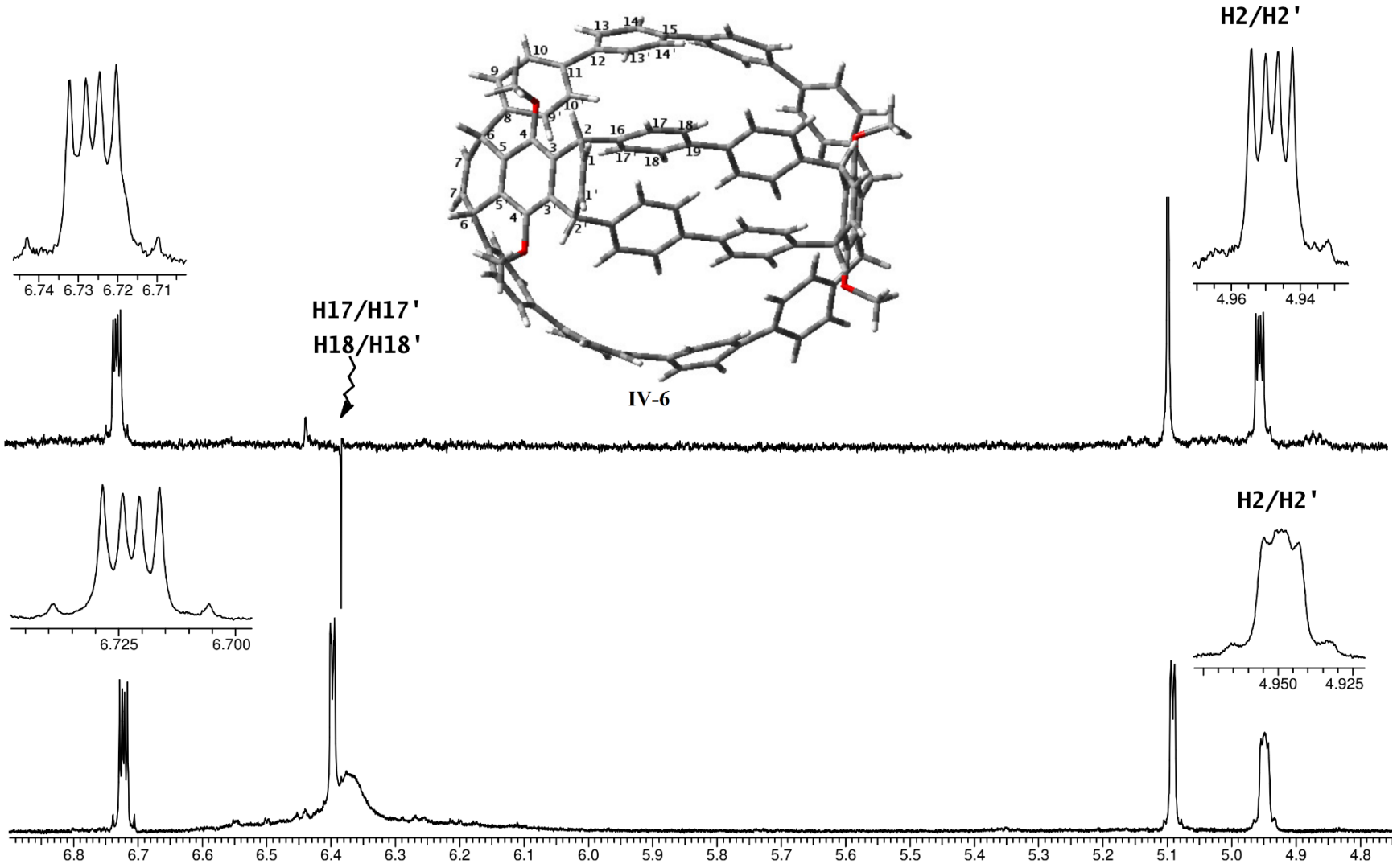

gCOSY

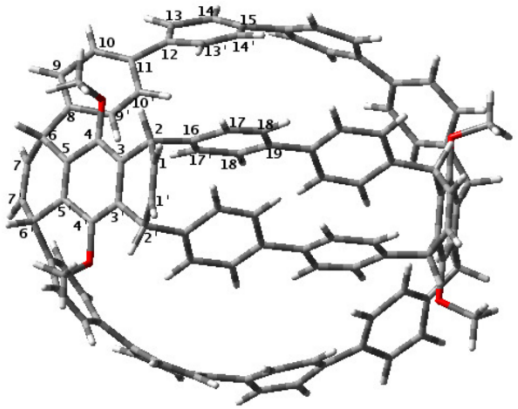

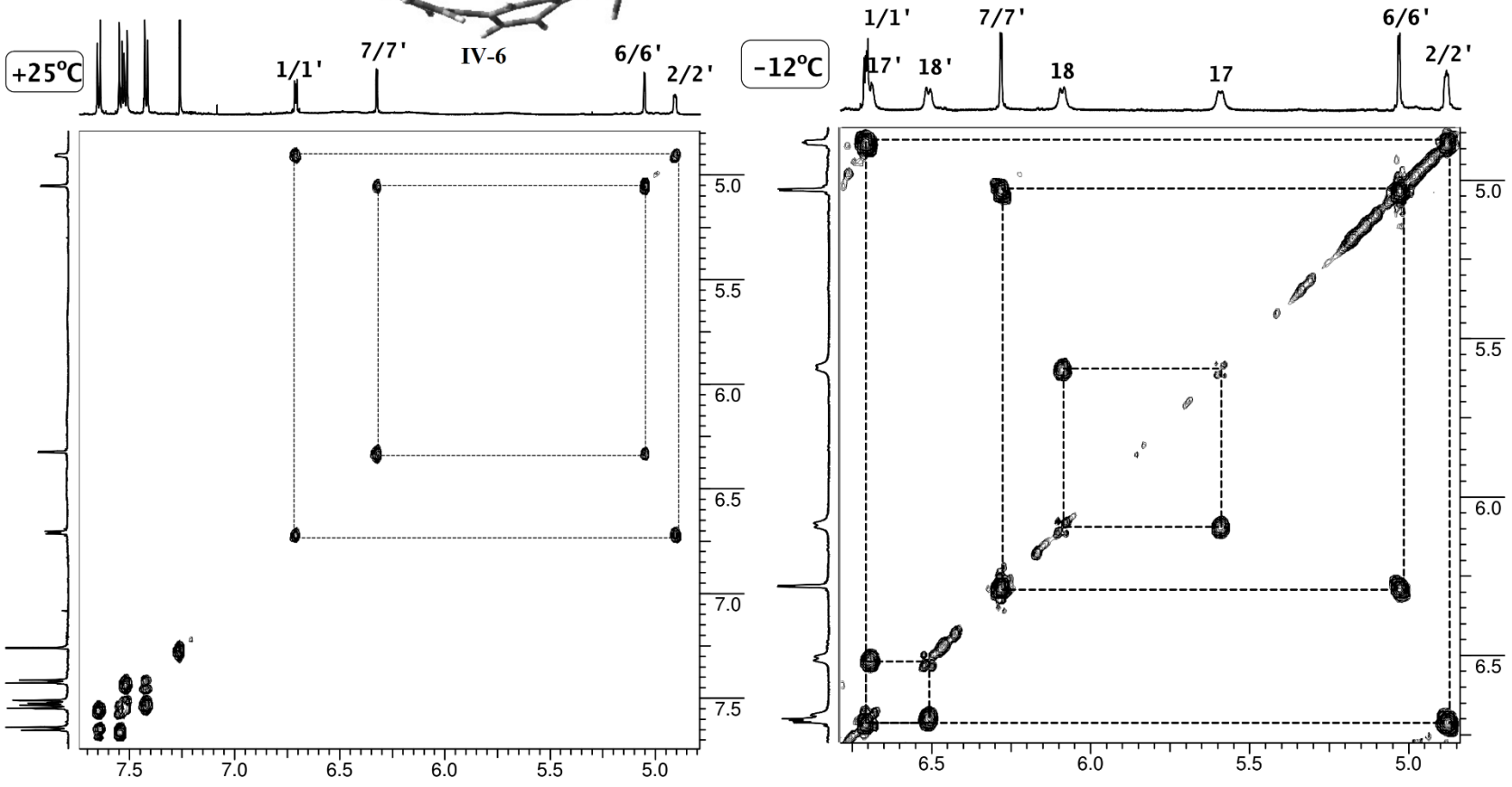

Expanded portions of the **NOESY** spectrum at **+25°C**

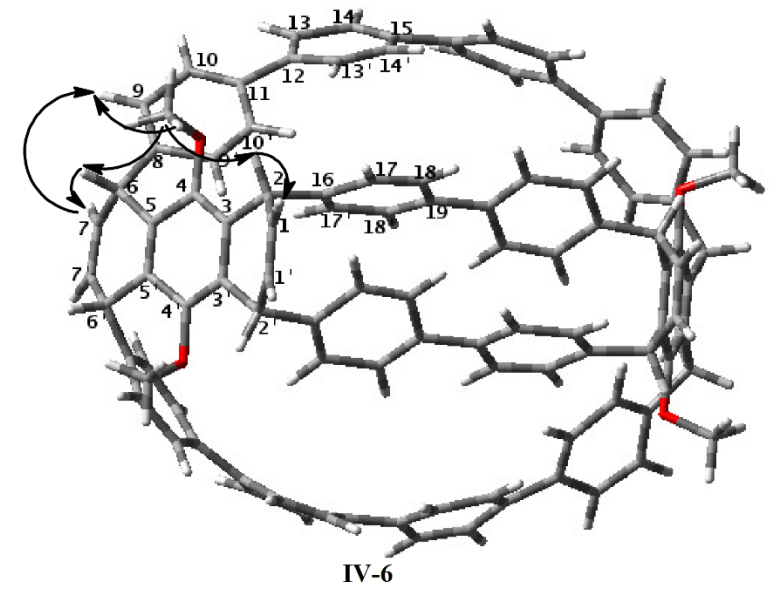

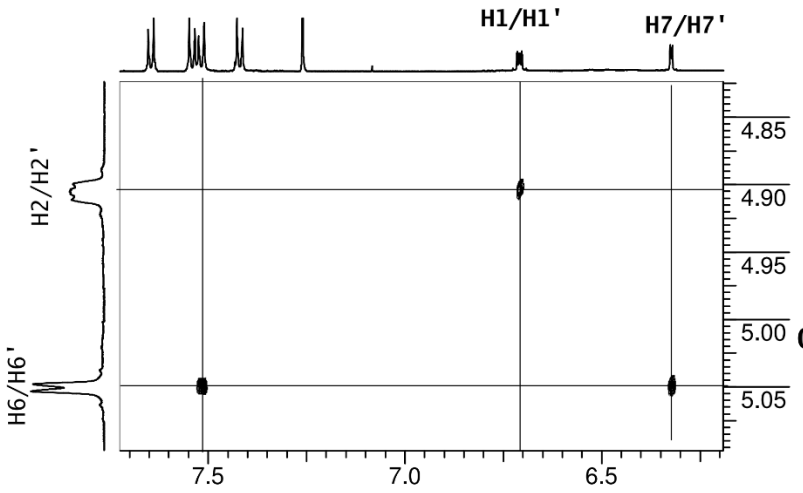

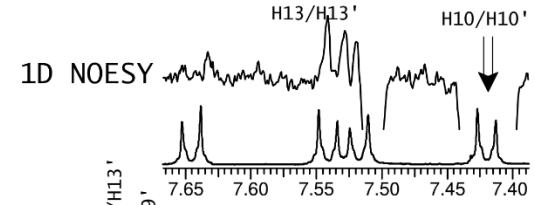

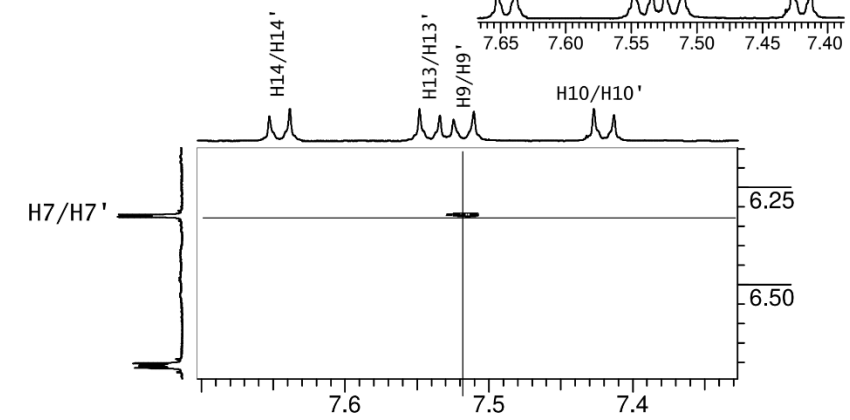

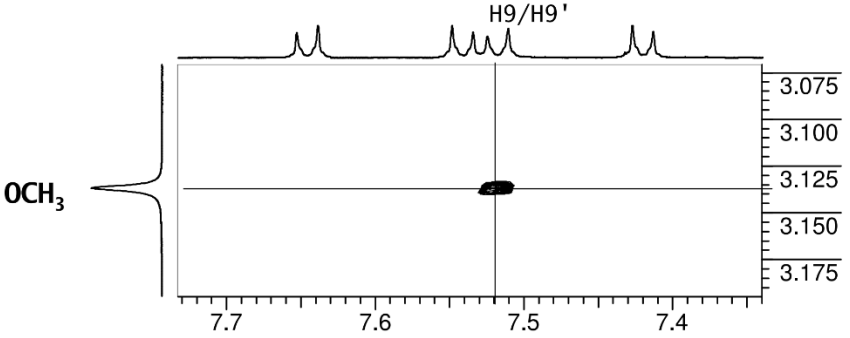

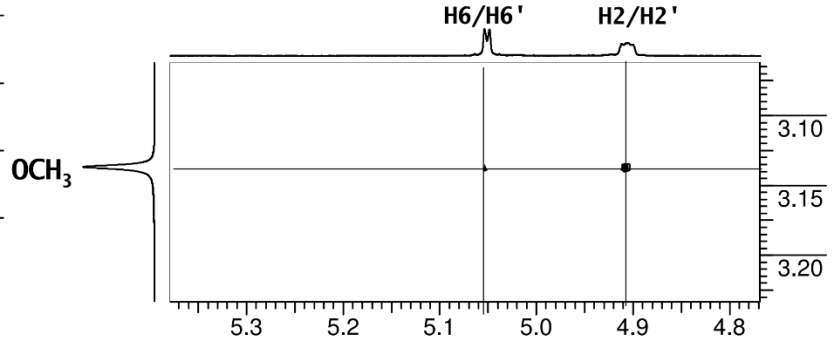

Expanded portion of the **NOESY** spectrum at **-5°C**

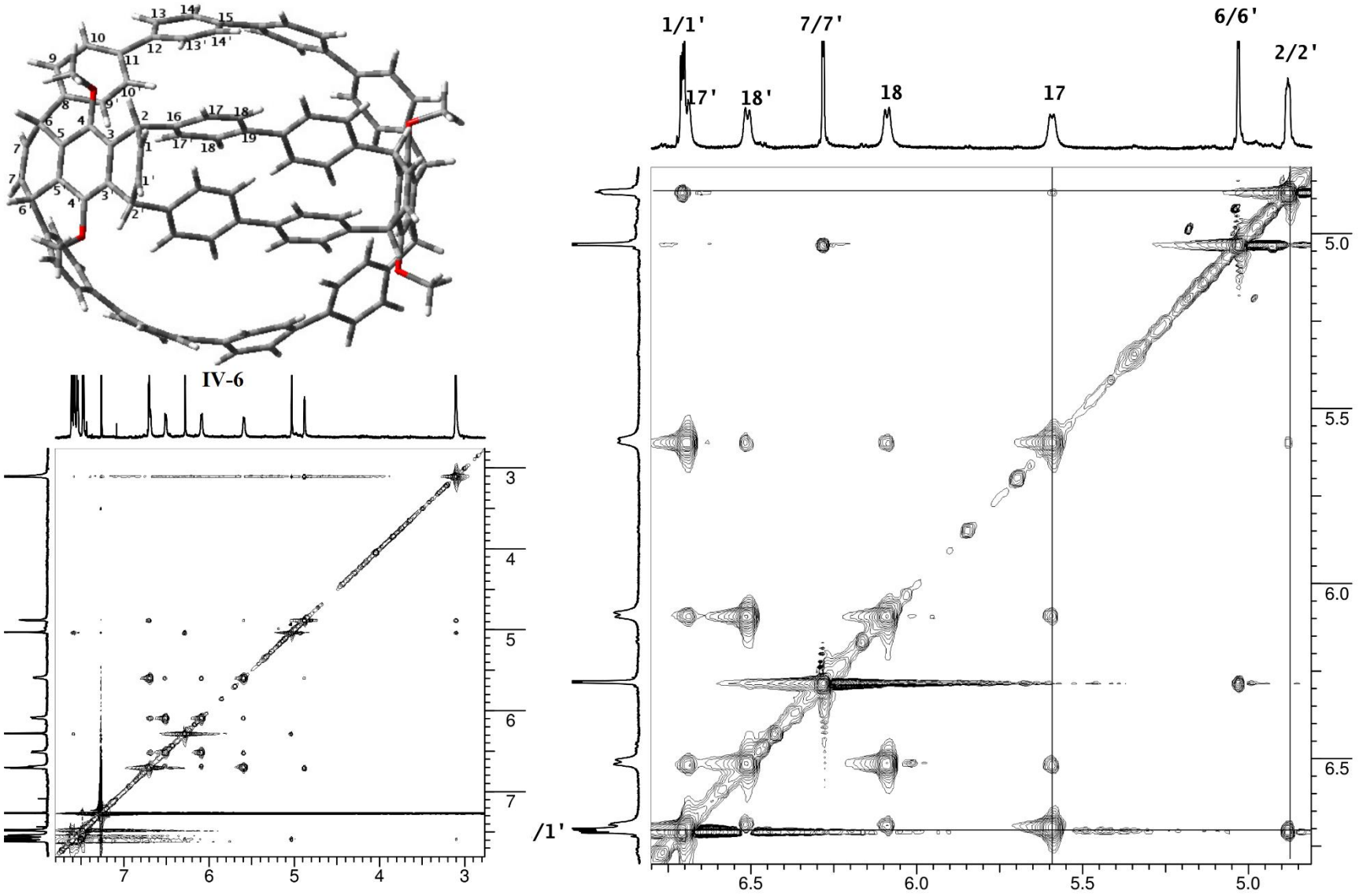

gHSQCAD

One-bond correlations at +25°C and -12°C

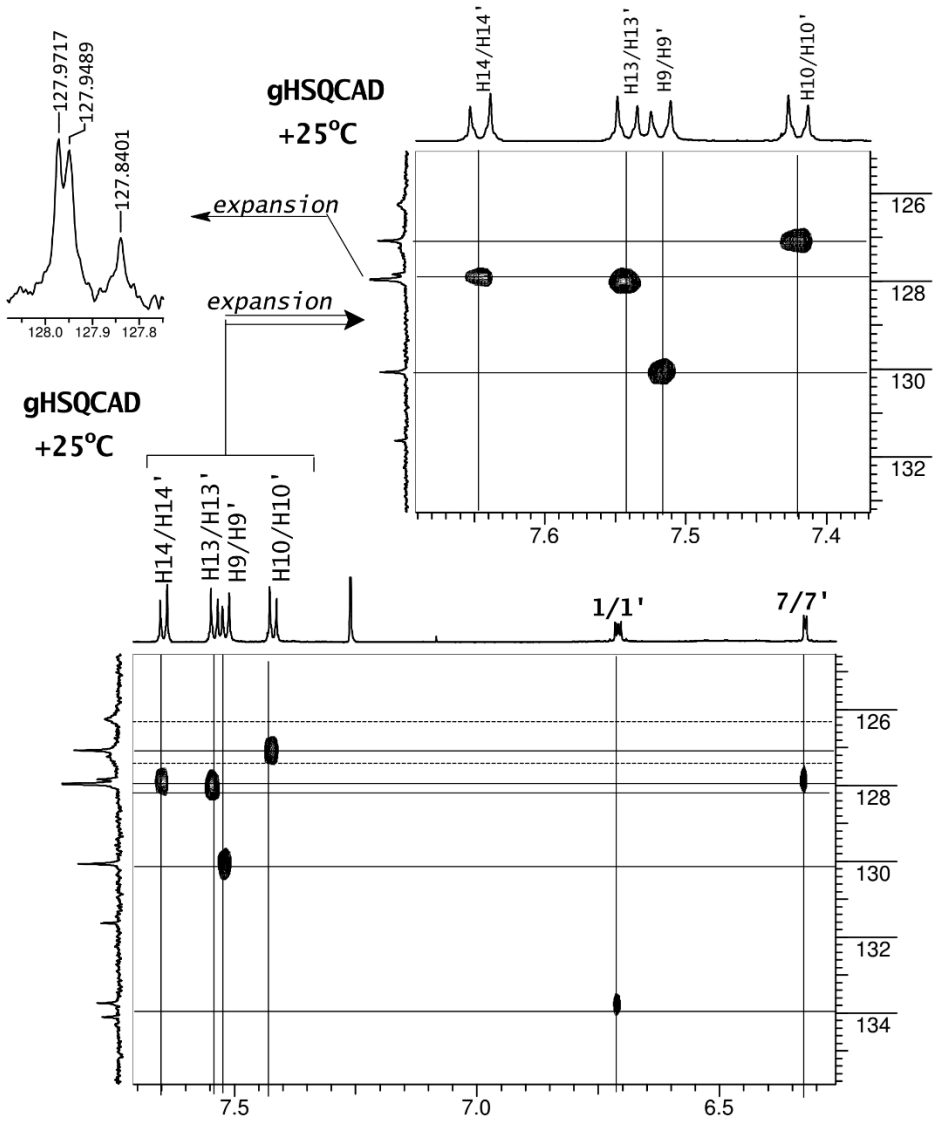

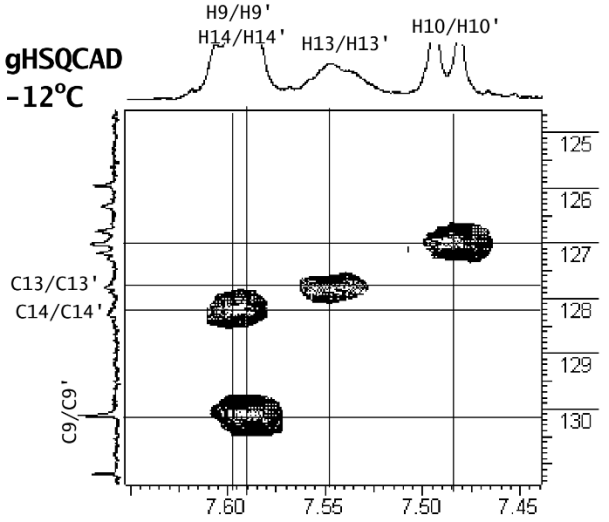

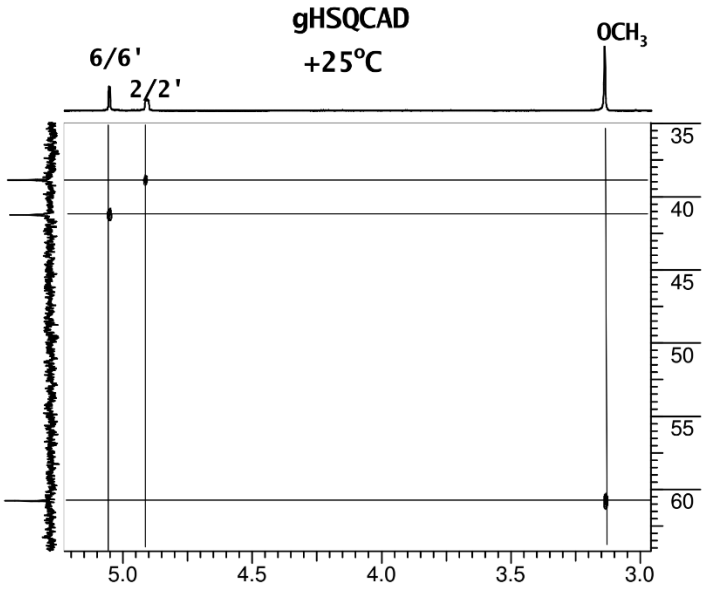

gHSQCAD

One-bond correlations at -12°C

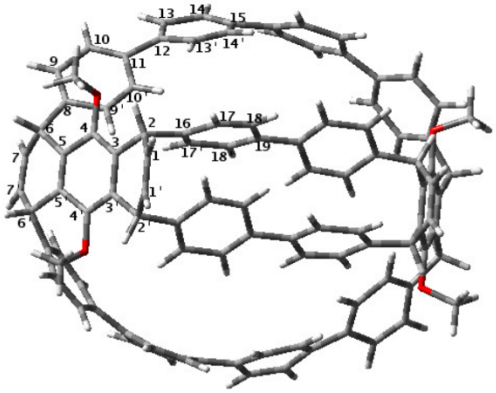

IV-6

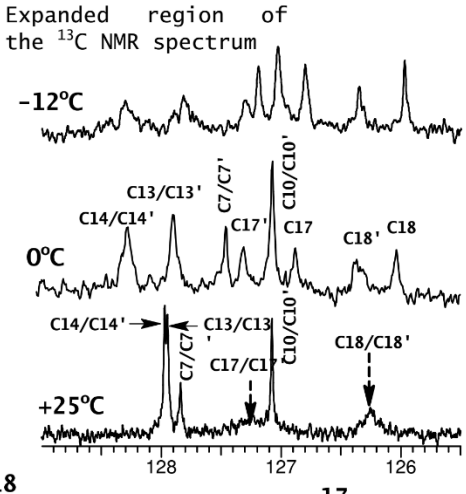

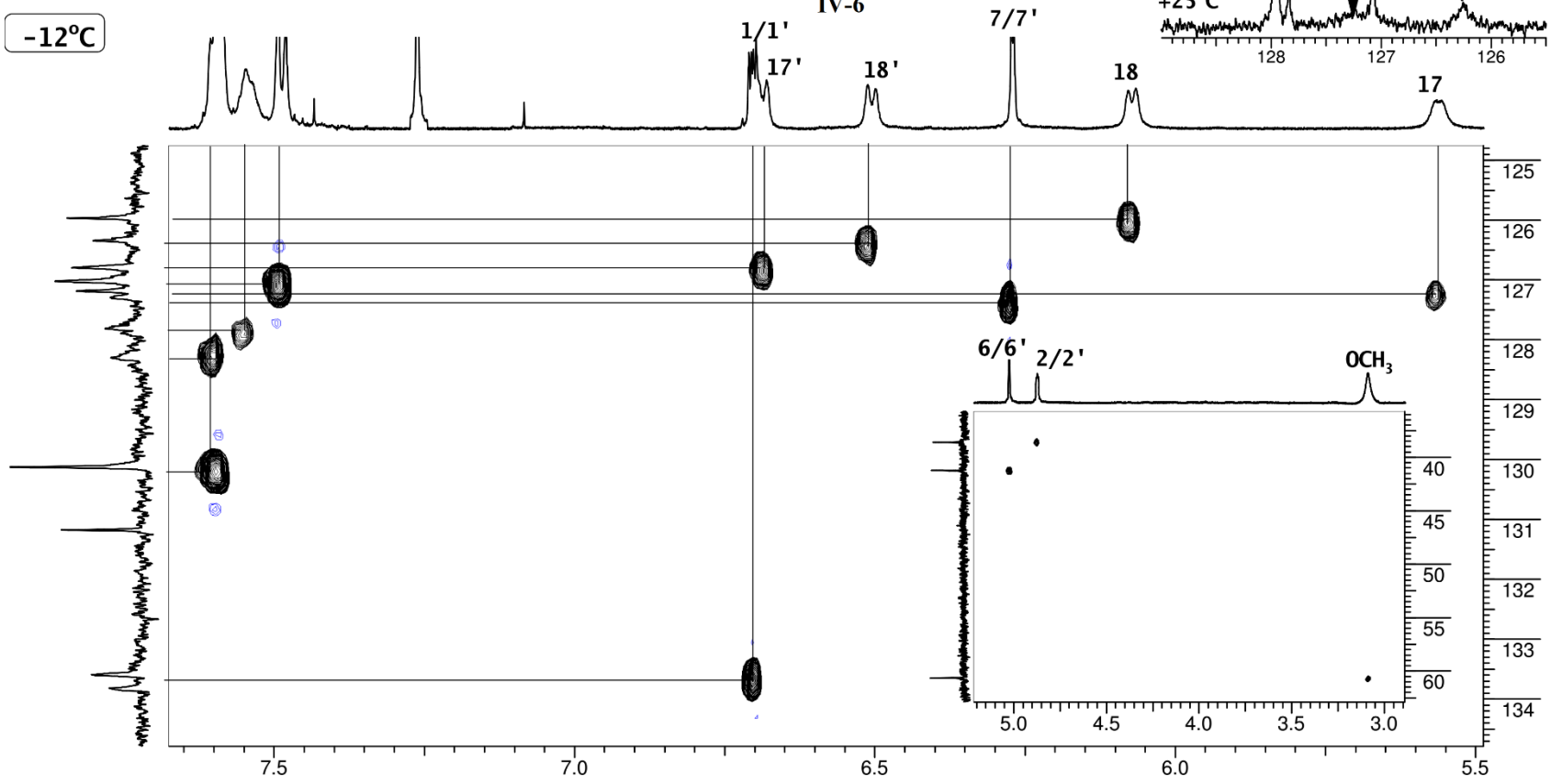

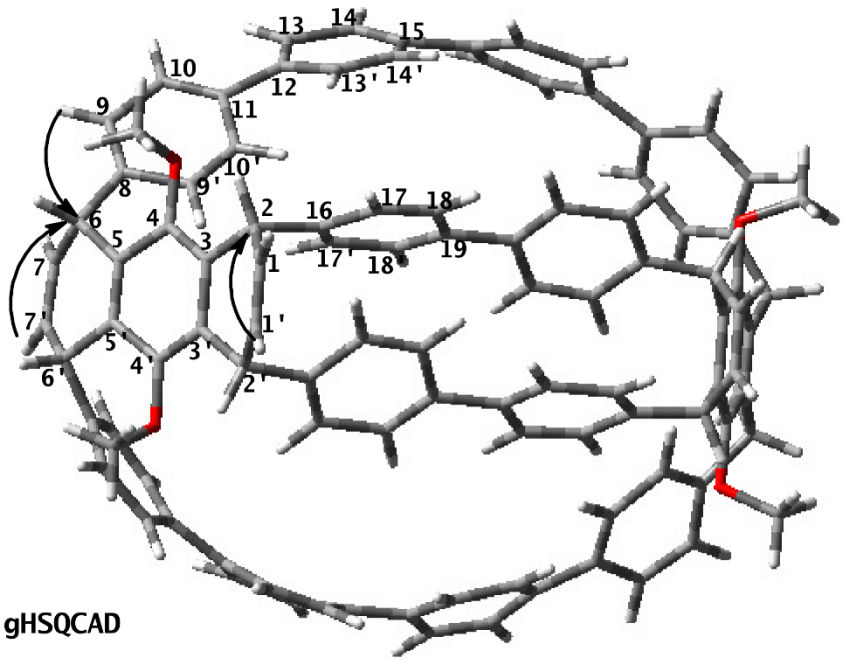

IV-6

gHSQCAD

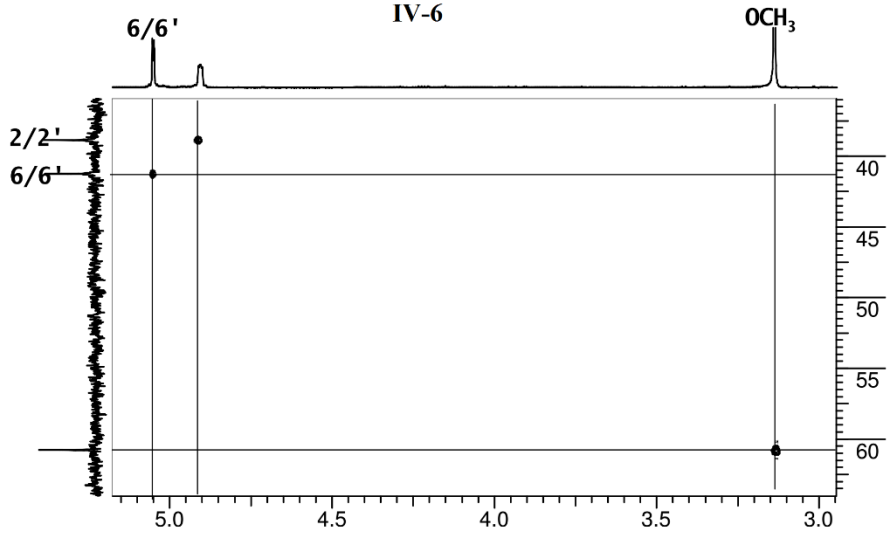

gHMBCAD

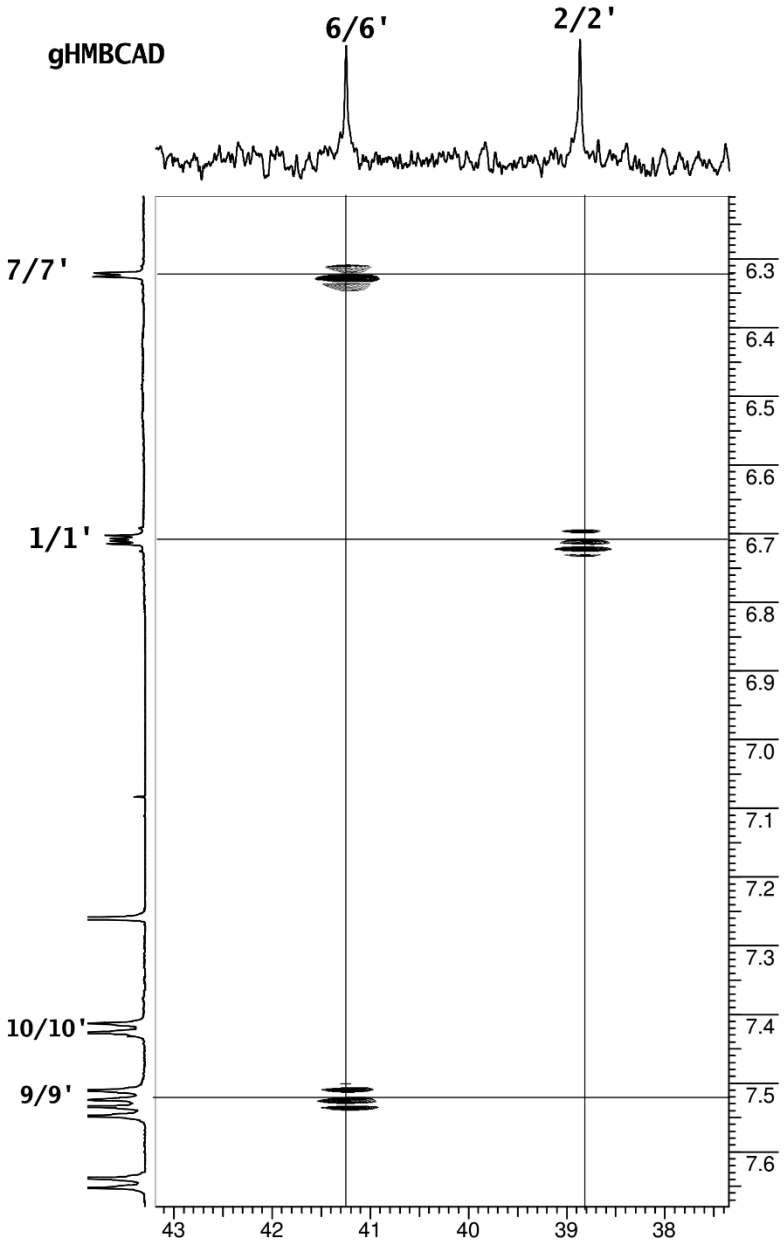

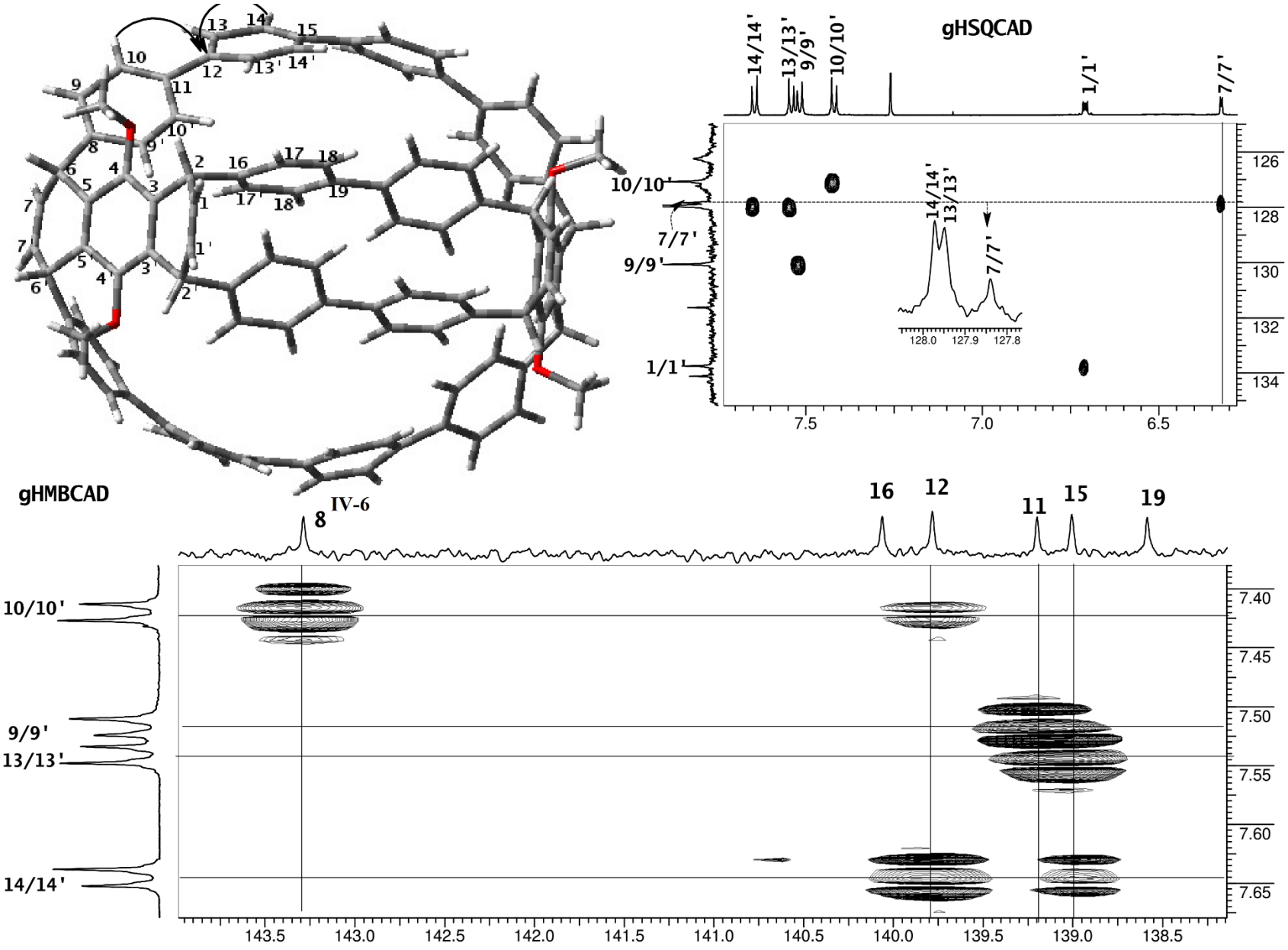
gHSQCAD
14/14'
13/13'
9/9'
10/10'
1/1'
7/7'
gHMBCAD
IV-6
8
16
12
11
15
19
10/10'
9/9'
13/13'
14/14'

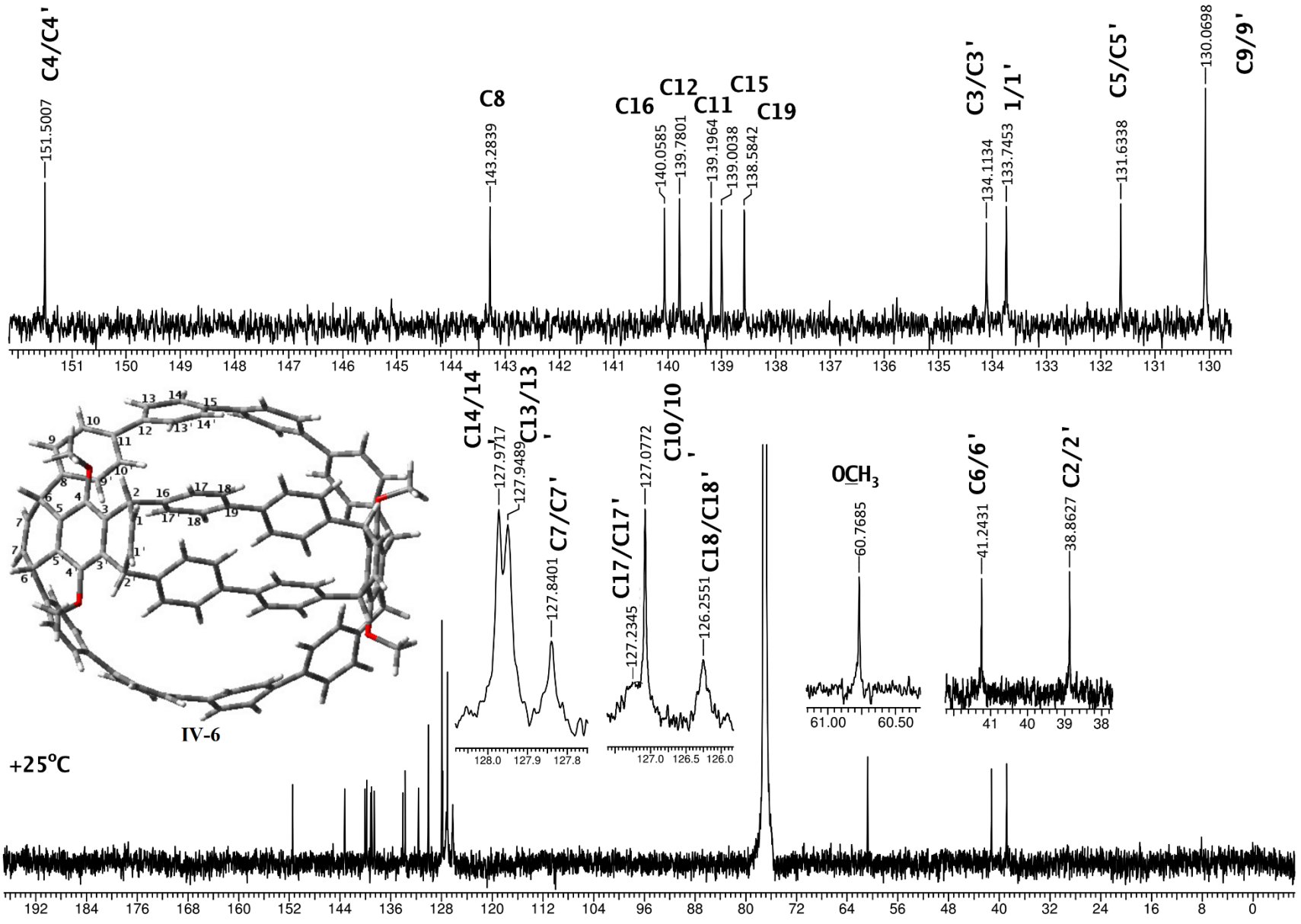
C4/C4'
151.5007
C8
143.2839
C16
C12
C11
C15
C19
140.0585
139.7801
139.1964
139.0038
138.5842
C3/C3'
1/1'
134.1134
133.7453
C5/C5'
131.6338
130.0698
C9/9'
C14/14'
C13/13'
127.9717
127.9489
C7/C7'
127.8401
C17/C17'
C10/10'
127.0772
127.2345
C18/C18'
126.2551
OCH3
60.7685
C6/6'
41.2431
C2/2'
38.8627
IV-6
+25°C

Expanded portions of the ^{13}C NMR spectrum at +25°C and at -12°C

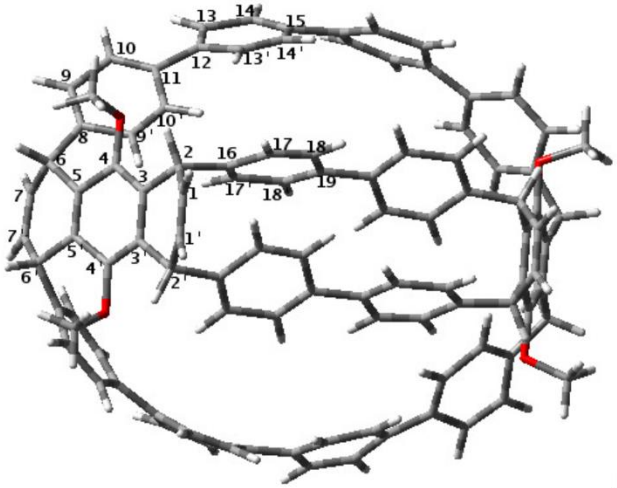

IV-6

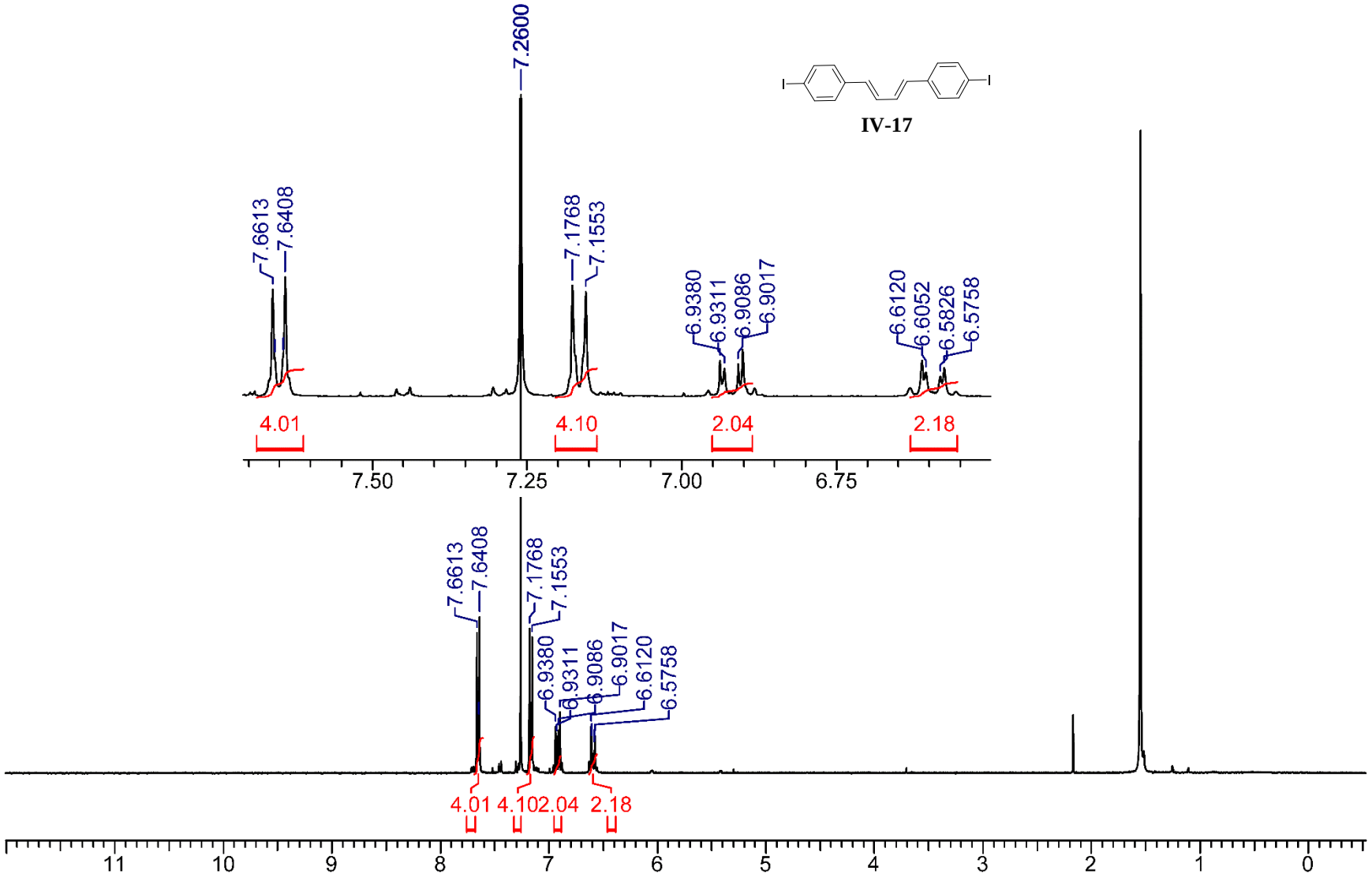
7.2600
7.6613
7.6408
7.1768
7.1553
6.9380
6.9311
6.9086
6.9017
6.6120
6.6052
6.5826
6.5758
4.01
4.10
2.04
2.18
7.50
7.25
7.00
6.75
IV-17
11
10
9
8
7
6
5
4
3
2
1
0

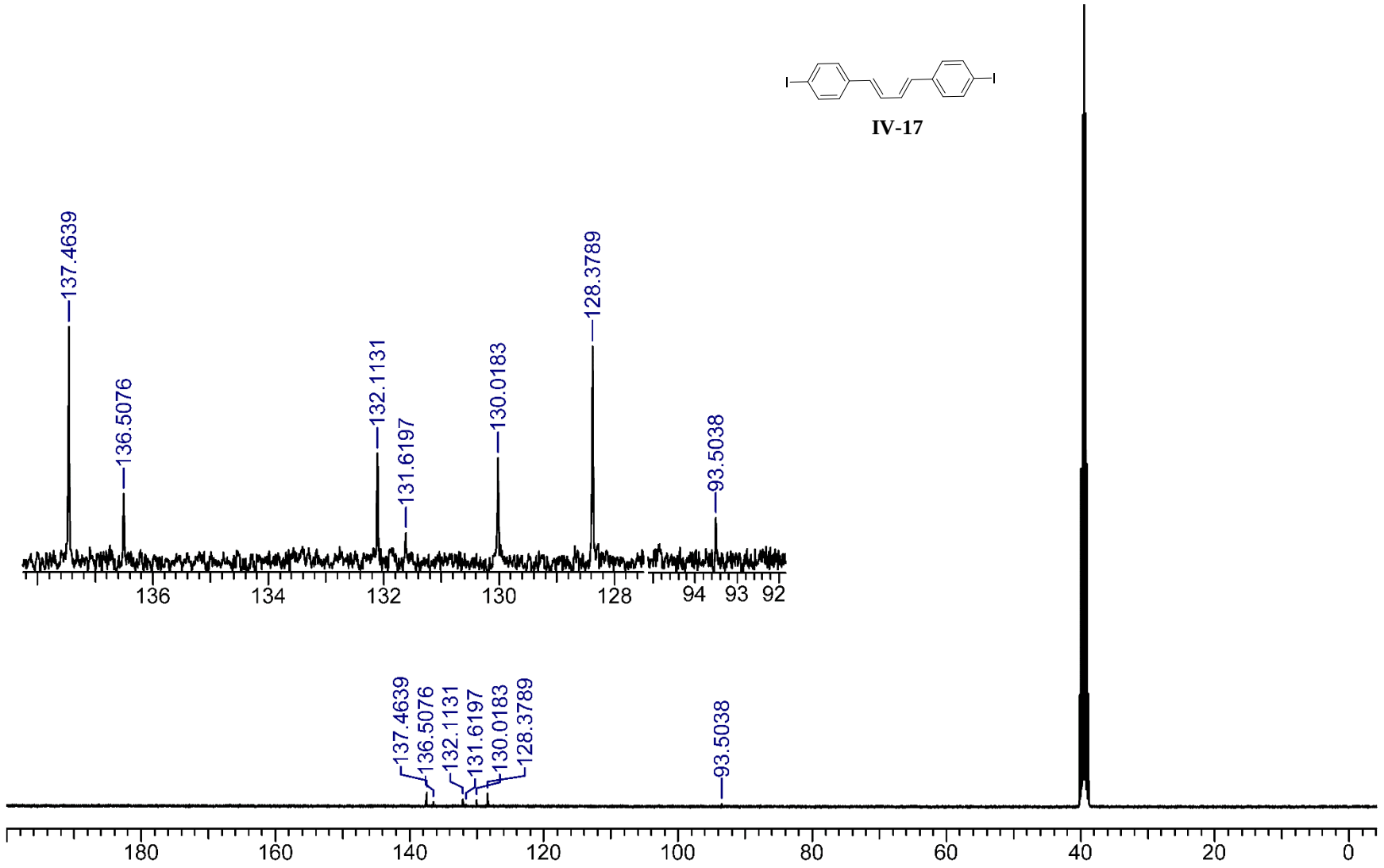
IV-17
137.4639
136.5076
132.1131
131.6197
130.0183
128.3789
93.5038
180
160
140
120
100
80
60
40
20
0
136
134
132
130
128
94
93
92

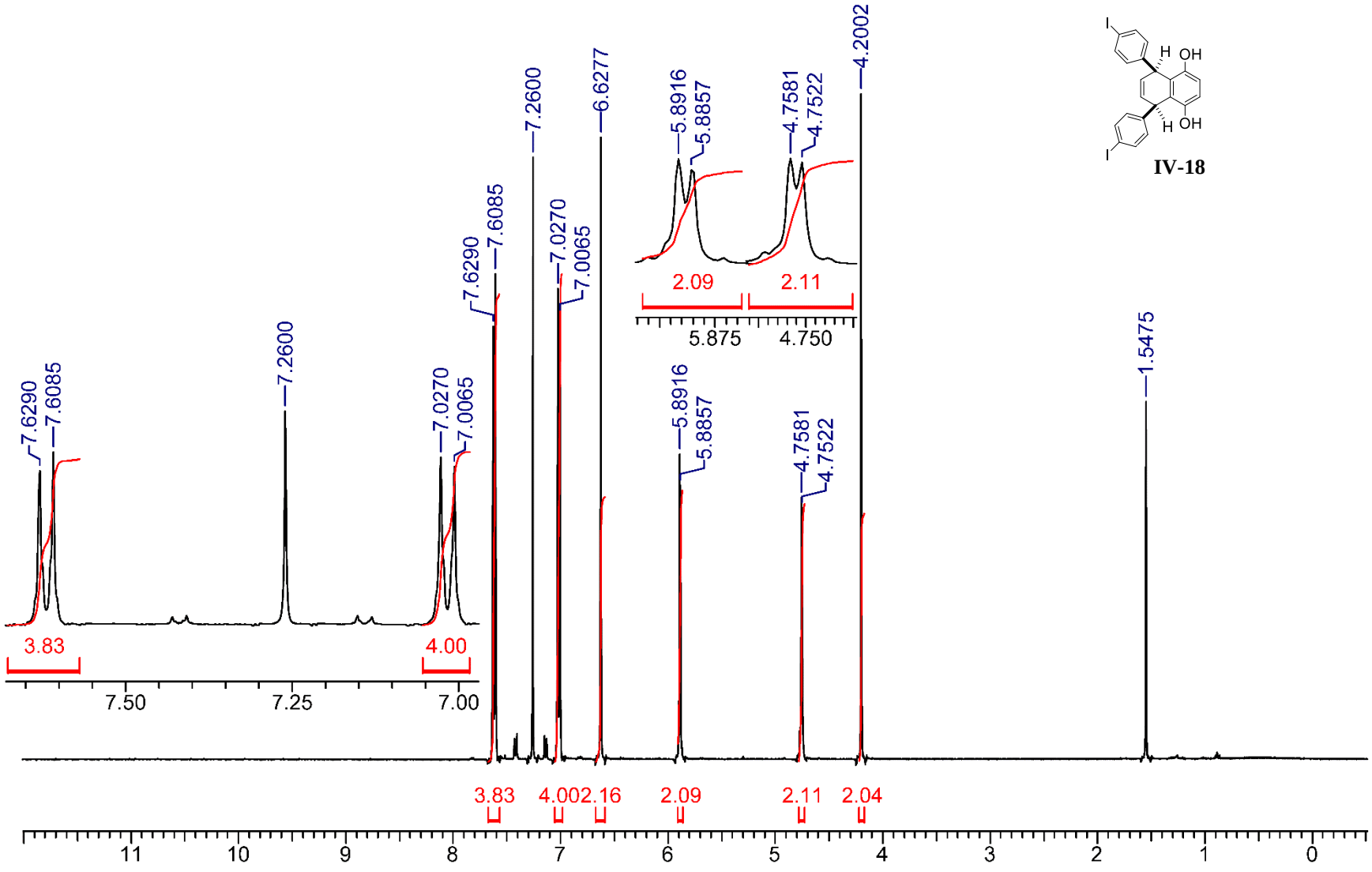
7.6290
7.6085
7.2600
7.0270
7.0065
6.6277
5.8916
5.8857
4.7581
4.7522
4.2002
1.5475
3.83
4.00
2.16
2.09
2.11
2.04
IV-18

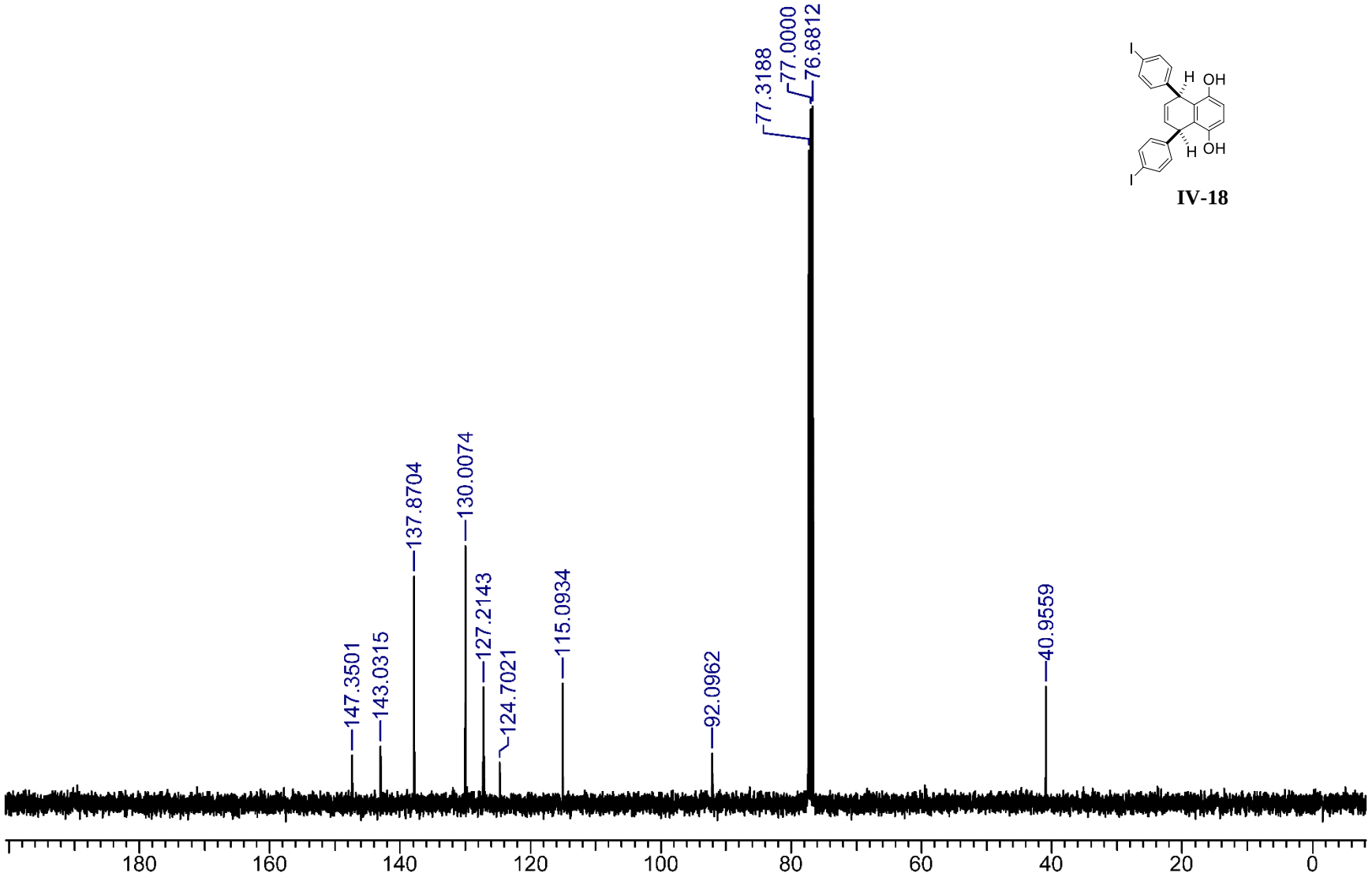
77.3188
77.0000
76.6812
147.3501
143.0315
137.8704
130.0074
127.2143
124.7021
115.0934
92.0962
40.9559
180
160
140
120
100
80
60
40
20
0
I
H
OH
H
OH
I

IV-18

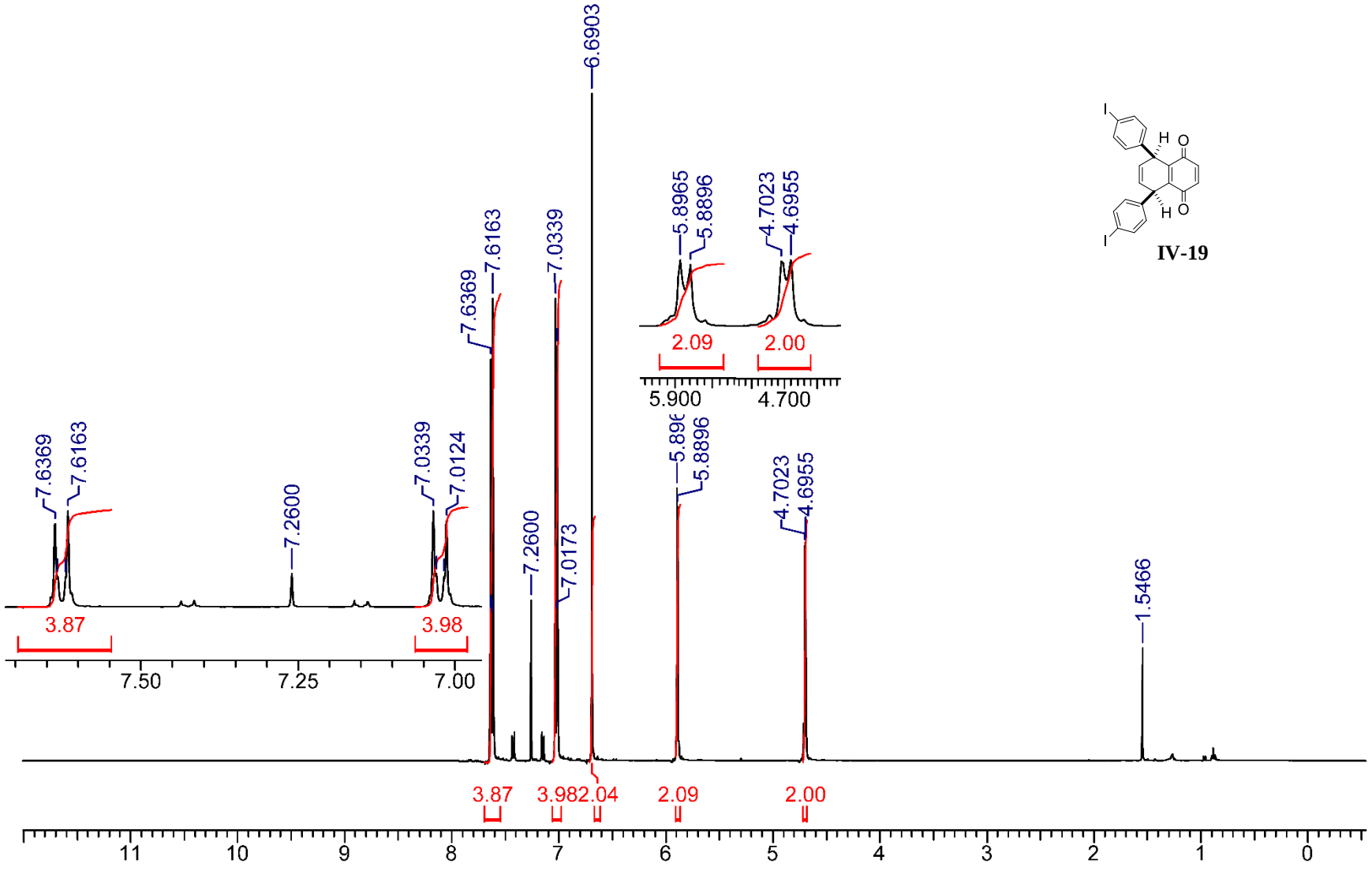
6.6903
7.6369
7.6163
7.0339
7.2600
7.0173
5.8965
5.8896
4.7023
4.6955
1.5466
3.87
3.98
2.04
2.09
2.00
IV-19

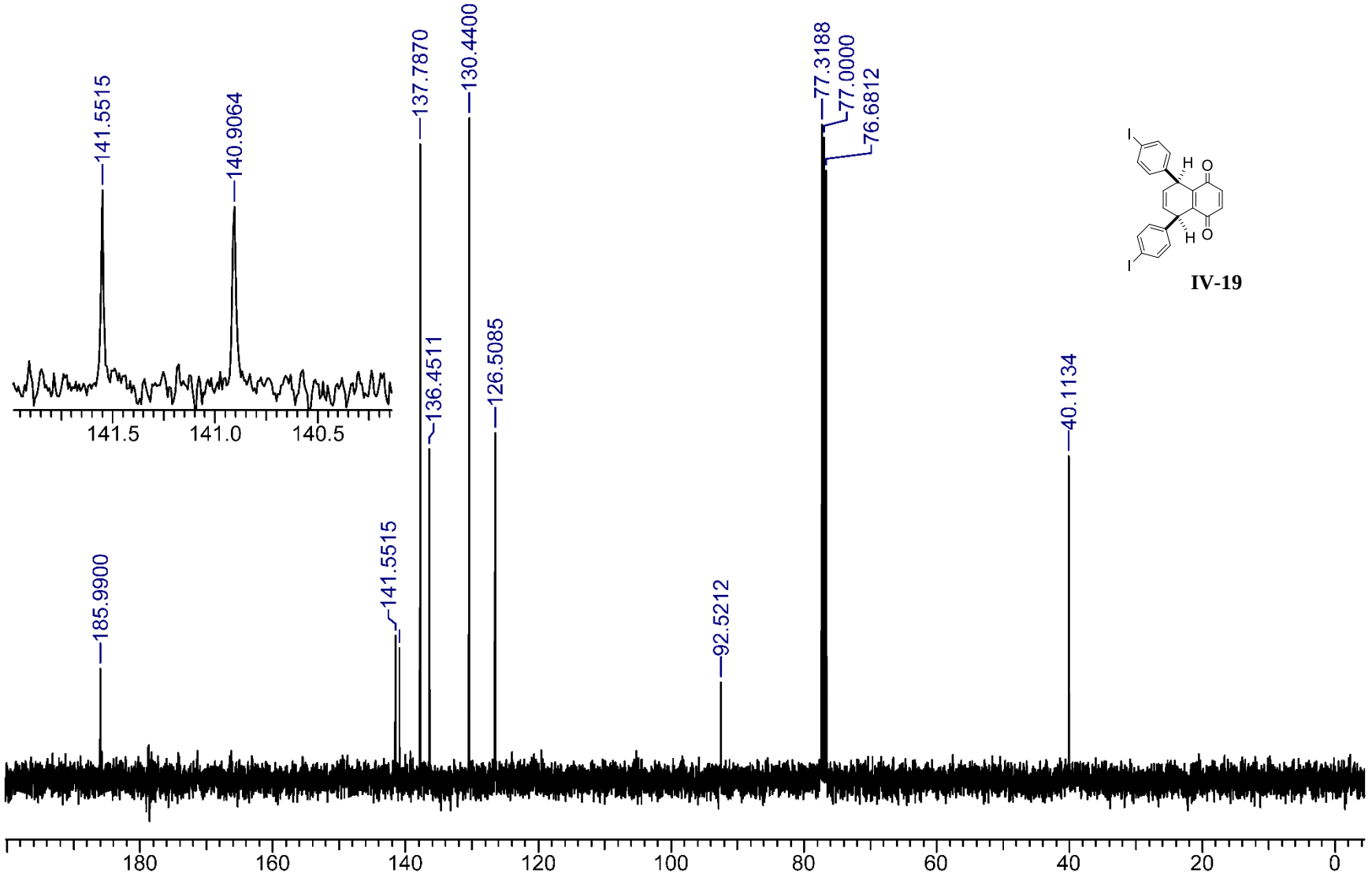
141.5515
140.9064
137.7870
130.4400
77.3188
77.0000
76.6812
136.4511
126.5085
40.1134
185.9900
141.5515
92.5212
141.5
141.0
140.5
180
160
140
120
100
80
60
40
20
0

IV-19

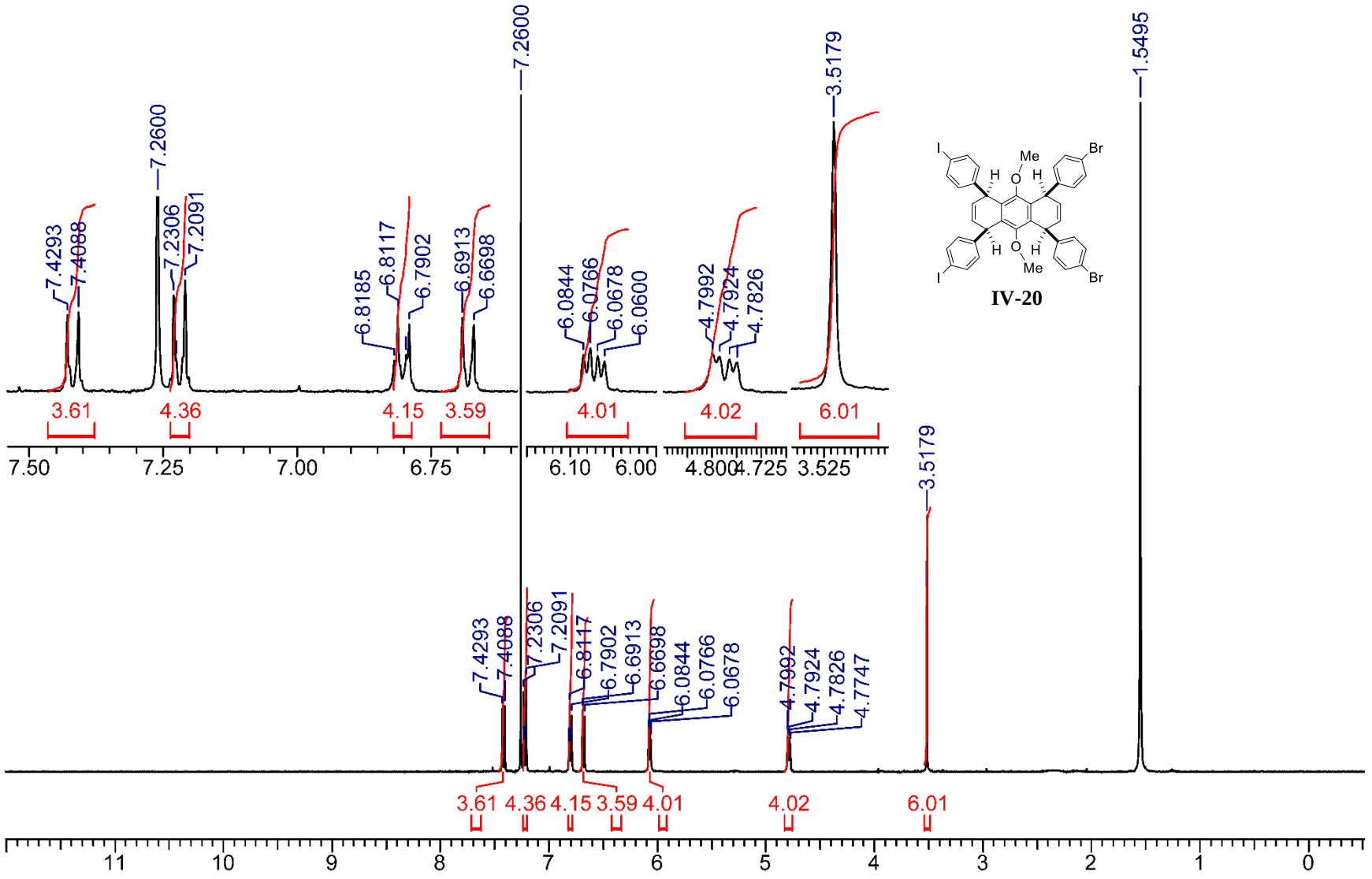
7.4293
7.4088
7.2600
7.2306
7.2091
6.8185
6.8117
6.7902
6.6913
6.6698
7.2600
6.0844
6.0766
6.0678
6.0600
4.7992
4.7924
4.7826
3.5179
1.5495
3.61
4.36
4.15
3.59
4.01
4.02
6.01
7.50
7.25
7.00
6.75
6.10
6.00
4.800
4.725
3.525
3.5179
7.4293
7.4088
7.2306
7.2091
6.8117
6.7902
6.6913
6.6698
6.0844
6.0766
6.0678
4.7992
4.7924
4.7826
4.7747
3.61
4.36
4.15
3.59
4.01
4.02
6.01
11
10
9
8
7
6
5
4
3
2
1
0

IV-20

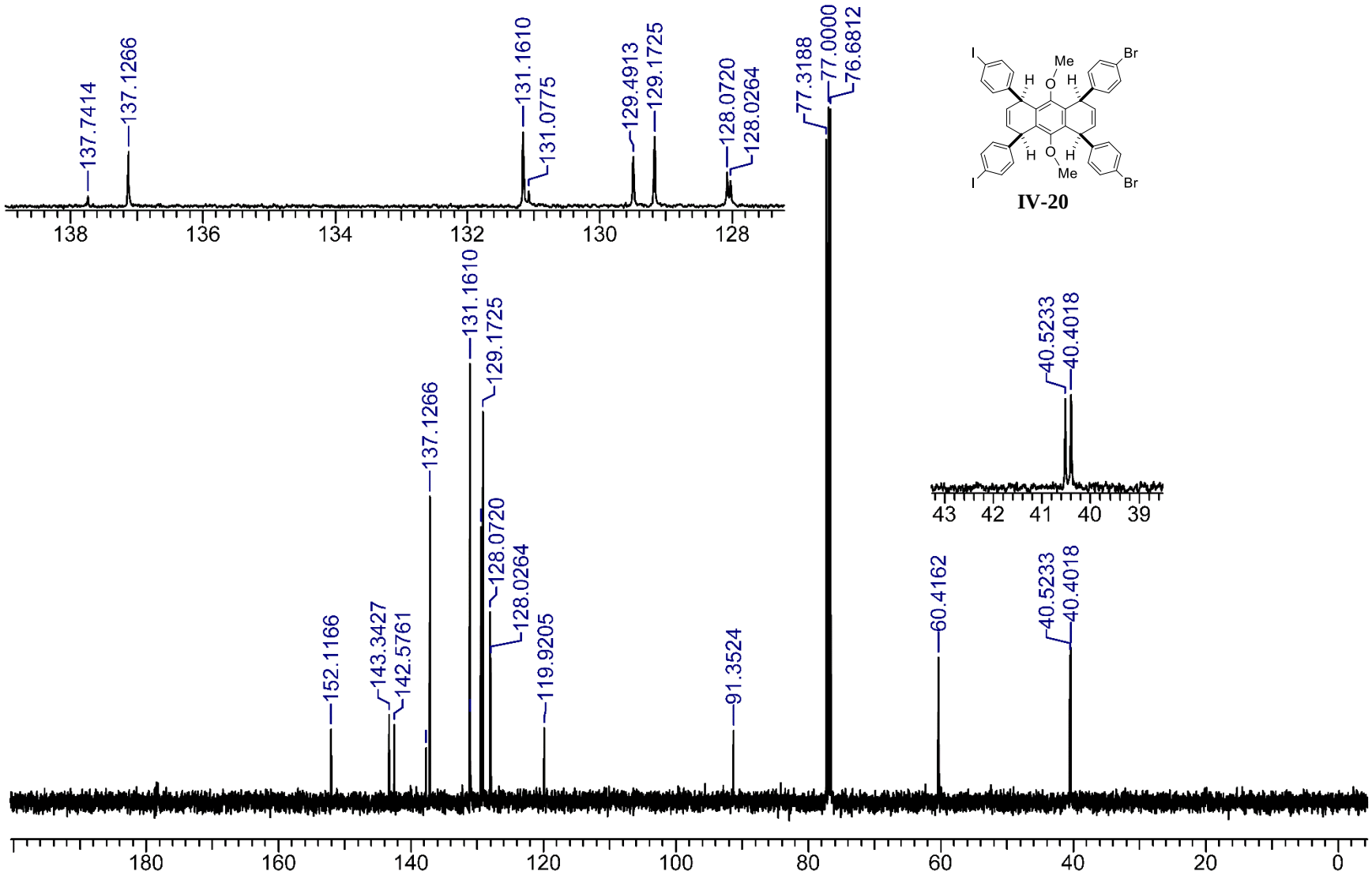
137.7414
137.1266
131.1610
131.0775
129.4913
129.1725
128.0720
128.0264
77.3188
77.0000
76.6812
138
136
134
132
130
128
I
Br
Me
O
H
IV-20
131.1610
129.1725
137.1266
128.0720
128.0264
152.1166
143.3427
142.5761
119.9205
91.3524
60.4162
40.5233
40.4018
43
42
41
40
39
180
160
140
120
100
80
60
40
20
0

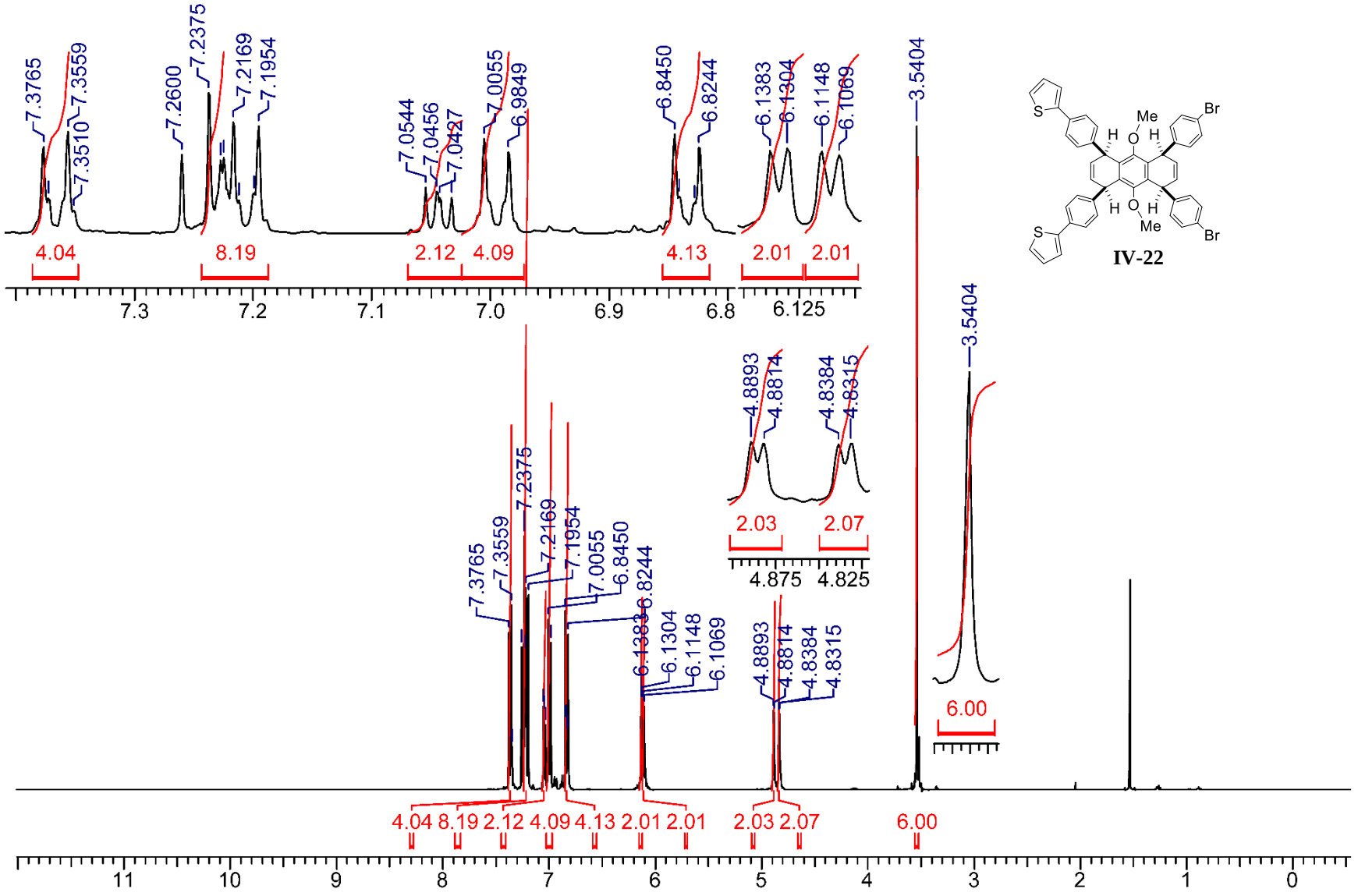
7.3765
7.3559
7.3510
7.2600
7.2375
7.2169
7.1954
7.0544
7.0456
7.0427
7.0055
6.9849
6.8450
6.8244
6.1383
6.1304
6.1148
6.1069
3.5404
4.8893
4.8814
4.8384
4.8315
4.04
8.19
2.12
4.09
4.13
2.01
2.01
2.03
2.07
6.00
Me
Br
S
H
O
IV-22

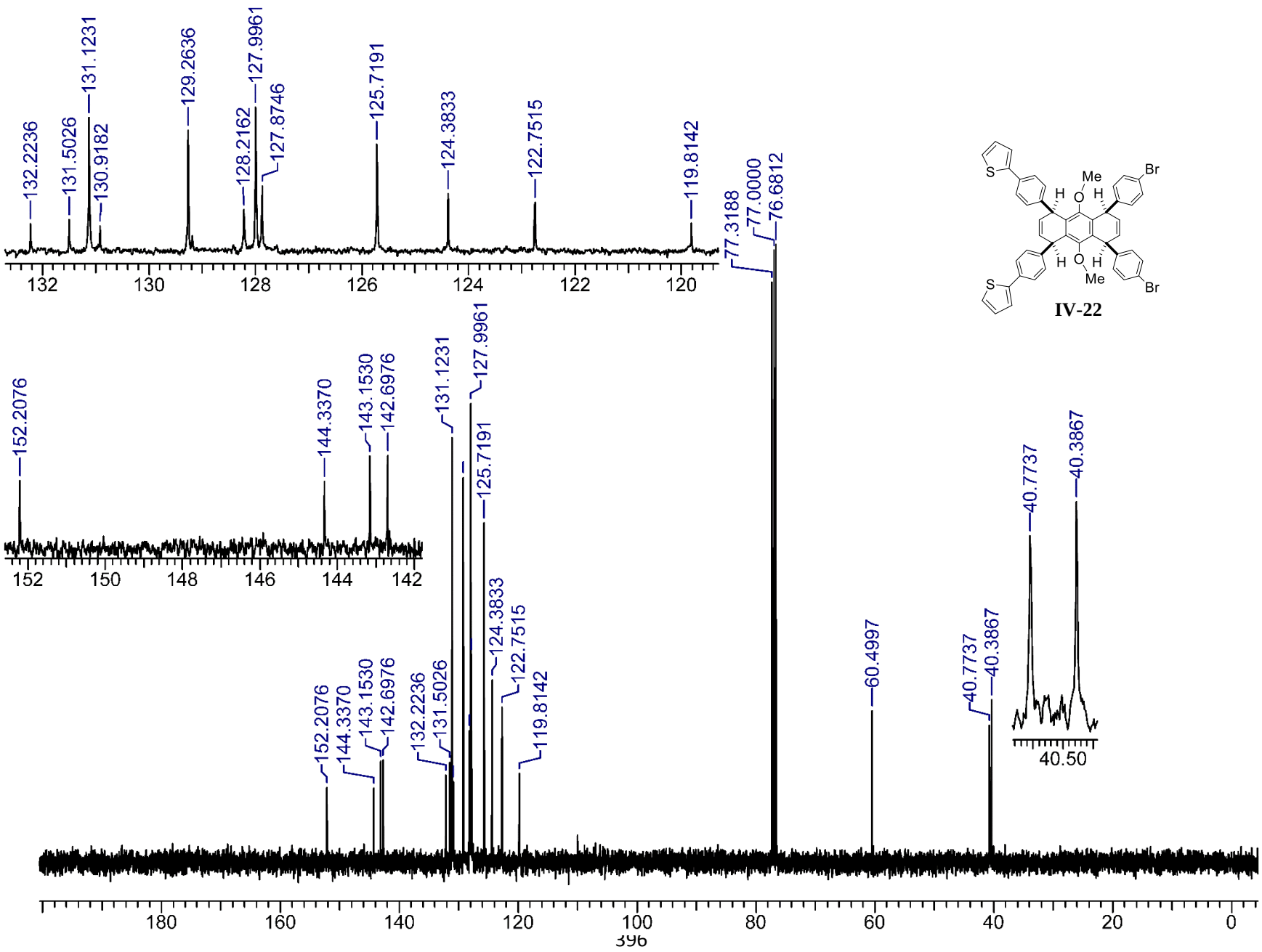
132.2236
131.5026
131.1231
130.9182
129.2636
128.2162
127.9961
127.8746
125.7191
124.3833
122.7515
119.8142
77.3188
77.0000
76.6812
152.2076
144.3370
143.1530
142.6976
131.1231
127.9961
125.7191
124.3833
122.7515
119.8142
132.2236
131.5026
60.4997
40.7737
40.3867
Me
Br
S
H
O
IV-22

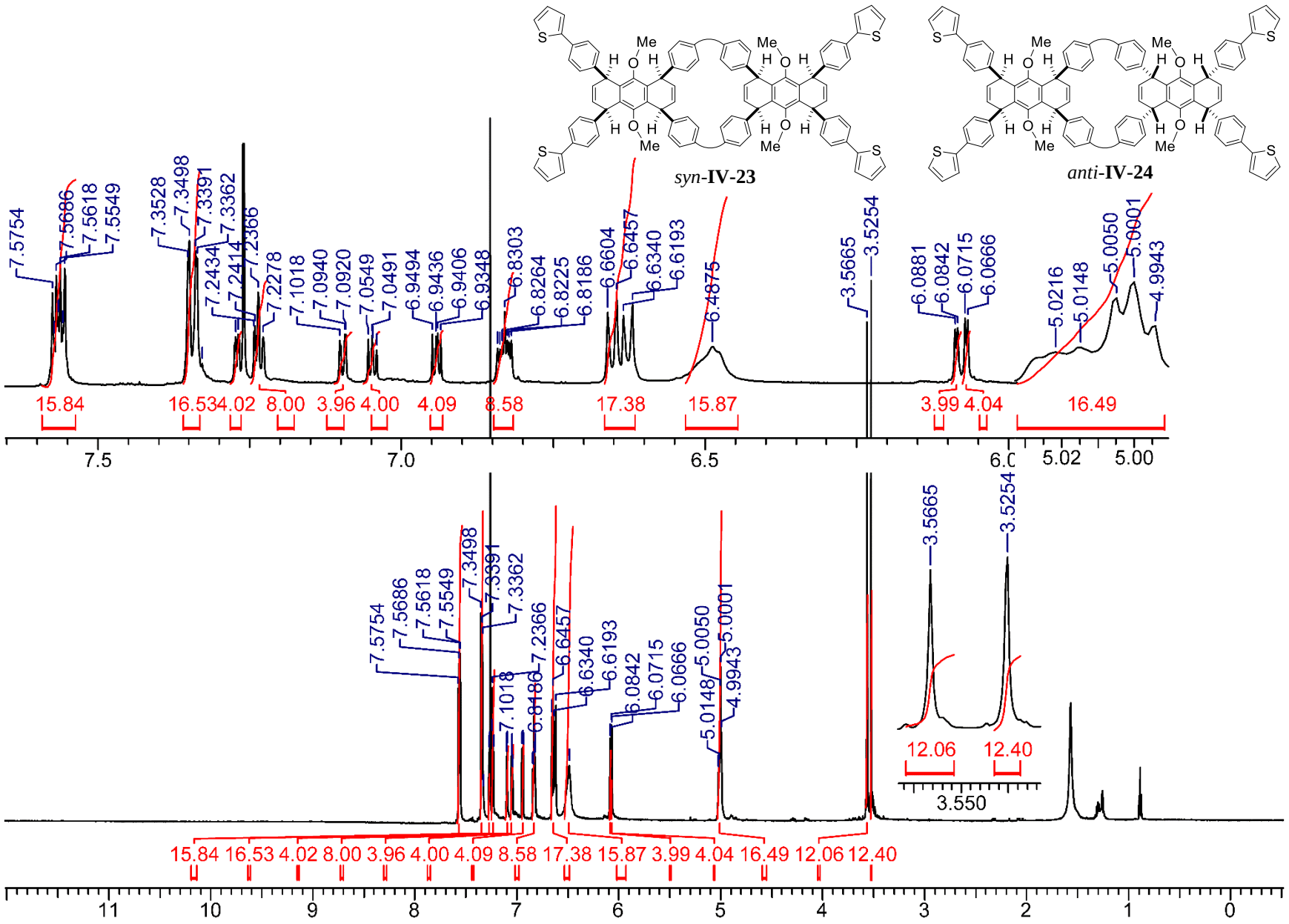
syn-IV-23
anti-IV-24
7.5754
7.5686
7.5618
7.5549
7.3528
7.3498
7.3391
7.3362
7.2434
7.2414
7.2366
7.2278
7.1018
7.0940
7.0920
7.0549
7.0491
6.9494
6.9436
6.9406
6.9348
6.8303
6.8264
6.8225
6.8186
6.6604
6.6457
6.6340
6.6193
6.4875
3.5665
3.5254
6.0881
6.0842
6.0715
6.0666
5.0216
5.0148
5.0050
5.0001
4.9943
15.84
16.53
4.02
8.00
3.96
4.00
4.09
8.58
17.38
15.87
3.99
4.04
16.49
12.06
12.40
3.550

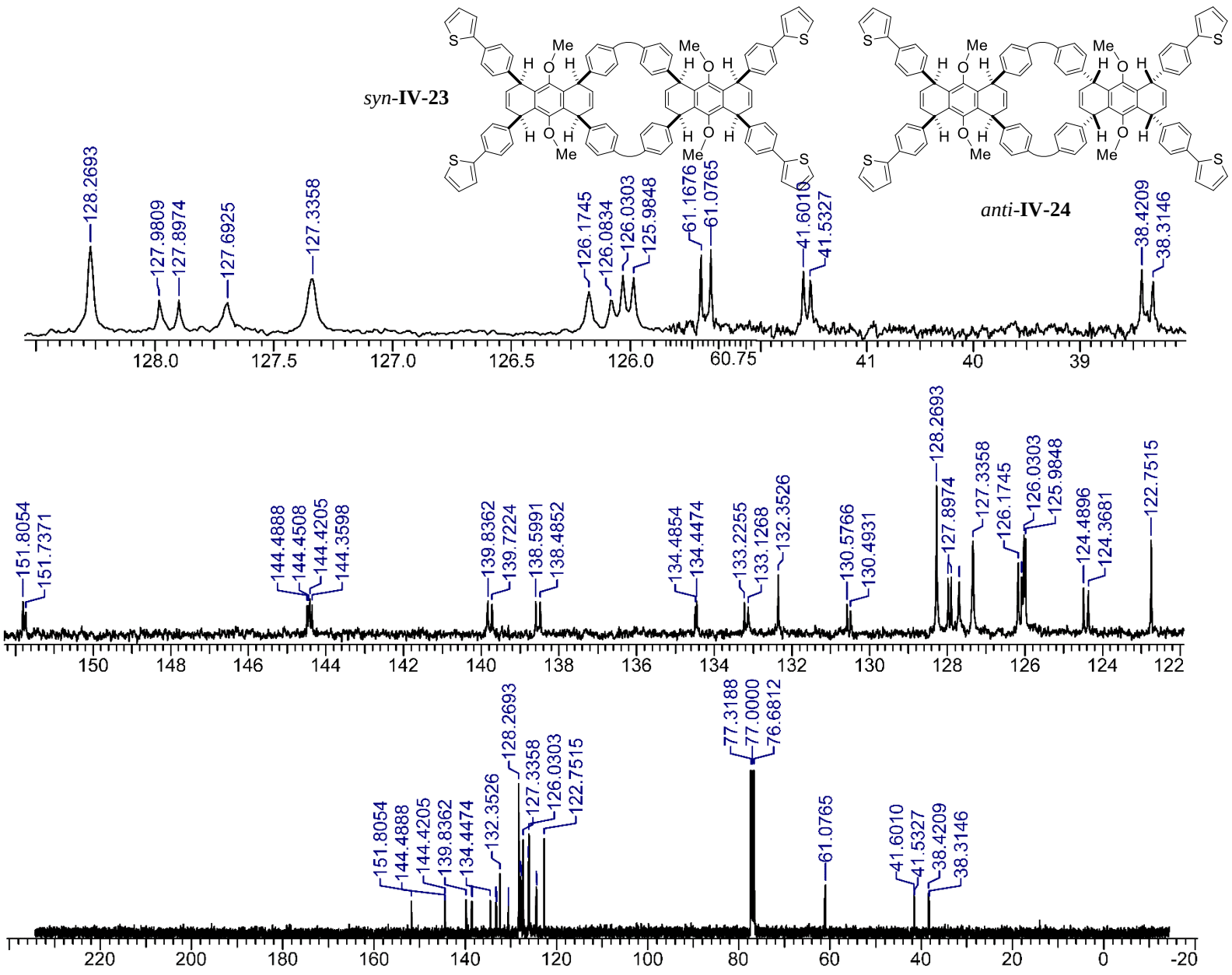
syn-IV-23
anti-IV-24
128.2693
127.9809
127.8974
127.6925
127.3358
126.1745
126.0834
126.0303
125.9848
61.1676
61.0765
41.6010
41.5327
38.4209
38.3146
151.8054
151.7371
144.4888
144.4508
144.4205
144.3598
139.8362
139.7224
138.5991
138.4852
134.4854
134.4474
133.2255
133.1268
132.3526
130.5766
130.4931
128.2693
127.8974
127.3358
126.1745
126.0303
125.9848
124.4896
124.3681
122.7515
77.3188
77.0000
76.6812
61.0765
41.6010
41.5327
38.4209
38.3146

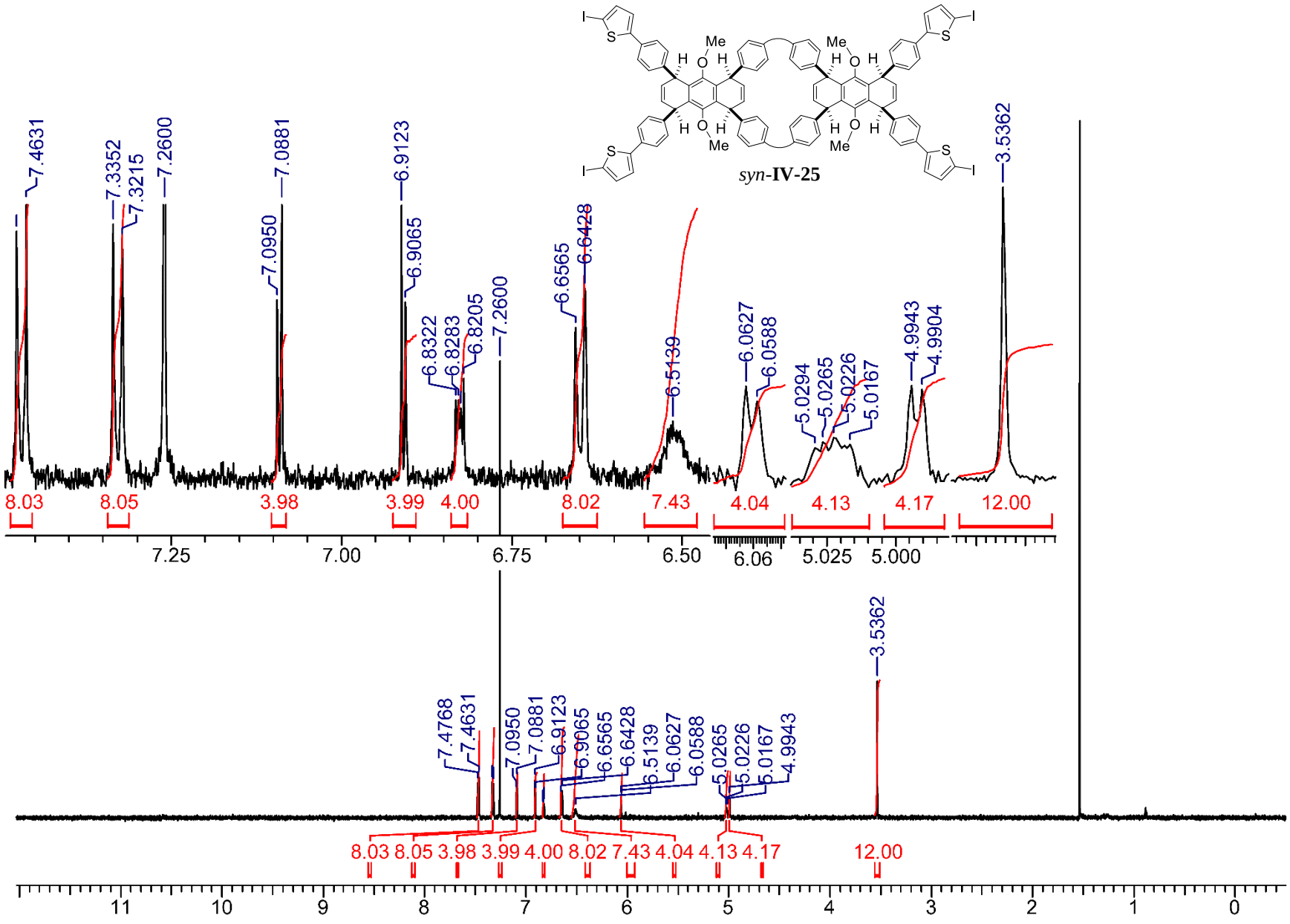
syn-IV-25
7.4631
7.3352
7.3215
7.2600
7.0881
7.0950
6.9123
6.9065
6.8322
6.8283
6.8205
7.2600
6.6565
6.6428
6.5139
6.0627
6.0588
5.0294
5.0265
5.0226
5.0167
4.9943
4.9904
3.5362
8.03
8.05
3.98
3.99
4.00
8.02
7.43
4.04
4.13
4.17
12.00
7.25
7.00
6.75
6.50
6.06
5.025
5.000
7.4768
7.4631
7.0950
7.0881
6.9123
6.9065
6.6565
6.6428
6.5139
6.0627
6.0588
5.0265
5.0226
5.0167
4.9943
3.5362
8.03 8.05 3.98 3.99 4.00 8.02 7.43 4.04 4.13 4.17
12.00
11
10
9
8
7
6
5
4
3
2
1
0

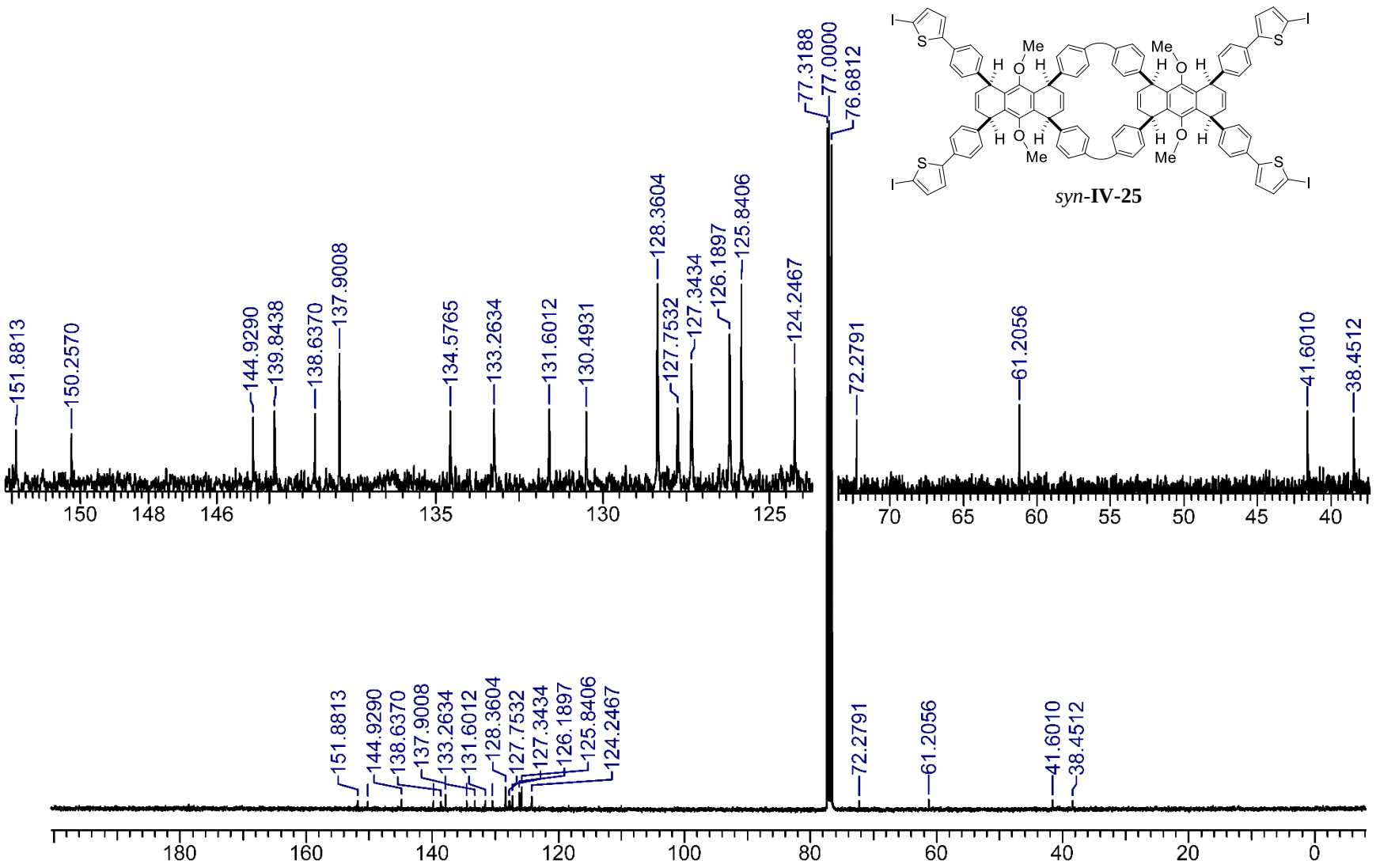
151.8813
150.2570
144.9290
139.8438
138.6370
137.9008
134.5765
133.2634
131.6012
130.4931
128.3604
127.7532
127.3434
126.1897
125.8406
124.2467
77.3188
77.0000
76.6812
72.2791
61.2056
41.6010
38.4512
Me
H
O
S
I
syn-IV-25

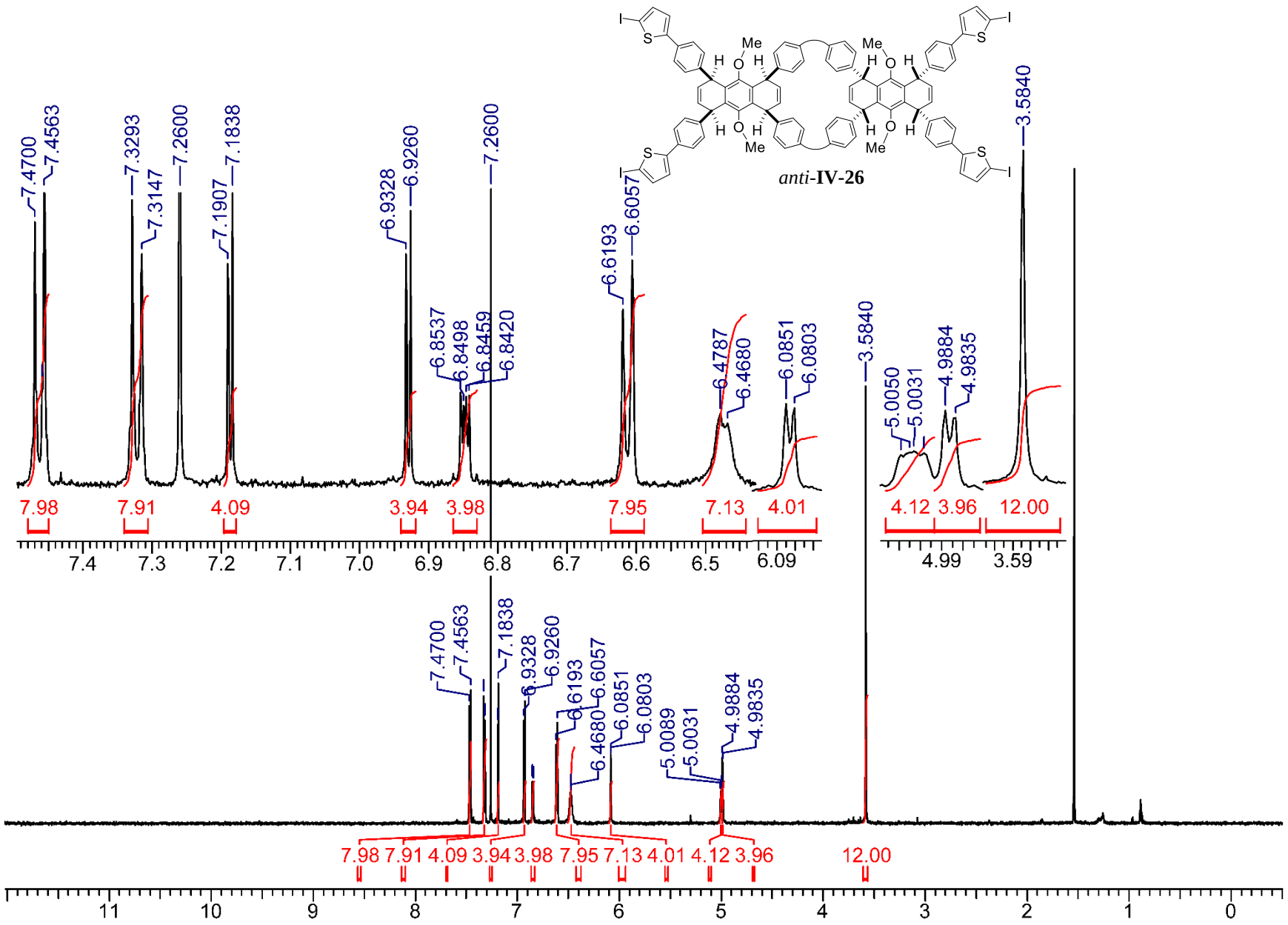
anti-IV-26
7.4700
7.4563
7.3293
7.3147
7.2600
7.1907
7.1838
6.9328
6.9260
6.8537
6.8498
6.8459
6.8420
6.6193
6.6057
6.4787
6.4680
6.0851
6.0803
5.0050
5.0031
4.9884
4.9835
3.5840
7.98
7.91
4.09
3.94
3.98
7.95
7.13
4.01
4.12
3.96
12.00

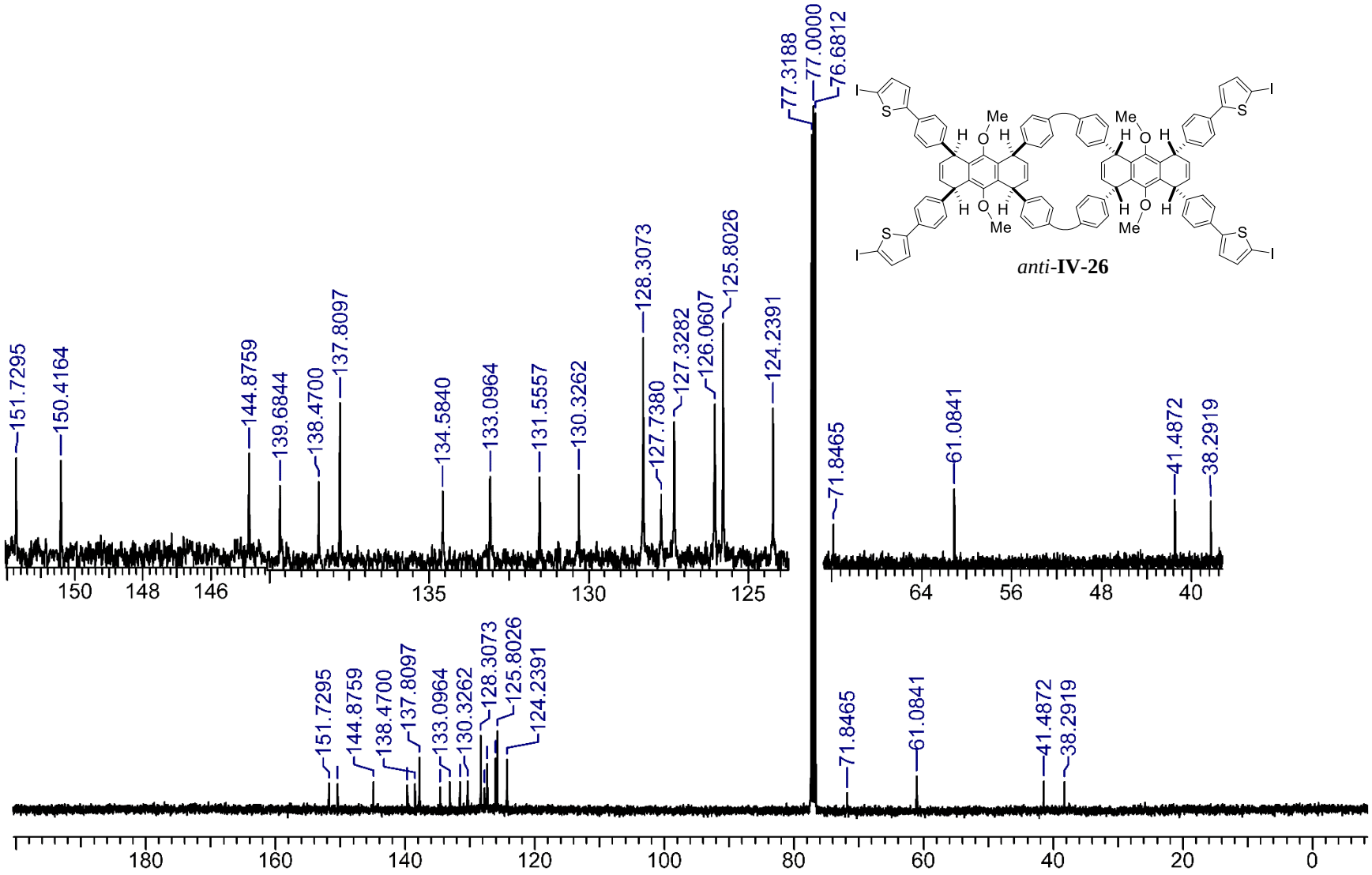
77.3188
77.0000
76.6812
151.7295
150.4164
144.8759
139.6844
138.4700
137.8097
134.5840
133.0964
131.5557
130.3262
128.3073
127.7380
127.3282
126.0607
125.8026
124.2391
71.8465
61.0841
41.4872
38.2919
Me
H
O
S
I

anti-**IV-26**

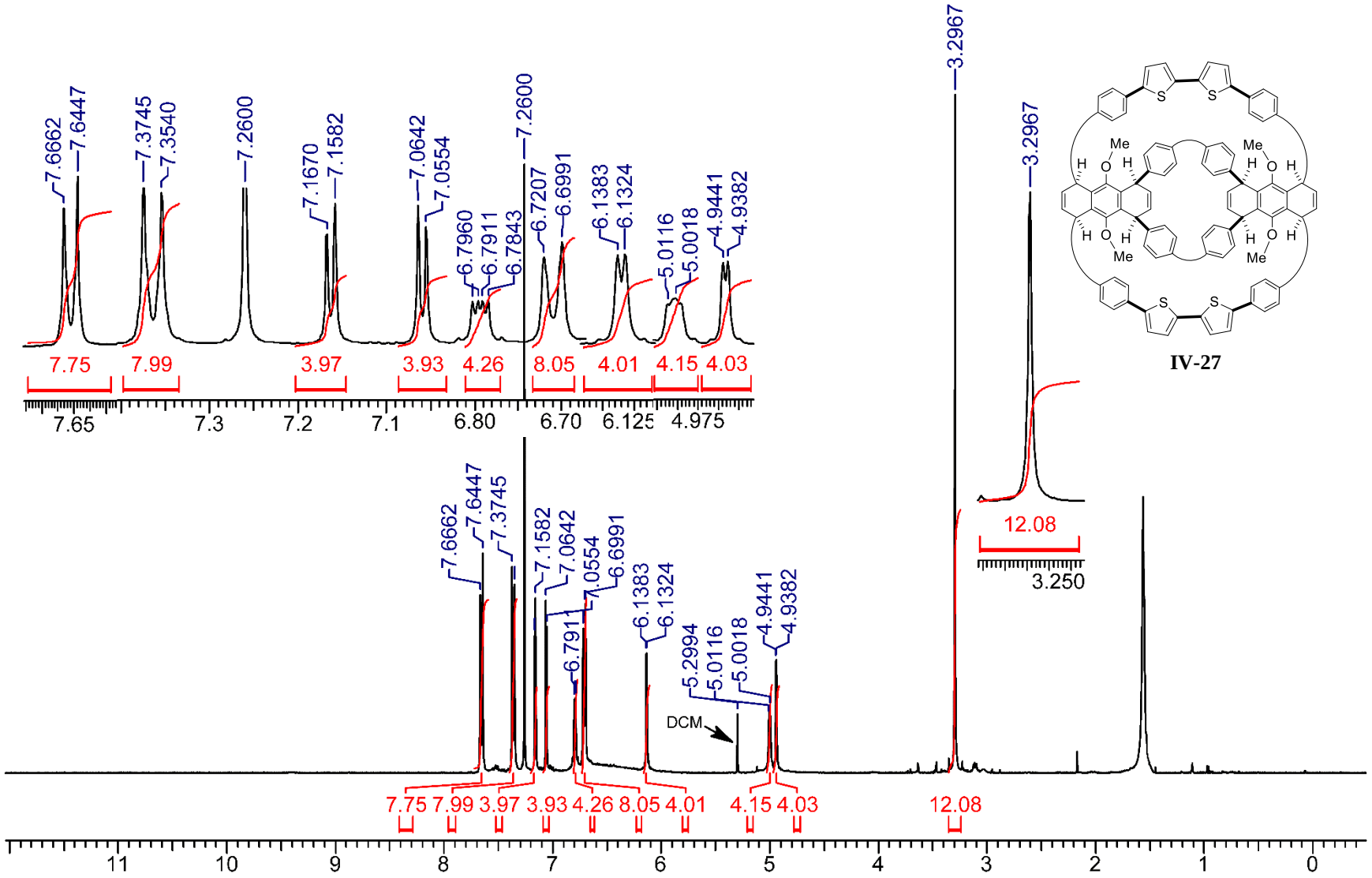
7.6662
7.6447
7.3745
7.3540
7.2600
7.1670
7.1582
7.0642
7.0554
6.7960
6.7911
6.7843
6.7207
6.6991
6.1383
6.1324
5.0116
5.0018
4.9441
4.9382
3.2967
7.75
7.99
3.97
3.93
4.26
8.05
4.01
4.15
4.03
12.08
3.250
DCM
IV-27

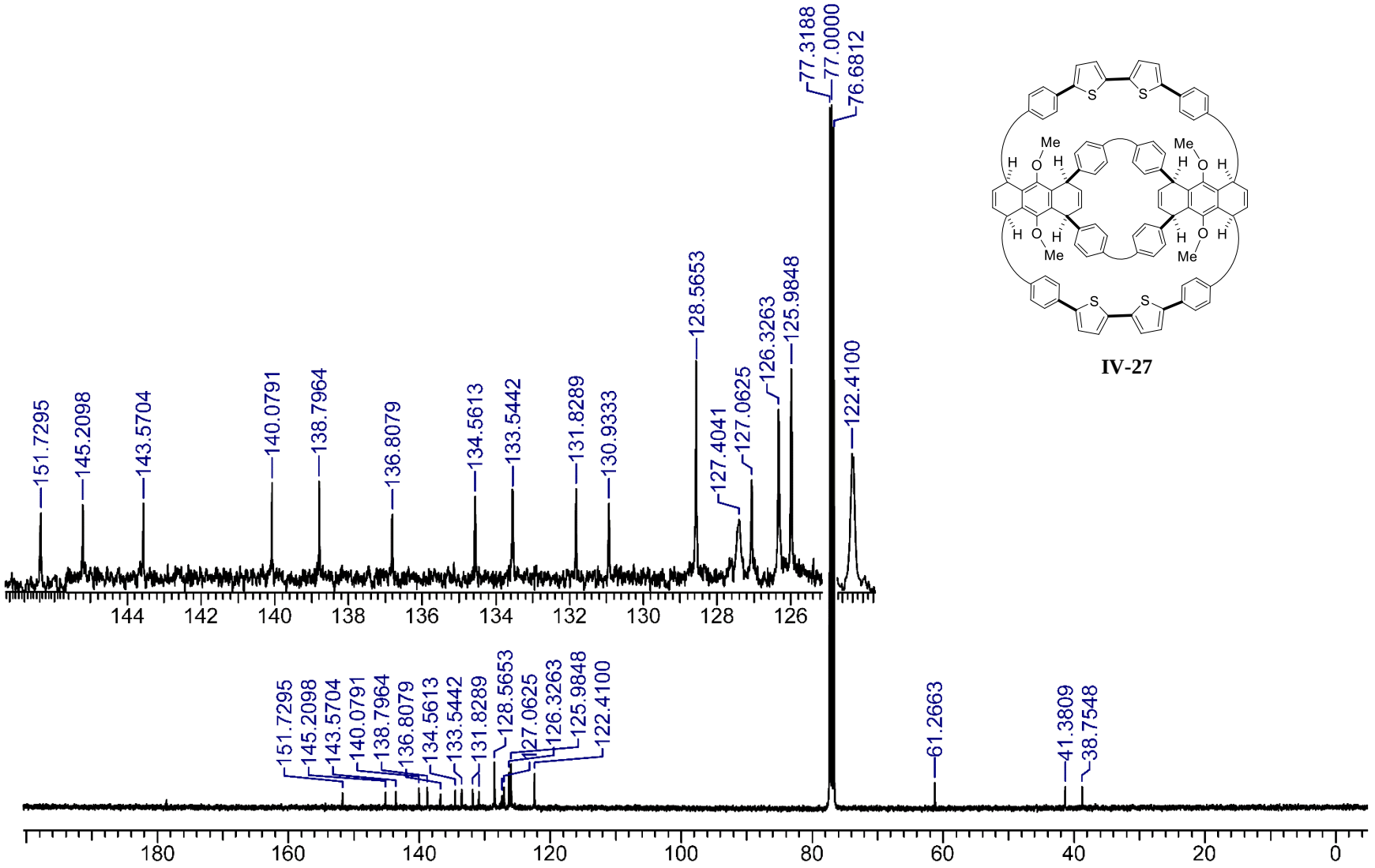
77.3188
77.0000
76.6812
128.5653
127.4041
127.0625
126.3263
125.9848
122.4100
151.7295
145.2098
143.5704
140.0791
138.7964
136.8079
134.5613
133.5442
131.8289
130.9333
61.2663
41.3809
38.7548
144
142
140
138
136
134
132
130
128
126
180
160
140
120
100
80
60
40
20
0

IV-27

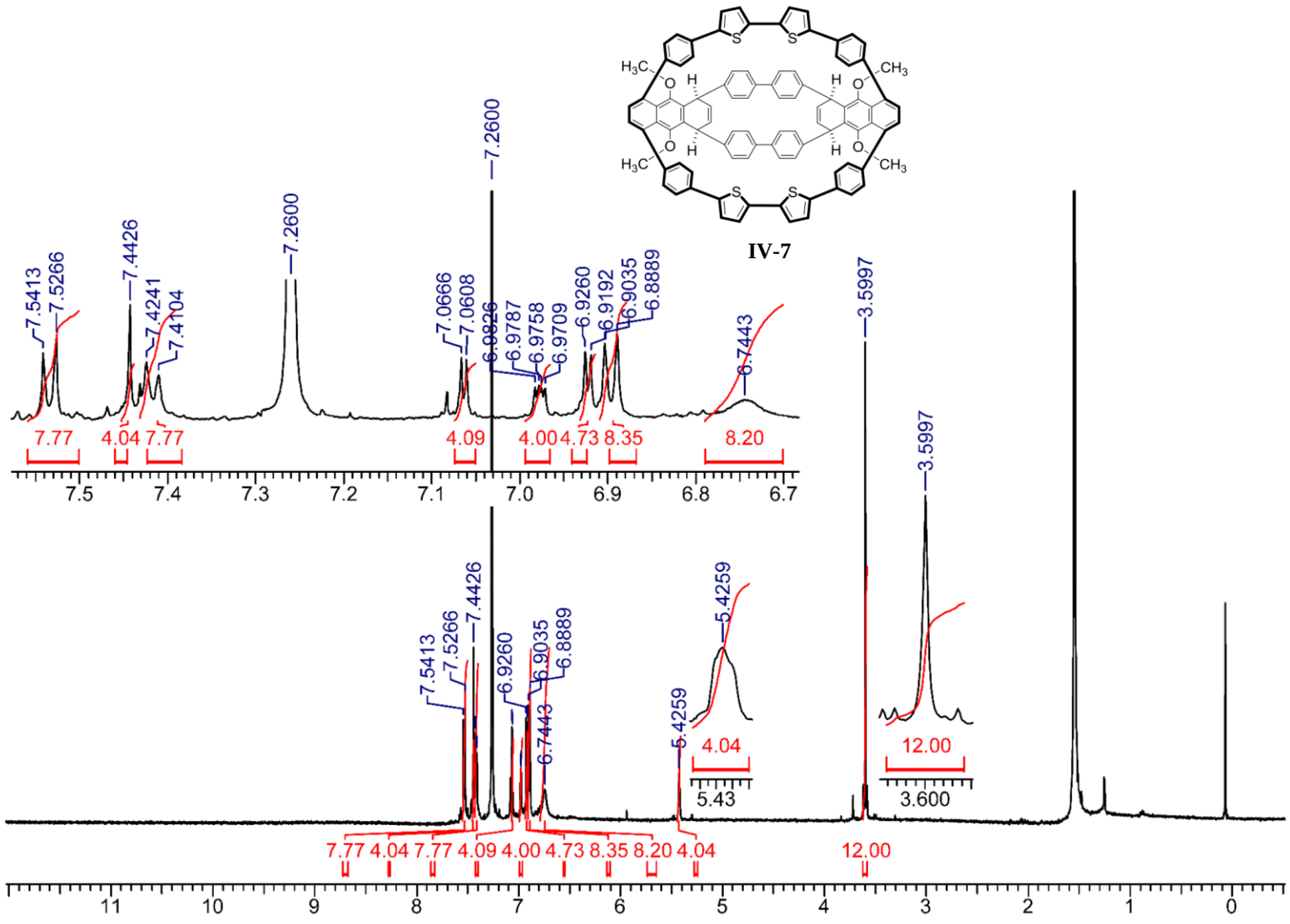
IV-7
7.5413
7.5266
7.4426
7.4241
7.4104
7.2600
7.0666
7.0608
6.9787
6.9758
6.9709
6.9260
6.9192
6.9035
6.8889
6.7443
3.5997
5.4259
7.77
4.04
7.77
4.09
4.00
4.73
8.35
8.20
12.00
5.43
3.600

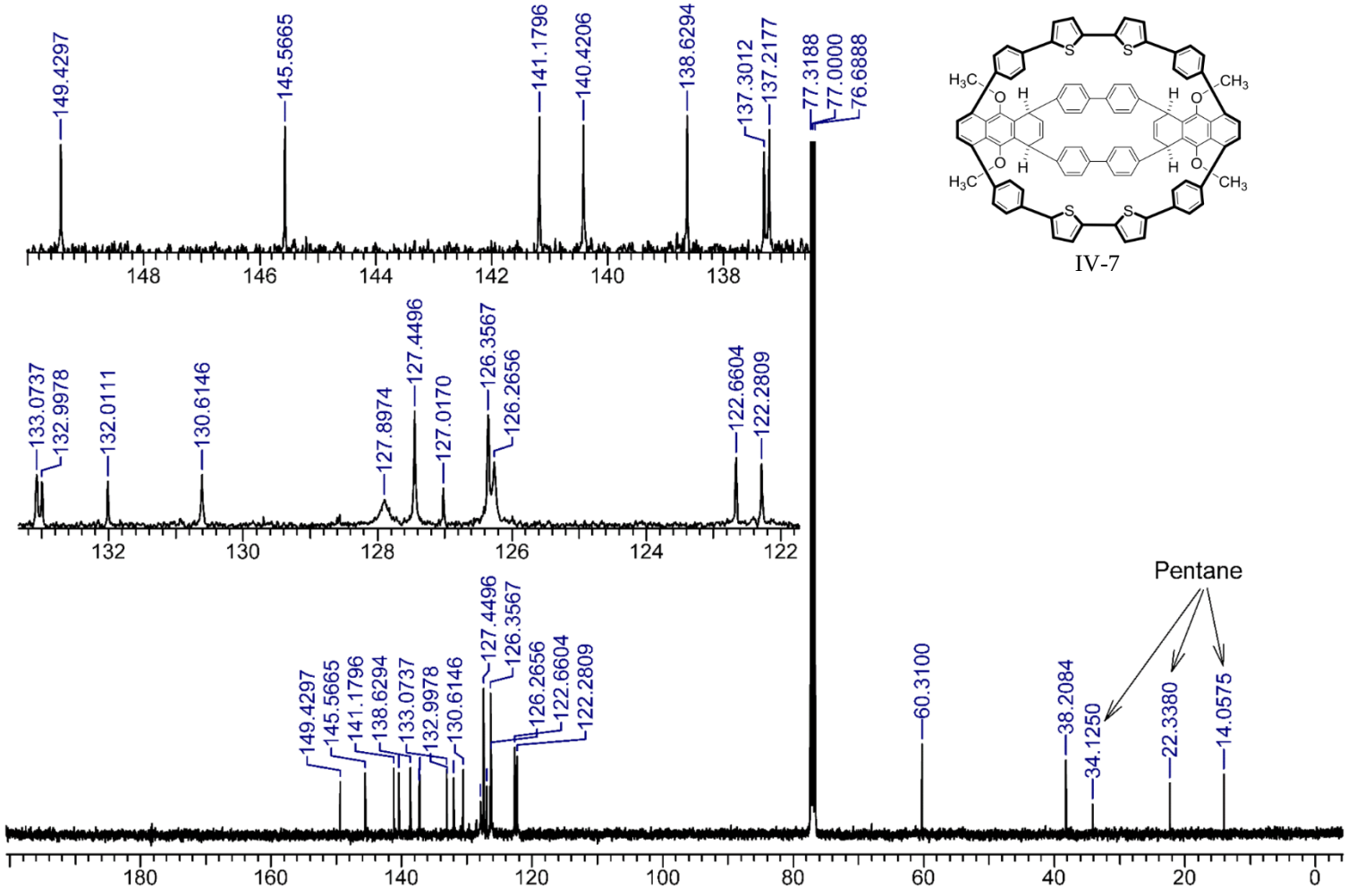
149.4297
145.5665
141.1796
140.4206
138.6294
137.3012
137.2177
77.3188
77.0000
76.6888
148
146
144
142
140
138
133.0737
132.9978
132.0111
130.6146
127.8974
127.4496
127.0170
126.3567
126.2656
122.6604
122.2809
132
130
128
126
124
122
Pentane
149.4297
145.5665
141.1796
138.6294
133.0737
132.9978
130.6146
127.4496
126.3567
126.2656
122.6604
122.2809
60.3100
38.2084
34.1250
22.3380
14.0575
180
160
140
120
100
80
60
40
20
0

IV-7

List of Publication

1. Behzad Farajidizaji, Haresh Thakellapalli, Shuangjiang Li, Changfeng Huang, Notashia N. Baughman, Novruz G. Akhmedov, Brian V. Popp, Jeffrey L. Petersen, and Kung K. Wang*. "Synthesis of Cycloparaphenylenes Bearing Furan-2,5-diyl or 2,2'-Bifuran-5,5'-diyl Units in the Macrocyclic Structures." *Chem. Eur. J*. 2016, *22*, 16420–16424.

2. Behzad Farajidizaji, Haresh Thakellapalli, Changfeng Huang, Shuangjiang Li, Novruz G. Akhmedov, Brian V. Popp, Jeffrey L. Petersen, and Kung K. Wang*. "Synthesis and Characterization of Functionalized [12]Cycloparaphenylenes Containing Four Alternating Biphenyl and Naphthyl Units." *J. Org. Chem.* 2017, *82*, 4458−4464.

3. **Behzad Farajidizaji**, Haresh Thakellapalli, Novruz G. Akhmedov, and Kung K. Wang * ''Synthesis of Molecular Nanohoops Bearing a Tetrahydro[6]cycloparaphenylene Fused to a Hydrogenated or a Thiophene-Inserted Cycloparaphenylene'' (Just accepted to *J. Org. Chem*).

4. Shuangjiang Li, Merfat Aljahdli, Haresh Thakellapalli, **Behzad Farajidizaji**, Novruz G. Akhmedov and Kung K. Wang* "Synthesis and Structure of a Functionalized [9]Cycloparaphenylene Bearing Three Indeno[2,1-a]fluorene-11,12-dione-2,9-diyl Units." *Org. Lett.* **2017**, *19*, 4078−4081.

5. Haresh Thakellapalli, Shuangjiang Li, **Behzad Farajidizaji**, Notashia N. Baughman, Novruz G. Akhmedov, Brian V. Popp and Kung K. Wang* "Synthesis and Characterization of 2,7-Di-2-thienyl-9H-fluoren-9-one-Containing Macrocycles" *Org. Lett.* **2017**, *19*, 2674−2677.

6. Changfeng Huang, Shuangjiang Li, Haresh Thakellapalli, Behzad Farajidizaji, Yiwei Huang, Novruz G Akhmedov, Brian V. Popp, Jeffrey L. Petersen and, Kung K. Wang*. "Synthesis of Partially Hydrogenated Cycloparaphenylenes with Bent and Fused Structures Bearing Armchair Carbon Nanotube-like Connections." *J. Org. Chem.* 2017, *82*, 1166−1174.

7. Shuangjiang Li, Changfeng Huang, Haresh Thakellapalli, **Behzad Farajidizaji**, Brian V. Popp, Jeffrey L. Petersen, and Kung K. Wang*. "Syntheses and Structures of Functionalized [9]Cycloparaphenylenes as Carbon Nanohoops Bearing Carbomethoxy and *N*-Phenylphthalimido Groups." *Org. Lett.* **2016**, *18*, 2268−2271.

8. Haresh Thakellapalli, **Behzad Farajidizaji**, Trevor W. Butcher, Novruz G. Akhmedov, Brian V. Popp, Jeffrey L. Petersen, and Kung K. Wang*. “Syntheses and Structures of Thiophene-Containing Cycloparaphenylenes and Related Carbon Nanohoops.” *Org. Lett.* **2015**, *17*, 3470−3473.